frontiers | Research Topics

New insights into renal fibrosis and therapeutic effects of natural products, volume II

Edited by
Dan-Qian Chen and Zhiyong Guo

Published in
Frontiers in Pharmacology

ISSN 1664-8714
ISBN 978-2-83251-428-3
DOI 10.3389/978-2-83251-428-3

About Frontiers

Frontiers is more than just an open access publisher of scholarly articles: it is a pioneering approach to the world of academia, radically improving the way scholarly research is managed. The grand vision of Frontiers is a world where all people have an equal opportunity to seek, share and generate knowledge. Frontiers provides immediate and permanent online open access to all its publications, but this alone is not enough to realize our grand goals.

Frontiers journal series

The Frontiers journal series is a multi-tier and interdisciplinary set of open-access, online journals, promising a paradigm shift from the current review, selection and dissemination processes in academic publishing. All Frontiers journals are driven by researchers for researchers; therefore, they constitute a service to the scholarly community. At the same time, the *Frontiers journal series* operates on a revolutionary invention, the tiered publishing system, initially addressing specific communities of scholars, and gradually climbing up to broader public understanding, thus serving the interests of the lay society, too.

Dedication to quality

Each Frontiers article is a landmark of the highest quality, thanks to genuinely collaborative interactions between authors and review editors, who include some of the world's best academicians. Research must be certified by peers before entering a stream of knowledge that may eventually reach the public - and shape society; therefore, Frontiers only applies the most rigorous and unbiased reviews. Frontiers revolutionizes research publishing by freely delivering the most outstanding research, evaluated with no bias from both the academic and social point of view. By applying the most advanced information technologies, Frontiers is catapulting scholarly publishing into a new generation.

What are Frontiers Research Topics?

Frontiers Research Topics are very popular trademarks of the *Frontiers journals series*: they are collections of at least ten articles, all centered on a particular subject. With their unique mix of varied contributions from Original Research to Review Articles, Frontiers Research Topics unify the most influential researchers, the latest key findings and historical advances in a hot research area.

Find out more on how to host your own Frontiers Research Topic or contribute to one as an author by contacting the Frontiers editorial office: frontiersin.org/about/contact

New insights into renal fibrosis and therapeutic effects of natural products, volume II

Topic editors

Dan-Qian Chen — Northwest University, China

Zhiyong Guo — Second Military Medical University, China

Citation

Chen, D.-Q., Guo, Z., eds. (2023). *New insights into renal fibrosis and therapeutic effects of natural products, volume II*. Lausanne: Frontiers Media SA.

doi: 10.3389/978-2-83251-428-3

Table of contents

frontiers | Frontiers in Pharmacology

TYPE Editorial
PUBLISHED 28 October 2022
DOI 10.3389/fphar.2022.1053408

OPEN ACCESS

EDITED BY
Giuseppe Remuzzi,
Istituto di Ricerche Farmacologiche Mario Negri IRCCS, Italy

REVIEWED BY
Yue-Yu Gu,
The Chinese University of Hong Kong, China

*CORRESPONDENCE
Dan-Qian Chen,
chendanqian2013@163.com
Yu-Ping Tang,
yupingtang@sntcm.edu.cn

SPECIALTY SECTION
This article was submitted to Renal Pharmacology, a section of the journal Frontiers in Pharmacology

RECEIVED 25 September 2022
ACCEPTED 13 October 2022
PUBLISHED 28 October 2022

CITATION
Chen D-Q, Guo Y, Guo Z-Y and Tang Y-P (2022), Editorial: New insights into renal fibrosis and therapeutic effects of natural products volume II. *Front. Pharmacol.* 13:1053408. doi: 10.3389/fphar.2022.1053408

Editorial: New insights into renal fibrosis and therapeutic effects of natural products volume II

Dan-Qian Chen[1,2]*, Yan Guo[3], Zhi-Yong Guo[4] and Yu-Ping Tang[1]*

[1]Key Laboratory of Shaanxi Administration of Traditional Chinese Medicine for TCM Compatibility, Shaanxi University of Chinese Medicine, Xi'an, China, [2]Department of Emergency, China-Japan Friendship Hospital, Beijing, China, [3]Department of Internal Medicine, University of New Mexico, Albuquerque, NM, United States, [4]Department of Nephrology, Changhai Hospital, Naval Medical University, Shanghai, China

KEYWORDS

natural product, renal fibrosis, therapeutic target, active component, Chinese herbal medicine

Editorial on the Research Topic
New Insights into Renal Fibrosis and Therapeutic Effects of Natural Products, Volume II

Introduction

Renal fibrosis which begins as an abnormal tissue regeneration process is the final and common outcome of various chronic kidney diseases (CKD) (Li et al., 2022). Sustained chronic inflammation, myofibroblast activation, epithelial-to-mesenchymal transition (EMT) and extracellular matrix (ECM) accumulation are the major characteristics of renal fibrosis (Chen et al., 2018a). Renin angiotensin aldosterone system is the first-line therapy for CKD in clinics. Although the blockade of renin angiotensin aldosterone system attenuates renal fibrosis, their effects are limited and hardly delay renal fibrosis and CKD progression (Romero et al., 2015). The therapeutic candidate and strategy that specifically target the pathogenesis of fibrosis are urgently needed, which highlights the importance of identifying novel therapeutic targets and mechanisms.

Natural products have been recognized as promising therapeutic candidates for renal fibrosis and CKD treatment, and have yielded favorable efficacy in clinics (Chen et al., 2018b). However, the mechanisms underlying natural products against renal fibrosis are partially unclear which hinders their clinical application. Emerging evidences are beneficial to provide comprehensive acknowledge and guide clinical rational use of natural products.

The present Research Topic aims to collate manuscripts reporting or describing new insights into renal fibrosis and therapeutic effects of natural products. After rigorous peer

reviews, a total of 16 manuscripts were published. These manuscripts report the novel mechanisms of renal fibrosis, the therapeutic effects and targets of natural products, and the high-quality evidences from clinical trials.

New insights into the underlying mechanisms of renal fibrosis

Several novel therapeutic targets and strategies for renal fibrosis in diabetic kidney disease (DKD) are discussed. Liang et al. identified E2F transcription factor 1 (E2F1) as a promising therapeutic target for DKD treatment by acting on the senescence of renal tubular epithelial cells. E2F1 was upregulated in high-glucose-induced renal tubular epithelial cells and DKD animal model. Treatment with metformin suppressed cellular senescence of renal tubular epithelial cells to alleviate renal injury through modulating E2F1. Xiao et al. explored the anti-fibrotic mechanism of bone morphogenetic protein (BMP)-7 in diabetic tubulointerstitial fibrosis. Functionally, BMP-7 alleviated diabetic renal injury by upregulating Id2 protein levels through the BMP-7–MAPK signaling pathway. Further experiments demonstrated that oxymatrine ameliorated EMT process to delay DKD progression by suppressing renal tubulointerstitial fibrosis *via* BMP-7–MAPK pathway. Guo et al. identified insulin-like growth factor-1 receptor (IGF1R) as a novel therapeutic target for DKD treatment *via* modulating EMT process. Treatment with sodium-glucose cotransporter 2 (SGLT2) inhibitor, dapagliflozin, significantly decreased IGF1R levels in plasma samples from patients with DKD and DKD animal model. The suppression of SGLT2/IGF1R/PI3K signaling served as a key mediator in blocking EMT process. Zhang et al. explored the relationship between serum metabolites and gut microbiota in DKD. They found that isomaltose, D-mannose, galactonic acid, citramalic acid, and prostaglandin B2 significantly increased, while 3-(2-hydroxyethyl)-indole, 3-methylindole, and indoleacrylic acid decreased in the DKD model, which involved in the dysfunction of *g_Eubacterium_nodatum_group*, *g_Lactobacillus*, and *g_Faecalibaculum*. These results reveal the potential metabolic and microbial targets for DKD treatment.

Autophagy is traditionally known for its vital role in maintaining homeostasis, structure, and function of the kidney (Chen et al., 2022). Fu et al. found a novel mechanism that persistent autophagy after acute kidney injury (AKI) was detrimental, which induced pro-fibrotic cytokines in renal tubular cells, promoted renal fibrosis and CKD progression. Treatment with autophagy inhibitors substantially blocked repeated low dose cisplatin-induced secretion of pro-fibrotic cytokines in renal tubular cells. In addition, Zhou et al. highlighted the important role of microRNAs in primary membranous nephropathy (MN) progression under PM2.5 exposure. Multiple microRNAs participated in primary MN progression and treatment under PM2.5 exposure through immune system cells by acting on the imbalance of Th17/Treg, indicating Th17/Treg balance/imbalance as new insights of primary MN and its therapeutic value.

New insights into therapeutic effects of natural products against renal fibrosis

Zhao et al. carried out an integrative network pharmacology-based approach and experimental verification to confirm the anti-fibrotic effect of Jian-Pi-Yi-Shen formula (JPYSF) in kidney. Functionally, JPYSF suppressed EMT process to attenuate renal fibrosis *via* inactivating Wnt3a/β-catenin signaling pathway and enhancing E-cadherin expression in 5/6 nephrectomy-induced renal fibrosis rats. Jia et al. reported the anti-fibrotic effect and underlying mechanism of Tongluo Yishen (TLYS) decoction on renal interstitial fibrosis. TLYS decoction exhibited favorable efficacy in improving renal function, delaying renal interstitial fibrosis progression, and inhibiting pyroptosis in unilateral ureteral obstruction rats. TLYS also attenuated hypoxia-induced NRK-52E cell damage *via* the suppression of the NLRP3-mediated pyroptosis. Shenkang injection (SKI) is a commonly used herbal formula in China, and Wang et al. investigated the underlying mechanism of Shenkang injection against renal fibrosis and CKD. Shenkang injection and its active component rhein suppressed kidney function decline and EMT *via* inhibiting renin angiotensin system activation and the hyperactive Wnt/β-catenin signalling pathway in adenine-induced rats and Ang II-induced HK-2 and NRK-49F cells. Focal segmental glomerulosclerosis (FSGS) accounts for nearly 20% of nephrotic syndrome in children and 40% in adults, with characteristics of fibrosis in glomeruli and interstitium. Tan et al. found that Yi-Shen-Hua-Shi (YSHS) granule prevented nephrotic syndrome progression in clinical and animal models of FSGS. A network pharmacology-based and experimental approaches were used to identify that BMP2/Smad signaling pathway was vital for YSHS granule to attenuate FSGS.

Liu et al. discussed the therapeutic mechanisms of Chinese herbal medicine in attenuating renal interstitial fibrosis including increased ECM, renal tubular epithelial cell phenotype transformation, oxidative stress, renal interstitial fibroblast proliferation, activation, and phenotypic transformation, and the activation of cytokines and inflammatory cells. TGF-β, NF-κB, Wnt/β-Catenin, hedgehog, notch, and MAPK-related signaling pathways are the common intervening targets of Chinese herbal medicine. Wang et al. reviewed the pathophysiological rationale for MN treatments and highlighted its clinical diagnosis by autoantibodies against the phospholipase A2 receptor (PLA2R) and thrombospondin type-1 domain-containing protein 7A (THSD7A) antigens. *Astragalus membranaceus*, *Tripterygium wilfordii*, and Astragaloside IV have exhibited beneficial effects for the treatment of MN clinically. Chen et al. reported the latest progress of quercetin, a

natural flavonoid, in treating CKD. Quercetin exhibited protection in both AKI and CKD through anti-hyperglycemic, anti-oxidative effects, autophagy promotion, senolytic mechanisms. Tan et al. concluded the potential mechanisms of Cordyceps against renal fibrosis, and its mechanisms involved in the inhibition of oxidative stress and inflammation, the suppression of apoptosis, the modulation of autophagy, and the reduction of extracellular matrix deposition and fibroblast activation. Clinical trials have confirmed the beneficial efficacy of Cordyceps against CKD, but the low quality and significant heterogeneity of Cordyceps preparations prohibit their extensive use. Further evidences from clinical trials are needed for natural products to boost the application beyond China and Asia.

New insights into clinical therapeutic effects of natural products against renal fibrosis

Here, two multicenter randomized controlled clinical trials provide favorable evidences for natural products against renal fibrosis. Chen et al. carried out a multicenter randomized controlled clinical trial to confirm the nephroprotection of Chuan Huang Fang (CHF) on CKD patients who suffered AKI. Compared to the reduced glutathione (RG)-treated group, more reductions of Scr, BUN, UA, and better improvement of eGFR were observed in RG + CHF group, and the levels of urinary AKI biomarkers and renal fibrosis biomarkers were lower, highlighting CHF as a promising therapeutic candidate. Persistent inflammation associated with recurrent urinary tract infection (rUTI) is a crucial inducement of inflammation-driven renal fibrosis. A multicenter, randomized, controlled clinical trial from Li et al. reported that Tailin formulation (TLF, a Chinese herbal formulation for rUTI treatment) combined with continuous low-dose antibiotic therapy (CLAT) exhibited more favorable efficacy than CLAT alone in reducing rUTI recurrence, the non-infection-related physical symptoms and tubular fibrosis.

Conclusion

The Research Topic 'New Insights into Renal Fibrosis and Therapeutic Effects of Natural Products, Volume II' have collected worthy studies and contributions on the subject of renal fibrosis, highlighting the promising therapeutic property of natural products in pre-clinical and clinical contexts. We hope that you enjoy and gain from the Research Topic which will surely inspire additional natural products-based research in the future.

Author contributions

D-QC wrote the first draft of the manuscript. YG, Y-PT and Z-YG reviewed and revised this editorial. All authors approved the submitted version.

Conflict of interest

The authors declare that the research was conducted in the absence of any commercial or financial relationships that could be construed as a potential conflict of interest.

Publisher's note

References

Chen, D. Q., Feng, Y. L., Cao, G., and Zhao, Y. Y. (2018a). Natural products as a source for antifibrosis therapy. *Trends Pharmacol. Sci.* 39, 937–952. doi:10.1016/j.tips.2018.09.002

Chen, D. Q., Guo, Y., Li, X., Zhang, G. Q., and Li, P. (2022). Small molecules as modulators of regulated cell death against ischemia/reperfusion injury. *Med. Res. Rev.* 2022, 2067–2101. doi:10.1002/med.21917

Chen, D. Q., Hu, H. H., Wang, Y. N., Feng, Y. L., Cao, G., and Zhao, Y. Y. (2018b). Natural products for the prevention and treatment of kidney disease. *Phytomedicine* 50, 50–60. doi:10.1016/j.phymed.2018.09.182

Li, L., Fu, H., and Liu, Y. (2022). The fibrogenic niche in kidney fibrosis: Components and mechanisms. *Nat. Rev. Nephrol.* 18, 545–557. doi:10.1038/s41581-022-00590-z

Romero, C. A., Orias, M., and Weir, M. R. (2015). Novel RAAS agonists and antagonists: Clinical applications and controversies. *Nat. Rev. Endocrinol.* 11, 242–252. doi:10.1038/nrendo.2015.6

frontiers | Frontiers in Pharmacology

ORIGINAL RESEARCH
published: 14 April 2022
doi: 10.3389/fphar.2022.872988

Characteristics of Serum Metabolites and Gut Microbiota in Diabetic Kidney Disease

Bo Zhang[1,2], Yuzhou Wan[2], Xuefeng Zhou[2], Haojun Zhang[2], Hailing Zhao[2], Liang Ma[2], Xi Dong[2], Meihua Yan[2], Tingting Zhao[1,2] and Ping Li[2]**

[1]Graduate School of Peking Union Medical College, Chinese Academy of Medical Sciences and Peking Union Medical College, Beijing, China, [2]Beijing Key Laboratory for Immune-Mediated Inflammatory Diseases, Institute of Clinical Medical Sciences, China–Japan Friendship Hospital, Beijing, China

Disturbance of circulating metabolites and disorders of the gut microbiota are involved in the progression of diabetic kidney disease (DKD). However, there is limited research on the relationship between serum metabolites and gut microbiota, and their involvement in DKD. In this study, using an experimental DKD rat model induced by combining streptozotocin injection and unilateral nephrectomy, we employed untargeted metabolomics and 16S rRNA gene sequencing to explore the relationship between the metabolic profile and the structure and function of gut microbiota. Striking alterations took place in 140 serum metabolites, as well as in the composition and function of rat gut microbiota. These changes were mainly associated with carbohydrate, lipid, and amino acid metabolism. In these pathways, isomaltose, D-mannose, galactonic acid, citramalic acid, and prostaglandin B2 were significantly upregulated. 3-(2-Hydroxyethyl)indole, 3-methylindole, and indoleacrylic acid were downregulated and were the critical metabolites in the DKD model. Furthermore, the levels of these three indoles were restored after treatment with the traditional Chinese herbal medicine Tangshen Formula. At the genera level, *g_Eubacterium_nodatum*_group, *g_Lactobacillus*, and *g_Faecalibaculum* were most involved in metabolic disorders in the progression of DKD. Notably, the circulating lipid metabolites had a strong relationship with DKD-related parameters and were especially negatively related to the mesangial matrix area. Serum lipid indices (TG and TC) and UACR were directly associated with certain microbial genera. In conclusion, the present research verified the anomalous circulating metabolites and gut microbiota in DKD progression. We also identified the potential metabolic and microbial targets for the treatment of DKD.

Keywords: gut microbiota, diabetic kidney disease, carbohydrate metabolism, lipid metabolism, serum metabolites, amino acid metabolism

OPEN ACCESS

Edited by:
Zhiyong Guo,
Second Military Medical University, China

Reviewed by:
Yifei Zhong,
Longhua Hospital, China
Yi-Gang Wan,
Nanjing University, China

****Correspondence:***
Tingting Zhao
ttfrfr@163.com
Ping Li
lp8675@163.com

Specialty section:
This article was submitted to Renal Pharmacology, a section of the journal Frontiers in Pharmacology

Received: *10 February 2022*
Accepted: *18 March 2022*
Published: *14 April 2022*

Citation:
Zhang B, Wan Y, Zhou X, Zhang H, Zhao H, Ma L, Dong X, Yan M, Zhao T and Li P (2022) Characteristics of Serum Metabolites and Gut Microbiota in Diabetic Kidney Disease. Front. Pharmacol. 13:872988. doi: 10.3389/fphar.2022.872988

INTRODUCTION

Diabetic kidney disease (DKD) is one of the most prevalent microvascular complications of diabetes mellitus and is the main cause of end-stage renal disease in developed countries and the developed regions of China (Ma, 2018; Johansen et al., 2021). The poor prognosis of DKD severely reduces the quality of life and imposes a substantial financial burden on patients. The pathogenesis of DKD remains unclear, and there is a lack of comprehensive awareness of the

progression of DKD (Winther et al., 2020; Jin and Ma, 2021), which severely restricts its prevention and diagnosis.

Metabolites are both the substrates and products of cellular basal metabolism. With advances in metabolomics, abnormal biological pathways can now be detected in the disease state, especially in DKD, which involves various metabolic pathways and complicated pathogenic mechanisms (Johnson et al., 2016; Rinschen et al., 2019). In addition, the metabolites are produced not only by the host organism but also by the gut microbiota in large portions, such as short chain fatty acids (Li et al., 2020a; Hu et al., 2020) and uremic toxins (Kikuchi et al., 2019; Winther et al., 2019), which are highly involved in DKD. The number of genes encoded by gut microorganisms is high in humans. Furthermore, the plethora of active metabolites, particularly those uniquely produced by gut microbiota, have profound implications on the health of the host.

In the present research, we used untargeted metabolomics and 16S rRNA gene sequencing to explore the relationship and possible mechanisms between the shift in host serum metabolic profile and intestinal flora disorder in the experimental DKD rat model induced by combining streptozotocin injection and unilateral nephrectomy. The results indicated that disorders in the serum metabolites and gut microbiota principally involved carbohydrate, lipid, and amino acid metabolism. This was verified by the restoration of the serum metabolites and gut microbiota after treatment with the traditional Chinese herbal medicine Tangshen Formula (TSF).

METHODS

Animals and Experimental Design

This study was conducted in the Experimental Animal Center of the Institute of Clinical Medicine, China–Japan Friendship Hospital [Beijing, China, permit number: SYXK (Jing) 2016-0043]. Adult (6- to 8-weeks old) male Wistar rats (180–220 g) were purchased from Beijing Huafukang Biotechnology Co. Ltd. [Beijing, China, license number: SCXK (Jing) 2019-0008]. The animals of each experimental group were raised together in specific-pathogen-free (SPF) environment with controlled temperature and humidity (20–25°C, 65–75% humidity) and maintained under light–dark cycle (12 h light/12 h dark). The rats were given free access to standard laboratory animal feed and water.

TSF was extracted from the following seven herbs: astragalus root [*Astragalus membranaceus* (Fisch.) Bge.], burning bush twig [*Euonymus alatus* (Thunb.) Sieb.], rehmannia root (*Rehmannia glutinosa* Libosch.), bitter orange (*Citrus aurantium* L.), cornus fruit (*Cornus officinalis* Sieb. et Zucc), rhubarb root and rhizome (*Rheum palmatum* L.), and notoginseng root [*Panax notoginseng* (Burk.) F.H. Chen] (Li et al., 2015). TSF preparation was conducted by the Beijing Institute of Clinical Pharmacy (Beijing, China) and quality control performed according to the criteria published in the *Chinese Pharmacopoeia* (2015 edition).

Following an adaptation period of 1 week, 30 rats were randomly divided into a sham group and a DKD-model group based on weight (10 and 20 rats, respectively). The DKD-model group underwent unilateral nephrectomy. The sham group was subjected to sham surgery that involved opening the abdominal cavity and exposing the kidney through stripping the renal capsule. Following a period of 1 week after surgery, the DKD rats were administered streptozotocin intraperitoneally (STZ; 40 mg/kg; Sigma-Aldrich, St. Louis, MO, United States) as previously described (Tang et al., 2019). The sham rats were injected with the same volume of citrate buffer solution (0.1 mol/L, pH = 4.2). Blood glucose was detected after 3 days and animals with blood glucose levels >16.7 mmol/L were designated as successful models. A total of 20 rats met the criteria for model building and were separated into two equal groups (DKD and TSF).

A dose of TSF of 4.8 g/kg/d was equivalent to 85 g/d of the raw herbs for DKD patients (Zhang et al., 2011). The sham and DKD rats received gavages of solvent (CMC-Na aqueous solution) only. After 20 weeks, all rats were housed in metabolic cages (Suzhou Fengshi Laboratory Animal Equipment, Jiangsu Province, China), and their urine was collected for 24 h under fasting condition except for access to water. All animals were then anesthetized by intraperitoneal injection of 1% sodium pentobarbital (1 ml/kg; Sigma-Aldrich), and then sacrificed. The colon contents, serum, and renal tissues were collected for subsequent examinations. The protocol in this study was approved by the Ethics Committee of the China–Japan Friendship Hospital (No. 180115).

Histology and Pathologic Analysis of Renal Tissue

The renal tissues preserved in 10% neutral formalin were dehydrated, embedded in paraffin, and sectioned to 3-μm thick sections. They were subjected to periodic acid–Schiff (PAS), Masson trichrome, and hematoxylin and eosin (H&E) staining. Under ×400 magnification, 20 glomeruli from each rat were randomly chosen to view the mesangial matrices that had been stained with PAS. This was followed by semiquantitative analysis using the Image-Pro Plus 6.0 software (Media Cybernetics, Rockville, MD, United States). Under ×200 magnification, 10 areas were randomly selected from each sample, and a semiquantitative analysis of the area of collagen fiber, which had been stained with Masson trichrome, was performed. Inflammatory infiltration, which was highlighted using H&E staining, was assessed using Image-Pro Plus 6.0 software. The scoring criteria of inflammatory infiltration was: 0, no inflammatory infiltration; 1, <25%; 2, 25–50%; 3, 50–75%; and 4, >75% of renal tubular injury.

Untargeted Analysis of Serum Metabolites

The serum samples were added to the extract solvent, and the extraction was diluted after grinding, ultrasonic processing, and centrifugation. The supernatant was further separated using an Agilent 1290 Infinity II series UHPLC System (Agilent Technologies, Santa Clara, CA, United States), equipped with

a Waters ACQUITY UPLC BEH Amide column (100 × 2.1 mm, 1.7 μm). Then, mass spectrometry data were obtained using a Triple TOF 6600 mass spectrometer (SCIEX, Redwood City, CA, United States). Data management was conducted as follows: The metabolite features that were only detected in < 20% of the experimental samples or in <50% of the QC samples were removed from subsequent analysis. The missing values of raw data were filled by half of the minimum value, and data normalization performed by internal standardization. Features with relative standard deviation (RSD) >30% were excluded. Then, the differential metabolites were filtered from statistical analysis. Markedly altered metabolites were determined based on the following criteria: 1) VIP value >1 using OPLS-DA analysis, and 2) p-value < 0.05 obtained by Student's unpaired t-test. The metabolite pathways were searched using databases, including KEGG (http://www.kegg.jp), HMDB (http://www.hmdb.ca), and MetaboAnalyst (http://www.metaboanalyst.ca).

Exploration of Gut Microbial Communities

Fresh colon contents were collected and immediately frozen at −80°C until tested. Microbial DNA was extracted using the PowerSoil DNA Isolation Kit (MO BIO Laboratories, Carlsbad, CA, United States), according to the manufacturer's instructions. The V3-4 regions of the 16S rRNA gene were amplified, and the PCR products were purified using an AMPure XP kit (Beckman Coulter Life Sciences, Indianapolis, IN, United States).

High-quality PCR products were sequenced on a MiSeq PE300 high-throughput sequencing system (Illumina, San Diego, CA, United States), and technical support was provided by Beijing Allwegene Technology (Beijing, China). Quality control processing of the raw data included removing sequences that were shorter than 230 bp using the UPARSE-OTU algorithm (v2.7.1; USEARCH software, https://drive5.com/uparse) and deleting chimeric sequences using the UCHIME algorithm (USEARCH; https://www.drive5.com/usearch/manual/uchime_algo.html) based on the "Gold database." With a 97% sequence similarity level, clean tags were clustered into operational taxonomic units (OTUs) using UPARSE. The alpha diversity indices, namely, Chao1, Shannon, and Simpson were analyzed by the QIIME (v1.8.0; http://qiime.org/1.8.0) software to clarify diversity and abundance of the microbial community. Partial least-squares discrimination analysis (PLS-DA) was conducted for beta diversity to delineate the differences in intestinal flora between the groups.

Statistical Analyses

The data involved in the present study were presented as means ± SEM. Statistical analyses were conducted using GraphPad Prism (v8.0.2; https://www.graphpad.com/scientific-software/prism), Origin software (2021; OrginLab, Northampton, MA, United States), and R software (v4.1.1; R Foundation, https://www.r-project.org/foundation). The significant differences between the two groups were analyzed by Student's unpaired t-test or Mann–Whitney U test. The significant differences of genera were assessed using Wilcoxon rank-sum test and LEfSe analysis. The differential concentration of the serum metabolites was determined by the Student's unpaired t-test and OPLS-DA models (VIP>1). p-value <0.05 was regarded as statistically significant.

RESULTS

Physiologic and Biochemical Parameters Were Altered in Diabetic Kidney Disease Rats

The body weight in the DKD rats was lower than that in the sham group after 20 weeks of TSF treatment (**Figure 1A**). Compared to the sham rats, the urine volume and urinary albumin to creatinine ratio (UACR) were markedly increased in the DKD group (**Figure 1B**). These outcomes were in line with typical characteristics of the diabetic rat model, including polyuria and emaciation (Committee of the Japan Diabetes Society on the Diagnostic Criteria of Diabetes Mellitus et al., 2010). Moreover, the rise in the UACR was a typical manifestation of renal impairment. The serum biochemical parameters, such as the fasting blood glucose (FBG), blood urea nitrogen (BUN), and total cholesterol (TC) levels were significantly increased in the DKD group. Albumin was reduced in DKD rats when compared with that in sham rats (**Figure 1C**).

Renal Injury in Diabetic Kidney Disease Rats and the Effects of Tangshen Formula Treatment

PAS, Masson trichrome, and H&E staining of the renal tissue are shown in **Figure 1D**. In the sham group, the tubular epithelial cells were tightly arranged; there was no obvious inflammatory cell infiltration although a small amount of collagen fiber deposition was noted. In the DKD group, there were clear pathologic phenomena in the kidneys, including collagen fiber deposition, glomerular mesangial matrix expansion, glomerular basement membrane thickening, and moderate inflammatory cell infiltration. The aforementioned pathologies were significantly improved in the TSF group. Semi-quantification of renal damage showed that TSF treatment could significantly improve kidney damage in rats with DKD (**Figures 1E–G**).

Changes in Serum Metabolite Profiling Between the Diabetic Kidney Disease and Sham Rats

The serum samples from the DKD and sham rats underwent untargeted metabolic analysis using UHPLC-QE-MS. A total of 476 metabolites were detected after data management. The OPLS-DA model was established between the sham and DKD groups. The R^2Y value of this model was 0.994 and showed a good interpretation rate. The Q^2 parameter of the model was 0.606 (p < 0.05), indicating that the model has good predictive ability. The result of the OPLS-DA score plots showed that the samples could be divided into two clusters (**Figure 2A**). The S-plot from the OPLS-DA analysis and 205 metabolites was selected with a VIP

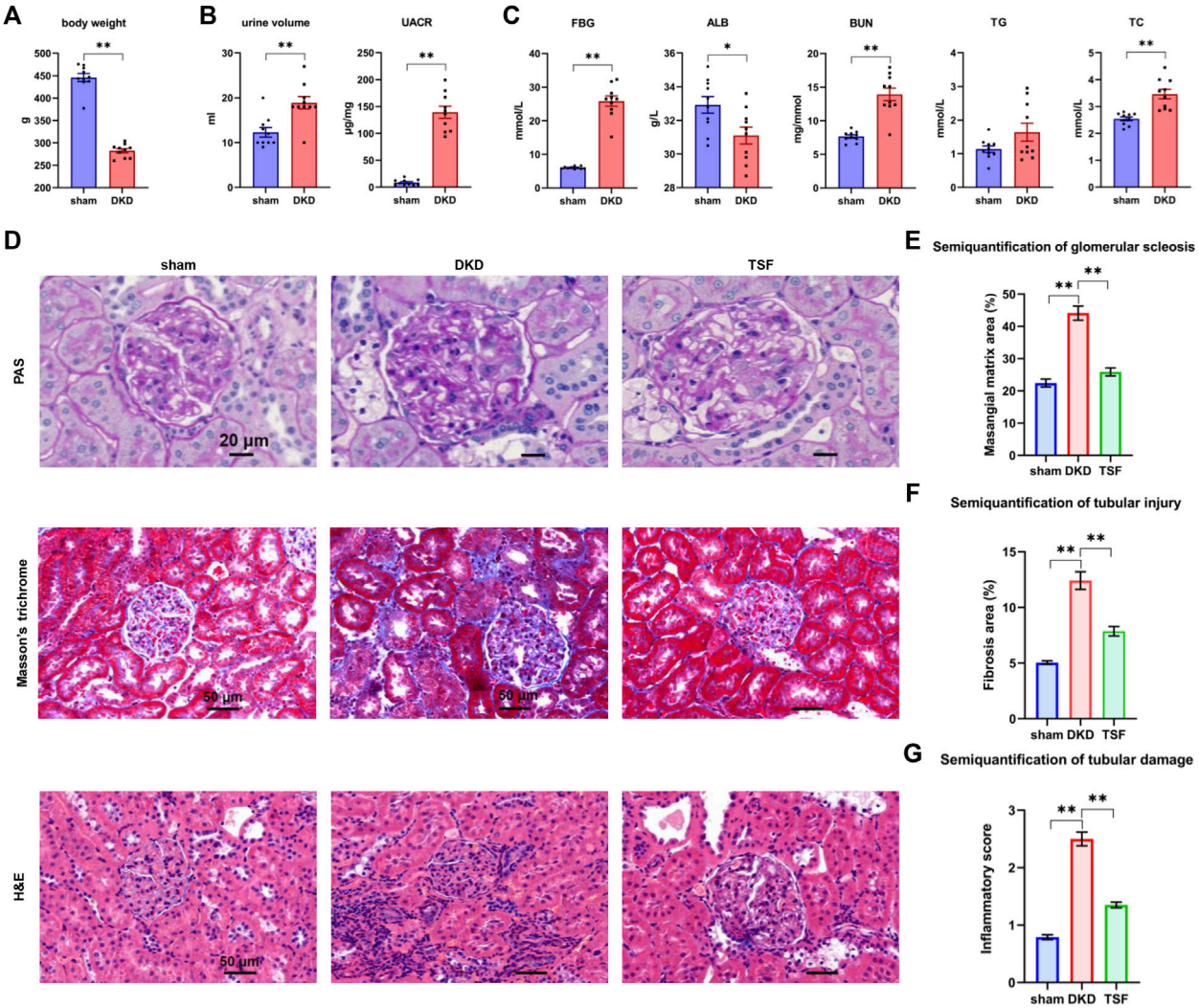

FIGURE 1 | Significant shift in physiologic and biochemical parameters and kidney pathology in DKD rats, and the effects of TSF treatment on renal damage. **(A)** Body weight of rats in the sham and DKD groups. *$p < 0.05$, **$p < 0.01$, versus sham rats. **(B)** Urinary parameters of sham and DKD rats. **(C)** Biochemical parameters in rat serum in the sham and DKD groups. **(D)** H&E, Masson trichrome, and PAS staining. **(E–G)** Semi-quantification of mesangial matrix, fibrosis area, and inflammatory scores based on PAS, Masson trichrome, and H&E staining, respectively. *$p < 0.05$, **$p < 0.01$.

score >1 (**Figure 2B**). Among them, 140 differential metabolites were identified according to the selection criteria, which included 95 significantly upregulated and 45 downregulated substances (**Figure 2C**). Overall, these compounds mainly contained carbohydrates, lipids, amino acids, nucleosides, nucleotides, and their derivatives. Notably, all the carbohydrates, nucleosides, and nucleotides showed significantly elevated characteristics; 17 of 26 lipids and lipid-like molecules were increased; and 16 of 29 amino acids were decreased in the DKD serum (**Table 1**).

The KEGG pathway differential enrichment analysis of the metabolites was conducted, and the top 20 pathways based on the *p*-values were revealed (**Figure 2D**). The citric acid cycle had the highest impact value (0.15) among the 55 pathways enriched. The impact value of phenylalanine, tyrosine, and tryptophan biosynthesis, aminoacyl-tRNA biosynthesis, and arginine biosynthesis was 0.1471, 0.1346, and 0.1304, respectively. A total of 12 differentially expressed metabolites were involved in the biosynthesis of amino acids, and 8 differential metabolites were in ABC transporters.

Further filtering of the different metabolites was conducted based on the condition log2 fold change >1 or <−1, and 30 metabolites were ultimately screened out. The relative content of 27 substances was elevated in the DKD serum, which included products from carbohydrate metabolism (isomaltose, citramalic acid, and D-glucuronolactone), prostaglandins (B2 and D2) and bile acids (cholic acid, chenodeoxycholate, deoxycholic acid, and lithocholic acid), amino acids and analogs (L-homoserine and indole-2-

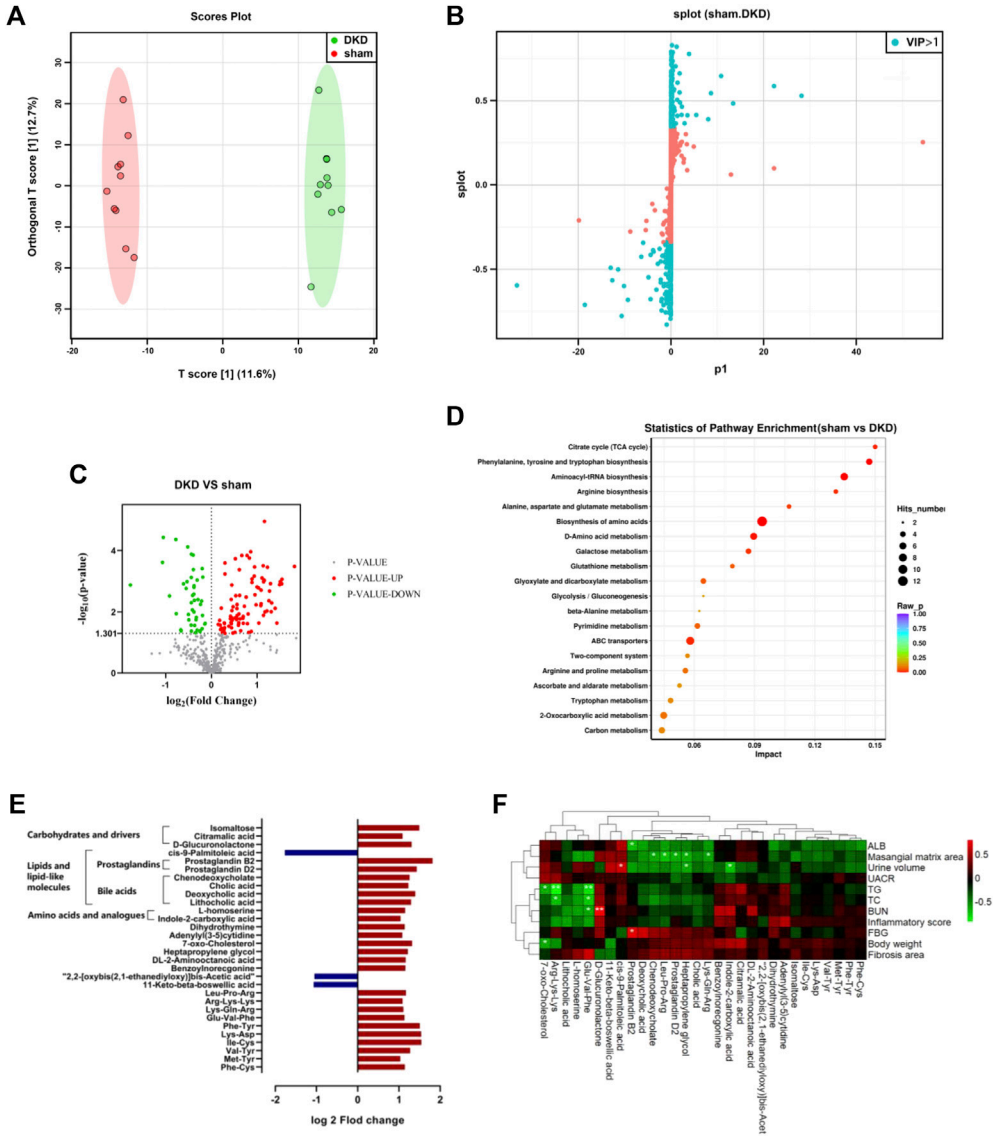

FIGURE 2 | Significantly altered circulating metabolic profile in the DKD group. **(A)** OPLS-DA plots with scores of the first two principal components. **(B)** S-plots of the OPLS-DA model from sham and DKD rats. **(C)** Volcano plot of the different metabolites obtained according to the screening criteria from sham and DKD rats. **(D)** Bubble plot of the KEGG pathway enrichment analysis of 315 markedly different metabolites. **(E)** Further screening from differential serum metabolites according to the following condition: log2 fold change>1 or < −1. **(F)** Correlation analysis between base parameters related to DKD, semi-quantification of renal damage, and 30 differential serum metabolites using Spearman's rank correlation (*p < 0.05, **p < 0.01).

TABLE 1 | Distribution and changes of differential metabolites in DKD serum.

		Total	Upregulated	Downregulated
Carbohydrates and drivers		15	15	0
Lipids and lipid-like molecules		26	17	9
Amino acids	Basic amino acid	7	2	5
	Other amino acid	11	7	4
	Tryptophan derivatives	8	2	6
	Amino acid derivatives	3	2	1
Nucleosides, nucleotides, and analogs		11	11	0

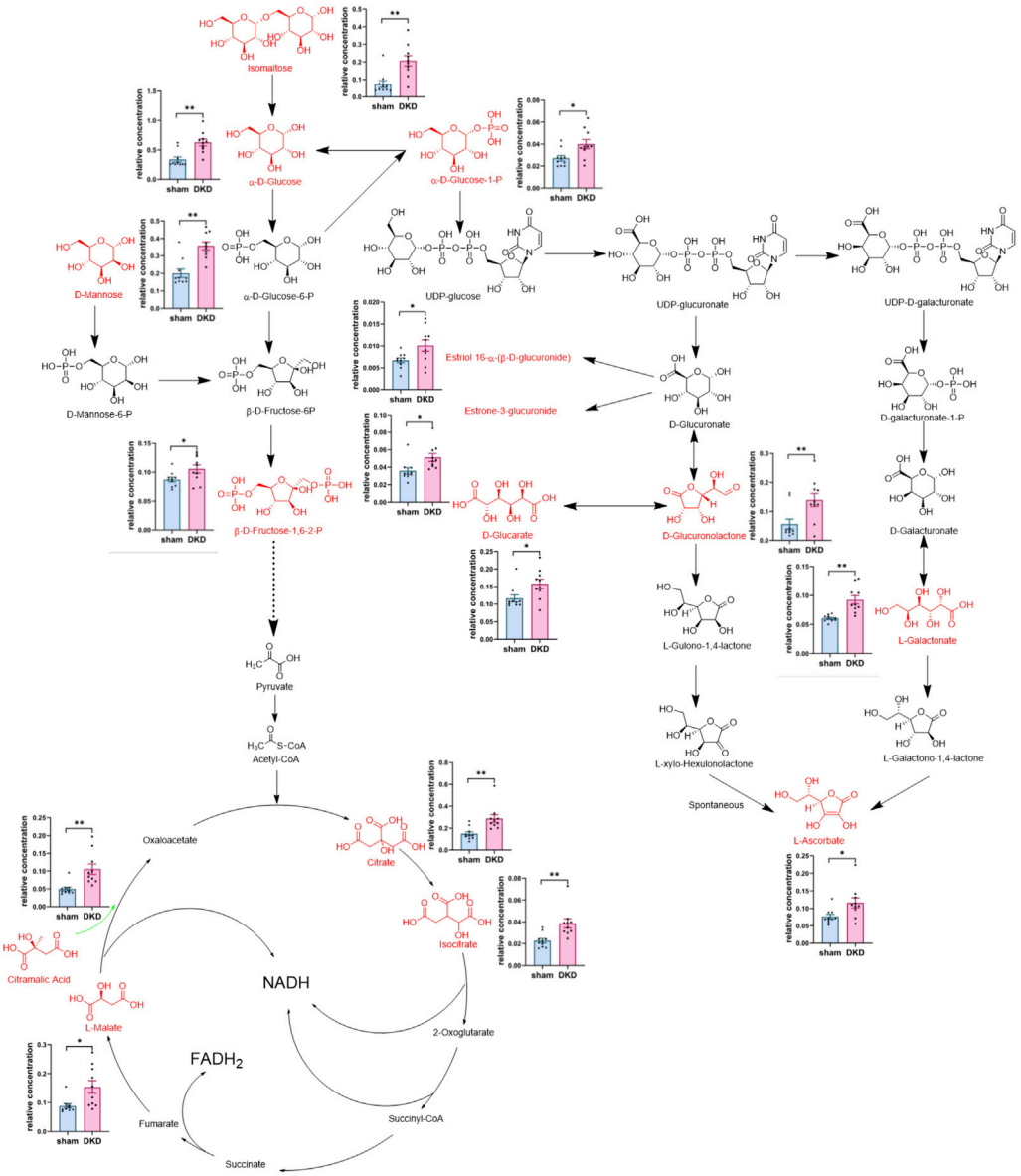

FIGURE 3 | Analysis of 15 markedly elevated metabolites in carbohydrate metabolism. Note: Carbohydrates highlighted in red and their relative concentrations shown in column scatter plot (*p < 0.05, **p < 0.01).

carboxylic acid), among others. While three substances decreased in the DKD serum, cis-9-palmitoleic acid was greatly decreased among all serum metabolites in DKD rats (**Figure 2E**).

The Spearman correlation heat map showed the correlation between base parameters related to DKD, semi-quantification of renal damage, and serum differences. Prostaglandin B2, chenodeoxycholate, 7-oxo-cholesterol, indole-2-carboxylic acid, heptapropylene glycol, prostaglandin D2, and cis-9-palmitoleic acid had a strong correlation with DKD-related base parameters. In particular, lipid metabolites had conspicuous association with DKD-related parameters, including prostaglandin D2 and chenodeoxycholate, which were negatively related to the mesangial matrix area. Furthermore, 7-oxo-cholesterol was negatively related to body weight, while cis-9-palmitoleic acid was positively related to urine volume (**Figure 2F**).

Analysis of Metabolites in Carbohydrate and Amino Acid Metabolism

We further analyzed the metabolic pathways of significantly increased serum carbohydrates and found α-D-glucose, β-D-fructose-1,6-bisphosphate, and α-D-glucose-1-phosphate were involved in glycolysis/gluconeogenesis; citrate, isocitrate, L-malate, and citramalic acid participated in the citric acid

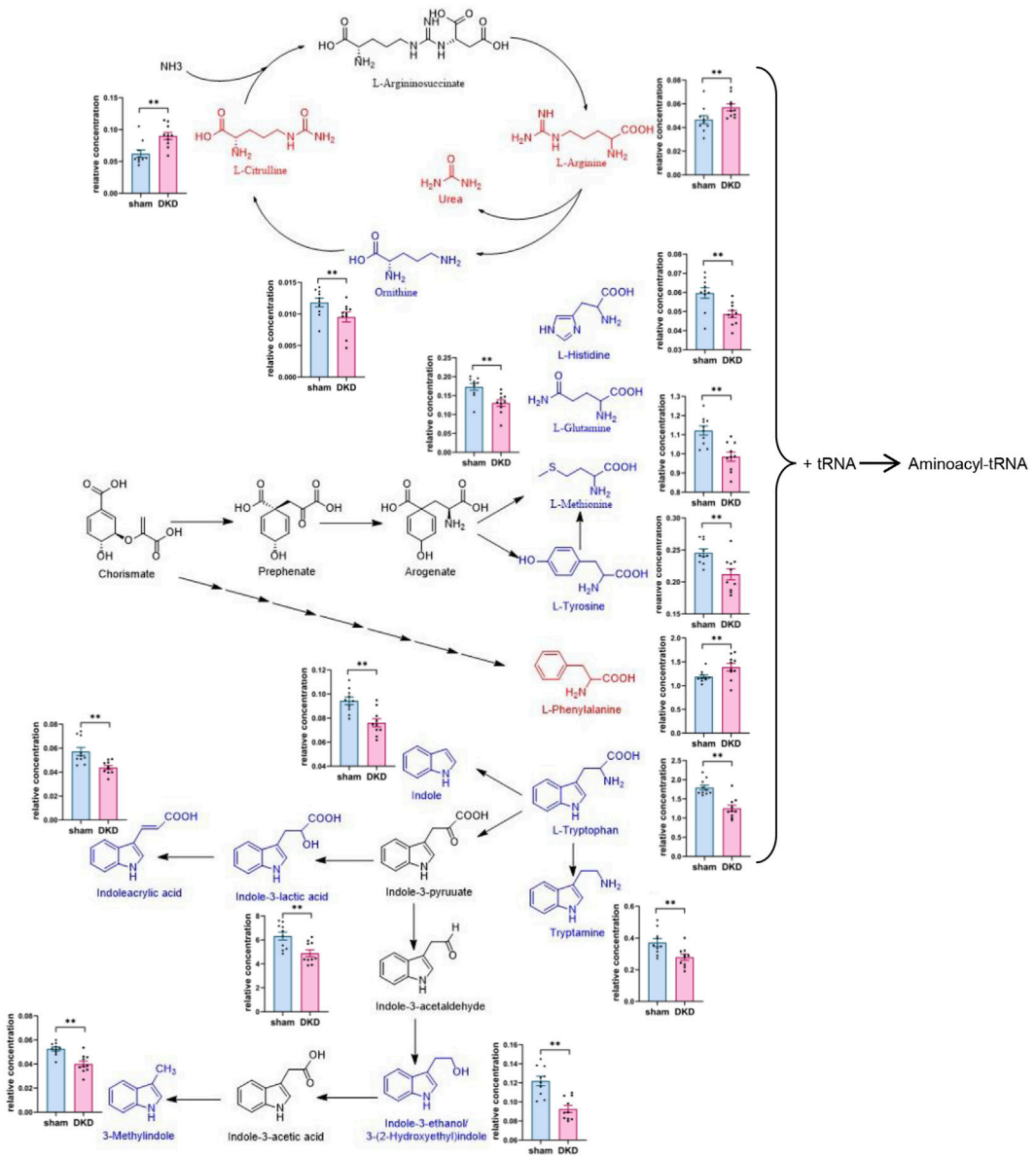

FIGURE 4 | Analysis of amino acid biosynthesis and metabolism. Note: Elevated metabolites are highlighted in red, reduced metabolites are shown in blue, and their relative concentrations are shown in column scatter plot (*$p < 0.05$, **$p < 0.01$).

cycle; isomaltose was involved in starch metabolism; D-mannose was involved in mannose metabolism; and D-glucuronolactone, D-glucarate, estriol 16α-(β-D-glucuronide), estrone-3-glucuronide, L-galactonate, and L-ascorbate were associated with ascorbate and aldarate metabolism (**Figure 3**). Similarly, we demonstrated the relationship between amino acid biosynthesis and metabolism, which had a higher impact value (**Figure 4**). The results indicated that L-arginine and L-citrulline were elevated, while ornithine declined in the ornithine cycle. Tryptophan and its derivatives, namely, tryptamine, indole, DL-indole-3-lactic acid, indoleacrylic acid, 3-(2-hydroxyethyl) indole, and 3-methylindole, were all decreased in the DKD serum. Among the aromatic amino acids, L-phenylalanine was raised, whereas tyrosine and methionine were reduced. L-glutamine and L-histidine were diminished in the DKD rats when compared with those in the sham rats.

Comparison of Gut Microbiome Between Sham and Diabetic Kidney Disease Rats

DNA was extracted from fresh colon contents and sequenced, obtaining an average of 61,776 quality-controlled sequences per sample. A total of 1,227 OTUs were obtained with cluster analysis, and 1,217 OTUs

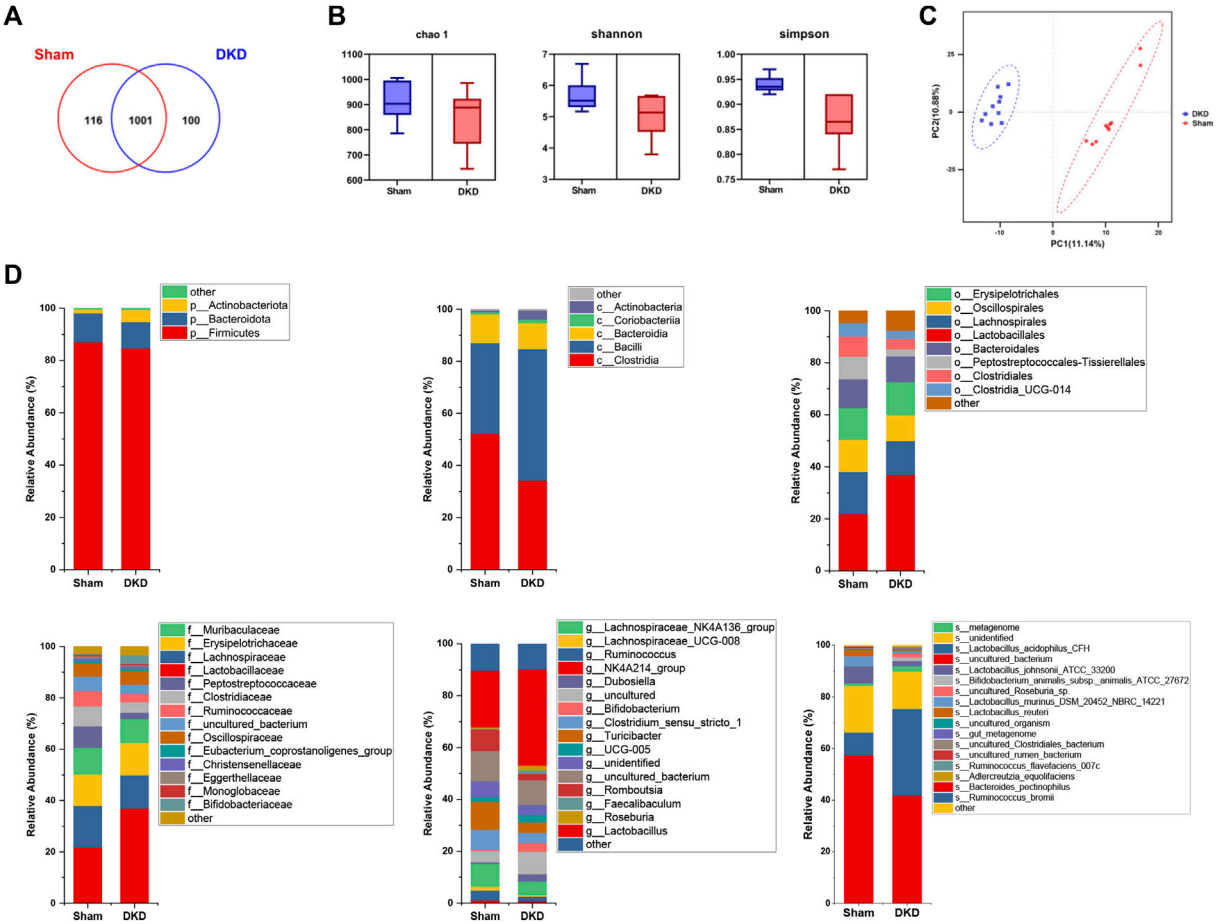

FIGURE 5 | Altered bacterial taxa in DKD rats. **(A)** Venn diagram of OTU distribution between samples from sham and DKD rats. **(B)** Alpha-diversity indices of Chao1, Shannon, and Simpson of gut microbiota between sham and DKD rats. **(C)** PLS-DA of gut bacterial communities from the sham and DKD groups. **(D)** Taxonomic distributions of bacteria from colon content 16S rDNA sequencing data at the phylum to genus level between sham and DKD rats.

remained after pumping analysis. A total of 116 OTUs were unique to the sham group and 100 OTUs belonged specifically to the DKD group (**Figure 5A**). Chao1, Shannon, and Simpson indices characterized the α-diversity of microbial communities and were 910.60 ± 23.25, 5.68 ± 0.16, and 0.94 ± 0.01 in sham rats and 843.00 ± 38.10, 5.06 ± 0.20, and 0.87 ± 0.02 in the DKD rats, respectively (**Figure 5B**). The sham and DKD groups were markedly separated based on PLS-DA (**Figure 5C**).

Annotation of OTUs and microbial composition analysis were presented for each classification level. At the phylum level, 1,217 OTUs were assigned to 8 phyla. *Firmicutes* was the most dominant phylum and accounted for more than 80%. At the class level, *Clostridia*, *Bacilli*, and *Bacteroidia* occupied more than 90% of the total detected classes. *Lactobacillales* and *Lactobacillaceae* were the predominant bacteria at the order and family levels, respectively. At the genus level, the *NK4A214_group* had the highest relative abundance. The relative genus-level abundance of gut microbiota varied significantly among the DKD and sham groups (**Figure 5D**). We conclude that DKD dramatically alters the structure of the gut microbiota.

Analysis of Significantly Altered Gut Taxa in Diabetic Kidney Disease Rats

Based on LEfSe analysis, 35 taxa were screened out, including 18 significantly decreased and 17 increased taxa ($p < 0.05$). *p_Actinobacteriota* was markedly increased in the DKD group (4.76 ± 0.89%) when compared to the sham group (1.43 ± 0.18%). *c_Clostridia* was detected at an average of 34.3% in DKD rats when compared to the 52.2% in sham rats ($p < 0.05$), whereas *c_Bacilli* (50.44 ± 2.92% in the DKD group and 34.89 ± 2.57% in the sham group, $p < 0.05$) and *c_Actinobacteria* (3.43 ± 0.84% and 0.56 ± 0.22% in the DKD and sham groups, respectively) had the opposite shift (**Figure 6A**). There were 39 genera that were significantly different among the sham and DKD groups (**Figure 6B**). *g_Turicibacter*, *g_Romboutsia*, *g_Ruminococcus*, *g_Lachnospiraceae_UCG-008*, etc. were markedly reduced in DKD rats, while *g_Lactobacillus*, *g_Bifidobacterium*, *g_Dubosiella*,

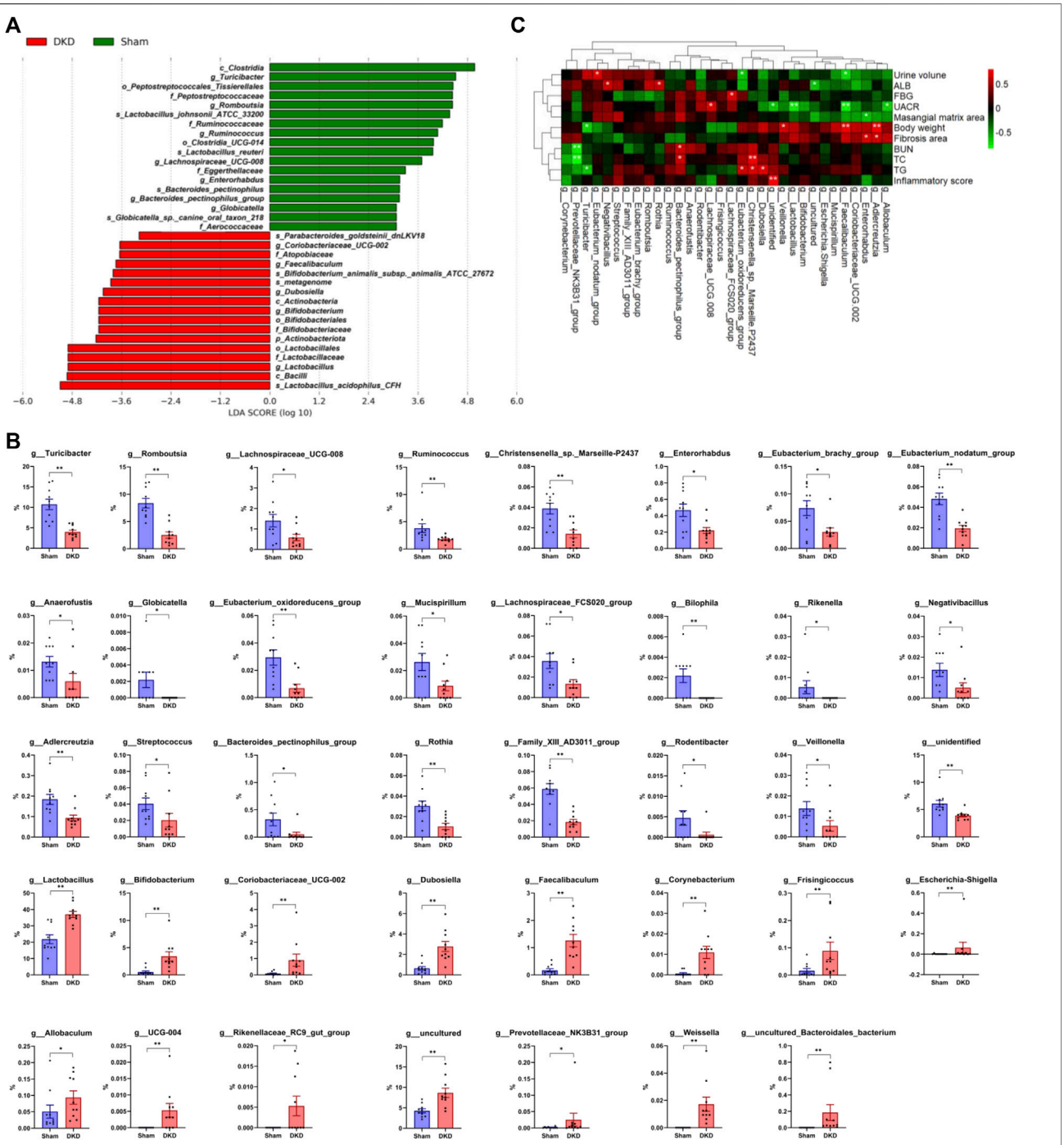

FIGURE 6 | Differential gut microbiome in DKD rats compared to sham rats. **(A)** LDA score of the significantly discriminant taxa between the two groups (LDA score >3.0, Wilcoxon rank-sum test, $p < 0.05$). **(B)** Bar graphs of the significant differences in the relative abundance of 39 genera between sham and DKD rats selected by Wilcoxon test analysis and p-value < 0.05. $^{*}p < 0.05$, $^{**}p < 0.01$, versus sham rats. **(C)** Spearman rank correlation between DKD-related base parameters and differential genera (selected from Wilcoxon rank-sum test, $p < 0.05$) displayed in heat map cluster analysis ($^{*}p < 0.05$, $^{**}p < 0.01$).

g_Coriobacteriaceae_UCG-002, and *g_Faecalibaculum* were significantly elevated in the DKD group compared with the sham group.

The correlation between DKD-related base parameters and markedly differential genera was analyzed (**Figure 6C**). *g_Allobaculum*, *g_Adlercreutzia*, *g_Enterorhabdus*,

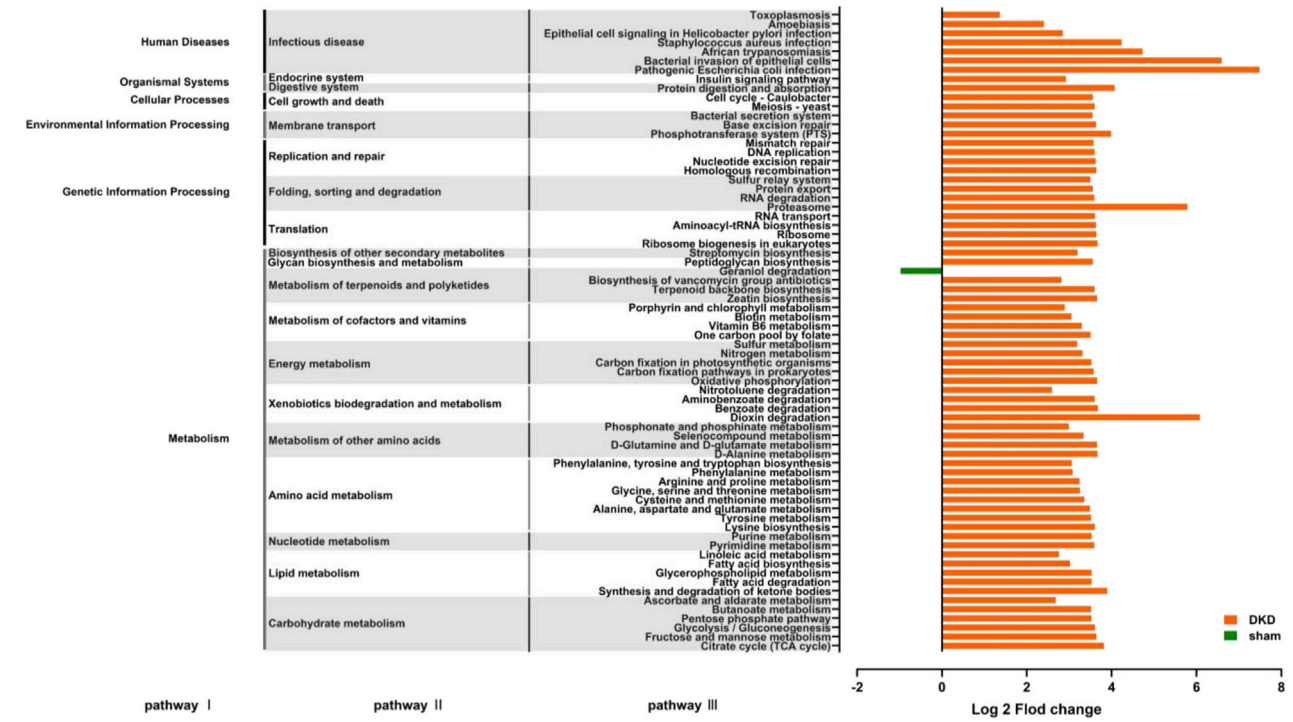

FIGURE 7 | Predicting the effects of changes in the structure and abundance of intestinal flora on functional pathways. A total of 70 predictive pathways were screened out using Wilcoxon rank-sum test ($p < 0.05$).

g_Coriobacteriaceae_UCG-002, *g_Faecalibaculum*, *g_Mucispirillum*, *g_Escherichia–Shigella*, *g_uncultured*, *g_Bifidobacterium*, *g_Lactobacillus*, *g_Veillonella*, *g_unidentified*, *g_Dubosiella*, *g_Christensenella_sp._Marseille-P2437*, and *g_Eubacterium_oxidoreducens_group* were clustered together and had a negative correlation with urine volume, ALB, FBG, UACR, and mesangial matrix area and had a positive correlation with body weight, fibrosis area, BUN, TC, TG, and inflammatory score. In addition, *g_Lachnospiraceae_FCS020_group* had a positive correlation with FBG, *g_Lachnospiraceae_UCG-008* had a positive correlation with UACR, *g_Bacteroides_pectinophilus_group* had a positive correlation with BUN and TC, *g_Rothia* and *g_Negativibacillus* had positive correlations with ALB, *g_Eubacterium_nodatum_group* had a positive correlation with urine volume, while *g_Turicibacter* had a negative correlation with body weight and BUN, and *g_Prevotellaceae_NK3B31_group* had a negative correlation with BUN and TC.

Prediction of Functional Changes in Intestinal Flora in Diabetic Kidney Disease Rats

Functional prediction was conducted based on the 16S rRNA gene sequencing data using PICRUSt analysis. There were 70 significantly altered pathways, including 45 metabolic pathways (**Figure 7**) ($p < 0.05$, Wilcoxon rank-sum test). In carbohydrate metabolism, the citric acid cycle, fructose and mannose metabolism, glycolysis/gluconeogenesis, the pentose phosphate pathway, and ascorbate and aldarate metabolism were significantly enriched, which were consistent with the abnormal accumulation of circulating carbohydrates. In lipid metabolism, fatty acid biosynthesis, metabolism, and enrichment were all improved, and correspondingly, disturbance of circulating fatty acids and their metabolites occurred. In amino acid metabolism, phenylalanine, tyrosine and tryptophan biosynthesis, phenylalanine metabolism, tyrosine metabolism, and arginine and proline metabolism were enriched, which coincided with the results that the concentration of L-phenylalanine, L-arginine, and L-citrulline were elevated, while L-tyrosine, L-tryptamine, and ornithine decreased in the DKD serum. This demonstrated a strong relationship between metabolites and gut microbiota in the DKD rats. In addition to the metabolic pathways, there were 25 pathways involved in human diseases, organismal systems, cellular processes, environmental information processing, and genetic information processing (**Figure 7**).

There were four metabolic pathways obtained by the KEGG enrichment analysis. These were dioxin degradation, proteasome, pathogenic *Escherichia coli* infection, and bacterial invasion of the epithelial cells. The number of differential genes annotated to the abovementioned pathways was extremely elevated (log2 fold change value >5) in the DKD group. Notably, the number of differential genes annotated to geraniol degradation, the exclusive pathway, was decreased.

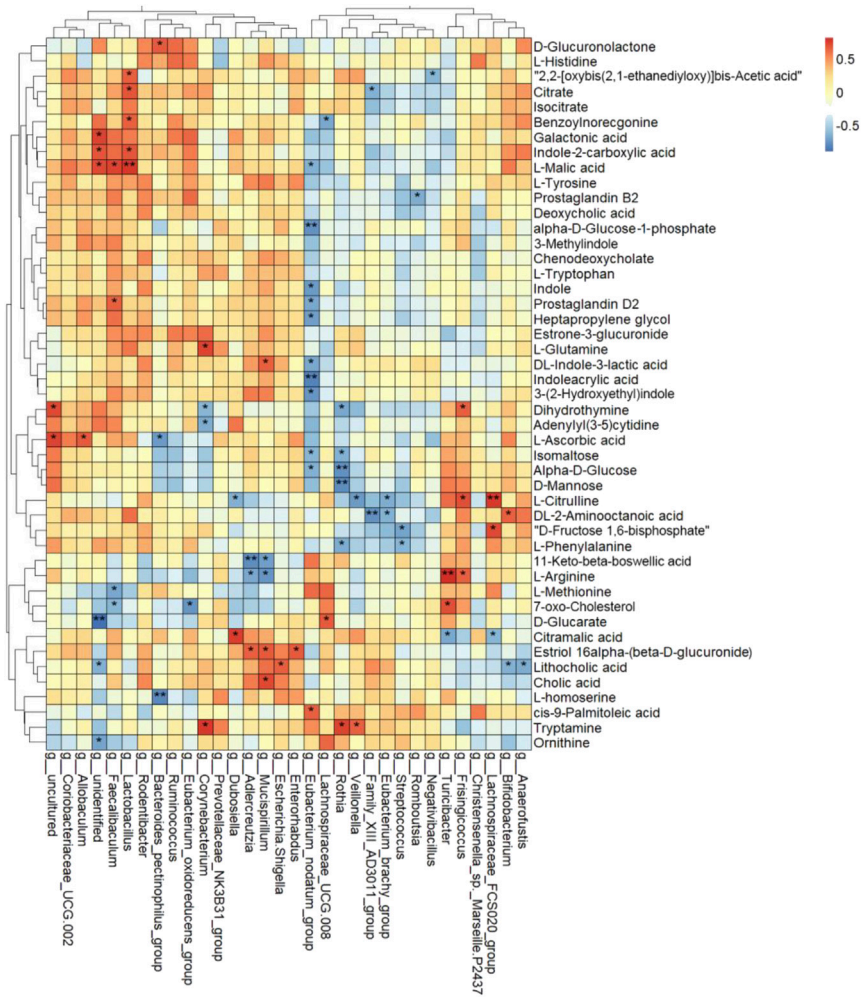

FIGURE 8 | Heat map cluster analysis of the correlation among differential serum metabolites and differential genera using Spearman rank correlation (*$p < 0.05$, **$p < 0.01$).

Analysis of the Interaction Between Serum Metabolites and Gut Microbiota in Diabetic Kidney Disease Rats

To further study the correlations between serum metabolites and gut microbiota, Spearman correlation was performed (**Figure 8**). There was a complex interaction between serum metabolites and gut microbiota. A total of 27 of 32 genera had notable relationships with circulating differential metabolites. *g_Eubacterium_nodatum_group*, *g_Rothia*, *g_Lactobacillus*, *g_Mucispirillum*, *g_Faecalibaculum*, and *g_Corynebacterium* were all significantly correlated with at least 4 serum metabolites. More importantly, *g_Eubacterium_nodatum_group* had a significantly negative relationship with 10 metabolites and a positive relationship with 1 metabolite, indicating the potential impact on DKD metabolism. *g_Lactobacillus* and *g_Faecalibaculum* were high in abundance and were correlated with four and five serum differences, respectively. The above three genera showed a significant effect on DKD.

Furthermore, D-mannose, alpha-D-glucose, and isomaltose were clustered together and had strong negative correlations with *g_Eubacterium_nodatum_group* and *g_Rothia*. Galactonic acid, L-malic acid, and indole-2-carboxylic acid were clustered and positively correlated with *g_Lactobacillus* and *g_Faecalibaculum* and negatively correlated with *g_Eubacterium_nodatum_group* and *g__Lachnospiraceae_UCG-008*. Lithocholic acid, cholic acid, and estriol-16-alpha-(beta-D-glucuronide) were clustered and had positive correlations with *g_Enterorhabdus*, *g_Escherichia–Shigella*, *g_Mucispirillum,* and *g_Adlercreutzia*. DL-indole-3-lactic acid, indoleacrylic acid, 3-(2-hydroxyethyl)indole were clustered, and indole, prostaglandin D2, and heptapropylene glycol were clustered. All of them had a negative correlation with *g_Eubacterium_nodatum_group*.

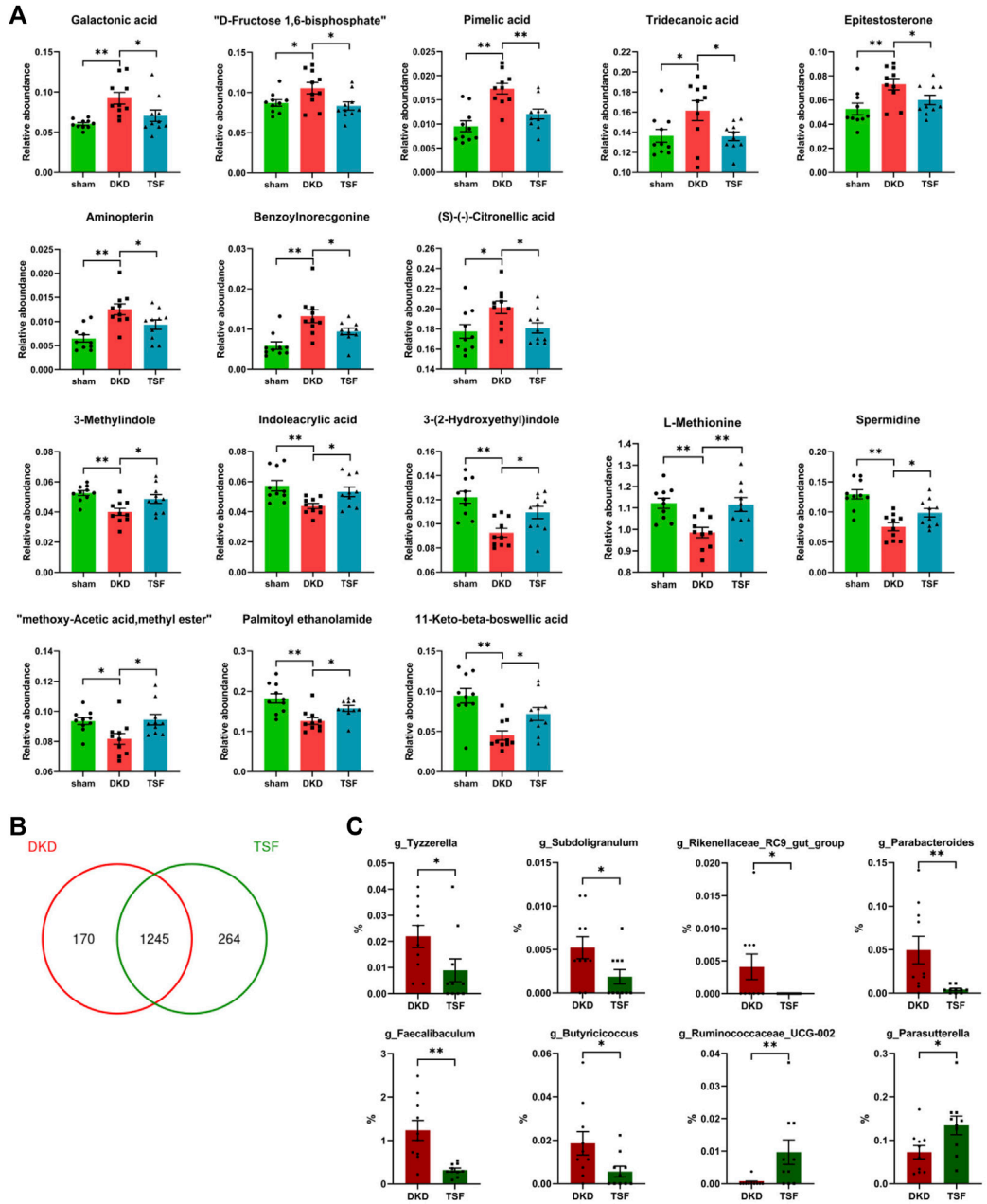

FIGURE 9 | Effects of TSF treatment on serum metabolites and gut microbiota. **(A)** TSF treatment significantly improved levels of 16 metabolites in DKD rats as determined using Wilcoxon rank-sum test (*$p < 0.05$, **$p < 0.01$). **(B)** Effect of TSF treatment on gut microbiota at the OTU level. **(C)** Relative abundance of genera changes in the TSF group compared with the DKD group.

Effect of Tangshen Formula Treatment on Serum Metabolites in Diabetic Kidney Disease Rats

After 20 weeks of TSF treatment, disturbances of 16 serum metabolites in DKD rats were significantly attenuated. Eight of the metabolites that were excessively accumulated in the serum of DKD rats were reduced in the TSF group. These metabolites included galactonic acid, D-fructose-1, 6-bisphosphate, medium- and long-chain fatty acids (pimelic acid and tridecanoic acid), androgen (epitestosterone), among others. Eight metabolites that were markedly reduced in DKD rats and whose relative abundances were significantly elevated after TSF treatment were tryptophan [3-methylindole, indoleacrylic acid, and 3-(2-hydroxyethyl)indole], amino acids and derivatives (L-methionine and spermidine), and other substances (**Figure 9A**).

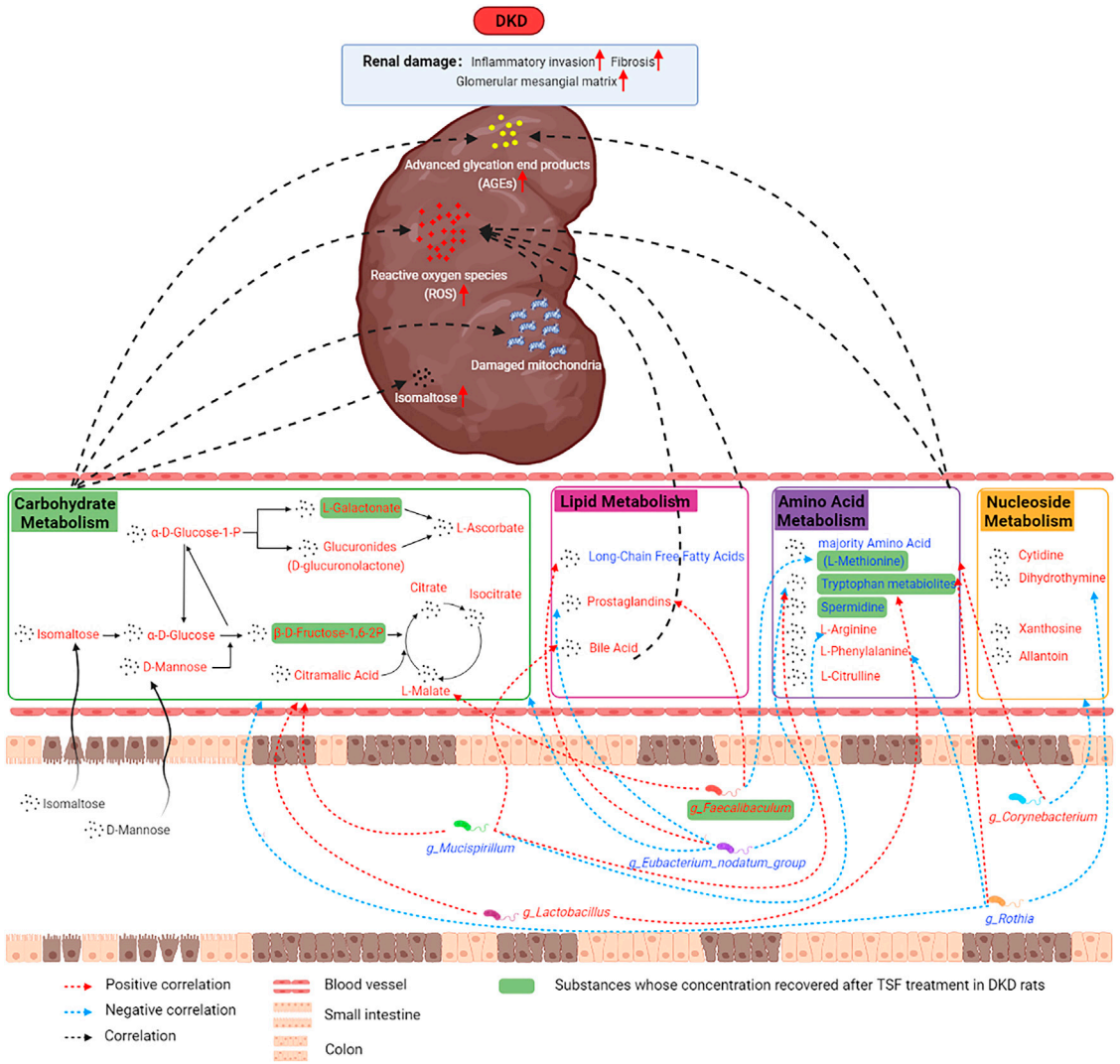

FIGURE 10 | The mechanism diagram illustrated the potential mechanisms between altered serum metabolic profiles, disturbances in gut microbiota, and kidney damage in DKD.

Finally, TSF treatment greatly altered the structure and composition of gut microbiota. At the OTU level, the number of unique OTUs in TSF rats was 264 compared with 170 OTUs in DKD rats (**Figure 9B**). There were eight genera that were altered in the TSF group, and of note, TSF treatment restored the OTU relative abundance of g_Faecalibaculum and g_Rikenellaceae_RC9_gut_group (**Figure 9C**).

DISCUSSION

In the current research, we used untargeted metabolomics to study the shift in the metabolic profile of the DKD rat serum and utilized 16S rRNA gene sequencing to analyze the changes in the structure and function of the gut microbiota. We further explored the relationship and role of the microbiota in the progression of DKD. Our results indicate that the metabolic profile of DKD rats and the composition and structure of their gut microbiota were altered. These changes were associated with the metabolism of carbohydrates, lipids, amino acids, and nucleotides. In these metabolic pathways, isomaltose, D-mannose, galactonic acid, citramalic acid, and prostaglandin B2 were significantly upregulated. 3-(2-hydroxyethyl)indole, 3-methylindole, and indoleacrylic acid were downregulated and were the critical metabolites, and *g_Eubacterium_nodatum_group*, *g_Lactobacillus*, and *g_Faecalibaculum* were important functional bacteria in the DKD model. Furthermore, the levels of these three indoles were restored after treatment with the traditional Chinese herbal medicine Tangshen Formula (**Figure 10**).

We found that alpha-D-glucose, alpha-D-glucose 1-phosphate, and "D-Fructose 1,6-bisphosphate"—which are

involved in glycolysis/gluconeogenesis—and citrate, isocitrate, and L-malate—which are involved in the citric acid cycle—were all elevated in the DKD serum. Studies have pointed out that the glycolysis and citric acid cycle metabolites accumulate in the kidneys in the early stage of diabetes (Hasegawa et al., 2020) and abnormal glycolysis and accumulation of toxic glucose metabolites are linked to kidney damage in diabetic patients and models (Qi et al., 2017; Srivastava et al., 2018; Li et al., 2020b; Liu et al., 2021). Moreover, glycolysis and the citric acid cycle in the DKD serum are disturbed, and abnormal increases in dihydroxyacetone phosphate and succinyl-CoA are positively related to mitochondria damage (Jiang et al., 2019). Citramalic acid is a metabolite of gut microbiota and an analog of L-malate that competitively inhibits the metabolism of L-malate. In our research, citramalic acid was elevated in DKD rats, which concurs with the results of O'Kell et al. (2021) in their study on diabetic dogs. We further confirmed that the disorder of glycolysis/gluconeogenesis and citrate cycle and the abnormal accumulation of intermediate metabolites in the serum play an outstanding role in DKD progression.

In our study, we discovered that isomaltose and D-mannose were elevated in the DKD serum. We had previously studied the renal cortex metabolomics in DKD rats and demonstrated the abnormal accumulation of maltose and mannose in the kidneys (the fold change of DKD/sham was 498.56 for maltose and 7.43 for mannose) (Zhao et al., 2012). Isomaltose is the end product of starch digestion and is hydrolyzed into glucose, which is then absorbed in the small intestine. Therefore, an abnormal elevation of isomaltose in the DKD serum might be due to the downregulation of activity or content of isomaltose, and intestinal barrier impairment. The toxic effect of isomaltose on the kidneys is not well understood and needs further study. D-mannose is also derived from food and is absorbed directly into the blood and excreted intact in the urine without metabolization. Any remaining mannose in the system is mainly utilized for nonenzymatic glycation, the activity of which has been found to be five times that of glucose (Sharma et al., 2014). Advanced glycation end products participate in the progression of DKD through multiple modes of action (Vlassara et al., 2012; Azegami et al., 2021). Moreover, in our study, we found that isomaltose, D-mannose, and glucose were highly associated with differential genera of the microbiota.

Another interesting discovery was that the circulating oxidation products of carbohydrates, namely, D-glucuronolactone, D-glucarate, and galactonic acid, were greatly elevated in the DKD group when compared with the sham group, which might indicate excessive oxidative stress in DKD rats. In line with this viewpoint, we found a marked decline in serum L-methionine, which could be methylated to generate L-(+)-cysteine in the body. The latter is one of the three amino acids that synthesize glutathione (GSH). GSH is an important antioxidant that participates in a variety of redox reactions and can effectively improve oxidative stress (Fahrmann et al., 2015). In the present investigation, the elevation in circulating D-glucuronolactone was correlated positively with the serum level of BUN. Moreover, *g_Bacteroides_pectinophilus_group* had a positive association with D-glucuronolactone and BUN. We also found that the concentration of the three glucuronides in the renal cortex of DKD rats was more than five times that in the sham group. Of note, 2-phenylethanol glucuronide in the renal cortex was 27 times that in sham rats in our previous study (Zhao et al., 2012). Thus, it appears that excessive accumulation of glucuronides in the renal cortex was involved in kidney injury. However, the role of *g_Bacteroides_pectinophilus_group* in this process needs more exploration. In addition, we found that L-ascorbate, another well-known endogenous antioxidant (Al-Shamsi et al., 2006; Kazmierczak-Baranska et al., 2020), was elevated in the DKD serum. This might be a self-regulation response to the oxidative stress state.

Our results indicate that there were several DKD-associated changes in lipid metabolism. DKD rats displayed decreased levels of long-chain free fatty acids, such as arachidonic acid, cis-9-palmitoleic acid, palmitic acid, "all cis-(6,9,12)-linolenic acid," and myristic acid. Free fatty acids have beneficial effects against DKD. One fatty acid, cis-9-palmitoleic acid, has been found to attenuate hyperglycemia by promoting β-cell proliferation under low glucose concentration, improving β-cell secretion and inhibiting the expression of pro-inflammatory genes (Maedler et al., 2001; Yang et al., 2011).

Consistent with this finding, the metabolites of arachidonic acid, namely, prostaglandin B2 and prostaglandin D2, were markedly elevated in the DKD group when compared with the sham group. Prostaglandins have many physiological effects, such as responding to inflammation, and regulating the immune system and blood pressure (Yao and Narumiya, 2019). Prostaglandin E2 contributes to the increase in renal blood flow through afferent arteriole dilation (Ren et al., 2013; Asirvatham-Jeyaraj et al., 2019) and is involved in insulin resistance (Robertson, 1983). The resulting changes in the DKD kidney include renal hemodynamic alteration, glomerular hypertension, and decrease in glomerular filtration rate (Alicic et al., 2017). Prostaglandin B2 has been found to reduce mean arterial pressure and increase renal blood flow (Marchand et al., 1973; Hall and Jaitly, 1976). In our study, prostaglandin B2 was the most elevated among all the metabolites and was positively correlated with the FBG level and negatively correlated with the ALB level. Therefore, prostaglandin B2 and E2 may act similarly, that is, their accumulation can lead to insulin resistance and accelerate kidney damage, but in our study, prostaglandin B2 was elevated, whereas prostaglandin E2 was not elevated.

The interaction between prostaglandins and gut microbiota is being studied intensely. Prostaglandin E2 was found to be synthesized by the commensal fungus *Meyerozyma guilliermondii*, and prostaglandin E2 production in the liver

has been shown to be positively correlated with excessive growth of gut fungi (Sun et al., 2020). Our results indicate that prostaglandin B2 has a negative correlation with *g_Romboutsia*, and prostaglandin D2 was positively correlated with *g_Faecalibaculum* and negatively correlated with *g_Eubacterium_nodatum_group*.

Bile acids are derived from cholesterol through oxidation of liver enzymes and aid in fat digestion and absorption. Bile acids are being investigated for their regulatory effects on the metabolism of lipids, glucose, and energy, as well as their involvement in immunologic processes such as signaling molecules (McGlone and Bloom, 2019). In the present study, the levels of bile acid in the DKD rats' serum, namely, chenodeoxycholate, lithocholic acid, cholic acid, and deoxycholic acid, were significantly higher than in the sham group. Elevated levels of bile acids have also been found in the feces of DKD mice (Zhao et al., 2019) and in patients with end-stage renal disease (Wang et al., 2020). Proposed mechanisms of bile acids causing kidney damage such as disruption of the intestinal barrier and allowing bacterial toxins to enter the systemic circulation (Ramezani and Raj, 2014), oxidative stress, and promoting the release of inflammatory cells (Chávez-Talavera et al., 2017). The gut microbiota metabolize primary bile acids into secondary bile acids through deconjugation, dehydrogenation, and dihydroxylation (Caesar, 2019). Chenodeoxycholic acid undergoes 7-dehydroxylation to produce lithocholic acid with *Clostridium* and *Eubacterium* participating in 7-dehydroxylation (Jia et al., 2018). In our study, we found lithocholic acid was positively correlated with *g_Escherichia–Shigella* and was negatively correlated with *g_Bifidobacterium* and *g_Anaerofustis*, which implies that the three genera are involved in 7-dehydroxylation.

DKD rats were treated with TSF, a traditional Chinese medicine compound with verified therapeutic action against DKD in animal experiments (Zhang et al., 2011) and clinical trials (Li et al., 2015). Following TSF treatment, metabolite disorders in the serum and gut microbiota imbalance were partially restored, and damage to the renal cortex was ameliorated. Recovery of circulating galactonic acid and L-methionine levels following TSF treatment further demonstrated the important role of oxidative stress in DKD. We also found that levels of indole derivatives [namely, 3-(2-hydroxyethyl)indole, 3-methylindole, and indoleacrylic acid], as well as spermidine (an amino acid metabolite), were recovered after TSF treatment but were decreased in the DKD group. Indole and derivatives are converted from tryptophan under the action of gut microbiota and have a wide range of biologic functions. Indoleacrylic acid improves the integrity of the intestinal barrier through promoting the differentiation of the intestinal goblet cells and mucus secretion from the intestinal goblet cells. Furthermore, indoleacrylic acid possesses antioxidant and anti-inflammatory functions (Wlodarska et al., 2017). Studies have found that 3-methylindole is an antioxidant that prevents lipid peroxidation in lung tissue (Adams et al., 1987; Kiorpes et al., 1988). Research indicates that 3-(2-hydroxyethyl) indole shows antimicrobial activity against *Staphylococcus aureus, Salmonella enterica*, and *Lactobacillus plantarum* (Roager and Licht, 2018). Spermidine is a polyamine that has diverse metabolic functions such as inhibiting hemoglobin glycosylation and lipid peroxidation (Méndez and Balderas, 2006) and has the potential to prevent DKD complications. Therefore, amino acids, especially tryptophan and its metabolites, are highly involved in the development of DKD.

Taken together, the metabolite disturbances that we identified were mainly concentrated in the metabolism of carbohydrates, lipids, and amino acids, as well as in related functional bacteria. Our finding that disruption of amino acid metabolism, especially disordered tryptophan metabolism, was in line with the results of studies in DKD patients (Winther et al., 2020; Zhang et al., 2021). However, we did not find abnormal accumulation of typical uremic toxins in middle-stage DKD rat serum, which might be due to the fact that the most significant accumulation of uremic toxins occurred during progression to end-stage renal disease. Zhang et al. (2021) compared end-stage (eGFR <15 ml/min/1.73 m^2) and non–end-stage renal disease (eGFR ≥15 ml/min/1.73 m^2) with type 2 DKD patients and demonstrated an anomalously elevated hippurate. Similarly, Winther et al. (2020) in comparing type 1 diabetic patients with macroalbuminuria and those with normo- or microalbuminuria found that serum indoxyl sulphate was elevated, while those abnormal rises did not occur in individuals with microalbuminuria and those with normoalbuminuria.

We discovered novel metabolites and gut genera involved in carbohydrate metabolism and lipid metabolism. TSF treatment attenuated the abnormal levels of metabolites and gut microbiota dysbiosis. In the future, we should validate our results in samples from DKD patients and confirm the mechanism for potential functional molecules *in vivo* and *in vitro*. In addition, fecal microbiota transplantation to identify specific bacterial species will support exploration of the underlying mechanisms in DKD and TSF treatment.

CONCLUSION

In the present investigation, disturbances in the metabolic profile in the serum and gut microbiota were the main cause of imbalances in carbohydrate, lipid, and amino acid metabolism, as well as of renal damage, thus the importance of the aforementioned in the progression of DKD. Anomalously upregulated isomaltose, D-mannose, galactonic acid, citramalic acid, and prostaglandin B2 and downregulated 3-(2-hydroxyethyl)indole, 3-methylindole, and indoleacrylic acid were the critical metabolites in these pathways. Additionally, *g_Eubacterium_nodatum_group*, *g_Lactobacillus*, and *g_Faecalibaculum* were the most involved in metabolic disorders in DKD rats.

DATA AVAILABILITY STATEMENT

The datasets presented in this study can be found in online repositories. The names of the repository/repositories and accession number(s) can be found below: National Center for Biotechnology Information (NCBI) BioProject database under accession number PRJNA812954.

ETHICS STATEMENT

The animal study was reviewed and approved by the Ethics Committee of the China–Japan Friendship Hospital.

AUTHOR CONTRIBUTIONS

BZ and TZ wrote the manuscript draft. BZ, YW, XZ, HZ (4th author), HZ (5th author), LM, XD, and MY performed the experiments. TZ and PL supervised the experiments. BZ and TZ analyzed the data. All authors contributed to the article and approved the submitted version.

FUNDING

This study was supported by the National Natural Science Foundation of China (No: 81973627, 82174296, 82074221, and 81873140), Beijing Natural Science Foundation (No: 7212195), and Innovation Team and Talents Cultivation Program of National Administration of Traditional Chinese Medicine (No: ZYYCXTD-C-202005).

ACKNOWLEDGMENTS

The authors thank Nissi S. Wang, MSc, for content editing of the manuscript.

SUPPLEMENTARY MATERIAL

The Supplementary Material for this article can be found online at: https://www.frontiersin.org/articles/10.3389/fphar.2022.872988/full#supplementary-material

REFERENCES

Adams, J. D., Jr, Heins, M. C., and Yost, G. S. (1987). 3-Methylindole Inhibits Lipid Peroxidation. *Biochem. Biophys. Res. Commun.* 149 (1), 73–78. doi:10.1016/0006-291x(87)91606-8

Al-Shamsi, M., Amin, A., and Adeghate, E. (2006). Effect of Vitamin C on Liver and Kidney Functions in normal and Diabetic Rats. *Ann. N. Y Acad. Sci.* 1084, 371–390. doi:10.1196/annals.1372.031

Alicic, R. Z., Rooney, M. T., and Tuttle, K. R. (2017). Diabetic Kidney Disease: Challenges, Progress, and Possibilities. *Clin. J. Am. Soc. Nephrol.* 12 (12), 2032–2045. doi:10.2215/CJN.11491116

Asirvatham-Jeyaraj, N., Jones, A. D., Burnett, R., and Fink, G. D. (2019). Brain Prostaglandin D2 Increases Neurogenic Pressor Activity and Mean Arterial Pressure in Angiotensin II-Salt Hypertensive Rats. *Hypertension* 74 (6), 1499–1506. doi:10.1161/HYPERTENSIONAHA.119.13175

Azegami, T., Nakayama, T., Hayashi, K., Hishikawa, A., Yoshimoto, N., Nakamichi, R., et al. (2021). Vaccination against Receptor for Advanced Glycation End Products Attenuates the Progression of Diabetic Kidney Disease. *Diabetes* 70 (9), 2147–2158. doi:10.2337/db20-1257

Caesar, R. (2019). Pharmacologic and Nonpharmacologic Therapies for the Gut Microbiota in Type 2 Diabetes. *Can. J. Diabetes* 43 (3), 224–231. doi:10.1016/j.jcjd.2019.01.007

Chávez-Talavera, O., Tailleux, A., Lefebvre, P., and Staels, B. (2017). Bile Acid Control of Metabolism and Inflammation in Obesity, Type 2 Diabetes, Dyslipidemia, and Nonalcoholic Fatty Liver Disease. *Gastroenterology* 152 (7), 1679–e3. doi:10.1053/j.gastro.2017.01.055

Committee of the Japan Diabetes Society on the Diagnostic Criteria of Diabetes MellitusSeino, Y., Nanjo, K., Tajima, N., Kadawoki, T., Kashiwagi, A., Araki, E., et al. (2010). Report of the Committee on the Classification and Diagnostic Criteria of Diabetes Mellitus. *J. Diabetes Investig.* 1 (5), 212–228. doi:10.1111/j.2040-1124.2010.00074.x

Fahrmann, J., Grapov, D., Yang, J., Hammock, B., Fiehn, O., Bell, G. I., et al. (2015). Systemic Alterations in the Metabolome of Diabetic NOD Mice Delineate Increased Oxidative Stress Accompanied by Reduced Inflammation and Hypertriglyceremia. *Am. J. Physiol. Endocrinol. Metab.* 308 (11), E978–E989. doi:10.1152/ajpendo.00019.2015

Hall, D. W., and Jaitly, K. D. (1976). Structure-activity Relationships in a Series of 11-deoxy Prostaglandins. *Prostaglandins* 11 (3), 573–587. doi:10.1016/0090-6980(76)90106-4

Hasegawa, S., Tanaka, T., Saito, T., Fukui, K., Wakashima, T., Susaki, E. A., et al. (2020). The Oral Hypoxia-Inducible Factor Prolyl Hydroxylase Inhibitor Enarodustat Counteracts Alterations in Renal Energy Metabolism in the Early Stages of Diabetic Kidney Disease. *Kidney Int.* 97 (5), 934–950. doi:10.1016/j.kint.2019.12.007

Hu, Z. B., Lu, J., Chen, P. P., Lu, C. C., Zhang, J. X., Li, X. Q., et al. (2020). Dysbiosis of Intestinal Microbiota Mediates Tubulointerstitial Injury in Diabetic Nephropathy via the Disruption of Cholesterol Homeostasis. *Theranostics* 10 (6), 2803–2816. doi:10.7150/thno.40571

Jia, W., Xie, G., and Jia, W. (2018). Bile Acid-Microbiota Crosstalk in Gastrointestinal Inflammation and Carcinogenesis. *Nat. Rev. Gastroenterol. Hepatol.* 15 (2), 111–128. doi:10.1038/nrgastro.2017.119

Jiang, H., Shao, X., Jia, S., Qu, L., Weng, C., Shen, X., et al. (2019). The Mitochondria-Targeted Metabolic Tubular Injury in Diabetic Kidney Disease. *Cell Physiol Biochem* 52 (2), 156–171. doi:10.33594/000000011

Jin, Q., and Ma, R. C. W. (2021). Metabolomics in Diabetes and Diabetic Complications: Insights from Epidemiological Studies. *Cells* 10 (11), 2832–2869. doi:10.3390/cells10112832

Johansen, K. L., Chertow, G. M., Foley, R. N., Gilbertson, D. T., Herzog, C. A., Ishani, A., et al. (2021). US Renal Data System 2020 Annual Data Report: Epidemiology of Kidney Disease in the United States. *Am. J. Kidney Dis.* 77 (4 Suppl. 1), A7–A8. doi:10.1053/j.ajkd.2021.01.002

Johnson, C. H., Ivanisevic, J., and Siuzdak, G. (2016). Metabolomics: beyond Biomarkers and towards Mechanisms. *Nat. Rev. Mol. Cel Biol* 17 (7), 451–459. doi:10.1038/nrm.2016.25

Kazmierczak-Baranska, J., Adamus-Grabicka, A., Boguszewska, K., and Karwowski, B. T. (2020). Two Faces of Vitamin C-Antioxidative and Pro-oxidative Agent. *Nutrients* 12 (5), 12051501. doi:10.3390/nu12051501

Kikuchi, K., Saigusa, D., Kanemitsu, Y., Matsumoto, Y., Thanai, P., Suzuki, N., et al. (2019). Gut Microbiome-Derived Phenyl Sulfate Contributes to Albuminuria in Diabetic Kidney Disease. *Nat. Commun.* 10 (1), 1835–1851. doi:10.1038/s41467-019-09735-4

Kiorpes, A. L., Sword, J. W., and Hoekstra, W. G. (1988). Effect of 3-methylindole on Respiratory Ethane Production in Selenium and Vitamin E Deficient Rats. *Biochem. Biophys. Res. Commun.* 153 (2), 535–539. doi:10.1016/s0006-291x(88)81127-6

Li, J., Liu, H., Takagi, S., Nitta, K., Kitada, M., Srivastava, S. P., et al. (2020). Renal Protective Effects of Empagliflozin via Inhibition of EMT and Aberrant

Glycolysis in Proximal Tubules. *JCI Insight* 5 (6), e129034. doi:10.1172/jci.insight.129034

Li, P., Chen, Y., Liu, J., Hong, J., Deng, Y., Yang, F., et al. (2015). Efficacy and Safety of Tangshen Formula on Patients with Type 2 Diabetic Kidney Disease: a Multicenter Double-Blinded Randomized Placebo-Controlled Trial. *PLoS One* 10 (5), e0126027. doi:10.1371/journal.pone.0126027

Li, Y. J., Chen, X., Kwan, T. K., Loh, Y. W., Singer, J., Liu, Y., et al. (2020). Dietary Fiber Protects against Diabetic Nephropathy through Short-Chain Fatty Acid-Mediated Activation of G Protein-Coupled Receptors GPR43 and GPR109A. *J. Am. Soc. Nephrol.* 31 (6), 1267–1281. doi:10.1681/ASN.2019101029

Liu, H., Takagaki, Y., Kumagai, A., Kanasaki, K., and Koya, D. (2021). The PKM2 Activator TEPP-46 Suppresses Kidney Fibrosis via Inhibition of the EMT Program and Aberrant Glycolysis Associated with Suppression of HIF-1α Accumulation. *J. Diabetes Investig.* 12 (5), 697–709. doi:10.1111/jdi.13478

Ma, R. C. W. (2018). Epidemiology of Diabetes and Diabetic Complications in China. *Diabetologia* 61 (6), 1249–1260. doi:10.1007/s00125-018-4557-7

Maedler, K., Spinas, G. A., Dyntar, D., Moritz, W., Kaiser, N., and Donath, M. Y. (2001). Distinct Effects of Saturated and Monounsaturated Fatty Acids on Beta-Cell Turnover and Function. *Diabetes* 50 (1), 69–76. doi:10.2337/diabetes.50.1.69

Marchand, G. R., Greenberg, S., Wilson, W. R., and Williamson, H. E. (1973). Effects of Prostaglandin B2 on Renal Hemodynamics and Excretion. *Proc. Soc. Exp. Biol. Med.* 143 (4), 938–940. doi:10.3181/00379727-143-37445

McGlone, E. R., and Bloom, S. R. (2019). Bile Acids and the Metabolic Syndrome. *Ann. Clin. Biochem.* 56 (3), 326–337. doi:10.1177/0004563218817798

Méndez, J. D., and Balderas, F. L. (2006). Inhibition by L-Arginine and Spermidine of Hemoglobin Glycation and Lipid Peroxidation in Rats with Induced Diabetes. *Biomed. Pharmacother.* 60 (1), 26–31. doi:10.1016/j.biopha.2005.08.004

O'Kell, A. L., Wasserfall, C., Guingab-Cagmat, J., Webb-Roberston, B. M., Atkinson, M. A., and Garrett, T. J. (2021). Targeted Metabolomic Analysis Identifies Increased Serum Levels of GABA and Branched Chain Amino Acids in Canine Diabetes. *Metabolomics* 17 (11), 100. doi:10.1007/s11306-021-01850-y

Qi, W., Keenan, H. A., Li, Q., Ishikado, A., Kannt, A., Sadowski, T., et al. (2017). Pyruvate Kinase M2 Activation May Protect against the Progression of Diabetic Glomerular Pathology and Mitochondrial Dysfunction. *Nat. Med.* 23 (6), 753–762. doi:10.1038/nm.4328

Ramezani, A., and Raj, D. S. (2014). The Gut Microbiome, Kidney Disease, and Targeted Interventions. *J. Am. Soc. Nephrol.* 25 (4), 657–670. doi:10.1681/ASN.2013080905

Ren, Y., D'Ambrosio, M. A., Garvin, J. L., Wang, H., and Carretero, O. A. (2013). Prostaglandin E2 Mediates Connecting Tubule Glomerular Feedback. *Hypertension* 62 (6), 1123–1128. doi:10.1161/HYPERTENSIONAHA.113.02040

Rinschen, M. M., Ivanisevic, J., Giera, M., and Siuzdak, G. (2019). Identification of Bioactive Metabolites Using Activity Metabolomics. *Nat. Rev. Mol. Cel Biol* 20 (6), 353–367. doi:10.1038/s41580-019-0108-4

Roager, H. M., and Licht, T. R. (2018). Microbial Tryptophan Catabolites in Health and Disease. *Nat. Commun.* 9 (1), 3294–3313. doi:10.1038/s41467-018-05470-4

Robertson, R. P. (1983). Prostaglandins, Glucose Homeostasis, and Diabetes Mellitus. *Annu. Rev. Med.* 34, 1–12. doi:10.1146/annurev.me.34.020183.000245

Sharma, V., Ichikawa, M., and Freeze, H. H. (2014). Mannose Metabolism: More Than Meets the Eye. *Biochem. Biophys. Res. Commun.* 453 (2), 220–228. doi:10.1016/j.bbrc.2014.06.021

Srivastava, S. P., Li, J., Kitada, M., Fujita, H., Yamada, Y., Goodwin, J. E., et al. (2018). SIRT3 Deficiency Leads to Induction of Abnormal Glycolysis in Diabetic Kidney with Fibrosis. *Cell Death Dis* 9 (10), 997–1010. doi:10.1038/s41419-018-1057-0

Sun, S., Wang, K., Sun, L., Cheng, B., Qiao, S., Dai, H., et al. (2020). Therapeutic Manipulation of Gut Microbiota by Polysaccharides of Wolfiporia Cocos Reveals the Contribution of the Gut Fungi-Induced PGE2 to Alcoholic Hepatic Steatosis. *Gut Microbes* 12 (1), 1830693. doi:10.1080/19490976.2020.1830693

Tang, J., Wysocki, J., Ye, M., Vallés, P. G., Rein, J., Shirazi, M., et al. (2019). Urinary Renin in Patients and Mice with Diabetic Kidney Disease. *Hypertension* 74 (1), 83–94. doi:10.1161/HYPERTENSIONAHA.119.12873

Vlassara, H., Uribarri, J., Cai, W., Goodman, S., Pyzik, R., Post, J., et al. (2012). Effects of Sevelamer on HbA1c, Inflammation, and Advanced Glycation End Products in Diabetic Kidney Disease. *Clin. J. Am. Soc. Nephrol.* 7 (6), 934–942. doi:10.2215/CJN.12891211

Wang, X., Yang, S., Li, S., Zhao, L., Hao, Y., Qin, J., et al. (2020). Aberrant Gut Microbiota Alters Host Metabolome and Impacts Renal Failure in Humans and Rodents. *Gut* 69 (12), 2131–2142. doi:10.1136/gutjnl-2019-319766

Winther, S. A., Henriksen, P., Vogt, J. K., Hansen, T. H., Ahonen, L., Suvitaival, T., et al. (2020). Gut Microbiota Profile and Selected Plasma Metabolites in Type 1 Diabetes without and with Stratification by Albuminuria. *Diabetologia* 63 (12), 2713–2724. doi:10.1007/s00125-020-05260-y

Winther, S. A., Øllgaard, J. C., Tofte, N., Tarnow, L., Wang, Z., Ahluwalia, T. S., et al. (2019). Utility of Plasma Concentration of Trimethylamine N-Oxide in Predicting Cardiovascular and Renal Complications in Individuals with Type 1 Diabetes. *Diabetes Care* 42 (8), 1512–1520. doi:10.2337/dc19-0048

Wlodarska, M., Luo, C., Kolde, R., d'Hennezel, E., Annand, J. W., Heim, C. E., et al. (2017). Indoleacrylic Acid Produced by Commensal Peptostreptococcus Species Suppresses Inflammation. *Cell Host Microbe* 22 (1), 25–e6. doi:10.1016/j.chom.2017.06.007

Yang, Z. H., Miyahara, H., and Hatanaka, A. (2011). Chronic Administration of Palmitoleic Acid Reduces Insulin Resistance and Hepatic Lipid Accumulation in KK-Ay Mice with Genetic Type 2 Diabetes. *Lipids Health Dis.* 10 (120), 120. doi:10.1186/1476-511X-10-120

Yao, C., and Narumiya, S. (2019). Prostaglandin-cytokine Crosstalk in Chronic Inflammation. *Br. J. Pharmacol.* 176 (3), 337–354. doi:10.1111/bph.14530

Zhang, H., Li, P., Burczynski, F. J., Gong, Y., Choy, P., Sha, H., et al. (2011). Attenuation of Diabetic Nephropathy in Otsuka Long-Evans Tokushima Fatty (OLETF) Rats with a Combination of Chinese Herbs (Tangshen Formula). *Evid. Based Complement. Alternat Med.* 2011, 613737. doi:10.1155/2011/613737

Zhang, Q., Zhang, Y., Zeng, L., Chen, G., Liu, M., Sheng, H., et al. (2021). The Role of Gut Microbiota and Microbiota-Related Serum Metabolites in the Progression of Diabetic Kidney Disease. *Front. Pharmacol.* 12, 757508. doi:10.3389/fphar.2021.757508

Zhao, J., Zhang, Q. L., Shen, J. H., Wang, K., and Liu, J. (2019). Magnesium Lithospermate B Improves the Gut Microbiome and Bile Acid Metabolic Profiles in a Mouse Model of Diabetic Nephropathy. *Acta Pharmacol. Sin* 40 (4), 507–513. doi:10.1038/s41401-018-0029-3

Zhao, T., Zhang, H., Zhao, T., Zhang, X., Lu, J., Yin, T., et al. (2012). Intrarenal Metabolomics Reveals the Association of Local Organic Toxins with the Progression of Diabetic Kidney Disease. *J. Pharm. Biomed. Anal.* 60, 32–43. doi:10.1016/j.jpba.2011.11.010

Conflict of Interest: The authors declare that the research was conducted in the absence of any commercial or financial relationships that could be construed as a potential conflict of interest.

Publisher's Note: All claims expressed in this article are solely those of the authors and do not necessarily represent those of their affiliated organizations, or those of the publisher, the editors, and the reviewers. Any product that may be evaluated in this article, or claim that may be made by its manufacturer, is not guaranteed or endorsed by the publisher.

frontiers | Frontiers in Pharmacology

ORIGINAL RESEARCH
published: 17 May 2022
doi: 10.3389/fphar.2022.873023

Network Pharmacology and Experimental Verification Strategies to Illustrate the Mechanism of Jian-Pi-Yi-Shen Formula in Suppressing Epithelial–Mesenchymal Transition

Yuan Zhao[1], Xiangbin Li[2], Fochang Wang[1], Shiying Huang[1], Hanqian Du[3], Shunmin Li[1] and Jianping Chen[1]**

[1]Shenzhen Key Laboratory of Hospital Chinese Medicine Preparation, Shenzhen Traditional Chinese Medicine Hospital, The Fourth Clinical Medical College of Guangzhou University of Chinese Medicine, Shenzhen, China, [2]Shenzhen Hospital of Beijing University of Chinese Medicine (Longgang), Shenzhen, China, [3]Institute of Chinese Materia Medica, China Academy of Chinese Medical Sciences, Beijing, China

OPEN ACCESS

Edited by:
Zhiyong Guo,
Second Military Medical University, China

Reviewed by:
Dingkun Gui,
Shanghai Jiao Tong University, China
Rishov Goswami,
Dana–Farber Cancer Institute, United States

***Correspondence:**
Shunmin Li
zyylishunmin@163.com
Jianping Chen
lycjp@126.com

Specialty section:
This article was submitted to Renal Pharmacology, a section of the journal Frontiers in Pharmacology

Received: 10 February 2022
Accepted: 24 March 2022
Published: 17 May 2022

Citation:
Zhao Y, Li X, Wang F, Huang S, Du H, Li S and Chen J (2022) Network Pharmacology and Experimental Verification Strategies to Illustrate the Mechanism of Jian-Pi-Yi-Shen Formula in Suppressing Epithelial–Mesenchymal Transition. Front. Pharmacol. 13:873023. doi: 10.3389/fphar.2022.873023

Jian-Pi-Yi-Shen formula (JPYSF), a traditional Chinese medicine, has been recommended to treat renal fibrosis for decades. Previous studies had shown that JPYSF could inhibit epithelial–mesenchymal transition (EMT), an important regulatory role in renal fibrosis. However, the mechanism of JPYSF action is largely unknown. In this study, network pharmacology and experimental verification were combined to elucidate and identify the potential mechanism of JPYSF against renal fibrosis by suppressing EMT at molecular and pathway levels. Network pharmacology was first performed to explore the mechanism of JPYSF against renal fibrosis targeting EMT, and then a 5/6 nephrectomy (5/6 Nx)-induced rat model of renal fibrosis was selected to verify the predictive results by Masson's trichrome stains and western blot analysis. Two hundred and thirty-two compounds in JPYSF were selected for the network approach analysis, which identified 137 candidate targets of JPYSF and 4,796 known therapeutic targets of EMT. The results of the Gene Ontology (GO) function enrichment analysis included 2098, 88, and 133 GO terms for biological processes (BPs), molecular functions (MFs), and cell component entries, respectively. The top 10 enrichment items of BP annotations included a response to a steroid hormone, a metal ion, oxygen levels, and so on. Cellular composition (CC) is mainly enriched in membrane raft, membrane microdomain, membrane region, etc. The MF of JPYSF analysis on EMT was predominately involved in proximal promoter sequence-specific DNA binding, protein heterodimerization activity, RNA polymerase II proximal promoter sequence-specific DNA binding, and so on. The involvement signaling pathway of JPYSF in the treatment of renal fibrosis targeting EMT was associated with anti-fibrosis,

Abbreviations: JPYSF, Jian-Pi-Yi-Shen Formula; EMT, epithelial–mesenchymal transition; 5/6 Nx, 5/6 nephrectomy; TCM, traditional Chinese medicine; CTS, chemicals-shared target genes-signal pathway; BP, biological process; CC, cell component; MF, molecular function; SD, Sprague–Dawley.

anti-inflammation, podocyte protection, and metabolism regulation. Furthermore, the *in vivo* experiments confirmed that JPYSF effectively ameliorated interstitial fibrosis and inhibited the overexpression of α-SMA, Wnt3a, and β-catenin, and increased the expression of E-cadherin by wnt3a/β-catenin signaling pathway in 5/6 Nx-induced renal fibrosis rats. Using an integrative network pharmacology-based approach and experimental verification, the study showed that JPYSF had therapeutic effects on EMT by regulating multi-pathway, among which one proven pathway was the Wnt3a/β-catenin signaling pathway. These findings provide insights into the renoprotective effects of JPYSF against EMT, which could suggest directions for further research of JPYSF in attenuating renal fibrosis by suppressing EMT.

Keywords: Jian-Pi-Yi-Shen formula, renal fibrosis, epithelial–mesenchymal transition, network pharmacology, Wnt3a/β-catenin signaling pathway

INTRODUCTION

Renal fibrosis can lead to the progressive loss of renal function, with the characteristic of the proliferation of renal intrinsic cells, activation of renal interstitial fibroblasts, and deposition of extracellular matrix, which is the most common cause of kidney failure (Zhao et al., 2021). A large part of interstitial myofibroblasts, the main effector cells of renal fibrosis, are derived from tubular epithelial cells of the affected kidneys via epithelial–mesenchymal transition (EMT) (Hu et al., 2021). EMT, one of the main mechanisms of renal fibrosis, had been found to contribute to ongoing fibrosis in kidney disease through a variety of signal pathways, which ultimately led to renal function impairment, and then developed into chronic renal disease and end-stage renal disease. Despite extensive studies, the current treatment strategies of western medicine can hardly reverse the progression of renal fibrosis, underscoring the need to develop an alternative therapeutic approach to reverse or stop the progression. Traditional Chinese medicine (TCM), with the feature of multi-component, multi-target, and multi-channel, can enhance body functions and reduce drug toxicity through the synergistic actions of their main active ingredients, which could be a rich source for drug discovery. The experimental models and clinical studies have proved that TCM and its extracts have made great progress in the prevention or even treatment of renal fibrosis, and effectively inhibited the development of EMT in recent years (Xu et al., 2021).

Jian-Pi-Yi-Shen Formula (JPYSF) is derived from the addition and subtraction of "Yupingfeng San" and "Sijing Pills" (recorded in Shengji Zonglu). JPYSF has been prescribed for patients with chronic kidney disease in clinics, which consists of *Astragalus mongholicus* Bunge (*A. mongholicus*), *Dioscorea oppositifolia* L. (*D. oppositifolia*.), *Salvia miltiorrhiza* Bge. (*S. miltiorrhiza*), *Atractylodes macrocephala* Koidz. (*A. macrocephala*), *Cistanche deserticola* Ma (*C. deserticola*), *Amomum kravanh* Pierre ex Gagnep. (*A. kravanh*), *Rheum palmatum* L. (*R. palmatum*), and *Glycyrrhiza uralensis* Fisch. (*G. uralensis*). Adopting the two-complement five-way method, the two complement mainly consists of "tonifying the kidney" and "tonifying the spleen." *A. mongholicus*, *A. macrocephala*., *D. oppositifolia*., and *C. deserticola* were used as spleen and kidney supplements (Zhong et al., 2016). *A. mongholicus* was used for nourishing the qi of the five viscera, and it was an important medicine for nourishing the qi of the spleen and kidney. "Five-way" means to make sure that feces, urine, sweat, breath, and blood are unobstructed. *R. palmatum*, *A. macrocephala*, and *C. deserticola* were used to pass bowel movements, having the functions of loosening the bowel to relieve constipation (Zhong et al., 2016). *A. mongholicus* and *A. macrocephala* were used for urination, having a diuretic effect (Fu et al., 2014). *A. kravanh*, which has the effect of warming middle energizer, dissipating hygrosis and regulating *qi*, and promoting sweat and breathing well, was used to drain sweat and breath. *S. miltiorrhiza* and *R. palmatum* were used to promote blood circulation, having the effect of promoting blood circulation and removing blood stasis (Mei et al., 2019; Pei et al., 2020). *G. uralensis* was used for invigorating the spleen and harmonizing herbs. Taken together, JPYSF, the combined use of all the above-mentioned herbs, has the effects of invigorating the spleen and kidney, promoting blood circulation, and removing turbidity. Previous pharmaceutical studies have revealed that JPYSF had effectiveness in the treatment of chronic kidney disease and renal fibrosis (Liu et al., 2018; Lu et al., 2018; Chen et al., 2019). However, the composition of JPYSF is complex and its mechanism of action is not clear enough, which limits its wide clinical application.

Network pharmacology is a theory based on systems biology and has been commonly used in the modern research of TCM in recent years. It emphasizes the multichannel regulation of signaling pathways, which is in accord with the characteristics of multi-components and multi-targets of Chinese medicine. Therefore, network pharmacology has become a new effective approach in TCM research at the molecular level (Zhang et al., 2021).

In this study, the integrated strategy of network pharmacology and verification *in vivo*, we first explored the main active ingredients, targets, and signal pathways of JPYSF in the treatment of EMT, and then the animal experiment was carried out to verify the effect of JPYSF against renal fibrosis by inhibiting EMT. The research may lay a good theoretical foundation for further study on developing new drugs for renal fibrosis.

METHODS

Network Pharmacology Analysis

Determination of the Active Components of Jian-Pi-Yi-Shen Formula

All chemical ingredients from the eight herbal medicines of JPYSF were collected from an online database, including a traditional Chinese medicine system pharmacology database and an analysis platform (TCMSP, https://tcmspw.com/tcmsp.php), Integrative Pharmacology-based Research Platform of Traditional Chinese Medicine (TCMIP) v2.0 (Xu et al., 2019; Su et al., 2021), and previous pieces of literature (Wang F et al., 2020). All chemical ingredients were employed to evaluate the degree of drug absorption based on the criteria of oral bioavailability (OB ≥ 30%) and drug-like (DL ≥ 0.18) (mean value for all molecules within the DrugBank database).

Target Screening of Active Components of Jian-Pi-Yi-Shen Formula and Epithelial–Mesenchymal Transition

The target screening of components was predicted using TCMIP v2.0, TCMSP, the Swiss Target Prediction (http://www.swisstargetprediction.ch/) databases, and previous pieces of literature. The candidate's therapeutic genes related to EMT were acquired from the OMIM (https://www.omim.org/) (Amberger et al., 2019), GeneCards (https://www.genecards.org/), and Drugbank (https://go.drugbank.com/) using "epithelial–mesenchymal transition" as the keyword. Then, all targets were converted into gene names by the UniProt database (https://www.uniprot.org/).

Protein–Protein Interaction Network Construction and Analysis

The interaction networks of the common targets of JPYSF and EMT were constructed by the STRING platform (https://www.string-db.org/). To identify the potential hub nodes of JPYSF in the treatment of EMT, the minimum required interaction score was set as the highest confidence 0.9. "hide disconnected nodes in the network" was ticked in network display options. String_interactions.tsv was then exported. Network visualization and analysis were performed using Cytoscape 3.7.1 software.

Gene Ontology and KEGG Pathway Enrichment Analysis

The coexistent targets of JPYSF and EMT were conducted on VENNY 2.1 website (https://bioinfogp.cnb.csic.es/tools/venny/index.html), and the Venn diagram was then prepared. The coexistent targets were analyzed using R (https://www.r-project.org/) software for the GO and KEGG enrichment analysis. The threshold was set to $p < 0.05$. The results were visually displayed in the form of bubble charts and histograms. The biological processes (BPs), molecular functions (MFs), and cellular compositions (CCs) were included in the GO enrichment analysis.

Network Construction of "Chemicals-Shared Target Genes-Signal Pathway"

The network of CTS was constructed with Cytoscape 3.7.1 software. The nodes in the network diagram are targets, chemicals, or signal pathways. The edge means that there is an interactive relationship between a certain target and a certain signal pathway, a component and a certain target, or a certain target and a certain target.

Experimental Verification

Samples and Sample Preparation

All the raw herbs were obtained from Shenzhen Huahui Pharmaceutical Co., Ltd. (Shenzhen, China) and were authenticated by Shangbin Zhang. The extraction of JPYSF was conducted as previously described (Chen et al., 2019). In brief, *A. mongholicus*, *A. macrocephala*, *D. oppositifolia*, *C. deserticola*, *A. kravanh*, *S. miltiorrhiza*, *R. palmatum*, and *G. uralensis* were mixed in the ratio of 30:10:30:10:10:15:10:6. The detailed methods were as described previously (Wang YN et al., 2020). The extract was freeze-dried and stored at −80°C. The powder was re-dissolved in ddH_2O as a JPYSF sample. The yield of the extract was 30.8%. The extract being used here was chemically analyzed by HPLC-MS, as indicated in **Supplementary Figure S1** according to previously established standards (Wang F et al., 2020), which guaranteed the repeatability of biological results.

Animals

All animal experiments were in accord with the ethics committee of Guangzhou University of Chinese Medicine and the National Institutes of Health Guideline for the care and use of laboratory animals. Forty male Sprague–Dawley (SD) rats weighing between 180 and 220 g were supplied by Guangdong Medical Laboratory Animal Center (Foshan, China). All the rats were housed under controlled conditions (12-h light/12-h dark cycle) in a specific pathogen-free animal facility with free access to rodent food and drinking water. Either 5/6 nephrectomy (5/6 Nx) or sham operation (sham) was performed on SD rats. The 5/6 Nx operation was conducted in a two-step surgery as described previously (Chen et al., 2019). In brief, upper and lower two-thirds of the left kidneys of 30 rats were ablated, and two weeks later, the right kidneys of the animals were removed under anesthesia with sodium pentobarbital (50 mg/kg, intraperitoneal injection). Laparotomy was performed on rats in the sham-operated group, manipulation of the renal pedicles but without destructing the renal tissue, and then replaced intact. Twelve weeks after the second surgery, all rats were randomly classified into four groups for 6 weeks as follows: the sham group that was given a gavage of distilled water, the model group (5/6 Nx) that was given a gavage of distilled water, and the JPYSF group (2.73, 10.89 g/kg) (Liu et al., 2018; Zheng et al., 2020). All rats were anesthetized with sodium pentobarbital by intraperitoneal injection (50 mg/kg). The kidneys were removed and preserved for further analysis.

Masson's Trichrome Stains

The kidneys of the rats were fixed with 10% neutral formaldehyde and then paraffin embedding and sectioning were carried out. Pathological changes in the kidney were evaluated by Masson's

trichrome stains. The experimental process and quantitative methods were performed as previously described (Lu et al., 2018).

Western Blot Analysis

The cortex tissues of the kidneys were lysed with RIPA lysis buffer. Equal amounts of lysates were loaded and electrophoresed through 10% SDS-polyacrylamide gels, and then transferred to the PVDF membrane. Following blocking in 5% non-fat milk for 2 h at room temperature, the membranes were incubated with various primary antibodies at 4°C overnight. The primary antibodies included α-SMA (1:1,000, Cell Signaling Technology, Beverly, MA, United States), E-cadherin (1:1,000, Cell Signaling Technology, Beverly, MA, United States), Wnt3a (1:1,000, Abcam, Cambridge, MA, United States), β-catenin (1:1,000, Abcam, Cambridge, MA, United States), and GAPDH (1:5,000, Abcam, Cambridge, MA, United States). Then, the membranes were incubated in HRP-conjugated secondary antibodies for 2 h at room temperature. HRP activity was visualized using Tanon-6100C (Guangzhou Yuwei Biotechnology Instrument Co., Ltd., Guangzhou, China).

Statistical Analysis

Data were expressed as mean ± standard deviation. One-way analysis of variance (ANOVA) was used to determine the level of statistical significance followed by Tukey's multiple comparison tests. There was a significant difference if the '*p*' value was less than 0.05.

RESULTS

Network Pharmacology to Illustrate the Mechanism of Jian-Pi-Yi-Shen Formula in Suppressing Epithelial–Mesenchymal Transition

Compounds in Jian-Pi-Yi-Shen Formula

There were 232 compounds in JPYSF that were being screened by the conditions of OB value ≥ 30% and DL value ≥ 0.18. Among them, 6 compounds were in *A. macrocephala*, 16 compounds were in *R. palmatum*, 67 compounds were in *S. miltiorrhiza*, 9 compounds were in *A. kravanh*, 89 compounds were in *G. uralensis*, 14 compounds were in *A. mongholicus*, 4 compounds were in *C. deserticola*, and 16 compounds were in *D. oppositifolia*. Luteolin was the common compound derived from both *S. miltiorrhiza* and *A. kravanh*; Jaranol was the common ingredient of *A. kravanh*, *G. uralensis*, and *A. mongholicus*. Mairin and calycosin co-existed in *A. mongholicus* and *G. uralensis*. Quercetin existed in *G. uralensis*, *A. mongholicus*, *A. kravanh*, and *C. deserticola*. (3S,8S,9S,10R,13R,14S,17R)-10,13-Dimethyl-17-[(2R,5S)-5-propan-2-yloctan-2-yl]-2,3,4,7,8,9,11,12,14,15,16,17-dodecahydro-1H-cyclopenta[a]phenanthren-3-ol was present in *A. mongholicus* and *A. macrocephala*. Isorhamnetin, formononetin, and kaempferol were present in *A. mongholicus* and *G. uralensis*. β-sitosterol was present in both *C. deserticola* and *R. palmatum*. Sucrose was present in *A. mongholicus* and *D. oppositifolia*. The aforesaid compounds in JPYSF can be found in **Supplementary Table S1**.

Target Collection of Epithelial–Mesenchymal Transition and Active Ingredients of Jian-Pi-Yi-Shen Formula

Fifty-nine EMT-related targets were identified in the DrugBank database, 4,770 targets in the GeneCards database, and 7 targets in the OMIM database. There were 4796 EMT-related targets after removing the duplicate values (**Supplementary Table S2**). Excluding duplicate targets, a total of 137 candidate targets were queried in JPYSF (**Supplementary Table S3**). As shown in **Figure 1A**, there were 100 common targets in both EMT and JPYSF. Among them, 87 targets interacted with others (**Figure 1B**). HSP90AA1 was the most frequent target, followed by CTNNB1, ESR1, RELA, and FOS. The top 30 targets in action frequency are shown in **Figure 1C**.

Gene Ontology Function and KEGG Signal Pathway Enrichment Analysis of Common Targets

To better summarize the specific functions of JPYSF in EMT, 100 common targets were imported into R software for GO function annotation and KEGG pathway enrichment. The results showed that a total of 2098 GO terms for BP, 88 GO terms for CC, and 133 GO terms for MF with statistical significance ($p < 0.05$) were obtained (**Supplementary Table S4**). As shown in **Figure 2**, the top 10 enrichment items of BP annotations included response to a steroid hormone, response to a metal ion, response to oxygen levels, and so on. CC was mainly enriched in the membrane raft, membrane microdomain, membrane region, etc. The MF of JPYSF analysis on EMT was predominately involved in proximal promoter sequence-specific DNA binding, protein heterodimerization activity, RNA polymerase II proximal promoter sequence-specific DNA binding, etc. Genes that were classified in the pathway analysis were heavily involved in the PI3K-Akt signaling pathway, NF-kappa B signaling pathway, Toll-like receptor signaling pathway, Wnt signaling pathway, JAK-STAT signaling pathway, AMPK signaling pathway, Autophagy–animal, Hedgehog signaling pathway, mTOR signaling pathway, and TGF-beta signaling pathway (**Figure 3**). Genes enriched in signaling pathways are demonstrated in **Supplementary Table S5**.

Network Construction of CTS and Analysis

According to the KEGG enrichment analysis results, the network of CTS was established to systematically explain the mechanism of JPYSF on EMT. There were 343 nodes that interacted with other nodes in the network. The rose font represented the top 10 pathways, the blue font represented the bioactive components, and the red font represented the common target genes of JPYSF and EMT (**Figure 4**). According to the topological parameters results of the network, the average degree value was 12.6006, the average betweenness centrality value was 0.0060, and the average

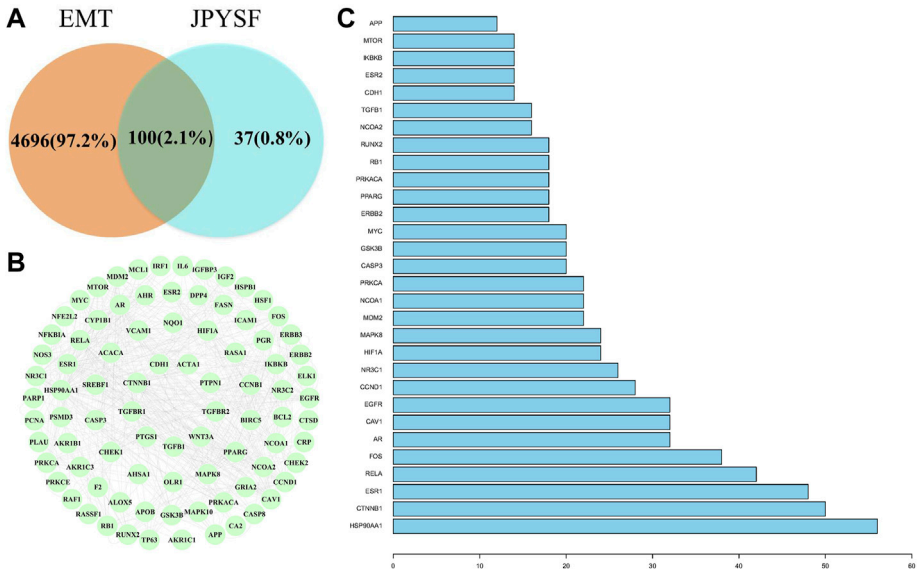

FIGURE 1 | The interaction of shared targets between Jian-Pi-Yi-Shen formula (JPYSF) active ingredients and epithelial–mesenchymal transition (EMT). **(A)**. The Venn diagram; **(B)** 87 connected nodes in the network; and **(C)** The top 30 targets in action frequency.

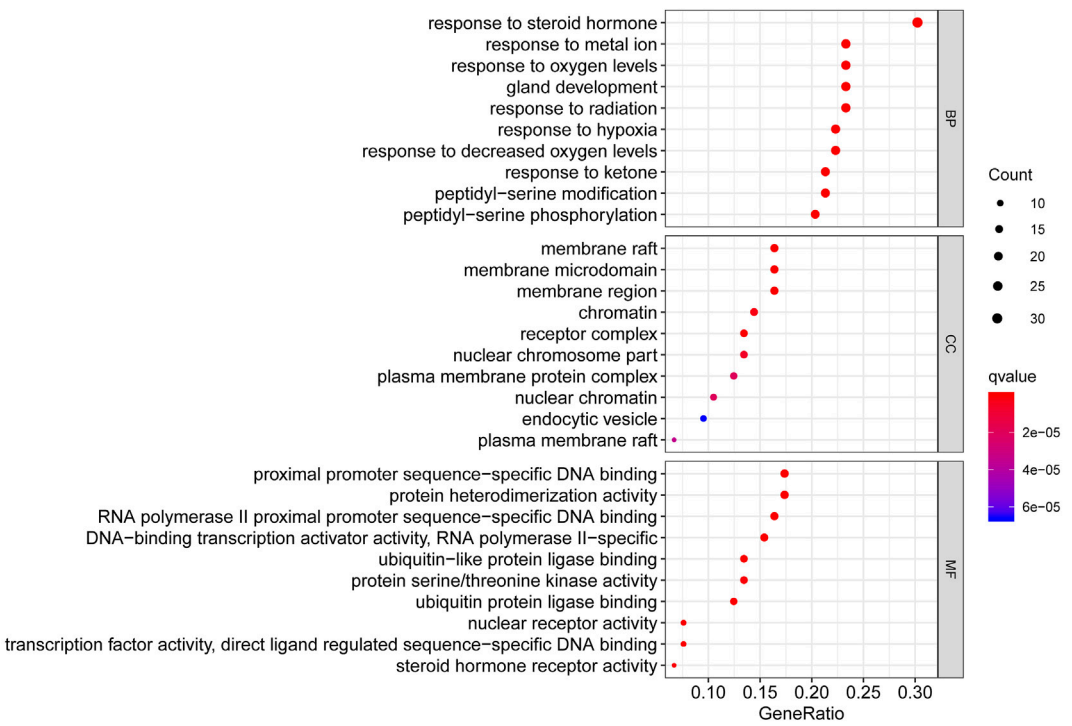

FIGURE 2 | The top 10 pathways for the GO enrichment analysis based on the common targets of the Jian-Pi-Yi-Shen formula (JPYSF) and epithelial–mesenchymal transition (EMT).

closeness centrality value was 0.3365. In the network, the nodes with the topological parameters above the average degree, betweenness centrality, and closeness centrality of the C-T-S network were the core targets and the core chemicals of JPYSF in the treatment of EMT to relieve renal fibrosis (**Figure 5**). The core targets were NCOA2, HSP90AA1, PTGS1, PRKACA, ESR1, GSK3B, PPARG, AR, PRSS1, F2, F10, ACHE, CHRM1, DPP4, NCOA1, RELA, CHRM3, ESR2, CCND1, F7, CHRM2, BCL2, and CHRNA7. Core molecules included quercetin (MOL000098), kaempferol (MOL000422), luteolin (MOL000006), naringenin

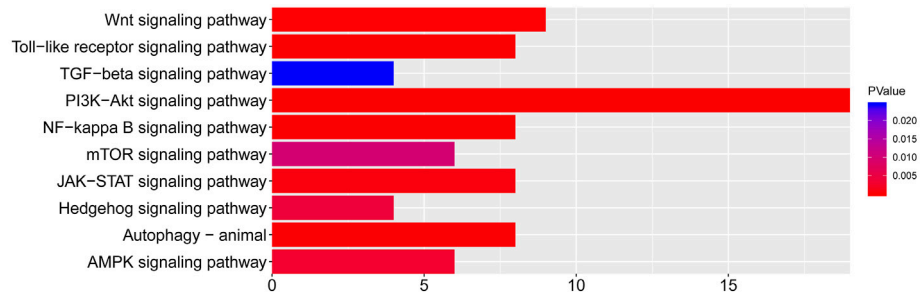

FIGURE 3 | The top 10 pathways for the KEGG pathway are enriched from the common targets between JPYSF and epithelial–mesenchymal transition (EMT).

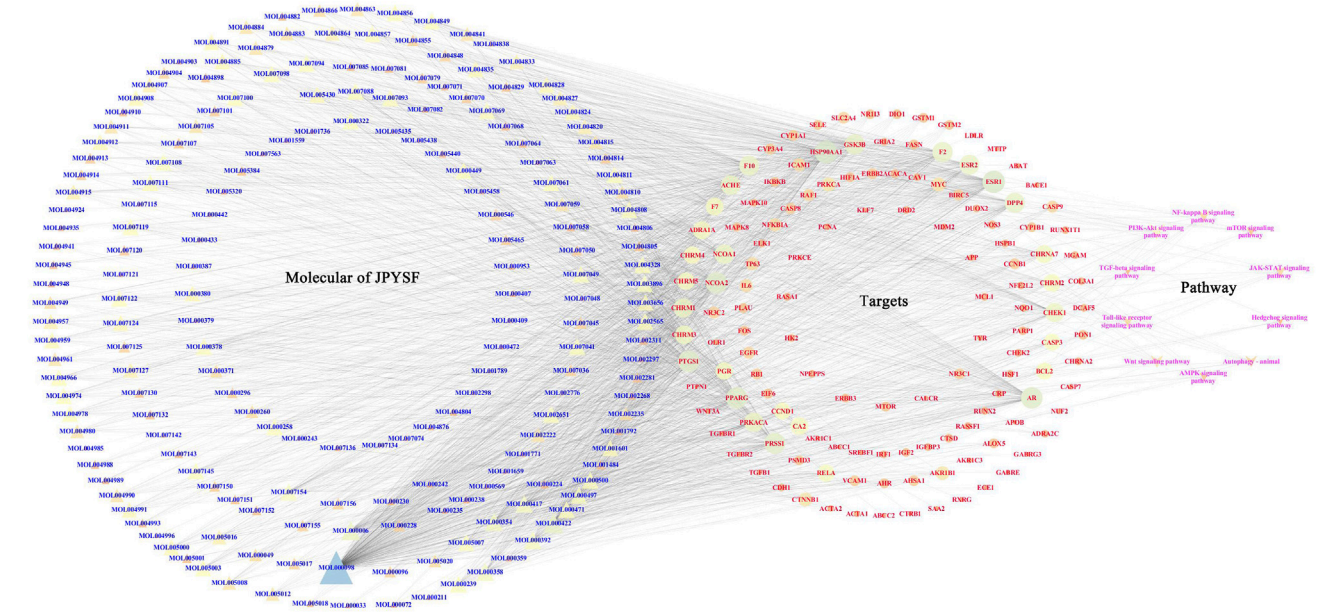

FIGURE 4 | The "chemicals-shared target genes-signal pathway "(C-T-S) network. The blue fonts represent the components of JPYSF, the red fonts represent the targets of JPYSF components and epithelial–mesenchymal transition (EMT), and the rose fonts represent the signaling pathway.

(MOL004328), isorhamnetin (MOL000354), Tanshinone IIA(MOL007154), aloe-emodin (MOL000471), stigmasterol (MOL000449), beta-sitosterol (MOL000358), salviolone (MOL007145), cryptotanshinone (MOL007088), licochalcone A(MOL000497), 7-O-methylisomucronulatol (MOL000378), kadsurenone (MOL000322), miltionone I(MOL007119), 4-methylenemiltirone (MOL007049), and medicarpin (MOL002565).

Jian-Pi-Yi-Shen Formula Administration Significantly Reduced Epithelial–Mesenchymal Transition by Inhibiting the Wnt3a/β-Catenin Pathway in Renal Fibrosis of 5/6 Nx Rats

As shown in **Figures 6A,B**, 5/6 Nx rats showed obvious interstitial fibrosis by extensive blue staining of the tubulointerstitial area, which was 6 times that of the sham group in quantitative analysis ($p < 0.001$). Tubular atrophy and interstitial fibrosis in 5/6 Nx rats were significantly ameliorated in both 2.73 g/kg and 10.89 g/kg JPYSF groups.

To investigate whether JPYSF improved kidney fibrosis by restraining EMT, the protein expression of α-SMA and E-cadherin in the kidney tissues of 5/6 Nx rats was detected by western blot. As shown in **Figures 6C,D**, the results indicated that the expression of α-SMA was significantly up-regulated, and E-cadherin was reduced in 5/6 Nx rats compared with the sham group. The expression pattern was reversed by JPYSF administration in 5/6 Nx rats. In both 2.73 and 10.89 g/kg doses of JPYSF groups, the protein expression of α-SMA was decreased than that in the model group; while E-cadherin expression was increased than that in the model group by JPYSF administration at 10.89 g/kg. According to the analysis results of network pharmacology, the highest number of targets was in the Wnt signaling pathway and the most significant *p* value

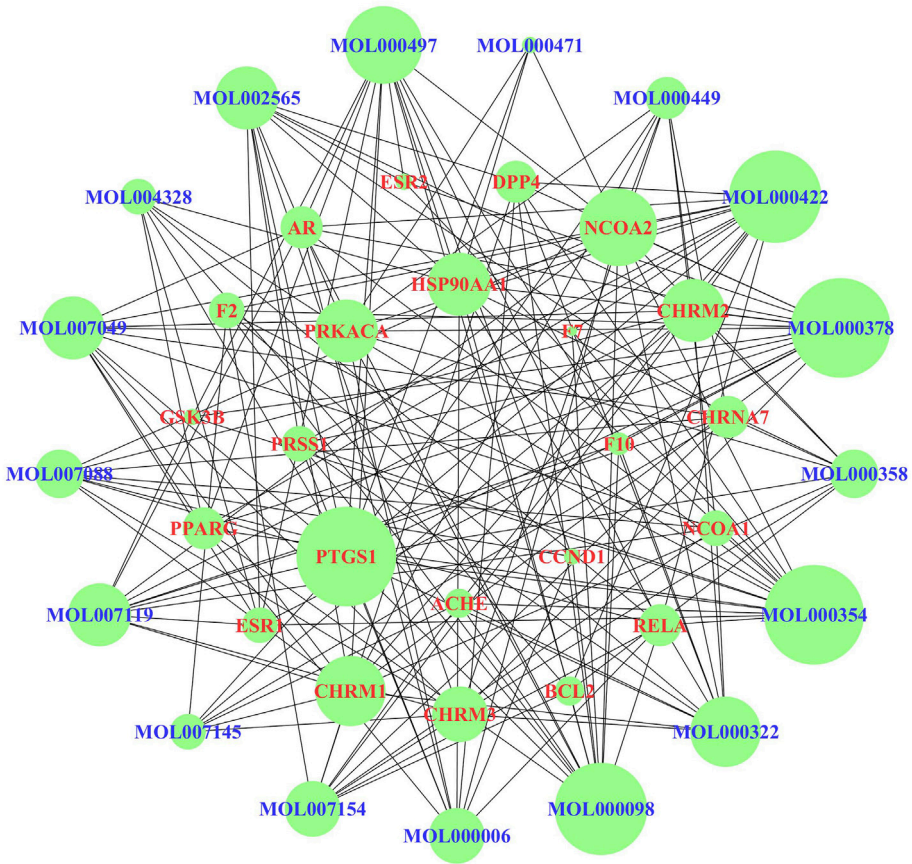

FIGURE 5 | The core targets and compounds in the "chemicals-shared target genes-signal pathway" (C-T-S) network. The nodes with a larger area have a larger degree value.

was in the enriched anti-fibrosis signaling pathway. Therefore, the protein expression of Wnt3a and β-catenin was calculated. The protein levels of both Wnt3a and β-catenin were increased in the model group than those in the sham group, and the changes were significantly reversed by the JPYSF treatment. The western blot results showed that JPYSF administration significantly alleviated EMT by inhibiting the Wnt3a/β-catenin pathway.

DISCUSSION

JPYSF, a classic prescription of hospital preparations, has been used clinically to treat renal fibrosis as an effective and safe TCM. Previous studies confirmed that JPYSF significantly decreased fibrotic area to ameliorate interstitial fibrosis and down-regulated fibrosis-associated protein expression such as fibronectin and type IV collagen in 5/6 Nx rats (Liu et al., 2018; Lu et al., 2018; Chen et al., 2019). These results indicated that JPYSF could inhibit EMT, one of the main mechanisms of renal fibrosis. However, the bioactive components and multi-target mechanisms of JPYSF on EMT have not yet been fully studied. It is therefore of great importance to comprehensively investigate the pharmacological mechanisms of JPYSF on EMT to alleviate renal fibrosis.

First, network pharmacology was employed to explore the potential active ingredients and targets of JPYSF. Second, the common targets were the intersection targets between the potential targets of JPYSF and EMT-associated targets, and then they were identified to build a protein interaction network. According to the string database, the top 30 targets with action frequency are shown in **Figure 1C**. Some genes, such as HSP90AA1 and RELA have been associated with the pathogenesis of EMT. Studies have found that HSP90AA1 exhibited anti-hepatic fibrosis effects in LX-2 cells (Chen CH. et al., 2021), and EMT was reported to be suppressed by RELA/p65 through integrin-mediated signaling (Roupakia et al., 2021). Third, the GO functional and KEGG enrichment analyses were carried out to further understand the mechanism of JPYSF. The enrichment analysis results predicted that the therapeutic effects of JPYSF against EMT might be involved in anti-fibrosis (the Wnt signaling pathway, the JAK-STAT signaling pathway, the Hedgehog signaling pathway, and the TGF-beta signaling pathway), anti-inflammation (the PI3K-Akt signaling pathway, the NF-kappa B signaling pathway, and the Toll-like receptor signaling pathway), podocyte protection (the Autophagy–animal and the mTOR signaling pathway), and metabolism regulation (the AMPK signaling pathway). In accordance with previous

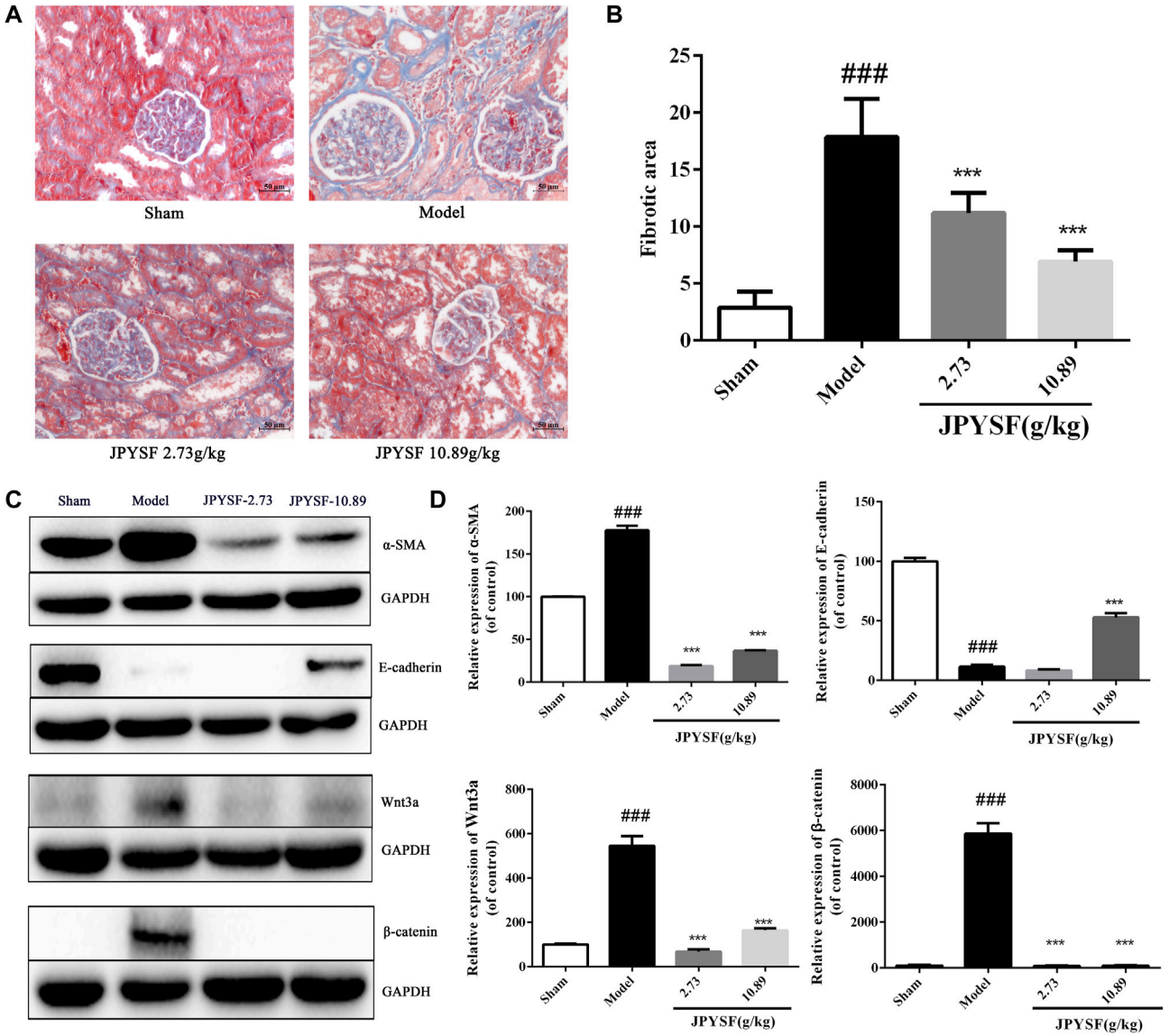

FIGURE 6 | JPYSF administration significantly reduces renal fibrosis by alleviating EMT in 5/6 nephrectomy (Nx) rats. **(A)** Representative images of renal tissue are shown by Masson staining from the sham group, model group, the JPYSF 2.73 g/kg group, and the JPYSF 10.89 g/kg group (200×). **(B)** Quantitative analysis of the fibrotic area. Data were presented as the mean ± SEM, $n = 10$ rats per group ($^{###}$, $p < 0.001$, compared with the sham group; ***,$p < 0.001$, compared with the model group). **(C)** Relative protein expression of α-SMA, E-cadherin, Wnt3a, and β-catenin in the kidney cortex tissues of the sham, model, 2.73, and 10.89 g/kg Jian-Pi-Yi-Shen formula (JPYSF) groups by western blot analysis. Representative bands show the relative expression of α-SMA, E-cadherin, Wnt3a, and β-catenin. **(D)** Quantitative analysis of protein expressions of α-SMA, E-cadherin, Wnt3a, and β-catenin by densitometry based on western blot images. $^{###}$, $p < 0.001$, compared with the Sham group; ***, $p < 0.001$, compared with the model group.

studies, these results indicated that the above pathways had important effects on the progression and advancement of EMT. Among them, the Wnt/β-catenin pathway is the best researched anti-fibrosis pathway related to EMT (ChenQ et al., 2021; Gao, et al., 2020). Therefore, the Wnt/β-catenin pathway may play a crucial role in JPYSF against EMT. Other anti-fibrosis signal pathways were also reported in the EMT process. For instance, EMT and glomerulosclerosis in rats with chronic kidney disease were suppressed by JAK/STAT signaling pathway (Zhao et al., 2019), and cyclosporine-A-induced renal fibrosis was ameliorated by chrysin by the inhibition of TGF-beta-induced EMT (Nagavally et al., 2021). In addition, the PI3K-Akt signaling pathway, a major regulator of anti-inflammation, has been reported to prevent renal fibrosis by attenuating renal tubular epithelial cell–mesenchymal transition (Hu et al., 2021; Zhang Q et al., 2020; Wang et al., 2019). In line with this, JPYSF inhibited the inflammation via suppression of the NF–kappa B signaling pathway (Lu et al., 2018). Then, the network of CTS and core CTS

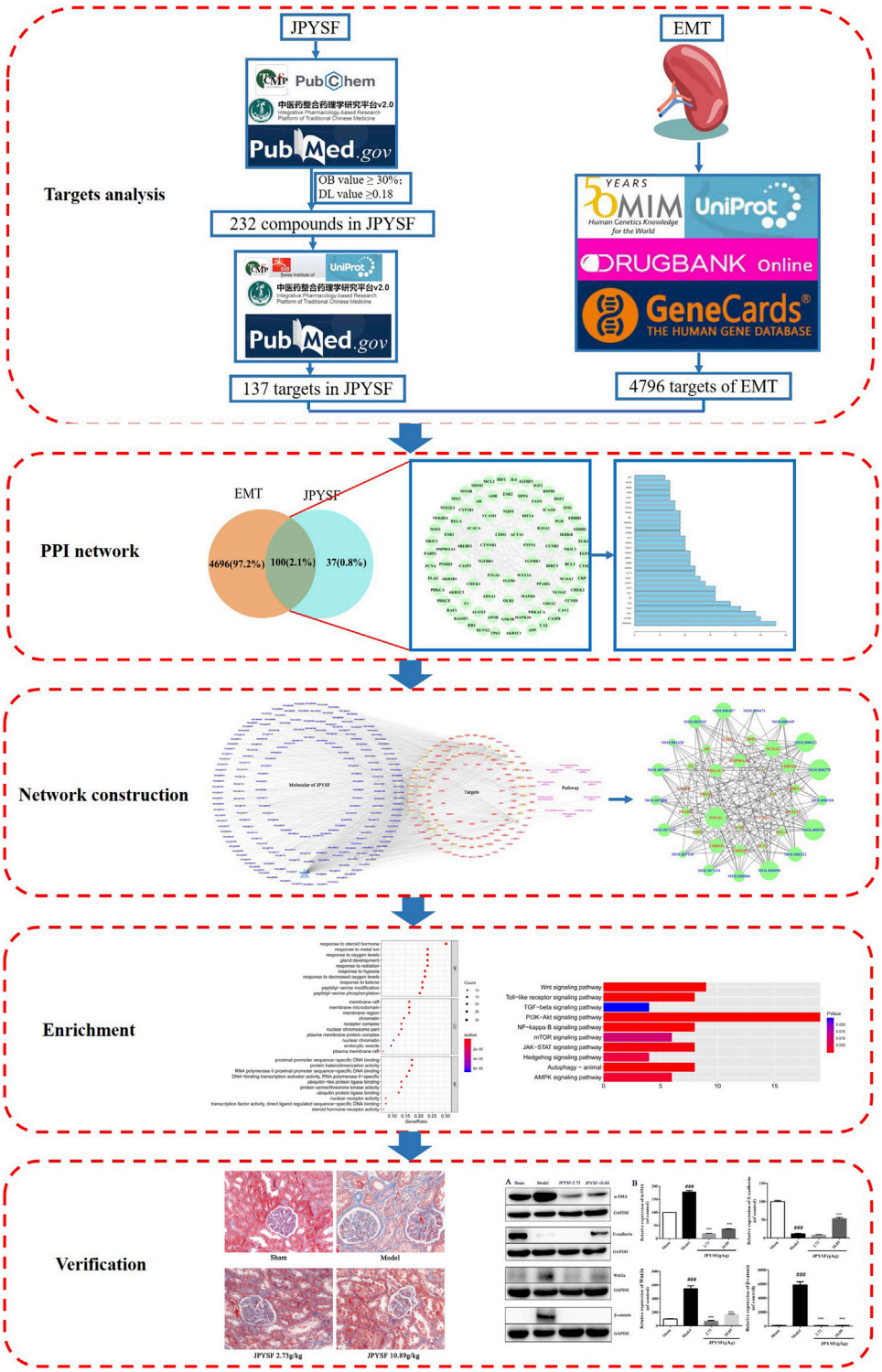

FIGURE 7 | The workflow of the system's pharmacology analysis and experimental verification of Jian-Pi-Yi-Shen formula (JPYSF) in suppressing epithelial–mesenchymal transition (EMT).

were performed to comprehensively predict the core compounds, target genes, and mechanism of JPYSF on EMT, as shown in **Figures 4**, **5**. Degree centrality is the most direct and important parameter of the node among the three topological characteristic parameters. The node with a greater degree is more important in the network. The closeness between a node and other nodes in the network was reflected by closeness centrality. The node that is closer to other nodes has greater proximity centrality. Between centrality means the number of shortest paths through a node. The results of the topological analysis of the C-T-S network showed that 17 core components and 23 core targets had higher values than the average degree centrality value, closeness centrality value, and between centrality value. All the compounds that might participate in the regulatory processes of JPYSF in EMT were considered as potential active ingredients. In support of this, several previous studies have shown that quercetin (Elumalai et al., 2021), kaempferol (Ji et al., 2020), luteolin (Cao et al., 2020), naringenin (Li et al., 2021), isorhamnetin, Tanshinone IIA (Fu et al., 2021), cryptotanshinone (Zhang Z et al., 2020), and aloe-emodin (Liu et al., 2021) had well-established roles in EMT. Taken together, our results demonstrate that the core components may be the effective ingredients of JPYSF for the EMT treatment.

Finally, the 5/6 Nx-induced renal fibrosis rat model was selected to evaluate the therapeutic effects of JPYSF on EMT to verify the network pharmacology prediction. As expected, JPYSF treatment significantly ameliorated interstitial fibrosis in 5/6 Nx rats by Masson staining analysis (**Figure 6**). In our previous studies, we have reported that JPYSF notably reduced the expression levels of fibronectin and type IV collagen by immunofluorescence analysis in renal fibrosis of 5/6 Nx rats (Liu et al., 2018). We, therefore, expect a similar outcome that the other markers of fibrosis can be identified. Furthermore, α-SMA, a mesenchymal cytoskeletal marker, and E-cadherin, an intercellular epithelial adhesion molecule, were selected to assess whether JPYFS had a modulating effect on EMT. The Wnt/β-catenin pathway, the best-enriched anti-fibrosis pathway related to EMT, was chosen to test the predicted molecular mechanisms and verify the accuracy of network pharmacology prediction. Consistently, the western blot analysis detected that JPYSF markedly up-regulated expressions of E-cadherin, Wnt3a, and β-catenin, and down-regulated expression of α-SMA in 5/6 Nx rats. In agreement with this, our previous studies have reported that JPYSF notably reduced the increased levels of fibronectin and type IV collagen in renal fibrosis of 5/6 Nx rats (Liu et al., 2018). Moreover, it has been reported that astragaloside IV up-regulates the decreased expressions of E-cadherin and occludin, whereas it down-regulates expressions of N-cadherin and vimentin in high glucose-induced EMT cells (Wang YN et al., 2020). Therefore, we assume that JPYSF could regulate other epithelial markers and mesenchymal markers. To support this notion, astragaloside IV, which is an active ingredient from *A. mongholicus*, is considered as the monarch drug, the ingredient that provides the principal curative action on the main syndrome in JPYS prescription and has also been identified within JPYSF by HPLC-MS analysis in the current study (**Supplementary Figure S1**). Since most of the EMT markers are cell- and drug-treatment-specific, checking the expression of EMT markers in the specific context by JPYSF would be the future potential work. Collectively, these results provide evidence that JPYSF could regulate EMT by inhibiting the Wnt3a/β-catenin pathway.

However, there were some limitations of research, such as the core compound with no effective dose, which still needed further experiments to identify. Moreover, the direct regulatory relationship of JPYSF in EMT and the Wnt3a/β-catenin pathway by gene knockout animal experiments and cell experiments would be our future potential work for a better understanding of this signaling pathway.

CONCLUSIONS

In this research, a combining approach of systematic network pharmacology and experimental verification were employed to determine therapeutic targets and pharmacological mechanisms of a complex herbal formulation, JPYSF, against EMT. The results suggested that 17 core compounds such as quercetin, kaempferol, luteolin, naringenin, and 23 core targets such as NCOA2, HSP90AA1, and PTGS1 might play an important role in JPYSF-treated renal fibrosis. The multi-target synergetic mechanisms of JPYSF in EMT mainly consist of four therapeutic aspects including anti-fibrosis, anti-inflammation, podocyte protection, and metabolism regulation. *In vivo* experiment data showed that JPYSF significantly ameliorated interstitial fibrosis by Masson staining and exerted the regulation of EMT by inhibiting the Wnt3a/β-catenin pathway (**Figure 6**). In summary, our study provides a basis and guidance for JPYSF research and its clinical application in the treatment of EMT, offering insights into the multi-target mechanisms by the system's pharmacology approach (**Figure 7**).

DATA AVAILABILITY STATEMENT

The original contributions presented in the study are included in the article/**Supplementary Material**, further inquiries can be directed to the corresponding author.

ETHICS STATEMENT

The animal study was reviewed and approved by the Guangzhou University of Chinese Medicine.

AUTHOR CONTRIBUTIONS

YZ conceived and designed the experiments; XL undertook the network pharmacology analysis. FW and SH conducted the animal experimental and Masson's trichrome stains of the

kidneys; YZ performed the western blot experiment and drafted the manuscript; HD assisted in finding the literature when writing the first draft of the article. JC and SL designed the experiments and provided revisions and comments to the manuscript. All authors reviewed and approved the final manuscript.

FUNDING

This study was primarily supported by the Natural Science Foundation of China (81804052, 82004248), the Traditional Chinese Medicine Bureau of Guangdong Province (20201320), the Sanming Project of Medicine in Shenzhen (SZZYSM202111002), and the Shenzhen Science and Technology Plan Project (JSGG20191129102216637).

SUPPLEMENTARY MATERIAL

The Supplementary Material for this article can be found online at: https://www.frontiersin.org/articles/10.3389/fphar.2022.873023/full#supplementary-material

Supplementary Figure S1 | HPLC-MS chromatograms of JPYSF extract. The notations are as follows: 1: Acteoside; 2: Calycosin 7-O-glucoside; 3: Liquiritin; 4: Rosmarinic acid; 5: Salvianolic acid A; 6: Calycosin; 7: Astragaloside IV; 8: Formononetin; 9: Rhein; 10: Dioscin; 11: Atractylenolide I; 12: Tanshinone IIA.

REFERENCES

Amberger, J. S., Bocchini, C. A., Scott, A. F., and Hamosh, A. (2019). OMIM.org: Leveraging Knowledge across Phenotype-Gene Relationships. *Nucleic Acids Res.* 47 (D1), D1038–D1043. doi:10.1093/nar/gky1151

Cao, D., Zhu, G. Y., Lu, Y., Yang, A., Chen, D., Huang, H. J., et al. (2020). Luteolin Suppresses Epithelial-Mesenchymal Transition and Migration of Triple-Negative Breast Cancer Cells by Inhibiting YAP/TAZ Activity. *Biomed. Pharmacother.* 129, 110462. doi:10.1016/j.biopha.2020.110462

Chen, C. H., Ke, G. M., Lin, P. C., and Lin, K. D. (2021). Therapeutic DNA Vaccine Encoding CEMIP (KIAA1199) Ameliorates Kidney Fibrosis in Obesity through Inhibiting the Wnt/β-Catenin Pathway. *Biochim. Biophys. Acta Gen. Subj.* 1865 (12), 130019. doi:10.1016/j.bbagen.2021.130019

Chen, J., Wang, F., Huang, S., Liu, X., Li, Z., Qi, A., et al. (2019). Jian-Pi-Yi-Shen Decoction Relieves Renal Anemia in 5/6 Nephrectomized Rats: Production of Erythropoietin via Hypoxia-Inducible Factor Signaling. *Evid. Based. Complement. Alternat. Med.* 2019, 2807926. doi:10.1155/2019/2807926

Chen, Q., Wang, Y., Ma, F., Han, M., Wang, Z., Xue, P., et al. (2021). Systematic Profiling of the Effective Ingredients and Mechanism of Scabiosa Comosa and S. Tschilliensis against Hepatic Fibrosis Combined with Network Pharmacology. *Sci. Rep.* 11 (1), 2600. doi:10.1038/s41598-021-81399-x

Elumalai, P., Ezhilarasan, D., and Raghunandhakumar, S. (2021). Quercetin Inhibits the Epithelial to Mesenchymal Transition through Suppressing Akt Mediated Nuclear Translocation of β-Catenin in Lung Cancer Cell Line. *Nutr. Cancer*, 1–13. doi:10.1080/01635581.2021.1957487

Fu, J., Wang, Z., Huang, L., Zheng, S., Wang, D., Chen, S., et al. (2014). Review of the Botanical Characteristics, Phytochemistry, and Pharmacology of Astragalus Membranaceus (Huangqi). *Phytother Res.* 28 (9), 1275–1283. doi:10.1002/ptr.5188

Fu, K., Shao, L., Mei, L., Li, H., Feng, Y., Tian, W., et al. (2021). Tanshinone ⅡA Inhibits the Lipopolysaccharide-Induced Epithelial-Mesenchymal Transition and Protects Bovine Endometrial Epithelial Cells from Pyolysin-Induced Damage by Modulating the NF-κB/Snail2 Signaling Pathway. *Theriogenology* 176, 217–224. doi:10.1016/j.theriogenology.2021.10.001

Gao, F., Zhang, Y., Yang, Z., Wang, M., Zhou, Z., Zhang, W., et al. (2020). Arctigenin Suppressed Epithelial-Mesenchymal Transition through Wnt3a/β-Catenin Pathway in PQ-Induced Pulmonary Fibrosis. *Front. Pharmacol.* 11, 584098. doi:10.3389/fphar.2020.584098

Hu, S., Hu, H., Wang, R., He, H., and Shui, H. (2021). microRNA-29b Prevents Renal Fibrosis by Attenuating Renal Tubular Epithelial Cell-Mesenchymal Transition through Targeting the PI3K/AKT Pathway. *Int. Urol. Nephrol.* 53 (9), 1941–1950. doi:10.1007/s11255-021-02836-4

Ji, X., Cao, J., Zhang, L., Zhang, Z., Shuai, W., and Yin, W. (2020). Kaempferol Protects Renal Fibrosis through Activating the BMP-7-Smad1/5 Signaling Pathway. *Biol. Pharm. Bull.* 43 (3), 533–539. doi:10.1248/bpb.b19-01010

Li, Q., Liu, S., Yang, G., Li, M., Qiao, P., and Xue, Q. (2021). Naringenin Inhibits Autophagy and Epithelial-mesenchymal Transition of Human Lens Epithelial Cells by Regulating the Smad2/3 Pathway. *Drug Dev. Res.*, 1–8. doi:10.1002/ddr.21868

Liu, W., Gu, R., Lou, Y., He, C., Zhang, Q., and Li, D. (2021). Emodin-induced Autophagic Cell Death Hinders Epithelial-Mesenchymal Transition via Regulation of BMP-7/tgf-B1 in Renal Fibrosis. *J. Pharmacol. Sci.* 146 (4), 216–225. doi:10.1016/j.jphs.2021.03.009

Liu, X., Chen, J., Liu, X., Wang, D., Zheng, P., Qi, A., et al. (2018). Jian-Pi-Yi-Shen Formula Ameliorates Chronic Kidney Disease: Involvement of Mitochondrial Quality Control Network. *BMC Complement. Altern. Med.* 18 (1), 340. doi:10.1186/s12906-018-2395-2

Lu, J., Liu, X., Liao, Y., Wang, D., Chen, J., and Li, S. (2018). Jian-Pi-Yi-Shen Formula Regulates Inflammatory Cytokines Production in 5/6 Nephrectomized Rats via Suppression of NF-Kb Activation. *Evid. Based. Complement. Alternat. Med.* 2018, 7203547. doi:10.1155/2018/7203547

Mei, X. D., Cao, Y. F., Che, Y. Y., Li, J., Shang, Z. P., Zhao, W. J., et al. (2019). Danshen: a Phytochemical and Pharmacological Overview. *Chin. J. Nat. Med.* 17 (1), 59–80. doi:10.1016/S1875-5364(19)30010-X

Nagavally, R. R., Sunilkumar, S., Akhtar, M., Trombetta, L. D., and Ford, S. M. (2021). Chrysin Ameliorates Cyclosporine-A-Induced Renal Fibrosis by Inhibiting TGF-B1-Induced Epithelial-Mesenchymal Transition. *Int. J. Mol. Sci.* 22 (19), 10252. doi:10.3390/ijms221910252

Pei, L., Shen, X., Qu, K., Tan, C., Zou, J., Wang, Y., et al. (2020). Exploration of the Two-Way Adjustment Mechanism of Rhei Radix et Rhizoma for Cardiovascular Diseases. *Comb. Chem. High Throughput Screen.* 23 (10), 1100–1112. doi:10.2174/1386207323666200521120308

Roupakia, E., Chavdoula, E., Karpathiou, G., Vatsellas, G., Chatzopoulos, D., Mela, A., et al. (2021). Canonical NF-Kb Promotes Lung Epithelial Cell Tumour Growth by Downregulating the Metastasis Suppressor CD82 and Enhancing Epithelial-To-Mesenchymal Cell Transition. *Cancers (Basel)* 13 (17), 4302. doi:10.3390/cancers13174302

Su, Z., Zeng, K., Feng, B., Tang, L., Sun, C., Wang, X., et al. (2021). Kun-Dan Decoction Ameliorates Insulin Resistance by Activating AMPK/mTOR-Mediated Autophagy in High-Fat Diet-Fed Rats. *Front. Pharmacol.* 12, 670151. doi:10.3389/fphar.2021.670151

Wang, F., Huang, S., Chen, Q., Hu, Z., Li, Z., Zheng, P., et al. (2020). Chemical Characterisation and Quantification of the Major Constituents in the Chinese Herbal Formula Jian-Pi-Yi-Shen Pill by UPLC-Q-TOF-MS/MS and HPLC-QQQ-MS/MS. *Phytochem. Anal.* 31 (6), 915–929. doi:10.1002/pca.2963

Wang, J., Zhu, H., Huang, L., Zhu, X., Sha, J., Li, G., et al. (2019). Nrf2 Signaling Attenuates Epithelial-To-Mesenchymal Transition and Renal Interstitial Fibrosis via PI3K/Akt Signaling Pathways. *Exp. Mol. Pathol.* 111, 104296. doi:10.1016/j.yexmp.2019.104296

Wang, Y. N., Zhao, S. L., Su, Y. Y., Feng, J. X., Wang, S., Liao, X. M., et al. (2020). Astragaloside IV Attenuates High Glucose-Induced EMT by Inhibiting the TGF-β/Smad Pathway in Renal Proximal Tubular Epithelial Cells. *Biosci. Rep.* 40 (6), 1–13. doi:10.1042/BSR20190987

Xu, H., Wu, T., and Huang, L. (2021). Therapeutic and Delivery Strategies of Phytoconstituents for Renal Fibrosis. *Adv. Drug Deliv. Rev.* 177, 113911. doi:10.1016/j.addr.2021.113911

Xu, H. Y., Zhang, Y. Q., Liu, Z. M., Chen, T., Lv, C. Y., Tang, S. H., et al. (2019). ETCM: an Encyclopaedia of Traditional Chinese Medicine. *Nucleic Acids Res.* 47 (D1), D976–D982. doi:10.1093/nar/gky987

Zhang, J., Zhao, J., Ma, Y., Wang, W., Huang, S., Guo, C., et al. (2021). Investigation of the Multi-Target Mechanism of Guanxin-Shutong Capsule in Cerebrovascular Diseases: A Systems Pharmacology and Experimental Assessment. *Front. Pharmacol.* 12, 650770. doi:10.3389/fphar.2021.650770

Zhang, Q., Gan, C., Liu, H., Wang, L., Li, Y., Tan, Z., et al. (2020). Cryptotanshinone Reverses the Epithelial-Mesenchymal Transformation Process and Attenuates Bleomycin-Induced Pulmonary Fibrosis. *Phytother. Res.* 34 (10), 2685–2696. doi:10.1002/ptr.6699

Zhang, Z., Wu, W., Fang, X., Lu, M., Wu, H., Gao, C., et al. (2020). Sox9 Promotes Renal Tubular Epithelial-mesenchymal Transition and Extracellular Matrix Aggregation via the PI3K/AKT Signaling Pathway. *Mol. Med. Rep.* 22 (5), 4017–4030. doi:10.3892/mmr.2020.11488

Zhao, D., Zhu, X., Jiang, L., Huang, X., Zhang, Y., Wei, X., et al. (2021). Advances in Understanding the Role of Adiponectin in Renal Fibrosis. *Nephrology (Carlton)* 26 (2), 197–203. doi:10.1111/nep.13808

Zhao, S. Q., Shen, Z. C., Gao, B. F., and Han, P. (2019). microRNA-206 Overexpression Inhibits Epithelial-Mesenchymal Transition and Glomerulosclerosis in Rats with Chronic Kidney Disease by JAK/STAT Signaling Pathway. *J. Cel Biochem.* 120 (9), 14604–14617. doi:10.1002/jcb.28722

Zheng, L., Chen, S., Wang, F., Huang, S., Liu, X., Yang, X., et al. (2020). Distinct Responses of Gut Microbiota to Jian-Pi-Yi-Shen Decoction Are Associated with Improved Clinical Outcomes in 5/6 Nephrectomized Rats. *Front. Pharmacol.* 11, 604. doi:10.3389/fphar.2020.00604

Zhong, L. L. D., Zheng, G., Da Ge, L., Lin, C. Y., Huang, T., Zhao, L., et al. (2016). Chinese Herbal Medicine for Constipation: Zheng-Based Associations Among Herbs, Formulae, Proprietary Medicines, and Herb-Drug Interactions. *Chin. Med.* 11, 28. doi:10.1186/s13020-016-0099-4

Conflict of Interest: The authors declare that the research was conducted in the absence of any commercial or financial relationships that could be construed as a potential conflict of interest.

Publisher's Note: All claims expressed in this article are solely those of the authors and do not necessarily represent those of their affiliated organizations, or those of the publisher, the editors, and the reviewers. Any product that may be evaluated in this article, or claim that may be made by its manufacturer, is not guaranteed or endorsed by the publisher.

frontiers | Frontiers in Pharmacology

SYSTEMATIC REVIEW
published: 26 May 2022
doi: 10.3389/fphar.2022.907108

Recent Advances in Clinical Diagnosis and Pharmacotherapy Options of Membranous Nephropathy

Yan-Ni Wang[1], Hao-Yu Feng[1], Xin Nie[1], Ya-Mei Zhang[2], Liang Zou[3], Xia Li[1,4], Xiao-Yong Yu[5]* and Ying-Yong Zhao[1]**

[1]Faculty of Life Science & Medicine, Northwest University, Xi'an, China, [2]Key Disciplines of Clinical Pharmacy, Clinical Genetics Laboratory, Affiliated Hospital and Clinical Medical College of Chengdu University, Chengdu, China, [3]School of Food and Bioengineering, Chengdu University, Chengdu, China, [4]Department of General Practice, Xi'an International Medical Center Hospital, Northwest University, Xi'an, China, [5]Department of Nephrology, Shaanxi Traditional Chinese Medicine Hospital, Xi'an, China

OPEN ACCESS

Edited by:
Zhiyong Guo, Second Military Medical University, China

Reviewed by:
Liu Baoli, Capital Medical University, China
Yuan Li, Affiliated Hospital of Nantong University, China

***Correspondence:**
Xia Li
lixia.1966@163.com
Xiao-Yong Yu
gub70725@126.com
Ying-Yong Zhao
Zhaoyybr@163.com

Specialty section:
This article was submitted to Renal Pharmacology, a section of the journal Frontiers in Pharmacology

Received: *29 March 2022*
Accepted: *25 April 2022*
Published: *26 May 2022*

Citation:
Wang Y-N, Feng H-Y, Nie X, Zhang Y-M, Zou L, Li X, Yu X-Y and Zhao Y-Y (2022) Recent Advances in Clinical Diagnosis and Pharmacotherapy Options of Membranous Nephropathy. Front. Pharmacol. 13:907108. doi: 10.3389/fphar.2022.907108

Membranous nephropathy (MN) is the most common cause of nephrotic syndrome among adults, which is the leading glomerular disease that recurs after kidney transplantation. Treatment for MN remained controversial and challenging, partly owing to absence of sensitive and specific biomarkers and effective therapy for prediction and diagnosis of disease activity. MN starts with the formation and deposition of circulating immune complexes on the outer area in the glomerular basement membrane, leading to complement activation. The identification of autoantibodies against the phospholipase A_2 receptor (PLA_2R) and thrombospondin type-1 domain-containing protein 7A (THSD7A) antigens illuminated a distinct pathophysiological rationale for MN treatments. Nowadays, detection of serum anti-PLA_2R antibodies and deposited glomerular PLA_2R antigen can be routinely applied to MN. Anti-PLA_2R antibodies exhibited much high specificity and sensitivity. Measurement of PLA_2R in immune complex deposition allows for the diagnosis of PLA_2R-associated MN in patients with renal biopsies. In the review, we critically summarized newer diagnosis biomarkers including PLA_2R and THSD7A tests and novel promising therapies by using traditional Chinese medicines such as *Astragalus membranaceus*, *Tripterygium wilfordii*, and Astragaloside IV for the treatment of MN patients. We also described unresolved questions and future challenges to reveal the diagnosis and treatments of MN. These unprecedented breakthroughs were quickly translated to clinical diagnosis and management. Considerable advances of detection methods played a critical role in diagnosis and monitoring of treatment.

Keywords: chronic kidney disease, idiopathic membranous nephropathy, membranous nephropathy, traditional Chinese medicine, *Astragalus membranaceus*, *Tripterygium wilfordii*, Astragaloside IV, Shenqi particle

Abbreviation: CBSA, cationic bovine serum albumin; CKD, chronic kidney disease; ELISA, enzyme-linked immunosorbent assay; GBM, glomerular basement membrane; IMN, idiopathic membranous nephropathy; MN, membranous nephropathy; NEP, neutral endopeptidase; NF-κB, nuclear factor-κB; PLA_2R, M-type phospholipase A_2 receptor; THSD7A, thrombospondin type-1 domain-containing protein 7A.

1 INTRODUCTION

Membranous nephropathy (MN) is one of the most common causes of formation of nephrotic syndrome in adults, accounting for 30% incidence of patients (1.7/100000/year), with a 67% male preponderance and a high incidence in humans aged 30–50 years (Bally et al., 2016). It is unwonted in children (Liu et al., 2020a; Tamura, 2021). MN mainly affects renal glomerulus, particularly podocytes in glomerulus, indicating that podocytes play a critical role in regulating renal permeability to various molecules including proteins (Ronco and Debiec, 2020). In healthy individuals, albumin and macromolecule proteins are not filtered, while in a milieu called nephrotic syndrome, many proteins are leaked and excreted through urine, leading to a reduction in serum albumin and generalized edema development (Ronco and Debiec, 2020; Medina Rangel et al., 2021).

This condition can be "primary" or "idiopathic" for patients that did not present disease association (70–80% of patients), or for patients that present disease association, such as infections, lupus erythematosus, malignancy, or drug toxicity (Moroni and Ponticelli, 2020; Cravedi et al., 2019). Exogenous antigens may pass *via* the glomerular basement membrane (GBM), become planted under the podocyte surface layer, and following the combination with circulating antibodies (Cravedi et al., 2019) (**Figure 1**). Circulating immune complexes separate and reform in the subepithelial space (Moroni and Ponticelli, 2020). Idiopathic membranous nephropathy (IMN) is a kidney-specific non-inflammatory autoimmune disease, and circulating autoantibodies bind to autoantigens on the podocyte surface layer (Moszczuk et al., 2021). About 40% of IMN patients could suffer spontaneous remission. However, the rest of 30% showed a poor outcome to immunosuppressive treatment and finally reached end-stage renal disease treated by dialysis and transplantation (Tesar and Hruskova, 2021; Passerini et al., 2019; Xipell et al., 2018; Molina Andújar et al., 2022; da Silva et al., 2018), which were two leading therapies for patients with end-stage renal disease (Zhang et al., 2020a; Sawhney and Gill, 2020; Wu et al., 2021a; Bacharaki et al., 2021; Chang et al., 2021; Chuengsaman et al., 2021; Gambino et al., 2021). Approximately, 40% patients accept kidney grafts

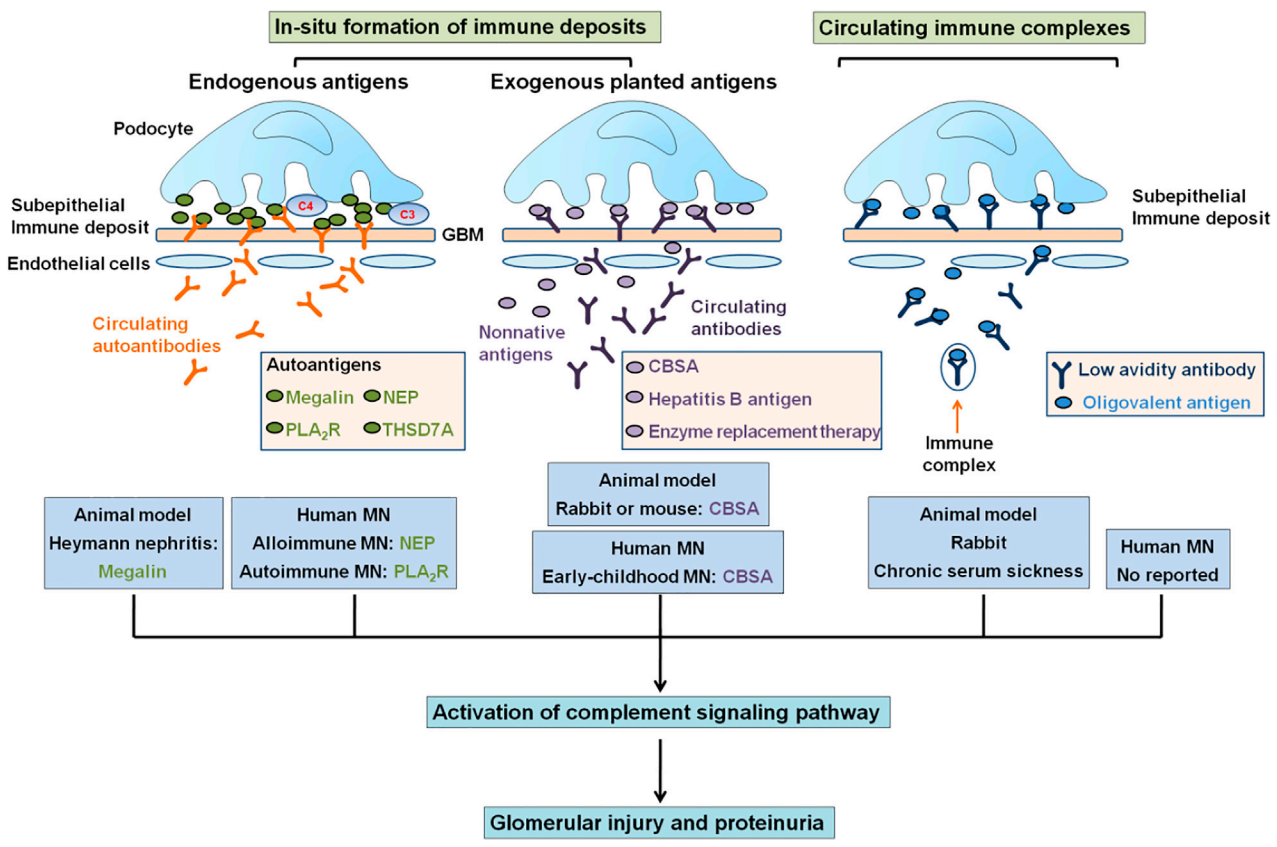

FIGURE 1 | Mechanisms of formation of subepithelial immune complex deposits. The depositions of subepithelial immune complexes might form either *in situ* immune complexes or circulating immune complexes that contained circulating antibodies binding to endogenous antigens (megalin, NEP, PLA_2R, and THSD7A) in podocytes or to exogenous antigens (CBSA, hepatitis B antigen, and enzyme replacement therapy) planted in GBM. In total, four endogenous antigenic targets have been identified, including megalin in Heymann nephritis, NEP in alloimmune neonatal MN, and PLA_2R and THSD7A in IMN. In total, four circulating exogenous antibodies can target surface-exposed intrinsic podocyte antigens to cause capping and shedding of *in situ* antigen–antibody complex into underlying GBM. CBSA, enzyme from enzyme replacement therapy, and hepatitis B antigen may traverse GBM and bind under podocyte as planted antigens and also as target for circulating antibodies. In addition, circulating immune complexes deposited in the subepithelial region.

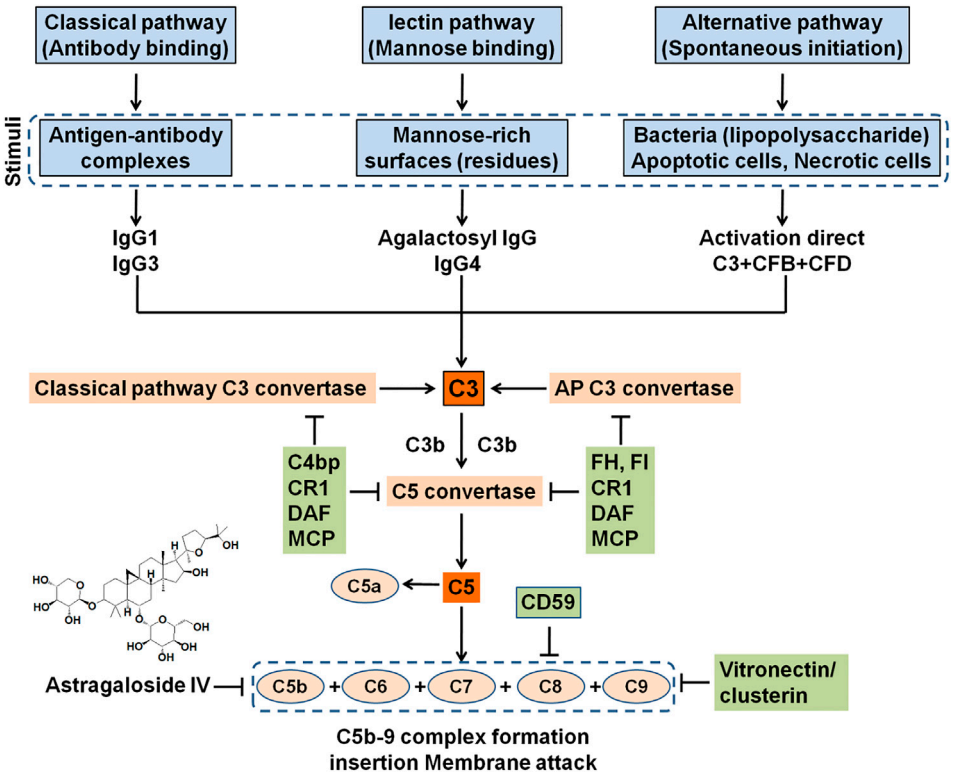

FIGURE 2 | Activation of complement system-induced formation of MAC (C5b-9). Complement could be activated by three pathways including classical, lectin, and alternative signaling pathways, which came together toward production of C5 convertase and formation of C5b that bound to C6, C7, C8, and multiple C9 to generate the MAC. This process could be mostly inhibited by circulating inhibitors, podocyte-positive regulatory proteins, and natural products such as Astragaloside IV. However, this inhibitory effect might be devastated at high levels of complement. MAC could insert into the podocyte membrane, even in sublytic quantity, evoked cell injury under a lack of inflammation condition.

that lead to recurrence, and about 45% patients lose the graft (Passerini et al., 2019; Robson and Kitching, 2021; Uffing et al., 2021). Treatment with costly drugs and potential adverse effects of drugs remain challenging (Gauckler et al., 2021). The most important points of precision therapy are the discovery of the accurate etiology and pathogenesis in IMN.

The feature of IMN is immune complex deposition along the subepithelial region of GBM, which leads to a membrane-like thickening of GBM (Liu et al., 2020b; Gu et al., 2021) (**Figure 1**). The immune complexes are composed of several components, such as IgG4, antigens that are eluded, and membrane attack complex, which is formed by complement components to produce C5b–9 (Gu et al., 2021; Hu et al., 2021) (**Figure 2**). IgG4 is the most main IgG subclass deposited in IMN, although altered IgG1 is also involved in the deposited immune complexes, IgG1-3 exceeds IgG4 deposition in secondary MN patients (Lönnbro-Widgren et al., 2015; Xu et al., 2020; Ronco et al., 2021). Subepithelial immune complex formation deposits and activation of complement are directly associated with functional lesion of the glomerular capillary wall, which leads to urine protein in absence of inflammatory cells (Xu et al., 2020; Gu et al., 2021) (**Figure 2**).

Based on the natural IMN history, IMN has a classic rule of thirds including one-third patients with spontaneous remission, one-third patients with sustaining proteinuria, and one-third patients with progression of kidney failure (McQuarrie et al., 2012). Although spontaneous remission is a common feature of IMN, IMN causes end-stage renal disease in nearly 40% of patients after 10 years (Ronco et al., 2021). Interventions remain controversial and challenging owing to adverse effect using immunosuppressive treatment, and, apart from proteinuria, few sensitive and reliable biomarkers are used for the prediction of disease activity and outcome because of the fact that antigens targeted by antibodies remain enigmatic (Moszczuk et al., 2021; Tesar and Hruskova, 2021). Taken together, an essential improvement of IMN diagnosis, monitoring, treatment, and prognosis is the elucidation of pathogenic mechanisms.

In the past several decades, important advances have been achieved in the illumination of the mechanisms of molecular pathogenesis of human MN (Gu et al., 2021; Xu et al., 2020). In addition, several latest publications have shown that MN was associated with the dysbiosis of gut microbiota and dysregulation of long non-coding RNAs (Zhang et al., 2020b; Dong et al., 2020; Luan et al., 2022; Jin et al., 2019). These advances were inspired by using animal models of IMN, including Heymann nephritis and cationic bovine serum albumin (CBSA)–induced MN (Jiang et al., 2020). The model of Heymann nephritis put forward the concept

that a podocyte antigen, namely, megalin, was a target of antibody-forming *in situ* immune complexes, whereas CBSA-induced MN first reflected the case of planted antigen (**Figure 1**). Jones (1957) first reported MN as a specific disease entity. Subsequently, the recognition that autoimmune response to antigen-induced MN was first reported in an animal model in 1959. The rats were injected by using extracts from proximal tubular cells that mediated immune complex deposition on the subepithelial capillary wall region in the glomerular that were similar to those found in MN patients, strongly indicated the possibility of an immune-induced pathogenesis mechanism (Heymann et al., 1959). These immunocomplexes included IgG antibody–targeting megalin, which was expressed on both rat podocytes and tubuli (Kerjaschki and Farquhar, 1982), but not on podocytes in human. In humans, progress in MN started in 2002 with the discovery of target antigen, namely, neutral endopeptidase (NEP, also known as neprilysin) as a targeting antigen in baby of a woman with NEP deficiency (Debiec et al., 2002). Anti-NEP alloantibodies was generated by the mother-passed placenta and bound to NEP expressed in fetal podocytes (Debiec et al., 2002), which showed the role of autoantibody in human MN pathogenesis. This result showed the proof of concept that podocyte antigens were associated with human MN, as is the paradigm for megalin in rats, and laid the foundation for the identification of a novel causal antigen M-type phospholipase A_2 receptor (PLA_2R), which is the first podocyte autoantigen identified in human IMN in 2009 (Beck et al., 2009). In 2014, this was followed by the discovery of a second antigen, namely, thrombospondin type-1 domain-containing 7A (THSD7A) in human IMN (Tomas et al., 2014). PLA_2R-related and THSD7A-related MN accounted for about 70% and 1–5% of IMN patients, respectively (Zhang et al., 2021a). A genome-wide association study indicated that single nucleotide polymorphisms in the *PLA_2R* gene were closely related to IMN, which again revealed the involvement of this antigen by using an untargeted genetic approach (Xu et al., 2020; Yoshikawa and Asaba, 2020). Other antigens including aldose reductase, superoxide dismutase-2, and α-enolase were also found in human, although their function remains to be established because they were not detected on normal podocyte surfaces (Prunotto et al., 2010). In addition, endogenous podocyte antigens and exogenous antigens including CBSA were also involved in patients with early-childhood MN (Ayalon and Beck, 2015; Jiang et al., 2020). Taken together, these studies exhibited a new era for the diagnosis, monitoring, and prognosis of MN from early infancy to adulthood. In this article, we summarize the traditional diagnostic method for MN and review recent improvements in diagnostics and the treatment of MN.

2 DIAGNOSIS OF MEMBRANOUS NEPHROPATHY

2.1 Traditional Diagnosis Approach

On the patients with nephrotic syndrome, after diagnosis for secondary causes, a renal biopsy was subsequently performed, which was a gold standard for MN diagnosis. The membranous summarized microscopic characteristic of capillary wall thickening in glomeruli, which led to subepithelial IgG accumulation. Immune complex depositions produced a spiked appearance and formed granular lines. Electron microscopy analysis further confirmed electron-dense subepithelial immune complexes, which were often accompanied by foot process effacement in podocyte. If the diagnosis was established, Kidney Disease: Improving Global Outcomes advised a 6-month observation, as there are many patients of spontaneous remission of MN. However, it takes more than a year to reach spontaneous remission.

2.2 Newer Diagnosis Approach

Renal biopsy is a gold standard in the analysis and detection of the pattern of MN damage. However, standard light and electron microscopic results could not reflect nature of MN (Xie et al., 2020). The distinction between IMN and secondary MN is the main challenge in the diagnosis of MN, in particular malignancy-related MN in patients. It is a common practice to exclude secondary causes of the lesion of MN on the basis of physical examination, pathological analysis, and laboratory examination. An assessment of the immunopathologic features from the biopsy specimen may get discriminative information (Ronco and Debiec, 2015). A sole subepithelial location of the immune complex deposits is typical characteristics of IMN. The deposition of C1q was hardly observed in IMN but could be found in other secondary causes, especially in systemic lupus erythematosus. IgG subclass staining could help to classify MN. The deposits of IgG1, IgG2, and IgG3 usually distribute in secondary MN, while many amounts of IgG4 are characteristic for IMN, indicating the fact that PLA_2R antibody and THSD7A antibody are mostly of the IgG4 subclass.

2.2.1 Phospholipase A_2 Receptor Test for Diagnosis and Monitoring

Although the underlying mechanism of PLA_2R in the pathogenesis of IMN is still unknown, the presence of anti-PLA_2R antibodies is highly specific for IMN (Logt et al., 2021; Nieto-Gañán et al., 2021). A low occurrence of PLA_2R antibodies was found in secondary MN (Porcelli et al., 2021), but in these patients, coincidental occurrence of IMN with related disease might be included. The level of PLA_2R antibodies was detected in patients with other cause-induced nephrotic syndrome or healthy controls (Tomas et al., 2021). Several findings suggest that anti-PLA_2R antibodies were associated with disease activity (Jurubită et al., 2021; Logt et al., 2021).

The commercial immunofluorescent test (Euroimmun, Lübeck, Germany) was applied to diagnosis. Anti-PLA_2R antibodies occurred in serum of 52–86% of MN patients (Hofstra and Wetzels, 2012). Detections by using either Western blot or immunofluorescent approaches, and immunofluorescent tests have a lower sensitivity than the Western blot technique (Hoxha et al., 2017). The studies included patients with different ethnicity, long-standing disease, and treated in remission. It was also reported that initially antibodies against PLA_2R lacked in serum of patients

with PLA_2R-related MN. An earlier study showed 10 patients with PLA_2R antigen staining positive in immune complexes in the renal biopsy specimen from a cohort of 42 patients, with no measurable serum antibodies (Debiec and Ronco, 2011). Subsequent results showed that antibodies against PLA_2R indeed were absent at disease the onset and could be detected during follow-up analysis (Ramachandran et al., 2015; van de Logt et al., 2015). We hypothesized that antibodies combined with antigen of podocytes with high affinity and only be detected when binding sites in renal tissues are saturated (van de Logt et al., 2015). Of note, the same research group also reported three patients with a high circulating concentration of antibodies against PLA_2R who did not have detectable PLA_2R in the glomeruli (Debiec and Ronco, 2011). This phenomenon attracts little attention. The immunofluorescent analysis only allowed semi-quantitative evaluation of antibodies against PLA_2R by dilution steps. The enzyme-linked immunosorbent assay (ELISA) provided a precise quantitation for antibodies against PLA_2R. A commercially available ELISA (Euroimmun) was introduced to clinical practice and widespread application (Dähnrich et al., 2013; Zhu et al., 2022). This ELISA determined total antibodies against PLA_2R IgG. However, PLA_2R antigen was observed in immune deposits in some patients, which suggested rapid clearance of antibodies and deposition in glomeruli. Conversely, determination of circulating antibodies was not always related to the presence of the antigen in the immune complex deposits, which indicated that not all antibodies to PLA_2R are pathogenic. Evaluation of both circulating anti-PLA_2R antibodies and PLA_2R in kidney biopsy could better select patients for accurate therapy. In addition, anti-PLA_2R antibodies showed a high diagnostic ability on IMN for the population with diabetic kidney disease (Wang et al., 2020a).

2.2.2 Thrombospondin Type-1 Domain-Containing Protein 7A Test for Diagnosis and Monitoring

So far, THSD7A antibodies were not detected in healthy individuals or patients with other renal and systemic diseases (Tomas et al., 2014), presenting a 100% specificity for the damage of MN. However, another study has demonstrated that circulating autoantibodies against human podocyte antigen THSD7A was found in 5–10% of MN patients who did not present circulating anti-PLA_2R autoantibodies (Tomas et al., 2014). The percentages of THSD7A-related IMN range from 3% to 9% in Europe and the United States. Notably, in large-scale THSD7A-associated MN patients, a tumor was found from diagnosis of MN (Hoxha et al., 2016). Of note, chemotherapy initiation caused a decreasing THSD7A antibody followed by a reduction of proteinuria (Hoxha et al., 2016). These findings showed that the immune system discerned cancer THSD7A as a foreign antigen mediating THSD7A antibody production, the latter binding to THSD7A on the surface of podocyte *in situ*.

2.2.3 Combined Phospholipase A_2 Receptor and Thrombospondin Type-1 Domain-Containing Protein 7A Test for Diagnosis and Monitoring

It is presently uncertain whether there are patients with dual PLA_2R and THSD7A antibody positivity (Zhang et al., 2021a). When PLA_2R antibodies were detected in serum and there is no evidence for secondary MN, one may consider that patients do not undergo a kidney biopsy sample, provided that patients presented normal or only mild renal function decline. In patients with kidney function injury, a biopsy could help us to exclude a crescentic form of MN or concurrence of other diseases and evaluate the chronic damage degree.

3 TREATMENT OF MEMBRANOUS NEPHROPATHY

Currently, IMN patients are mainly treated with either calcineurin inhibitors, alkylating cytotoxic agents, B-cell depleting monoclonal antibody, or rituximab (Wang et al., 2018a; Hamilton et al., 2018; Yu et al., 2018). The use of calcineurin inhibitors led to a high relapse rate on their withdrawal. Alkylating cytotoxic agents were effective, but their use led to severely adverse effects. Rituximab-treated MN patients showed a decrease in anti-PLA_2R antibody levels in the follow-up period (Ramachandran et al., 2018). However, it is worth noting that some natural products exhibit an excellent efficacy for MN treatment (Feng et al., 2020; Lang et al., 2020; Lu et al., 2021).

3.1 Immunosuppressive Treatment

Kidney Disease: Improving Global Outcomes guidelines recommend that corticosteroids and alkylating agents including cyclophosphamide or chlorambucil are prescribed for 6 months for MN patients with nephrotic syndrome after 6–12 months as a conservative treatment or with decreased baseline renal function (Stevens and Levin, 2013). However, these therapies showed some severe adverse effects. The severity of side effects had important drawbacks in this therapy. Therefore, the classical combined therapy should be optimized (Chen et al., 2020a). The latest results indicated that remission at first 3 months were higher in the steroid–tacrolimus group than in the steroid–cyclophosphamide group over an 18-month period (Zou et al., 2020). Although the incidence of adverse effects was not different between two groups, the incidence after first 3 months was decreased in the steroid–tacrolimus group. Levels of 24-h urinary protein and serum albumin improved in the steroid–tacrolimus group more than those in the steroid–cyclophosphamide group (Zou et al., 2020).

Hoxha et al. (2014)reported that antibody levels were significantly reduced after 3 months of immunosuppressive treatment by 81% and proteinuria by 39% in 133 MN patients with positive anti-PLA_2R antibody. Patients with remission after 12 months presented decreased levels of anti-PLA_2R antibodies at baseline compared to patients with no remission. Moreover, patients with high anti-PLA_2R antibody concentrations achieved remission later than patients with low concentrations. The antibody concentrations remained increased in patients who did not achieve proteinuria remission.

Alternatively, decreasing proteinuria concentrations without an immunological response could not be interpreted as real

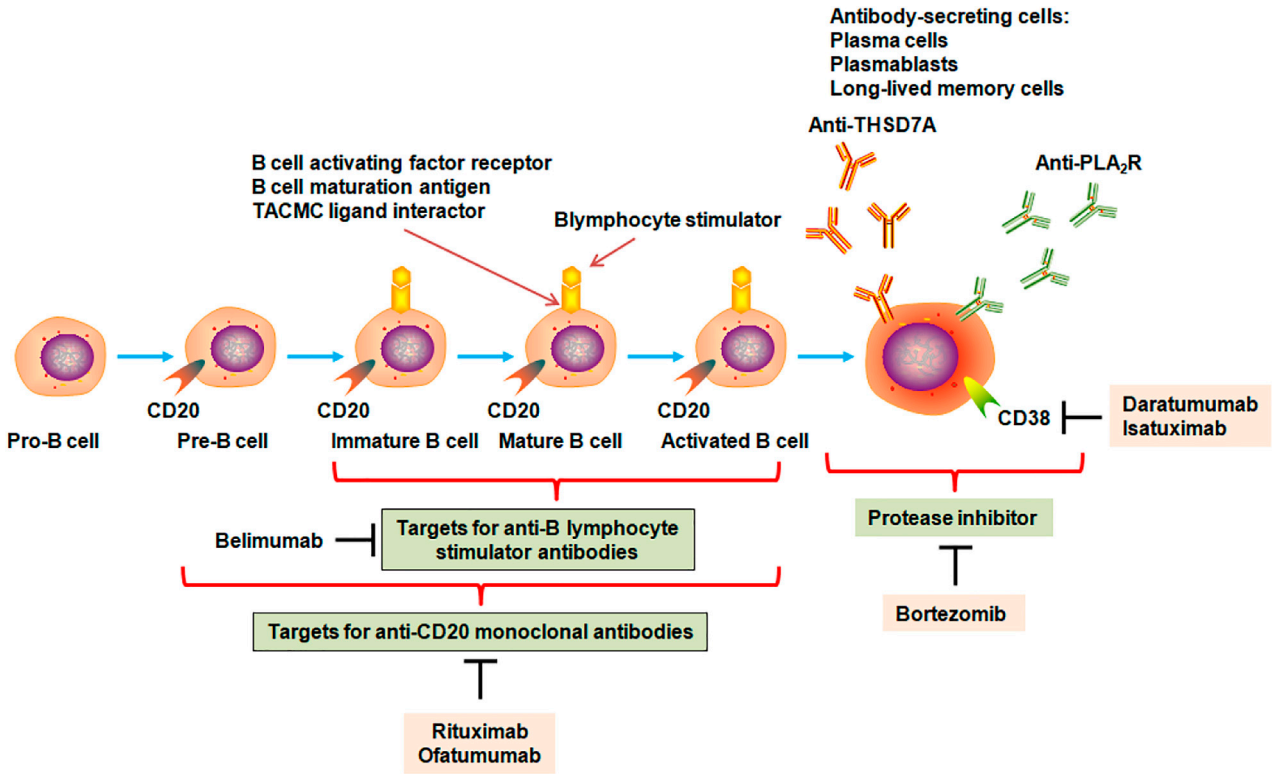

FIGURE 3 | Targets for monoclonal antibodies in B cells for the MN therapy strategy. B cells originated from bone marrow stem cells as pro-B cells and mature to pre-B cells, immature B cells, mature B cells, and activated B cells, which could form plasma cells, plasmablasts, and long-lived memory plasma cells that could secrete antibodies such as immunoglobulin A, immunoglobulin E, immunoglobulin G, and immunoglobulin M. Autoreactive B-cell clones could generate anti-PLA_2R and anti-THSD7A antibodies. When B cells became mature, they generated many biomarkers that were considered targets for monoclonal antibodies. Monoclonal antibodies rituximab and ofatumumab could bind and inhibit a number of CD20-positive B cells but not mature plasma cells, plasmablasts, and memory plasma cells that could not produce CD20 antigen. Plasma cells produced CD38 and could be a target for anti-CD38 antibodies by daratumumab and isatuximab. Immature, mature, and activated B cells produced receptors for B-lymphocyte stimulator including B-cell activating factor receptor, B-cell maturation antigen, transmembrane activator, and calcium-modulating cyclophilin (TACMC) ligand interactor. Belimumab could inhibit B-cell differentiation into plasma cells by suppressing interaction between B-lymphocyte stimulator and its receptors. Bortezomib, a proteasome inhibitor, could inhibit antibody production by mediating plasma cell apoptosis, while anti-CD38 antibodies daratumumab and isatuximab could directly mediate plasma cell cytolysis.

remission. There is an increasing risk of relapse when treatment by frequently using cyclosporine is withdrawn. Persistence of the high anti-PLA_2R antibody titer is a sign of ongoing immunologic activity that was associated with ongoing podocyte injury despite decreased proteinuria concentrations. Therefore, the efficacy of any immunosuppressive treatment need to be assessed based on immunologic remission induction (Bomback and Fervenza, 2018). Anti-PLA_2R positivity reappearance and/or an elevation in the previously lower titer of anti-PLA_2R antibody was a clear indicator of the impending relapse of MN, sometimes preceding the rise of proteinuria concentrations. Serial detection methods of anti-PLA_2R antibodies during immunosuppressive treatment could improve personalized treatment of MN.

3.2 Rituximab

After nearly 40 years of empirical treatment, the identification of newer anti-PLA_2R and anti-THSD7A autoantibodies was an unprecedented breakthrough for the understanding of underlying pathophysiological mechanisms of MN and its interventions specifically aimed at preventing antibody production (**Figure 3**). Rituximab was one of the first-line drugs for the treatment of moderate and high-risk IMN. The latest study demonstrated that 91 patients treated by rituximab achieved anti-PLA_2R antibody depletion at 6 months; 58.2% of patients showed clinical remission at 12 months (Gao et al., 2021). Further analysis indicated that high proteinuria levels and persistent positive anti-PLA_2R antibodies could be independent risk factors for no remission. The remission rate treated using rituximab as an initial regimen was increased compared to rituximab as an alternative regimen. In addition, 45 adverse events occurred in 37 patients. Rituximab effect was determined for the patients with PLA_2R-associated MN and stage four or five chronic kidney disease (CKD) (Hanset et al., 2020). In total, 10 treatment courses caused an increase in an estimated glomerular filtration rate and remission of nephrotic syndrome. In contrast, four patients treated by rituximab were unsuccessful and required chronic hemodialysis within 1 year. Immunological remission was observed after 11 treatments and was related to response. However, three patients showed severe adverse events (Hanset et al., 2020). These findings suggest that rituximab

showed effective and reasonably safe in PLA_2R-related MN with stage four or five CKD. Immunological remission is related to a beneficial clinical outcome.

Prior to the finding that anti-PLA_2R autoantibodies affected MN pathogenesis, *in vivo* animal experiments had consistently demonstrated that antibodies generated by autoreactive B-cell clones triggered events that led to glomerular barrier damage and proteinuria development (Brglez et al., 2020). Consistent with these findings, cyclophosphamide showed an inhibitory effect on production of B-cell antibody in MN, adding to the non-specific antimitotic and immunosuppressive nature that induced some side effects. A monoclonal antibody against B-cell surface antigen CD20 has performed whether targeted B-cell depletion with inhibition of autoantibody production ameliorated MN patients while reduced side effects of immunosuppressants and steroids. Therefore, rituximab, as an anti-CD20 monoclonal antibody (**Figure 3**), was used in MN patients. MN patients treated by rituximab showed reduced levels of circulating anti-PLA_2R antibody and proteinuria within several months (Gao et al., 2021; Gauckler et al., 2021). Ruggenenti et al. (2015) demonstrated that rituximab-treated patients with IMN showed a partial or complete remission, whereas anti-PLA_2R antibody-positive patients showed a remission demonstrated by a decrease in antibody titer before treatment. These patients presented complete antibody depletion 6 months after the beginning of rituximab regimen. The finding from all patients showed that depletion of anti-PLA_2R antibodies preceded complete remission. Early decreasing of anti-PLA_2R antibody titer by 50% was in line with a reduction in proteinuria levels by 50% by 10 months, whereas rituximab was not associated with polymorphisms of PLA_2R1.

Recently, it was reported that early response to either cyclosporine or rituximab was complete, and partial remission was observed in 130 patients treated by cyclosporine or rituximab, which showed similar results. However, partial or complete remission was faster in rituximab-treated patients than cyclosporine-treated patients at 24 months Fervenza et al. (2019). However, cyclosporine was withdrawn at 12 months, which reflected the risk of early relapse after cyclosporine withdrawal. Of note, the reduction of anti-PLA_2R antibodies was faster in rituximab-treated patients than the cyclosporine-treated patients (Fervenza et al., 2019). These findings illuminated that immunological remission by depleting anti-PLA_2R antibodies was promising for clinical remission.

Recently, a randomized and open-label controlled experiment was performed on 86 patients with IMN and nephrotic syndrome and assigned 43 each to receive 6-month cyclical intervention with the corticosteroid–cyclophosphamide group or sequential intervention with the tacrolimus–rituximab group (Fernández-Juárez et al., 2021). The results showed 83.7% of patients treated by the corticosteroid–cyclophosphamide group and 51.8% of patients treated by the tacrolimus–rituximab group exhibited complete or partial remission at 24 months. Complete remission occurred in 60% of patients treated by the corticosteroid–cyclophosphamide group and 26% of patients treated by the tacrolimus–rituximab group (Fernández-Juárez et al., 2021). Anti-PLA_2R titers were significantly decreased in both groups, but the proportion of anti-PLA_2R-positive patients who showed anti-PLA_2R antibody depletion was higher at 3 and 6 months in the corticosteroid–cyclophosphamide group than the tacrolimus–rituximab group (Fernández-Juárez et al., 2021). Severe adverse effects were similar in both groups. Therefore, the corticosteroid–cyclophosphamide treated remission in many patients with IMN compared to tacrolimus–rituximab. In addition, Tian et al. (2022)assessed the efficacy and safety of tacrolimus combined with corticosteroids in patients with IMN and reported that 75 patients with renal biopsy MN and nephrotic syndrome were treated by rituximab or non-immunosuppressant. The depletion of anti-PLA_2R was demonstrated at 6 months in 50% of patients intervened by rituximab and only in 12% of patients intervened by non-immunosuppressant Dahan et al. (2017).

3.3 Pharmacological Effects of Natural Products on Membranous Nephropathy

Natural products or traditional Chinese medicines have been long used in patients and considered an alternative therapeutic strategy for prevention and treatment of glomerular-associated diseases including MN (Feng et al., 2020), glomerulonephritis (Gianassi et al., 2019; Wang et al., 2021), diabetes (Chen et al., 2020b; Wang et al., 2020b; Fang et al., 2021; Su et al., 2021; He et al., 2022), and diabetic nephropathy (Li et al., 2020a; Yang et al., 2020; Wang, 2021; Xuan et al., 2021; Yang and Wu, 2021; Zhou et al., 2021; Liu et al., 2022). Earlier finding have demonstrated that a 77-year-old woman with IMN was treated by *Astragalus membranaceus* and achieved clinical remission without using immunosuppressive therapy (Ahmed et al., 2007). A multicenter randomized controlled clinical study assessed efficacy and safety of Shenqi particle for patients with IMN. Shenqi particle showed a beneficial effect on patients with IMN and nephrotic syndrome (Chen et al., 2013). In addition, Jian Pi Qu Shi formula treatment showed improvement in 15 patients, who failed to respond immunosuppressive therapy, and showed that 80% of the patients achieved clinical remission, whereas no obvious adverse effects were observed after 1-year follow-up (Shi et al., 2018). Similarly, Shulifenxiao formula as a clinical cocktail therapy also showed a beneficial intervention effect on steroid and immunosuppressant-resistant refractory IMN patients (Cui et al., 2021). Therefore, these formulas might be an alternative therapy for steroid and general immunosuppressant-resistant IMN patients. The combination of *Tripterygium wilfordii* multi-glycosides and prednisone is considered an effective therapy for IMN. The remission probability was similar for both *Tripterygium wilfordii* multi-glycosides and tacrolimus (Jin et al., 2020). Traditional Chinese medicines also could improve immunosuppressant efficacy. Wuzhi capsule could increase blood FK506 concentration in patients with IMN (Zhang et al., 2019). These studies have indicated that traditional Chinese medicines can effectively improve IMN and reduce proteinuria, but the underlying mechanism is still elusive.

Mechanistically, Wu et al. recently reported that 24-h urine protein level was significantly decreased, and kidney histological injury was restored in the CBSA-induced rats treated by Wenyang

Lishui decoction. Similarly, an *in vitro* experiment showed that the apoptosis rate was increased in CBSA-induced mouse podocytes, while it was decreased when treated by Wenyang Lishui decoction, which was associated with downregulation of p53 mRNA and protein expression and upregulation of Bcl-2 mRNA and protein expression (Lu et al., 2020). An earlier study has revealed that Astragaloside IV might ameliorate complement attack complex-mediated podocyte lesion *via* inhibiting extracellular-regulated protein kinase expression (Zheng et al., 2012) (**Figure 2**). Recently, Tian et al. (2019)revealed that administration of Sanqi oral solution mitigated MN by lowering proteinuria, increasing serum albumin, and retarding renal damages in the experimental rat model of MN induced by CBSA. Sanqi oral solution also inhibited depositions of C3 and IgG and restored the protein expressions of podocin and synaptopodin, which were associated with the nuclear factor-κB (NF-κB) signaling pathway (Tian et al., 2019). The NF-κB signaling pathway plays an important role in immune modulation. Recent studies revealed that the NF-κB pathway was involved in the pathogenesis of MN (Sutariya et al., 2017). Liu et al. (2019)demonstrated that Zhenwu decoction reduced urine protein levels and alleviated kidney damage in the rat model of MN; furthermore, treatment with Zhenwu decoction could downregulate the protein expressions of IgG, C3, and desmin as well as upregulate podocin expression in glomerulus. The same research group demonstrated that Zhenwu decoction inhibited the advanced glycation end by suppressing the expression of receptor for advanced glycation end products in podocyte, which reduced oxidative stress in podocyte (Wu et al., 2016). These findings revealed that natural products ameliorate MN through targeting inflammation. However, MN is a non-inflammatory autoimmune disease of the kidney glomerulus. Taken together, the underlying mechanism should be investigated in the future.

In addition, Yu et al. (2020) reported that Chinese herbal injections were demonstrated to be superior to treatment of chemical drugs alone in the treatment of primary nephrotic syndrome and might be beneficial for patients with primary nephrotic syndrome. The combination of chemical drugs and Yinxingdamo injection and chemical drugs and Danhong injection had the potential to be the best Chinese herbal injections relative to total clinical effectiveness, serum albumin, and 24-h urinary protein excretion. Moreover, Li et al. (2020b) and Li et al. (2020c) demonstrated that Zhen-Wu-Tang could ameliorate immunoglobulin A nephropathy in rats.

3.4 Future Therapy and Directions

The integrated assessment of the levels of autoantibody and albumin in serum and proteinuria in patients could provide MN diagnosis and individually tailored treatment protocols. Traditional, toxic, and non-specific immunosuppressant will be replaced by safe and disease-specific agents, such as B-cell-targeting anti-CD20 antibodies (**Figure 3**), providing a new treatment paradigm based on the principles of precision medicine and personalized therapy. Although great advances were achieved in MN pathogenesis, a number of critical issues remain unsolved. For example, how the immune response is triggered and spreads remains unknown; the conditions that resulted in the appearance of PLA_2R epitope of podocytes and the events that mediated immunization are elusive; the aim of antigen-driven therapy has still not been fulfilled. Although anti-PLA_2R and anti-THSD7A antibodies as the leading diagnosis approaches were extensively applied to MN patients, some questions including autoimmune response, antigenic epitopes, and podocyte injury-associated with signaling pathways remain unresolved. In addition, when the patients have renal biopsy of MN, the clinicians need to answer two key issues. If patients are PLA_2R-positive, then what are the risk factors of progression to renal failure? If patients are PLA_2R-negative, then the causes of disease development and progression are primary or secondary?

Owing to the adverse effects of currently available immunosuppressive agents, a better understanding of MN pathomechanisms will provide more specific concept-directed therapy strategies. Based on the critical role of IgG antibodies in MN, targeting B lymphocytes by anti-CD20 antibody might be a specific and effective therapy to ameliorate MN by blocking antibody formation (**Figure 3**). However, responses are wide, and further research is needed to identify those patients who are benefitted by rituximab treatment and those who are non-effective. A clinical study showed that adrenocorticotropic hormone exerted its role through activated melanocortin receptors (MC1R–MC5R) that existed in the whole body were effective therapy for IMN patients who failed immunosuppressive treatment (Markell et al., 2019; Wu et al., 2021b). Melanocortin one receptor occurred in B cells, T cells, podocytes, and antigen-presenting cells. Melanocortin one receptor agonists could lower proteinuria, improve glomerular morphology, and retard oxidative stress in passive Heymann nephritis rats, which were associated with decrease in production of nephritogenic antibodies, direct targeting effect on podocytes, and stabilizing glomerular architecture. Further experiment should be performed to adrenocorticotropic hormone effect. The pathophysiological mechanisms have an important effect on patient care, including kidney biopsy, diagnosis, monitoring, and therapy.

Intriguingly, natural products are one of the most promising therapies for a broad spectrum of refractory diseases including coronavirus disease 2019 and its complications (Chen et al., 2018a; Chen et al., 2018b; Izzo et al., 2020; Yang et al., 2021a; Yang et al., 2021b; Zhang et al., 2021b; Singla et al., 2021; Zuo et al., 2021). Mounting natural products have been demonstrated to exhibit excellent efficacy for CKD treatment (Wang et al., 2018b; Zhang et al., 2020c; Geng et al., 2020; Meng et al., 2020; Miao et al., 2020; Lan, 2021; Li et al., 2021; Luo et al., 2021; Miao et al., 2022; Yu et al., 2022). Although a number of natural products could mitigate MN, the natural products in MN application are still in its infancy compared with CKD. Therefore, whether natural products can abolish MN, for which the study should be carried out on the animal models and patients with MN in the future.

DATA AVAILABILITY STATEMENT

The raw data supporting the conclusion of this article will be made available by the authors, without undue reservation.

AUTHOR CONTRIBUTIONS

Y-YZ designed and wrote the review. Y-NW, H-YF, XN, Y-MZ, LZ, XL, and X-YY revised the manuscript. All authors accepted the final version of the manuscript.

FUNDING

This study was supported by the National Key Research and Development Project (No. 2019YFC1709405) and National Natural Science Foundation of China (Nos. 82074002 and 81872985).

REFERENCES

Ahmed, M. S., Hou, S. H., Battaglia, M. C., Picken, M. M., and Leehey, D. J. (2007). Treatment of Idiopathic Membranous Nephropathy with the Herb Astragalus Membranaceus. *Am. J. Kidney Dis.* 50 (6), 1028–1032. doi:10.1053/j.ajkd.2007.07.032

Ayalon, R., and Beck, L. H., Jr. (2015). Membranous Nephropathy: Not Just a Disease for Adults. *Pediatr. Nephrol.* 30 (1), 31–39. doi:10.1007/s00467-013-2717-z

Bacharaki, D., Chrysanthopoulou, E., Grigoropoulou, S., Giannakopoulos, P., Simitsis, P., Frantzeskaki, F., et al. (2021). Siblings with Coronavirus Disease 2019 Infection and Opposite Outcome-The Hemodialysis's Better Outcome Paradox: Two Case Reports. *World J. Nephrol.* 10 (2), 21–28. doi:10.5527/wjn.v10.i2.21

Bally, S., Debiec, H., Ponard, D., Dijoud, F., Rendu, J., Fauré, J., et al. (2016). Phospholipase A2 Receptor-Related Membranous Nephropathy and Mannan-Binding Lectin Deficiency. *J. Am. Soc. Nephrol.* 27 (12), 3539–3544. doi:10.1681/ASN.2015101155

Beck, L. H., Jr., Bonegio, R. G., Lambeau, G., Beck, D. M., Powell, D. W., Cummins, T. D., et al. (2009). M-type Phospholipase A2 Receptor as Target Antigen in Idiopathic Membranous Nephropathy. *N. Engl. J. Med.* 361 (1), 11–21. doi:10.1056/NEJMoa0810457

Bomback, A. S., and Fervenza, F. C. (2018). Membranous Nephropathy: Approaches to Treatment. *Am. J. Nephrol.* 47 (Suppl. 1), 30–42. doi:10.1159/000481635

Brglez, V., Boyer-Suavet, S., Zorzi, K., Fernandez, C., Fontas, E., Esnault, V., et al. (2020). Personalized Medicine for PLA2R1-Related Membranous Nephropathy: A Multicenter Randomized Control Trial. *Front. Med. (Lausanne)* 7, 412. doi:10.3389/fmed.2020.00412

Chang, T.-Y., Wu, H.-H., Li, Y.-J., Liu, H.-L., Yeh, C.-H., Jian, H.-S., et al. (2021). Changes of Brain Functional Connectivity in End-Stage Renal Disease Patients Receiving Peritoneal Dialysis without Cognitive Decline. *Front. Med.* 8, 734410. doi:10.3389/fmed.2021.734410

Chen, D. Q., Feng, Y. L., Cao, G., and Zhao, Y. Y. (2018). Natural Products as a Source for Antifibrosis Therapy. *Trends Pharmacol. Sci.* 39 (11), 937–952. doi:10.1016/j.tips.2018.09.002

Chen, D. Q., Hu, H. H., Wang, Y. N., Feng, Y. L., Cao, G., and Zhao, Y. Y. (2018). Natural Products for the Prevention and Treatment of Kidney Disease. *Phytomedicine* 50, 50–60. doi:10.1016/j.phymed.2018.09.182

Chen, S., Ren, S., Wang, A. Y., Tran, H., Li, Z., Cheng, X., et al. (2020). Comparison of the Efficacy and Safety of Tacrolimus Monotherapy and Cyclophosphamide Combined with Glucocorticoid in the Treatment of Adult Primary Membranous Nephropathy: Protocol of a Multicenter, Randomized, Controlled, Open Study. *Trials* 21 (1), 219. doi:10.1186/s13063-020-4144-3

Chen, Y., Deng, Y., Ni, Z., Chen, N., Chen, X., Shi, W., et al. (2013). Efficacy and Safety of Traditional Chinese Medicine (Shenqi Particle) for Patients with Idiopathic Membranous Nephropathy: a Multicenter Randomized Controlled Clinical Trial. *Am. J. Kidney Dis.* 62 (6), 1068–1076. doi:10.1053/j.ajkd.2013.05.005

Chen, Z. Q., Sun, X. H., Li, X. J., Xu, Z. C., Yang, Y., Lin, Z. Y., et al. (2020). Polydatin Attenuates Renal Fibrosis in Diabetic Mice through Regulating the Cx32-Nox4 Signaling Pathway. *Acta Pharmacol. Sin.* 41 (12), 1587–1596. doi:10.1038/s41401-020-0475-6

Chuengsaman, P., Narenpitak, S., and Sritippayawan, S. (2021). Efficacy and Safety of Recombinant Human Erythropoietin (Hema-Plus®) for Management of Anemia in Thai Patients on Peritoneal Dialysis. *World J. Nephrol.* 10 (6), 109–121. doi:10.5527/wjn.v10.i6.109

Cravedi, P., Jarque, M., Angeletti, A., Favà, À., Cantarelli, C., and Bestard, O. (2019). Immune-monitoring Disease Activity in Primary Membranous Nephropathy. *Front. Med.* 6, 241. doi:10.3389/fmed.2019.00241

Cui, H., Fu, F. Q., Liu, B., Liu, W. J., and Liu, Y. N. (2021). Herbal Medicine "Shulifenxiao" Formula for Nephrotic Syndrome of Refractory Idiopathic Membranous Nephropathy. *Front. Pharmacol.* 12, 675406. doi:10.3389/fphar.2021.675406

da Silva, A. Q. B., de Sandes-Freitas, T. V., Mansur, J. B., Medicina-Pestana, J. O., and Mastroianni-Kirsztajn, G. (2018). Clinical Presentation, Outcomes, and Treatment of Membranous Nephropathy after Transplantation. *Int. J. Nephrol.* 2018, 3720591. doi:10.1155/2018/3720591

Dahan, K., Debiec, H., Plaisier, E., Cachanado, M., Rousseau, A., Wakselman, L., et al. (2017). Rituximab for Severe Membranous Nephropathy: a 6-month Trial with Extended Follow-Up. *J. Am. Soc. Nephrol.* 28 (1), 348–358. doi:10.1681/ASN.2016040449

Dähnrich, C., Komorowski, L., Probst, C., Seitz-Polski, B., Esnault, V., Wetzels, J. F., et al. (2013). Development of a Standardized ELISA for the Determination of Autoantibodies against Human M-type Phospholipase A_2 Receptor in Primary Membranous Nephropathy. *Clin. Chim. Acta* 421, 213–218. doi:10.1016/j.cca.2013.03.015

Debiec, H., Guigonis, V., Mougenot, B., Decobert, F., Haymann, J. P., Bensman, A., et al. (2002). Antenatal Membranous Glomerulonephritis Due to Anti-neutral Endopeptidase Antibodies. *N. Engl. J. Med.* 346 (26), 2053–2060. doi:10.1056/NEJMoa012895

Debiec, H., and Ronco, P. (2011). PLA2R Autoantibodies and PLA2R Glomerular Deposits in Membranous Nephropathy. *N. Engl. J. Med.* 364 (7), 689–690. doi:10.1056/NEJMc1011678

Dong, R., Bai, M., Zhao, J., Wang, D., Ning, X., and Sun, S. (2020). A Comparative Study of the Gut Microbiota Associated with Immunoglobulin a Nephropathy and Membranous Nephropathy. *Front. Cell Infect. Microbiol.* 10, 557368. doi:10.3389/fcimb.2020.557368

Fang, C. Y., Lou, D. Y., Zhou, L. Q., Wang, J. C., Yang, B., He, Q. J., et al. (2021). Natural Products: Potential Treatments for Cisplatin-Induced Nephrotoxicity. *Acta Pharmacol. Sin.* 42 (12), 1951–1969. doi:10.1038/s41401-021-00620-9

Feng, Z., Liu, W., Jiang, H. X., Dai, H., Gao, C., Dong, Z., et al. (2020). How Does Herbal Medicine Treat Idiopathic Membranous Nephropathy? *Front. Pharmacol.* 11, 994. doi:10.3389/fphar.2020.00994

Fernández-Juárez, G., Rojas-Rivera, J., Logt, A. V., Justino, J., Sevillano, A., Caravaca-Fontán, F., et al. (2021). The STARMEN Trial Indicates that Alternating Treatment with Corticosteroids and Cyclophosphamide Is Superior to Sequential Treatment with Tacrolimus and Rituximab in Primary Membranous Nephropathy. *Kidney Int.* 99 (4), 986–998. doi:10.1016/j.kint.2020.10.014

Fervenza, F. C., Appel, G. B., Barbour, S. J., Rovin, B. H., Lafayette, R. A., Aslam, N., et al. (2019). Rituximab or Cyclosporine in the Treatment of Membranous Nephropathy. *N. Engl. J. Med.* 381 (1), 36–46. doi:10.1056/NEJMoa1814427

Gambino, G., Catalano, C., Marangoni, M., Geers, C., Moine, A. L., Boon, N., et al. (2021). Case Report: Homozygous Pathogenic Variant P209L in the TTC21B Gene: a Rare Cause of End Stage Renal Disease and Biliary Cirrhosis Requiring Combined Liver-Kidney Transplantation. A Case Report and Literature Review. *Front. Med.* 8, 795216. doi:10.3389/fmed.2021.795216

Gao, S., Cui, Z., Wang, X., Zhang, Y. M., Wang, F., Cheng, X. Y., et al. (2021). Rituximab Therapy for Primary Membranous Nephropathy in a Chinese Cohort. *Front. Med. (Lausanne)* 8, 663680. doi:10.3389/fmed.2021.663680

Gauckler, P., Shin, J. I., Alberici, F., Audard, V., Bruchfeld, A., Busch, M., et al. (2021). Rituximab in Membranous Nephropathy. *Kidney Int. Rep.* 6 (4), 881–893. doi:10.1016/j.ekir.2020.12.035

Geng, X. Q., Ma, A., He, J. Z., Wang, L., Jia, Y. L., Shao, G. Y., et al. (2020). Ganoderic Acid Hinders Renal Fibrosis via Suppressing the TGF-β/Smad and MAPK Signaling Pathways. *Acta Pharmacol. Sin.* 41 (5), 670–677. doi:10.1038/s41401-019-0324-7

Gianassi, I., Allinovi, M., Caroti, L., and Cirami, L. C. (2019). Broad Spectrum of Interferon-Related Nephropathies-Glomerulonephritis, Systemic Lupus Erythematosus-like Syndrome and Thrombotic Microangiopathy: A Case

Report and Review of Literature. *World J. Nephrol.* 8 (7), 109–117. doi:10.5527/wjn.v8.i7.109

Gu, Y., Xu, H., and Tang, D. (2021). Mechanisms of Primary Membranous Nephropathy. *Biomolecules* 11 (4), 513. doi:10.3390/biom11040513

Hamilton, P., Kanigicherla, D., Venning, M., Brenchley, P., and Meads, D. (2018). Rituximab versus the Modified Ponticelli Regimen in the Treatment of Primary Membranous Nephropathy: a Health Economic Model. *Nephrol. Dial. Transpl.* 33 (12), 2145–2155. doi:10.1093/ndt/gfy049

Hanset, N., Esteve, E., Plaisier, E., Johanet, C., Michel, P. A., Boffa, J. J., et al. (2020). Rituximab in Patients with Phospholipase A2 Receptor-Associated Membranous Nephropathy and Severe CKD. *Kidney Int. Rep.* 5 (3), 331–338. doi:10.1016/j.ekir.2019.12.006

He, J. Y., Hong, Q., Chen, B. X., Cui, S. Y., Liu, R., Cai, G. Y., et al. (2022). Ginsenoside Rb1 Alleviates Diabetic Kidney Podocyte Injury by Inhibiting Aldose Reductase Activity. *Acta Pharmacol. Sin.* 43 (2), 342–353. doi:10.1038/s41401-021-00788-0

Heymann, W., Hackel, D. B., Harwood, S., Wilson, S. G., and Hunter, J. L. (1959). Production of Nephrotic Syndrome in Rats by Freund's Adjuvants and Rat Kidney Suspensions. *Proc. Soc. Exp. Biol. Med.* 100 (4), 660–664. doi:10.3181/00379727-100-24736

Hofstra, J. M., and Wetzels, J. F. (2012). Anti-PLA_2R Antibodies in Membranous Nephropathy: Ready for Routine Clinical Practice? *Neth J. Med.* 70 (3), 109–113.

Hoxha, E., Beck, L. H., Wiech, T., Tomas, N. M., Probst, C., Mindorf, S., et al. (2017). An Indirect Immunofluorescence Method Facilitates Detection of Thrombospondin Type 1 Domain-Containing 7A-specific Antibodies in Membranous Nephropathy. *J. Am. Soc. Nephrol.* 28 (2), 520–531. doi:10.1681/ASN.2016010050

Hoxha, E., Thiele, I., Zahner, G., Panzer, U., Harendza, S., and Stahl, R. A. (2014). Phospholipase A2 Receptor Autoantibodies and Clinical Outcome in Patients with Primary Membranous Nephropathy. *J. Am. Soc. Nephrol.* 25 (6), 1357–1366. doi:10.1681/ASN.2013040430

Hoxha, E., Wiech, T., Stahl, P. R., Zahner, G., Tomas, N. M., Meyer-Schwesinger, C., et al. (2016). A Mechanism for Cancer-Associated Membranous Nephropathy. *N. Engl. J. Med.* 374 (20), 1995–1996. doi:10.1056/NEJMc1511702

Hu, W., Li, G., Lin, J., Dong, W., Yu, F., Liu, W., et al. (2021). M2 Macrophage Subpopulations in Glomeruli Are Associated with the Deposition of IgG Subclasses and Complements in Primary Membranous Nephropathy. *Front. Med. (Lausanne)* 8, 657232. doi:10.3389/fmed.2021.657232

Izzo, A. A., Teixeira, M., Alexander, S. P. H., Cirino, G., Docherty, J. R., George, C. H., et al. (2020). A Practical Guide for Transparent Reporting of Research on Natural Products in the British Journal of Pharmacology: Reproducibility of Natural Product Research. *Br. J. Pharmacol.* 177 (10), 2169–2178. doi:10.1111/bph.15054

Jiang, H. X., Feng, Z., Zhu, Z. B., Xia, C. H., Zhang, W., Guo, J., et al. (2020). Advances of the Experimental Models of Idiopathic Membranous Nephropathy (Review). *Mol. Med. Rep.* 21 (5), 1993–2005. doi:10.3892/mmr.2020.11014

Jin, L. W., Pan, M., Ye, H. Y., Zheng, Y., Chen, Y., Huang, W. W., et al. (2019). Down-regulation of the Long Non-coding RNA XIST Ameliorates Podocyte Apoptosis in Membranous Nephropathy via the miR-217-TLR4 Pathway. *Exp. Physiol.* 104 (2), 220–230. doi:10.1113/EP087190

Jin, Y., Zhang, J., Wang, Y., Xiao, X., and Zhang, Q. (2020). Tripterygium Wilfordii Multiglycosides Combined with Prednisone in the Treatment of Idiopathic Membranous Nephropathy: A Protocol for a Systematic Review and Meta-Analysis. *Med. Baltim.* 99 (5), e18970. doi:10.1097/MD.0000000000018970

Jones, D. B. (1957). Nephrotic Glomerulonephritis. *Am. J. Pathol.* 33 (2), 313–329.

Jurubită, R., Obrișcă, B., Sorohan, B., Achim, C., Micu, G. E., Mircescu, G., et al. (2021). Clinical Phenotypes and Predictors of Remission in Primary Membranous Nephropathy. *J. Clin. Med.* 10 (12), 2624. doi:10.3390/jcm10122624

Kerjaschki, D., and Farquhar, M. G. (1982). The Pathogenic Antigen of Heymann Nephritis Is a Membrane Glycoprotein of the Renal Proximal Tubule Brush Border. *Proc. Natl. Acad. Sci. U. S. A.* 79 (18), 5557–5561. doi:10.1073/pnas.79.18.5557

Lan, H.-y. (2021). The Yin and Yang Role of Transforming Growth Factor-β in Kidney Disease. *Integr. Med. Nephrol. Androl.* 8 (1), 1. doi:10.4103/imna.imna_17_21

Lang, R., Wang, X., Liang, Y., Yan, L., Shi, B., and Yu, R. (2020). Research Progress in the Treatment of Idiopathic Membranous Nephropathy Using Traditional Chinese Medicine. *J. Transl. Int. Med.* 8 (1), 3–8. doi:10.2478/jtim-2020-0002

Li, H., Lu, R., Pang, Y., Li, J., Cao, Y., Fu, H., et al. (2020). Zhen-Wu-Tang Protects IgA Nephropathy in Rats by Regulating Exosomes to Inhibit NF-Kb/nlrp3 Pathway. *Front. Pharmacol.* 11, 1080. doi:10.3389/fphar.2020.01080

Li, J., Cao, Y., Lu, R., Li, H., Pang, Y., Fu, H., et al. (2020). Integrated Fecal Microbiome and Serum Metabolomics Analysis Reveals Abnormal Changes in Rats with Immunoglobulin A Nephropathy and the Intervention Effect of Zhen Wu Tang. *Front. Pharmacol.* 11, 606689. doi:10.3389/fphar.2020.606689

Li, N., Zhao, T., Cao, Y., Zhang, H., Peng, L., Wang, Y., et al. (2020). Tangshen Formula Attenuates Diabetic Kidney Injury by Imparting Anti-pyroptotic Effects via the TXNIP-NLRP3-GSDMD axis. *Front. Pharmacol.* 11, 623489. doi:10.3389/fphar.2020.623489

Li, S. S., Sun, Q., Hua, M. R., Suo, P., Chen, J. R., Yu, X. Y., et al. (2021). Targeting the Wnt/β-Catenin Signaling Pathway as a Potential Therapeutic Strategy in Renal Tubulointerstitial Fibrosis. *Front. Pharmacol.* 12, 719880. doi:10.3389/fphar.2021.719880

Liu, B., Lu, R., Li, H., Zhou, Y., Zhang, P., Bai, L., et al. (2019). Zhen-Wu-tang Ameliorates Membranous Nephropathy Rats through Inhibiting NF-Kb Pathway and NLRP3 Inflammasome. *Phytomedicine* 59, 152913. doi:10.1016/j.phymed.2019.152913

Liu, W., Gao, C., Liu, Z., Dai, H., Feng, Z., Dong, Z., et al. (2020). Idiopathic Membranous Nephropathy: Glomerular Pathological Pattern Caused by Extrarenal Immunity Activity. *Front. Immunol.* 11, 1846. doi:10.3389/fimmu.2020.01846

Liu, X. Q., Jiang, L., Li, Y. Y., Huang, Y. B., Hu, X. R., Zhu, W., et al. (2022). Wogonin Protects Glomerular Podocytes by Targeting Bcl-2-Mediated Autophagy and Apoptosis in Diabetic Kidney Disease. *Acta Pharmacol. Sin.* 43 (1), 96–110. doi:10.1038/s41401-021-00721-5

Liu, Z. N., Cui, Z., He, Y. D., Zhang, Y. M., Wang, F., Wang, X., et al. (2020). Membranous Nephropathy in Pregnancy. *Am. J. Nephrol.* 51 (4), 304–317. doi:10.1159/000505175

Logt, A. V., Justino, J., Vink, C. H., van den Brand, J., Debiec, H., Lambeau, G., et al. (2021). Anti-PLA2R1 Antibodies as Prognostic Biomarker in Membranous Nephropathy. *Kidney Int. Rep.* 6 (6), 1677–1686. doi:10.1016/j.ekir.2021.04.002

Lönnbro-Widgren, J., Ebefors, K., Mölne, J., Nyström, J., and Haraldsson, B. (2015). Glomerular IgG Subclasses in Idiopathic and Malignancy-Associated Membranous Nephropathy. *Clin. Kidney J.* 8 (4), 433–439. doi:10.1093/ckj/sfv049

Lu, H., Luo, Y., Su, B., Tang, S., Chen, G., Zhang, L., et al. (2020). Wenyang Lishui Decoction Ameliorates Podocyte Injury in Membranous Nephropathy Rat and Cell Models by Regulating P53 and Bcl-2. *Evid. Based Complement. Altern. Med.* 2020, 6813760. doi:10.1155/2020/6813760

Lu, Z., Liu, W., Gao, H., Chen, W., Ge, W., Li, F., et al. (2021). Traditional Chinese Medicine as an Adjunct Therapy in the Treatment of Idiopathic Membranous Nephropathy: A Systematic Review and Meta-Analysis. *PLoS One* 16 (5), e0251131. doi:10.1371/journal.pone.0251131

Luan, S., Zhang, S., Pan, L., Hu, W., Cui, H., Wei, X., et al. (2022). Salivary Microbiota Analysis of Patients with Membranous Nephropathy. *Mol. Med. Rep.* 25 (5), 190. doi:10.3892/mmr.2022.12706

Luo, L. P., Suo, P., Ren, L. L., Liu, H. J., Zhang, Y., and Zhao, Y. Y. (2021). Shenkang Injection and its Three Anthraquinones Ameliorates Renal Fibrosis by Simultaneous Targeting IκB/NF-κb and Keap1/Nrf2 Signaling Pathways. *Front. Pharmacol.* 12, 800522. doi:10.3389/fphar.2021.800522

Markell, M., Brar, A., Bhela, S., Patel, A., and Salifu, M. (2019). Use of Repository Corticotropin Gel (Acthar) in Progressive Nephrotic Syndrome Secondary to Transplant Glomerulopathy: a Report of Three Cases. *Kidney Med.* 1 (1), 31–35. doi:10.1016/j.xkme.2018.12.003

McQuarrie, E. P., Stirling, C. M., and Geddes, C. C. (2012). Idiopathic Membranous Nephropathy and Nephrotic Syndrome: Outcome in the Era of Evidence-Based Therapy. *Nephrol. Dial. Transpl.* 27 (1), 235–242. doi:10.1093/ndt/gfr220

Medina Rangel, P. X., Priyadarshini, A., and Tian, X. (2021). New Insights into the Immunity and Podocyte in Glomerular Health and Disease: From Pathogenesis to Therapy in Proteinuric Kidney Disease. *Integr. Med. Nephrol. Androl.* 28, 1707. doi:10.1681/ASN.2017010027

Meng, J., Sai-Zhen, W., He, J. Z., Zhu, S., Huang, B. Y., Wang, S. Y., et al. (2020). Ganoderic Acid A Is the Effective Ingredient of Ganoderma Triterpenes in Retarding Renal Cyst Development in Polycystic Kidney Disease. *Acta Pharmacol. Sin.* 41 (6), 782–790. doi:10.1038/s41401-019-0329-2

Miao, H., Cao, G., Wu, X. Q., Chen, Y. Y., Chen, D. Q., Chen, L., et al. (2020). Identification of Endogenous 1-aminopyrene as a Novel Mediator of Progressive Chronic Kidney Disease via Aryl Hydrocarbon Receptor Activation. *Br. J. Pharmacol.* 177 (15), 3415–3435. doi:10.1111/bph.15062

Miao, H., Wu, X. Q., Wang, Y. N., Chen, D. Q., Chen, L., Vaziri, N. D., et al. (2022). 1-Hydroxypyrene Mediates Renal Fibrosis through Aryl Hydrocarbon Receptor Signalling Pathway. *Br. J. Pharmacol.* 179 (1), 103–124. doi:10.1111/bph.15705

Molina Andújar, A., Lucas, A., Escudero, V. J., Rovira, I., Matute, P., Ibañez, C., et al. (2022). Antiphospholipase A_2 Receptor Antibody-Positive Membranous Nephropathy in the Kidney Donor: Lessons from a Serendipitous Transplantation. *Am. J. Transpl.* 22 (1), 299–303. doi:10.1111/ajt.16813

Moroni, G., and Ponticelli, C. (2020). Secondary Membranous Nephropathy. A Narrative Review. *Front. Med.* 7, 611317. doi:10.3389/fmed.2020.611317

Moszczuk, B., Kiryluk, K., Pączek, L., and Mucha, K. (2021). Membranous Nephropathy: from Research Bench to Personalized Care. *J. Clin. Med.* 10 (6), 1205. doi:10.3390/jcm10061205

Nieto-Gañán, I., Iturrieta-Zuazo, I., Rita, C., and Carrasco-Sayalero, Á. (2021). Comparison of 3 Anti-pla2r Inmmunoassaysfor the Diagnosis of Idiopathic Membranous Nephropathy in an European Population. A Pilot Study. *Clin. Immunol.* 227, 108729. doi:10.1016/j.clim.2021.108729

Passerini, P., Malvica, S., Tripodi, F., Cerutti, R., and Messa, P. (2019). Membranous Nephropathy (MN) Recurrence after Renal Transplantation. *Front. Immunol.* 10, 1326. doi:10.3389/fimmu.2019.01326

Porcelli, B., Guarnieri, A., Ferretti, F., Garosi, G., Terzuoli, L., Cinci, F., et al. (2021). Diagnostic Accuracy of Anti-phospholipase A2 Receptor (PLA2R) Antibodies in Idiopathic Membranous Nephropathy: an Italian Experience. *J. Nephrol.* 34 (2), 573–579. doi:10.1007/s40620-020-00888-w

Prunotto, M., Carnevali, M. L., Candiano, G., Murtas, C., Bruschi, M., Corradini, E., et al. (2010). Autoimmunity in Membranous Nephropathy Targets Aldose Reductase and SOD2. *J. Am. Soc. Nephrol.* 21 (3), 507–519. doi:10.1681/ASN.2008121259

Ramachandran, R., Kumar, V., Nada, R., and Jha, V. (2015). Serial Monitoring of Anti-pla2r in Initial PLA2R-Negative Patients with Primary Membranous Nephropathy. *Kidney Int.* 88 (5), 1198–1199. doi:10.1038/ki.2015.310

Ramachandran, R., Yadav, A. K., Kumar, V., Inamdar, N., Nada, R., Gupta, K. L., et al. (2018). Temporal Association between PLA2R Antibodies and Clinical Outcomes in Primary Membranous Nephropathy. *Kidney Int. Rep.* 3 (1), 142–147. doi:10.1016/j.ekir.2017.09.001

Robson, K. J., and Kitching, A. R. (2021). Recurrent Membranous Nephropathy after Transplantation: Donor Antigen and HLA Converge in Defining Risk. *Kidney Int.* 99 (3), 545–548. doi:10.1016/j.kint.2020.10.044

Ronco, P., and Debiec, H. (2020). Molecular Pathogenesis of Membranous Nephropathy. *Annu. Rev. Pathol.* 15, 287–313. doi:10.1146/annurev-pathol-020117-043811

Ronco, P., and Debiec, H. (2015). Pathophysiological Advances in Membranous Nephropathy: Time for a Shift in Patient's Care. *Lancet* 385 (9981), 1983–1992. doi:10.1016/S0140-6736(15)60731-0

Ronco, P., Plaisier, E., and Debiec, H. (2021). Advances in Membranous Nephropathy. *J. Clin. Med.* 10 (4), 607. doi:10.3390/jcm10040607

Ruggenenti, P., Debiec, H., Ruggiero, B., Chianca, A., Pellé, T., Gaspari, F., et al. (2015). Anti-Phospholipase A2 Receptor Antibody Titer Predicts Post-Rituximab Outcome of Membranous Nephropathy. *J. Am. Soc. Nephrol.* 26 (10), 2545–2558. doi:10.1681/ASN.2014070640

Sawhney, H., and Gill, S. S. (2020). Renal Transplant Recipient Seizure Practical Management. *World J. Nephrol.* 9 (1), 1–8. doi:10.5527/wjn.v9.i1.1

Shi, B., Zhang, R. R., Liang, Y., Wang, X. H., Lang, R., and Yu, R. H. (2018). Efficacy of Traditional Chinese Medicine Regimen Jian Pi Qu Shi Formula for Refractory Patients with Idiopathic Membranous Nephropathy: a Retrospective Case-Series Study. *Evid. Based Complement. Altern. Med.* 2018, 5854710. doi:10.1155/2018/5854710

Singla, R. K., He, X., Chopra, H., Tsagkaris, C., Shen, L., Kamal, M. A., et al. (2021). Natural Products for the Prevention and Control of the COVID-19 Pandemic: Sustainable Bioresources. *Front. Pharmacol.* 12, 758159. doi:10.3389/fphar.2021.758159

Stevens, P. E., and Levin, A. (2013). Evaluation and Management of Chronic Kidney Disease: Synopsis of the Kidney Disease: Improving Global Outcomes 2012 Clinical Practice Guideline. *Ann. Intern Med.* 158 (11), 825–830. doi:10.7326/0003-4819-158-11-201306040-00007

Su, J., Gao, C., Xie, L., Fan, Y., Shen, Y., Huang, Q., et al. (2021). Astragaloside II Ameliorated Podocyte Injury and Mitochondrial Dysfunction in Streptozotocin-Induced Diabetic Rats. *Front. Pharmacol.* 12, 638422. doi:10.3389/fphar.2021.638422

Sutariya, B., Taneja, N., and Saraf, M. (2017). Betulinic Acid, Isolated from the Leaves of Syzygium Cumini (L.) Skeels, Ameliorates the Proteinuria in Experimental Membranous Nephropathy through Regulating Nrf2/NF-Kb Pathways. *Chem. Biol. Interact.* 274, 124–137. doi:10.1016/j.cbi.2017.07.011

Tamura, H. (2021). Trends in Pediatric Nephrotic Syndrome. *World J. Nephrol.* 10 (5), 88–100. doi:10.5527/wjn.v10.i5.88

Tesar, V., and Hruskova, Z. (2021). Autoantibodies in the Diagnosis, Monitoring, and Treatment of Membranous Nephropathy. *Front. Immunol.* 12, 593288. doi:10.3389/fimmu.2021.593288

Tian, R., Wang, L., Chen, A., Huang, L., Liang, X., Wang, R., et al. (2019). Sanqi Oral Solution Ameliorates Renal Damage and Restores Podocyte Injury in Experimental Membranous Nephropathy via Suppression of NFκB. *Biomed. Pharmacother.* 115, 108904. doi:10.1016/j.biopha.2019.108904

Tian, Z., Wang, M., Huang, C., Gao, W., Zhu, Y., Zhang, F., et al. (2022). Efficacy and Safety of Tacrolimus Combined with Corticosteroids in Patients with Idiopathic Membranous Nephropathy: a Systematic Review and Meta-Analysis of Randomized Controlled Trials. *Int. Urol. Nephrol.* 1, 1. doi:10.1007/s11255-022-03169-6

Tomas, N. M., Beck, L. H., Meyer-Schwesinger, C., Seitz-Polski, B., Ma, H., Zahner, G., et al. (2014). Thrombospondin Type-1 Domain-Containing 7A in Idiopathic Membranous Nephropathy. *N. Engl. J. Med.* 371 (24), 2277–2287. doi:10.1056/NEJMoa1409354

Tomas, N. M., Huber, T. B., and Hoxha, E. (2021). Perspectives in Membranous Nephropathy. *Cell Tissue Res.* 385 (2), 405–422. doi:10.1007/s00441-021-03429-4

Uffing, A., Hullekes, F., Riella, L. V., and Hogan, J. J. (2021). Recurrent Glomerular Disease after Kidney Transplantation: Diagnostic and Management Dilemmas. *Clin. J. Am. Soc. Nephrol.* 16 (11), 1730–1742. doi:10.2215/CJN.00280121

van de Logt, A. E., Hofstra, J. M., and Wetzels, J. F. (2015). Serum Anti-pla2r Antibodies Can Be Initially Absent in Idiopathic Membranous Nephropathy: Seroconversion after Prolonged Follow-Up. *Kidney Int.* 87 (6), 1263–1264. doi:10.1038/ki.2015.34

Wang, M., Chen, D. Q., Chen, L., Cao, G., Zhao, H., Liu, D., et al. (2018). Novel Inhibitors of the Cellular Renin-Angiotensin System Components, Poricoic Acids, Target Smad3 Phosphorylation and Wnt/β-Catenin Pathway against Renal Fibrosis. *Br. J. Pharmacol.* 175 (13), 2689–2708. doi:10.1111/bph.14333

Wang, Q., Dong, Z. Y., Zhang, W. G., Liu, X. M., Qu, Y. L., Duan, S. W., et al. (2020). Diagnostic Efficacy of Serum Anti-phospholipase A2 Receptor Antibodies for Idiopathic Membranous Nephropathy in Patients with Diabetic Kidney Disease. *Clin. Chim. Acta* 502, 222–226. doi:10.1016/j.cca.2019.11.004

Wang, W., Long, H., Huang, W., Zhang, T., Xie, L., Chen, C., et al. (2020). Bu-Shen-Huo-Xue Decoction Ameliorates Diabetic Nephropathy by Inhibiting Rac1/PAK1/p38MAPK Signaling Pathway in High-Fat Diet/Streptozotocin-Induced Diabetic Mice. *Front. Pharmacol.* 11, 587663. doi:10.3389/fphar.2020.587663

Wang, X., Cui, Z., Zhang, Y. M., Qu, Z., Wang, F., Meng, L. Q., et al. (2018). Rituximab for Non-responsive Idiopathic Membranous Nephropathy in a Chinese Cohort. *Nephrol. Dial. Transpl.* 33 (9), 1558–1563. doi:10.1093/ndt/gfx295

Wang, Y. W., Zeng, Q., and Yu, R. H. (2021). Treatment of Membranoproliferative Glomerulonephritis with Traditional Chinese Medicine and Rituximab: A Case Report. *Integr. Med. Nephrol. Androl.* 8, 3.

Wang, Y. (2021). Xiaochaihu Decoction in Diabetic Kidney Disease: A Study Based on Network Pharmacology and Molecular Docking Technology. *Integr. Med. Nephrol. Androl.* 8, 13.

Wu, J., Liu, B., Liang, C., Ouyang, H., Lin, J., Zhong, Y., et al. (2016). Zhen-Wu-tang Attenuates Cationic Bovine Serum Albumin-Induced Inflammatory Response in Membranous Glomerulonephritis Rat through Inhibiting AGEs/RAGE/NF-κB Pathway Activation. *Int. Immunopharmacol.* 33, 33–41. doi:10.1016/j.intimp.2016.01.008

Wu, L., Lai, J., Ling, Y., Weng, Y., Zhou, S., Wu, S., et al. (2021). A Review of the Current Practice of Diagnosis and Treatment of Idiopathic Membranous Nephropathy in China. *Med. Sci. Monit.* 27, e930097. doi:10.12659/MSM.930097

Wu, X., Zhong, Y., Meng, T., Ooi, J. D., Eggenhuizen, P. J., Tang, R., et al. (2021). Patient Survival between Hemodialysis and Peritoneal Dialysis Among End-Stage Renal Disease Patients Secondary to Myeloperoxidase-ANCA-Associated Vasculitis. *Front. Med. (Lausanne)* 8, 775586. doi:10.3389/fmed.2021.775586

Xie, J., Liu, L., Mladkova, N., Li, Y., Ren, H., Wang, W., et al. (2020). The Genetic Architecture of Membranous Nephropathy and its Potential to Improve Non-invasive Diagnosis. *Nat. Commun.* 11 (1), 1600. doi:10.1038/s41467-020-15383-w

Xipell, M., Rodas, L. M., Villarreal, J., Molina, A., Reinoso-Moreno, J., Blasco, M., et al. (2018). The Utility of Phospholipase A2 Receptor Autoantibody in Membranous Nephropathy after Kidney Transplantation. *Clin. Kidney J.* 11 (3), 422–428. doi:10.1093/ckj/sfx128

Xu, Z., Chen, L., Xiang, H., Zhang, C., and Xiong, J. (2020). Advances in Pathogenesis of Idiopathic Membranous Nephropathy. *Kidney Dis. (Basel)* 6 (5), 330–345. doi:10.1159/000507704

Xuan, C., Xi, Y. M., Zhang, Y. D., Tao, C. H., Zhang, L. Y., and Cao, W. F. (2021). Yiqi Jiedu Huayu Decoction Alleviates Renal Injury in Rats with Diabetic Nephropathy by Promoting Autophagy. *Front. Pharmacol.* 12, 624404. doi:10.3389/fphar.2021.624404

Yang, F., Zhang, Q., Yuan, Z., Teng, S., Cui, L., Xue, F., et al. (2021). Signaling Potential Therapeutic Herbal Medicine Prescription for Treating COVID-19 by Collaborative Filtering. *Front. Pharmacol.* 12, 759479. doi:10.3389/fphar.2021.759479

Yang, K., Bai, Y., Yu, N., Lu, B., Han, G., Yin, C., et al. (2020). Huidouba Improved Podocyte Injury by Down-Regulating NOX4 Expression in Rats with Diabetic Nephropathy. *Front. Pharmacol.* 11, 587995. doi:10.3389/fphar.2020.587995

Yang, Y., and Wu, C. (2021). Traditional Chinese Medicine in Ameliorating Diabetic Kidney Disease via Modulating Gut Microbiota. *Integr. Med. Nephrol. Androl.* 8, 8. doi:10.4103/imna.imna_28_21

Yang, Z.-H., Wang, B., Ma, Q., Wang, L., Lin, Y.-X., Yan, H.-F., et al. (2021). Potential Mechanisms of Action of Chinese Patent Medicines for COVID-19: a Review. *Front. Pharmacol.* 12, 668407. doi:10.3389/fphar.2021.668407

Yoshikawa, M., and Asaba, K. (2020). Single-nucleotide Polymorphism Rs4664308 in PLA2R1 Gene Is Associated with the Risk of Idiopathic Membranous Nephropathy: a Meta-Analysis. *Sci. Rep.* 10 (1), 13119. doi:10.1038/s41598-020-70009-x

Yu, H., Han, M., Lin, W., Wang, L., Liu, P., Yang, K., et al. (2020). Efficacy of Chinese Herbal Injections for the Treatment of Primary Nephrotic Syndrome: a Bayesian Network Meta-Analysis of Randomized Controlled Trials. *Front. Pharmacol.* 11, 579241. doi:10.3389/fphar.2020.579241

Yu, X., Cai, J., Jiao, X., Zhang, S., Liu, H., and Ding, X. (2018). Response Predictors to Calcineurin Inhibitors in Patients with Primary Membranous Nephropathy. *Am. J. Nephrol.* 47 (4), 266–274. doi:10.1159/000488728

Yu, X. Y., Sun, Q., Zhang, Y. M., Zou, L., and Zhao, Y. Y. (2022). TGF-β/Smad Signaling Pathway in Tubulointerstitial Fibrosis. *Front. Pharmacol.* 13, 860588. doi:10.3389/fphar.2022.860588

Zhang, J., Luo, D., Lin, Z., Zhou, W., Rao, J., Li, Y., et al. (2020). Dysbiosis of Gut Microbiota in Adult Idiopathic Membranous Nephropathy with Nephrotic Syndrome. *Microb. Pathog.* 147, 104359. doi:10.1016/j.micpath.2020.104359

Zhang, P., Huang, W., Zheng, Q., Tang, J., Dong, Z., Jiang, Y., et al. (2021). A Novel Insight into the Role of PLA2R and THSD7A in Membranous Nephropathy. *J. Immunol. Res.* 2021, 8163298. doi:10.1155/2021/8163298

Zhang, Q. H., Huang, H. Z., Qiu, M., Wu, Z. F., Xin, Z. C., Cai, X. F., et al. (2021). Traditional Uses, Pharmacological Effects, and Molecular Mechanisms of Licorice in Potential Therapy of COVID-19. *Front. Pharmacol.* 12, 719758. doi:10.3389/fphar.2021.719758

Zhang, Y., Bian, S. Z., Yang, K., Wang, Y., Tang, S., Wang, W., et al. (2020). Baseline Soluble Anti-erythropoietin Antibody Level Is an Independent Associated Factor for Follow-Up Erythropoietin Demand in Maintenance Dialysis Patients with End-Stage Renal Disease: a Prospective Cohort Study. *Front. Med. (Lausanne)* 7, 109. doi:10.3389/fmed.2020.00109

Zhang, Z., Lu, X., Dong, L., Ma, J., and Fan, X. (2019). Clinical Observation on the Effect of Wuzhi Soft Capsule on FK506 Concentration in Membranous Nephropathy Patients. *Med. Baltim.* 98 (48), e18150. doi:10.1097/MD.0000000000018150

Zhang, Z. H., He, J. Q., Zhao, Y. Y., Chen, H. C., and Tan, N. H. (2020). Asiatic Acid Prevents Renal Fibrosis in UUO Rats via Promoting the Production of 15d-PGJ2, an Endogenous Ligand of PPAR-γ. *Acta Pharmacol. Sin.* 41 (3), 373–382. doi:10.1038/s41401-019-0319-4

Zheng, R., Deng, Y., Chen, Y., Fan, J., Zhang, M., Zhong, Y., et al. (2012). Astragaloside IV Attenuates Complement Membranous Attack Complex Induced Podocyte Injury through the MAPK Pathway. *Phytother. Res.* 26 (6), 892–898. doi:10.1002/ptr.3656

Zhou, X. F., Wang, Y., Luo, M. J., and Zhao, T. T. (2021). Tangshen Formula Attenuates Renal Fibrosis by Downregulating Transforming Growth Factor β1/Smad3 and LncRNA-MEG3 in Rats with Diabetic Kidney Disease. *Integr. Med. Nephrol. Androl.* 8, 1. doi:10.4103/imna.imna_22_21

Zhu, H., Xu, L., Liu, X., Liu, B., Zhai, C., Wang, R., et al. (2022). Anti-PLA2R Antibody Measured by ELISA Predicts the Risk of Vein Thrombosis in Patients with Primary Membranous Nephropathy. *Ren. Fail* 44 (1), 594–600. doi:10.1080/0886022X.2022.2057861

Zou, H., Jiang, F., and Xu, G. (2020). Effectiveness and Safety of Cyclophosphamide or Tacrolimus Therapy for Idiopathic Membranous Nephropathy. *Intern Med. J.* 50 (5), 612–619. doi:10.1111/imj.14446

Zuo, H. L., Lin, Y. C., Huang, H. Y., Wang, X., Tang, Y., Hu, Y. J., et al. (2021). The Challenges and Opportunities of Traditional Chinese Medicines against COVID-19: a Way Out from a Network Perspective. *Acta Pharmacol. Sin.* 42 (6), 845–847. doi:10.1038/s41401-021-00645-0

Conflict of Interest: The authors declare that the research was conducted in the absence of any commercial or financial relationships that could be construed as a potential conflict of interest.

Publisher's Note: All claims expressed in this article are solely those of the authors and do not necessarily represent those of their affiliated organizations, or those of the publisher, the editors, and the reviewers. Any product that may be evaluated in this article, or claim that may be made by its manufacturer, is not guaranteed or endorsed by the publisher.

frontiers | Frontiers in Pharmacology

ORIGINAL RESEARCH
published: 30 May 2022
doi: 10.3389/fphar.2022.918732

Persistent Activation of Autophagy After Cisplatin Nephrotoxicity Promotes Renal Fibrosis and Chronic Kidney Disease

Ying Fu[1], *Yu Xiang*[1], *Wenwen Wu*[1], *Juan Cai*[1], *Chengyuan Tang*[1] *and Zheng Dong*[1,2]*

[1]*Department of Nephrology, Hunan Key Laboratory of Kidney Disease and Blood Purification, The Second Xiangya Hospital at Central South University, Changsha, China,* [2]*Department of Cellular Biology and Anatomy, Medical College of Georgia at Augusta University and Charlie Norwood VA Medical Center, Augusta, GA, United States*

Autophagy, a highly conserved catabolic pathway in eukaryotic cells, contributes to the maintenance of the homeostasis and function of the kidney. Upon acute kidney injury (AKI), autophagy is activated in renal tubular cells to act as an intrinsic protective mechanism. However, the role of autophagy in the development of chronic kidney pathologies including renal fibrosis after AKI remains unclear. In this study, we detected a persistent autophagy activation in mouse kidneys after nephrotoxicity of repeated low dose cisplatin (RLDC) treatment. 3-methyladenine (3-MA) and chloroquine (CQ), respective inhibitors of autophagy at the initiation and degradation stages, blocked autophagic flux and improved kidney repair in post-RLDC mice, as indicated by kidney weight, renal function, and less interstitial fibrosis. *In vitro*, RLDC induced a pro-fibrotic phenotype in renal tubular cells, including the production and secretion of pro-fibrotic cytokines. Notably, autophagy inhibitors blocked RLDC-induced secretion of pro-fibrotic cytokines in these cells. Together, the results indicate that persistent autophagy after AKI induces pro-fibrotic cytokines in renal tubular cells, promoting renal fibrosis and chronic kidney disease.

Keywords: autophagy, cisplatin, kidney injury and repair, renal fibrosis, profibrotic growth factor

OPEN ACCESS

Edited by:
Zhiyong Guo,
Second Military Medical University, China

Reviewed by:
Ming Chang Hu,
University of Texas Southwestern Medical Center, United States
Jinu Kim,
School of Medicine, Jeju National University, South Korea
Marta Tapparo,
University of Turin, Italy

***Correspondence:**
Zheng Dong
zdong@augusta.edu

Specialty section:
This article was submitted to Renal Pharmacology, a section of the journal Frontiers in Pharmacology

Received: *12 April 2022*
Accepted: *26 April 2022*
Published: *30 May 2022*

Citation:
Fu Y, Xiang Y, Wu W, Cai J, Tang C and Dong Z (2022) Persistent Activation of Autophagy After Cisplatin Nephrotoxicity Promotes Renal Fibrosis and Chronic Kidney Disease. Front. Pharmacol. 13:918732. doi: 10.3389/fphar.2022.918732

INTRODUCTION

Nephrotoxicity is a major limiting factor in the clinical use of cisplatin, a widely used chemotherapy drug that typically results in acute kidney injury (AKI) in 30% of cancer patients (Miller et al., 2010). Even with measures to reduce the acute toxicity, such as repeated low-dose cisplatin (RLDC) therapy (Bennis et al., 2014), the patients receiving cisplatin treatment are still at risk of progressive decline in renal function and the development of chronic kidney disease (CKD) (Skinner et al., 2009). Recent

Abbreviations: AKI, acute kidney injury; ATG, autophagy-related gene; α-SMA, alpha-smooth muscle actin; BSA, bovine serum albumin; BUMPT, Boston University mouse proximal tubular cell line; CKD, chronic kidney disease; CQ, chloroquine; COL-1, collagen type I; CTGF, connective tissue growth factor; DMEM, Dulbecco's modified eagle medium; ECM, extracellular matrix; FN, fibronectin; GFR, glomerular filtration rate; HE, hematoxylin-eosin staining; IHC, immunohistochemistry; IF, immunofluorescence; mTOR, mammalian target of rapamycin; PDGF, platelet-derived growth factor; RLDC, repeated low dose cisplatin; SDS, sodium dodecyl sulfate; Scr, serum creatinine; TGF-β, transforming growth factor-β; TASCC, mTOR-autophagy spatial coupling compartments; VIM, vimentin; 3-MA, 3-methyladenine.

studies have begun to understand the chronic effect of cisplatin nephrotoxicity by using the animal models of RLDC treatment (Torres et al., 2016; Black et al., 2018; Sharp et al., 2018; Shi et al., 2018; Fu et al., 2019; Landau et al., 2019; Sears and Siskind, 2021). For example, we showed that, after 4 weekly injections of 8 mg/kg cisplatin, mice had chronic renal damage, interstitial fibrosis, gradual decline of renal function within 6 months (Fu et al., 2019). In addition, we developed an *in vitro* model of RLDC by treating cultured renal tubular cells repeatedly low doses of cisplatin, which led to pro-fibrotic changes in these cells characterized by the production of pro-fibrotic cytokines (Fu et al., 2019).

Renal tubulointerstitial fibrosis is a common pathological feature of progressive CKD, which is characterized by excessive deposition of extracellular matrix (ECM) in the interstitial space. Interstitial fibrosis is also a pathological feature of maladaptive kidney repair following AKI, which involves a complex interaction between multiple pathways, such as inflammation, cell cycle arrest, mitochondrial damage, autophagy and senescence, to name just a few (Grgic et al., 2012; Venkatachalam et al., 2015; Basile et al., 2016; Humphreys et al., 2016). Under this condition, renal tubular cells may undergo a dramatic change to assume a secretory phenotype for the release of profibrotic cytokines, which stimulate interstitial fibroblasts for fibrosis (Geng et al., 2009; Lan et al., 2012). Multiple mechanisms, such as cycle arrest and senescence, may contribute to the phenotypic change in renal tubular cells during maladaptive kidney repair (Ferenbach and Bonventre, 2015; Venkatachalam et al., 2015; Humphreys et al., 2016; Liu B. et al., 2018).

Autophagy is a conserved lysosomal pathway for degrading cytoplasmic components, which is critical for maintaining renal homeostasis, structure, and function (Tang et al., 2020). In AKI, autophagy is activated as an intrinsic protective mechanism in renal tubular cells (Periyasamy-Thandavan et al., 2008; Jiang et al., 2012; Tang et al., 2018; Deng et al., 2021). However, the role of autophagy in kidney repair after AKI, especially its involvement in the development of interstitial fibrosis, remains unclear and highly controversial (Choi, 2020; Tang et al., 2020). In this regard, autophagy contributes to tubular atrophy, cell death and senescence during the development of chronic kidney pathologies, leading to renal fibrosis (Koesters et al., 2010; Li et al., 2010; Forbes et al., 2011; Xu et al., 2013; Baisantry et al., 2016; Livingston et al., 2016). However, autophagy may degrade extracellular matrix proteins, such as collagen type I, and thereby suppress fibrosis (Kim S. et al., 2012; Ding et al., 2014; Li et al., 2016). It is important to examine the role of autophagy in renal fibrosis by using different models.

In this study, we have investigated autophagy in maladaptive kidney repair and associated renal fibrosis after cisplatin nephrotoxicity induced by RLDC. We show that autophagy was persistently activated during maladaptive kidney repair after RLDC treatment in mice. Autophagy inhibitors given after RLDC improved kidney repair and ameliorated renal fibrosis, supporting a pathogenic role of autophagy in maladaptive kidney repair. Mechanistically, we demonstrate that autophagy in proximal tubules may promote fibrosis by synergistically inducing tubular cell death, tubular atrophy, and especially the production of pro-fibrotic factors such as CTGF, and TGFB.

MATERIALS AND METHODS

Animals

Male C57BL/6 mice (8 weeks of age) purchased from SJA Laboratory Animal Corporation (Changsha, Hunan, China) were housed in the pathogen-free animal facility of the Second Xiangya Hospital under a 12-h light-dark cycle with free access to food and water. Mice received saline vehicle or 8 mg/kg cisplatin (Hansoh Pharma, Jiangsu, China) via intraperitoneal injection once a week for 4 weeks (Fu et al., 2019). For intervention, animals were randomly divided into four groups: saline administration group (vehicle), cisplatin + saline group, cisplatin + chloroquine (CQ) group and cisplatin + 3-methyladenine (3-MA) group (n = 6/group). After the last cisplatin injection, CQ (60 mg/kg/day), 3-MA (20 mg/kg/day) or saline was administered to mice by intraperitoneal injection for seven consecutive days. Both chloroquine (C6628) and 3-methyladenine (M9281) were purchased from Sigma-Aldrich. Animals were sacrificed at 1 week, 1 month, or 6 months after the last cisplatin injection to collect samples. The kidneys were fresh frozen in liquid nitrogen or fixed in 10% neutral buffered formalin. All animal experiments were conducted in accordance with a protocol approved by the Institutional Animal Care and Use Committee of the Second Xiangya Hospital of Central South University.

Cell Culture and Treatment

The Boston University mouse proximal tubular cell line (BUMPT) was originally obtained from Dr. Lieberthal (Boston University) and cultured in DMEM medium with 10% FBS and 10% streptomycin as previously (Fu et al., 2019). To observe the fibrotic phenotype and apoptosis induced by different cisplatin concentrations, BUMPT cells were subjected to four cycles of treatment with 0, 0.5, 1, 2 or 5 μM cisplatin. Each cycle consisted of 7 h of cisplatin incubation and 17 h of recovery in cisplatin-free medium. Also, to observe the changes in autophagy and fibrosis phenotypes at different time points under 2 μM cisplatin, we collected cell samples at the end of cycles 0, 1, 2, 3, and 4, respectively. For CQ or 3-MA treatment, cells were subjected to four cycles of treatment with 2 μM cisplatin, and then incubated with 20 μM chloroquine (CQ) or 10 mM 3-methyladenine (3-MA) for 17 h in cisplatin-free medium. For detection of autophagic flux in cells, BUMPT cells were transiently transfected with mRFP-GFP-LC3 (ptfLC3, Addgene plasmid 21,074). Cells were processed 24 h after transfection. RFP and GFP fluorescence images were collected by confocal microscopy (Zeiss, United States). The numbers of GFP-LC3 puncta per cell and RFP-LC3 puncta per cell were counted separately using ImageJ. The number of autophagosomes was represented by GFP dots, and the number of autolysosomes was obtained by subtracting GFP dots from RFP dots. The number of autolysosomes was divided by the total number of RFP spots to express the autophagic flux rate.

Assessment of Serum Creatinine

Serum creatinine was measured by using a commercial kit (DICT-500) from BioAssay Systems as previously described (Tang et al., 2018). In brief, blood samples were collected for coagulation and centrifugation at room temperature to collect serum. Serum samples were added to a pre-warmed (37°C) reaction mixture and the absorbance at 510 nm was monitored kinetically at 0 and 5 min of reaction. Creatinine levels (mg/dl) were then calculated based on standard curves.

Transcutaneous Measurement of Glomerular Filtration Rate

GFR was measured in mice by transcutaneously monitoring the clearance of FITC-labeled sinistrin. Briefly, mice were anesthetized with isoflurane through an inhalation anesthesia device. A small patch on the flank of the mice was then shaved, and the transdermal GFR monitors were adhered to the skin using a double-sided adhesive patch (MediBeacon, Mannheim, Germany). Devices were secured on the mouse by wrapping with medical tape. FITC-sinistrin (7 mg/100 g b. w.) was injected via a tail vein. Mice were placed back in their cages separately, and GFR was monitored for 1–2 h. The devices were then removed, and data were analyzed using elimination kinetics curve of FITC-sinistrin as previously described (Ellery et al., 2015; Fu et al., 2019).

Histological Staining

Hematoxylin and eosin staining. Kidney tissues were fixed with 4% paraformaldehyde, embedded in paraffin, and cut into 4 μm sections for hematoxylin and eosin staining. The renal cortex and outer medulla were examined. The degree of morphological changes was determined by light microscopy in a blinded fashion. The following measures were chosen as an indication of morphological damage to the kidney after treatment with vehicle or cisplatin: tubular necrosis, loss of the brush border, proximal tubule degradation, tubular casts, presence of inflammatory cells, and interstitial fibrosis. These measures were evaluated on a scale of 0–4, which ranged from not present 0) to mild 1), moderate 2), severe 3), and very severe 4).

Masson trichrome staining. Masson trichrome staining was performed to evaluate collagen fibrils in renal tissues using the reagents from Servicebio (Wuhan, China). For quantification, 10-20 positive collagen-stained fields (× 100 magnification) were randomly selected from each section and analyzed by Image-Pro Plus 6.0. The ratio of the blue-stained area to the area of the entire field (glomeruli, tubule lumina, and blood vessels, if any, excluded) was assessed and expressed as a percentage of the fibrotic area.

Immunofluorescence Staining

For immunofluorescence of LC3B, a modified immunofluorescence staining protocol was performed as previously described (35). Briefly, kidney tissue sections were deparaffinized and subjected to antigen retrieval in a buffer with EDTA. The following steps were performed using the Tyramide SuperBoost™ Kit and Alexa Fluor™ Tyramides (Thermo Fisher Scientific, United States). The slides were incubated with 3% hydrogen peroxide solution for 1 h at room temperature. After washing with PBS, they were incubated with blocking buffer for 1 h, and then exposed to 1:5,000 anti-LC3 (NB100-2220, Novus Biologicals) overnight at 4°C, followed by incubation with Alexa Fluor 594-conjugated goat anti-rabbit IgG for 1 h at room temperature. After washing with PBS, the slides were incubated in tyramide working solution and then reaction stop reagent. For quantification, 10 to 20 random fields (800 magnification) were selected for each tissue to evaluate the LC3B puncta in each tubule; For fluorescent staining of collagen I, slides were washed with PBS and fixed with cold methanol:acetone (1:1) for 10 min at room temperature. After washing, fixed cells were blocked with 10% normal goat serum for 30 min. Cells were then incubated with anti-collagen I (AF7001, Affinity, Jiangsu, China) overnight at 4°C and exposed to goat anti-rabbit IgG conjugated to Alexa Fluor 594 for 1 h at room temperature. Hoechst 33,342 was used as a counterstain of the nucleus.

ELISA

ELISA kits of CTGF(CSB-E07877 m), TGF-β1 (CSB-E04726 months) were from CUSABIO BIOTECH (Wuhan, China). Briefly, cell specimens were centrifuged at 1,000 g for 15 min at 4°C to collect cell culture supernatants. 100 μl standard and test samples were added to the wells respectively, covered with stickers after mixing, and incubated at 37 °C for 2 h. Then 100 μl biotin-labeled antibody working solution was added to each well and incubated at 37 °C for 1 h. The plate was washed three times, and 100 μl horseradish peroxidase-labeled avidin working solution was added to each well, and incubated at 37°C for 1 h. Then, 90 μl substrate solution was added in sequence, and the color was developed at 37°C for 15–30 min in the dark. 50 μl stop solution was added to stop the reaction. The optical density (OD value) of each well was measured with a microplate reader at a wavelength of 450 nm within 5 min after the reaction was terminated. A standard curve was constructed by measuring OD of the standards. Finally, the sample concentration was calculated according to the equation of the standard curve.

Immunoblot Analysis

Renal cortical and outer medulla tissues were lysed using 2% SDS buffer with 1% protease inhibitor cocktail (P8340, Sigma-Aldrich). Protein concentration was determined using a Pierce BCA protein assay kit (no. 23225) from Thermo Scientific. Equal amounts of proteins were separated by SDS-polyacrylamide gels and then transferred onto polyvinylidene difluoride membranes. Membranes were blocked with 5% fat-free milk or 5% BSA for 1 h and subsequently incubated with primary antibodies at 4°C overnight and secondary antibodies for 1 h at room temperature. Primary antibodies used in present study were from following sources: anti-Vimentin 5,741) and anti-cleaved Caspase-3 (Asp175) 9,661) from Cell Signaling Technology; anti-LC3B (NB100-2220) from Novus Biologicals; anti-α-Smooth Muscle Actin (ab5694) and anti-Fibronectin (ab2413) from Abcam; anti-GAPDH (10494-1-AP) from Proteintech; anti-

TABLE 1 | Primer sequences used for quantitative qPCR.

Gene	Forward	Reverse
Tgfβ	*5′- GAGCCCGAAGCGGACTACTA-3′*	*5′-GTTGTTGCGGTCCACCATT-3′*
Ctgf	*5′- GACCCAACTATGATGCGAGCC-3′*	*5′-TCCCACAGGTCTTAGAACAGG-3′*
Pdgfβ	*5′-TCTCTGCTGCTACCTGCGTCTG-3′*	*5′-CGTCTTGCACTCGGCGATTACAG-3′*
Gapdh	*5′-AGGTCGGTGTGAACGGATTTG-3′*	*5′-GGGGTCGTTGATGGCAACA-3′*

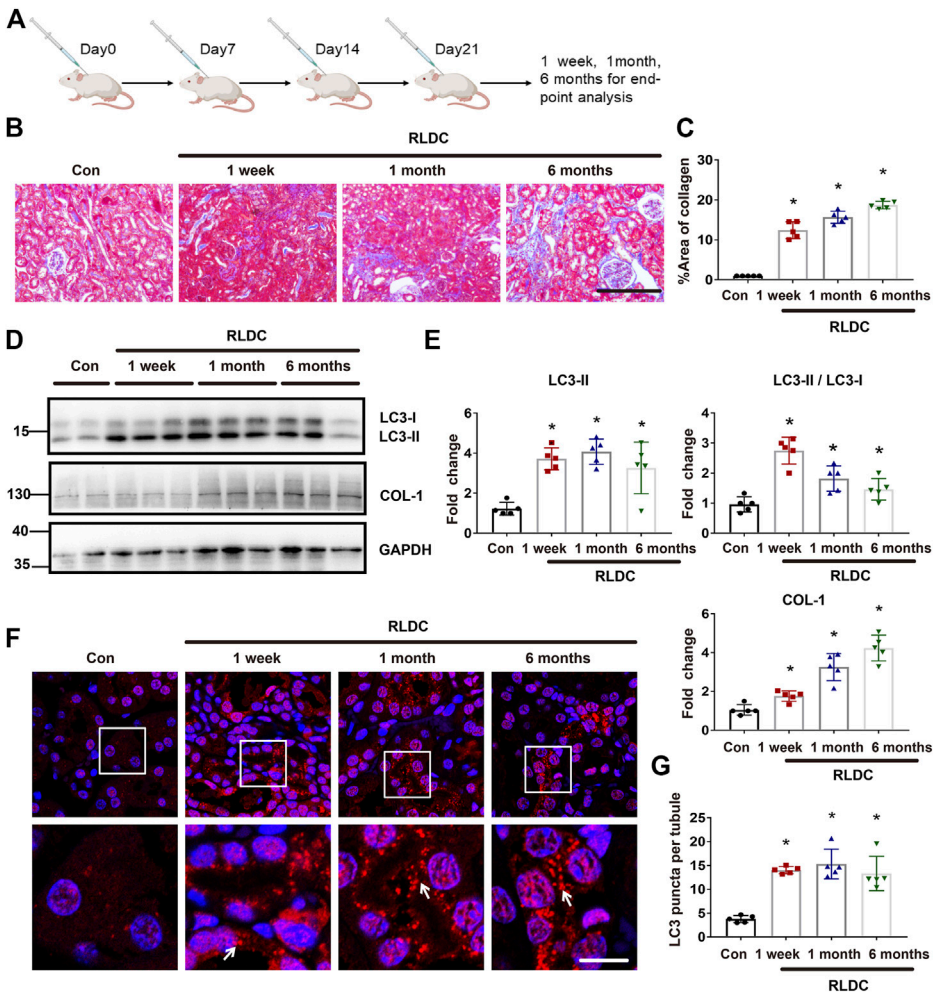

FIGURE 1 | Persistent autophagy activation in kidneys after RLDC treatment in mice. Male C57BL/6 mice were injected weekly with 8 mg/kg cisplatin for 4 weeks (RLDC) or with saline as control (Con) to collect samples at 1 week, 1 month and 6 months later. **(A)** The schematic representation of the RLDC model regimen. **(B)** Masson staining of kidney tissues. ($n = 5$, bar = 50 μm). **(C)** Statistical analysis of the area of collagen deposition in Masson staining. **(D)** Representative immunoblots of LC3, COL-1 and GAPDH (loading control) in kidney tissues ($n = 5$). **(E)** Densitometry of LC3II, LC3II/LC3I and COL-1. The experiments were normalized according to GAPDH expression. The protein level of control group (Con) was arbitrarily set as 1, and the signals of other conditions were normalized with the control group to indicate their protein fold changes. **(F)** Representative images of immunofluorescence staining of LC3B. ($n = 5$). **(G)** Statistical analysis of the number of LC3B spots per renal tubule. All quantitative data are expressed as mean ± SEM. *$p < 0.05$ vs the control group (Con).

Collagen 1 (AF7001) from Affinity; all secondary antibodies for immunoblot analysis from Thermo Fisher Scientific. Antigen-antibody complexes on the membranes were detected with an enhanced chemiluminescence kit from Thermo Scientific. For quantification, protein bands were analyzed with ImageJ software.

Quantitative Real-Time PCR

Total RNA from kidney tissues and cells was extracted with TRIzol reagents from CWBIO (Jiangsu, China) according to the manufacturer's protocol. cDNA was synthesized using Taqman RT reagents (TaKaRa, Japan). Quantitative real-time PCR was performed using the TB Green Premix Ex Taq II

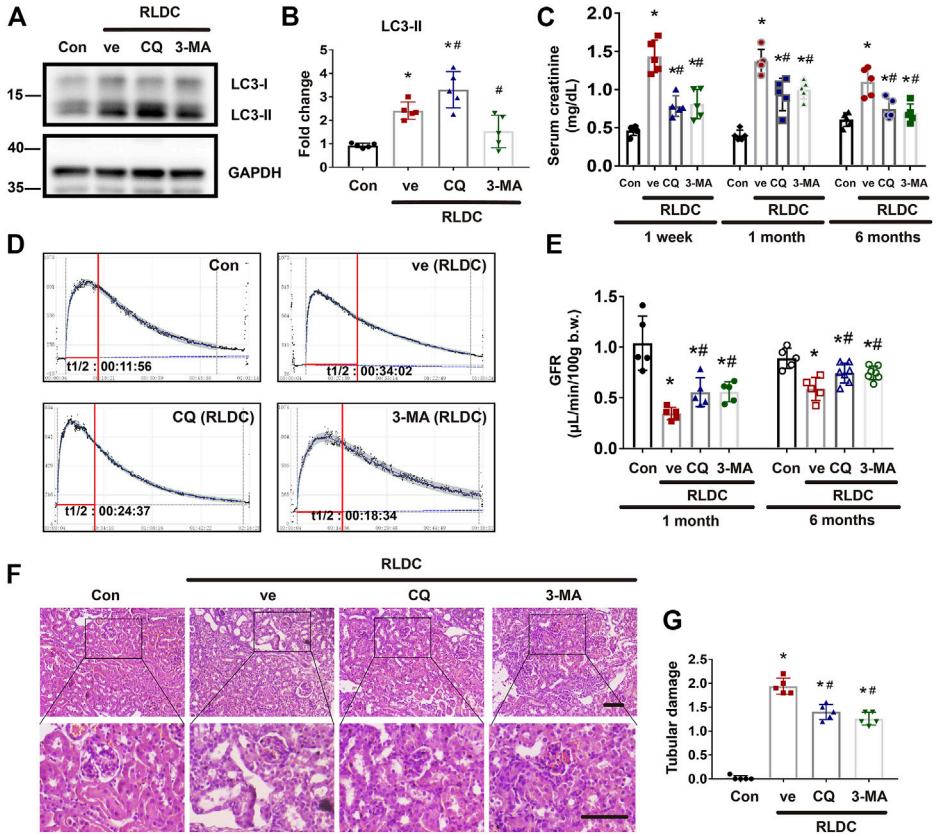

FIGURE 2 | Pharmacologic inhibition of autophagy alleviates renal dysfunction and tubular damage in post-RLDC kidneys. Male C57BL/6 mice were injected weekly with 8 mg/kg cisplatin for 4 weeks (RLDC) or with saline as control (Con). After the final dose, the mice were injected with 60 mg/kg/day chloroquine (CQ), 20 mg/kg/day 3-methyladenine (3-MA), or saline as vehicle solution (ve) for 7 days. **(A)** Representative immunoblots of LC3-I, LC3-II and GAPDH (loading control) in kidney tissues ($n = 5$). **(B)** Densitometry of LC3II. The experiments were normalized according to GAPDH expression. The protein level of control group (Con) was arbitrarily set as 1, and the signals of other conditions were normalized with the control group to indicate their protein fold changes. **(C)** Effect of autophagy inhibitor on serum creatinine at 1 week, 1 month and 6 months after RLDC treatment. ($n = 5$). **(D)** Representative tracing curves of FITC-sinistrin clearance in mice. ($n = 5$). **(E)** GFR measurement by transcutaneously monitoring FITC-sinistrin clearance ($n = 5$). **(F)** Representative histology images of hematoxylin-eosin staining of kidney tissues in renal cortex and outer medulla. ($n = 5$, bar = 50 μm). **(G)** Pathological score of tubular damage. Quantitative data are expressed as mean ± SEM. $^{*}p < 0.05$ vs the control group (Con), $^{\#}p < 0.05$ vs. (RLDC + vehicle) group.

reagent (TaKaRa) on a LightCycler96 Real-Time PCR System. Relative expression was normalized to the expression levels of GAPDH. The primer sequences used for qPCR are shown in **Table 1**.

Statistics

All *in vivo* qualitative data are representative of at least six individual animals and *in vitro* qualitative data are representative of at least five independent experiments. Morphological analysis was performed in a blinded fashion. Quantitative data are presented as mean ± SD. Statistical analysis was performed using GraphPad Prism seven software. The statistical differences of multiple groups were determined by performing multiple comparisons with ANOVA followed by Tukey's posttests, while statistical differences between two groups were determined by two-tailed unpaired or paired Student's *t* test. The value of $p < 0.05$ was considered significantly different.

RESULTS

Persistent Autophagy Activation in Kidneys After RLDC Treatment in Mice

C57BL/6 mice were subjected to RLDC treatment that included 4 weekly injections of 8 mg/kg cisplatin (**Figure 1A**). Consistent with our previous work (Fu et al., 2019), we detected renal interstitial fibrosis at 1 week, 1 month, and 6 months after RLDC treatment by Masson staining (**Figures 1B,C**) and immunoblot analysis of collagen-I (COL-1), a fibrosis marker protein (**Figures 1D,E**). Interestingly, we detected autophagy activation at all these time points after RLDC treatment (**Figures 1D,E**). At 1 week after RLDC treatment, the autophagy marker LC3B-II increased in renal tissue to approximately 4 times over control, and was maintained at this high level at 1 and 6 months (**Figures 1D,E**). In immunofluorescence analysis, control mouse kidneys showed ~4 LC3-positive spots per proximal tubule, which was increased ~15 at 1 week, 1 month, and 6 months after RLDC treatment (**Figures 1F,G**). These results

indicate that autophagy is persistently induced during maladaptive kidney repair after cisplatin nephrotoxicity.

Pharmacologic Inhibition of Autophagy Alleviates Renal Dysfunction and Tubular Damage in Post-RLDC Kidneys

To delineate the role of autophagy in maladaptive kidney repair, we studied the effects of two pharmacological inhibitors of autophagy, 3-methyladenine (3-MA) and chloroquine (CQ). 3-MA is a class III phosphatidylinositol 3-kinase inhibitor that suppresses the initial step of autophagosome formation, whereas CQ is a lysosomotropic weak base that inhibits autophagosome fusion with lysosomes and autophagic degradation (Klionsky et al., 2021). We first examined LC3 by immunoblotting. As expected, CQ induced LC3-II accumulation, whereas 3-MA reduced LC3-II formation (**Figures 2A,B**). For renal function, compared with the normal saline group, the serum creatinine level increased by more than 2 times at 1 week after RLDC treatment. However, the serum creatinine increase in post-RLDC mice was significantly reduced by CQ and 3-MA (**Figure 2C**). Moreover, we measured glomerular filtration rate (GFR) by monitoring the clearance of injected FITC-sinistrin. As shown by the clearance curves, the half-life (t1/2) of excreted FITC-sinistrin was significantly prolonged after the RLDC regimen, indicative of a decline of renal function after RLDC treatment (**Figure 2D**). Notably, both CQ and 3-MA reduced the half-life of FITC excretion and increased the clearance in post-RLDC mice (**Figure 2D**). For quantification, we calculated the GFR of these mice. As shown in **Figure 2E**, the GFR value of post-RLDC mice was 0.4–0.5 μl/min/100 g b. w., half of the control mice, which was improved to 0.5–0.7 μl/min/100 g b. w. by CQ and 3-MA after 1-month RLDC regimen. And the GFR value of 6-months-RLDC mice was 0.5–0.7 μl/min/100 g b. w, which was improved to 0.8–0.9 μl/min/100 g b. w. by CQ and 3-MA. Moreover, post-RLDC kidneys developed a series of pathological features, including interstitial inflammation, tubular cell death, phenotypic transition of resident renal cells, proliferation and activation of fibroblasts, and excessive ECM deposition, leading to renal fibrosis (Torres et al., 2016; Black et al., 2018; Fu et al., 2019). Histological analysis by hematoxylin-eosin staining showed that at 1 month after RLDC, renal tubules were significantly damaged, manifested by extensive necrosis of proximal tubules, cast formation, and tubular cell atrophy. There were also tubular dilation and obvious expansion of the interstitium. These pathological changes were attenuated by CQ, which reduced significantly tubular atrophy and lowered tubule damage score (**Figures 2F,G**). Similar effects were shown for 3-MA, the other autophagy inhibitor tested. Taken together, these results suggest that persistent autophagy in the kidney may contribute to the development of renal pathologies and the decline of renal function after RLDC treatment.

Inhibition of Autophagy Suppresses Interstitial Fibrosis After RLDC Regimen

Next, we specifically analyzed the role of autophagy in renal fibrogenesis in post-RLDC kidneys. Following RLDC treatment, renal interstitial fibrosis was significantly induced. Both CQ and 3-MA partially but significantly reduced the expression of fibrosis proteins in post-RLDC mouse kidneys, including fibronectin (FN), a-SMA and vimentin (VIM) (**Figure 3A**). This conclusion was substantiated by densitometry analysis of the immunoblots (**Figure 3B**). Masson staining further verified that CQ and 3-MA significantly reduced interstitial collagen fibril deposition in post-RLDC kidneys (**Figure 3C**). Morphometry showed that RLDC induced 15–17% of interstitial fibrosis at 1 month after RLDC treatment, which was reduced to 9–10% by CQ and 3-MA, and 19–20% of collagen deposition at 6 months, which was reduced to 10–12% by CQ and 3-MA (**Figure 3D**). The inhibitory effects of CQ and 3-MA support a role of autophagy in renal fibrogenesis during maladaptive kidney repair after cisplatin nephrotoxicity.

RLDC Treatment Induces Autophagy and Fibrotic Phenotypes in Bumpt Cells

We recently established an *in vitro* model of RLDC treatment, in which mouse kidney proximal tubular BUMPT cells were treated with low concentrations of cisplatin for 7 h daily for 4 days (Fu et al., 2019). In this model, we examined the induction of autophagy along with fibrotic changes. It was found that the fibrosis marker fibronectin (FN) was not induced until the second cycle of cisplatin exposure, whereas the autophagy marker LC-3II was elevated after the first cycle (**Figures 4A,B**). Morphologically, confluent BUMPT cells formed cobblestone monolayers typical of epithelium with evident cell junctions. After RLDC incubation, the cells changed to a spindle-shaped, fibroblast-like morphology (**Figure 4C**). We further analyzed autophagy by expressing the mRFP-GFP-LC3 tandem plasmid. Following transfection, the cells showed only minimal punctate staining under control conditions. After RLDC treatment, the cells had a large number of green GFP-LC3 and red mRFP-LC3 puncta (**Figures 4D,E**). The puncta with both GFP-LC3 and mRFP-LC3 signals were autophagosomes and appeared yellow in overlapping images. Once fused with lysosomes, the acid-sensitive GFP fluorescence disappeared, while the acid-insensitive RFP signal remained to indicate autolysosomes. We counted the GFP-LC3 puncta and the mRFP-LC3 puncta to calculate the autophagic flux rate (Livingston et al., 2016; Livingston et al., 2019; Klionsky et al., 2021), which increased from 8% in control cells to about 40% in RLDC-treated cells (**Figure 4F**). These results indicate that RLDC dynamically activate autophagy in renal tubular cells, showing the induction of autophagosome formation and the maturation into autolysosomes.

Inhibition of Autophagy Suppresses Fibrotic Phenotype Changes in RLDC-Treated BUMPT Cells

Next, we investigated the effect of autophagy inhibition on fibrotic changes *in vitro*. To do this, BUMPT cells were incubated subjected to repeated treatment with 2uM cisplatin in the absence or presence of CQ and 3-MA. Both CQ and 3-MA ameliorated RLDC-induced cellular spindle-shaped

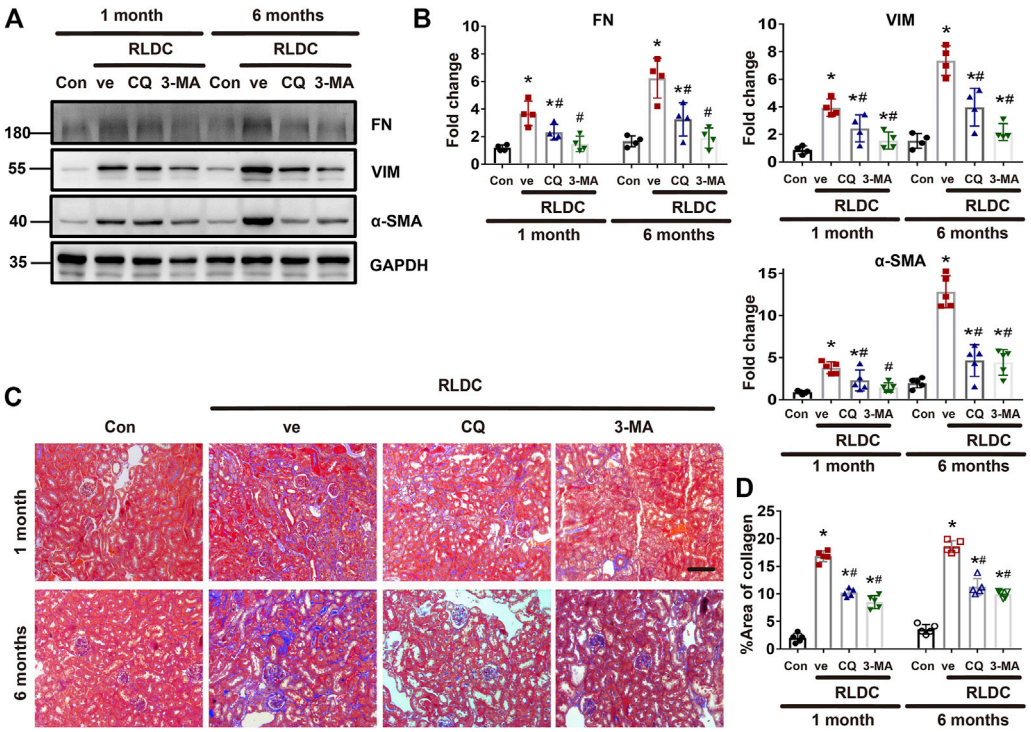

FIGURE 3 | Inhibition of autophagy suppresses interstitial fibrosis after RLDC regimen. Male C57BL/6 mice were injected weekly with 8 mg/kg cisplatin for 4 weeks (RLDC) or with saline as control (Con). After the final dose, the mice were injected with 60 mg/kg/day chloroquine (CQ), 20 mg/kg/day 3-methyladenine (3-MA), or saline as vehicle solution (ve) for 7 days. **(A)** Representative immunoblots of FN, VIM, a-SMA and GAPDH (loading control) in kidney tissues ($n = 5$). **(B)** Densitometry of FN, VIM, and a-SMA. The experiments were normalized according to GAPDH expression. The protein level of control group (Con) was arbitrarily set as 1, and the signals of other conditions were normalized with the control group to indicate their protein fold changes. **(C)** Masson staining of kidney tissues. ($n = 5$, bar = 50 μm). **(D)** Statistical analysis of area of collagen deposition in Masson staining images. Data are expressed as mean ± SEM. $^{*}p < 0.05$ vs the control group (Con), $^{\#}p < 0.05$ vs. (RLDC + vehicle) group.

morphological changes (**Figure 5A**). As expected, CQ blocked autophagic flux resulting in LC3B-II increase, whereas 3-MA decreased LC3B-II production (**Figure 5B**). Under this condition, CQ and 3-MA reduced RLDC-induced accumulation of fibrotic marker proteins like COL-1 and VIM (**Figures 5B,C**). Immunofluorescence staining also confirmed that autophagy inhibited reduced collagen I in RLDC-treated cells (**Figure 5D**). Taken together, these results suggest that autophagy activation by RLDCs may contribute to the production of fibrotic protein markers and the induction of fibrotic phenotypes in proximal tubular cells.

Autophagy Inhibitors Suppress the Expression and Secretion of Pro-fibrotic Growth Factors in RLDC-Treated Bumpt Cells

Mechanistically, we hypothesized that autophagy might promote renal fibrosis by inducing the expression and secretion of pro-fibrotic cytokines in kidney tubular cells. To test this possibility, after RLDC treatment, BUMPT cells were given CQ, 3-MA, or saline as control. We analyzed the expression of pro-fibrotic growth factors *Ctgf*, *Tgfβ* and *Pdgfβ* (Kok et al., 2014; Lee et al., 2015). RLDC induced mRNA expression of *Ctgf*, *Tgfβ* and *Pdgfβ*, and the former two were attenuated by both CQ and 3-MA (**Figure 6A**). To examine the secretion of these factors, we collected cell culture media for ELISA. The results showed that after RLDC treatment, the secretion of CTGF and TGFB by BUMPT cells increased 2-3-fold (**Figure 6B**). 3-MA treatment significantly reduced the secretion of CTGF and TGFB, while CQ only affected the secretion of TGFB. These results suggest that autophagy inhibitors reduce the induction of fibrotic phenotypes probably by reducing the expression and secretion of specific pro-fibrotic cytokines.

DISCUSSION

The role of autophagy in maladaptive kidney repair including especially renal fibrosis has been very controversial (Kim S. et al., 2012; Kim W. et al., 2012; Bernard et al., 2014; Ding et al., 2014; Li et al., 2016; Livingston et al., 2016; Shu et al., 2021). In previous work, we characterized the key features of maladaptive kidney repair in mice after RLDC treatment, including persistent inflammation, progressive interstitial fibrosis, "atubular" glomerulus and renal function decline, and further established an *in vitro* model of RLDC treatment of cultured renal tubular cells (Fu et al., 2019). Using these models, we have examined

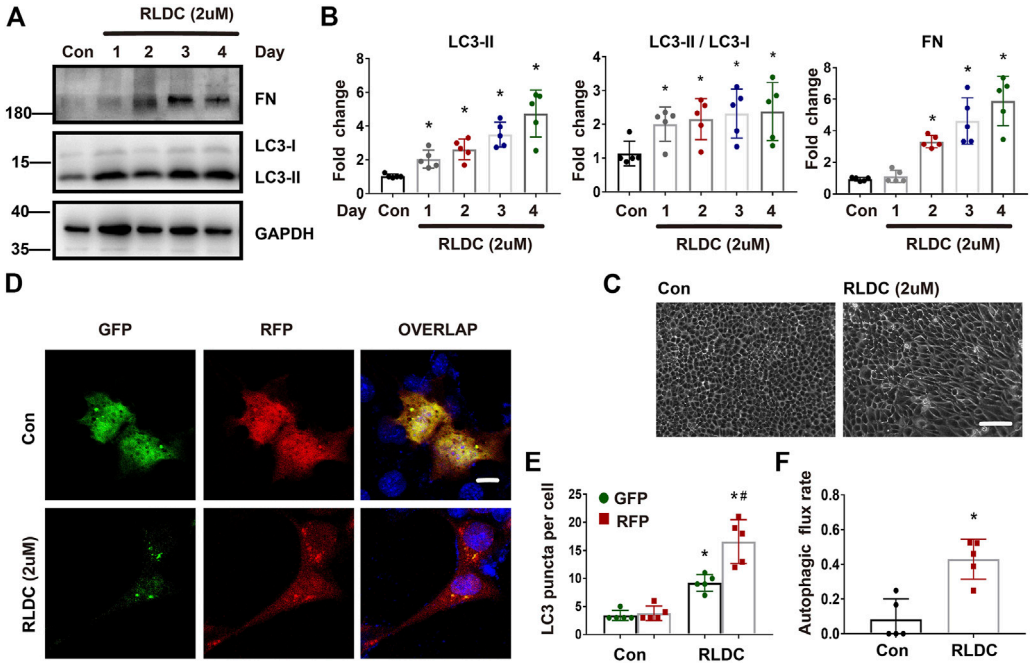

FIGURE 4 | RLDC treatment induces autophagy and fibrotic phenotypes in BUMPT cells. BUMPT cells were incubated with 2 μM cisplatin for 7 h each day for 4 days (RLDC) or without cisplatin exposure (Con). **(C–F)**. **(A)** Representative immunoblots of FN, LC3-I, LC3-II and GAPDH (loading control) in cells after different cycles of cisplatin treatment. (n = 5). **(B)** Densitometry of FN and LC3-II, LC3II/LC3I. The experiments were normalized according to GAPDH expression. The protein level of control group (Con) was arbitrarily set as 1, and the signals of other conditions were normalized with the control group to indicate their protein fold changes. **(C)** Morphologies of control and RLDC-treated cells. (bar = 50 μm). **(D)** BUMPT cells were transiently transfected with mRFP-GFP-LC3. RFP and GFP fluorescence images were collected at 24 h after transfection by confocal microscopy. **(E)** The numbers of GFP-LC3 puncta per cell and RFP-LC3 puncta per cell were counted separately using ImageJ. The number of autophagosomes is represented by GFP dots, and the number of autolysosomes was obtained by subtracting GFP dots from RFP dots. (n = 5). **(F)** Autophagic flux rate. (n = 5). Quantitative data are expressed as mean ± SEM. *p < 0.05 vs the control group (Con).

autophagy in maladaptive kidney repair and renal fibrosis after cisplatin nephrotoxicity. We detected persistent autophagy after RLDC treatment in mice and in renal tubular cells. By using pharmacological inhibitors targeting different stages of autophagy, we further demonstrated that autophagy contributes to RLDC-induced renal fibrosis *in vivo* and fibrotic phenotypes in proximal tubular cells. We also found that inhibition of autophagy reduced the degree of tubular atrophy and histopathological damage, and protected against chronic renal function decline. In the cultured renal proximal tubular cells, RLDC induced accumulation of fibrotic protein markers and secretion of pro-fibrotic growth factors, which was attenuated by autophagy inhibitors. Taken together, these results support a critical role of autophagy in maladaptive kidney repair and interstitial fibrosis following cisplatin nephrotoxicity. Mechanistically, autophagy may promote fibrosis by coordinating and inducing the production and secretion of pro-fibrotic cytokines.

We have previously shown that in nephrotoxic AKI, induction of autophagy prevents tubular cell damage and death (Periyasamy-Thandavan et al., 2008; Jiang et al., 2012; Liu J. et al., 2018; Wang et al., 2018). As for the role of autophagy in maladaptive repair, we reported the role of autophagy in unilateral ureteral obstruction (UUO) mice in 2016 (Livingston et al., 2016). In that study, autophagy was induced persistently in UUO kidneys, especially in renal tubules. Remarkably, pharmacological inhibition of autophagy with CQ and 3-MA as well as ablation of autophagy-related gene 7 (Atg7) specifically from kidney proximal tubules reduced interstitial fibrosis in UUO, indicating that tubular autophagy in renal tubules promotes renal fibrosis. Consistently, blockade of autophagy suppressed TGFB1-induced fibrotic changes in cultured renal tubular cells. Furthermore, our recent study demonstrated the reciprocal regulation between endoplasmic reticulum stress and autophagy in chronic kidney injury and fibrosis (Shu et al., 2021). Specifically, autophagy was activated during ER stress and led to renal fibrosis. These observations are consistent with our current study, which demonstrates the pro-fibrotic function of autophagy during maladaptive kidney repair after cisplatin nephrotoxicity. However, Kim and others reported that in UUO rats, inhibition of autophagy with 30 mg/kg 3-MA increased tubular apoptosis and interstitial fibrosis (Kim W. et al., 2012), an observation that was opposite to what we found. The cause of this discrepancy might be the disparity between the model species, as well as the difference in 3-MA dosing. Of note, 3-MA, in addition to its ability to inhibit class III PI3-kinase and associated autophagy, it may also inhibit class I PI3-kinases that regulate various cellular signaling such as membrane trafficking and mTORC1 activation (Mizushima et al., 2010). Taking this into consideration, high doses

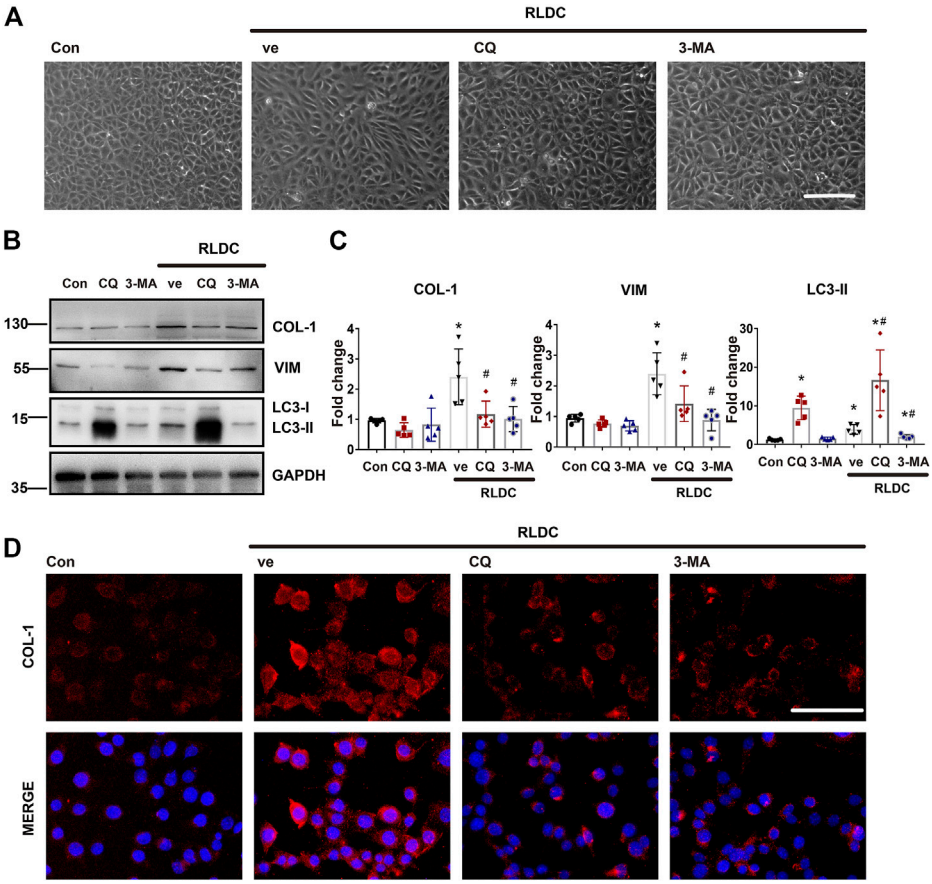

FIGURE 5 | Inhibition of autophagy suppresses fibrotic phenotype changes in RLDC-treated BUMPT cells. BUMPT cells were incubated with 2 μM cisplatin for 7 h each day for 4 days (RLDC) or without cisplatin exposure (Con). After the last 7 h of cisplatin treatment, cells were incubated with 20 μM chloroquine (CQ) or 10 mM 3-methyladenine (3-MA) for 17 h in cisplatin-free medium. Cells were collected for morphological observation or biochemical analyses. **(A)** Cell morphology under light microscope after RLDC induction with or without CQ and 3-MA. (bar = 50 μm). **(B)** Representative immunoblots of COL-1, VIM, LC3-I, LC3-II and GAPDH (loading control). ($n = 5$). **(C)** Densitometry of COL-1, VIM, and LC3-II. The experiments were normalized according to GAPDH expression. The protein level of control group (Con) was arbitrarily set as 1, and the signals of other conditions were normalized with the control group to indicate their protein fold changes. **(D)** Immunofluorescence of COL-1. (n = 5, bar = 50 μm). Quantitative data are expressed as mean ± SEM. $^{*}p < 0.05$ vs the control group (Con). $^{\#}p < 0.05$ vs. (RLDC + vehicle) group.

of 3-MA may produce adverse effects that are not dependent on autophagy, thereby impairing tubular cell viability. In this regard, Kim et al. used 1.5 times higher dosage of 3-MA than we did. Furthermore, they showed only an early but transient induction of autophagy (within 1 week) in the rat proximal tubules, whereas autophagy remained persistently activated for 6 months after RLDC treatment in our study. Pertaining to this, Li et al. showed that sustained autophagy in proximal tubules may inhibit tubular proliferation and repair during the recovery phase (Li et al., 2014). The pro-fibrotic role of tubular autophagy was also demonstrated by the study of Baisantry et al. (Baisantry et al., 2016), in which proximal tubule autophagy-related 5 (Atg5) knockout mice showed less interstitial fibrosis and improved renal function 30 days after ischemia/reperfusion injury. In contrast, Li et al. reported that selective ablation of Atg5 in proximal renal tubules significantly aggravated G2/M arrest, COL1 production, and fibrosis in UUO mice (Li et al., 2016). Although both studies tested Atg5 knockout mice, they examined renal fibrosis in different disease models. Therefore, the role of autophagy in renal fibrosis and chronic kidney disease may depend on the experimental model, animal species, and the timing or duration of autophagy activation.

For the mechanism whereby autophagy promotes renal fibrosis, we hypothesized that autophagy may promote a pro-fibrotic phenotype in renal tubular cells, which produce and secrete pro-fibrotic cytokines. To initially test this possibility, in this study we examined representative pro-fibrotic cytokines, such as TGFB, CTGF, and PDGFB. The expression of these pro-fibrotic growth factors was significantly increased after RLDC treatment (**Figure 6**). Notably, autophagy inhibition attenuated the production of TGFB and CTGF, but not PDGFB. This observation indicates that, rather than general effects, autophagy promotes specific pro-fibrotic cytokines. In addition, we observed that the two

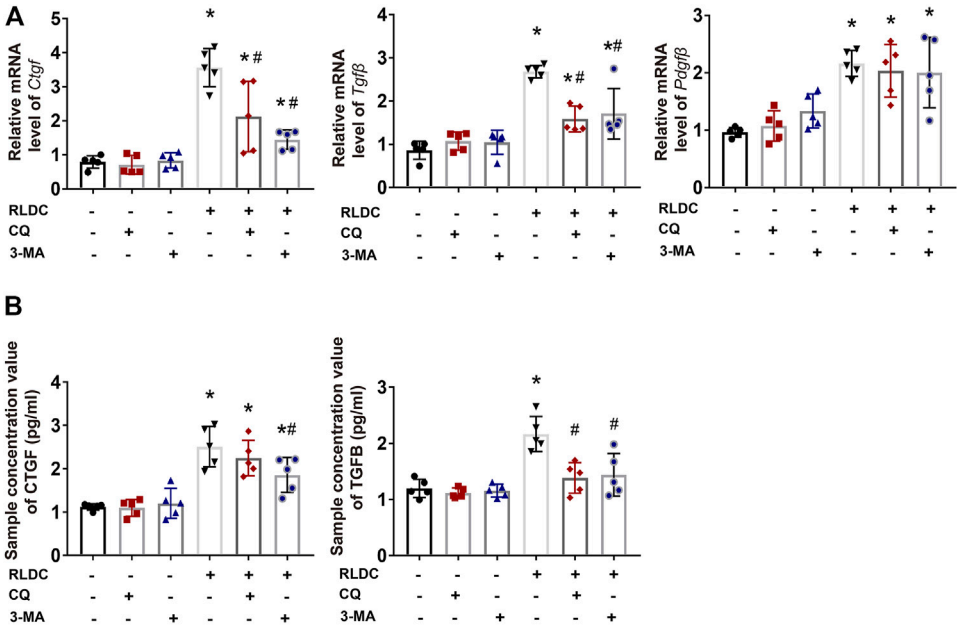

FIGURE 6 | Autophagy inhibitors suppress the expression and secretion of pro-fibrotic growth factors in RLDC-treated BUMPT cells. BUMPT cells were incubated with 2 μM cisplatin for 7 h each day for 4 days (RLDC) or without cisplatin exposure (Con). After the last 7 h of cisplatin treatment, cells were incubated with 20 μM chloroquine (CQ) or 10 mM 3-methyladenine (3-MA) for 17 h in cisplatin-free medium. **(A)** The mRNA levels of *Ctgf, Tgfbβ* and *Pdgfβ* in cells quantified by qRT-PCR showing the inhibitory effect of CQ and 3-MA ($n = 5$). Data are normalized to *Gapdh* and expressed as fold change compared to controls. **(B)** CTGF and TGFB in cell culture medium detected by Elisa. ($n = 5$). Data are expressed as mean ± SEM. $^{*}p < 0.05$ vs the control group (Con). $^{\#}p < 0.05$ vs. (RLDC + vehicle) group.

autophagy inhibitors, CQ and 3-MA, had different effects on TGFB and CTGF. For example, the inhibitory effect of 3-MA on CTGF is stronger than that of CQ, and it further affects the secretion of CTGF. The stronger effect of 3-MA may be due to its synergistic actions. It is known that, some PI3 kinase inhibitors, in addition to inhibiting autophagosome formation, may also inhibit mTOR by targeting its ATP-binding site (Mizushima et al., 2010). Furthermore, in addition to renal tubular cells, autophagy-regulated production of pro-fibrotic secretory proteins has also been demonstrated in fibroblasts. For instance, in a model of chronic serum starvation of fibroblasts, sustained autophagy activates MTORC2 signaling, resulting in enhanced expression and secretion of CTGF, which favors the transformation of fibroblasts into myofibroblasts (Bernard et al., 2014).

It remains unclear how autophagy promotes the expression and secretion of specific pro-fibrotic factors. As eluded above, we speculate that persistent autophagy may lead to phenotypic changes in renal tubular cells. Especially, autophagy may promote cell cycle arrest, metabolic shift, and/or senescence, which are known to contribute to maladaptive kidney repair including interstitial fibrosis (Venkatachalam et al., 2015; Zheng et al., 2019; Tang et al., 2020; Kitada and Koya, 2021). In a recent study, Canaud and others demonstrated the formation of mTOR-autophagy spatial coupling compartments (TASCCs), which promoted the secretion of profibrotic factors during maladaptive kidney repair (Canaud et al., 2019). Future studies should examine the effect of autophagy blockade on cell cycle arrest, senescence, and the formation of TASCCs after RLDC treatment. One limitation of this study is the possible off-target effects of the autophagy inhibitors. As mentioned above, 3-MA may also inhibit the class I PI3-kinases and, in turn, regulate various cellular signaling such as membrane trafficking and mTORC1 activation (Mizushima et al., 2010). In addition to interfering with autophagic flux, CQ in endosomes/lysosomes also inhibits post-translational modification of newly synthesized proteins in endoplasmic reticulum or trans-Golgi network vesicles (e.g, glyco-syltransferases and proteases involved in the post translational processing that requires low pH) (Yoon et al., 2010; Ferreira et al., 2021). In addition, CQ could activate the transcriptional response of p53 to induce the activation of p53-regulated genes such as apoptotic gene targets (pig3 and bax) (Ferreira et al., 2021). In view of these off-target effects, we tested both 3-MA and CQ in the present study. Since these two inhibitors had similar inhibitory effects on renal fibrosis in post-RLDC kidneys, the results provide relatively reliable evidence for the pro-fibrotic role of autophagy in this model. We also tested rapamycin (1 mg/kg) as autophagy inducer in a pilot experiment, which did not have significant effects on renal function or Masson's staining of renal fibrosis after RLDC treatment in mice. But, rapamycin reduced the

expression of some fibrosis proteins like fibronectin and vimentin. Our explanation is that this effect of rapamycin was due to its inhibition of mTOR and related protein synthesis, and not due to its effect on autophagy.

In conclusion, in this study we have detected persistent autophagy activation in both *in vivo* and *in vitro* RLDC models of maladaptive kidney repair after cisplatin nephrotoxicity. We have further demonstrated that inhibition of autophagy improved kidney repair and attenuated renal interstitial fibrosis in these models, suggesting a critical role of autophagy in the development of chronic kidney problems after cisplatin nephrotoxicity. The pro-fibrotic function of autophagy is associated with its coordinated regulation of tubular cell death and the production and secretion of pro-fibrotic cytokines. Targeting autophagy may provide a new strategy to reduce renal fibrosis to prevent the progression of related renal diseases including CKD.

CHEMICAL COMPOUNDS

Chemical compounds studied in this article: Cisplatin (PubChem CID: 5702198); Chloroquine (PubChem CID: 2719); 3-Methyladenine (PubChem CID: 135398661).

DATA AVAILABILITY STATEMENT

The original contributions presented in the study are included in the article/**Supplementary Material**, further inquiries can be directed to the corresponding author.

ETHICS STATEMENT

The animal study was reviewed and approved by Animal Ethics Committee of The Second Xiangya Hospital of Central South University.

AUTHOR CONTRIBUTIONS

ZD and YF designed this study; YF performed most of the experiments; YF, YX, WW, and JC contributed to data analysis; ZD and YF analyzed results; CT and JC provided suggestions for manuscript preparation; ZD and YF contributed to manuscript writing.

FUNDING

This study was financially supported by National Natural Science Foundation of China (81720108008, 82090024), National Key R&D Program of China (2020YFC2005000), the Natural Science Foundation of Hunan Province (2020JJ5798) and the Fundamental Research Funds for the Central Universities of Central South University (2021zzts0392).

SUPPLEMENTARY MATERIAL

The Supplementary Material for this article can be found online at: https://www.frontiersin.org/articles/10.3389/fphar.2022.918732/full#supplementary-material

REFERENCES

Baisantry, A., Bhayana, S., Rong, S., Ermeling, E., Wrede, C., Hegermann, J., et al. (2016). Autophagy Induces Prosenescent Changes in Proximal Tubular S3 Segments. *J. Am. Soc. Nephrol.* 27 (6), 1609–1616. doi:10.1681/ASN.2014111059

Basile, D., Bonventre, J., Mehta, R., Nangaku, M., Unwin, R., Rosner, M., et al. (2016). Progression after AKI: Understanding Maladaptive Repair Processes to Predict and Identify Therapeutic Treatments. *J. Am. Soc. Nephrol.* 27 (3), 687–697. doi:10.1681/ASN.2015030309

Bennis, Y., Savry, A., Rocca, M., Gauthier-Villano, L., Pisano, P., and Pourroy, B. (2014). Cisplatin Dose Adjustment in Patients with Renal Impairment, Which Recommendations Should We Follow? *Int. J. Clin. Pharm.* 36 (2), 420–429. doi:10.1007/s11096-013-9912-7

Bernard, M., Dieudé, M., Yang, B., Hamelin, K., Underwood, K., and Hébert, M. (2014). Autophagy Fosters Myofibroblast Differentiation through MTORC2 Activation and Downstream Upregulation of CTGF. *Autophagy* 10 (12), 2193–2207. doi:10.4161/15548627.2014.981786

Black, L., Lever, J., Traylor, A., Chen, B., Yang, Z., Esman, S., et al. (2018). Divergent Effects of AKI to CKD Models on Inflammation and Fibrosis. *Am. J. Physiol. Ren. Physiol.* 315 (4), F1107–F18. doi:10.1152/ajprenal.00179.2018

Canaud, G., Brooks, C. R., Kishi, S., Taguchi, K., Nishimura, K., Magassa, S., et al. (2019). Cyclin G1 and TASCC Regulate Kidney Epithelial Cell G-M Arrest and Fibrotic Maladaptive Repair. *Sci. Transl. Med.* 11 (476), eaav4754. doi:10.1126/scitranslmed.aav4754

Choi, M. (2020). Autophagy in Kidney Disease. *Annu. Rev. Physiol.* 82, 297–322. doi:10.1146/annurev-physiol-021119-034658

Deng, Z., Sun, M., Wu, J., Fang, H., Cai, S., An, S., et al. (2021). SIRT1 Attenuates Sepsis-Induced Acute Kidney Injury via Beclin1 Deacetylation-Mediated Autophagy Activation. *Cell death Dis.* 12 (2), 217. doi:10.1038/s41419-021-03508-y

Ding, Y., Kim, S., Lee, S., Koo, J., Wang, Z., and Choi, M. (2014). Autophagy Regulates TGF-β Expression and Suppresses Kidney Fibrosis Induced by Unilateral Ureteral Obstruction. *J. Am. Soc. Nephrol.* 25 (12), 2835–2846. doi:10.1681/ASN.2013101068

Ellery, S., Cai, X., Walker, D., Dickinson, H., and Kett, M. (2015). Transcutaneous Measurement of Glomerular Filtration Rate in Small Rodents: through the Skin for the Win? *Nephrol. Carlt. Vic.* 20 (3), 117–123. doi:10.1111/nep.12363

Ferenbach, D., and Bonventre, J. (2015). Mechanisms of Maladaptive Repair after AKI Leading to Accelerated Kidney Ageing and CKD. *Nat. Rev. Nephrol.* 11 (5), 264–276. doi:10.1038/nrneph.2015.3

Ferreira, P., Sousa, R., Ferreira, J., Militão, G., and Bezerra, D. (2021). Chloroquine and Hydroxychloroquine in Antitumor Therapies Based on Autophagy-Related Mechanisms. *Pharmacol. Res.* 168, 105582. doi:10.1016/j.phrs.2021.105582

Forbes, M., Thornhill, B., and Chevalier, R. (2011). Proximal Tubular Injury and Rapid Formation of Atubular Glomeruli in Mice with Unilateral Ureteral Obstruction: a New Look at an Old Model. *Am. J. Physiol. Ren. Physiol.* 301 (1), F110–F117. doi:10.1152/ajprenal.00022.2011

Fu, Y., Cai, J., Li, F., Liu, Z., Shu, S., Wang, Y., et al. (2019). Chronic Effects of Repeated Low-Dose Cisplatin Treatment in Mouse Kidneys and Renal Tubular Cells. *Am. J. Physiol. Ren. Physiol.* 317 (6), F1582–F92. doi:10.1152/ajprenal.00385.2019

Geng, H., Lan, R., Wang, G., Siddiqi, A., Naski, M., Brooks, A., et al. (2009). Inhibition of Autoregulated TGFbeta Signaling Simultaneously Enhances Proliferation and Differentiation of Kidney Epithelium and Promotes Repair Following Renal Ischemia. *Am. J. Pathol.* 174 (4), 1291–1308. doi:10.2353/ajpath.2009.080295

Grgic, I., Campanholle, G., Bijol, V., Wang, C., Sabbisetti, V., Ichimura, T., et al. (2012). Targeted Proximal Tubule Injury Triggers Interstitial

Fibrosis and Glomerulosclerosis. *Kidney Int.* 82 (2), 172–183. doi:10.1038/ki.2012.20

Humphreys, B., Cantaluppi, V., Portilla, D., Singbartl, K., Yang, L., Rosner, M., et al. (2016). Targeting Endogenous Repair Pathways after AKI. *J. Am. Soc. Nephrol.* 27 (4), 990–998. doi:10.1681/ASN.2015030286

Jiang, M., Wei, Q., Dong, G., Komatsu, M., Su, Y., and Dong, Z. (2012). Autophagy in Proximal Tubules Protects against Acute Kidney Injury. *Kidney Int.* 82 (12), 1271–1283. doi:10.1038/ki.2012.261

Kim, S., Na, H., Ding, Y., Wang, Z., Lee, S., and Choi, M. (2012). Autophagy Promotes Intracellular Degradation of Type I Collagen Induced by Transforming Growth Factor (TGF)-β1. *J. Biol. Chem.* 287 (15), 11677–11688. doi:10.1074/jbc.M111.308460

Kim, W., Nam, S., Song, H., Ko, J., Park, S., Kim, H., et al. (2012). The Role of Autophagy in Unilateral Ureteral Obstruction Rat Model. *Nephrol. Carlt. Vic.* 17 (2), 148–159. doi:10.1111/j.1440-1797.2011.01541.x

Kitada, M., and Koya, D. (2021). Autophagy in Metabolic Disease and Ageing. *Nat. Rev. Endocrinol.* 17 (11), 647–661. doi:10.1038/s41574-021-00551-9

Klionsky, D., Abdel-Aziz, A., Abdelfatah, S., Abdellatif, M., Abdoli, A., Abel, S., et al. (2021). Guidelines for the Use and Interpretation of Assays for Monitoring Autophagy (4th Edition). *Autophagy* 17 (1), 1–382. doi:10.1080/15548627.2015.1100356

Koesters, R., Kaissling, B., Lehir, M., Picard, N., Theilig, F., Gebhardt, R., et al. (2010). Tubular Overexpression of Transforming Growth Factor-Beta1 Induces Autophagy and Fibrosis but Not Mesenchymal Transition of Renal Epithelial Cells. *Am. J. Pathol.* 177 (2), 632–643. doi:10.2353/ajpath.2010.091012

Kok, H., Falke, L., Goldschmeding, R., and Nguyen, T. (2014). Targeting CTGF, EGF and PDGF Pathways to Prevent Progression of Kidney Disease. *Nat. Rev. Nephrol.* 10 (12), 700–711. doi:10.1038/nrneph.2014.184

Lan, R., Geng, H., Polichnowski, A., Singha, P., Saikumar, P., McEwen, D., et al. (2012). PTEN Loss Defines a TGF-β-Induced Tubule Phenotype of Failed Differentiation and JNK Signaling during Renal Fibrosis. *Am. J. Physiol. Ren. Physiol.* 302 (9), F1210–F1223. doi:10.1152/ajprenal.00660.2011

Landau, S., Guo, X., Velazquez, H., Torres, R., Olson, E., Garcia-Milian, R., et al. (2019). Regulated Necrosis and Failed Repair in Cisplatin-Induced Chronic Kidney Disease. *Kidney Int.* 95 (4), 797–814. doi:10.1016/j.kint.2018.11.042

Lee, S., Kim, S., and Choi, M. (2015). Therapeutic Targets for Treating Fibrotic Kidney Diseases. *Transl. Res. J. lab. Clin. Med.* 165 (4), 512–530. doi:10.1016/j.trsl.2014.07.010

Li, H., Peng, X., Wang, Y., Cao, S., Xiong, L., Fan, J., et al. (2016). Atg5-mediated Autophagy Deficiency in Proximal Tubules Promotes Cell Cycle G2/M Arrest and Renal Fibrosis. *Autophagy* 12 (9), 1472–1486. doi:10.1080/15548627.2016.1190071

Li, L., Wang, Z., Hill, J., and Lin, F. (2014). New Autophagy Reporter Mice Reveal Dynamics of Proximal Tubular Autophagy. *J. Am. Soc. Nephrol. JASN.* 25 (2), 305–315. doi:10.1681/ASN.2013040374

Li, L., Zepeda-Orozco, D., Black, R., and Lin, F. (2010). Autophagy Is a Component of Epithelial Cell Fate in Obstructive Uropathy. *Am. J. pathology* 176 (4), 1767–1778. doi:10.2353/ajpath.2010.090345

Liu, B., Tang, T., Lv, L., and Lan, H. (2018). Renal Tubule Injury: a Driving Force toward Chronic Kidney Disease. *Kidney Int.* 93 (3), 568–579. doi:10.1016/j.kint.2017.09.033

Liu, J., Livingston, M., Dong, G., Tang, C., Su, Y., Wu, G., et al. (2018). Histone Deacetylase Inhibitors Protect against Cisplatin-Induced Acute Kidney Injury by Activating Autophagy in Proximal Tubular Cells. *Cell death Dis.* 9 (3), 322. doi:10.1038/s41419-018-0374-7

Livingston, M., Ding, H., Huang, S., Hill, J., Yin, X., and Dong, Z. (2016). Persistent Activation of Autophagy in Kidney Tubular Cells Promotes Renal Interstitial Fibrosis during Unilateral Ureteral Obstruction. *Autophagy* 12 (6), 976–998. doi:10.1080/15548627.2016.1166317

Livingston, M., Wang, J., Zhou, J., Wu, G., Ganley, I., Hill, J., et al. (2019). Clearance of Damaged Mitochondria via Mitophagy Is Important to the Protective Effect of Ischemic Preconditioning in Kidneys. *Autophagy* 15 (12), 2142–2162. doi:10.1080/15548627.2019.1615822

Miller, R., Tadagavadi, R., Ramesh, G., and Reeves, W. (2010). Mechanisms of Cisplatin Nephrotoxicity. *Toxins* 2 (11), 2490–2518. doi:10.3390/toxins2112490

Mizushima, N., Yoshimori, T., and Levine, B. (2010). Methods in Mammalian Autophagy Research. *Cell* 140 (3), 313–326. doi:10.1016/j.cell.2010.01.028

Periyasamy-Thandavan, S., Jiang, M., Wei, Q., Smith, R., Yin, X., and Dong, Z. (2008). Autophagy Is Cytoprotective during Cisplatin Injury of Renal Proximal Tubular Cells. *Kidney Int.* 74 (5), 631–640. doi:10.1038/ki.2008.214

Sears, S., and Siskind, L. (2021). Potential Therapeutic Targets for Cisplatin-Induced Kidney Injury: Lessons from Other Models of AKI and Fibrosis. *J. Am. Soc. Nephrol.* 32 (7), 1559–1567. doi:10.1681/asn.2020101455

Sharp, C., Doll, M., Megyesi, J., Oropilla, G., Beverly, L., and Siskind, L. (2018). Subclinical Kidney Injury Induced by Repeated Cisplatin Administration Results in Progressive Chronic Kidney Disease. *Am. J. Physiol. Ren. Physiol.* 315 (1), F161–F72. doi:10.1152/ajprenal.00636.2017

Shi, M., McMillan, K., Wu, J., Gillings, N., Flores, B., Moe, O., et al. (2018). Cisplatin Nephrotoxicity as a Model of Chronic Kidney Disease. *Lab. Invest. a J. Tech. Methods Pathol.* 98 (8), 1105–1121. doi:10.1038/s41374-018-0063-2

Shu, S., Wang, H., Zhu, J., Liu, Z., Yang, D., Wu, W., et al. (2021). Reciprocal Regulation between ER Stress and Autophagy in Renal Tubular Fibrosis and Apoptosis. *Cell death Dis.* 12 (11), 1016. doi:10.1038/s41419-021-04274-7

Skinner, R., Parry, A., Price, L., Cole, M., Craft, A., and Pearson, A. (2009). Persistent Nephrotoxicity during 10-year Follow-Up after Cisplatin or Carboplatin Treatment in Childhood: Relevance of Age and Dose as Risk Factors. *Eur. J. cancer* 45 (18), 3213–3219. doi:10.1016/j.ejca.2009.06.032

Tang, C., Han, H., Yan, M., Zhu, S., Liu, J., Liu, Z., et al. (2018). PINK1-PRKN/PARK2 Pathway of Mitophagy Is Activated to Protect against Renal Ischemia-Reperfusion Injury. *Autophagy* 14 (5), 880–897. doi:10.1080/15548627.2017.1405880

Tang, C., Livingston, M., Liu, Z., and Dong, Z. (2020). Autophagy in Kidney Homeostasis and Disease. *Nat. Rev. Nephrol.* 16 (9), 489–508. doi:10.1038/s41581-020-0309-2

Torres, R., Velazquez, H., Chang, J., Levene, M., Moeckel, G., Desir, G., et al. (2016). Three-Dimensional Morphology by Multiphoton Microscopy with Clearing in a Model of Cisplatin-Induced CKD. *J. Am. Soc. Nephrol. JASN* 27 (4), 1102–1112. doi:10.1681/ASN.2015010079

Venkatachalam, M., Weinberg, J., Kriz, W., and Bidani, A. (2015). Failed Tubule Recovery, AKI-CKD Transition, and Kidney Disease Progression. *J. Am. Soc. Nephrol.* 26 (8), 1765–1776. doi:10.1681/ASN.2015010006

Wang, Y., Tang, C., Cai, J., Chen, G., Zhang, D., Zhang, Z., et al. (2018). PINK1/Parkin-mediated Mitophagy Is Activated in Cisplatin Nephrotoxicity to Protect against Kidney Injury. *Cell death Dis.* 9 (11), 1113. doi:10.1038/s41419-018-1152-2

Xu, Y., Ruan, S., Wu, X., Chen, H., Zheng, K., and Fu, B. (2013). Autophagy and Apoptosis in Tubular Cells Following Unilateral Ureteral Obstruction Are Associated with Mitochondrial Oxidative Stress. *Int. J. Mol. Med.* 31 (3), 628–636. doi:10.3892/ijmm.2013.1232

Yoon, Y., Cho, K., Hwang, J., Lee, S., Choi, J., and Koh, J. (2010). Induction of Lysosomal Dilatation, Arrested Autophagy, and Cell Death by Chloroquine in Cultured ARPE-19 Cells. *Invest. Ophthalmol. Vis. Sci.* 51 (11), 6030–6037. doi:10.1167/iovs.10-5278

Zheng, K., He, Z., Kitazato, K., and Wang, Y. (2019). Selective Autophagy Regulates Cell Cycle in Cancer Therapy. *Theranostics* 9 (1), 104–125. doi:10.7150/thno.30308

Conflict of Interest: The authors declare that the research was conducted in the absence of any commercial or financial relationships that could be construed as a potential conflict of interest.

Publisher's Note: All claims expressed in this article are solely those of the authors and do not necessarily represent those of their affiliated organizations, or those of the publisher, the editors and the reviewers. Any product that may be evaluated in this article, or claim that may be made by its manufacturer, is not guaranteed or endorsed by the publisher.

frontiers | Frontiers in Pharmacology

ORIGINAL RESEARCH
published: 02 June 2022
doi: 10.3389/fphar.2022.900346

BMP-7 Upregulates Id2 Through the MAPK Signaling Pathway to Improve Diabetic Tubulointerstitial Fibrosis and the Intervention of Oxymatrine

Yawen Xiao[1,2], *Dan Liang*[1,2], *Zhiyang Li*[1,2], *Zhaowei Feng*[1,2], *Zhiping Yuan*[3], *Fan Zhang*[1,2], *Yuanyuan Wang*[1,2], *Yuxia Zhou*[1,2], *Mingjun Shi*[1,2], *Lingling Liu*[1,2], *Ying Xiao*[1,2]* and *Bing Guo*[1,2]*

[1]Guizhou Provincial Key Laboratory of Pathogenesis and Drug Research on Common Chronic Diseases, Guizhou Medical University, Guizhou, China, [2]Department of Pathophysiology, Guizhou Medical University, Guizhou, China, [3]School Hospital, Guizhou Medical University, Guiyang, China

Diabetic kidney disease is one of the most serious microvascular complications of diabetes. It progresses irreversibly to end-stage renal disease if left untreated. Bone morphogenetic protein (BMP)-7 is a negative regulator of organ fibrosis and may also play an essential role in tubulointerstitial fibrosis. This study aimed to investigate the precise role and potential molecular mechanisms of BMP-7 in the progression of diabetic nephropathy. In this study, BMP-7 was overexpressed *in vivo* after the replication of the diabetic rat model using streptozotocin. The results showed that BMP-7 inhibited the phosphorylation of related mitogen-activated protein kinase (MAPK) pathways while upregulating the inhibitor of differentiation (Id2) expression and effectively ameliorated pathological renal injury. Further *in vitro* validation showed that the inhibition of the phosphorylation of MAPKs at a high glucose concentration in renal tubular epithelial cells was followed by the upregulation of Id2 protein expression, suggesting that BMP-7 could improve diabetic nephropathy by upregulating Id2 protein levels through the BMP-7–MAPK signaling pathway. Previous laboratory studies found that oxymatrine improved renal fibrotic lesions. However, the exact mechanism is unclear. The present study showed that oxymatrine treatment in a diabetic rat model upregulated BMP-7 protein expression and inhibited MAPK pathway protein phosphorylation levels. These results suggested that oxymatrine improved the epithelial-to-mesenchymal transition process in the early stage of diabetic kidney disease by regulating the BMP-7–MAPK pathway and ameliorated renal tubulointerstitial fibrosis.

Keywords: BMP-7, Id2, MAPKs, oxymatrine, tubulointerstitial fibrosis

OPEN ACCESS

Edited by:
Zhiyong Guo,
Second Military Medical University, China

Reviewed by:
Zhonghui Zhu,
Capital Medical University, China
Miyuki Kobara,
Kyoto Pharmaceutical University, Japan

***Correspondence:**
Ying Xiao
yxhx20060725@126.com
Bing Guo
guobingbs@126.com

Specialty section:
This article was submitted to Renal Pharmacology, a section of the journal Frontiers in Pharmacology

Received: *20 March 2022*
Accepted: *13 May 2022*
Published: *02 June 2022*

Citation:
Xiao Y, Liang D, Li Z, Feng Z, Yuan Z, Zhang F, Wang Y, Zhou Y, Shi M, Liu L, Xiao Y and Guo B (2022) BMP-7 Upregulates Id2 Through the MAPK Signaling Pathway to Improve Diabetic Tubulointerstitial Fibrosis and the Intervention of Oxymatrine. Front. Pharmacol. 13:900346. doi: 10.3389/fphar.2022.900346

INTRODUCTION

Diabetic kidney disease (DKD) is one of the most common and severe chronic microvascular complications of diabetes mellitus (DM). Tubulointerstitial fibrosis (TIF) is considered to be the "final common pathway" to renal function loss in DKD. Renal function and prognosis in patients with DKD may ultimately be more related to TIF than to classical and early glomerular changes (Bonner et al., 2020). Increasing evidence shows that the epithelial-to-mesenchymal transition

(EMT) plays a vital role in the TIF process (Liu et al., 2019). Renal fibrosis involves the deposition of the fibrotic matrix and scarring in response to severe or persistent injury. Despite its involvement in the wound healing process, persistent fibrosis can damage tissue structure and organ function, eventually leading to renal failure. Chronic injury to the kidney promotes multiple pathological changes, including EMT, which exerts its pro-fibrotic function by secreting collagen I, III, and V and fibronectin, leading to the accumulation of extracellular matrix (ECM) and, ultimately, tubulointerstitial fibrosis (Yuqing et al., 2021). Many genes and proteins are known to be involved in this complex and influential process of EMT. However, the specific regulatory mechanisms remain unclear, especially regarding the changes in the expression of negative regulators that may play an equally important role in the fibrosis process and their regulatory mechanisms.

Bone morphogenetic proteins (BMPs) are homodimeric members of the transforming growth factor β (TGF-β) superfamily (Aluganti Narasimhulu and Singla, 2021). Kidneys are considered the primary site of BMP-7 synthesis during embryonic and postnatal development (Mo et al., 2021). BMP-7 is an essential regulator for maintaining the typical phenotype of renal tubular epithelial cells. The level of BMP-7 is significantly reduced while increased levels of BMP-7 expression can inhibit EMT in various animal models of acute kidney injury or chronic renal fibrosis (Mo et al., 2021). During renal fibrosis, the effect of BMP-7 to impede the development of fibrosis involves reversing glomerular hypertrophy, reducing tubular atrophy, maintaining the tubular epithelial cell phenotype, delaying the EMT process, and inhibiting ECM synthesis (Sun et al., 2017). As the HDAC inhibitor, SFN prevents diabetes-induced renal fibrosis through epigenetic upregulation of BMP-7 (Kong et al., 2021). BMP-7 effectively inhibits TGF-β1-induced EMT by inhibiting Wnt3/β-linked protein and TGF-β1/Smad2/3 signaling pathways (Song et al., 2020). The collagen formation mediated by TGF-β can be inhibited by BMP-7, and this inhibition is accomplished by BMP-7-induced expression of Inhibitor of differentiation 2 (Id2) in murine pulmonary myofibers. Id2 can bind to the type I collagen A2 promoter to form a heterodimer, rendering it inactive transcriptionally (Kim et al., 2015). Id2 is a negative regulatory protein of nuclear transcription factors widely present in mammalian cells. It is a member of the helix-loop-helix family of transcription factors (Ito et al., 2021). Recent studies have shown that reduced Id2 protein expression plays a vital role in developing fibrosis in various organ tissues. Id2 overexpression after myocardial infarction was found to inhibit cardiac fibrosis (Yin et al., 2019). The overexpression of Id2 maintains the alveolar epithelial cell phenotype in pulmonary fibrosis, attenuating pulmonary fibrosis (Yang et al., 2015). A previous study by our group (Xiao et al., 2019) suggested that the EMT process in renal tubular epithelial cells might be associated with the decrease in Id2 expression. The addition of different doses of BMP-7 (100 and 200 ng/ml) to renal tubular epithelial cells cultured in a high-glucose environment *in vitro* showed that BMP-7 induced the upregulation of Id2 expression in renal tubular epithelial cells cultured in a high concentration of glucose, restored E-cadherin expression, and delayed EMT in renal tubular epithelial cells (Liu et al., 2016), suggesting that BMP-7 regulated Id2 expression in renal tubular epithelial cells under the high-glucose status. However, how BMP-7 regulates Id2 expression in renal tubular epithelial cells is not well understood.

Mitogen-activated protein kinases (MAPKs) regulate various cellular programs, including embryogenesis, proliferation, differentiation, and apoptosis, based on cues from the cell surface, metabolic state, and cellular environment. The MAPK pathway is activated in several glomerular and tubulointerstitial diseases, including diabetic nephropathy; together, they mediate signaling in fibrosis. The inhibition of the MAPK signaling pathway reverses EMT progression and renal fibrosis (Yuqing et al., 2021). Many studies have shown that the MAPK pathway regulates EMT as a non-Smad signaling pathway. The inhibition of the MAPK signaling pathway reversed EMT progression and renal fibrosis (Li et al., 2017; Geng et al., 2020). However, most studies focused on the regulation of these proteins at a single site. Whether BMP-7 regulates Id2 through an MAPK signaling pathway during the transdifferentiation of diabetic renal tubular epithelial cells to mesenchymal cells and the development of renal tubular–interstitial fibrosis has not been reported.

Oxymatrine (OMT) is a quinacrine alkaloid extracted from *Scutellaria baicalensis* with an extensive source and a molecular structure of $C_{15}H_{24}N_2O_2$ and a molecular weight of 264.360 g/mol. It is confirmed that the protective mechanism of OMT is mainly related to anti-inflammatory, anti-oxidative stress, anti- or pro-apoptotic, antifibrotic, metabolic modulation, and anti-nociception effects *in vitro* and *in vivo*. In addition, OMT can affect various signaling pathways, cells, and cytokines, and maximum therapeutic results can be achieved through these combined effects (Lan et al., 2020). Pre-laboratory studies found that OMT could delay the process of high glucose–induced EMT in renal tubular epithelial cells; the possible mechanism was to facilitate DKD tubulointerstitial fibrosis by inhibiting the transcriptional activation of Twist protein on downstream EMT-related target genes through the upregulation of Id2 expression (Ying et al., 2020). However, the specific mechanism of OMT for Id2 regulation remains to be further investigated.

In summary, BMP-7 has a negative role in regulating EMT in renal tubular epithelial cells in diabetic nephropathy. Still, the specific mechanism of BMP-7 regulation of EMT needs to be studied in depth. Another study confirmed the protective effect of oxymatrine on high glucose–induced renal tubular epithelial cell injury. Based on the aforementioned theories and previous studies, this study applied a holistic animal and cellular model, employing a type I diabetic rat model and cultured renal tubular epithelial cells (NRK-52E) with high glucose as the study subjects, and used gene therapy with the overexpression of BMP-7 adeno-associated virus, OMT, MAPK pathway inhibitors, and other multi-method interventions to investigate the effects of BMP-7 on downstream fibrogenic-related signaling pathways and OMT. We investigated the effect of BMP-7 on downstream fibrogenic signaling pathways and the possible regulatory mechanism of OMT on early DKD–related pathophysiological processes.

TABLE 1 | Virus sequence.

	Bmp7 (rat,NM_001191856)
pHS-AVC-LW1529	5′-ATGCACGTGCGCTCGCTGCGCGCTGCGGCGCCACACAGCTTCGTGGCGCTCTGGGCGCCTCTGTTCTTGCTG CGCTCTGCCTTGGCCGACTTCAGCCTGGACAACGAGGTGCACTCCAGTTTCATCCACCGGCGCCTCCGCAGTCAG GAGCGGCGGGAGATGCAGCGGGAAATCCTGTCCATCTTGGGCTTGCCCCATCGTCCGCGCCCGCACCTCCAGGGA AAACATAATTCGGCGCCCATGTTCATGTTGGACCTGTACAACGCCATGGCGGTGGAGGAGAGTGGGCCGGACGGA CAGGGCTTCTCCTACCCCTACAAGGCCGTCTTCAGTACCCAGGGTCCCCCTTTGGCCAGCCTGCAGGACAGCCAC TTCCTCACCGACGCCGACATGGTCATGAGCTTCGTCAACCTAGTGGAGCACGACAAGGAATTCTTCCACCCTCGATAC CACCATCGAGAGTTCCGGTTTGATCTTTCCAAGATCCCCGAGGGAGAGGCGGTGACCGCAGCCGAGTTCAGGATC TATAAGGACTACATCCGGGAGCGGTTTGACAACGAGACCTTCCAGATCACAGTCTATCAGGTGCTCCAGGAGCACTCA GGCAGGGAGTCCGACCTCTTCTTGCTGGACAGCCGTACCATCTGGGCTTCTGAGGAGGGCTGGTTGGTATTTGAC ATCACAGCCACCAGCAACCACTGGGTGGTCAACCCTCGGCACAACCTGGGCTTACAGCTCTCCGTGGAGACCCTG GATGGGCAGAGCATCAACCCCAAGTTGGCAGGCCTGATTGGACGGCATGGACCCCAGAACAAGCAACCCTTCATG GTGGCCTTCTTCAAGGCCACGGAGGTTCATCTCCGTAGCATCCGGTCCACGGGGGGCAAACAACGCAGCCAGAAC CGCTCCAAGACTCCAAAGAACCAAGAGGCACTGAGGATGGCCAGTGTGGCAGAAAACAGCAGCAGTGACCAGAGG CAGGCCTGCAAGAAACACGAGCTGTATGTTAGCTTCCGAGACCTTGGCTGGCAGGACTGGATCATCGCACCTGAA GGCTATGCTGCCTACTACTGTGAGGGAGAGTGTGCCTTCCCTCTGAACTCCTACATGAACGCCACCAACCATGCTATC GTCCAGACACTGGTTCACTTCATCAACCCAGACACCGTACCCAAGCCCTGCTGTGCCCCCACCCAGCTCAACGCG ATATCTGTCCTCTACTTCGACGACAGCTCCAACGTCATCCTGAAGAAGTACAGAAACATGGTGGTCCGGGCCTGTGGC TGCCAC-3′

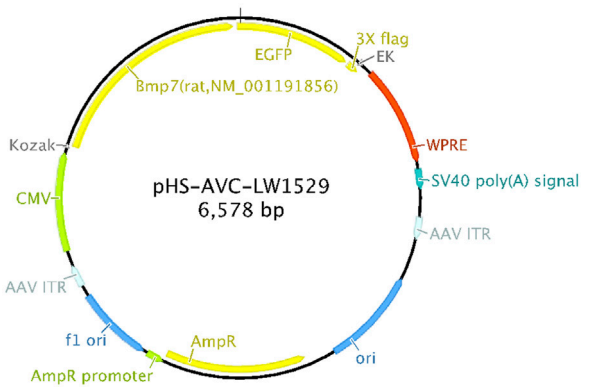

FIGURE 1 | Schematic diagram of overexpressed adeno-associated virus backbone.

MATERIALS AND METHOD

Experimental Subjects

Sprague–Dawley (SD) rats were purchased from Beijing Huafukang Biotechnology Co., Ltd. and weighed 160 ± 20 g. The rats were randomly divided into normal control group (NC group), diabetes mellitus model group (DM group), DM + overexpressed BMP-7 group (rAAV + BMP-7 group), and oxymatrine intervention group (OMT group). The type 1 diabetes model was replicated using a single streptozotocin (STZ) (concentration of 55 mg/kg) tail vein injection and randomly divided into NC and DM groups. The model was considered successful with blood glucose greater than or equal to 16.7 mmo/L and maintained stable. The adeno-associated virus overexpressing BMP-7 (rAAV + BMP-7) was given by tail vein injection in the sixth week of model formation as the rAAV + BMP-7 group. The adeno-associated virus (dissolved in sterile saline) was injected intravenously at a dose of 1.5×10^{12}/animal and continuously fed for 8 weeks before death. The rats in the DM model were treated with OMT starting in the sixth week as the OMT group and injected intraperitoneally (120 mg/kg per rat) daily for 8 weeks before death. Blood and urine samples were collected and tested for relevant biochemical parameters in rats using biochemical assay kits. The sample size for statistical analysis of each independent group was 6 (n = 6).

The *in vivo* overexpression of the BMP-7 sequence is shown in **Table 1**, and the schematic diagram of adeno-associated virus construction is shown in **Figure 1**.

The experimental cells were NRK-52E cells (renal tubular epithelial cell line) derived from ATCC. Cell culture was performed using a glucose concentration of 5.5 mmol/L as the normal group and 30 mmol/L glucose concentration as the high glucose stimulation group, respectively. Westernblot experiments of cells were performed using the results of three batches of cells and counted.

Reagents

The following reagents and instruments were used in the study: STZ (Sigma, United States). Total protein, creatinine, glucose, triglyceride, and cholesterol biochemical assay kits (Nanjing Jiancheng Company); immunohistochemistry SP two-step assay reagent (Beijing Zhongsun Jinqiao Biotechnology Co. Ltd.); Talent qPCR fluorescence quantification kit (Beijing Tiangen Biotechnology Co., Ltd.), BMP-7, FN, Id2, and GAPDH primers (Shanghai Biotechnology Engineering Service Co., Ltd.); low-sugar DMEM (5.5 mmol/L glucose) (Gibco Invitrogen, United States); fetal bovine serum (FBS) (Biological Industries, Israel); human recombinant BMP-7 (rhBMP-7; PeproTech); immunoprecipitation (Co-IP) kit (Thermo, United States); lipofectamine 2000 (Invitrogen, United States); rabbit anti-BMP-7 polyclonal antibody, rabbit anti-Vimentin polyclonal antibody, and rabbit anti-Col-III polyclonal antibody (Wuhan Proteintech Company); rabbit anti-α-SMA polyclonal antibody, rabbit anti-p38 polyclonal antibody, rabbit anti-p-p38 polyclonal antibody, rabbit anti-Erk1/2

TABLE 2 | Primer sequences of RT-qPCR.

Primer	Primer sequences	Tm
BMP-7	F: CGT AGC ATC CGG TCC AC R: CAG CTC GTG TTT CTT GCA G	55.0 (°C)
Fibronectin	F: ATT GCC TAC TCG CAG CTT R: ACG GGA TCA CAC TTC CAC	54.4 (°C)
Id2	F: TGC TAC TCC AAG CTC AAG G R: GTG TTC AGG GTG GTC AGC	55.6 (°C)
GADPH	F: GAC ATG CCG CCT GGA GAA AC R: AGC CCA GGA TGC CCT TTA GT	59.0 (°C)

antibody, and rabbit anti-p-Erk1/2 polyclonal antibody (Cell Signaling Technology); mouse anti-JNK monoclonal antibody, mouse anti-p-JNK monoclonal antibody (Santa Cruz, United States); mouse anti-Col-IV monoclonal antibody and rabbit anti-Id2 polyclonal antibody (Sigma, United States); rabbit anti-FN polyclonal antibody (Abcam); direct labeled secondary anti-GADPH-HRP antibody (Wuhan Ltd.); and SP600125 (JNK inhibitor), SB203580 (p38 inhibitor), and SCH772984 (Erk1/2 inhibitor) (Cell Signaling Technology).

Histopathological Observation of Kidney Tissues

Kidney tissues were fixed in 4% paraformaldehyde and dehydrated using gradients of alcohol, half benzene and half alcohol, benzene, half benzene, and half wax; fixed by paraffin embedding and sectioned (3 μm) with a microtome; and the sections were used for HE staining, Masson staining, PAS staining, and immunohistochemical staining. Paraffin sections were baked at 60°C for 2 h; treated with xylene and gradient alcohol to chemical wax to water; stained using HE, Masson, and PAS staining kits; dehydrated; sealed with neutral resin; and observed microscopically. Similar methods were used for immunohistochemical staining with labeled antibodies.

Western Blot Analysis for Protein Detection and PCR for RNA Detection

For analyses, 0.1 g of kidney tissue was added to 700 μl of lysate. 10% SDS-polyacrylamide gel was used to separate the protein, which was transferred to the PVDF membrane and blocked with skimmed milk. The membrane was intercepted according to different molecular weights and incubated with different primary antibodies. The p38, Erk, JNK, p-p38, p-Erk, and p-JNK antibodies (1:1000) were purchased from Cell Signaling Technology. BMP-7, Collagen III, and Vimentin (1:1000) were purchased from Proteintech. Collagen Ⅳ antibody (1:1000) was purchased from Sigma. FN antibody (1:1000) was purchased from Abcam and incubated overnight. The membrane was removed on the second day, washed three times with TBST (5 min/time), incubated with the secondary antibody (1:8000) for 2 h at room temperature, and exposed to Tanon apparatus.

Further, 0.1 g of tissue was lysed by adding 1 ml of TRIzol, and tissue RNA was extracted and reverse transcribed to obtain cDNA. Next, 20-μl Real-time PCR system (kit purchased from Tiangen) was prepared following the manufacturer's protocol and detected using Bio-Rad PCR instrument. PCR was performed using calculated values for statistical analysis of the results, calculated by the formula $2^{-\Delta\Delta Ct}$.

PCR primer sequences are shown in **Table 2**.

Cell Experimental Grouping and Treatment

The cells requiring experimental treatment were inoculated in six-well plates at the time of passage. When the cells were in good growth condition and the fusion degree reached 70%, they were transferred to a low-sugar medium without FBS and synchronized for 12 h. The cells were divided into normal sugar (NG), high sugar (HG), and their additive/cytokine groups. The cell proteins were collected after 48 h, and cell immunofluorescence experiments were performed.

Main Analysis Methods and Software

Data were statistically analyzed using SPSS25.0 and expressed as mean ± standard deviation. ANOVA was used for comparison between multiple groups of factors. Independent-samples *t* test was used for comparison between two groups, and differences were considered statistically significant at $p \leq 0.05$. ImageJ 180 was used for image processing. Statistical software IBM SPSS statistics 19.0 was used for data processing. GraphPad Prism 5 was used to draw charts.

Cell Immunofluorescence Staining

The cell suspension was inoculated into a 6-well plate/12-well plate lined with a cell crawl (the cell crawl was baked with an alcohol lamp, put into a six-well plate, and washed once with sterile saline). The suspension was transferred to a normal-sugar and a high-sugar medium when the fusion degree reached 50%, and removed after 48 h of incubation. The cells were washed three times with PBS, 5 min each time, fixed with 4% paraformaldehyde at room temperature for 20 min, and again washed three times with PBS, 5 min each time. They were treated with 0.5% Triton X-100 at room temperature for 20 min, and again washed three times with PBS, 5 min each time. For serum closure, the cells were aspirated with PBS, mixed with 10% BSA dropwise (BSA powder freshly prepared), and closed at 37°C for 30 min. The closure solution was washed off, primary antibodies were added dropwise, and the suspension was diluted with 1% BSA and refrigerated at 4°C overnight. The suspension was taken out from the refrigerator the next day for re-warming, the primary antibodies were recovered, and the cells were washed with PBS three times, 5 min each time. Secondary antibody incubation: CY3 sheep anti-mouse IgG (1:100) and FITC sheep anti-rabbit IgG (1:200) were added dropwise, and the cells were incubated at 37°C for 1 h in the absence of light and washed three times with PBS, 5 min each time. DAPI was added dropwise to re-stain nuclei, and the cells were incubated for 5 min in the absence of light and washed four times with PBS, 5 min each time. The excess liquid was absorbed from the crawling film with an absorbent paper, and the film was sealed with a sealer containing a fluorescence quencher and observed under a fluorescence microscope.

TABLE 3 | Detection of renal function and metabolism-related indicators in each group.

Group	NC	DM	OMT	rAAV + BMP-7
Glucose (mmol/L)	5.54 ± 1.12	36.75 ± 4.46*	23.43 ± 4.77#	34.49 ± 4.43
Triglyceride (mmol/L)	0.75 ± 0.10	2.24 ± 1.23*	0.74 ± 0.19#	1.90 ± 1.17
Cholesterol (mmol/L)	1.38 ± 0.24	2.58 ± 0.36*	1.60 ± 0.17#	2.55 ± 0.17
Urine creatinine (μmol/L)	8581.85 ± 2755.24	748.42 ± 244.37*	1151.42 ± 137.67#	1216.42 ± 143.98#
Serum creatinine (μmol/L)	15.78 ± 3.52	150.62 ± 55.10*	21.04 ± 16.68#	28.28 ± 12.07#
Creatinine clearance rate (ml/min)	8.71 ± 3.34	0.64 ± 0.26*	6.46 ± 3.92#	5.95 ± 2.80#
24 h urinay protein quantity (mg)	13.42 ± 3.27	47.74 ± 14.74*	26.95 ± 10.30#	31.52 ± 8.71#

*p < 0.05 vs. NC; #p < 0.05vs. DM; Ccr (ml/min) = urinary creatinine(μmol/l) × urine volume(ml/min)/blood creatinine(μmol/l).

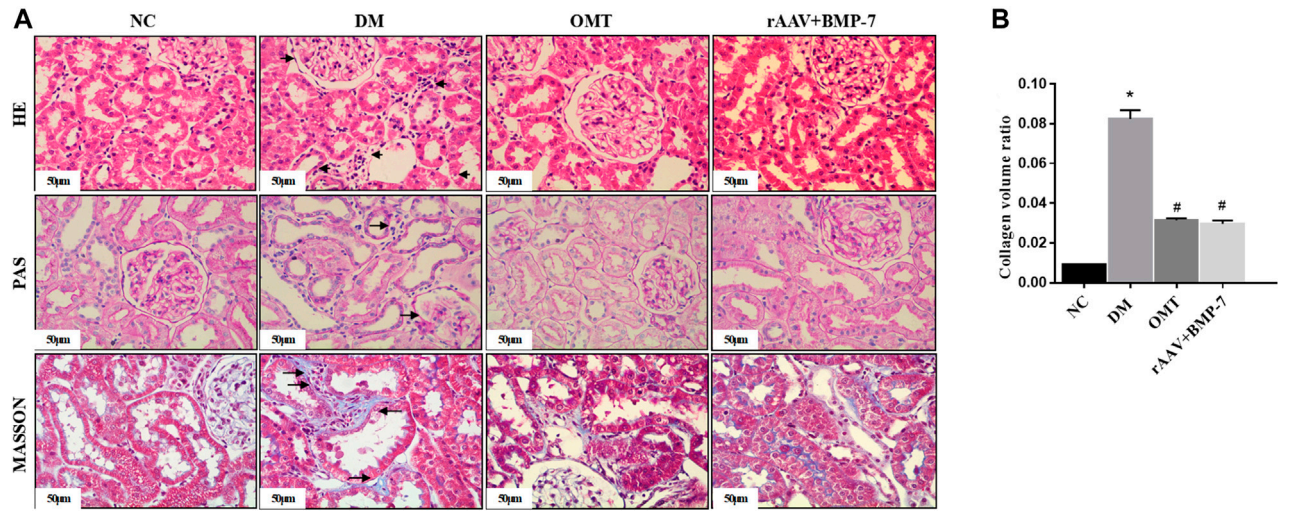

FIGURE 2 | Paraffin sections of rat kidney tissues in each group were stained with HE, PAS, and MASSON(scale bar is 50 μm), and the ratio of collagen area to the total area of the tissue under each field was counted, *p < 0.05 vs. NC group, #p < 0.05 vs. DM group.

RESULTS AND CONCLUSION

Changes in Biochemical Indices and Pathological Staining in Rats

As shown in **Table 3**, the blood glucose level was significantly higher in the DM group compared with the NC group. The blood glucose in the DM rats decreased after OMT treatment but was still higher than normal, suggesting that OMT could interfere with the blood glucose level *in vivo* but did not achieve an effective therapeutic effect. The blood glucose level did not change significantly after the injection of BMP-7 adeno-associated virus, suggesting that BMP-7 did not affect the process of DKD by regulating the blood glucose level. The levels of triglycerides and total cholesterol increased in the DM group and decreased after OMT treatment, but did not significantly improve in the rAAV + BMP-7 group, suggesting that OMT had a therapeutic effect on lipid metabolism in early DKD. In contrast, BMP-7 did not have a significant effect on lipid metabolism in DKD. The 24-h urine protein quantification reflected that DM rats showed some renal damage compared with that in the NC group. The 24-h urine protein quantification reflected that DM rats showed some renal injury, which was improved by OMT. It also improved in the rAAV + BMP-7 group, suggesting that BMP-7 played a role in promoting the improvement in renal injury in early DKD.

HE staining and PAS staining showed that the glomerular lamina propria cells in the NC group did not show significant hyperplasia, the thylakoid region did not show significant widening, the basement membrane did not show significant thickening, the renal tubules were tightly arranged and did not show atrophy, the epithelial cells did not show significant granular and vacuolar degeneration, the renal interstitium did not show abnormalities, and the small vessels did not show glassy degeneration and thickening (**Figures 2A,B**). The DM group showed mild segmental hyperplasia of thylakoid cells and stroma, no significant thickening of basement membrane, small focal atrophy of renal tubules (atrophy area less than 10%), granular and vacuolar degeneration of epithelial cells in focal areas, small focal lymphocytic infiltration and fibrous tissue hyperplasia in the renal interstitium (shown by arrows in the figure), and no glassy degeneration and significant thickening of small vessel walls. In the OMT group and the rAAV + BMP-7 intervention group, there was a reduction in the area of small focal tubular atrophy compared with the DM group, an improvement in microscopic

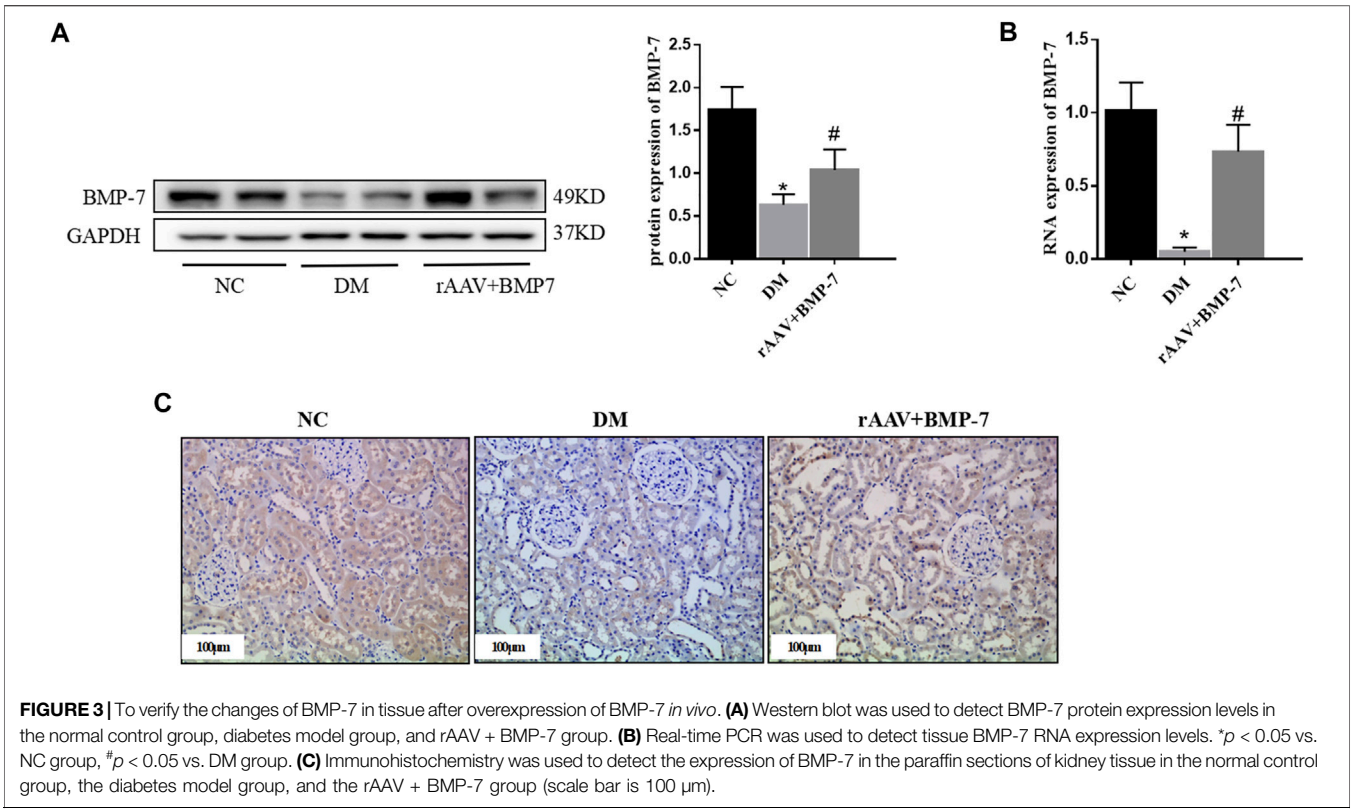

FIGURE 3 | To verify the changes of BMP-7 in tissue after overexpression of BMP-7 *in vivo*. **(A)** Western blot was used to detect BMP-7 protein expression levels in the normal control group, diabetes model group, and rAAV + BMP-7 group. **(B)** Real-time PCR was used to detect tissue BMP-7 RNA expression levels. $^{*}p < 0.05$ vs. NC group, $^{\#}p < 0.05$ vs. DM group. **(C)** Immunohistochemistry was used to detect the expression of BMP-7 in the paraffin sections of kidney tissue in the normal control group, the diabetes model group, and the rAAV + BMP-7 group (scale bar is 100 μm).

epithelial cell morphology, less lymphocytic infiltration in the renal interstitium, and a reduction in the area of fibrous tissue hyperplasia. The results of Masson staining and statistical analysis of collagen volume showed that the blue collagen deposition in the tubular interstitium significantly increased in the DM group compared with the NC group. The OMT and rAAV + BMP-7 intervention groups showed some collagen distribution and reduced fibrosis. The results suggested that the overexpression of BMP-7 and OMT treatment improved renal injury and inhibited the development of fibrosis.

BMP-7 Ameliorated Tubulointerstitial Fibrosis in DKD

Adeno-associated viruses carrying the overexpressed BMP-7 gene were constructed and then injected into the tail vein 6 weeks after DM modeling. The results showed that the protein and RNA expression levels of BMP-7 decreased in the DM group, while BMP-7 protein (**Figure 3A**) and RNA (**Figure 3B**) expression levels significantly increased in the rAAV + BMP-7 group compared with the DM group. The immunohistochemical results (**Figure 3C**) showed that the expression of BMP-7 significantly decreased in the kidneys of rats in the DM group; the expression increased after the injection of the overexpressed adeno-associated virus compared with that in the DM group. The results suggested that the expression of BMP-7 decreased under the high-glucose condition. In contrast, the expression level of BMP-7 was significantly higher in the rAAV + BMP-7 group than in the DM group, and the model was successfully replicated.

Western blot analysis results showed that the expression of Vimentin and α-SMA increased in the DM group compared with the NC group, suggesting that EMT occurred in the DM group, while the expression of Col III, Col IV, and FN increased, suggesting that ECM deposition in the kidney tissue increased in the DM group (**Figure 4A**). The levels of the aforementioned indicators decreased In the rAAV + BMP-7 group, suggesting that the expression of BMP-7 was upregulated after the tail vein injection of BMP-7 adeno-associated virus, which could promote the improvement in the EMT process and decrease in ECM deposition. Immunohistochemistry showed an increase in FN deposition in the interstitial kidney tissue in the DM group compared with the NC group and a decrease in the rAAV + BMP-7 group compared with the DM group (**Figure 4B**). Real-time PCR showed a decrease in the RNA level of FN in the rAAV + BMP-7 group compared with the DM group (**Figure 4C**). These results suggested that the restoration of BMP-7 expression could inhibit the fibrosis-related process in DM rats.

Pre-laboratory studies confirmed that BMP-7 improved the EMT- and ECM-related indexes in high glucose–stimulated NRK-52E cells. The expression of FN (**Figure 5A**) and α-SMA (**Figure 5B**) in NRK-52E cells was detected by cellular immunofluorescence. The results verified that the expression of FN and α-SMA reduced after the administration of BMP-7 cytokine compared with that in the HG group. These results suggested that *in vitro* BMP-7 delayed the EMT process in renal tubular epithelial cells under the high-glucose status.

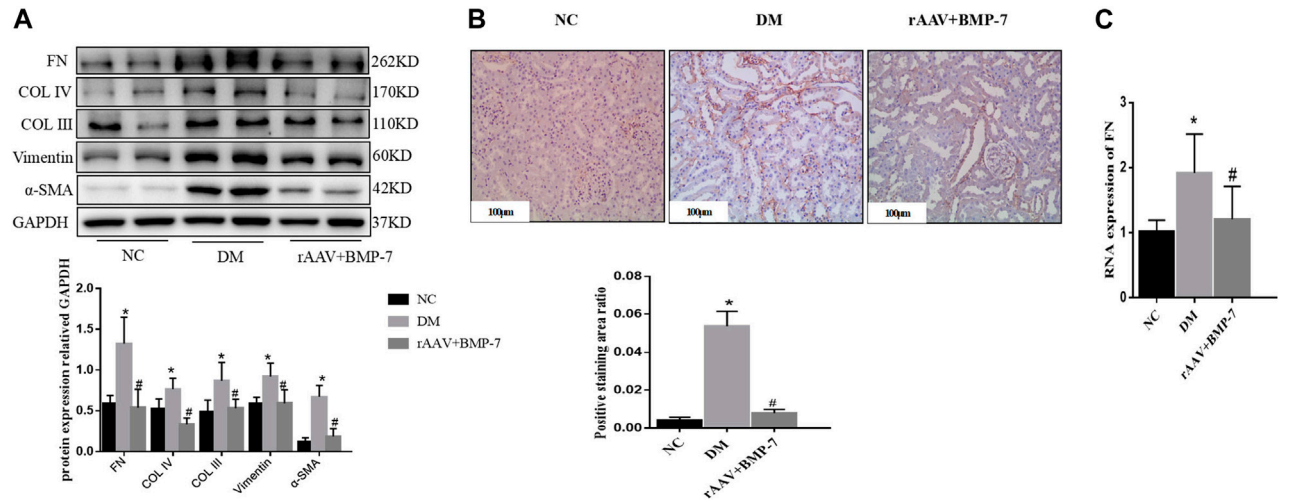

FIGURE 4 | Detection of fibrosis-related index levels after overexpression of BMP-7 *in vivo*. **(A)** Western blot was used to detect EMT and ECM related indexes in the normal control group, diabetes model group, and rAAV + BMP-7 group, *$p < 0.05$ vs. NC group, #$p < 0.05$ vs. DM group. **(B)** Immunohistochemistry was used to detect the expression of FN in the paraffin sections of kidney tissue in the normal control group, the diabetes model group, and the rAAV + BMP-7 group, and the ratio of the positive staining area to the total tissue area under each field was counted. *$p < 0.05$ vs. NC group, #$p < 0.05$ vs. DM group (scale bar is 100 μm) **(C)** Real-time PCR was used to detect tissue FN RNA expression levels. *$p < 0.05$ vs. NC group, #$p < 0.05$ vs. DM group.

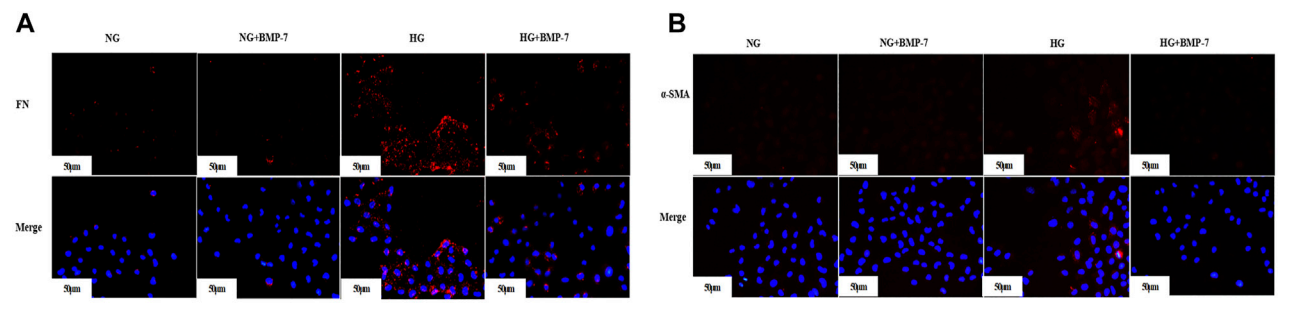

FIGURE 5 | (A) The expression of FN in cells was detected by immunofluorescence (scale bar is 50 μm). **(B)** The expression of α-SMA in cells was detected by immunofluorescence (scale bar is 50 μm).

BMP-7 Upregulated Id2 Expression and its Possible Signaling Pathway

Western blot analysis showed that the protein expression level of Id2 in the DM group significantly decreased in the kidney tissues, and the protein level of Id2 increased after the overexpression of BMP-7 (**Figure 6A**). Fluorescence quantitative PCR results showed that the RNA expression of Id2 reduced in the DM group compared with the NC group (**Figure 6B**). At the same time, its RNA expression level was upregulated after the overexpression of BMP-7. The immunohistochemical results showed that Id2 was abundantly expressed in the cytoplasm and nucleus of renal tubular epithelial cells in the NC group, while it was significantly reduced in the DM group and increased in the rAAV + BMP-7 group compared with the DM group (**Figure 6C**). The results suggested that Id2 expression was reduced in the high-glucose status and upregulated by the overexpression of BMP-7.

Pre-laboratory studies confirmed that the addition of BMP-7 to NRK-52E cells cultured in standard- and high-glucose medium also upregulated Id2 expression. The cellular immunofluorescence results showed that Id2 expression in HG-cultured NRK-52E cells was significantly lower compared with that in the NG group, and Id2 expression increased after the addition of BMP-7 cytokine treatment (**Figure 7**). The results verified that BMP-7 could upregulate Id2 expression in NRK-52E cells.

The Western blot analysis showed that the phosphorylation levels of p38, Erk1/2, and JNK significantly increased in renal tissues in the DM group, and the activation of p38, Erk1/2, and JNK was significantly inhibited after the overexpression of BMP-7 (**Figure 8A**). The results suggested that the overexpression of BMP-7 could inhibit the activation of the nonclassical MAPK pathway.

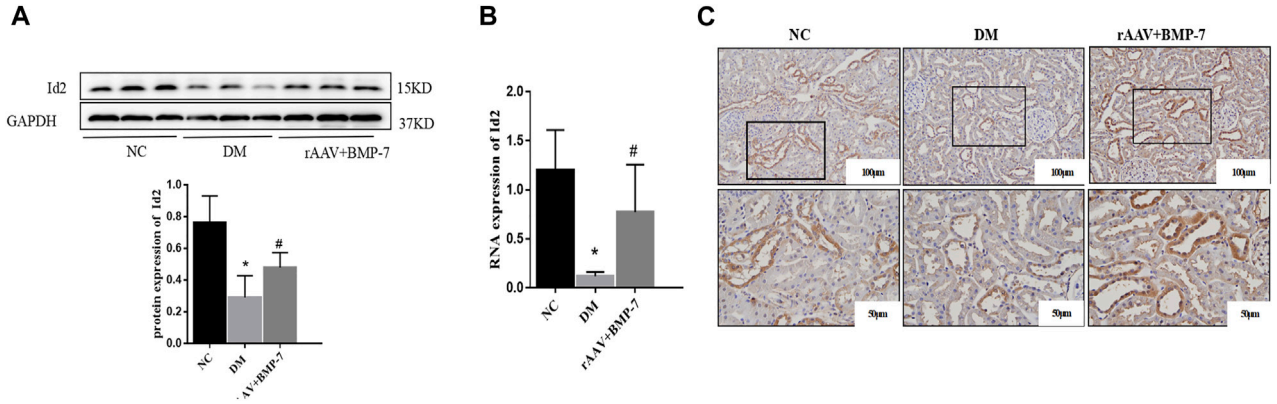

FIGURE 6 | To verify the changes in protein and mRNA levels of Id2 after overexpression of BMP-7 *in vivo*. **(A)** Western blot was used to detect Id2 protein expression levels in the normal control group, diabetes model group, and rAAV + BMP-7 group, *$p < 0.05$ vs. NC group, #$p < 0.05$ vs. DM group. **(B)** Real-time PCR was used to detect tissue Id2 RNA expression levels. *$p < 0.05$ vs. NC group, #$p < 0.05$ vs. DM group. **(C)** Immunohistochemistry was used to detect the expression of Id2 in the paraffin sections of kidney tissue in the normal control group, the diabetes model group, and the rAAV + BMP-7 group (scale bar are 100 and 50 μm).

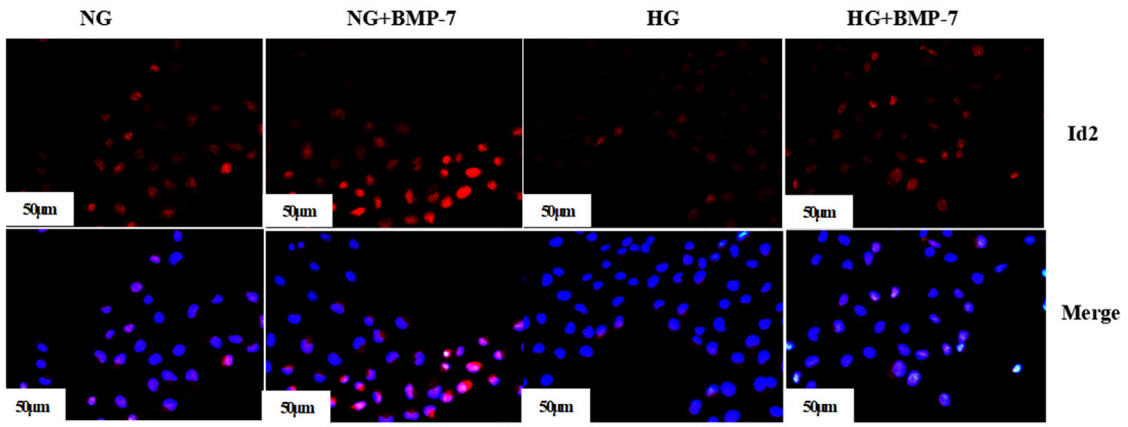

FIGURE 7 | The expression of Id2 in cells was detected by immunofluorescence (scale bar is 50 μm).

Three inhibitors of MAPK family, SP600125 (JNK inhibitor), SB203580 (p38 inhibitor), and SCH772984 (Erk1/2 inhibitor), were added to NRK-52E cells for 2 h and then transferred to serum-containing high-glucose medium for 48 h. The cell proteins were extracted, and Western blot analysis was performed to detect the change in Id2 expression. The results showed that the protein expression level of Id2 was upregulated after the addition of the three inhibitors compared with that in the DMSO-stimulated control (HC) group (**Figure 8B**). The results suggested that the expression of Id2 increased when the activation of the MAPK (p38, Erk1/2, and JNK) signaling pathway was inhibited.

OMT Affected the BMP-7–MAPK Signaling Pathway to Improve Fibrosis

Western blot results showed that the protein expression levels of FN, Col IV, and Col III decreased in DM rats after OMT intervention compared with that in the DM group, suggesting a decrease in ECM deposition (**Figure 9A**). The expression of Vimentin and α-SMA decreased, suggesting that the EMT process was slowed down and the degree of fibrosis was improved. Immunohistochemical results showed that FN deposition reduced and α-SMA expression relatively decreased in the renal tissues of DM rats after OMT treatment (**Figure 9B**). These results suggested that oxymatrine has a significant ameliorative effect on DKD kidney injury.

Pre-laboratory studies confirmed that OMT improved the EMT- and ECM-related indexes in high glucose–stimulated NRK-52E cells. The expression of FN (**Figure 10A**) and α-SMA (**Figure 10B**) in NRK-52E cells was detected by cellular immunofluorescence. The results showed a relative reduction in FN and α-SMA expression in high-glucose-stimulated NRK-52E cells after OMT intervention. The results verified that OMT could

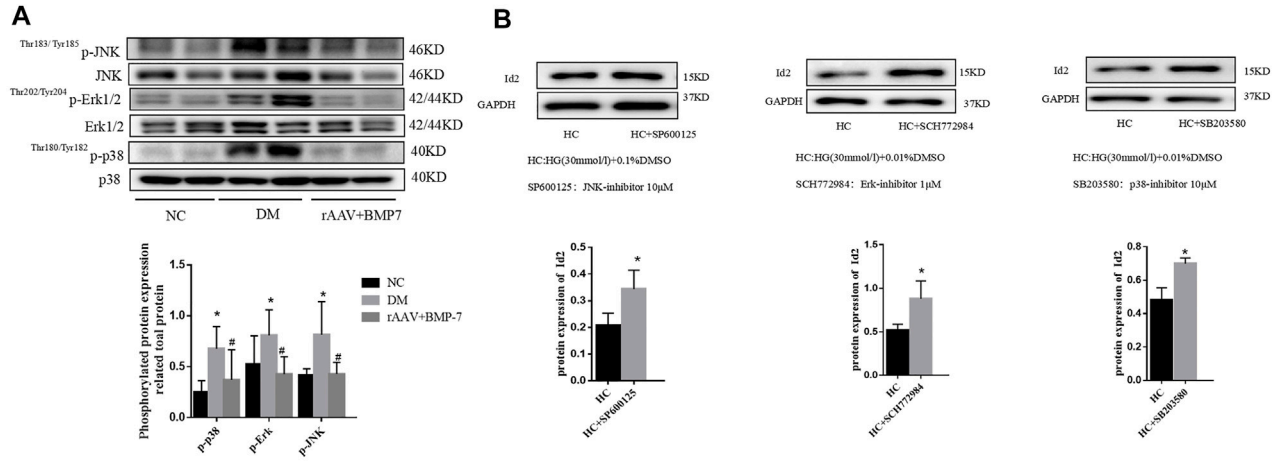

FIGURE 8 | (A) Western blot was used to detect the phosphorylation of p38, Erk1/2, and JNK in the normal control group, diabetes model group, rAAV + BMP-7 group, $^{*}p < 0.05$ vs. NC group, $^{\#}p < 0.05$ vs. DM group. **(B)** The expression of Id2 in cells was detected by Western blot, $^{*}p < 0.05$ vs. HC group.

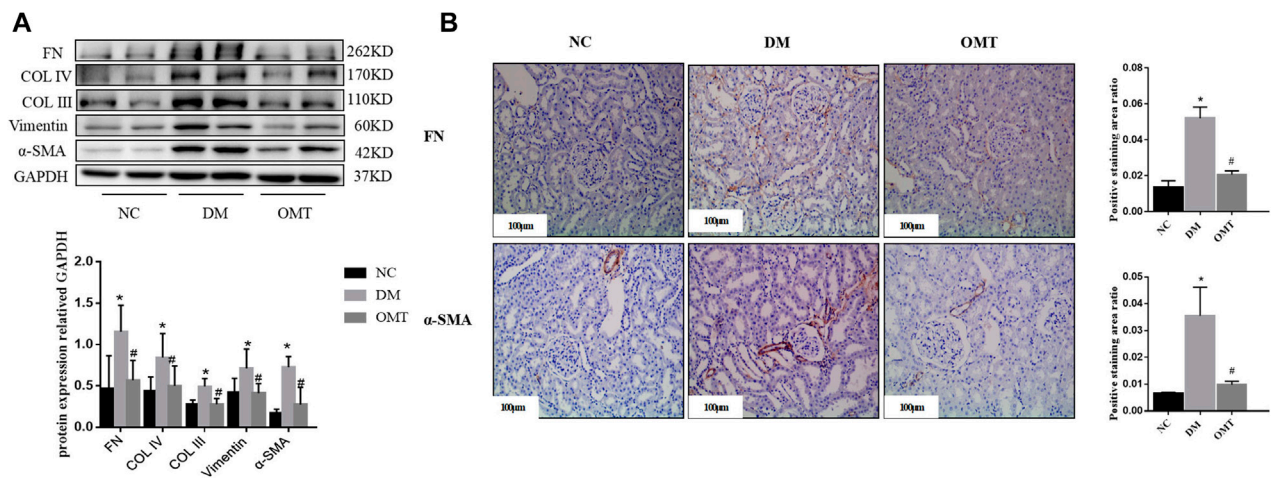

FIGURE 9 | Detection of fibrosis changes after OMT treatment *in vivo*. **(A)** Changes in the expression of EMT and ECM-related indicators in the normal control group, diabetes model group, OMT intervention group, $^{*}p < 0.05$ vs. NC group, $^{\#}p < 0.05$ vs. DM group **(B)** Immunohistochemical technology was used to detect the expression of FN and α-SMA in paraffin sections of rat kidney tissues in each group (scale bar is 100 μm), and the ratio of the positive staining area to the total area of the tissue under each field was counted, $^{*}p < 0.05$ vs. NC group, $^{\#}p < 0.05$ vs. DM group.

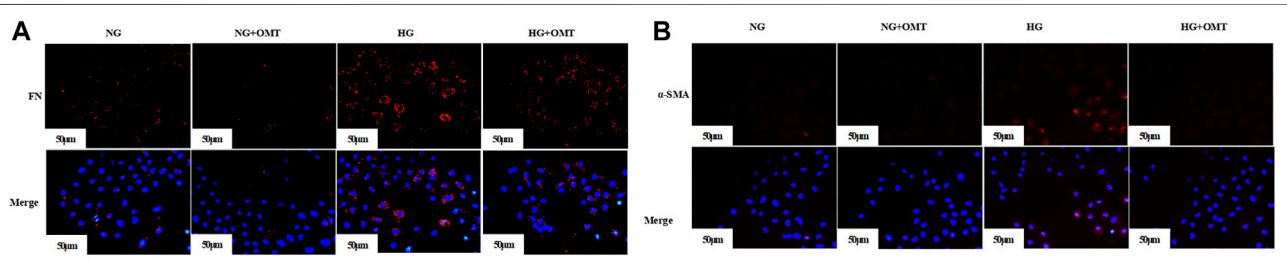

FIGURE 10 | (A) The expression of FN in cells was detected by immunofluorescence (scale bar is 50 μm). **(B)** The expression of α-SMA in cells was detected by immunofluorescence (scale bar is 50 μm).

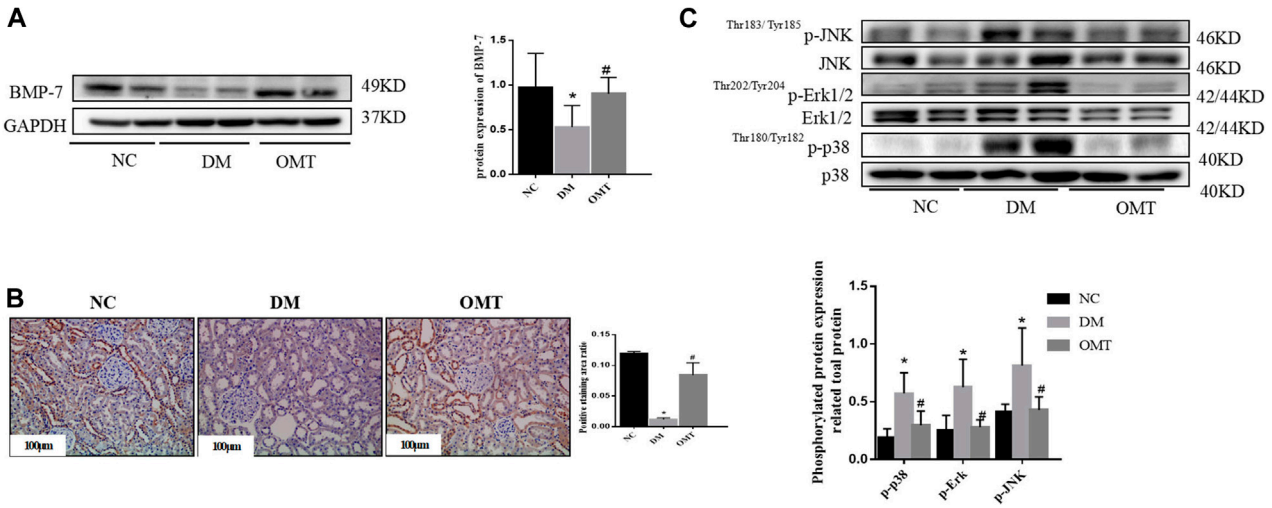

FIGURE 11 | (A) Detection of BMP-7 proteins after OMT intervention. Western blot was used to detect the change of BMP-7 expression level after OMT intervention, *p < 0.05 vs. NC group, #p < 0.05 vs. DM group. **(B)** The immunohistochemical technique was used to detect the expression of BMP-7 in the paraffin sections of rat kidney tissues in each group (scale bar is 100 μm), and the ratio of the positive staining area to the total area of the tissue under each field was counted, *p < 0.05 vs. NC group, #p < 0.05 vs. DM Group **(C)** Detection of MAPK pathway-related proteins after OMT intervention. Western blot was used to detectp38, Erk and JNK phosphorylation levels after OMT intervention, *p < 0.05 vs. NC group, #p < 0.05 vs. DM group.

reduce ECM deposition in high-glucose-stimulated NRK-52E cells.

OMT has a certain ameliorative effect on renal injury in early DKD, but its exact mechanism of action is not fully understood. The Western blot analysis showed that OMT treatment increased the protein expression level of BMP-7 (**Figure 11A**). Immunohistochemistry showed that BMP-7 expression significantly increased in the kidneys after OMT intervention (**Figure 11B**). Meanwhile, the phosphorylation levels of MAPK p38, Erk1/2, and JNK were inhibited after OMT treatment (**Figure 11C**). The results suggested that OMT could upregulate the expression of BMP-7 in DKD kidney tissues and then inhibited the activation of MAPKs.

DISCUSSION

DKD can be defined as persistent microalbuminuria and impaired glomerular filtration leading to the deterioration of renal function and ultimately morbidity and mortality in patients. Proteinuria is a characteristic clinical biomarker of DKD in patients with diabetes (Danta et al., 2021). In this study, STZ was used to partially destroy the pancreatic β-cells of SD rats to replicate the type 1 diabetes model. The results of biochemical-related indexes showed elevated blood glucose levels and significantly increased expression levels of triglycerides and total cholesterol in the DM group compared with the NC group, suggesting successful replication of the diabetes model. The 24-h urine protein quantification significantly increased, suggesting early renal injury in the DM group.

The main manifestations of early renal pathology in DKD include proliferation and hypertrophy of renal cells, thickening of the glomerular basement membrane, and expansion of the ECM (Akhtar et al., 2020); they are associated with the EMT process. This process leads to massive myofibroblast activation and proliferation. It increases ECM secretion through pro-fibrogenic factors. Increased ECM cannot be degraded rapidly, leading to excessive accumulation of glomerular and tubulointerstitial ECM and causes renal functional impairment. The pathomorphological staining showed mild segmental hyperplasia of thylakoid cells and stroma, tubular atrophy, and interstitial fibrous tissue hyperplasia in the DM group, suggesting glomerular and tubulointerstitial fibrotic lesions in the kidney. Western blot results showed that the expression of mesenchymal cell markers α-SMA and Vimentin significantly increased in the DM group compared with the NC group rats, suggesting a significant increase in the expression of FN, Col IV, and Col III and the presence of excessive ECM deposition. These results indicated that the rats in the DM group had early kidney injury.

Recent studies have confirmed the ability of Id2 to resist organ fibrosis by inhibiting the EMT process (Saika et al., 2006; Jibing et al., 2015). Veerasamy et al., (2013) showed that Id2 reduction was essential for TGF-β-induced α-SMA expression in human proximal tubular epithelial cells. Pre-laboratory studies showed that the downstream-related protein expression of EMT could be inhibited by upregulating Id2 expression. The results of the present study further confirmed that the Id2 expression level in the kidneys was reduced in the DM group compared with the NC group. However, the specific targets of Id2 regulation of EMT-related proteins remain to be clarified. As a critical transcription factor regulating EMT, Snail is involved in the EMT process in DKD (Bai et al., 2016). In the OSCC model, Id2 could bind to Snail and thus regulate the EMT process

(JingPing et al., 2015; Kamata et al., 2016; Sumida et al., 2016). Id2 bound to the SNAG domain of Snai1 at the β4 promoter in normal murine mammary gland cells, and hence the function of Snai1 was inhibited (Cheng et al., 2013). In this study, the Western blot analysis (**Supplementary Figure S1A**) after the transfection of cells with Id2 siRNA showed that the protein expression level of Snail remained unchanged after the knockdown of Id2. The results of Co-IP (**Supplementary Figure S1B**) and immunofluorescence double staining (**Supplementary Figure S1C**) showed that Id2 bound and co-localized with Snail, which again verified that Id2 did not affect Snail expression.

Under physiological conditions, some positive regulators of fibrogenesis are tightly controlled by negative regulators, and the expression of these negative regulators is often reduced in organ tissues with fibrotic lesions. It may be an essential factor contributing to the development of fibrosis. Domestic and foreign scholars demonstrated that BMP-7 was an antifibrotic cytokine with a significant antifibrotic effect (Sun et al., 2017; Song et al., 2020; Kong et al., 2021; Mo et al., 2021). In this study, Western blot results showed that the expression level of BMP-7 was significantly lower in the DM group rats than in the NC group rats. The immunohistochemical results showed that the expression of BMP-7 decreased in the kidney tissues of the DM group rats. As a negative regulation–related protein of DKD, BMP-7 cytokine treatment in NRK-52E cells significantly improved the EMT- and ECM-related indexes (Xiao et al., 2019). In addition, we used adeno-associated virus as a vector to construct an animal model overexpressing BMP-7. The results showed that the expression levels of Col III, Col IV, and FN, the fibrosis-related indexes in kidney tissues, were downregulated after the overexpression of BMP-7 compared with those in the DM group. The 24-h urine protein quantification of the kidney function–related indexes significantly decreased but the metabolism-related indexes were not significantly changed. The morphological staining suggested that the degree of interstitial fibrosis reduced after the overexpression of BMP-7, which confirmed the protective effect of BMP-7 on renal injury in DM rats. In addition, BMP-7 cytokine intervention was given to NRK-52E cells cultured *in vitro* with a high glucose concentration; the expression of ECM-related proteins reduced after the addition of BMP-7. These results suggested that BMP-7 improved tubulointerstitial fibrosis by delaying the EMT process; however, the specific regulatory mechanism of BMP-7 on fibrosis remains unclear.

The MAPK family plays essential roles in a variety of signaling pathways, including inflammation, oxidative stress, and apoptosis. Excessive activation of the MAPK pathway promotes the EMT process in renal tubular epithelial cells, suggesting that the MAPK pathway is involved in the progression of early DKD (Geng et al., 2020). In the present study, Western blot results showed that the phosphorylation levels of P38, Erk1/2, and JNK significantly increased in the DM group, indicating that the MAPK pathway (p38, Erk1/2, and JNK) was in an activated state in the chronic kidney injury model in diabetic rats. One study found that BMP-7 treatment given to db/db mice inhibited tubular inflammatory responses by suppressing p38 and Erk1/2 signaling pathways (Li et al., 2015). *In vitro*, BMP-7 ameliorated glucose-induced oxidative stress by inhibiting JNK phosphorylation (Ching-Hua et al., 2009). The results of this study showed that the levels of MAPKs p38, Erk1/2, and JNK phosphorylation significantly decreased after the overexpression of BMP-7 *in vivo*, suggesting that BMP-7 could delay the EMT process and ECM deposition by inhibiting the activation of MAPKs under the high-glucose status, and thus improved fibrosis.

Another study found that BMP-7 increased Id2 expression to exert antifibrotic effects in organ fibrosis models (Kim et al., 2015). The results of the present study showed that the expression level of Id2 increased after the overexpression of BMP-7 in DM rats, suggesting that BMP-7 could improve organ fibrosis by upregulating the expression of Id2. We cultured NRK-52E renal tubular epithelial cells *in vitro* and administered three MAPK phosphorylation inhibitors separately after high-glucose stimulation for 48 h to further investigate the regulatory mechanism of BMP-7 on Id2. The results showed that the expression level of Id2 was elevated after the addition of MAPK inhibitors. The *in vitro* and *in vivo* results suggested that BMP-7 might upregulate Id2 expression by inhibiting the phosphorylation of the MAPK pathway.

Herbal medicine has potential clinical benefits as primary or alternative therapy for treating diabetic neuropathy due to its multi-targeted function. A large number of studies have emphasized the molecular mechanism of bioactive compounds of traditional Chinese medicine and Raynaud's protective effect, which are involved in the signaling pathways of glucose/lipid metabolism regulation and exert antioxidant, anti-inflammatory, anti-fibrosis, and podocyte-protective effects (Tang et al., 2021). OMT has been shown to play a therapeutic role in visceral fibrosis, the exact mechanism of which is still poorly understood. The results of the present study showed that the 24-h urine protein quantification of renal function-related indexes and metabolic indexes, including glucose, triglycerides, and cholesterol, improved to different degrees, and pathomorphological staining showed a relative improvement in renal fibrotic lesions after the administration of OMT intraperitoneally to DM rats, confirming the therapeutic effect of OMT on renal injury in rats with early DKD. Western blot results showed that the expression Vimentin and α-SMA was downregulated compared with that in the DM group. It suggested that the EMT process was slowed down in the OMT group. The expression of FN, Col V, and Col III decreased, suggesting that ECM deposition was relatively reduced, which confirmed that the intervention of OMT improved the renal fibrosis process. Another study verified that the levels of p38, Erk1/2, and JNK phosphorylation were inhibited after the *in vitro* intervention of OMT in microglia (Dong et al., 2019). In the present study, the levels of p38, Erk1/2, and JNK phosphorylation were downregulated in the kidneys of rats in the OMT group compared with the DM group, suggesting that oxymatrine might regulate the EMT process in DKD kidneys by inhibiting MAPK phosphorylation levels. Further study showed that the expression level of BMP-7 in rat kidney tissues increased after OMT treatment. The protein expression level detected by Western blot was consistent with the immunohistochemical results of kidney tissues, suggesting that OMT could upregulate the expression level

of BMP-7 *in vivo*. All these results suggested that OMT affected the BMP-7–MAPK pathway and thus improved the development of renal fibrosis in DKD.

In summary, OMT affected the expression of BMP-7 and then inhibited the phosphorylation level of MAPKs, the nonclassical pathway of BMP-7. Consequently, the expression of Id2 was upregulated, which inhibited the transcriptional activation of downstream target genes by binding to the EMT-related transcription factor Snail. This delayed the EMT process and ECM deposition in diabetic kidney fibrosis and improved the renal injury in early DKD, thus providing an experimental basis for clinical treatment and pharmacological intervention in early DKD.

DATA AVAILABILITY STATEMENT

The original contributions presented in the study are included in the article/**Supplementary Material**, further inquiries can be directed to the corresponding authors.

ETHICS STATEMENT

The animal study was reviewed and approved by Institutional Animal Ethics Committee of Guizhou Medical University, Guiyang, China.

AUTHOR CONTRIBUTIONS

YaX: Contributed significantly to the conception or design of the work and acquired, analyzed and interpreted data for the work. DL, ZL and ZF: Assisted in obtaining and analyzing data. FZ, YW, YZ, MS and ZY: Critical revision of important intellectual content. YiX and BG agreed to be responsible for all aspects of the work and to ensure that issues related to the accuracy or completeness of any part of the work are properly investigated and resolved.

FUNDING

This study was supported by the National Natural Science Foundation of China (grant no. 81860656 and grant no. 81860135), and the Guizhou Province Science and Technology Foundation [grant no. Guizhou Science and Technology Foundation-ZK[2021] Focus 010].

SUPPLEMENTARY MATERIAL

The Supplementary Material for this article can be found online at: https://www.frontiersin.org/articles/10.3389/fphar.2022.900346/full#supplementary-material

REFERENCES

Akhtar, M., Taha, N. M., Nauman, A., Mujeeb, I. B., and Al-Nabet, A. D. M. H. (2020). Diabetic Kidney Disease: Past and Present. *Adv. Anat. Pathol.* 27, 87–97. doi:10.1097/PAP.0000000000000257

Aluganti Narasimhulu, C., and Singla, D. K. (2021). Amelioration of Diabetes-induced Inflammation Mediated Pyroptosis, Sarcopenia, and Adverse Muscle Remodelling by Bone Morphogenetic Protein-7. *J. Cachexia, Sarcopenia Muscle* 12, 403–420. doi:10.1002/jcsm.12662

Bai, X., Geng, J., Zhou, Z., Tian, J., and Li, X. (2016). MicroRNA-130b Improves Renal Tubulointerstitial Fibrosis via Repression of Snail-Induced Epithelial-Mesenchymal Transition in Diabetic Nephropathy. *Sci. Rep.* 6, 20475–204791. doi:10.1038/srep20475

Bonner, R., Albajrami, O., Hudspeth, J., and Upadhyay., A. (2020). Diabetic Kidney Disease. *Prim. Care Clin. Office Pract.* 47, 645–659. doi:10.1016/j.pop.2020.08.004

Chang, C., Yang, X., Pursell, B., and Mercurio, A. M. (2013). Id2 Complexes with the SNAG Domain of Snai1 Inhibiting Snai1-Mediated Repression of Integrin β4. *Mol. Cell Biol.* 33, 3795–3804. doi:10.1128/MCB.00434-13

Ching-Hua, Y., Chang, C.-K., Cheng, M.-F., Lin, H.-J., and Cheng, J.-T. (2009). The Antioxidative Effect of Bone Morphogenetic Protein-7 against High Glucose-Induced Oxidative Stress in Mesangial Cells. *Biochem. Biophysical Res. Commun.* 382, 292–297. doi:10.1016/j.bbrc.2009.03.011

Danta, C. C., Boa, A. N., Bhandari, S., Sathyapalan, T., and Xu, S.-Z. (2021). Recent Advances in Drug Discovery for Diabetic Kidney Disease. *Expert Opin. Drug Discov.* 16, 447–461. doi:10.1080/17460441.2021.1832077

Dong, P., Ji, X., Han, W., and Han, H. (2019). Oxymatrine Exhibits Anti-neuroinflammatory Effects on Aβ1-42-Induced Primary Microglia Cells by Inhibiting NF-Kb and MAPK Signaling Pathways. *Int. Immunopharmacol.* 74, 105686. doi:10.1016/j.intimp.2019.105686

Geng, X.-q., Ma, A., He, J.-z., Wang, L., Jia, Y.-l., Shao, G.-y., et al. (2020). Ganoderic Acid Hinders Renal Fibrosis via Suppressing the TGF-β/Smad and MAPK Signaling Pathways. *Acta Pharmacol. Sin.* 41, 670–677. doi:10.1038/s41401-019-0324-7

Ito, J., Minemura, T., Wälchli, S., Niimi, T., Fujihara, Y., Kuroda, S. i., et al. (2021). Id2 Represses Aldosterone-Stimulated Cardiac T-type Calcium Channels Expression. *Ijms* 22, 3561. doi:10.3390/ijms22073561

Jibing, Y., Velikoff, M., Agarwal, M., Disayabutr, S., Wolters, P. J., and Kim, K. (2015). Overexpression of Inhibitor of DNA-Binding 2 Attenuates Pulmonary Fibrosis through Regulation of C-Abl and Twist. *Am. J. Pathology* 185 (4), 1001–1011. doi:10.1016/j.ajpath.2014.12.008

JingPing, Z., ZhenLin, G., MeiLing, Z., MengYing, H., XiaoHui, X., DeTao, T., et al. (2015). Snail Interacts with Id2 in the Regulation of TNF-α-Induced Cancer Cell Invasion and Migration in OSCC. *Am. J. Cancer Res.* 5, 1680–1691.

Kamata, Y. U., Tomoki, S., Yosuke, K., Akiko, I., Wataru, K., and Yoshihide, M. (2016). Introduction of ID2 Enhances Invasiveness in ID2-null Oral Squamous Cell Carcinoma Cells via the SNAIL Axis. *Cancer Genomics Proteomics* 13, 493–498. doi:10.21873/cgp.20012

Kim, H. M., Ryu, B., Lee, J. S., Choi, J.-H., and Jang, D. S. (2015). Schisandrosides A-D, Dibenzocyclooctadiene Lignan Glucosides from the Roots of Schisandra Chinensis. *Chem. Pharm. Bull.* 63, 746–751. doi:10.1248/cpb.c15-00400

Kong, L., Wang, H., Li, C., Cheng, H., Cui, Y., Liu, L., et al. (2021). Sulforaphane Ameliorates Diabetes-Induced Renal Fibrosis through Epigenetic Up-Regulation of BMP-7. *Diabetes Metab. J.* 45, 909–920. doi:10.4093/dmj.2020.0168

Lan, X., Zhao, J., Zhang, Y., Chen, Y., Liu, Y., and Xu, F. (2020). Oxymatrine Exerts Organ- and Tissue-Protective Effects by Regulating Inflammation, Oxidative Stress, Apoptosis, and Fibrosis: From Bench to Bedside. *Pharmacol. Res.* 151, 104541. doi:10.1016/j.phrs.2019.104541

Li, R. X., Yiu, W. H., Wu, H. J., Wong, D. W., Chan, L. Y., Lin, M., et al. (2015). BMP7 Reduces Inflammation and Oxidative Stress in Diabetic Tubulopathy. *Clin. Sci. (Lond)* 128, 269–280. doi:10.1042/CS20140401

Li, Z., Liu, X., Wang, B., Nie, Y., Wen, J., Wang, Q., et al. (2017). Pirfenidone Suppresses MAPK Signalling Pathway to Reverse Epithelial-Mesenchymal Transition and Renal Fibrosis. *Nephrol. Carlt.* 22, 589–597. doi:10.1111/nep.12831

Liu, L., Wang, Y., Yan, R., Li, S., Shi, M., Xiao, Y., et al. (2016). Oxymatrine Inhibits Renal Tubular EMT Induced by High Glucose via Upregulation of SnoN and

Inhibition of TGF-β1/Smad Signaling Pathway. *PLoS One* 11, e0151986. doi:10.1371/journal.pone.0151986

Liu, L., Wang, Y., Yan, R., Liang, L., Zhou, X., Liu, H., et al. (2019). BMP-7 Inhibits Renal Fibrosis in Diabetic Nephropathy via miR-21 Downregulation. *Life Sci.* 238, 116957. doi:10.1016/j.lfs.2019.116957

Mo, S., Cui, Y., Sun, K., Wang, H., Peng, X., Ou, L., et al. (2021). High Sodium Chloride Affects BMP-7 and 1α-Hydroxylase Levels through NCC and CLC-5 in NRK-52E Cells. *Ecotoxicol. Environ. Saf.* 225, 112762. doi:10.1016/j.ecoenv.2021.112762

Saika, S., Ikeda, K., Yamanaka, O., Flanders, K. C., Ohnishi, Y., Nakajima, Y., et al. (2006). Adenoviral Gene Transfer of BMP-7, Id2, or Id3 Suppresses Injury-Induced Epithelial-To-Mesenchymal Transition of Lens Epithelium in Mice. *Am. J. Physiology-Cell Physiology* 290, C282–C289. doi:10.1152/ajpcell.00306.2005

Song, Y., Lv, S., Wang, F., Liu, X., Cheng, J., Liu, S., et al. (2020). Overexpression of BMP-7 R-everses TGF-β1-induced E-pithelial-mesenchymal T-ransition by A-ttenuating the Wnt3/β-catenin and/Smad2/3 S-ignaling P-athways in HK-2 C-ells. *Mol. Med. Rep.* 21, 833–841. doi:10.3892/mmr.2019.10875

Sumida, T., Ishikawa, A., Nakano, H., Yamada, T., Mori, Y., and Desprez, P. Y. (2016). Targeting ID2 Expression Triggers a More Differentiated Phenotype and Reduces Aggressiveness in Human Salivary Gland Cancer Cells. *Genes cells.* 21, 915–920. doi:10.1111/gtc.12389

Sun, L., Zou, L.-X., and Chen, M.-J. (2017). Make Precision Medicine Work for Chronic Kidney Disease. *Med. Princ. Pract.* 26, 101–107. doi:10.1159/000455101

Tang, G., Li, S., Zhang, C., Chen, H., Wang, N., and Feng, Y. (2021). Clinical Efficacies, Underlying Mechanisms and Molecular Targets of Chinese Medicines for Diabetic Nephropathy Treatment and Management. *Acta Pharm. Sin. B* 11, 2749–2767. doi:10.1016/j.apsb.2020.12.020

Veerasamy, M., Phanish, M., and Dockrell, M. E. (2013). Smad Mediated Regulation of Inhibitor of DNA Binding 2 and its Role in Phenotypic Maintenance of Human Renal Proximal Tubule Epithelial Cells. *PLoS One* 8, e51842. doi:10.1371/journal.pone.0051842

Xiao, Y., Jiang, X., Peng, C., Zhang, Y., Xiao, Y., Liang, D., et al. (2019). Corrigendum to "BMP-7/Smads-Induced Inhibitor of Differentiation 2(Id2) Upregulation and Id2/Twist Interaction Was Involved in Attenuating Diabetic Renal Tubulointerstitial Fibrosis" [Int. J. Biochem. Cell Biol. 116 (November) (2019) 105613]. *Int. J. Biochem. Cell Biol.* 117, 105623. doi:10.1016/j.biocel.2019.105623

Yang, J., Velikoff, M., Agarwal, M., Disayabutr, S., Wolters, P. J., and Kim, K. K. (2015). Overexpression of Inhibitor of DNA-Binding 2 Attenuates Pulmonary Fibrosis through Regulation of C-Abl and Twist. *Am. J. Pathology* 185, 1001–1011. doi:10.1016/j.ajpath.2014.12.008

Yin, L., Liu, M.-x., Li, W., Wang, F.-y., Tang, Y.-h., and Huang, C.-x. (2019). Over-Expression of Inhibitor of Differentiation 2 Attenuates Post-Infarct Cardiac Fibrosis through Inhibition of TGF-β1/Smad3/HIF-1α/IL-11 Signaling Pathway. *Front. Pharmacol.* 10, 1349. doi:10.3389/fphar.2019.01349

Ying, X., Can, P., Yawen, X., Dan, L., Zhiping, Y., Zhiyang, L., et al. (2020). Oxymatrine Inhibits Twist-Mediated Renal Tubulointerstitial Fibrosis by Upregulating Id2 Expression. *Front. Physiol.* 19, 599. doi:10.3389/fphys.2020.00599.eCollection2020

Yuqing, Z., De, J., Xiaomin, K., Rongrong, Z., Yuting, S., Fengmei, L., et al. (2021). Signaling Pathways Involved in Diabetic Renal Fibrosis. *Front. Cell Dev. Biol.* 12, 696542. doi:10.3389/fcell.2021.696542

Conflict of Interest: The authors declare that the research was conducted in the absence of any commercial or financial relationships that could be construed as a potential conflict of interest.

Publisher's Note: All claims expressed in this article are solely those of the authors and do not necessarily represent those of their affiliated organizations, or those of the publisher, the editors and the reviewers. Any product that may be evaluated in this article, or claim that may be made by its manufacturer, is not guaranteed or endorsed by the publisher.

frontiers | Frontiers in Pharmacology

REVIEW
published: 13 June 2022
doi: 10.3389/fphar.2022.900491

Research Progress of Chinese Herbal Medicine Intervention in Renal Interstitial Fibrosis

*Xiao-Yuan Liu[1], Xu-Bin Zhang[2], Ya-Feng Zhao[1], Kai Qu[1] and Xiao-Yong Yu[1]**

[1]Department of Nephrology, Shaanxi Provincial Hospital of Traditional Chinese Medicine, Xi'an, China, [2]Department of Orthopaedic, Xi'an Hospital of Traditional Chinese Medicine, Xi'an, China

Chronic kidney diseases usually cause renal interstitial fibrosis, the prevention, delay, and treatment of which is a global research hotspot. However, no definite treatment options are available in modern medicine. Chinese herbal medicine has a long history, rich varieties, and accurate treatment effects. Hitherto, many Chinese herbal medicine studies have emerged to improve renal interstitial fibrosis. This paper reviews the mechanisms of renal interstitial fibrosis and recent studies on the disease intervention with Chinese herbal medicine through literature search, intend to reveal the importance of Chinese herbal medicine in renal interstitial fibrosis. The results show that Chinese herbal medicine can improve renal interstitial fibrosis, and the effects of Chinese herbal medicine on specific pathological mechanisms underlying renal interstitial fibrosis have been explored. Additionally, the limitations and advantages of Chinese herbal medicine in the treatment of renal interstitial fibrosis, possible research directions, and new targets of Chinese herbal medicine are discussed to provide a basis for studies of renal interstitial fibrosis.

Keywords: chronic kidney disease, renal interstitial fibrosis, Chinese herbal medicine, mechanism, research progress

OPEN ACCESS

Edited by:
Dan-Qian Chen,
Northwest University, China

Reviewed by:
Zou Chuan,
Guangdong Provincial Hospital of Chinese Medicine, China
Yong'An Ye,
Beijing University of Chinese Medicine, China

****Correspondence:***
Xiao-Yong Yu
gub70725@126.com

Specialty section:
This article was submitted to Renal Pharmacology, a section of the journal Frontiers in Pharmacology

Received: *20 March 2022*
Accepted: *18 May 2022*
Published: *13 June 2022*

Citation:
Liu X-Y, Zhang X-B, Zhao Y-F, Qu K and Yu X-Y (2022) Research Progress of Chinese Herbal Medicine Intervention in Renal Interstitial Fibrosis. Front. Pharmacol. 13:900491. doi: 10.3389/fphar.2022.900491

INTRODUCTION

Chronic kidney disease (CKD) is a global public health problem with low public awareness, high prevalence rate and medical cost, and poor prognosis (Mills et al., 2015; Hill et al., 2016). In 2017, 697.5 million patients had CKD, representing 9.1% of the global population. The number of cardiovascular deaths due to CKD in 2017 was 2.6 million, accounting for 4.6% of all deaths worldwide, making CKD the 12th leading cause of death worldwide (GBD Chronic Kidney Disease Collaboration, 2020). Regardless of the etiology of CKD, the final pathologic outcome is renal fibrosis (Zhou et al., 2016; Szeto, 2017). Renal fibrosis is a dynamic, multifactorial process involving complex and overlapping sequences of initiation, activation changes, subsequent execution, and eventual progression (Zhou et al., 2013). Upon persistent injury, inflammatory infiltration constitutes the first step of fibrosis, which appear as cell proliferation, fibroblast activation, and phenotypic transformation of renal tubular epithelial cells and endothelial cells. After activation, fibrotic signals mediate the process. Various cytokines are involved, resulting in hypoxia, renal tubular atrophy, scar formation, and eventually, renal failure. Renal fibrosis includes glomerulosclerosis and renal interstitial fibrosis (RIF). RIF is the pathological outcome of the vast majority of CKD. However, no targeted, clear, and effective prevention and control measures for RIF exist. Therefore, early prevention, delay, and reversal of RIF is a hot spot of current global medical research (Liu,

2011). Recent clinical research shows that modern medicine has succeeded in improving RIF to a certain extent; however, the clinical effect is still unsatisfactory. Moreover, accumulating evidence shows that traditional Chinese medicine, including extracts and compound preparations, is quite effective in preventing and treating RIF. For example, studies have shown that Astragalus can reduce TGF-β1 expression and Smad2/3 phosphorylation in mice with unilateral ureteral obstruction (UUO), thereby antagonizing the epithelial-mesenchymal transition (EMT) process and improving RIF (Shan et al., 2016). Hk-2 human proximal tubule epithelial cells were treated with angiotensin II (ANG-II) to induce EMT. After treatment with Fuzheng Huayu prescription, miR-21 expression and AKT phosphorylation were reduced and EMT was reversed (Wang Q. L. et al., 2020). This article reviews the research progress of Chinese herbal medicine intervention in RIF, in order to provide target ideas and references for clinical research.

PATHOLOGICAL MECHANISMS OF RIF

The pathological process of RIF is complex and related to the increase of extracellular matrix (ECM), EMT, oxidative stress, and the effect of various cytokines (**Figure 1**).

Increased ECM

Similar to all other organs, the hallmark of renal fibrosis is the excessive sedimentation of ECM. ECM is a very intricate network structure consisting of collagen, elastin, a variety of glycoproteins, and other components, which constitute the basement membrane and interstitial space. In addition to providing scaffolding and organ stability, ECM has many other functions, including its role in phlogosis. The composition of ECM depends on the functions of the respective kidney chamber (ie., glomeruli, tubulointerstitium, and blood vessels). Clinically, ECM plays a significant role in CKD. It can participate in the occurrence of uncommon kidney diseases, promote renal fibrosis, and thus accelerate the pace of CKD. The catabolism of ECM is mainly associated with two substances, matrix metalloproteinases and tissue inhibitors of metalloproteinases, which are disordered when fibrosis occurs (Bulow and Boor, 2019). ECM plays a very important role in maintaining normal tissue structure and function as well as the process of cell growth and differentiation. It is in a dynamic balance of continuous metabolic renewal, degradation, and remodeling. Excessive deposition of ECM is the main cause of RIF (Razzaque and Taguchi, 2002). ECM overdeposition and sedimentation are significant characteristic landmarks of fibrosis (Djudjaj and Boor, 2019).

Renal Tubular Epithelial Cell Phenotype Transformation

Renal tubular epithelial phenotypic transformation (EMT) is characterized by the transformation of the epithelial phenotype into a fibroblast-like mesenchymal phenotype, in which E-cadherin expression is reduced, and N-cadherin expression is increased. Epithelial cells lose top base polarity and, on the other hand, intercellular adhesion and gain mesenchymal properties (Liu et al., 2020; Li L. et al., 2021). This change is critical, not just in renal fibrosis, but in various biological processes such as cancer progression, organization palingenesis, embryo growth, and wound coalescence. In RIF, the effect of EMT is very clear: a large amount of evidence shows that EMT is a pivotal step in the launch of renal interstitial myofibroblasts. Thus, the precaution and treatment of EMT is a new direction in the study of renal fibrosis. Numerous studies have shown that EMT has three main effects on renal injury: affecting TEC role, leading to G2 stage cell period stasis, and dysregulating the balance between repair and fibrosis. As such, EMT is considered one of the most important processes leading to interstitial fibrosis (Liu, 2006; Thiery et al., 2009; Zhou et al., 2022).

Oxidative Stress

Oxidative stress accelerates the progression of RIF, meaning that when the body is exposed to adverse stimuli, the balance between the oxidant and antioxidant systems in the body is lost, the generation of reactive oxygen species is abnormally increased, and the body is damaged by oxidative stress, causing damage in various ways. The increase of reactive oxygen species and the decrease of antioxidant enzyme activity are closely related to the production of obstructive renal injury. The accumulation of reactive oxygen species can directly cause pathological damage to various renal cells. In addition, it can stimulate the expression of fibrosis-related factors, accelerate the multiplication of fibroblasts, inhibit the degradation of ECM, and ultimately aggravate renal fibrosis (McCarty, 2006; Mittal et al., 2014; Ren et al., 2017). In addition, the excessive accumulation of reactive oxygen species will destroy the structure and function of cells, directly injuring the kidney. On the other hand, reactive oxygen species can be used as signaling molecules to participate in intracellular signaling pathways (such as nuclear transcription factor-κB [NF-κB]), and can influence key enzymes in kidney cells to initiate growth factor signaling and the transcription of a variety of cytokines, causing RIF (Rhyu et al., 2005).

Renal Interstitial Fibroblast Proliferation, Activation, and Phenotypic Transformation

Renal interstitial fibroblasts are the main effector cells of fibrogenesis, and their massive proliferation and activation are the precursors for the production of excess ECM. Fibroblasts are reticulated in the kidney and are positioned between capillaries and epithelial cells to reinforce organization structure. Fibroblasts are star-shaped and contain a very dense endoplasmic reticulum, collagen particles, and many actin filaments. Interstitial fibroblasts are linked to the tubular and capillary basement membrane, which is facilitated by many cells. When inactive, stromal fibroblasts can generate erythropoietin. They can also secrete small proteins, such as fibroblast specific protein 1. Under normal conditions, fibroblasts produce a moderate amount of ECM to maintain stromal stability. However, under pathological

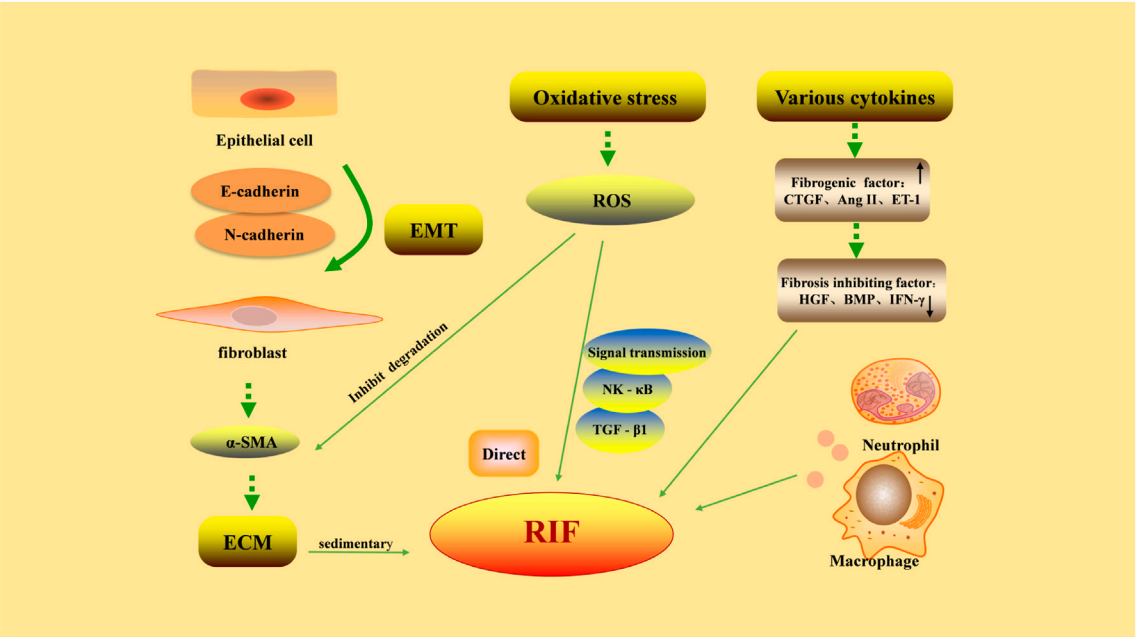

FIGURE 1 | Pathological factors in renal interstitial fibrosis. Excessive deposition of extracellular matrix (ECM) is the main cause of renal interstitial fibrosis. Epithelial-mesenchymal transition (EMT) refers to the phenotypic transformation of epithelial cells to fibroblast-like cells by acquiring a mesenchymal morphology, through decreased expression of E-cadherin and increased expression of N-cadherin. The proliferation of fibroblasts is the precursor of ECM overproduction. The factors promoting/inhibiting fibrosis restrict each other, and the dynamic balance is lost, leading to the formation of fibrosis. The damaged part of renal interstitium can be rapidly infiltrated by a large number of inflammatory cells, aggravating fibrosis. The abnormal increase in reactive oxygen species (ROS) generation during oxidative stress can directly induce pathological damage to various renal cells and reduce the degradation of ECM by mesangial cells. On the other hand, ROS can participate in intracellular signaling pathways as a signaling molecule, causing RIF.

conditions, fibroblasts can be activated by pro-fibrotic cytokines and certain stresses, generate α-SMA, causing an excessive ECM accumulation and obtaining myofibroblast phenotype. Myofibroblasts are the main cells that synthesize TGF-β1, and their number is closely related to the degree of RIF. They also secrete fibronectin, which provides scaffolds for the deposition of other ECM components and the formation of collagen fibers, leading to RIF (Eddy, 1996; Liu, 2011).

Cytokines and Inflammatory Cells

Factors that promote fibrosis mainly include TGF-β1, endothelin-1 (ET-1), platelet-derived growth factor (PDGF), and tumor necrosis factor (TNF-α). Some of the main factors that inhibit fibrosis are hepatocyte growth factor (HGF), interferon-γ (IFN-γ), and bone morphogenetic protein (BMP). The promoting and inhibitory factors restrict each other and form a dynamic balance, thereby maintaining the normal morphological structure and function of the kidney. When the promoting effect is enhanced or the inhibitory effect is weakened, this dynamic balance is lost, resulting in the formation of fibrosis. A large number of inflammatory cells such as macrophages, lymphocytes, and monocytes can infiltrate rapidly into the damaged renal interstitium. Macrophages play an important role in the process of renal fibrosis, and many related studies have been conducted in recent years, showing that the extent of macrophage infiltration is positively correlated with renal disease. Following renal injury, macrophages change from M1 type to M2 type and express factors that promote fibroblast activation. On the other hand, macrophages can directly take part in the production of ECM, and excessive deposition of ECM aggravates RIF (Pan et al., 2015; Wang Y. Y. et al., 2017; Yan et al., 2021). TNF-α is also involved in RIF as a key player that mediates inflammatory reaction in multiple cells, such as macrophages, mesangial cells, and renal tubular epithelial cells. TNF-α can launch NF-κB, MAPK, and other signaling pathways, resulting in fibrosis. These signaling pathways further promote the activation of TNF-α by increasing the extent of many inflammatory factors. Serum TNF-α standard is closely related to the severity of renal injury (Liu Y. et al., 2021; Taguchi et al., 2021).

MECHANISMS OF RIF INTERVENTION

RIF refers to many signaling pathways and a variety of cytokines; the pathological process is complex and dynamic. There are many studies on the intervention of Chinese herbal medicines in RIF, including single herbs, Chinese herbal extracts, and Chinese herbal compound preparations. Specific mechanisms of intervention in RIF are summarized in this section.

Regulation of TGF-β Signaling Pathway

In 1985, studies of the TGF-β family appeared, including molecular cloning of its signal transduction mediators. After this, researchers used cloning and genetic, biochemical, and

other methods to identify similar polypeptides of TGF-β1, which constitute members of the TGF-β family. A total of 33 TGF-β -associated polypeptides are encoded in the mammalian genome based on the completed gene sequencing (Derynck et al., 1985). TGF-β belongs to the category of dimer peptides and has many functions, including the regulation of cell multiplication and cell differentiation and participating in the immune response. Numerous lines of evidence, including upregulation of TGF-β signaling in the glomerulus or tubulointerstitium, increased TGF-β-induced renal fibrosis, and amelioration of renal fibrosis through anti-TGF-β treatment, support the role of TGF-β in fibrosis associated with kidney diseases. TGF-β competence was significantly increased in glomerular diseases. TGF-β1 expression was also positively correlated with fibrosis in biopsy specimens (Yoshioka et al., 1993). TGF-β1 first binds to the membrane-bound TGF-β1 type II receptor and then activates the Smad signal. It is mainly responsible for the accumulation of ECM, not only by upregulating the gene of ECM but also by enhancing the production of plasminogen activator inhibitors and other substances, aggravating the production of ECM, and further inducing fibrosis (Li Z. et al., 2018). In addition, TGF-β1 can aggravate the progression of RIF through the induction of EMT (Yan et al., 2019). TGF-β can reduce the decomposition of the cell matrix and increase the composition of metalloproteinase inhibitors by decreasing the composition of metalloproteinases (Isaka, 2018). TGF-β itself is a very critical profibrotic factor, but its role can be affected during the fibrosis process. Cytokines such as IL-1 promote the effects of TGF-β. Conversely, certain substances, including vitamin D receptors, inhibit TGF-β activity and thus the activation of fibroblasts (Wu et al., 2009; Palumbo-Zerr et al., 2015).

In traditional Chinese medicine, comfrey has been widely used for thousands of years and is mainly produced in Xinjiang, China. Comfrey has a variety of pharmacological effects, including anti-inflammation, antiviral, and anti-tumor activities. Studies have reported that shikonin can significantly prevent the loss of E-cadherin in diabetic nephropathy (DN) mice, attenuate the expression of TGF-β1-induced mesenchymal markers, and inhibit TGF-β1/Smad-mediated EMT (Li Z. et al., 2018). Xiexin soup contains rhubarb, rhizoma coptidis, and Scutellaria baicalensis and has been used to treat diabetes for years. According to the pharmacodynamic evaluation, Coptis alkaloids (A), Rhubarb polysaccharides (P), and Scutellaria flavonoids (F) were identified as the main active ingredients, namely the APF components. APF negatively regulated the TGF-β1/Smad pathway in DN mice and decreased NF-κB phosphorylation in the kidney of mice, suggesting that APF inhibits NF-κB signaling and its effect on inflammation. APF is a combination of herbs that can achieve therapeutic effects through multiple pathways (Wu et al., 2015). Dendrobium mixture can reduce the level of glucose and lipids and improve insulin resistance. On the one hand, dendrobium mixture can lower blood glucose standard in DN DB/DB mice and, on the other hand, restrain TGF-β1/Smads passage, thereby inhibiting renal EMT and fibrosis (Chen et al., 2021a). Astragalus has a wide range of medicinal uses. Astragalus includes astragaloside IV, Astragalus polysaccharide, various amino acids, total astragalus saponins, carotenoids, and other components. Astragalus in UUO rats can partially prevent renal myofibroblast activation by preventing EMT in obstructive nephropathy, induce HGF expression, inhibit TGF-β1 expression, and significantly reduce renal interstitial fibrosis (Zuo et al., 2009). The traditional Chinese medicine compound preparation Huangqi Decoction improves renal interstitial fibrosis in a dose-dependent manner in UUO mice. The decoction can downregulate TGF-β/Smad conduction and recede the EMT process in addition to avoiding the excessive accumulation of ECM, thus postponing RIF (Zhao et al., 2016). Rhubarb and Astragalus Capsules, medicinal plants rhubarb and AM, attenuate apoptosis by regulating the p38 MAPK pathway and alleviate RIF in UUO rats (Zeng et al., 2020). Compound Jincao Granules is composed of Jincao, psyllium, corn silk, and Shiwei. It is a classic formula for the treatment of urinary calculi. This formula can prevent calcium oxalate crystal-induced kidney damage in mice by impacting the TGF-β/Smad conduction (Liu et al., 2020). Rhubarb is widely used in the treatment of CKD. Taking adenine-induced chronic tubulointerstitial fibrosis in rats as the research object, it was shown that rhubarb extract treatment could reduce renal damage and improve renal function. The rhubarb extract inhibited RIF mainly by regulating the TGF-β/Smad conduction (Zhang et al., 2018). TGF-β1 can act in an either autocrine or paracrine fashion. Safflower has a wide range of effects, including antioxidative and inflammation suppressive actions, and safflower extract can act by inhibiting autocrine TGF-β signaling, thereby inhibiting renal interstitial fibrosis in UUO rats (Yang et al., 2008). The traditional Chinese medicine compound Shenqi Jiedu granules is a commonly used formula for the treatment of CKD in the clinic. With astragalus, angelica, salvia, and other ingredients, it has the functions of invigorating the kidney, promoting blood circulation, and detoxifying. Research shows that, combined with P311, Shenqi Jiedu granules can reduce pathological changes such as RIF, tubular dilation, and atrophy in rat kidneys, and its mechanism may be related to EMT and the TGF-β-Smad-Ilk signaling pathway (Cai et al., 2017). From the perspective of traditional Chinese medicine theory, many scholars believe that "kidney Yang deficiency" is one of the reasons for the occurrence of renal fibrosis. "Tonifying kidney Yang deficiency" is also the main criterion in the prevention and treatment of RIF. Shenqi Pill is composed of Rehmannia glutinosa, Danpi, Poria, Chinese yam, Alisma, and other components. Shenqi Pill can improve renal interstitial fibrosis in rats with adenine-induced renal injury by regulating TGF-β1/Smads conduction (Chen et al., 2017). Another research showed that the traditional Chinese medicine prescription Yougui Pill could improve RIF by regulating TGF-β1/Smads conduction (Wang L. et al., 2015). Tanshinone IIA is the most abundant diterpene quinone in the rhizome of Salvia miltiorrhiza. It has been used for the treatment of CKD in many countries for more than 2000 years. Tanshinone IIA attenuated TGF-β/Smad and NF-κB conduction and inhibited inflammation, thereby reducing RIF in 5/6 nephrectomized rats with CKD (Wang D. T. et al., 2015). Saponins are a class of phytochemicals that exist in a variety of plants, including ginsenosides. Previous studies have

suggested that total ginsenosides have a profound protective effect in acute myocardial ischemia, and ginsenosides can simultaneously inhibit TGF-β1/Smad, NF-κB conduction, activation of Nrf2-ARE conduction to attenuate renal fibrosis (Gao et al., 2021). Many patients with hypertension will develop CKD and experience the pathological changes of RIF, leading to renal failure. Qingxuan Antihypertensive soup is a Chinese herbal medicine formula that can significantly reduce patients' hypertension. Previous research has reported that it can reduce the excessive accumulation of ECM and thereby reduce RIF by decreasing the TGF-β1/Smad conduction in spontaneously hypertensive rats (Liu W. et al., 2017). The Shenkang VII recipe is a commonly used composition for the treatment of CKD. Studies have shown that it can improve renal function by reducing ECM deposition in the kidney and the expression of inflammatory mediators. In addition, the Shenkang VII recipe inhibited the activation of TGF/Smad, NF-kB, and SHH signal transduction in UUO rats, slowing the progression of renal fibrosis (Zhou et al., 2020). Dioscorea, a common Chinese herbal medicine. β-hydroxybutyric acid (β-HB) (10 mM) to induce renal interstitial fibroblast (NRK) cells. Studies have shown that diosgenin inhibited TGF-β signaling pathway and antagonized EMT, thereby reducing RIF (Liu et al., 2012). Hirudin has a clear medicinal effect and is a commonly used thrombin inhibitor. Hirudin can improve RIF and has many advantages, including safety and low cost, which has attracted the attention of many researchers. Hirudin can inhibit inflammation and reduce the activation of the TGF-β pathway, thereby inhibiting EMT and improving RIF (Xie et al., 2020; Lin et al., 2022).

Regulation of NF-κB Signaling Pathway

NF-κB protein has its own family and plays important roles in the body, including inflammatory response and immune processes. Transcription factors adjust the function of multiple genes including cell growth, development, and death (Vallabhapurapu and Karin, 2009). Oxidative stress can lead to RIF through the NF-κB pathway. When epithelial cells are hypoxic, the NF-κB pathway is activated. The main function of the NF-κB pathway in the body is to cause inflammation and promote fibrosis of tissues (Liu M. et al., 2017). The NF-κB pathway also regulates the activation of EMT-related Snail1 and exacerbates fibrosis. Transglutaminase promoter is an inducer that increases TGF-β expression and, on the other hand, accelerates ECM accumulation and exacerbates fibrosis by enhancing NF-κB expression through a positive feedback pathway (Bitzer et al., 2000; Chen et al., 2008; Ghiazza et al., 2010). Toll-like receptor 4 (TLR4) is an inflammatory stimulator and the acceptor of lipopolysaccharide (LPS), which is a significant element of the external membrane of Gram-negative bacteria that can irritate the activation of inflammatory conduction. Compared to other transcription factors, NF-κB is relatively conserved and plays an important role in many processes, including post-infection regulation of the immune system. The NF-κB signaling pathway can be activated by TLR4. There are a great many pathways that can initiate NF-κB signaling, which can be categorized as the canonical and noncanonical pathways. Among them, the activation of inflammatory receptors is a canonical pathway. Several TNF receptor members recruit TRAF2 and TRAF3 signals to initiate the NF-κB signal in a non-canonical fashion (Morgan and Liu, 2011). In mammals, the most widely studied member of the NF-κB/Rel family is P65, whose activation is influenced by multifarious stimuli and is associated with a variety of cells, such as inflammatory and apoptotic factors (Yde et al., 2011; Basak et al., 2012). In addition, activated p65 has been implicated in various inflammatory diseases, such as RIF (Fujihara et al., 2007). NF-κB is a hinge intermediary in inflammatory infiltration, which is mediated by excessive cell multiplication, ECM accumulation, and apoptosis (Barkett and Gilmore, 1999).

Curcumin is a chemical produced by the rhizome of turmeric with pharmacological effects of antioxidant, anti-fibrotic, anti-inflammatory, and anti-proliferative activities. The results of previous research showed that curcumin reduced RIF in UUO mice, mainly preventing the EMT process, inhibiting inflammatory response, and slowing down the excessive accumulation of ECM (Wang Z. et al., 2020). Fuzheng Huayu prescription is a commonly used Chinese herbal medicine prescription in the clinic. The role of the prescription is to promote blood circulation and remove blood stasis, replenish essence, and nourish yin. Studies have shown that it can attenuate mercuric chloride-induced renal interstitial fibrosis in rats by resisting oxidative stress and regulating the NF-κB signaling pathway (Yuan et al., 2017). Artemisinin is a very good antimalarial drug and is widely used around the world. Artemisia annua has many other functions, such as regulating the body's immune function. Studies have shown that artemisinin can reduce RIF in rats with 5/6 nephrectomy by downregulating the NF-κB/NLRP3 signaling pathway, thereby providing renal protection (Wen et al., 2019). Zhenwu Decoction is a traditional Chinese medicine prescription with definite clinical efficacy. PPARγ has a variety of biological effects, including antagonizing the activation of TGF-β1 and NF-κB signals and the multiplication of mesangial cells. PPARγ also has biological functions such as anti-inflammatory and anti-fibrotic activities and regulation of lipid metabolism. Zhenwu Decoction inhibited the activation of the TGF-β1 signaling pathway and promoted the activity of PPARγ in UUO rats, thereby improving RIF (Li S. et al., 2018). Maslinic acid, a pentacyclic triterpene, using UUO mouse kidney and NRK49F cells treated with TGF-β, maslinic acid can disturb the MyD88, inhibit Smad4 nuclear activity, and improve the changes of renal fibrosis. In addition, hawthorn acid reduced NF-κB signaling and improved fibrosis (Sun et al., 2021). Coreopsis is an ethnic medicine. Local Uyghurs consume it as an herbal tea to treat high blood pressure and diarrhea. Coreopsis have anti-inflammatory, lipid-regulating, and blood sugar-regulating effects. In diabetic kidney cells, NF-κB expression is significantly increased, and NF-κB can reach the nucleus, induce inflammatory infiltration, and accelerate the progression of renal fibrosis. Studies have shown that in high glucose-induced rat glomerular mesangial cells, coreopsis ameliorates fibrosis through the TGF-β1/SMADS/AMPK/NF-κB axis (Yao et al., 2019). Resveratrol, a polyphenol with anticancer, anti-inflammatory, and antioxidant properties, can modulate Hsp70 expression in the kidneys of 5/6 nephrectomized uremic rats, and, at the same time, inhibit NF-

κB expression, thereby exerting a renal protective effect (Feng et al., 2020). Cordyceps sinensis is an entomopathogenic fungus, which has been widely used in the clinic for centuries with definite curative effects in heart palpitations, epilepsy, and convulsions in children. N6-(2-hydroxyethyl) adenosine (HEA), derived from cicadas, is a compound that has pharmacological activities such as antagonizing inflammation. Studies have shown that HEA exerts advantageous effects on UUO-induced RIF in mice by regulating the NF-κB/TGF-β1/Smad axis, inhibiting inflammation, and activating renal fibroblasts (Zheng et al., 2018). The clinical studies of Astragalus membranaceus are extensive. Astragaloside IV is a very important physiological component of Astragalus membranaceus, which has multifarious activities such as vasodilation, prevention of endothelial dysfunction, improvement of myocardial cell energy metabolism, as well as anti-inflammatory and antioxidant activities. Studies have shown that Astragaloside IV reduces ECM accumulation and inflammatory cell infiltration in UUO-induced renal fibrosis and significantly attenuates inflammatory response. On the other hand, it inhibited lPS-induced inflammatory infiltration in epithelial cells, decreased NF-κB signaling both *in vivo* and *in vitro*, thereby delaying RIF (Zhou et al., 2017b). Quercetin is a natural compound widely found in Chinese herbs such as jujube and sophorae. Researchers have studied the effect of quercetin on kidney injury in UUO mice. The results showed that quercetin inhibited NF-κB signal transduction, regulated M1/M2 macrophage polarization, and improved RIF (Lu et al., 2018).

Regulation of MAPK-Related Signaling Pathways

Mitogen-activated protein kinase (MAPK) is a widely conserved, versatile protein that takes part in many cellular activities. Many stimuli outside the cell activate MAPK, and its activation appears in the order of MAPK kinase kinase (MAPKKK), MAPKK kinase (MAPKK), and MAPK. There are many members of the MAPK family, and more than four are well-known, including extracellular signal-regulated kinase 1/2 (ERK1/2), C-Jun-amino terminal kinase (JNK), P38, and ERK5 (Nishimoto and Nishida, 2006). The P38 MAPK pathway carries out signal transduction in cells and plays an important role by participating in the inflammatory infiltration and producing fibrotic substances and profibrotic mediators. P38 has been implicated in ECM synthesis in the pathogenesis of fibrosis (Lee et al., 2019). JNK signaling promotes the manufacturing of inflammation and profibrotic molecules by tubular epithelial cells, as well as the dedifferentiation of tubular cells towards a mesenchymal phenotype. JNK signaling pathway and other signaling pathways crosstalk and participate in physiological and pathological activities in the body. JNK signaling pathway is most closely related to the TGF-β/SMAD signaling pathway. When activated, JNK enhances the activity of the TGF-β signaling pathway. Therefore, inhibition of p38 MAPK or TGF-β1 protein expression may be an effective strategy to alleviate RIF (Grynberg et al., 2017).

Puerarin (PR) from the puerarin plant has been comprehensively used in the clinic to treat a variety of diseases, including cardiovascular, brain, and lung injuries. A study showed that puerarin could inhibit the activation of MAPK in UUO mice and attenuate RIF (Zhou et al., 2017a). Gardeniside, an iridoid glycoside compound, is one of the most active components obtained from gardenia fruit. Autophagy is the process of recycling damaged cells and proteins and a very conserved cellular process that functions to maintain intercellular homeostasis. Autophagy is an important therapeutic target for DN; studies have shown that geniposide can increase MAPK activity in DN mice, enhance ULK1-mediated autophagy response, reduce AKT activity, thereby blocking oxidative stress, phlegmonosis, and renal fibrosis in diabetic kidneys (Dusabimana et al., 2021). Kangxianling is a traditional Chinese herbal formula that can cause more than 1,000 characteristic genes to be upregulated in azithromycin nephropathy rats, triggering the downstream launch of Wnt, TGF-β, and MAPK pathways to achieve the inhibition of RIF (Jiang et al., 2020). Astragaloside IV, as one of the most important pharmacological components of Astragalus membranaceus, has a wide range of pharmacological effects, including antagonizing inflammation, lowering blood pressure and hypoglycemia, and protecting the myocardium. Studies have shown that it inhibits TGF-β1-induced ERK1/2, p38 MAPK, phosphorylation of JNK, and IkBa, suggesting that astragaloside IV exerts anti-fibrotic effects through MAPK and NF-kB signaling pathways (Che et al., 2015). The main medicine in huangkui capsule is Huangkui, a traditional Chinese medicine. Huangkui capsule can obviously improve the renal fibrosis of diabetic nephropathy patients. Modulation of oxidative stress and p38MAPK/Akt pathway reduces renal fibrosis in rats with diabetic nephropathy compared with lipoic acid (Mao et al., 2015). In ginkgo biloba injection, the main drug is ginkgo biloba, clinical application of which is mature and has proven effects in the treatment of cardiovascular diseases. Clinical studies on ginkgo biloba leaf are also extensive. Ginkgo biloba leaf can inhibit inflammation and apoptosis, thus preventing testicular damage. On the other hand, ginkgo biloba leaf can downregulate the p38 MAPK signaling pathway and antagonize organ fibrosis (Li et al., 2017; Wang R. et al., 2017; Gevrek et al., 2018; Wang A. et al., 2018). Recent studies have shown that Ginkgo biloba can effectively improve cisplatin-induced post-renal interstitial fibrosis in rats with AKI by inhibiting renal cell apoptosis, which is mediated by downregulating the p38MAPK/TGF-β1 and p38MAPK/HIF-1α signaling axes (Liang et al., 2021). Salidroside (Sal) is the main pharmacological component of rhodiola rosea in Chinese herbal medicine. Salidroside has many beneficial functions for the body, including antagonizing inflammation and protecting kidney. In addition, salidroside decreased the accumulation of ECM and inhibited the activity of TLR4/NF-κB and MAPK signaling pathways in UUO mice and HK-2 cells, delaying renal fibrosis (Li et al., 2019). The ERK signaling pathway can be activated by a variety of stimuli, including high glucose, and this activation can cause EMT. MicroRNAs (miRNAs) are non-coding, relatively short RNAs that have a role in adjusting cell function. Existing studies have shown that multifarious miRNAs are highly correlated with EMT. Mulberry leaf is a commonly used traditional Chinese medicine and is rich in ingredients. Pharmacodynamic studies have shown

that mulberry leaf and its functional compounds have the potential to prevent the development of DN, and network pharmacology has confirmed that mulberry leaf has anti-diabetic activities. Further studies showed that mulberry leaf extract could reduce the pathological changes of EMT induced by high glucose through the inhibition of the NADPH oxidase/ROS/ERK signaling axis. In addition, in HK-2 cells, mulberry leaf could increase the expression of MiR-302a and inhibit ZEB1, thereby inhibiting EMT (Ji et al., 2019). Interleukin-11 (IL-11) has its own biological function, and it belongs to the IL-6 system. When TGF-β signal is activated, it can greatly promote the activation of IL-11 and other fibrosis-related genes. IL-11 causes ERK1/2 activation in organ fibrosis, but not the JAK/STAT pathway. After IL-11 induced ERK1/2 activation, mRNA translation and fibrosis protein expression were further promoted. This is inconsistent with TGF-β activation. Another study confirmed that osthole directly affects IL-11-induced ERK1/2 signaling and alleviates renal fibrosis (Wu et al., 2021). Poricoic acid is the main chemical component of poria cocos. In a recent study, NRK-49F cells induced by TGF-β1 were used as the research object. The results showed that Poricoic acid could inhibit the activation of PDGF-C, Smad3, and MAPK pathways, thus reducing the excessive accumulation of ECM and improving RIF (Li Q. et al., 2021).

Regulation of Wnt/β-Catenin Signaling Pathway

The Wnt/β-catenin signaling pathway is important for many biological functions, such as promoting tissue production, maintaining cell stability, and the development of some diseases (MacDonald et al., 2009). Wnt/β-catenin signaling pathway also plays a significant role in renal disease, and many studies have reported that this signaling pathway is involved in the progression of diabetic nephropathy, adriamycin nephropathy, focal glomerulosclerosis and other diseases (Surendran et al., 2005; Dai et al., 2009; He et al., 2012; Naves et al., 2012). Different levels of Wnt/β-catenin and the interaction between Wnt/β-catenin signaling pathway and other pathways are important links leading to EMT. It is well established that the EMT process can directly lead to RIF. In conclusion, inhibition of Wnt/β-catenin signaling activity or blocking of this signal transduction is beneficial to alleviate RIF (Liu, 2010; He et al., 2013; Li et al., 2013). On the other hand, After activation of Wnt signal, β-catenin is activated accordingly, promoting the process of renal fibrosis. Wnt/β-catenin also regulates the activity of a variety of downstream mediators in cells, including snail 1, fibroblasts and macrophages 6 and components of the renin-angiotensin system, and others. When Wnt/β-catenin activation promotes RIF, it is not a single effect, but often combined with other signal transduction (Li S. S. et al., 2021).

Accumulating evidence suggests that Astragaloside IV (AS-IV) exerts renoprotective effects by anti-inflammatory action, reducing oxidative stress, and blocking NF-κB transmission, thereby inhibiting inflammatory infiltration, attenuating podocyte damage by modulating the MAPK pathway, and attenuating ROS produced to improve podocyte apoptosis. In addition, the study demonstrated that AS-IV can inhibit Wnt/β-catenin signal transduction in UUO rats, suggesting that astragaloside IV can reduce RIF and protect renal function (Wang et al., 2014). Qishen Yiqi Dropping Pill (QSYQ) has a good clinical effect on kidney disease, including astragalus, salvia, red sandalwood, and other drugs. β-catenin (β-catenin) is a key protein in Wnt signaling. Recent research indicates that QSYQ can reduce RIF in UUO rats due to the selective inhibition of β-catenin upregulation and downstream fibrotic effects (Zhou et al., 2016). Tangshenning is a compound preparation that can relieve the symptoms of edema and dysuria in DN patients. AS-IV is the main active ingredient of Tangshenning, which can prevent podocyte EMT in DN. Scholars have studied its effects on podocyte EMT and Wnt/β-catenin pathway. It inhibited the launch of the Wnt/β-catenin pathway in DN mice (Cui et al., 2021). Most Chinese medicine scholars believe that DN also includes blood stasis blocking collaterals and kidney collaterals. Studies have found significant ECM deposition in the tubulointerstitium and some glomeruli of DN rats, and high glucose could stimulate and induce the activation of Wnt/β-catenin pathway, leading to RIF in DN rats. Huayu tongluo can significantly inhibit the deposition of ECM and block the overresponse of the Wnt/β-catenin pathway, thus alleviating RIF (Bai L. et al., 2017). Curcumin can inhibit Wnt/β-catenin signaling in diabetic rats and attenuate the reaction of superoxide, TGF-β1, and fibronectin activity in renal mesangial cells by high glucose and alleviate the accumulation of ECM in diabetic nephropathy (Ho et al., 2016). Poria is a commonly used traditional Chinese medicine in clinical practice, and it has a series of biological effects, including inhibition of inflammation, regulation of blood lipids, and inhibition of oxidation. Using HK-2 cells and UUO mice as the research objects, the study showed that novel tetracyclic triterpenoids, namely pachylic acid ZC (PZC), pachylic acid ZD (PZD), and pachylic acid ZE (PZE), could block the overexpression of Wnt/β-catenin signal, thereby intercepting Smad3 phosphorylation and significantly attenuating RIF. Furthermore, PZC and PZD have stronger renoprotective effects compared to PZE (Wang M. et al., 2018). Salidroside is the main pharmacological component of rhodiola rosea, which has a variety of pharmacological effects, such as treating diabetes, inhibiting oxidative stress, and delaying aging. Using a mouse model of azithromycin nephropathy, the study showed that salidroside also has many pharmacological effects on the kidney. It can attenuate Wnt/β-catenin signaling, thereby reducing proteinuria, protecting podocyte, and protecting renal function. The results of this study demonstrated the renal protective effect of salidroside and laid the foundation for further studies on salidroside and kidney (Huang et al., 2019). Alisma is a well-known natural product with lipid-lowering and kidney-protecting properties. Triterpenoids are the main active ingredients. 25-O-methyl alismatil F (MAF) is a pharmacological component extracted from Alismatil alismatil. Scholars have studied the effect of MAF on normal mouse renal tubular epithelial cells (NRK-52E) induced by TGF-β1 and Angiotensin II (ANG) and normal mouse fibroblast (NRK-49F) EMT, confirming that it can selectively inhibit TGF-mediated Smad3 phosphorylation,

enhance Smad7 expression, inhibit Wnt/catenin signaling pathway, thereby attenuating EMT and relieving renal interstitial fibrosis (Chen et al., 2018). Tripterygium wilfordii is a common Chinese medicine. Studies have shown that tripterygium wilfordii treatment can reduce the expression of WNT-1 and β-catenin in renal tissues in diabetic rats, thereby alleviating fibrosis (Chang et al., 2018).

Regulation of PI3K/Akt/mTOR and JAK2/STAT3 Signaling Pathways

mTOR is a serine/threonine protein kinase, which plays an important role in regulating many cellular processes, mainly cell growth. mTOR forms two main complexes, mTOR compound 1 (mTORC1) and compound 2. In the body, mTORC1 is more important for the regulation of cell growth. MTORC1 relies on the phosphorylation of several downstream factors, including ribosomal protein S6 kinase β -1 (p70S6K) and other substances, for its physiological activity. mTORC1/p70S6K signaling has been reported to mediate EMT during DN. Astragalus invigorates qi and transports spleen. It has a wide range of clinical indications and safe and clear efficacy in certain conditions such as heart-related diseases, leucopenia, and diabetic nephropathy. Studies have shown the effects of astragaloside IV on EMT, involving the reduction of high glucose-induced EMT in renal tubular cells through mTORC1/p70S6K signaling and subsequent downregulation of transcription in HK-2 cells (Chen et al., 2019). The Janus kinase/signal transduction and transcription activator (JAK/STAT) pathway has many physiological functions, involving many growth factors and cytokines. The JAK/STAT pathway is involved in cell proliferation. JAK can activate STAT3 in response to TGF-β and other related cytokines, playing a role in promoting fibrosis. Shenkang (SK) is a very common prescription for the treatment of renal failure. In UUO mice, studies have shown that SK can inhibit the conduction of JAK2/STAT3 signaling and significantly improve RIF in mice (Qin et al., 2021). Some studies have shown that autophagy promotes the occurrence of diabetic nephropathy and plays an important role in the progression of diabetic nephropathy. At present, there are many researches on autophagy, which can keep cells stable by clearing damaged cells and proteins from the body. Adjustment of autophagy within the body involves many signal pathways and targets; the most classic pathway is the PI3K/AKT/mTOR axis, and the most common target is mTOR. mTOR can adjust autophagy in two opposite directions. mTOR is downstream of the PI3K/AKT axis, which determines the activity of mTOR. The mixture of Dendrobium can regulate the PI3K/AKT/mTOR signal conduction to interfere with autophagy, inhibit kidney fibrosis, delay DN progression, and protect the renal function (Chen et al., 2021b).

Regulation of Hedgehog and Notch Signaling Pathways

In mammals, the hedgehog signaling pathway is also very important in a variety of cellular signaling processes, particularly in embryonic cells. This pathway plays a pivotal role in the growth and development of animals. Shh is one of the important protein ligands of hedgehog proteins. Previous research has indicated that Shh activity increased significantly during fibrosis, suggesting a potential relationship between organ fibrosis and abnormal Shh signaling. Studies have shown that blocking the activation of Shh signaling helps inhibit RIF and prevent CKD progression. Polygonum cuspidatumt inhibits inflammatory infiltration and antagonizes oxidative stress, inhibiting tumor progression. Polysaccharides are an important pharmacological component of Polygonum cuspidatumt. Using UUO mice, researchers have studied the medicinal value of polysaccharides (BPPs) in Polygonum cuspidatum for relieving RIF and found that, BPP treatment could reduce ECM components and the activation of fibroblasts that produce these ECM components, resulting in a significant reduction in interstitial fibrosis. After BPP administration, the level of matrix metalloproteinase enzymes increased significantly in the body. In contrast, the levels of tissue inhibitors of metalloprotease were significantly reduced. The same case applied in HK-2 cells treated with TGF-β1. Furthermore, BPP administration decreases the expression of multiple transcription factors that regulate E-cadherin expression. The activation of the hedgehog pathway, the degree of EMT, and the degree of fibrosis are positively correlated. Studies have shown that BPP administration inhibited the hedgehog signaling pathway. Therefore, BPPs can suppress the EMT process by attenuating the activity of the hedgehog signal conduction, thereby improving RIF (Briscoe, 2009; Jenkins, 2009; Ding et al., 2012; Rauhauser et al., 2015; Li L. et al., 2021). Sedum is extracted from rhodiola rosea and widely used in the clinic. Studies have shown that Sedum extract can inhibit hedgehog signaling pathway and myofibroblast phenotypic transformation in UUO rats, thereby improving renal fibrosis (Bai Y. et al., 2017).

Many studies have shown that the Notch pathway can induce the EMT process and lead to fibrosis. Snail directly inhibits the transcription of E-cadherin, which brings about the loss of epithelial cell attachment and promotes the occurrence of EMT. Snail can regulate gene expression and is affected by a variety of signaling pathways, of which Notch signaling pathway is the most influential. Berberine (BBR) from Coptis chinensis and Phellodendron chinensis possesses a variety of pharmacological activities, including antibacterial, hypoglycemic, cholesterol-lowering, antitumor, and immunomodulatory properties. Using KKAy mice as animals to establish a DN mouse model, a study found that BBR administration may have indirec and direc pleiotropic effects on the Notch/Snail axis, inhibiting EMT, reducing RIF, and delaying the course of DN (Paznekas et al., 1999; Peinado et al., 2004; Katoh and Katoh, 2005; Herranz et al., 2008; Yang et al., 2017).

Inhibition of NLRP3 Inflammasome and EZH2 Activity Expression

Inflammatory status can have an adverse effect on kidney diseases and aggravate RIF. Inflammatory corpuscle is a protein complex that acts as a receptor and regulates inflammatory factors in the body. The NOD-like receptor family has many members, including pyrin domain 3 (NLRP3), which is a typical

TABLE 1 | Summary of Chinese herbal medicines that improve RIF-related mechanisms Single herb.

Chinese herbal medicine	Specific drug	Research object	Specific mechanism	References
Astragalus	Astragalus	UUO rat	↓TGF-β1/Smad ↓ EMT ↑ HGF	Zuo et al. (2009)
Rhubarb	Rhubarb	Chronic-renal tubulointerstitial fibrosis in rat	↓ TGF-β/Smad	Zhang et al. (2018)
Safflower	Safflower	UUO rat	↓ TGF-β	Yang et al. (2008)
Yam	Yam	β-Hydroxybutyric acid-induced fibroblasts	↓ TGF-β/Smad ↓ EMT	Liu et al. (2012)
Coreopsis	Coreopsis	Rat glomerular mesangial cell	↓TGF-β1/SMADS ↓AMPK/NF-κB	Yao et al. (2019)
Huangkui Capsules	Huangkui	DN rat	↓ p38MAPK/Akt	Mao et al. (2015)
Ginkgo biloba injection	Ginkgo biloba	Cisplatin- induced rat AKI	↓p38MAPK/TGF-1 ↓p38MAPK/HIF1α	Liang et al. (2021)
Mulberry leaves	Mulberry leaves	HK-2	↓NADPH oxidase/ROS/ERK	Ji et al. (2019)
Astragalus	Astragalus	UUO rat	↓ TGF-β1 ↓ EMT	Shan et al. (2016)
Tripterygium wilfordii	Tripterygium wilfordii	DN rat	↓Wnt-1/β-catenin	Chang et al. (2018)

↑: increase or activation; ↓: decrease or inhibition. UUO: unilateral ureteral obstruction; TGF-β1/Smad: transforming growth factor-beta1/Smad; EMT: Epithelial-mesenchymal transition; HGF: hepatocyte growth factor; AMPK: AMP-activated kinase protein; NF-κB: nuclear factor kappa beta; DN: diabetic nephropathy; p38MAPK: p38 mitogen-activated protein kinase; Akt: serine-threonine kinase; AKI: acute kidney injury; HIF-1α: hypoxia-inducible factor-1α; HK-2: human renal tubular epithelial cells; NADPH: nicotinamide adenine dinucleotide phosphate; ROS: reactive oxygen species; ERK: extracellular regulated protein kinases.

inflammasome thar forms a complex composed of adaptor proteins, including the caspase recruitment domain (ASC) and the serine protease caspases, Apoptosis-associated speck-like protein of enzyme 1 (Casp1). Renal tubular epithelial cell injury is caused by many factors, such as insufficient perfusion and severe obstruction; these injuries activate the NLRP3 inflammasome, which regulates the production of proinflammatory cytokines. The NLRP3 inflammasome has its own characteristics; it can respond to various non-exogenous harmful signals, which makes this inflammasome widely explored in the study of renal diseases. Danggui Buxue decoction was founded in the Jin Dynasty of China. The main components are Angelica sinensis and Astragalus root in a ratio of 1:5, which shows significant renal protection. Danggui Buxue Decoction can reduce RIF in UUO rats. The reason for this beneficial effect is that it affects the activity of NLRP3 and inhibits inflammatory infiltration (Wang et al., 2016). *In vitro* test results showed that andrographolide effectively inhibited high glucose-induced apoptosis and EMT. In addition, it can reduce HK-2 cell death. The reason is that andrographolide can inhibit the activation of the NOD-like receptor family and NLRP3 inflammasome, antagonize the EMT process, and improve mitochondrial dysfunction. *In vivo*, andrographolide also plays a role in inhibiting EMT and improving RIF (Liu W. et al., 2021).

EZH2 regulates gene expression through epigenetics, participates in many biological processes, and catalyzes the trimethylation of lysine 27 of histone H3 (H3K27me3). The expression of EZH2 and H3K27me3 were elevated in obstructed kidneys, and inhibition of EZH2 attenuated RIF. Overexpression of EZH2 is associated with multiple cancerous tissue types (Simon and Lange, 2008; Yang and Yu, 2013). Reducing the expression of EZH2 is beneficial to reduce cell proliferation, antagonize EMT, and prevent tumor progression (Lu et al., 2010). Reducing the expression of EZH2 can weaken TGF-β1 activity (Xiao et al., 2016). Emodin, the main component of the traditional Chinese medicine rhubarb, can delay the progression of CKD. Researchers have studied the effect of emodin on tubulointerstitial fibrosis and its mechanism, and the results showed that emodin inhibits RIF in UUO rats, which was associated with the reduction of EZH2 activity *in vitro* and *in vivo* (Xu et al., 2021).

DISCUSSION

RIF is the final pathological outcome of almost all CKDs and is a determinant and prognostic indicator of CKD progression. Pathophysiologically, RIF includes several stages. Cell activation and injury are the first steps. The second stage includes fibrotic signaling, in which various cells factors and signal pathways that can crosstalk with each other are included. Next, it enters the fibrosis stage, and ECM accumulates pathologically. The last stage is the occurrence of renal damage (Eddy, 2000). Overcoming RIF has been a global challenge. Based on the molecular mechanisms and targets of RIF, studies of modern medicine has produced abundant clinical results, associating the classical signaling pathways such as TGF-β, macrophages, stem cells, and autophagy, and significant progress has been made. However, there are no treatment modalities that can completely prevent and treat RIF.

Traditional Chinese medicine has a long history and definite curative effect, which emphasizes the unity of nature and man. Therefore, researches on the treatment of RIF with Chinese herbal medicine are abundant. The intervention forms include original Chinese herbal medicines, Chinese medicine extracts, and Chinese medicine compound preparations, involving the types of drugs such as invigorating qi and nourishing yin, removing blood stasis, promoting blood circulation, clearing heat and removing dampness, invigorating the kidney and detoxifying, and supporting yang qi. Several Chinese herbal

TABLE 2 | Summary of Chinese herbal medicines that improve RIF-related mechanisms Chinese herbal extract.

Chinese herbal medicine	Specific drug	Research object	Specific mechanism	References
Comfrey	Acetylshikonin	DN mouse	↑ E-cadherin ↓ TGF-β1/Smad ↓ EMT	Li et al. (2018b)
Salvia	Tanshinone	Nephrectomy in CKD rat	↓ TGF-β/Smad ↓ NF-κB	Wang et al. (2015a)
Ginseng	Ginsenosides	Natural aging rat	↓ TGF-β1/Smad ↓ NF-κB ↑ Nrf2-ARE	Gao et al. (2021)
Leech	Hirudin	UUO mice	↓ TGF-β ↓ EMT ↓ MCP-1	Lin et al. (2022)
Turmeric	Curcumin	UUO mice	↓ TLR4/NF-κB ↓ PI3K/AKT	Wang et al. (2020b)
Artemisia annua	Artemisinin	rats with 5/6 nephrectomy	↓ NF-κB/NLRP3	Wen et al. (2019)
Hawthorn	Hawthorn acid	UUO mice	↓ TGF-β ↓ NF-κB	Sun et al. (2021)
White hellebore	Resveratrol	5/6 nephrectomy uremic rat	↑ Hsp70 ↓ NF-κB	Feng et al. (2020)
Cicada Cordyceps	N6-(2-hydroxyethyl)adenosine	UUO induced mice	↓ NF-κB ↓ TGF-β1/Smad	Zheng et al. (2018)
Astragalus	Astragaloside IV	UUO mice	↓ TLR4 ↓ NF-κB	Zhou et al. (2017b)
Kudzu root	Puerarin	UUO mice	↓ MAPK	Zhou et al. (2017a)
Gardenia	Geniposide	DN mice	↑ MAPK ↓ AKT	Dusabimana et al. (2021)
Astragalus	Astragaloside IV	TGF-β1 induced mice	↓ MAPK ↓ NF-κB	Che et al. (2015)
Rhodiola	Salidroside	UUO mice	↓ TLR4/NF-κB ↓ MAPK	Li et al. (2019)
Cnidium	Osthole	UUO mice HK-2 cells	↓ TGF-β/Smad2/3 ↓ IL-11/ERK1/2	Wu et al. (2021)
Astragalus	Astragaloside IV	UUO rat	↓ Wnt/β-catenin	Wang et al. (2014)
Turmeric	Curcumin	DN rat	↓ Wnt/β-catenin	Ho et al. (2016)
Poria	Poria acid	HK-2 cells UUO mice	↓ Wnt/β-catenin	Wang et al. (2018b)
Rhodiola	Salidroside	Azithromycin nephropathy mouse model	↓ Wnt/β-catenin	Huang et al. (2019)
Alisma	25-O-methylalisol F	AngiotensinII-induced normal mice	↓ Wnt/β-catenin	Chen et al. (2018)
Astragalus	Astragaloside IV	High-glucose-induced renal tubular cells	↓mTORC1/p70S6K	Chen et al. (2019)
Knotweed	Polysaccharide	UUO mice	↓ TGF-β1 ↓ Hedgehog	Li et al. (2021a)
Coptis, Cork	Berberine	DN mice	↓ Notch/snail	Yang et al. (2017)
Andrographis	Andrographolide	Diabetic mice	↓ NLRP3	Liu et al. (2021a)
Rhubarb	Emodin	UUO rat	↓ EZH2	Xu et al. (2021)
Jujube	Quercetin	UUO mice	↓ NF-κB	Lu et al. (2018)
Rhodiola rosea	Sedum sarmentosum Bunge	UUO rat	↓Hedgehog	Bai et al. (2017b)
Poria cocos	Poricoic acid	NRK-49F	↓ PDGF-C ↓ TGF-β1 ↓ Smad3 ↓ MAPK	Li et al. (2021b)

↑: increase or activation; ↓: decrease or inhibition. Nrf2-ARE: nuclear factor erythroid 2-related factor 2-antioxidant response element; MCP-1: monocyte chemoattractant protein-1; TLR4: Toll-like receptor 4; PI3K: phosphatidylinositol 3 kinase; AKT: protein kinase B; NLRP3: NOD-like receptor protein 3; Hsp70: heat shock protein 70; MAPK: mitogen-activated protein kinase; IL-11: Interleukin-11; ERK1/2: extracellular regulated protein kinases; mTORC1: mammalian target of rapamycin complex 1; p70S6K: ribosomal protein S6 kinase β-1; EZH2: Enhancer of zeste homolog 2; NRK-49F: Rat normal kidney 49 fibroblast; PDGF-C: Platelet-derived growth factor C.

medicines can improve RIF in various ways, including astragalus and rhubarb. Chinese herbal medicine has great potential in the treatment of RIF. In terms of specific mechanisms, there are many studies on the regulation of various signaling pathways in RIF by Chinese herbal medicine, including the TGF-β/Smad, NF-κB, MAKP, Wnt/β-catenin, PI3K/Akt/mTOR, JAK2/STAT3, Hedgehog, and Notch signaling pathways. The TGF-β signaling pathway is the central signaling pathway in RIF. Downregulation of the TGF-β/Smad signaling pathway can inhibit EMT and accumulate ECM, thereby delaying the progression of RIF. Compared with Chinese herbal medicine, there are more clinical intervention studies on the TGF-β/Smad signaling pathway. However, it has also been shown that sustained inhibition of TGF- β has dual effects. Prolonged inhibition of the pathway may have adverse effects on the human body, such as affecting wound healing and

TABLE 3 | Summary of Chinese herbal medicines that improve RIF-related mechanisms Compound and Compound extract.

Chinese herbal medicine	Specific drug (etc)	Research object	Specific mechanism	References
Dendrobium mixture	Dendrobium, Astragalus, Salvia	DNdb/db mice	↓ TGF-β1/Smad ↓ EMT	Chen et al. (2021a)
Astragalus Soup	Astragalus, Poria, Melon	UUO mice	↓ TGF-β/Smad ↓ EMT	Zhao et al. (2016)
Rhubarb Astragalus Capsules	Rhubarb, Astragalus	UUO rat	↓TGF-β1/p38	Zeng et al. (2020)
Compound MoneyGrass Granules	Moneygrass, plantain seeds, corn silk	Calcium oxalate crystal-induced kidney injury in mice	↓ TGF-β/Smad	Liu et al. (2020)
ShenqiJiedu Granules	Astragalus, Angelica, Salvia	UUO rat	↓ EMT ↓ TGF-Smad-Ilk	Cai et al. (2017)
Shenqi Pill	Rehmannia, Danpi, Poria	Adenine-induced renal injury in rat	↓ TGF-β1/Smads	Chen et al. (2017)
Uguimaru	Rehmanniaglutinosa, aconite, cinnamon	UUO rat	↓ TGF-β1/Smad	Wang et al. (2015b)
Qingxuan antihypertensive soup	BambooRu, Poria, Gentian Grass	Spontaneously Hypertensive Rat	↓ TGF-β1/Smad ↓ ECM	Liu et al. (2017b)
ShenkangⅦ recipe	Polyporus, Money Grass, Sea Sand	UUO rat	↓ TGF/Smad ↓ NF-κB ↓ SHH	Zhou et al. (2020)
FuzhengHuayu Recipe	Salvia, Schisandra, Peach Kernel	mercuric chloride induced rat	↓ NF-κB	Yuan et al. (2017)
Zhenwu Soup	Peony, Poria,Ginger	UUO rat	↓ TGF-β1 ↑ PPARγ	Li et al. (2018a)
Anti - cellulite	Salvia, Jujube Achyranthes	Azithromycin nephropathy in rat	↓ Wnt ↓ TGF-β ↓ MAPK	Jiang et al. (2020)
QishenYiqi Dropping Pills	Astragalus, Salvia, Red Sandalwood	UUO rat	↓ β-catenin	Zhou et al. (2016)
removingblood stasisand dredging collaterals	Salvia, Dilong,Leech	DN rat	↓ Wnt/β-catenin	Bai et al. (2017a)
Shenkang	Safflower, Salvia, Astragalus	UUO mice	↓ JAK2/STAT3	Qin et al. (2021)
Dendrobium mixture	Dendrobium, Astragalus, Schisandra	DN rat	↓ PI3K/Akt/mTOR	Chen et al. (2021b)
Angelica sinensis soup	Astragalus, Angelica	UUO rat	↓ NLRP3	Wang et al. (2016)
FuzhengHuayu Soup	Cordycepssinensis powder, Danshen, Peach kernel	HK-2 cell	↓ miR-21 ↓ AKT ↓ EMT	Wang et al. (2020a)
Xiexin soup Rhubarb, Coptis, Scutellaria	Coptisalkaloids, rhubarb polysaccharides Scutellaria flavonoids	DN mice	↓ TGF-β1/Smad ↓ NF- κB	Wu et al. (2015)
Tangshenning Astragalus, Rhubarb, Chuanxiong	AS-IV	DN mice	↓ Wnt/β-catenin	Cui et al. (2021)

↑: increase or activation; ↓: decrease or inhibition. p38: p38 MAPK; TGF-Smad-Ilk: TGF-β1-Smad-ILK, pathway; ECM: extracellular matrix; SHH: sonic hedgehog signaling; PPARγ: Peroxisome Proliferator-Activated Receptor γ; JAK2/STAT3: Janus kinase2/signal transducer and activator of transcription3; mTOR: mammalian target of rapamycin; AS-IV: Astragaloside IV; miR-21:microRNA-21.

antagonizing inflammation (Luangmonkong et al., 2017). Therefore, for TGF-β/Smad inhibitory intervention, it is advocated to be moderate, so as not to damage the normal physiological functions of the body. Similarly, for the regulation of other signaling pathways and cellular molecules, there may also be scales to achieve the purpose of improving RIF without affecting the body's normal functions, but further research is needed to confirm this idea. In addition, Chinese herbal medicine has rich research on the intervention of the NF-κB, MAKP, and Wnt/β-catenin signaling pathways, which reflects the criticality and maturity of the above pathways in RIF research. On the other hand, Chinese herbal medicine can improve RIF by inhibiting the NLRP3 inflammasome and EZH2 gene expression. It can be seen that there are abundant studies on Chinese herbal medicine to delay RIF, and the overall efficacy is clear, as summarized in **Tables 1–3**. There are thousands of Chinese herbal medicines, with much more to be discovered and investigated. According to the existing research, Chinese herbal medicines, especially Chinese medicine compound preparations, have the advantages of multi-target intervention to improve RIF, and have broad research prospects. The advantages are worth further exploration. Current research has laid a solid foundation for the basic and clinical research of RIF in the future.

However, there are several limitations to the use of Chinese herbal medicines in RIF. For example, relatively few researches exist on the signaling pathways of RIF, such as Hedgehog and Notch, which need to be further elucidated. Second, a large number of molecules and mechanisms with pro-fibrotic or anti-fibrotic properties have been identified, and there are still many mechanisms in Chinese herbal medicine that have not been covered, which may also be a new direction for future research. Since fibrosis-related pathways or molecular mechanisms interfere with each other, finding targets that connect these

factors may also be a new direction for Chinese herbal medicine intervention. In addition, most of the interventions of Chinese herbal medicine in RIF are reflected as the overall curative effect. It is necessary to deeply explore the pharmacological components and mechanisms of specific drugs, analyze the pharmacological effects and mutual effects of each drug in the compound preparation, and detect the optimal dose and administration regimens. This is an inevitable trend for Chinese herbal medicine to improve RIF, which has a positive impact on the therapeutic significance of Chinese herbal medicine and global acceptance.

CONCLUDING REMARKS

To sum up, major breakthroughs and progress have been made in the research on Chinese herbal medicine to improve RIF, and the prevention and treatment of RIF is still a major challenge on a global scale. Because the RIF process is complex and involves dynamic changes, current research is limited in terms of the modeling time, and the inducing and influencing factors are single, the simulation research and research effect need to be further considered. Second, current research is based on cell and animal models; thus, much work is needed to elucidate clinical relevance. However, research thinking and methods continue to progress. Chinese herbal medicine has a long and profound history, and worthy of further exploration. Based on the research results of Chinese herbal medicine intervention in RIF, we believe that Chinese herbal medicine will greatly promote the progress in RIF prevention and treatment.

AUTHOR CONTRIBUTIONS

X-YY, and X-YL were responsible for the conception. X-YL wrote the manuscript. X-YL, X-BZ, Y-FZ and KQ prepared the figures and tables. X-YL are responsible for revising. X-YY checked the article. X-YL were responsible for the final approval of the version to be submitted. All authors read and approved the final manuscript.

FUNDING

This study was supported by the National Natural Science Foundation of China (No. 82174366).

REFERENCES

Bai, L., Huo, B., Chen, Z., Guo, Q., Xu, J., Fang, J., et al. (2017a). Effect of Huayu Tongluo Herbs on Reduction of Proteinuria via Inhibition of Wnt/β-Catenin Signaling Pathway in Diabetic Rats. *Evid. Based Complement. Altern. Med.* 2017, 3054145. doi:10.1155/2017/3054145

Bai, Y., Wu, C., Hong, W., Zhang, X., Liu, L., and Chen, B. (2017b). Anti-Fibrotic Effect of Sedum Sarmentosum Bunge Extract in Kidneys via the Hedgehog Signaling Pathway. *Mol. Med. Rep.* 16, 737–745. doi:10.3892/mmr.2017.6628

Barkett, M., and Gilmore, T. D. (1999). Control of Apoptosis by Rel/NF-kappaB Transcription Factors. *Oncogene* 18, 6910–6924. doi:10.1038/sj.onc.1203238

Basak, S., Behar, M., and Hoffmann, A. (2012). Lessons from Mathematically Modeling the NF-κB Pathway. *Immunol. Rev.* 246, 221–238. doi:10.1111/j.1600-065X.2011.01092.x

Bitzer, M., von Gersdorff, G., Liang, D., Dominguez-Rosales, A., Beg, A. A., Rojkind, M., et al. (2000). A Mechanism of Suppression of TGF-Beta/SMAD Signaling by NF-Kappa B/RelA. *Genes Dev.* 14, 187–197. doi:10.1101/gad.14.2.187

Briscoe, J. (2009). Making a Grade: Sonic Hedgehog Signalling and the Control of Neural Cell Fate. *EMBO J.* 28, 457–465. doi:10.1038/emboj.2009.12

Bülow, R. D., and Boor, P. (2019). Extracellular Matrix in Kidney Fibrosis: More Than Just a Scaffold. *J. Histochem Cytochem* 67, 643–661. doi:10.1369/0022155419849388

Cai, P., Liu, X., Xu, Y., Qi, F., and Si, G. (2017). Shenqi Detoxification Granule Combined with P311 Inhibits Epithelial-Mesenchymal Transition in Renal Fibrosis via TGF-β1-Smad-ILK Pathway. *Biosci. Trends* 11, 640–650. doi:10.5582/bst.2017.01311

Chang, B., Chen, W., Zhang, Y., Yang, P., and Liu, L. (2018). Tripterygium Wilfordii Mitigates Hyperglycemia-Induced Upregulated Wnt/β-Catenin Expression and Kidney Injury in Diabetic Rats. *Exp. Ther. Med.* 15, 3874–3882. doi:10.3892/etm.2018.5901

Che, X., Wang, Q., Xie, Y., Xu, W., Shao, X., Mou, S., et al. (2015). Astragaloside IV Suppresses Transforming Growth Factor-β1 Induced Fibrosis of Cultured Mouse Renal Fibroblasts via Inhibition of the MAPK and NF-κB Signaling Pathways. *Biochem. Biophys. Res. Commun.* 464, 1260–1266. doi:10.1016/j.bbrc.2015.07.116

Chen, H., Xu, Y., Yang, Y., Zhou, X., Dai, S., and Li, C. (2017). Shenqiwan Ameliorates Renal Fibrosis in Rats by Inhibiting TGF-β1/Smads Signaling Pathway. *Evid. Based Complement. Altern. Med.* 2017, 7187038. doi:10.1155/2017/7187038

Chen, H., Yang, T., Wang, M. C., Chen, D. Q., Yang, Y., and Zhao, Y. Y. (2018). Novel RAS Inhibitor 25-O-Methylalisol F Attenuates Epithelial-To-Mesenchymal Transition and Tubulo-Interstitial Fibrosis by Selectively Inhibiting TGF-β-Mediated Smad3 Phosphorylation. *Phytomedicine* 42, 207–218. doi:10.1016/j.phymed.2018.03.034

Chen, L., Zhang, J., Zhang, Y., Wang, Y., and Wang, B. (2008). Improvement of Inflammatory Responses Associated with NF-Kappa B Pathway in Kidneys from Diabetic Rats. *Inflamm. Res.* 57, 199–204. doi:10.1007/s00011-006-6190-z

Chen, X., Yang, Y., Liu, C., Chen, Z., and Wang, D. (2019). Astragaloside IV Ameliorates High Glucose-Induced Renal Tubular Epithelial-Mesenchymal Transition by Blocking mTORC1/p70S6K Signaling in HK-2 Cells. *Int. J. Mol. Med.* 43, 709–716. doi:10.3892/ijmm.2018.3999

Chen, Y., Lin, X., Zheng, Y., Yu, W., Lin, F., and Zhang, J. (2021a). Dendrobium Mixture Ameliorates Diabetic Nephropathy in db/db Mice by Regulating the TGF-β1/Smads Signaling Pathway. *Evid. Based Complement. Altern. Med.* 2021, 9931983. doi:10.1155/2021/9931983

Chen, Y., Zheng, Y., Lin, X., Zhang, J., Lin, F., and Shi, H. (2021b). Dendrobium Mixture Attenuates Renal Damage in Rats with Diabetic Nephropathy by Inhibiting the PI3K/Akt/mTOR Pathway. *Mol. Med. Rep.* 24, 590. doi:10.3892/mmr.2021.12229

Cui, F. Q., Gao, Y. B., Wang, Y. F., Meng, Y., Cai, Z., Shen, C., et al. (2021). Effect of Tang-Shen-Ning Decoction on Podocyte Epithelial-Esenchymal Transformation via Inhibiting Wnt/β-Catenin Pathway in Diabetic Mice. *Ann. Palliat. Med.* 10, 12921–12936. doi:10.21037/apm-20-602

Dai, C., Stolz, D. B., Kiss, L. P., Monga, S. P., Holzman, L. B., and Liu, Y. (2009). Wnt/beta-Catenin Signaling Promotes Podocyte Dysfunction and Albuminuria. *J. Am. Soc. Nephrol.* 20, 1997–2008. doi:10.1681/ASN.2009010019

Derynck, R., Jarrett, J. A., Chen, E. Y., Eaton, D. H., Bell, J. R., Assoian, R. K., et al. (1985). Human Transforming Growth Factor-beta Complementary DNA Sequence and Expression in Normal and Transformed Cells. *Nature* 316, 701–705. doi:10.1038/316701a0

Ding, H., Zhou, D., Hao, S., Zhou, L., He, W., Nie, J., et al. (2012). Sonic Hedgehog Signaling Mediates Epithelial-Mesenchymal Communication and Promotes Renal Fibrosis. *J. Am. Soc. Nephrol.* 23, 801–813. doi:10.1681/ASN.2011060614

Djudjaj, S., and Boor, P. (2019). Cellular and Molecular Mechanisms of Kidney Fibrosis. *Mol. Asp. Med.* 65, 16–36. doi:10.1016/j.mam.2018.06.002

Dusabimana, T., Park, E. J., Je, J., Jeong, K., Yun, S. P., Kim, H. J., et al. (2021). Geniposide Improves Diabetic Nephropathy by Enhancing ULK1-Mediated Autophagy and Reducing Oxidative Stress through AMPK Activation. *Int. J. Mol. Sci.* 22, 1651. doi:10.3390/ijms22041651

Eddy, A. A. (2000). Molecular Basis of Renal Fibrosis. *Pediatr. Nephrol.* 15, 290–301. doi:10.1007/s004670000461

Eddy, A. A. (1996). Molecular Insights into Renal Interstitial Fibrosis. *J. Am. Soc. Nephrol.* 7, 2495–2508. doi:10.1681/ASN.V7122495

Feng, S., Wang, J., Teng, J., Fang, Z., and Lin, C. (2020). Resveratrol Plays Protective Roles on Kidney of Uremic Rats via Activating HSP70 Expression. *Biomed. Res. Int.* 2020, 2126748. doi:10.1155/2020/2126748

Fujihara, C. K., Antunes, G. R., Mattar, A. L., Malheiros, D. M., Vieira, J. M., and Zatz, R. (2007). Chronic Inhibition of Nuclear Factor-kappaB Attenuates Renal Injury in the 5/6 Renal Ablation Model. *Am. J. Physiol. Ren. Physiol.* 292, F92–F99. doi:10.1152/ajprenal.00184.2006

Gao, Y., Yuan, D., Gai, L., Wu, X., Shi, Y., He, Y., et al. (2021). Saponins from Panax Japonicus Ameliorate Age-Related Renal Fibrosis by Inhibition of Inflammation Mediated by NF-κB and TGF-β1/Smad Signaling and Suppression of Oxidative Stress via Activation of Nrf2-ARE Signaling. *J. Ginseng Res.* 45, 408–419. doi:10.1016/j.jgr.2020.08.005

GBD Chronic Kidney Disease Collaboration (2020). Global, Regional, and National Burden of Chronic Kidney Disease, 1990-2017: A Systematic Analysis for the Global Burden of Disease Study 2017. *Lancet* 395, 709–733. doi:10.1016/S0140-6736(20)30045-3

Gevrek, F., Biçer, Ç., Kara, M., and Erdemir, F. (2018). The Ameliorative Effects of Ginkgo Biloba on Apoptosis, LH-R Expression and Sperm Morphology Anomaly in Testicular Torsion and Detorsion. *Andrologia* 50, e12969. doi:10.1111/and.12969

Ghiazza, M., Polimeni, M., Fenoglio, I., Gazzano, E., Ghigo, D., and Fubini, B. (2010). Does Vitreous Silica Contradict the Toxicity of the Crystalline Silica Paradigm? *Chem. Res. Toxicol.* 23, 620–629. doi:10.1021/tx900369x

Grynberg, K., Ma, F. Y., and Nikolic-Paterson, D. J. (2017). The JNK Signaling Pathway in Renal Fibrosis. *Front. Physiol.* 8, 829. doi:10.3389/fphys.2017.00829

He, J., Xu, Y., Koya, D., and Kanasaki, K. (2013). Role of the Endothelial-To-Mesenchymal Transition in Renal Fibrosis of Chronic Kidney Disease. *Clin. Exp. Nephrol.* 17, 488–497. doi:10.1007/s10157-013-0781-0

He, W., Tan, R. J., Li, Y., Wang, D., Nie, J., Hou, F. F., et al. (2012). Matrix Metalloproteinase-7 as a Surrogate Marker Predicts Renal Wnt/β-Catenin Activity in CKD. *J. Am. Soc. Nephrol.* 23, 294–304. doi:10.1681/ASN.2011050490

Herranz, N., Pasini, D., Díaz, V. M., Francí, C., Gutierrez, A., Dave, N., et al. (2008). Polycomb Complex 2 is Required for E-Cadherin Repression by the Snail1 Transcription Factor. *Mol. Cell Biol.* 28, 4772–4781. doi:10.1128/MCB.00323-08

Hill, N. R., Fatoba, S. T., Oke, J. L., Hirst, J. A., O'Callaghan, C. A., Lasserson, D. S., et al. (2016). Global Prevalence of Chronic Kidney Disease - A Systematic Review and Meta-Analysis. *PLoS One* 11, e0158765. doi:10.1371/journal.pone.0158765

Ho, C., Hsu, Y. C., Lei, C. C., Mau, S. C., Shih, Y. H., and Lin, C. L. (2016). Curcumin Rescues Diabetic Renal Fibrosis by Targeting Superoxide-Mediated Wnt Signaling Pathways. *Am. J. Med. Sci.* 351, 286–295. doi:10.1016/j.amjms.2015.12.017

Huang, X., Xue, H., Ma, J., Zhang, Y., Zhang, J., Liu, Y., et al. (2019). Salidroside Ameliorates Adriamycin Nephropathy in Mice by Inhibiting β-Catenin Activity. *J. Cell Mol. Med.* 23, 4443–4453. doi:10.1111/jcmm.14340

Isaka, Y. (2018). Targeting TGF-β Signaling in Kidney Fibrosis. *Int. J. Mol. Sci.* 19 (9), 2532. doi:10.3390/ijms19092532

Jenkins, D. (2009). Hedgehog Signalling: Emerging Evidence for Non-Canonical Pathways. *Cell Signal* 21, 1023–1034. doi:10.1016/j.cellsig.2009.01.033

Ji, T., Su, S. L., Zhu, Y., Guo, J. M., Qian, D. W. W., Tang, Y. P., et al. (2019). The Mechanism of Mulberry Leaves against Renal Tubular Interstitial Fibrosis through ERK1/2 Signaling Pathway Was Predicted by Network Pharmacology and Validated in Human Tubular Epithelial Cells. *Phytother. Res.* 33, 2044–2055. doi:10.1002/ptr.6390

Jiang, Y., Zhu, Y., Zhen, T., Li, J., Xing, K., He, L., et al. (2020). Transcriptomic Analysis of the Mechanisms of Alleviating Renal Interstitial Fibrosis Using the Traditional Chinese Medicine Kangxianling in a Rat Model. *Sci. Rep.* 10, 10682. doi:10.1038/s41598-020-67690-3

Katoh, M., and Katoh, M. (2005). Comparative Genomics on SNAI1, SNAI2, and SNAI3 Orthologs. *Oncol. Rep.* 14, 1083–1086. doi:10.3892/or.14.4.1083

Lee, J., An, J. N., Hwang, J. H., Lee, H., Lee, J. P., and Kim, S. G. (2019). p38 MAPK Activity Is Associated with the Histological Degree of Interstitial Fibrosis in IgA Nephropathy Patients. *PLoS One* 14, e0213981. doi:10.1371/journal.pone.0213981

Li, L., Zhou, G., Fu, R., He, Y., Xiao, L., Peng, F., et al. (2021a). Polysaccharides Extracted from balanophora Polyandra Griff (BPP) Ameliorate Renal Fibrosis and EMT via Inhibiting the Hedgehog Pathway. *J. Cell Mol. Med.* 25, 2828–2840. doi:10.1111/jcmm.16313

Li, Q., Ming, Y., Jia, H., and Wang, G. (2021b). Poricoic Acid A Suppresses TGF-β1-Induced Renal Fibrosis and Proliferation via the PDGF-C, Smad3 and MAPK Pathways. *Exp. Ther. Med.* 21, 289. doi:10.3892/etm.2021.9720

Li, R., Guo, Y., Zhang, Y., Zhang, X., Zhu, L., and Yan, T. (2019). Salidroside Ameliorates Renal Interstitial Fibrosis by Inhibiting the TLR4/NF-κB and MAPK Signaling Pathways. *Int. J. Mol. Sci.* 20 (5), 1103. doi:10.3390/ijms20051103

Li, R., Wang, Y., Liu, Y., Chen, Q., Fu, W., Wang, H., et al. (2013). Curcumin Inhibits Transforming Growth Factor-β1-Induced EMT via PPARγ Pathway, Not Smad Pathway in Renal Tubular Epithelial Cells. *PLoS One* 8, e58848. doi:10.1371/journal.pone.0058848

Li, S., Xiao, X., Han, L., Wang, Y., and Luo, G. (2018a). Renoprotective Effect of Zhenwu Decoction against Renal Fibrosis by Regulation of Oxidative Damage and Energy Metabolism Disorder. *Sci. Rep.* 8, 14627. doi:10.1038/s41598-018-32115-9

Li, S. S., Sun, Q., Hua, M. R., Suo, P., Chen, J. R., Yu, X. Y., et al. (2021c). Targeting the Wnt/β-Catenin Signaling Pathway as a Potential Therapeutic Strategy in Renal Tubulointerstitial Fibrosis. *Front. Pharmacol.* 12, 719880. doi:10.3389/fphar.2021.719880

Li, Y., Xiong, Y., Zhang, H., Li, J., Wang, D., Chen, W., et al. (2017). Ginkgo Biloba Extract EGb761 Attenuates Brain Death-Induced Renal Injury by Inhibiting Pro-Inflammatory Cytokines and the SAPK and JAK-STAT Signalings. *Sci. Rep.* 7, 45192. doi:10.1038/srep45192

Li, Z., Hong, Z., Peng, Z., Zhao, Y., and Shao, R. (2018b). Acetylshikonin from Zicao Ameliorates Renal Dysfunction and Fibrosis in Diabetic Mice by Inhibiting TGF-β1/Smad Pathway. *Hum. Cell* 31, 199–209. doi:10.1007/s13577-017-0192-8

Liang, T., Wei, C., Lu, S., Qin, M., Qin, G., Zhang, Y., et al. (2021). Ginaton Injection Alleviates Cisplatin-Induced Renal Interstitial Fibrosis in Rats via Inhibition of Apoptosis through Regulation of the p38MAPK/TGF-β1 and p38MAPK/HIF-1α Pathways. *Biomed. Rep.* 14, 38. doi:10.3892/br.2021.1414

Lin, Q., Long, C., Wang, Z., Wang, R., Shi, W., Qiu, J., et al. (2022). Hirudin, a Thrombin Inhibitor, Attenuates TGF-β-Induced Fibrosis in Renal Proximal Tubular Epithelial Cells by Inhibition of Protease-Activated Receptor 1 Expression via S1P/S1PR2/S1PR3 Signaling. *Exp. Ther. Med.* 23, 3. doi:10.3892/etm.2021.10924

Liu, M., Ning, X., Li, R., Yang, Z., Yang, X., Sun, S., et al. (2017a). Signalling Pathways Involved in Hypoxia-Induced Renal Fibrosis. *J. Cell Mol. Med.* 21, 1248–1259. doi:10.1111/jcmm.13060

Liu, S. F., Chang, S. Y., Lee, T. C., Chuang, L. Y., Guh, J. Y., Hung, C. Y., et al. (2012). Dioscorea Alata Attenuates Renal Interstitial Cellular Fibrosis by Regulating Smad- and Epithelial-Mesenchymal Transition Signaling Pathways. *PLoS One* 7, e47482. doi:10.1371/journal.pone.0047482

Liu, W., Liang, L., Zhang, Q., Li, Y., Yan, S., Tang, T., et al. (2021a). Effects of Andrographolide on Renal Tubulointersticial Injury and Fibrosis. Evidence of its Mechanism of Action. *Phytomedicine* 91, 153650. doi:10.1016/j.phymed.2021.153650

Liu, W., Lin, S., Cai, Q., Zhang, L., Shen, A., Chen, Y., et al. (2017b). Qingxuan Jiangya Decoction Mitigates Renal Interstitial Fibrosis in Spontaneously Hypertensive Rats by Regulating Transforming Growth Factor-β1/Smad Signaling Pathway. *Evid. Based Complement. Altern. Med.* 2017, 1576328. doi:10.1155/2017/1576328

Liu, W. R., Lu, H. T., Zhao, T. T., Ding, J. R., Si, Y. C., Chen, W., et al. (2020). Fu-Fang-Jin-Qian-Cao Herbal Granules Protect against the Calcium Oxalate-Induced Renal EMT by Inhibiting the TGF-β/smad Pathway. *Pharm. Biol.* 58, 1115–1122. doi:10.1080/13880209.2020.1844241

Liu, Y. (2011). Cellular and Molecular Mechanisms of Renal Fibrosis. *Nat. Rev. Nephrol.* 7, 684–696. doi:10.1038/nrneph.2011.149

Liu, Y. (2010). New Insights into Epithelial-Mesenchymal Transition in Kidney Fibrosis. *J. Am. Soc. Nephrol.* 21, 212–222. doi:10.1681/ASN.2008121226

Liu, Y. (2006). Renal Fibrosis: New Insights into the Pathogenesis and Therapeutics. *Kidney Int.* 69, 213–217. doi:10.1038/sj.ki.5000054

Liu, Y., Su, Y. Y., Yang, Q., and Zhou, T. (2021b). Stem Cells in the Treatment of Renal Fibrosis: A Review of Preclinical and Clinical Studies of Renal Fibrosis Pathogenesis. *Stem Cell Res. Ther.* 12, 333. doi:10.1186/s13287-021-02391-w

Lu, C., Han, H. D., Mangala, L. S., Ali-Fehmi, R., Newton, C. S., Ozbun, L., et al. (2010). Regulation of Tumor Angiogenesis by EZH2. *Cancer Cell* 18, 185–197. doi:10.1016/j.ccr.2010.06.016

Lu, H., Wu, L., Liu, L., Ruan, Q., Zhang, X., Hong, W., et al. (2018). Quercetin Ameliorates Kidney Injury and Fibrosis by Modulating M1/M2 Macrophage Polarization. *Biochem. Pharmacol.* 154, 203–212. doi:10.1016/j.bcp.2018.05.007

Luangmonkong, T., Suriguga, S., Bigaeva, E., Boersema, M., Oosterhuis, D., de Jong, K. P., et al. (2017). Evaluating the Antifibrotic Potency of Galunisertib in a Human *Ex Vivo* Model of Liver Fibrosis. *Br. J. Pharmacol.* 174, 3107–3117. doi:10.1111/bph.13945

MacDonald, B. T., Tamai, K., and He, X. (2009). Wnt/beta-Catenin Signaling: Components, Mechanisms, and Diseases. *Dev. Cell* 17, 9–26. doi:10.1016/j.devcel.2009.06.016

Mao, Z. M., Shen, S. M., Wan, Y. G., Sun, W., Chen, H. L., Huang, M. M., et al. (2015). Huangkui Capsule Attenuates Renal Fibrosis in Diabetic Nephropathy Rats through Regulating Oxidative Stress and p38MAPK/Akt Pathways, Compared to α-lipoic Acid. *J. Ethnopharmacol.* 173, 256–265. doi:10.1016/j.jep.2015.07.036

McCarty, M. F. (2006). Adjuvant Strategies for Prevention of Glomerulosclerosis. *Med. Hypotheses* 67, 1277–1296. doi:10.1016/j.mehy.2004.11.048

Mills, K. T., Xu, Y., Zhang, W., Bundy, J. D., Chen, C. S., Kelly, T. N., et al. (2015). A Systematic Analysis of Worldwide Population-Based Data on the Global Burden of Chronic Kidney Disease in 2010. *Kidney Int.* 88, 950–957. doi:10.1038/ki.2015.230

Mittal, M., Siddiqui, M. R., Tran, K., Reddy, S. P., and Malik, A. B. (2014). Reactive Oxygen Species in Inflammation and Tissue Injury. *Antioxid. Redox Signal* 20, 1126–1167. doi:10.1089/ars.2012.5149

Morgan, M. J., and Liu, Z. G. (2011). Crosstalk of Reactive Oxygen Species and NF-κB Signaling. *Cell Res.* 21, 103–115. doi:10.1038/cr.2010.178

Naves, M. A., Requião-Moura, L. R., Soares, M. F., Silva-Júnior, J. A., Mastroianni-Kirsztajn, G., and Teixeira, V. P. (2012). Podocyte Wnt/ss-Catenin Pathway Is Activated by Integrin-Linked Kinase in Clinical and Experimental Focal Segmental Glomerulosclerosis. *J. Nephrol.* 25, 401–409. doi:10.5301/jn.5000017

Nishimoto, S., and Nishida, E. (2006). MAPK Signalling: ERK5 versus ERK1/2. *EMBO Rep.* 7, 782–786. doi:10.1038/sj.embor.7400755

Palumbo-Zerr, K., Zerr, P., Distler, A., Fliehr, J., Mancuso, R., Huang, J., et al. (2015). Orphan Nuclear Receptor NR4A1 Regulates Transforming Growth Factor-β Signaling and Fibrosis. *Nat. Med.* 21, 150–158. doi:10.1038/nm.3777

Pan, B., Liu, G., Jiang, Z., and Zheng, D. (2015). Regulation of Renal Fibrosis by Macrophage Polarization. *Cell Physiol. Biochem.* 35, 1062–1069. doi:10.1159/000373932

Paznekas, W. A., Okajima, K., Schertzer, M., Wood, S., and Jabs, E. W. (1999). Genomic Organization, Expression, and Chromosome Location of the Human SNAIL Gene (SNAI1) and a Related Processed Pseudogene (SNAI1P). *Genomics* 62, 42–49. doi:10.1006/geno.1999.6010

Peinado, H., Ballestar, E., Esteller, M., and Cano, A. (2004). Snail Mediates E-Cadherin Repression by the Recruitment of the Sin3A/histone Deacetylase 1 (HDAC1)/HDAC2 Complex. *Mol. Cell Biol.* 24, 306–319. doi:10.1128/MCB.24.1.306-319.2004

Qin, T., Wu, Y., Liu, T., and Wu, L. (2021). Effect of Shenkang on Renal Fibrosis and Activation of Renal Interstitial Fibroblasts through the JAK2/STAT3 Pathway. *BMC Complement. Med. Ther.* 21, 12. doi:10.1186/s12906-020-03180-3

Rauhauser, A. A., Ren, C., Lu, D., Li, B., Zhu, J., McEnery, K., et al. (2015). Hedgehog Signaling Indirectly Affects Tubular Cell Survival after Obstructive Kidney Injury. *Am. J. Physiol. Ren. Physiol.* 309, F770–F778. doi:10.1152/ajprenal.00232.2015

Razzaque, M. S., and Taguchi, T. (2002). Cellular and Molecular Events Leading to Renal Tubulointerstitial Fibrosis. *Med. Electron Microsc.* 35, 68–80. doi:10.1007/s007950200009

Ren, Y., Du, C., Shi, Y., Wei, J., Wu, H., and Cui, H. (2017). The Sirt1 Activator, SRT1720, Attenuates Renal Fibrosis by Inhibiting CTGF and Oxidative Stress. *Int. J. Mol. Med.* 39, 1317–1324. doi:10.3892/ijmm.2017.2931

Rhyu, D. Y., Yang, Y., Ha, H., Lee, G. T., Song, J. S., Uh, S. T., et al. (2005). Role of Reactive Oxygen Species in TGF-Beta1-Induced Mitogen-Activated Protein Kinase Activation and Epithelial-Mesenchymal Transition in Renal Tubular Epithelial Cells. *J. Am. Soc. Nephrol.* 16, 667–675. doi:10.1681/ASN.2004050425

Shan, G., Zhou, X. J., Xia, Y., and Qian, H. J. (2016). Astragalus Membranaceus Ameliorates Renal Interstitial Fibrosis by Inhibiting Tubular Epithelial-Mesenchymal Transition *In Vivo* and *In Vitro*. *Exp. Ther. Med.* 11, 1611–1616. doi:10.3892/etm.2016.3152

Simon, J. A., and Lange, C. A. (2008). Roles of the EZH2 Histone Methyltransferase in Cancer Epigenetics. *Mutat. Res.* 647, 21–29. doi:10.1016/j.mrfmmm.2008.07.010

Sun, W., Byon, C. H., Kim, D. H., Choi, H. I., Park, J. S., Joo, S. Y., et al. (2021). Renoprotective Effects of Maslinic Acid on Experimental Renal Fibrosis in Unilateral Ureteral Obstruction Model via Targeting MyD88. *Front. Pharmacol.* 12, 708575. doi:10.3389/fphar.2021.708575

Surendran, K., Schiavi, S., and Hruska, K. A. (2005). Wnt-dependent Beta-Catenin Signaling Is Activated after Unilateral Ureteral Obstruction, and Recombinant Secreted Frizzled-Related Protein 4 Alters the Progression of Renal Fibrosis. *J. Am. Soc. Nephrol.* 16, 2373–2384. doi:10.1681/ASN.2004110949

Szeto, H. H. (2017). Pharmacologic Approaches to Improve Mitochondrial Function in AKI and CKD. *J. Am. Soc. Nephrol.* 28, 2856–2865. doi:10.1681/ASN.2017030247

Taguchi, S., Azushima, K., Yamaji, T., Urate, S., Suzuki, T., Abe, E., et al. (2021). Effects of Tumor Necrosis Factor-α Inhibition on Kidney Fibrosis and Inflammation in a Mouse Model of Aristolochic Acid Nephropathy. *Sci. Rep.* 11, 23587. doi:10.1038/s41598-021-02864-1

Thiery, J. P., Acloque, H., Huang, R. Y., and Nieto, M. A. (2009). Epithelial-Mesenchymal Transitions in Development and Disease. *Cell* 139, 871–890. doi:10.1016/j.cell.2009.11.007

Vallabhapurapu, S., and Karin, M. (2009). Regulation and Function of NF-kappaB Transcription Factors in the Immune System. *Annu. Rev. Immunol.* 27, 693–733. doi:10.1146/annurev.immunol.021908.132641

Wang, A., Yang, Q., Li, Q., Wang, X., Hao, S., Wang, J., et al. (2018a). Ginkgo Biloba L. Extract Reduces H2O2-Induced Bone Marrow Mesenchymal Stem Cells Cytotoxicity by Regulating Mitogen-Activated Protein Kinase (MAPK) Signaling Pathways and Oxidative Stress. *Med. Sci. Monit.* 24, 3159–3167. doi:10.12659/MSM.910718

Wang, D. T., Huang, R. H., Cheng, X., Zhang, Z. H., Yang, Y. J., and Lin, X. (2015a). Tanshinone IIA Attenuates Renal Fibrosis and Inflammation via Altering Expression of TGF-β/Smad and NF-κB Signaling Pathway in 5/6 Nephrectomized Rats. *Int. Immunopharmacol.* 26, 4–12. doi:10.1016/j.intimp.2015.02.027

Wang, L., Cao, A. L., Chi, Y. F., Ju, Z. C., Yin, P. H., Zhang, X. M., et al. (2015b). You-gui Pill Ameliorates Renal Tubulointerstitial Fibrosis via Inhibition of TGF-β/Smad Signaling Pathway. *J. Ethnopharmacol.* 169, 229–238. doi:10.1016/j.jep.2015.04.037

Wang, L., Chi, Y. F., Yuan, Z. T., Zhou, W. C., Yin, P. H., Zhang, X. M., et al. (2014). Astragaloside IV Inhibits the Up-Regulation of Wnt/β-Catenin Signaling in Rats with Unilateral Ureteral Obstruction. *Cell Physiol. Biochem.* 33, 1316–1328. doi:10.1159/000358699

Wang, L., Ma, J., Guo, C., Chen, C., Yin, Z., Zhang, X., et al. (2016). Danggui Buxue Tang Attenuates Tubulointerstitial Fibrosis via Suppressing NLRP3 Inflammasome in a Rat Model of Unilateral Ureteral Obstruction. *Biomed. Res. Int.* 2016, 9368483. doi:10.1155/2016/9368483

Wang, M., Chen, D. Q., Chen, L., Cao, G., Zhao, H., Liu, D., et al. (2018b). Novel Inhibitors of the Cellular Renin-Angiotensin System Components, Poricoic Acids, Target Smad3 Phosphorylation and Wnt/β-Catenin Pathway against Renal Fibrosis. *Br. J. Pharmacol.* 175, 2689–2708. doi:10.1111/bph.14333

Wang, Q. L., Tao, Y. Y., Xie, H. D., Liu, C. H., and Liu, P. (2020a). Fuzheng Huayu Recipe, a Traditional Chinese Compound Herbal Medicine, Attenuates Renal Interstitial Fibrosis via Targeting the miR-21/PTEN/AKT axis. *J. Integr. Med.* 18, 505–513. doi:10.1016/j.joim.2020.08.006

Wang, R., Zhang, H., Wang, Y., Song, F., and Yuan, Y. (2017a). Inhibitory Effects of Quercetin on the Progression of Liver Fibrosis through the Regulation of NF-κB/IκBα, P38 MAPK, and Bcl-2/Bax Signaling. *Int. Immunopharmacol.* 47, 126–133. doi:10.1016/j.intimp.2017.03.029

Wang, Y. Y., Jiang, H., Pan, J., Huang, X. R., Wang, Y. C., Huang, H. F., et al. (2017b). Macrophage-to-Myofibroblast Transition Contributes to Interstitial Fibrosis in Chronic Renal Allograft Injury. *J. Am. Soc. Nephrol.* 28, 2053–2067. doi:10.1681/ASN.2016050573

Wang, Z., Chen, Z., Li, B., Zhang, B., Du, Y., Liu, Y., et al. (2020b). Curcumin Attenuates Renal Interstitial Fibrosis of Obstructive Nephropathy by Suppressing Epithelial-Mesenchymal Transition through Inhibition of the TLR4/NF-κB and PI3K/AKT Signalling Pathways. *Pharm. Biol.* 58, 828–837. doi:10.1080/13880209.2020.1809462

Wen, Y., Pan, M. M., Lv, L. L., Tang, T. T., Zhou, L. T., Wang, B., et al. (2019). Artemisinin Attenuates Tubulointerstitial Inflammation and Fibrosis via the NF-κB/NLRP3 Pathway in Rats with 5/6 Subtotal Nephrectomy. *J. Cell Biochem.* 120, 4291–4300. doi:10.1002/jcb.27714

Wu, F., Zhao, Y., Shao, Q., Fang, K., Dong, R., Jiang, S., et al. (2021). Ameliorative Effects of Osthole on Experimental Renal Fibrosis *In Vivo* and *In Vitro* by Inhibiting IL-11/ERK1/2 Signaling. *Front. Pharmacol.* 12, 646331. doi:10.3389/fphar.2021.646331

Wu, J. S., Shi, R., Lu, X., Ma, Y. M., and Cheng, N. N. (2015). Combination of Active Components of Xiexin Decoction Ameliorates Renal Fibrosis through the Inhibition of NF-κB and TGF-β1/Smad Pathways in db/db Diabetic Mice. *PLoS One* 10, e0122661. doi:10.1371/journal.pone.0122661

Wu, M., Melichian, D. S., Chang, E., Warner-Blankenship, M., Ghosh, A. K., and Varga, J. (2009). Rosiglitazone Abrogates Bleomycin-Induced Scleroderma and Blocks Profibrotic Responses through Peroxisome Proliferator-Activated Receptor-Gamma. *Am. J. Pathol.* 174, 519–533. doi:10.2353/ajpath.2009.080574

Xiao, X., Senavirathna, L. K., Gou, X., Huang, C., Liang, Y., and Liu, L. (2016). EZH2 Enhances the Differentiation of Fibroblasts into Myofibroblasts in Idiopathic Pulmonary Fibrosis. *Physiol. Rep.* 4 (17), e12915. doi:10.14814/phy2.12915

Xie, Y., Lan, F., Zhao, J., and Shi, W. (2020). Hirudin Improves Renal Interstitial Fibrosis by Reducing Renal Tubule Injury and Inflammation in Unilateral Ureteral Obstruction (UUO) Mice. *Int. Immunopharmacol.* 81, 106249. doi:10.1016/j.intimp.2020.106249

Xu, L., Gao, J., Huang, D., Lin, P., Yao, D., Yang, F., et al. (2021). Emodin Ameliorates Tubulointerstitial Fibrosis in Obstructed Kidneys by Inhibiting EZH2. *Biochem. Biophys. Res. Commun.* 534, 279–285. doi:10.1016/j.bbrc.2020.11.094

Yan, H., Xu, J., Xu, Z., Yang, B., Luo, P., and He, Q. (2021). Defining Therapeutic Targets for Renal Fibrosis: Exploiting the Biology of Pathogenesis. *Biomed. Pharmacother.* 143, 112115. doi:10.1016/j.biopha.2021.112115

Yan, R., Wang, Y., Shi, M., Xiao, Y., Liu, L., Liu, L., et al. (2019). Regulation of PTEN/AKT/FAK Pathways by PPARγ Impacts on Fibrosis in Diabetic Nephropathy. *J Cell. Biochem.* 120, 6998–7014. doi:10.1002/jcb.27937

Yang, G., Zhao, Z., Zhang, X., Wu, A., Huang, Y., Miao, Y., et al. (2017). Effect of Berberine on the Renal Tubular Epithelial-To-Mesenchymal Transition by Inhibition of the Notch/Snail Pathway in Diabetic Nephropathy Model KKAy Mice. *Drug Des. Devel Ther.* 11, 1065–1079. doi:10.2147/DDDT.S124971

Yang, Y. A., and Yu, J. (2013). EZH2, an Epigenetic Driver of Prostate Cancer. *Protein Cell* 4, 331–341. doi:10.1007/s13238-013-2093-2

Yang, Y. L., Chang, S. Y., Teng, H. C., Liu, Y. S., Lee, T. C., Chuang, L. Y., et al. (2008). Safflower Extract: A Novel Renal Fibrosis Antagonist that Functions by Suppressing Autocrine TGF-Beta. *J. Cell Biochem.* 104, 908–919. doi:10.1002/jcb.21676

Yao, L., Li, J., Li, L., Li, X., Zhang, R., Zhang, Y., et al. (2019). Coreopsis Tinctoria Nutt Ameliorates High Glucose-Induced Renal Fibrosis and Inflammation via the TGF-β1/SMADS/AMPK/NF-κB Pathways. *BMC Complement. Altern. Med.* 19, 14. doi:10.1186/s12906-018-2410-7

Yde, P., Mengel, B., Jensen, M. H., Krishna, S., and Trusina, A. (2011). Modeling the NF-κB Mediated Inflammatory Response Predicts Cytokine Waves in Tissue. *BMC Syst. Biol.* 5, 115. doi:10.1186/1752-0509-5-115

Yoshioka, K., Takemura, T., Murakami, K., Okada, M., Hino, S., Miyamoto, H., et al. (1993). Transforming Growth Factor-Beta Protein and mRNA in Glomeruli in Normal and Diseased Human Kidneys. *Lab. Invest.* 68, 154–163.

Yuan, J. L., Tao, Y. Y., Wang, Q. L., Shen, L., and Liu, C. H. (2017). Fuzheng Huayu Formula Prevents Rat Renal Interstitial Fibrosis Induced by HgCl2 via Antioxidative Stress and Down-Regulation of Nuclear Factor-Kappa B Activity. *Chin. J. Integr. Med.* 23, 598–604. doi:10.1007/s11655-016-2540-z

Zeng, X., Cai, G., Liang, T., Li, Q., Yang, Y., Zhong, X., et al. (2020). Rhubarb and Astragalus Capsule Attenuates Renal Interstitial Fibrosis in Rats with Unilateral Ureteral Obstruction by Alleviating Apoptosis through Regulating Transforming Growth Factor beta1 (TGF-β1)/p38 Mitogen-Activated Protein Kinases (p38 MAPK) Pathway. *Med. Sci. Monit.* 26, e920720. doi:10.12659/MSM.920720

Zhang, Z. H., Li, M. H., Liu, D., Chen, H., Chen, D. Q., Tan, N. H., et al. (2018). Rhubarb Protect against Tubulointerstitial Fibrosis by Inhibiting TGF-β/Smad Pathway and Improving Abnormal Metabolome in Chronic Kidney Disease. *Front. Pharmacol.* 9, 1029. doi:10.3389/fphar.2018.01029

Zhao, J., Wang, L., Cao, A. L., Jiang, M. Q., Chen, X., Wang, Y., et al. (2016). HuangQi Decoction Ameliorates Renal Fibrosis via TGF-β/Smad Signaling Pathway *In Vivo* and *In Vitro*. *Cell Physiol. Biochem.* 38, 1761–1774. doi:10.1159/000443115

Zheng, R., Zhu, R., Li, X., Li, X., Shen, L., Chen, Y., et al. (2018). N6-(2-Hydroxyethyl) Adenosine from Cordyceps Cicadae Ameliorates Renal Interstitial Fibrosis and Prevents Inflammation via TGF-β1/Smad and NF-κB Signaling Pathway. *Front. Physiol.* 9, 1229. doi:10.3389/fphys.2018.01229

Zhou, D., Tan, R. J., Zhou, L., Li, Y., and Liu, Y. (2013). Kidney Tubular β-Catenin Signaling Controls Interstitial Fibroblast Fate via Epithelial-Mesenchymal Communication. *Sci. Rep.* 3, 1878. doi:10.1038/srep01878

Zhou, J., Jiang, H., Jiang, H., Fan, Y., Zhang, J., Ma, X., et al. (2022). The ILEI/LIFR Complex Induces EMT via the Akt and ERK Pathways in Renal Interstitial Fibrosis. *J. Transl. Med.* 20, 54. doi:10.1186/s12967-022-03265-2

Zhou, S. S., Ai, Z. Z., Li, W. N., Li, L., Zhu, X. Y., and Ba, Y. M. (2020). Shenkang VII Recipe Attenuates Unilateral Ureteral Obstruction-Induced Renal Fibrosis via TGF-β/Smad, NF-κB and SHH Signaling Pathway. *Curr. Med. Sci.* 40, 917–930. doi:10.1007/s11596-020-2255-4

Zhou, X., Bai, C., Sun, X., Gong, X., Yang, Y., Chen, C., et al. (2017a). Puerarin Attenuates Renal Fibrosis by Reducing Oxidative Stress Induced-Epithelial Cell Apoptosis via MAPK Signal Pathways *In Vivo* and *In Vitro*. *Ren. Fail* 39, 423–431. doi:10.1080/0886022X.2017.1305409

Zhou, X., Sun, X., Gong, X., Yang, Y., Chen, C., Shan, G., et al. (2017b). Astragaloside IV from Astragalus Membranaceus Ameliorates Renal Interstitial Fibrosis by Inhibiting Inflammation via TLR4/NF-κB *In Vivo* and *In Vitro*. *Int. Immunopharmacol.* 42, 18–24. doi:10.1016/j.intimp.2016.11.006

Zhou, Z., Hu, Z., Li, M., Zhu, F., Zhang, H., Nie, J., et al. (2016). QiShenYiQi Attenuates Renal Interstitial Fibrosis by Blocking the Activation of β-Catenin. *PLoS One* 11, e0162873. doi:10.1371/journal.pone.0162873

Zuo, C., Xie, X. S., Qiu, H. Y., Deng, Y., Zhu, D., and Fan, J. M. (2009). Astragalus Mongholicus Ameliorates Renal Fibrosis by Modulating HGF and TGF-beta in Rats with Unilateral Ureteral Obstruction. *J. Zhejiang Univ. Sci. B* 10, 380–390. doi:10.1631/jzus.B0820230

Conflict of Interest: The authors declare that the research was conducted in the absence of any commercial or financial relationships that could be construed as a potential conflict of interest.

Publisher's Note: All claims expressed in this article are solely those of the authors and do not necessarily represent those of their affiliated organizations, or those of the publisher, the editors and the reviewers. Any product that may be evaluated in this article, or claim that may be made by its manufacturer, is not guaranteed or endorsed by the publisher.

frontiers | Frontiers in Pharmacology

ORIGINAL RESEARCH
published: 15 June 2022
doi: 10.3389/fphar.2022.917428

Yi-Shen-Hua-Shi Granule Alleviates Adriamycin-Induced Glomerular Fibrosis by Suppressing the BMP2/Smad Signaling Pathway

Zhuojing Tan[1,2†], Yachen Si[3†], Yan Yu[1†], Jiarong Ding[4], Linxi Huang[4], Ying Xu[4], Hongxia Zhang[2], Yihan Lu[5], Chao Wang[2], Bing Yu[2*] and Li Yuan[1*]*

[1]Department of Nephrology, Affiliated Hospital of Nantong University, Nantong, China, [2]Department of Cell Biology, Naval Medical University (Second Military Medical University), Shanghai, China, [3]Department of Internal Medicine, No. 944 Hospital of Joint Logistics Support Force, Jiuquan, China, [4]Department of Nephrology, Changhai Hospital, Naval Medical University (Second Military Medical University), Shanghai, China, [5]Nanjing Medical University, Nanjing, China

OPEN ACCESS

Edited by:
Dan-Qian Chen,
Northwest University, China

Reviewed by:
Chunling Liang,
Guangdong Provincial Hospital of Chinese Medicine, China
Sean Eddy,
University of Michigan, United States

***Correspondence:**
Li Yuan
yuanlint@163.com
Bing Yu
smmucellyu@163.com
Chao Wang
wangchaosmmu@126.com

[†]These authors have contributed equally to this work and share first authorship

Specialty section:
This article was submitted to Renal Pharmacology, a section of the journal Frontiers in Pharmacology

Received: 11 April 2022
Accepted: 06 May 2022
Published: 15 June 2022

Citation:
Tan Z, Si Y, Yu Y, Ding J, Huang L, Xu Y, Zhang H, Lu Y, Wang C, Yu B and Yuan L (2022) Yi-Shen-Hua-Shi Granule Alleviates Adriamycin-Induced Glomerular Fibrosis by Suppressing the BMP2/Smad Signaling Pathway. Front. Pharmacol. 13:917428. doi: 10.3389/fphar.2022.917428

Focal segmental glomerulosclerosis (FSGS) is a common clinical condition with manifestations of nephrotic syndrome and fibrosis of the glomeruli and interstitium. Yi-Shen-Hua-Shi (YSHS) granule has been shown to have a good effect in alleviating nephrotic syndrome (NS) in clinical and in animal models of FSGS, but whether it can alleviate renal fibrosis in FSGS and its mechanism and targets are not clear. In this study, we explored the anti-fibrotic effect and the targets of the YSHS granule in an adriamycin (ADR)-induced FSGS model and found that the YSHS granule significantly improved the renal function of ADR-induced FSGS model mice and also significantly reduced the deposition of collagen fibers and the expression of mesenchymal cell markers FN, vimentin, and α-SMA in the glomeruli of ADR-induced FSGS mice, suggesting that the YSHS granule inhibited the fibrosis of sclerotic glomeruli. Subsequently, a network pharmacology-based approach was used to identify the potential targets of the YSHS granule for the alleviation of glomerulosclerosis in FSGS, and the results showed that the YSHS granule down-regulated the expressions of BMP2, GSTA1, GATS3, BST1, and S100A9 and up-regulated the expressions of TTR and GATM in ADR-induced FSGS model mice. We also proved that the YSHS granule inhibited the fibrosis in the glomeruli of ADR-induced FSGS model mice through the suppression of the BMP2/Smad signaling pathway.

Keywords: renal fibrosis (RF), focal segmental glomerulosclerosis (FSGS), Yi-Shen-Hua-Shi granule, BMP2, adriamycin

INTRODUCTION

FSGS accounts for 20% of NS in children and 40% in adults, with an increasing incidence rate (about seven patients per million). FSGS is one of the common causes of steroid-resistant nephrotic syndrome (SRNS) and end-stage renal disease (ESRD) in adults and children worldwide (Kopp, 2018; Hodson et al., 2022). The main clinical manifestations of patients with FSGS are NS (massive proteinuria, hypoproteinemia, edema, and hyperlipidemia),

hematuria, hypertension, and the impairment of renal function, etc. The pathological changes of FSGS include glomerulosclerosis, tubular atrophy, and interstitial fibrosis in the affected segments of renal tissues (D'Agati et al., 2011; Agrawal et al., 2018).

Renal fibrosis, which is the pathological repair of the damaged renal tissue caused by various chronic renal injuries, plays an important role in the progression of FSGS to ESRD. The proliferation of glomerular mesangial cells and renal tubulointerstitial fibroblasts, the accumulation of the extracellular matrix (ECM), and epithelial–mesenchymal transition (EMT) are involved in the progression of renal fibrosis (Liu, 2011; Dongre and Weinberg, 2019). The severity of renal fibrosis is closely related to the progress of renal insufficiency; thus, it is extremely important to find a targeted drug or treatment strategy that can effectively prevent the progression of renal fibrosis in FSGS. The mechanism of renal fibrosis is sophisticated, and many kinds of signal pathways, such as the transforming growth factor-β (TGF-β)/Smad signaling pathway (Yang et al., 2019), Wnt/β-catenin pathway (Miao et al., 2019), and Notch pathway (Yu et al., 2021), are involved in the progression of renal fibrosis. Therefore, the treatment of renal fibrosis may require a synergistic strategy to act on multiple targets and multiple signaling pathways to achieve better efficacy outcomes. Traditional Chinese medicine (TCM), which has the characteristics of multi-components and multi-targets, has achieved good therapeutic effect in the treatment of renal fibrosis-related diseases (Shen et al., 2018). The ErHuang Formula attenuates renal fibrosis in streptozotocin-induced diabetic nephropathy rats by inhibiting the CXCL6/JAK/STAT3 signaling pathway (Shen et al., 2019). Chinese herbal compound Tongxinluo inhibits renal fibrosis in diabetic nephropathy by preventing the transfer of TGF-β1 from glomerular endothelial cells to glomerular mesangial cells via exosomes (Wu et al., 2017).

The YSHS granule is a modern patent TCM drug approved by China National Medical Products Administration. It was derived from a TCM formula, Sheng-Yang-Yi-Wei decoction, which was first documented in the TCM classic Nei-Wai-Shang-Bian-Huo-Lun issued in 1247 AD. The formula is able to tonify the yang and spleen ('Sheng Yang Bu Pi' in Chinese), replenish the kidney, and resolve dampness ('Yi Shen Hua Shi' in Chinese), and increase urine excretion to reduce edema ('Li Shui Xiao Zhong' in Chinese) (Li, 2018). YSHS granule is composed of 16 herbs, including Ginseng Radix et Rhizoma (GRR), Astragali Radix (ASR), Atractylodis Macrocephalae Rhizoma (AMR), Poria (POR), Alismatis Rhizoma (ALR), Pinelliae Rhizoma Praeparatum Cum Alumine (PRP), Notopterygii Rhizoma et Radix (NRR), Angelicae Pubescentis Radix (APR), Saposhnikoviae Radix (SAR), Bupleuri Radix (BUR), Coptidis Rhizoma (COR), Paeoniae Radix Alba (PRA), Citri Reticulatae Pericarpium (CRP), Glycyrrhizae Radix et Rhizoma Praeparata Cum Melle (GRP), Zingiberis Rhizoma Recens (ZRR), and Jujubae Fructus (JUF). The YSHS granule has achieved good therapeutic effect on treating chronic glomerulonephritis (CGN) in clinic and C-BSA-induced CGN rat models (Zhao et al., 2019). However, the specific mechanism and the potential targets of YSHS against nephropathy remain unclear.

Network pharmacology offers an effective approach for investigating the multiple pharmacological effects of TCM from a molecular perspective (Hopkins, 2007). It can clarify the complex interactions between genes and proteins related to drugs or diseases by integrating cheminformatics, bioinformatics, system biology, and other related research fields. The systematic and holistic characteristics of network pharmacology are consistent with the complex mechanism of "multi-component, multi-target, and multi-pathway" within TCM (Hopkins, 2008). The identification of active components of TCM, component-targeting proteins, and disease-specific molecules is used to establish the component–target-disease network. The component–target interaction network contributes to clarify the molecular mechanism of TCM. The disease–target interaction network can be utilized to explore the pathogenesis (Niu et al., 2018). At present, an integration of network pharmacology and experimental validation has become an important measure to understand the targets of active components and the potential mechanism of TCM.

The ADR-induced renal injury model is an ideal FSGS model, which is often accompanied by glomerular and tubular fibroses (Wang et al., 2000). In this study, the potential active components and targets of the YSHS granule against glomerular injury in FSGS were predicted with network pharmacology. Moreover, the key targets were further verified by experiments. On the basis of the results, the characteristics and functions of the key targets were analyzed and discussed, which laid the foundation of the molecular mechanism of the YSHS granule against ADR-induced FSGS.

MATERIALS AND METHODS

Reagents

Doxorubicin hydrochloride (D807083, Macklin, China) was dissolved in 0.9% NaCl to make a 1 mg/ml solution. The YSHS granule was provided by Guangzhou Consun Pharmaceutical Co., Ltd., and was dissolved in deionized water to make a 200 mg/ml solution. Triglyceride assay kit (A110-1-1), total cholesterol assay kit (A111-1-1), creatinine assay kit (sarcosine oxidase) (C011-2-1), albumin assay kit (A028-2-1), and microalbumin assay kit (H127-1-2) were purchased from Nanjing Jiancheng Bioengineering Institute.

Real-Time Polymerase Chain Reaction

Total RNA was purified with the RNAiso Plus reagent (9,108, Takara). Then, cDNA was synthesized by the MMLV Reverse Transcriptase (M530A, Promega) according to the manufacturer's protocols. A real-time PCR analysis was performed on the LightCycler® 96 System (Roche) in the 20 μL reaction mixture containing 10 μL 2 × ChamQ SYBR qPCR Master Mix (Q321-02, Vazyme), 0.2 mM forward primer, 0.2 mM reverse primer, and 0.5 μL cDNA. The PCR amplification conditions were as follows: annealing at 95°C for 10 s, amplification at 60°C for 30 s, and the number of cycles was

TABLE 1 | Primers used in the real-time PCR analysis.

Gene symbol	Forward primer (5′→3′)	Reverse primer (5′→3′)
Gapdh	TGCGACTTCAACAGCAACTCC	TGCTGTAGCCGTATTCATTGTC
Bmp2	TCTTCCGGGAACAGATACAGG	TGGTGTCCAATAGTCTGGTCA
Gsta1	GCAAGGAAGGCTTTCAAGATTCA	TTGCAAAATAGCCAGGATCAACA
Gsta3	GGGCTGATATTGCCCTGGTT	TGGCTGCCAGGTTGAAGAAA
Bst1	TGCTCGTTATGAGCTATGGGG	TCAAGTCCAGAGGCATTTTCC
S100a9	ATACTCTAGGAAGGAAGGACACC	TCCATGATGTCATTTATGAGGGC
Ttr	TTGCCTCGCTGGACTGGTA	TTACAGCCACGTCTACAGCAG
Gatm	TTGAGTACCGAGCGTACAGGT	TCCACGGAATGGATGGGATAAT
Igf1	CACATCATGTCGTCTTCACACC	GGAAGCAACACTCATCCACAATG
Ren	ACGGGTCCGACTTCACCAT	TGCCTAGAACACCGTCAAACT
Pck1	AGCATTCAACGCCAGGTTC	CGAGTCTGTCAGTTCAATACCAA
Alb	TGCTTTTTCCAGGGGTGTGTT	TTACTTCCTGCACTAATTTGGCA
Pah	GAGCCTGAGGAACGACATTGG	CTGATTGGCGAATCTGTCCAG
Ctsv	ATCGCCACCAGAAGCACA	AAACGCCCAACAAGACCC
Dcxr	ACTGTGCTGGCGTTGAAGG	CGGGTCCCACATTGCTTAGG
Tnnc1	GCGGTAGAACAGTTGACAGAG	CCAGCTCCTTGGTGCTGAT

set to 40. The primers were summarized in **Table 1**. All samples were examined thrice. The fold changes of each target gene were calculated using the $2^{-\triangle\triangle Ct}$ method relative to GAPDH.

Western Blot

Western blots were performed as described previously (Li et al., 2022). In brief, the total protein was prepared with RIPA buffer (89,901, ThermoFisher), quantified by BCA kit (23,225, ThermoFisher), separated by SDS-PAGE electrophoresis, and was transferred to PVDF membranes. Then, the membranes were blocked with 5% skimmed milk powder for 30 min, and incubated with a primary antibody at 4°C overnight. The membranes were washed with TBST for three times, and incubated with an HRP-conjugated secondary antibody at 37°C for 1 h. The immune complexes were visualized by using Pierce™ ECL Western Blotting Substrate (32,132, ThermoFisher). The primary antibodies are listed as follows: E-cadherin (#3195, diluted 1:2000), N-cadherin (#4061, diluted 1:2000), Vimentin (#5741, diluted 1:2000), and α-SMA (#19245, diluted 1:2000) from Cell Signaling Technology, MMP9(PAA553Mu01, diluted 1:2000) from Cloud-Clone Corp, BMP2(66,383-1-lg, diluted 1:2000), beta actin (66,009-1-lg, diluted 1:5,000), and Alpha Tubulin (66,031-1-lg, diluted 1: 5,000) from Proteintech.

Histopathological Analyses

Hematoxylin and Eosin (H&E), immunohistochemistry (IHC), and immunoflurosence (IF) staining were performed as our previous report (Yu et al., 2020). For immunostaining, the rehydrated sections were immersed in Tris-EDTA buffer (pH 9.0) and heated at 121°C for 2 min to repair the antigen. The endogenous peroxidase activity was blocked with 3% H_2O_2 for 10 min at room temperature. The non-specific binding site was blocked with 1% BSA for 20 min at room temperature. The sections were incubated with primary antibodies at 4 °C overnight. For IHC staining, the sections were incubated with HRP-conjugated secondary antibodies at 37°C for 30 min, and visualized with DAB Substrate (34,002, ThermoFisher). For IF staining, the sections were incubated with fluorescein-conjugated secondary antibodies at 37°C for 30 min, then the nuclei were counter stained with DAPI. The primary antibodies are listed as follows: rabbit anti-NPHS2 (20384-1-AP, diluted 1:200), mouse anti-BMP2 (66,383-1-lg, diluted 1:200) and rabbit anti-Fibronectin (15613-1-AP, diluted 1:200) from ProteinTech Group, rabbit anti-Vimentin (#5741, diluted 1:200) and rabbit anti-α-SMA (#19245, diluted 1:200) from Cell Signaling Technology. The secondary antibodies are listed as follows: Peroxidase AffiniPure goat anti-rabbit IgG (H+L) (111-035-003, diluted 1:400), Peroxidase AffiniPure goat anti-mouse IgG (H+L) (115-035-003, diluted 1:400), and Cy™3 AffiniPure goat anti-rabbit IgG (H+L) (111-165-003, diluted 1:400) from Jackson ImmunoResearch.

For Sirius Red staining, the hydrated sections were stained with a Sirius Red staining kit (SJ1207, Shuangjian Biotech, China) according the manufacturer's instruction. For Masson staining, the hydrated sections were stained with Masson's Trichrome Stain Kit (G1340) from Solarbio (Beijing China) according the manufacturer's instruction. For PAS staining, the hydrated sections were stained by the Glycogen Periodic Acid Schiff (PAS/Hematoxylin) Stain Kit (G1281) from Solarbio (Beijing China) according to the manufacturer-provided user manual.

The extent of glomerular sclerosis was assessed by examining all glomeruli on a kidney cross-section and calculating the percentage involved (Angeletti et al., 2020).

Identification of Active Components and Targets of the Yi-Shen-Hua-Shi Granule

The chemical components of the YSHS granule were obtained from the reported literature (Chan et al., 2021). The Traditional Chinese Medicine Systems Pharmacology database (TCMSP, https://tcmspw.com/tcmsp.php) was used to assess the pharmacokinetics of these components (Ru et al., 2014). Active components with an oral bioavailability (OB) ≥ 30% and drug similarity (DL) ≥ 0.18 were selected for subsequent analysis (Xu et al., 2012). The target proteins of the active

components in the YSHS granule were achieved from PharmMapper (http://www.lilab-ecust.cn/pharmmapper/) (Liu et al., 2010).

Screening for Differentially Expressed Genes of Focal Segmental Glomerulosclerosis

Expression profiling data from GSE129973 were obtained from the GEO database (http://www.ncbi.nlm.nih.gov/geo/). The data platform was GPL17586 HTA-2_0 Affymetrix Human Transcriptome 2.0 Array, consisting of 20 normal and 20 FSGS samples. Transcriptome comparison of glomeruli from kidneys with FSGS and glomeruli from the unaffected portion of tumor nephrectomies was progressed. The GEO2R web tool (http://www.ncbi.nlm.nih.gov/geo/geo2r/) using the limma package (version 3.26.8) based on the R language (version 3.2.3) was utilized to screen differentially expressed genes (DEGs) with the criteria of adjusted p-value < 0.05 and |Log2FC| > 1.

Construction of the Component–Target–Disease Network

The targets of the YSHS granule against FSGS were achieved by taking the intersection of the target proteins of active components in the YSHS granule and the DEGs of FSGS. A component–target–disease network was constructed based on the targets of the YSHS granule against FSGS with the Cytoscape (http://cytoscape.org) software (Shannon et al., 2003).

Gene Ontology and Kyoto Encyclopedia of Genes and Genomes Pathway Enrichment Analysis

ClusterProfiler software package in R platform was adopted to conduct gene ontology (GO) and kyoto encyclopedia of genes and genomes (KEGG) pathway enrichment analyses based on the targets of the YSHS granule against FSGS (Yu et al., 2012). The process and pathway with $p < 0.05$ were considered significant.

Animal Experiments

Male BALB/c mice were provided by Shanghai SLAC Lab Animal Co., Ltd., and were kept in standard pathogen-free conditions. All animal experiments were met with the Guidance for the Care and Use of Laboratory Animals and were approved by the Institutional Ethics Committee of Naval Medical University. The mice were randomly divided into three groups: The first group was the control group treated with saline by gavage administration. The second group was treated with doxorubicin hydrochloride (10 mg/kg body weight) by single intravenous injection to establish the mouse FSGS model, and then was randomly divided into two groups: the ADR group and the ADR + YSHS group, which were separately treated with saline and indicated dosage of the YSHS granule by gavage administration after ADR injection for 12 h. The third group was the YSHS group only treated with the indicated dosage of the YSHS granule by gavage administration. Each group was given saline or YSHS granule by gavage administration once a day for 28 days. Urine was collected on the last day. On the 29th day, all the mice were anesthetized by intraperitoneal injection of 1.25% tribromoethanol, the whole blood was collected by eyeball extraction and set up at room temperature for 2 h, then, the serum was collected by the centrifugation at 4,000 rpm for 10 min. The levels of ALB, Cr, TG, and TC in the serum were measured according the manufacturer's instruction. The right kidney was used for RNA and protein extraction. The left kidney was fixed with 4% paraformaldehyde, and then was paraffin-emdedded and sectioned at 3–7 μm.

Urine Albumin and Creatinine Quantification

12 h-urine samples were collected in metabolic cages from individual mice on the last day of molding. Urinary creatinine and urinary albumin were determined using commercial assay kits from Nanjing Jiancheng Bioengineering Institute. Urinary albumin excretion was expressed as the ratio of urinary albumin to creatinine.

Statistical Analysis

All experimental data were shown as mean ± SD and analyzed by one-way analysis of variance (ANOVA) using Prism, version 8, for Windows (GraphPad Software Inc.). $P < 0.05$ was considered statistically significant.

RESULTS

Yi-Shen-Hua-Shi Granule Alleviates Renal Injury in the Adriamycin-Induced Focal Segmental Glomerulosclerosis Model

To determine the optimal therapeutic dose of the YSHS granule for the alleviation of renal injury in the ADR-induced FSGS mouse model, the doses of 2,000, 4,000 and 8,000 mg/kg body weight of the YSHS granule were administered by gavage once daily, and the urinary albumin/creatinine ratio (UACR), which is one of the most sensitive and reliable response indicators of early renal injury (Basset et al., 2022), was measured after 4 weeks of intragastric administration of the YSHS granule. The results showed that the UACR decreased after intragastric administration of three doses of the YSHS granule, but the therapeutic effects of 4,000 and 8,000 mg/kg body weight were better than that of 2,000 mg/kg body weight. Moreover, there was no significant difference between the therapeutic effects of 4,000 and 8,000 mg/kg body weight (**Figure 1A**). Therefore, the dosage of 4,000 mg/kg body weight was used as the optimal treatment dose for the following study. In addition, the intragastric administration of the YSHS granule at doses of 2,000, 4,000, and 8,000 mg/kg body weight to healthy mice alone did not cause obviously change in the UACR (**Figure 1B**), indicating that YSHS had no significant toxicity to the kidney. To further clarify the therapeutic effect of the YSHS granule, we performed biochemical assays on mouse serum specimens, and the results showed that the YSHS granule elevated serum albumin (**Figure 1C**) and reduced serum creatinine (**Figure 1D**), triglyceride

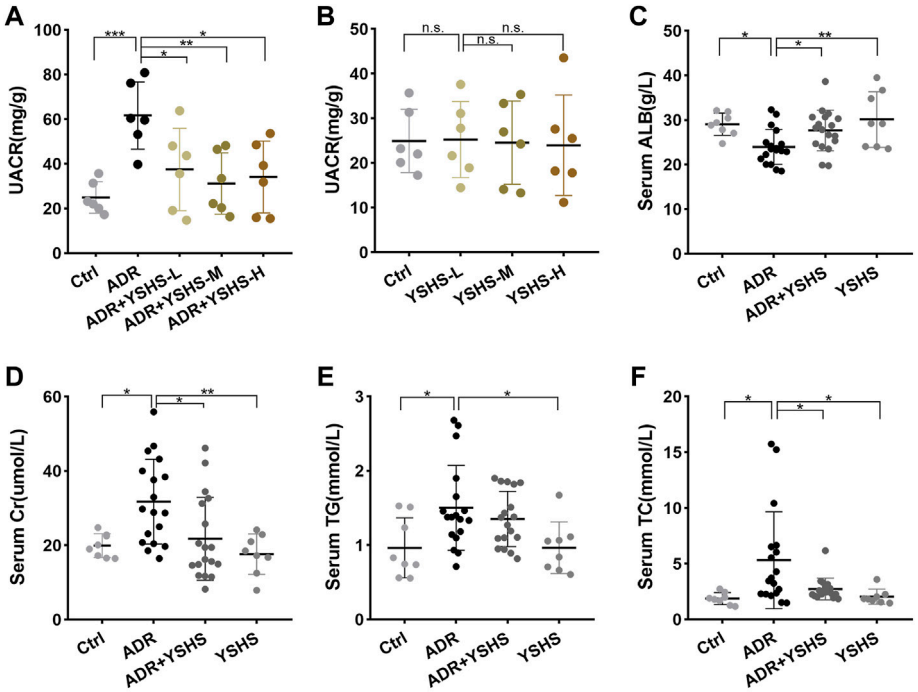

FIGURE 1 | YSHS granule mitigates kidney injury and proteinuria in ADR-induced nephropathy. **(A)** At the end of the fourth week of intragastric administration, 12 h-urine samples were collected. The UACR (mg/g) was evaluated from mice in Ctrl, ADR, and ADR with three different concentrations of YSHS treatment groups. **(B)** Three different doses of YSHS did not cause significant changes in UACR in healthy mice. **(C–F)** Serum albumin (ALB) **(C)**, creatinine (Cr) **(D)**, triglyceride (TG) **(E)** , and total cholesterol (TC) **(F)** were evaluated in the mice of the indicated groups. The data represent mean ± SD, one-way ANOVA analysis followed by Tukey post-hoc tests as appropriate for multiple comparisons. $^{*}p < 0.05$, $^{**}p < 0.01$, $^{***}p < 0.001$, n. s., no significant.

(**Figure 1E**), and total cholesterol (**Figure 1F**), which met the criteria for an effective treatment of FSGS.

To clarify the effect of the YSHS granule on the morphological structure of glomeruli in the ADR-induced FSGS mouse model, a series of pathological tests were performed. The results of HE and PAS staining showed that compared with the control group, ADR caused obvious glomerular segmental sclerosis, the formation of undifferentiated cells on the surface of the basement membrane adhering to the wall of Bowman's capsule, the dilatation and structural disorder of proximal tubules, a large number of protein casts in the tubular lumen, and extensive interstitial infiltration of inflammatory cells (**Figures 2A,B**). In contrast, the incidence and extent of glomerulosclerosis were significantly reduced in FSGS model mice after treatment with the YSHS granule (**Figure 2C**). Podocytes are an important component of the glomerular filtration membrane, and the damage to the filtration membrane is a key factor in causing proteinuria (Angeletti et al., 2020). The results of immunofluorescence staining showed that the number of podocytes in the glomeruli of the FSGS mouse model induced by ADR was significantly reduced, indicating that ADR had a significant damaging effect on podocytes, while the treatment with the YSHS granule significantly increased the number of podocytes in the glomeruli of the FSGS model (**Figures 2D,E**), suggesting that YSHS granule could reduce the damage of ADR on podocytes. These data suggest that YSHS granule has a promising therapeutic effect on ADR-induced focal segmental glomerulosclerosis.

Yi-Shen-Hua-Shi Alleviates Glomerular Fibrosis in the Focal Segmental Glomerulosclerosis Model

Renal fibrosis is a fundamental pathological change in the development of a chronic kidney disease to the end stage, and it is involved in the glomerular sclerosis of FSGS model mice induced by ADR (Djudjaj and Boor, 2019). Therefore, we detected the expression of fibrosis-related markers in the kidneys of ADR-induced FSGS model mice treated with the YSHS granule by using Western blot, and the results showed that the expression of epithelial cell marker E-cadherin was up-regulated, the expression of mesenchymal cell markers N-cadherin, Vimentin, and α-SMA were obviously down-regulated, and the level of matrix metalloproteinase MMP9, which functions to degrade the extracellular matrix, was increased in the kidney, of YSHS granule-treated ADR-induced FSGS model mice compared with the FSGS model group (**Figures 3A,B**).

To further clarify whether the fibrosis of sclerotic glomeruli in ADR-induced FSGS model can be attenuated by the YSHS granule, we performed Sirius Red and Masson staining and the results showed that the deposition of collagen fibers in the

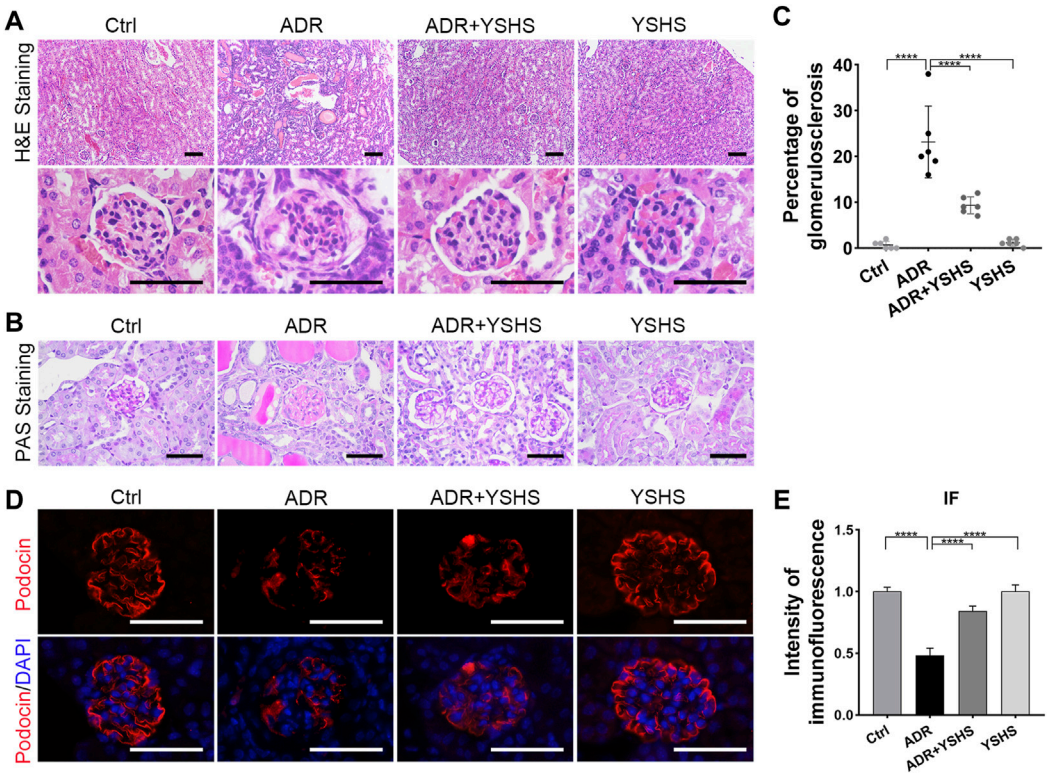

FIGURE 2 | YSHS granule ameliorates glomerular injury in the FSGS model. **(A)** Representative H&E staining of the renal sections in the indicated groups. **(B)** Representative PAS staining of the renal sections in the indicated groups. **(C)** The percentage of glomerulosclerosis in each group. **(D)** Representative IF staining of podocin (red) in the indicated groups. DAPI was used to visualize the cell nucleus (blue). **(E)** The quantification of the intensity of podocin revealed that the YSHS granule significantly increased the expression of podocin in the glomeruli of the FSGS model. All glomeruli from one section of 6 mice in each group were analyzed and the data were shown as mean ± SD, one-way ANOVA analysis followed by Tukey post-hoc tests as appropriate for multiple comparisons, ****$p < 0.0001$. scale bar: 50 μm.

glomeruli of ADR-induced FSGS model mice were obviously increased, while the deposition of collagen fibers in the glomeruli of FSGS model mice were significantly decreased by the YSHS granule treatment via intragastric administration (**Figures 3C,D**). In addition, the results of immunohistochemical staining showed that the YSHS granule not only significantly reduced the expression of Fibronectin (FN) (**Figure 3E**) and Vimentin (**Figure 3F**) in the glomeruli of FSGS model mice, but also significantly reduced the expression of α-SMA (**Figure 3G**) on the renal capsule wrapped outside the glomeruli.

These results indicated that the YSHS granule not only reduced the deposition of extracellular matrix, but also promoted the degradation of extracellular matrix by up-regulating the expression of MMP9, thus alleviating glomerular fibrosis induced by ADR, and effectively delaying the progress of chronic kidney diseases.

Identification of the Targets of the Yi-Shen-Hua-Shi Granule Against Focal Segmental Glomerulosclerosis With Network Pharmacology

According to the reported literature, a total of 105 chemical components were detected in the YSHS granule by using high performance liquid chromatography coupled with electrospray ionization tandem quadrupole time-of-fight mass spectrometry (HPLC-Q-TOF/MS) (Chan et al., 2021). Then, these components were searched in the TCMSP platform and 17 active components were obtained with the criteria of OB ≥ 30% and DL ≥ 0.18, as shown in **Table 2**. The 17 active components were respectively entered into the PharmMapper server and 423 target proteins that interact with these components were found (**Supplementary Table S1**). According to the expression profiling data of glomeruli from kidneys with FSGS from GSE129973, a total of 468 DEGs were identified, which consist of 197 up-regulated and 271 down-regulated genes (**Supplementary Table S2**). A Venn analysis between 423 target proteins of the YSHS granule and 468 DEGs of FSGS revealed 15 overlapping targets, which may play crucial roles in the protective effects of YSHS on FSGS (**Figure 4A**). To visualize the relationship between the active components of the YSHS granule and the targets of the YSHS granule against FSGS, a component-target-disease network was constructed by using Cytoscape (**Figure 4B**). In the network, the red node (1) represents YSHS; the yellow nodes (10) represent Chinese herbal medicinal ingredients; the purple nodes (17) represent active chemical components; the blue node (1) represents FSGS; and the green nodes (Hopkins, 2007) represent the targets of the YSHS granule against FSGS.

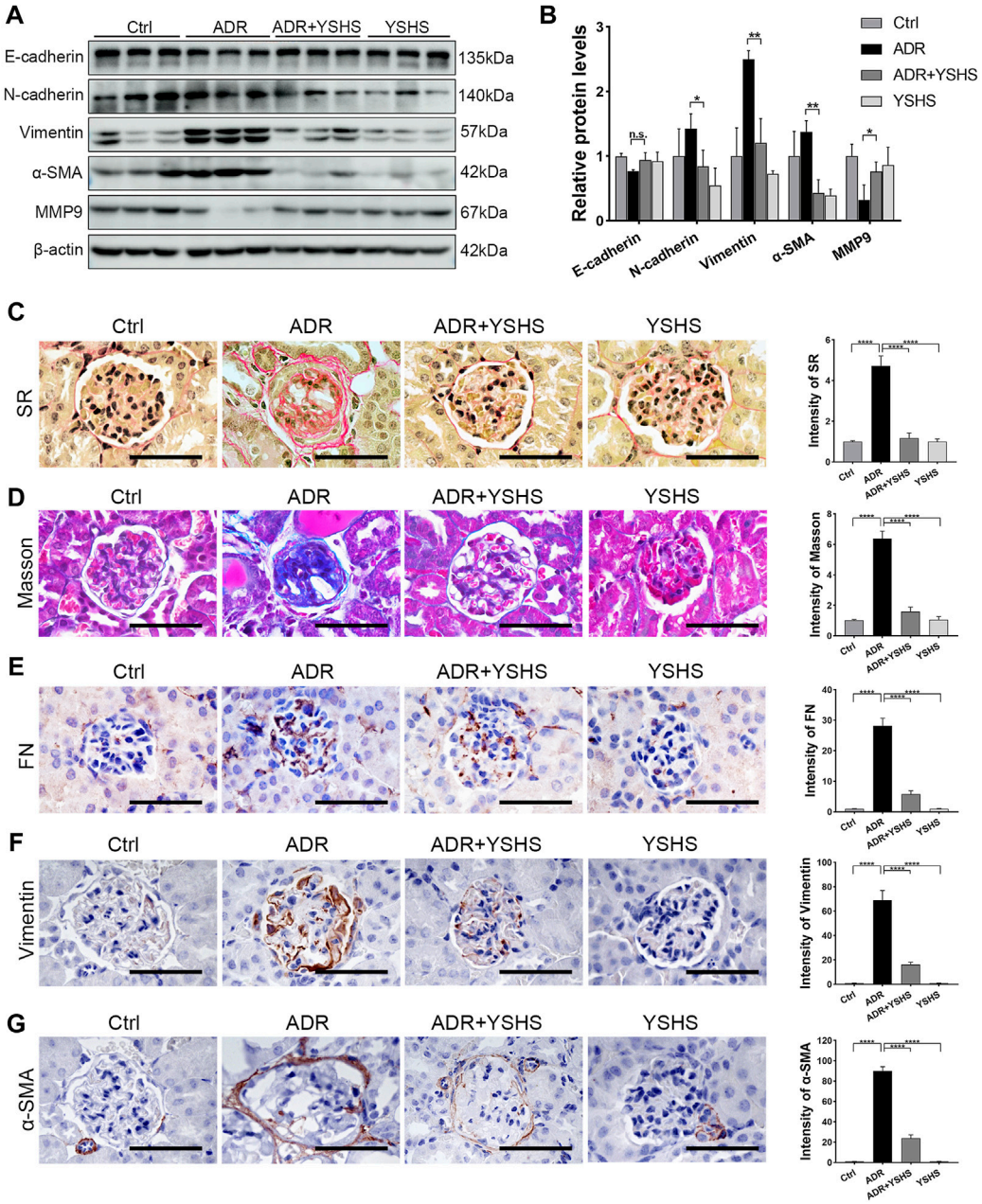

FIGURE 3 | YSHS granule relieves glomerular fibrosis in the FSGS model. **(A)** Western blot analysis shows the expression levels of the indicated proteins extracted from kidney tissues in each group. **(B)** The quantification of the relative intensities of blots showed that the YSHS granule reduced the expression of N-cadherin, Vimentin, and α-SMA in ADR-induced FSGS models. *N* = 3 in each group, the data were shown as mean ± SD, one-way ANOVA analysis followed by Tukey post-hoc tests as appropriate for multiple comparisons, $^{*}p < 0.05$, $^{**}p < 0.01$. **(C–D)** The results of Sirius Red (SR) staining **(C)** and Masson staining **(D)** showed that the YSHS granule obviously decreased the accumulation of collagen fibers in glomerulus of ADR-induced FSGS model mice. **(E–G)** The results of IHC staining FN **(E)**, Vimentin **(F),** and α-SMA **(G)** showed that the YSHS granule obviously decreased the expression of FN, α-SMA, and Vimentin in the glomerulus of ADR-induced FSGS model mice. *N* = 6 in each group, the data were shown as mean ± SD, one-way ANOVA analysis followed by Tukey post-hoc tests as appropriate for multiple comparisons, $^{****}p < 0.0001$. scale bar: 50 μm.

The Characteristics and Functions of Prediction Targets

To investigate the biological functions of the predicted targets, GO and KEGG pathway enrichment analyses were conducted. The results of the GO enrichment analysis include three categories: biological process (BP), cellular component (CC), and molecular function (MF) (**Supplementary Tables S3–S5**). The top 10 items of BP, CC, and MF in GO enrichment were visualized via bubble charts (**Figures 4C–E**). These results

TABLE 2 | Active components of the YSHS granule.

Mol Id	Component	Formula	OB (%)	DL	Source
MOL006710	Fraxin	$C_{16}H_{18}O_{10}$	36.76	0.42	NRR
MOL007004	Albiflorin	$C_{23}H_{28}O_{11}$	30.25	0.77	PRA
MOL001924	Paeoniflorin	$C_{23}H_{28}O_{11}$	53.87	0.79	PRA
MOL011737	Divaricatacid	$C_{16}H_{16}O_{7}$	87.00	0.32	SAR
MOL004903	Liquiritin	$C_{21}H_{22}O_{9}$	65.69	0.74	GRP
MOL004792	Nodakenin	$C_{20}H_{24}O_{9}$	57.12	0.69	NRR, APR
MOL013079	Praeruptorin A	$C_{21}H_{22}O_{7}$	46.46	0.53	SAR
MOL000392	Formononetin	$C_{16}H_{12}O_{4}$	69.67	0.21	ASR, GRP
MOL002644	Phellopterin	$C_{17}H_{16}O_{5}$	40.19	0.28	NRR, SAR
MOL011753	5-O-methylvisamminol	$C_{16}H_{18}O_{5}$	37.99	0.25	SAR
MOL013276	Poncirin	$C_{28}H_{34}O_{14}$	36.55	0.74	CRP
MOL000417	Calycosin	$C_{16}H_{12}O_{5}$	47.75	0.24	ASR, GRP
MOL006397	Jatrorrhizine	$C_{20}H_{20}NO_{4}$	30.44	0.75	COR
MOL000785	Palmatine	$C_{21}H_{22}NO_{4}$	64.60	0.65	COR
MOL004885	Licoisoflavanone	$C_{20}H_{18}O_{6}$	52.47	0.54	GRP
MOL001454	Berberine	$C_{20}H_{18}NO_{4}$	36.86	0.78	COR, JUF
MOL000289	Pachymic acid	$C_{33}H_{52}O_{5}$	33.63	0.81	POR

indicated that the YSHS granule might be involved in cellular oxidant detoxification, antioxidant activity, fatty acid binding, and insulin-like growth factor receptor binding to play protective roles in FSGS. The KEGG enrichment analysis identified 17 pathways (**Supplementary Table S6**) and the results were visualized by bubble charts (**Figure 4F**). A previous study found that impaired glutathione metabolism might be related to the acceleration of renal fibrosis progression (You et al., 2020). It can be inferred that the YSHS granule might alleviate renal fibrosis in FSGS by restoring glutathione metabolism disturbance. Taken together, the results of the GO and KEGG pathway enrichment analyses supported that the 15 predicted targets had the characteristics and functions as the therapeutic targets of the YSHS granule for treating FSGS.

The Expression Changes of the Predicted Targets in Focal Segmental Glomerulosclerosis Model Mice Treated With the Yi-Shen-Hua-Shi Granule

The expression changes of these 15 predicted target genes in FSGS model mice treated with the YSHS granule were evaluated by using real-time PCR assay. Results showed that the YSHS granule down-regulated the expressions of Bmp2, Gsta1, Gsta3, Bst1, and S100a9 (**Figure 5A**), and up-regulated the expressions of Ttr and Gatm (**Figure 5B**) in the kidney tissues of ADR-induced FSGS model mice, while there were no significant changes on the expressions of Igf1, Ren, Pck1, Alb, Pah, Ctsv, Dcxr, and Tnnc1. (**Figure 5C**).

Yi-Shen-Hua-Shi Granule Inhibits the Activity of the BMP2/Smad Signaling Pathway

It is well known that BMP2, a member of the TGF-β superfamily, is involved in the fibrosis process in a variety of tissues and cells through the Smad signaling pathway (Wang et al., 2012; Wang and Wu, 2018; Hong et al., 2020; Su et al., 2020). The protein expression of BMP2 was up-regulated in the kidney tissues of ADR-induced FSGS model, while the YSHS granule significantly decreased the expression of BMP2 in the ADR-induced FSGS model (**Figures 6A,B**), which was consistent with the expression trend of Bmp2 mRNA detected by Real-time PCR (**Figure 5A**). Simultaneously, the YSHS granule also decreased the expressions of Smad1 and p-Smad1/5 in the kidney of the FSGS model (**Figures 6A,B**). In addition, the results of immunohistochemistry further demonstrated that the YSHS granule reduced the expression of BMP2 in glomeruli of the ADR-induced FSGS model (**Figures 6C,D**). These results suggest that the YSHS granule attenuates glomerular fibrosis in the ADR-induced FSGS model by inhibiting the activity of the BMP2/Smad signaling pathway.

DISCUSSION

ADR is a potent cytotoxic antitumor drug, which can simultaneously inhibit the synthesis of cellular DNA and RNA, induce cell apoptosis, and have an obvious toxic damage to the glomeruli and renal tubules, eventually leading to FSGS with proteinuria, hyperlipidemia, and other clinical manifestations (Qiao et al., 2018). The occurrence of proteinuria is caused by the destruction of the glomerular filtration membrane. When the kidney is damaged by ADR, podocytes, the most important part of the filtration membrane, will fall off after being stimulated. Then, the exposed basement membrane adheres to the wall of Bowman's cyst and exudes plasma proteins. With the deposition of extracellular matrix, glomerulosclerosis is gradually formed (Wharram et al., 2005). In this study, we used the ADR-induced FSGS model in BALB/c mice to demonstrate that the YSHS granule can ameliorate renal injury in ADR-induced nephropathy, and found that both ADR-induced proteinuria and hyperlipidemia were significantly reduced after the

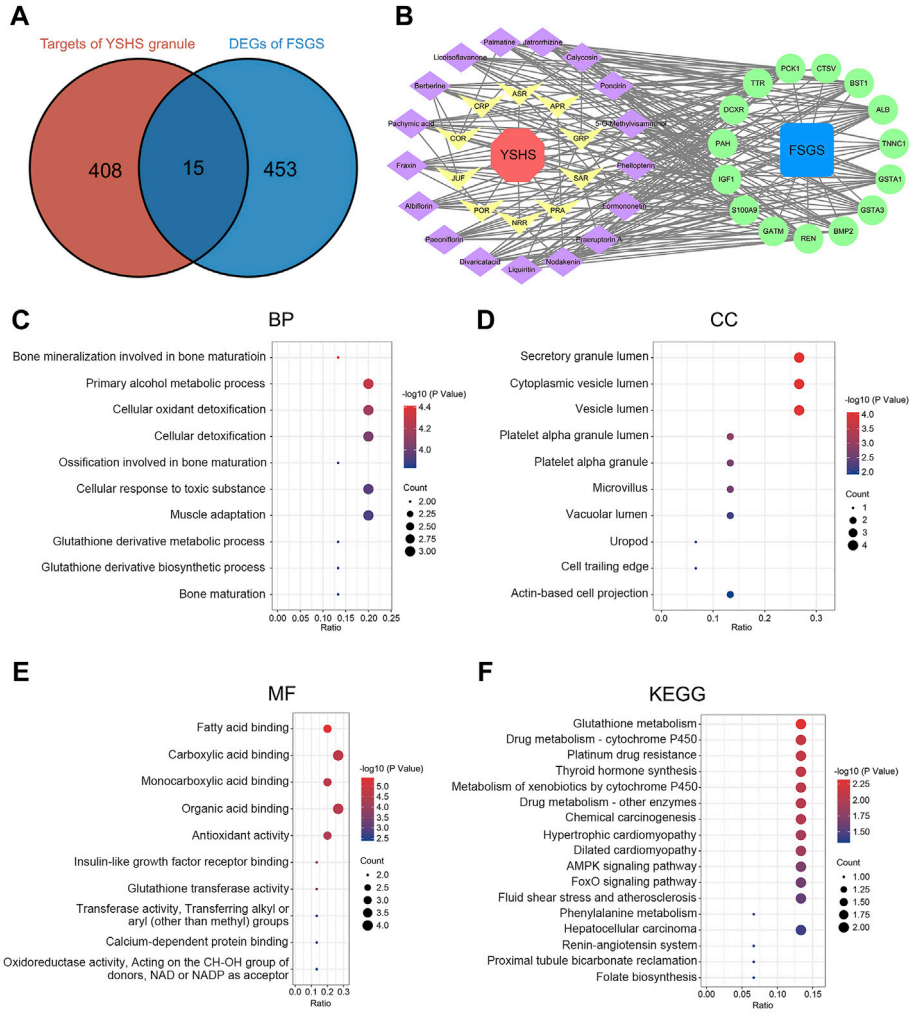

FIGURE 4 | Identification and analysis of the targets of the YSHS granule against FSGS. **(A)** Venn diagram of the targets of the YSHS granule and DEGs of glomeruli from kidneys with FSGS. **(B)** A network of the active components of the YSHS granule and the targets of the YSHS granule against FSGS, which was constructed by using Cytoscape. **(C–E)** The top 10 items of BP **(C)**, CC **(D)** and MF **(E)** in GO enrichment of the targets of the YSHS granule against FSGS. **(F)** KEGG pathway enrichment of the targets of the YSHS granule against FSGS.

intragastric administration of the YSHS granule to ADR-induced FSGS model mice.

Excessive deposition of extracellular matrix (ECM) is the core pathological change of renal fibrosis (Liu, 2006). Our results show that the YSHS granule reduced the accumulation of collagen fibers and FN in glomeruli caused by ADR, which are the main components of ECM. Meanwhile, the YSHS granule down-regulated the expression of α-SMA and Vimentin which were expressed in the activated myofibroblasts transformed from fibroblasts or epithelial cells (Mack and Yanagita, 2015; Djudjaj and Boor, 2019), and up-regulated matrix metalloproteinase MMP9 that degrades ECM (Yabluchanskiy et al., 2013). Here, we found that α-SMA was localized in the parietal layer of the renal capsule which is composed of a single layer of squamous epithelial cells, while Vimentin was mainly distributed in the glomerular interstitium, indicating that different types of epithelial cells underwent epithelial–mesenchymal transition under the stimulation of ADR. Therefore, the reduced expression of α-SMA and Vimentin in the ADR-induced FSGS model by the YSHS granule further suggested that the YSHS granule may prevent the progress of renal fibrosis in ADR-induced FSGS through the inhibition of EMT. However, which types of epithelial cells undergo EMT in the ADR-induced FSGS model and the mechanism of the YSHS granule inhibiting EMT still need to be further studied.

The most important feature of TCM is that it is composed of a variety of herbs and contains a variety of active ingredients. In this study, we identified 17 active ingredients from YSHS which is composed of 16 herbs. Some of these active ingredients have been reported to have anti-fibrotic effects. For example, paeoniflorin inhibited the epithelial–mesenchymal transition by downregulating the TGF-β/Smad signaling pathway, thereby improving pulmonary fibrosis and renal interstitial fibrosis

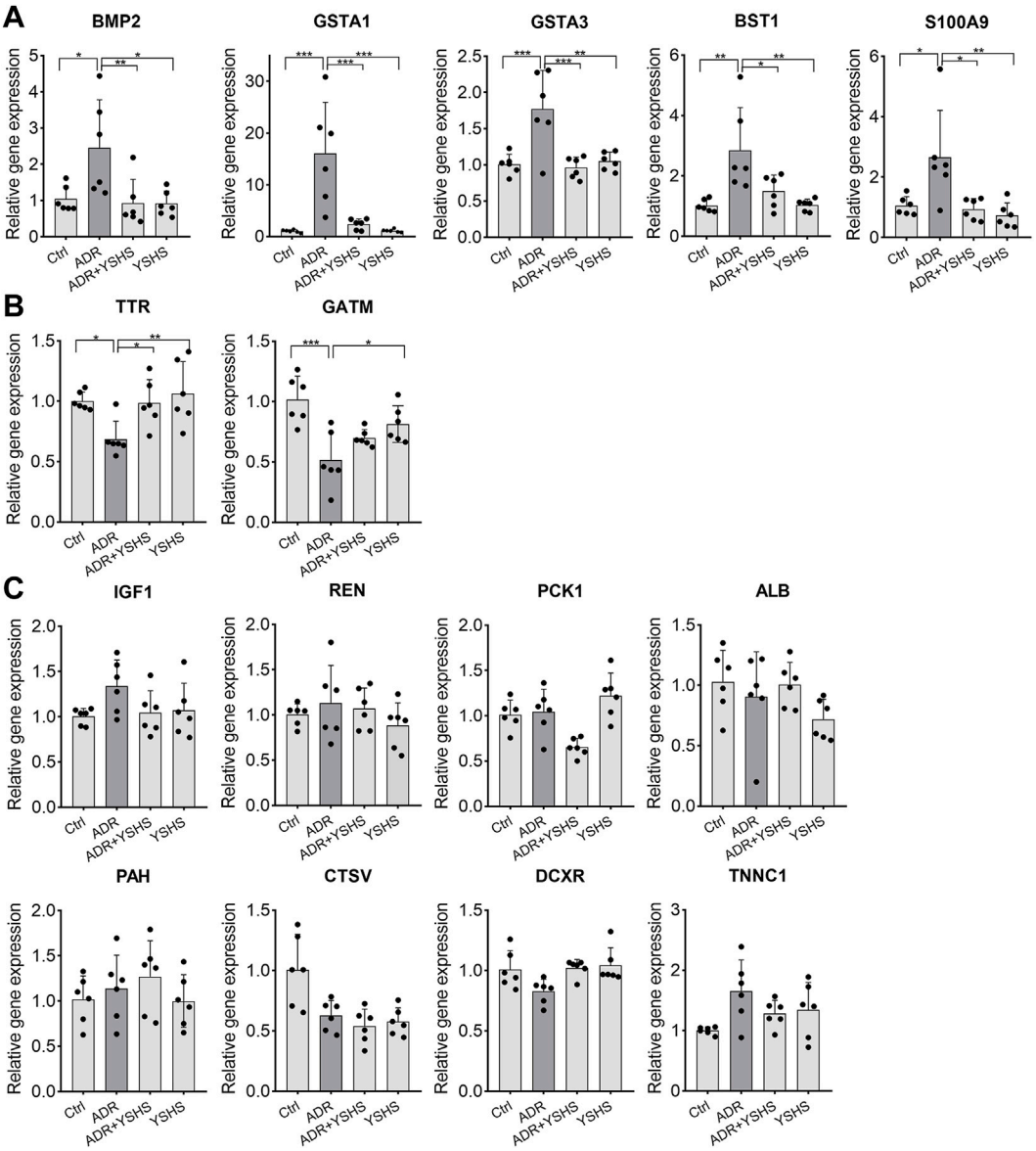

FIGURE 5 | Effects of the YSHS granule on the expression of predicted target genes in the ADR-induced FSGS model. **(A–C)** Real-Time PCR was performed to analyze the expression of these predicted targets. YSHS down-regulated the expressions of Bmp2, Gsta1, Gsta3, Bst1, and S100a9 **(A)**, and up-regulated the expression of Ttr and Gatm **(B)**, while it did not affect the expressions of Igf1, Ren, Pck1, Alb, Pah, Ctsv, Dcxr, and Tnnc1 **(C)** in the ADR-induced FSGS model. $N = 6$ in each group, the data were shown as mean ± SD, one-way ANOVA analysis followed by Tukey post-hoc tests as appropriate for multiple comparisons, $^{*}p < 0.05$, $^{**}p < 0.01$, $^{***}p < 0.001$.

(Zeng et al., 2013; Ji et al., 2016). Liquiritin prevented high fructose-induced myocardial fibrosis by inhibiting the NF-κB and MAPK signaling pathways (Zhang et al., 2016). Nodakenin inhibited UUO-induced renal fibrosis in mice and TGF-β1-treated renal epithelial cells, a classic model of cell fibrosis *in vitro*, by down-regulating the expression of Snail1 (Li et al., 2020). Formononetin activated the Nrf2/ARE signaling pathway through Sirt1, thereby ameliorating diabetic renal fibrosis (Zhuang et al., 2020). Calycosin ameliorated glomerulosclerosis and interstitial fibrosis in diabetic nephropathy by downregulating the IL33/ST2 signaling pathway (Elsherbiny et al., 2020). Berberine attenuated mesangial cell fibrosis via activating G protein-coupled bile acid receptor TGR5 and inhibiting the S1P2/MAPK signaling pathway (Yang et al., 2016). Although most of the active ingredients in the YSHS granule have been shown to have an anti-fibrotic effect in a variety of tissues, the anti-fibrotic effect and targets of these active ingredients in ADR-induced FSGS model remain unclear.

In this study, fifteen genes were predicted as the targets of the YSHS granule in the treatment of FSGS from the targets of the YSHS granule predicted from TCMSP and PharmMapper databases and the deferentially expressed genes from human

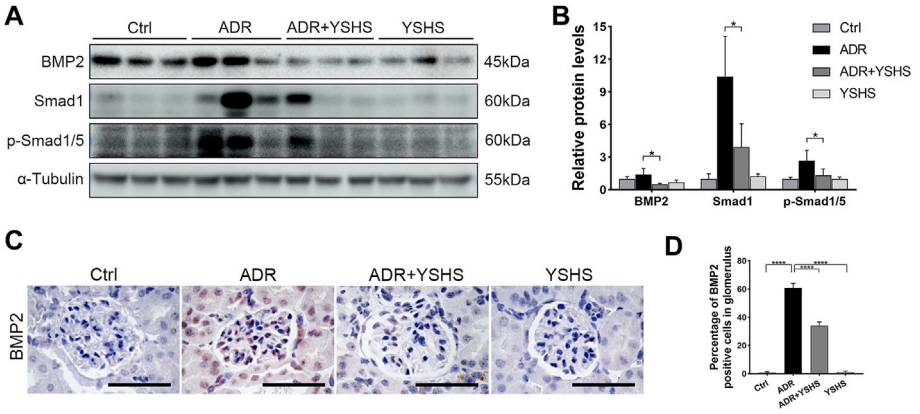

FIGURE 6 | YSHS granule inhibits the BMP2/Smad signaling pathway. **(A)** The expression of BMP2, Smad1, and p-Smad1/5 were determined by Western blot. α-Tubulin was used as a loading control. **(B)** The quantification of the relative intensities of blots showed that the YSHS granule reduced the protein expression of BMP2, Smad1, and p-Smad1/5 in the ADR-induced FSGS model. **(C)** Representative IHC staining of BMP2 in the indicated groups. **(D)** The quantification of the BMP2 positive cells in glomerulus revealed that the YSHS granule obviously decreased the expression of BMP2 in ADR-induced FSGS model. *N* = 6 in each group, the data were shown as mean ± SD, one-way ANOVA analysis followed by Tukey post-hoc tests as appropriate for multiple comparisons, $^{*}p < 0.05$, $^{****}p < 0.0001$. scale bar: 50 μm.

glomeruli in kidneys with FSGS expression profiles from the GSE129973 dataset based on the network pharmacological analysis, which is an innovative method to predict the targets of TCM based on the interaction of "disease-gene-target-drug". Then, seven genes, including BMP2, GSTA1, GSTA3, BST1, S100A9, TTR, and GATM, were identified as the targets of the YSHS granule in the treatment of ADR-induced FSGS by Real-time PCR analysis. Among these validated targets of YSHS, BMP2 belongs to the TGF-β superfamily, has a similar ligand structure, similar receptor-binding proteins, and similar downstream signaling cascades to TGF-β1 (Aashaq et al., 2022). Many researches demonstrated that BMP2 plays an important role in the occurrence, development, and outcome of renal interstitial fibrosis (Yang et al., 2009; Yang et al., 2011; Simone et al., 2012). Simone S et al. showed that BMP2 induced a profibrotic phenotype in adult human renal progenitor cells, such as increasing the expression of α-SMA, collagen I, and fibronectin protein (Simone et al., 2012), while, Yang YL et al. showed that BMP2 suppresses renal interstitial fibrosis (Yang et al., 2009; Yang et al., 2011). The role of BMP2 in renal fibrosis seems to be controversial. In our study, the expression of BMP2 was up-regulated in the ADR-induced FSGS model, while the expression of BMP2 was significantly inhibited after the intragastric administration of the YSHS granule. These data not only suggest that BMP2 is involved in the regulation of the fibrosis in the FSGS mouse model, but also suggest that BMP2 is one of the therapeutic targets in the treatment of fibrosis in the FSGS mouse model. However, the specific role of BMP2 in the regulation of fibrosis in the FSGS mouse model remains to be further clarified.

GSTA3, which is one of the most important members of the glutathione transferase family and is involved in the detoxification and cellular defense (Hayes et al., 2005), it was reported to attenuate renal interstitial fibrosis *in vivo* and *in vitro* by inhibiting the activity of the TGF-β1 signaling pathway (Xiao et al., 2016; Xiao et al., 2019) and inhibited liver fibrosis through the suppression of the MAPK and GSK-3β signaling pathways (Chen et al., 2019), suggesting that GSTA3 is an effective anti-fibrosis target. S100A9 was not only identified as a marker for idiopathic pulmonary fibrosis (Hara et al., 2012; Yamashita et al., 2021), but also aggravated dermal fibrosis induced by bleomycin in mice via activation of ERK1/2 MAPK and NF-κB pathways (Xu et al., 2018). In our study, we also found that the expression of S100A9 was up-regulated in the ADR-induced FSGS mouse model, indicating that S100A9 may promote glomerular fibrosis in the FSGS model. After intragastric administration of the YSHS granule, the expression of S100A9 decreased significantly, suggesting that it may be one of the effective targets for the YSHS granule to alleviate glomerular fibrosis in the FSGS model. GATM, which encodes the mitochondrial enzyme glycine amidinotransferase, is involved in creatine biosynthesis (Carney, 2018). Reichold, M. et al. showed that the accumulation of mutant GATM in the mitochondria of the proximal tubule, resulted in mitochondrial enlargement and elongation, eventually leading to renal tubular injury, renal Fanconi syndrome, and later in life, to fibrosis and progressive loss of renal function (Reichold et al., 2018), while another research showed that GATM knockout only caused neurological symptoms due to creatine deficiency but did not caused dysfunctions in renal and renal fibroses (Choe et al., 2013). Hence, whether GATM has an anti-fibrotic effect remains to be elucidated. The other three target genes (GSTA1, TTR, and BST1) have not been reported to be associated with fibrosis. Therefore, the role of these three targets in the treatment of renal fibrosis needs to be further clarified.

In summary, our research showed that the YSHS granule significantly improved the renal function and reduced the fibrosis in the glomeruli of ADR-induced FSGS model mice via suppressing of the BMP2/Smad signaling pathway. Our results indicated that the YSHS granule may be an effective drug to alleviate glomerular fibrosis in FSGS and BMP2 may be served as

an effective therapeutic target in the treatment of renal fibrosis and FSGS.

DATA AVAILABILITY STATEMENT

The datasets presented in this study can be found in online repositories. The names of the repository/repositories and accession number(s) can be found in the article/**Supplementary Material**.

ETHICS STATEMENT

The animal study was reviewed and approved by the Institutional Ethics Committee of Naval Medical University.

AUTHOR CONTRIBUTIONS

BY, LY, ZT, and CW designed this study. ZT, YS, BY, LH, YY, JD, YX, HZ, and YL performed the experiments and data analyses. BY, ZT, and YS wrote the manuscript. All authors read and approved the final manuscript.

FUNDING

This study was supported by the National Key R&D Program of China (2018YFA0107500 and 2019YFC1709402), National Natural Science Foundation of China (82,173,369 and 31,771,511), Foundation Strengthening Program in Technical Field of China (2019-JCJQ-JJ-068), Jiangsu Province TCM science and technology development plan project (YB201985), and Clinical and Experimental Research of YSHS Granule.

ACKNOWLEDGMENTS

The authors thank Guangzhou Consun Pharmaceutical Co., Ltd., for providing the YSHS granule.

SUPPLEMENTARY MATERIAL

The Supplementary Material for this article can be found online at: https://www.frontiersin.org/articles/10.3389/fphar.2022.917428/full#supplementary-material

REFERENCES

Aashaq, S., Batool, A., Mir, S. A., Beigh, M. A., Andrabi, K. I., and Shah, Z. A. (2022). TGF-β Signaling: A Recap of SMAD-Independent and SMAD-Dependent Pathways. *J. Cell Physiol.* 237, 59–85. doi:10.1002/jcp.30529

Agrawal, S., Zaritsky, J. J., Fornoni, A., and Smoyer, W. E. (2018). Dyslipidaemia in Nephrotic Syndrome: Mechanisms and Treatment. *Nat. Rev. Nephrol.* 14, 57–70. doi:10.1038/nrneph.2017.15510.1038/nrneph.2017.175

Angeletti, A., Cantarelli, C., Petrosyan, A., Andrighetto, S., Budge, K., D'Agati, V. D., et al. (2020). Loss of Decay-Accelerating Factor Triggers Podocyte Injury and Glomerulosclerosis. *J. Exp. Med.* 217 (9), e20191699. doi:10.1084/jem.20191699

Carney, E. F. (2018). GATM Mutations Cause Mitochondrial Abnormalities and Kidney Failure. *Nat. Rev. Nephrol.* 14, 414. doi:10.1038/s41581-018-0017-3

Chan, Y. C., Zhao, J., Hu, Q., Guo, H., and Yu, Z. L. (2021). Chemical Profile Assessment and Potential Bioactive Component Screening of a Chinese Patent Herbal Drug Yi-Shen-Hua-Shi Granule. *Nat. Product. Commun.* 16 (6), 1934578X2110216. doi:10.1177/1934578X211021691

Chen, H., Gan, Q., Yang, C., Peng, X., Qin, J., Qiu, S., et al. (2019). A Novel Role of Glutathione S-Transferase A3 in Inhibiting Hepatic Stellate Cell Activation and Rat Hepatic Fibrosis. *J. Transl. Med.* 17, 280. doi:10.1186/s12967-019-2027-8

Choe, C. U., Nabuurs, C., Stockebrand, M. C., Neu, A., Nunes, P., Morellini, F., et al. (2013). L-Arginine:Glycine Amidinotransferase Deficiency Protects from Metabolic Syndrome. *Hum. Mol. Genet.* 22, 110–123. doi:10.1093/hmg/dds407

D'Agati, V. D., Kaskel, F. J., and Falk, R. J. (2011). Focal Segmental Glomerulosclerosis. *N. Engl. J. Med.* 365, 2398–2411. doi:10.1056/NEJMra1106556

Basset, M., Milani, P., Ferretti, V. V., Nuvolone, M., Foli, A., Benigna, F., et al. (2022). Prospective Urinary Albumin/Creatinine Ratio for Diagnosis, Staging, and Organ Response Assessment in Renal AL Amyloidosis: Results From a Large Cohort of Patients. *Clin. Chem. Lab Med.* 60, 386–893. doi:10.1515/cclm-2021-0912

Djudjaj, S., and Boor, P. (2019). Cellular and Molecular Mechanisms of Kidney Fibrosis. *Mol. Asp. Med.* 65, 16–36. doi:10.1016/j.mam.2018.06.002

Dongre, A., and Weinberg, R. A. (2019). New Insights into the Mechanisms of Epithelial-Mesenchymal Transition and Implications for Cancer. *Nat. Rev. Mol. Cell Biol.* 20, 69–84. doi:10.1038/s41580-018-0080-4

Elsherbiny, N. M., Said, E., Atef, H., and Zaitone, S. A. (2020). Renoprotective Effect of Calycosin in High Fat Diet-Fed/STZ Injected Rats: Effect on IL-33/ST2 Signaling, Oxidative Stress and Fibrosis Suppression. *Chem. Biol. Interact.* 315, 108897. doi:10.1016/j.cbi.2019.108897

Hara, A., Sakamoto, N., Ishimatsu, Y., Kakugawa, T., Nakashima, S., Hara, S., et al. (2012). S100A9 in BALF Is a Candidate Biomarker of Idiopathic Pulmonary Fibrosis. *Respir. Med.* 106, 571–580. doi:10.1016/j.rmed.2011.12.010

Hayes, J. D., Flanagan, J. U., and Jowsey, I. R. (2005). Glutathione Transferases. *Annu. Rev. Pharmacol. Toxicol.* 45, 51–88. doi:10.1146/annurev.pharmtox.45.120403.095857

Hodson, E. M., Sinha, A., and Cooper, T. E. (2022). Interventions for Focal Segmental Glomerulosclerosis in Adults. *Cochrane Database Syst. Rev.* 2, CD003233. doi:10.1002/14651858.CD003233.pub3

Hong, O. K., Lee, S. S., Yoo, S. J., Lee, M. K., Kim, M. K., Baek, K. H., et al. (2020). Gemigliptin Inhibits Interleukin-1β-Induced Endothelial-Mesenchymal Transition via Canonical-Bone Morphogenetic Protein Pathway. *Endocrinol. Metab. Seoul.* 35, 384–395. doi:10.3803/EnM.2020.35.2.384

Hopkins, A. L. (2007). Network Pharmacology. *Nat. Biotechnol.* 25, 1110–1111. doi:10.1038/nbt1007-1110

Hopkins, A. L. (2008). Network Pharmacology: The Next Paradigm in Drug Discovery. *Nat. Chem. Biol.* 4, 682–690. doi:10.1038/nchembio.118

Ji, Y., Dou, Y. N., Zhao, Q. W., Zhang, J. Z., Yang, Y., Wang, T., et al. (2016). Paeoniflorin Suppresses TGF-β Mediated Epithelial-Mesenchymal Transition in Pulmonary Fibrosis through a Smad-Dependent Pathway. *Acta Pharmacol. Sin.* 37, 794–804. doi:10.1038/aps.2016.36

Kopp, J. B. (2018). Global Glomerulosclerosis in Primary Nephrotic Syndrome: Including Age as a Variable to Predict Renal Outcomes. *Kidney Int.* 93, 1043–1044. doi:10.1016/j.kint.2018.01.020

Li, D. Y. (2018). *Nei-Wai-Shang-Han-Bian-Huo-Lun*. Beijing: China Medical Science Press, 24p.

Li, J., Wang, L., Tan, R., Zhao, S., Zhong, X., and Wang, L. (2020). Nodakenin Alleviated Obstructive Nephropathy through Blunting Snail1 Induced Fibrosis. *J. Cell Mol. Med.* 24, 9752–9763. doi:10.1111/jcmm.15539

Li, X., Chen, W., Huang, L., Zhu, M., Zhang, H., Si, Y., et al. (2022). Sinomenine Hydrochloride Suppresses the Stemness of Breast Cancer Stem Cells by Inhibiting Wnt Signaling Pathway through Down-Regulation of WNT10B. *Pharmacol. Res.* 179, 106222. doi:10.1016/j.phrs.2022.106222

Liu, X., Ouyang, S., Yu, B., Liu, Y., Huang, K., Gong, J., et al. (2010). PharmMapper Server: A Web Server for Potential Drug Target Identification Using Pharmacophore Mapping Approach. *Nucleic Acids Res.* 38, W609–W614. doi:10.1093/nar/gkq300

Liu, Y. (2011). Cellular and Molecular Mechanisms of Renal Fibrosis. *Nat. Rev. Nephrol.* 7, 684–696. doi:10.1038/nrneph.2011.149

Liu, Y. (2006). Renal Fibrosis: New Insights into the Pathogenesis and Therapeutics. *Kidney Int.* 69, 213–217. doi:10.1038/sj.ki.5000054

Mack, M., and Yanagita, M. (2015). Origin of Myofibroblasts and Cellular Events Triggering Fibrosis. *Kidney Int.* 87, 297–307. doi:10.1038/ki.2014.287

Miao, J., Liu, J., Niu, J., Zhang, Y., Shen, W., Luo, C., et al. (2019). Wnt/β-Catenin/RAS Signaling Mediates Age-Related Renal Fibrosis and is Associated with Mitochondrial Dysfunction. *Aging Cell* 18, e13004. doi:10.1111/acel.13004

Niu, X., Zhang, J., Ni, J., Wang, R., Zhang, W., Sun, S., et al. (2018). Network Pharmacology-Based Identification of Major Component of Angelica Sinensis and its Action Mechanism for the Treatment of Acute Myocardial Infarction. *Biosci. Rep.* 38 (6), BSR20180519. doi:10.1042/BSR20180519

Qiao, J., Liu, Y., Jiang, Z., Yang, Y., Liu, W., and Han, B. (2018). Preparation and Renoprotective Effects of Carboxymethyl Chitosan Oligosaccharide on Adriamycin Nephropathy. *Carbohydr. Polym.* 201, 347–356. doi:10.1016/j.carbpol.2018.06.109

Reichold, M., Klootwijk, E. D., Reinders, J., Otto, E. A., Milani, M., Broeker, C., et al. (2018). Glycine Amidinotransferase (GATM), Renal Fanconi Syndrome, and Kidney Failure. *J. Am. Soc. Nephrol.* 29, 1849–1858. doi:10.1681/ASN.2017111179

Ru, J., Li, P., Wang, J., Zhou, W., Li, B., Huang, C., et al. (2014). TCMSP: A Database of Systems Pharmacology for Drug Discovery from Herbal Medicines. *J. Cheminform* 6, 13. doi:10.1186/1758-2946-6-13

Shannon, P., Markiel, A., Ozier, O., Baliga, N. S., Wang, J. T., Ramage, D., et al. (2003). Cytoscape: A Software Environment for Integrated Models of Biomolecular Interaction Networks. *Genome Res.* 13, 2498–2504. doi:10.1101/gr.1239303

Shen, Y. L., Jiang, Y. P., Li, X. Q., Wang, S. J., Ma, M. H., Zhang, C. Y., et al. (2019). ErHuang Formula Improves Renal Fibrosis in Diabetic Nephropathy Rats by Inhibiting CXCL6/JAK/STAT3 Signaling Pathway. *Front. Pharmacol.* 10, 1596. doi:10.3389/fphar.2019.01596

Shen, Y. L., Wang, S. J., Rahman, K., Zhang, L. J., and Zhang, H. (2018). Chinese Herbal Formulas and Renal Fibrosis: An Overview. *Curr. Pharm. Des.* 24, 2774–2781. doi:10.2174/1381612824666180829103355

Simone, S., Cosola, C., Loverre, A., Cariello, M., Sallustio, F., Rascio, F., et al. (2012). BMP-2 Induces a Profibrotic Phenotype in Adult Renal Progenitor Cells through Nox4 Activation. *Am. J. Physiol. Ren. Physiol.* 303, F23–F34. doi:10.1152/ajprenal.00328.2011

Su, Z., Zong, P., Chen, J., Yang, S., Shen, Y., Lu, Y., et al. (2020). Celastrol Attenuates Arterial and Valvular Calcification via Inhibiting BMP2/Smad1/5 Signalling. *J. Cell Mol. Med.* 24, 12476–12490. doi:10.1111/jcmm.15779

Wang, S., Sun, A., Li, L., Zhao, G., Jia, J., Wang, K., et al. (2012). Up-Regulation of BMP-2 Antagonizes TGF-β1/ROCK-Enhanced Cardiac Fibrotic Signalling through Activation of Smurf1/Smad6 Complex. *J. Cell Mol. Med.* 16, 2301–2310. doi:10.1111/j.1582-4934.2012.01538.x

Wang, Y., Wang, Y. P., Tay, Y. C., and Harris, D. C. (2000). Progressive Adriamycin Nephropathy in Mice: Sequence of Histologic and Immunohistochemical Events. *Kidney Int.* 58, 1797–1804. doi:10.1046/j.1523-1755.2000.00342.x

Wang, Y., and Wu, X. (2018). SMOC1 Silencing Suppresses the Angiotensin II-Induced Myocardial Fibrosis of Mouse Myocardial Fibroblasts via Affecting the BMP2/Smad Pathway. *Oncol. Lett.* 16, 2903–2910. doi:10.3892/ol.2018.8989

Wharram, B. L., Goyal, M., Wiggins, J. E., Sanden, S. K., Hussain, S., Filipiak, W. E., et al. (2005). Podocyte Depletion Causes Glomerulosclerosis: Diphtheria Toxin-Induced Podocyte Depletion in Rats Expressing Human Diphtheria Toxin Receptor Transgene. *J. Am. Soc. Nephrol.* 16, 2941–2952. doi:10.1681/ASN.2005010055

Wu, X. M., Gao, Y. B., Xu, L. P., Zou, D. W., Zhu, Z. Y., Wang, X. L., et al. (2017). Tongxinluo Inhibits Renal Fibrosis in Diabetic Nephropathy: Involvement of the Suppression of Intercellular Transfer of TGF-[Formula: See Text]1-Containing Exosomes from GECs to GMCs. *Am. J. Chin. Med.* 45, 1075–1092. doi:10.1142/S0192415X17500586

Xiao, Y., Liu, J., Peng, Y., Xiong, X., Huang, L., Yang, H., et al. (2016). GSTA3 Attenuates Renal Interstitial Fibrosis by Inhibiting TGF-Beta-Induced Tubular Epithelial-Mesenchymal Transition and Fibronectin Expression. *PLoS One* 11, e0160855. doi:10.1371/journal.pone.0160855

Xiao, Y., Zhang, Z., Fu, Y., Shan, H., Cui, S., and Wu, J. (2019). GSTA3 Regulates TGF-β1-Induced Renal Interstitial Fibrosis in NRK-52E Cells as a Component of the PI3K-Keap1/Nrf2 Pathway. *J. Int. Med. Res.* 47, 5787–5801. doi:10.1177/0300060519876796

Xu, X., Chen, Z., Zhu, X., Wang, D., Liang, J., Zhao, C., et al. (2018). S100A9 Aggravates Bleomycin-Induced Dermal Fibrosis in Mice via Activation of ERK1/2 MAPK and NF-κB Pathways. *Iran. J. Basic Med. Sci.* 21, 194–201. doi:10.22038/IJBMS.2018.19987.5255

Xu, X., Zhang, W., Huang, C., Li, Y., Yu, H., Wang, Y., et al. (2012). A Novel Chemometric Method for the Prediction of Human Oral Bioavailability. *Int. J. Mol. Sci.* 13, 6964–6982. doi:10.3390/ijms13066964

Yabluchanskiy, A., Ma, Y., Iyer, R. P., Hall, M. E., and Lindsey, M. L. (2013). Matrix Metalloproteinase-9: Many Shades of Function in Cardiovascular Disease. *Physiol. (Bethesda)* 28, 391–403. doi:10.1152/physiol.00029.2013

Yamashita, M., Utsumi, Y., Nagashima, H., Nitanai, H., and Yamauchi, K. (2021). S100A9/CD163 Expression Profiles in Classical Monocytes as Biomarkers to Discriminate Idiopathic Pulmonary Fibrosis from Idiopathic Nonspecific Interstitial Pneumonia. *Sci. Rep.* 11, 12135. doi:10.1038/s41598-021-91407-9

Yang, Q., Ren, G. L., Wei, B., Jin, J., Huang, X. R., Shao, W., et al. (2019). Conditional Knockout of TGF-βRII/Smad2 Signals Protects against Acute Renal Injury by Alleviating Cell Necroptosis, Apoptosis and Inflammation. *Theranostics* 9, 8277–8293. doi:10.7150/thno.35686

Yang, Y. L., Ju, H. Z., Liu, S. F., Lee, T. C., Shih, Y. W., Chuang, L. Y., et al. (2011). BMP-2 Suppresses Renal Interstitial Fibrosis by Regulating Epithelial-Mesenchymal Transition. *J. Cell Biochem.* 112, 2558–2565. doi:10.1002/jcb.23180

Yang, Y. L., Liu, Y. S., Chuang, L. Y., Guh, J. Y., Lee, T. C., Liao, T. N., et al. (2009). Bone Morphogenetic Protein-2 Antagonizes Renal Interstitial Fibrosis by Promoting Catabolism of Type I Transforming Growth Factor-Beta Receptors. *Endocrinology* 150, 727–740. doi:10.1210/en.2008-0090

Yang, Z., Li, J., Xiong, F., Huang, J., Chen, C., Liu, P., et al. (2016). Berberine Attenuates High Glucose-Induced Fibrosis by Activating the G Protein-Coupled Bile Acid Receptor TGR5 and Repressing the S1P2/MAPK Signaling Pathway in Glomerular Mesangial Cells. *Exp. Cell Res.* 346, 241–247. doi:10.1016/j.yexcr.2016.06.005

You, R., Zhou, W., Li, Y., Zhang, Y., Huang, S., Jia, Z., et al. (2020). Inhibition of ROCK2 Alleviates Renal Fibrosis and the Metabolic Disorders in the Proximal Tubular Epithelial Cells. *Clin. Sci. (Lond)* 134, 1357–1376. doi:10.1042/CS20200030

Yu, B., Li, H., Chen, J., He, Z., Sun, H., Yang, G., et al. (2020). Extensively Expanded Murine-Induced Hepatic Stem Cells Maintain High-Efficient Hepatic Differentiation Potential for Repopulation of Injured Livers. *Liver Int.* 40, 2293–2304. doi:10.1111/liv.14509

Yu, C., Xiong, C., Tang, J., Hou, X., Liu, N., Bayliss, G., et al. (2021). Histone Demethylase JMJD3 Protects against Renal Fibrosis by Suppressing TGFβ and Notch Signaling and Preserving PTEN Expression. *Theranostics* 11, 2706–2721. doi:10.7150/thno.48679

Yu, G., Wang, L. G., Han, Y., and He, Q. Y. (2012). clusterProfiler: An R Package for Comparing Biological Themes Among Gene Clusters. *OMICS* 16, 284–287. doi:10.1089/omi.2011.0118

Zeng, J., Dou, Y., Guo, J., Wu, X., and Dai, Y. (2013). Paeoniflorin of Paeonia Lactiflora Prevents Renal Interstitial Fibrosis Induced by Unilateral Ureteral Obstruction in Mice. *Phytomedicine* 20, 753–759. doi:10.1016/j.phymed.2013.02.010

Zhang, Y., Zhang, L., Zhang, Y., Xu, J. J., Sun, L. L., and Li, S. Z. (2016). The Protective Role of Liquiritin in High Fructose-Induced Myocardial Fibrosis via Inhibiting NF-κB and MAPK Signaling Pathway. *Biomed. Pharmacother.* 84, 1337–1349. doi:10.1016/j.biopha.2016.10.036

Zhao, J., Chan, Y. C., He, B., Duan, T. T., and Yu, Z. L. (2019). A Patent Herbal Drug Yi-Shen-Hua-Shi Granule Ameliorates C-BSA-Induced Chronic Glomerulonephritis and Inhabits TGFβ Signaling in Rats. *J. Ethnopharmacol.* 236, 258–262. doi:10.1016/j.jep.2019.02.044

Zhuang, K., Jiang, X., Liu, R., Ye, C., Wang, Y., Wang, Y., et al. (2020). Formononetin Activates the Nrf2/ARE Signaling Pathway via Sirt1 to Improve Diabetic Renal Fibrosis. *Front. Pharmacol.* 11, 616378. doi:10.3389/fphar.2020.616378

Conflict of Interest: The authors declare that the research was conducted in the absence of any commercial or financial relationships that could be construed as a potential conflict of interest.

Publisher's Note: All claims expressed in this article are solely those of the authors and do not necessarily represent those of their affiliated organizations, or those of the publisher, the editors, and the reviewers. Any product that may be evaluated in this article, or claim that may be made by its manufacturer, is not guaranteed or endorsed by the publisher.

frontiers | Frontiers in Pharmacology

ORIGINAL RESEARCH
published: 23 June 2022
doi: 10.3389/fphar.2022.926211

Metformin Improves the Senescence of Renal Tubular Epithelial Cells in a High-Glucose State Through E2F1

Dan Liang[1,2†], *Zhiyang Li*[1,2†], *Zhaowei Feng*[1,2], *Zhiping Yuan*[3], *Yunli Dai*[1,2], *Xin Wu*[1,2], *Fan Zhang*[1,2], *Yuanyuan Wang*[1,2], *Yuxia Zhou*[1,2], *Lingling Liu*[1,2], *Mingjun Shi*[1,2], *Ying Xiao*[1,2]* *and Bing Guo*[1,2]*

[1]*Guizhou Provincial Key Laboratory of Pathogenesis & Drug Research on Common Chronic Diseases, Guizhou Medical University, Guiyang, China,* [2]*Department of Pathophysiology, Guizhou Medical University, Guiyang, China,* [3]*University Town Hospital, Guizhou Medical University, Guiyang, China*

OPEN ACCESS

Edited by:
Dan-Qian Chen,
Northwest University, China

Reviewed by:
Reza Rahbarghazi,
Tabriz University of Medical Sciences, Iran
Shankar Munusamy,
Drake University, United States

***Correspondence:**
Ying Xiao
xiaoying@gmc.edu.cn
Bing Guo
guobingbs@126.com

[†]*These authors have contributed equally to this work*

Specialty section:
This article was submitted to Renal Pharmacology, a section of the journal Frontiers in Pharmacology

Received: *22 April 2022*
Accepted: *03 June 2022*
Published: *23 June 2022*

Citation:
Liang D, Li Z, Feng Z, Yuan Z, Dai Y, Wu X, Zhang F, Wang Y, Zhou Y, Liu L, Shi M, Xiao Y and Guo B (2022) Metformin Improves the Senescence of Renal Tubular Epithelial Cells in a High-Glucose State Through E2F1. Front. Pharmacol. 13:926211. doi: 10.3389/fphar.2022.926211

Diabetic kidney disease is a major cause of chronic kidney condition and the most common complication of diabetes. The cellular senescence participates in the process of diabetic kidney disease, but the specific mechanism is not yet clear. Cell cycle-related protein E2F transcription factor 1 (E2F1) is a member of the E2F transcription factor family, it plays a key role in cellular damage under HG conditions. In this study, we explored whether metformin improves a high-glucose-induced senescence and fibrosis of renal tubular epithelial cells through cell cycle-related protein E2F1. In the *in vivo* experiments, the recombinant adeno-associated virus (AAV-shE2F1) knockdown *E2F1* gene was injected into the tail vein of 16-weeks-old *db/db* mice for 8 weeks. The 16-week-old *db/db* mice were administered metformin (260 mg/kg/d) continuously for 8 weeks. The normal control group (NC) and diabetic model group (DM) were set up simultaneously. Mice renal tubular epithelial cells (mRTECs) were cultured *in vitro*. The cells were randomly divided into the following groups: normal glucose (NG, containing 5.5 mmol/L glucose), high glucose group (HG, containing 30 mmol/L glucose), NG/HG metformin intervention group (NG/HG + Met), NG/HG negative control siRNA transfection group (NG/HG + Control), NG/HG E2F1 siRNA transfection group (NG/HG + siRNA E2F1), HG metformin intervention and overexpression E2F1 plasmid transfection group (HG + Met + overexpress-E2F1). The expression of related indexes were detected by Western blot, real-time polymerase chain reaction (PCR), immunohistochemistry, and immunofluorescence. The results showed that E2F1 knockdown or metformin reduces the degree of renal fibrosis, DNA damage, and cellular senescence in the DM group; metformin also reduced the expression of E2F1. If E2F1 was overexpressed, the effects of metformin in delaying fibrosis and reducing DNA damage and cellular senescence could be weakened. Thus, metformin alleviates high-glucose-induced senescence and fibrosis of renal tubular epithelial cells by downregulating the expression of E2F1.

Keywords: metformin, diabetic kidney disease, DNA damage, renal tubular epithelial cells, fibrosis, E2F1

INTRODUCTION

Aging leads to physiological senescence in an organism, followed by various diseases that further facilitate cellular senescence. The senescent cells accumulate and damage various tissues and organs (Kirkland and Tchkonia, 2017), thus causing loss of function of the body. The production of senescent cells can be triggered by a variety of diseases, such as atherosclerosis, diabetes (Childs et al., 2015), osteoarthritis, and glaucoma (Calcinotto et al., 2019). If these senescent cells are not eliminated promptly, it would further affect the progression of the disease. Obesity and age are the major factors endangering type 2 diabetes, and both increase the burden of cells and promote cellular senescence (Palmer et al., 2019). Especially, obesity increases the level of senescence-associated markers, such as senescence-associated β-galactosidase (SA-β-Gal) activity and the production of senescence-associated secretory phenotype (SASP), such as proinflammatory cytokines interleukin-6 (IL-6) and tumor necrosis factor-α (TNF-α); the level of these inflammatory cytokines accelerate the senescence of neighboring cells (Burton and Faragher, 2018). The study demonstrated that hyperglycemia in type 1 and 2 diabetes models increases the DNA damage response and compromises the DNA repair that results in aging, increased inflammatory phenotype, and renal fibrosis (Kumar et al., 2020). Diabetic kidney disease (DKD) is a severe complication of diabetes mellitus (DM). The typical features of DKD are the thickening of the glomerular basement membrane, the extracellular matrix (ECM) alteration, and renal tubulointerstitial fibrosis (Bhxa et al., 2020). In recent years, the role of cellular senescence in DKD has gained increasing attention. Hyperglycemia accelerates the aging of glomerular mesangial cells and renal tubular epithelial cells and induces the secretion of SASP components, thus promoting inflammation and cellular senescence (Xiong and Zhou, 2019). Since the mechanisms of cellular senescence are complex, exploring its role in DKD would provide critical clues for treatment.

Metformin is a cost-effective and highly safe biguanide derivative widely used in cancer, cardiovascular disease, and kidney disease. It is one of the most commonly used drugs for the treatment of type 2 diabetes (Lv and Guo, 2020). Under the condition of high glucose, the survival rate of human umbilical vein endothelial cells decreased, and oxidative stress and chromosomal abnormalities occurred, indicating that diabetes hyperglycemia can interfere with the biochemical or biophysical properties of endothelial cells (Rezabakhsh et al., 2017). Moreover, high glucose also significantly reduced the viability of human umbilical vein endothelial cells and inhibited cell migration, while metformin significantly improved these characteristics, and promoted the angiogenic potential of endothelial cells, regulated the dynamics of endothelial cells under high glucose conditions, and improved the development of diabetic foot ulcers (Zolali et al., 2019). Furthermore, metformin alleviates the development of DKD by inhibiting the deposition of ECM and inflammation of glomerular mesangial cells by regulating the H19/miR-143-3p/TGF-β1 signaling pathway (Xu et al., 2020). It also reduces the production of oxidative stress during DKD through AMPK/SIRT1-FoxO1 pathway, enhances the autophagy response in the early stage of DKD, and reduces renal tubulointerstitial fibrosis (Ren et al., 2019; Wang et al., 2021). Metformin also exerts effects on diabetic retinopathy, aging, and cancer through mechanisms beyond nonapoptotic cell death, immunosuppression, and AMPK pathways (Hsu et al., 2021). In addition, metformin has a regulatory role in the renal aging process of DKD and delays the progress of DKD by reducing cellular senescence. Also, an active role is effectuated in high-glucose-induced renal tubular epithelial cells and *db/db* mice model through the MBNL1/miR-130a-3p/STAT3 pathway (Jiang et al., 2020). Metformin also reduces the loss of podocytes, mesangial cell apoptosis, and renal tubular epithelial cell senescence through the AMPK signal transduction pathway and exerts a renal protective role in DKD (Song et al., 2021). The anti-inflammatory and anti-fibrosis mechanisms of metformin and alleviation of cellular senescence in DKD are yet to be elucidated. Therefore, exploring the potential mechanism between metformin, DKD, and cellular senescence underlying the progression of DKD development is imperative.

Cell cycle-related protein E2F1 is a member of the E2F transcription factor family. It is involved in several biological processes, such as DNA damage response, cell migration and invasion, differentiation, metabolism, and cell cycle regulation (Roworth et al., 2015; Liang et al., 2016). E2F1 leads to hyperlipidemia and hyperglycemia in DM. Thus, inhibiting E2F1 activity prevents the hyperglycemia caused by obesity (Giralt et al., 2018). In the case of high glucose, the knockout of *E2F1* gene can save high-glucose-induced neuronal cell death (Wang et al., 2017). In addition, the regulatory effect of E2F1 on the cell cycle suggested a regulatory effect of E2F1 on cellular senescence. Moreover, P21 and P16, potent inhibitors of cell cycle-dependent kinase (CDK), blocked the phosphorylation of CDK-dependent retinoblastoma (RB) phosphorylation, leading to E2F1 inhibition and cell cycle arrest (Dick and Rubin, 2013). In addition, the overexpression of E2F1 induces senescence of normal cells (Xie et al., 2014). However, in human cancer cells, the expression of senescence markers increased after transfection with a small interference RNA (siRNA) to knock down the expression of E2F1 (Park et al., 2006). Together, these studies suggested that the regulation of E2F1 on cellular senescence is complex and unknown, and DKD is yet to be investigated.

In this study, we proved that high glucose causes renal tubular epithelial cell senescence by elevating the expression of E2F1, and metformin effectuates anti-fibrosis, reducing DNA damage response and anti-renal tubular epithelial cell aging by downregulating the expression of E2F1.

MATERIALS AND METHODS

DM Mouse Model Groups

A total of 30 specific pathogen-free (SPF) grade male *db/db* mice, 7-week-old, weighing 40 ± 5 g and 10 non-transgenic *db/m* mice with the same background at the same age, weighing 20 ± 5 g were

provided by GemPharmatech Co., Ltd. The batch number is BSK-DB T002407. The 7-week-old *db/m* mice comprised the normal control (NC) group. *db/db* mice were randomly and equally divided into DM group, AAV-shE2F1, and metformin (Met) groups. The mice were fed SPF grade feed, allowed pure water drinking *ad libitum*, and maintained at an appropriate temperature, humidity, and 12 h/day light. The AAV-shE2F1 group was injected the adeno-associated virus carrying the *E2F1* knockdown gene [Obio Technology (Shanghai) Corp. Ltd.] through the tail vein at week 16. The dose for each mouse was 2.4×10^{11} VG·/ml. The Met group was treated with metformin (Sino American Shanghai Squib Pharmaceutical Ltd.) by gavage at a dose of 260 mg/kg/d for 6 days/week and continuously for 8 weeks. All mice ate and drank water normally and were sacrificed at week 24. Mice urine, fasting serum, and kidney tissues were collected for the subsequent studies.

Detection of Biochemical Indexes of Mice

Blood glucose (BG) was measured using the glucose oxidase method. Blood urea nitrogen (BUN) was measured using the urease continuous monitoring method. Serum creatinine (S-CRE) was measured via the oxidase method. Total cholesterol (T-CHO) was measured using the cholesterol oxidase method. Triglyceride (TG) was measured using the phosphoglycerol oxidase method. Urinary microalbumin was measured by enzyme-linked immunosorbent assay (ELISA).

Histopathological Observation of Mice Kidney Tissues

The renal tissue sections were fixed with 4% neutral formaldehyde, embedded in paraffin, and stained with hematoxylin-eosin (HE), periodic acid Schiff (PAS), Masson, and Sirus red after dewaxing. The pathomorphological changes of renal tissue sections in the different groups of mice were observed under an ordinary optical microscope (OLYPUMS, Japan).

Cell Culture, Transfection, and Administration

mRTEC cell line was obtained from Otwo Biotech Inc. (Catalogue No: HTX2460). and cultured in medium (DMEM; Gibco, United States, low glucose, containing 5.5 mmol/L glucose) containing 10% fetal bovine serum (FBS; Biological Industries, Israel) in a constant temperature incubator under 5% CO_2 at 37°C. At 90% confluency, the cells were subcultured and used in subsequent experiments. E2F1 siRNA (Jima, Shanghai) and E2F1 overexpression plasmid (Yi le Biotech, Shanghai) were transfected into mRTECs, respectively. The negative control siRNA was transfected into the normal glucose/high glucose empty group (NG/HG + Control), the E2F1 siRNA was transfected into the normal glucose/high glucose knockdown group (NG/HG + siRNA E2F1). The cells cultured in normal glucose medium (5.5 mmol/L) and high glucose medium (30 mmol/L) containing 10% FBS were plated in a six-well plate for 72 h, followed by whole-protein extraction for subsequent experiments. Cell counting kit-8 (CCK-8; APEXBIO, United States) assay was used to detect the proliferation ability of mRTECs cultured in high-glucose after metformin (MedChemExpress, United States) intervention concentrations 10, 50, 100, and 150 μmol/L. The concentration of 50 μmol/L with maximal proliferation ability was selected for mRTEC intervention. Then, the cells were randomly divided into five groups: normal glucose/high glucose group (NG/HG), normal glucose/high glucose metformin intervention group (NG/HG + Met), high glucose metformin intervention and overexpression E2F1 plasmid transfection group (HG + Met + overexpress-E2F1) and cultured for 72 h for further experimental studies.

Western Blot

Mice renal cortical proteins were extracted and subjected to acrylamide gel electrophoresis. The proteins were detected by incubation with rabbit anti-E2F1 (Abcam, ab112580, 1:1,000), rabbit anti-ATM (Absin, abs131163, 1:1,000), rabbit anti-p-ATM (Absin, abs140239, 1:1,000), rabbit anti-Chk2 (Bioss, bs-1391R, 1:1,000), rabbit anti-p-Chk2 (Bioss, bs-3721R, 1:1,000), rabbit anti-P21 (Proteintech, 10355-1-AP, 1:1,000), rabbit anti-Fibronectin (Abcam, ab2413, 1:1,000), rabbit anti-Collagen III (Proteintech, 22734-1-AP, 1:1,000), and β-actin antibody-horseradish peroxidase (HRP)-conjugated (PMK, PMK058S, 1:5,000) antibodies at 4°C overnight. The next day, the polyvinylidene fluoride (PVDF; Millipore, United States) membranes were incubated with secondary antibodies at room temperature for 1 h and visualized by Smart-ECL (Beyotime Biotechnology, Shanghai) chemiluminescence solution, and the immunoreactive bands were analyzed quantitatively by Image J software.

Real-Time Polymerase Chain Reaction

Total RNA was extracted from mice renal cortex using TRIzol reagent (Ambion, Thermo, United States) and reverse transcribed into complementary DNA (cDNA). *E2F1*, *P21*, *Fibronectin*, and β-*actin* were amplified using cDNA as the template, with β-actin as an internal reference. The relative expression of *E2F1*, *P21*, and *Fibronectin* mRNA was calculated with the $2^{-\Delta\Delta Ct}$ method and analyzed statistically. The primer sequences (Biotech.Co., Ltd.) were as follows: *E2F1*: Forward: 5'-GAGAAGTCGCGCTATGAA ACCTC-3', Reverse: 5'-CCCAGTTCAGGTCAACGACAC-3' (annealing temperature 55.3°C); *P21*: Forward: 5'-TGTCTT GCACTCTGGTGTCTG-3', Reverse: 5'-ATCTGCGCTTGG AGTGATAGA-3' (annealing temperature 55.6°C); *Fibronectin*: Forward: 5'-GTCCATTGAGCTAACCAACCTC-3', Reverse: 5'-GCAGGAGATTTGTTAGGACCAC-3' (annealing temperature 55.8°C); *β-actin*: Forward: 5'-GTCCCTCACCCTCCCAAAAG-3', Reverse: 5'-GCTGCCTCAACACCTCAACCC-3' (annealing temperature 58.5°C).

Immunofluorescence of Kidney Tissue Sections

The tissue sections were dewaxed in doble distilled water (ddH_2O) before the antigen was retrieved by heating in citric

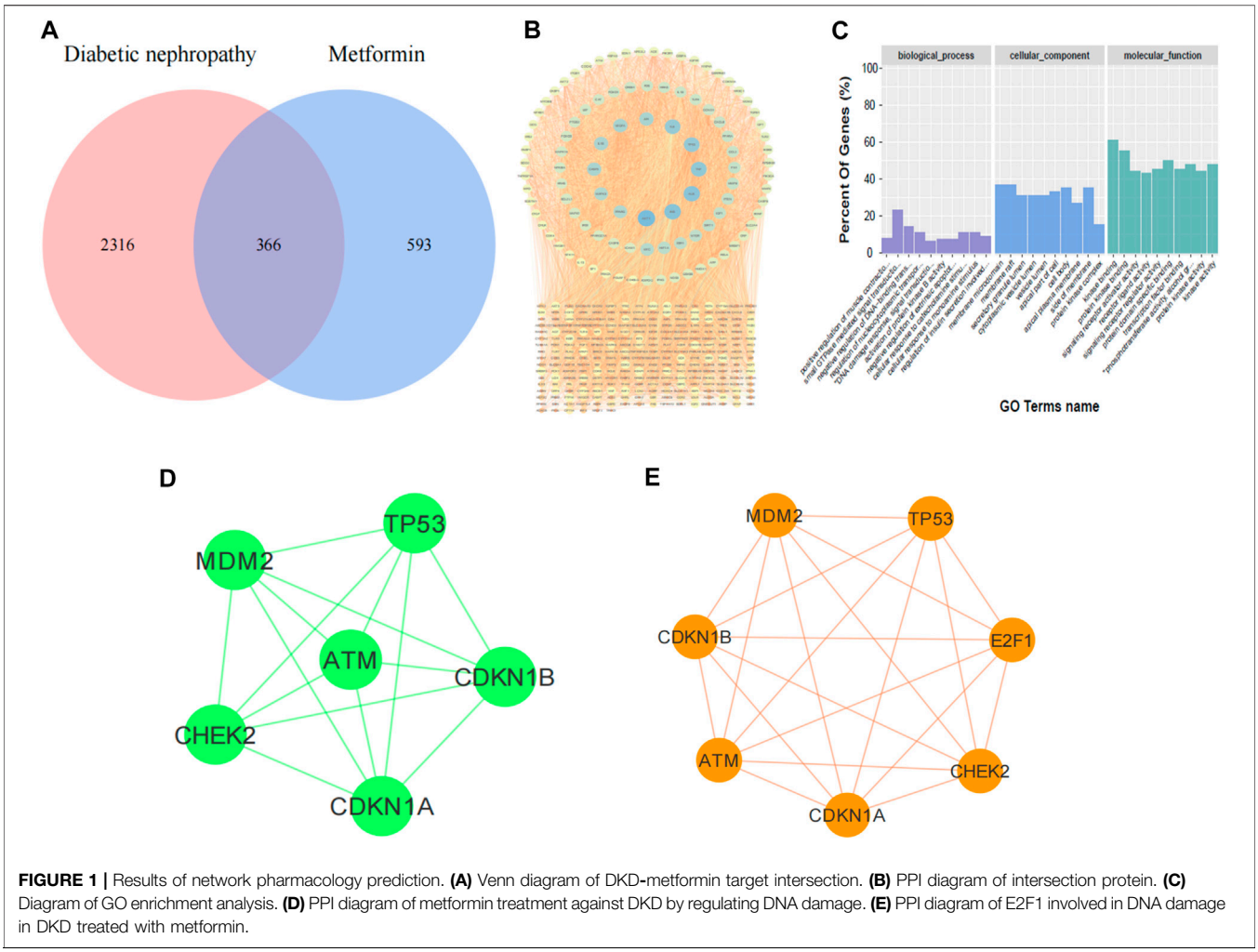

FIGURE 1 | Results of network pharmacology prediction. **(A)** Venn diagram of DKD-metformin target intersection. **(B)** PPI diagram of intersection protein. **(C)** Diagram of GO enrichment analysis. **(D)** PPI diagram of metformin treatment against DKD by regulating DNA damage. **(E)** PPI diagram of E2F1 involved in DNA damage in DKD treated with metformin.

TABLE 1 | Changes in BG, TG, T-CHO, S-CRE, BUN, and urine microalbumin of mice in each group (n = 6,*$p < 0.05$ vs. NC.$^{\#}p < 0.05$ vs. DM).

Group	NC	DM	Met	AAV-shE2F1
BG (mmol/L)	5.57 ± 1.35	23.25 ± 1.85*	13.39 ± 3.94$^{\#}$	16.11 ± 1.72$^{\#}$
TG (mmol/L)	1.09 ± 0.43	1.91 ± 0.44*	1.20 ± 0.20$^{\#}$	1.78 ± 0.32
T-CHO (mmol/L)	1.73 ± 0.64	5.18 ± 0.89*	1.84 ± 0.71$^{\#}$	4.78 ± 0.48
S-CRE (μmol/L)	21.28 ± 3.02	51.49 ± 10.74*	23.06 ± 8.66$^{\#}$	43.84 ± 7.48
BUN (mmol/L)	2.92 ± 0.82	8.68 ± 1.48*	4.43 ± 0.81$^{\#}$	4.66 ± 0.36$^{\#}$
MAU (ng/ml)	8.52 ± 1.79	131.89 ± 17.08*	21.02 ± 2.46$^{\#}$	27.27 ± 5.77$^{\#}$

acid in a microwave oven. Then, the sections were blocked with 3% hydrogen peroxide to remove endogenous catalase, permeabilized with 0.5% Triton X-100, washed with phosphate-buffered saline (PBS), blocked with 5% bovine serum albumin (BSA) at room temperature for 1 h, and incubated with mouse anti-E2F1 antibody (1:50) and mouse anti-P21 antibody (1:50) at 4°C overnight, followed by incubation with Cy3 antibody (1:200) at 37°C in the dark for 1 h. The nucleus was stained with DAPI (Solarbio, Beijing, China), and the tissue sections were sealed with an anti-fluorescence quencher, observed, and photographed under a fluorescence microscope (OLYPUMS, Japan).

Cellular Immunofluorescence

The cells were cultured in six-well plates and divided into groups according to the experiments. After the intervention, the cells were fixed with 4% paraformaldehyde, permeabilized with 0.5% TritonX-100, washed with PBS, and blocked with 10% BSA at 37°C for 30 min. The other steps were the same as those of tissue immunofluorescence.

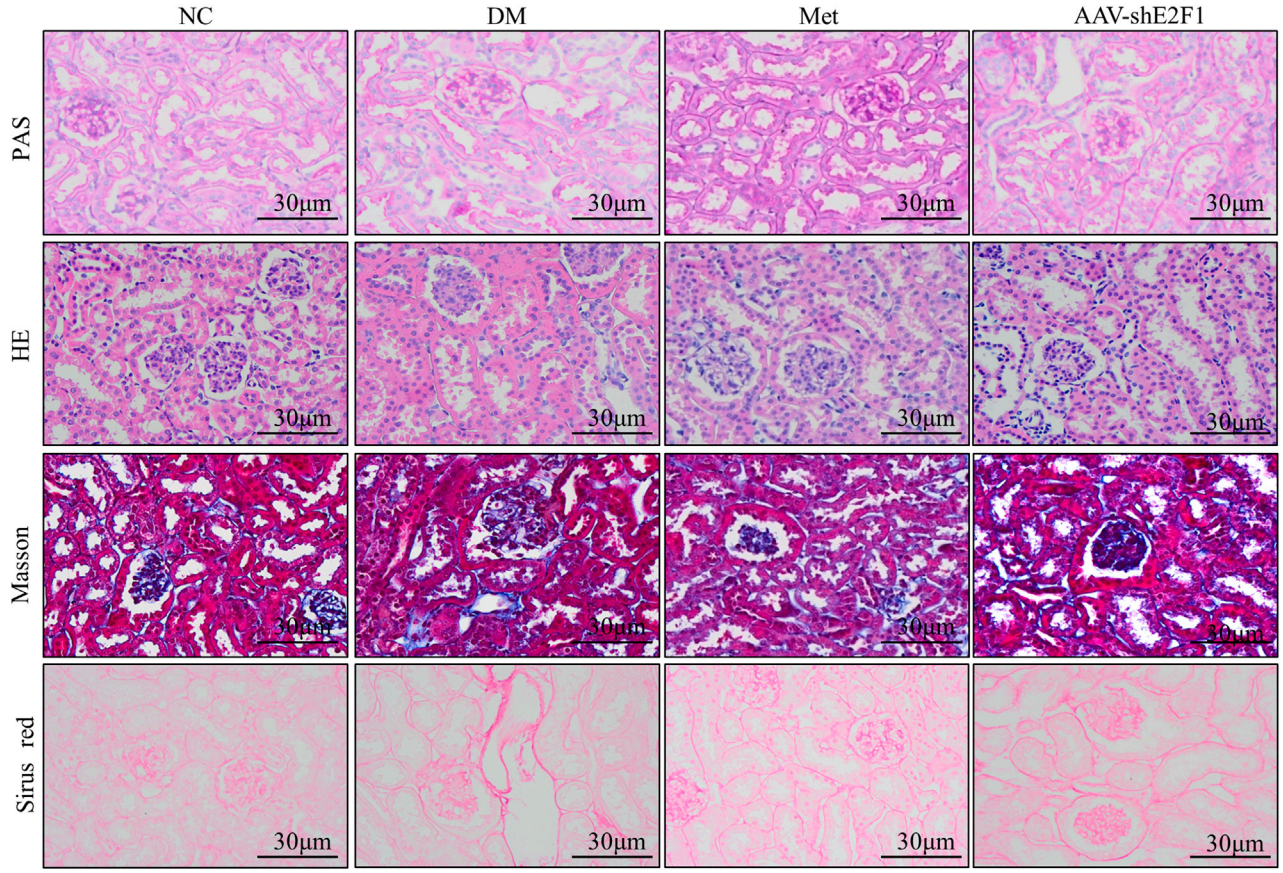

FIGURE 2 | Renal histopathological changes of mice in each group (PAS, HE, Masson, and Sirus red staining).

Immunohistochemistry

The procedure of tissue section dewaxing to hydrogen peroxide blocking was the same as that of tissue immunofluorescence, followed by PBS washes. Then, the sections were incubated with mouse anti-E2F1 antibody (1:50) and rabbit anti-Fibronectin antibodies (1:50) at 4°C overnight, followed by incubation with goat anti-mouse/rabbit IgG-labeled with HRP at room temperature for 20 min. Subsequently, the sections were stained with DAB [Gene Technology (Shanghai) Co., Ltd., GK500705]. The nucleus was stained with hematoxylin, dehydrated, sealed with neutral resin, observed, and photographed under an optical microscope.

β-Galactosidase Staining

The staining procedure was carried out according to the instructions of the kit (Cell Signaling Technology). After sealing, the sections were observed and imaged captured under the optical microscope.

Enzyme-Linked Immunosorbent Assay

The content of TNF-α and IL-6 in mouse tissue supernatant was detected using the Elabscience kit.

Network Pharmacology Analysis

The targets of metformin were obtained through relevant databases. The relevant targets of DKD were screened from the GeneCards database. The Venn diagram program obtained the putative targets of drugs for disease treatment. Metascape platform was used to annotate the intersecting proteins through gene ontology (GO). Protein-protein interaction (PPI) pathways were used to analyze the intersection proteins using the STRING database and Cytoscape software.

Statistical Analysis

The Western blot images were analyzed by Image J software. The experimental data were analyzed by SPSS 25.0 software and expressed as mean ± standard deviation (SD); one-way ANOVA was used for comparison among multiple groups, LSD test was used for comparison between the two groups, $p < 0.05$ indicated a statistically significant difference.

RESULTS

Results of Network Pharmacology

In order to identify the targets of metformin in the treatment of DKD, we retrieved 366 coincident targets of metformin and DKD from the database (**Figure 1A**). These coincident targets are putative targets of metformin in the treatment of DKD. The PPI network diagram was constructed for all proteins at the

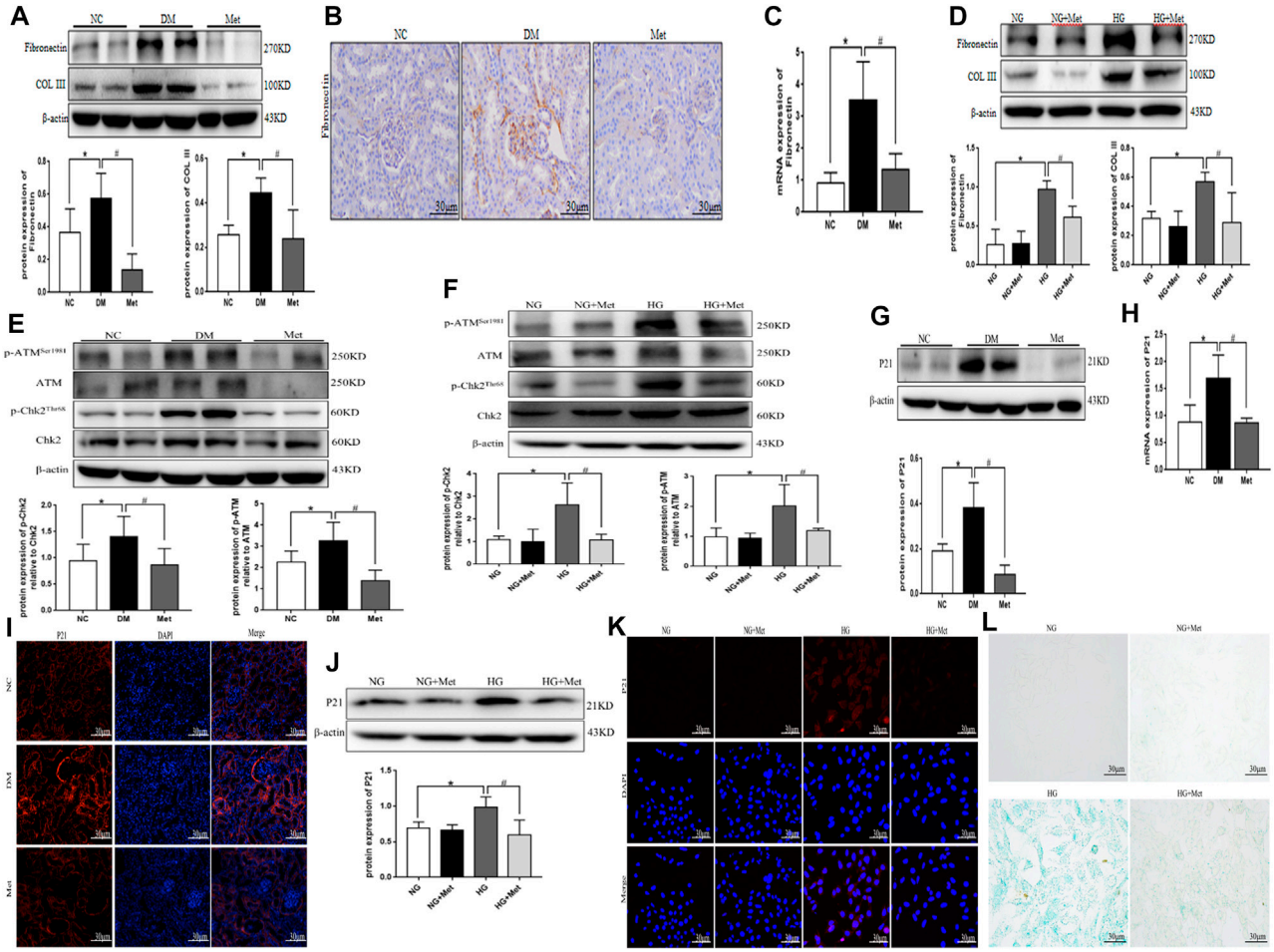

FIGURE 3 | Metformin improves the process of renal fibrosis and the degree of DNA damage and cellular senescence in the high-glucose state. **(A)** Western blot analysis of Fibronectin and COL III in renal cortex of mice in each group (n = 6, $^{*}p < 0.05$ vs. NC, $^{\#}p < 0.05$ vs. DM). **(B)** Immunohistochemical staining of Fibronectin in renal cortex of mice in each group. **(C)** Real-time PCR analysis of Fibronectin in renal cortex of mice in each group (n = 6, $^{*}p < 0.05$ vs. NC, $^{\#}p < 0.05$ vs. DM). **(D)** Western blot analysis of Fibronectin and COL III in mRTECs (n = 3, $^{*}p < 0.05$ vs. NG, $^{\#}p < 0.05$ vs. HG). **(E)** Western blot analysis of ATM, p-ATM^{Ser1981}, Chk2, and p-Chk2^{Thr68} in renal cortex of mice in each group (n = 6, $^{*}p < 0.05$ vs. NC, $^{\#}p < 0.05$ vs. DM). **(F)** Western blot analysis of ATM, p-ATM^{Ser1981}, Chk2, and p-Chk2^{Thr68} in mRTECs (n = 3, $^{*}p < 0.05$ vs. NG, $^{\#}p < 0.05$ vs. HG). **(G)** Western blot analysis of P21 in the renal cortex of mice in each group (n = 6, $^{*}p < 0.05$ vs. NC, $^{\#}p < 0.05$ vs. DM). **(H)** Real-time PCR analysis of P21 in the renal cortex of mice in each group (n = 6, $^{*}p < 0.05$ vs. NC, $^{\#}p < 0.05$ vs. DM). **(I)** Tissue immunofluorescence of P21 in renal cortex of mice in each group. **(J)** Western blot analysis of P21 in mRTECs (n = 3, $^{*}p < 0.05$ vs. NG, $^{\#}p < 0.05$ vs. HG). **(K)** Cellular immunofluorescence of P21 in mRTECs. **(L)** β-Galactosidase staining in mRTECs.

TABLE 2 | Content of IL-6 and TNF-α in the renal tissue supernatant of mice in each group (n = 6,$^{*}p < 0.05$ vs. NC.$^{\#}p < 0.05$ vs. DM).

Group	IL-6	TNF-α
NC	317.58 ± 178.71	228.76 ± 158.99
DM	505.74 ± 151.15*	482.26 ± 206.97*
Met	376.32 ± 71.57#	272.56 ± 126.05#

intersection (**Figure 1B**). The results of the GO enrichment analysis showed that biological processes, such as aging and DNA damage, were involved in identifying the potential targets of metformin in the treatment of DKD (**Figure 1C**). Therefore, the PPI network diagram of this process was constructed separately (**Figure 1D**). The core targets include ATM, Chk2, CDKN1A (P21), CDKN1B, MDM2, and TP53. Finally, the altered expression of P21, ATM, and Chk2 was observed in the subsequent experiments. Then, bioinformatics was utilized to identify the proteins that directly interact with E2F1. These were combined with the network pharmacology prediction targets and E2F1 interaction protein to construct the PPI network diagram (**Figure 1E**). The results showed that E2F1 was directly involved in the process of DNA damage in the treatment of DKD with metformin.

Changes in the Biochemical Indexes of Mice in Each Group

Compared to the NC group, BG, TG, T-CHO, S-CRE, BUN, and urine microalbumin levels were significantly increased in the DM

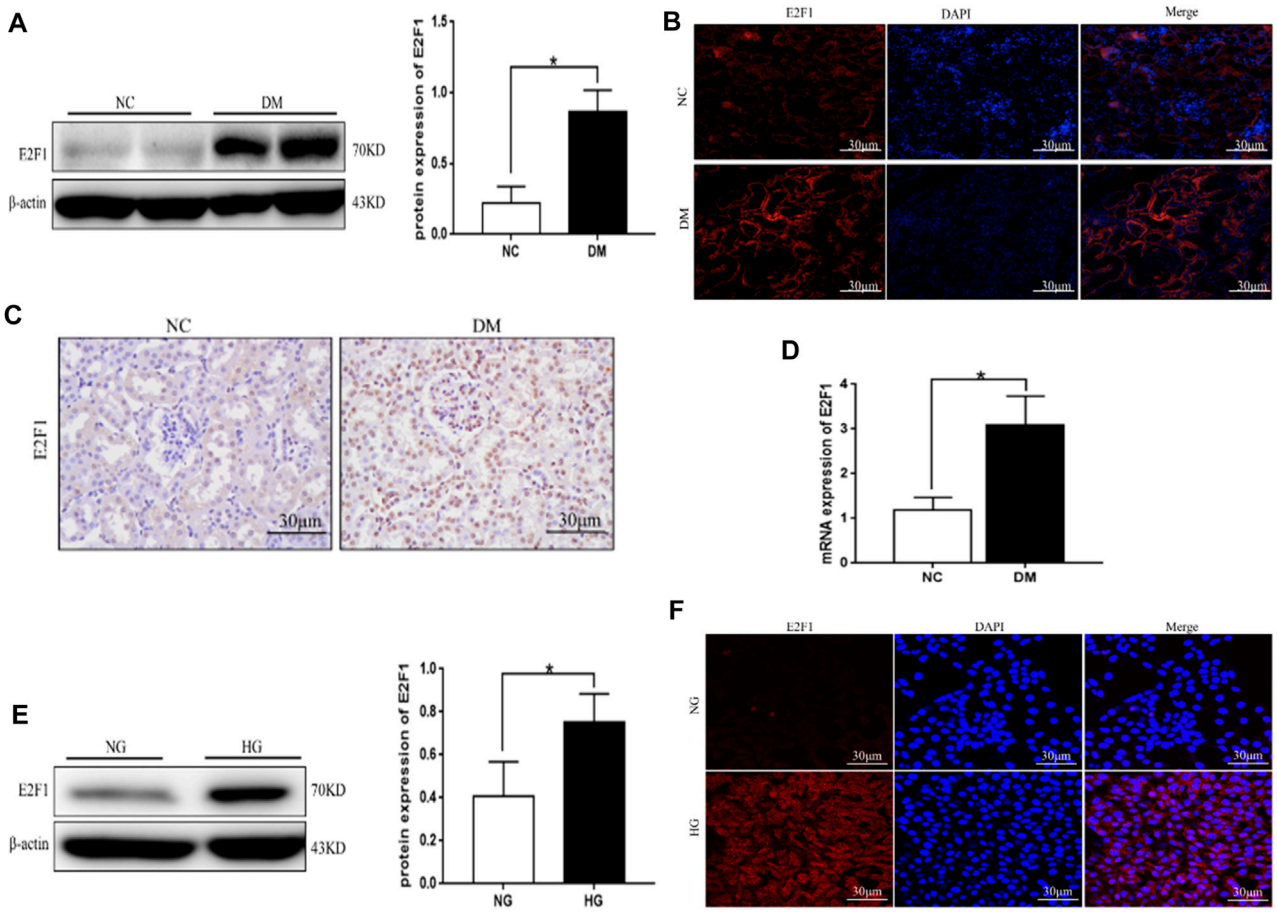

FIGURE 4 | High expression of E2F1 was observed in renal tubular epithelial cells in the high-glucose state. **(A)** Western blot analysis of E2F1 in the renal cortex of mice in each group (n = 6, *p < 0.05 vs. NC). **(B)** Tissue immunofluorescence of E2F1 in the renal cortex of mice in each group. **(C)** Immunohistochemical staining of E2F1 in the renal cortex of mice in each group. **(D)** Real-time PCR analysis of E2F1 in the renal cortex of mice in each group (n = 6, *p < 0.05 vs. NC). **(E)** Western blot analysis of E2F1 in mRTECs (n = 3, *p < 0.05 vs. NG). **(F)** Cellular immunofluorescence of E2F1 in mRTECs.

group. Compared to the DM group, the above indexes in the Met group showed an opposite trend, the levels of BG, BUN, and urine microalbumin were significantly decreased in the AAV-shE2F1 group, the levels of TG, cholesterol-CHO and S-CRE were no significant changes. (p < 0.05; **Table 1**).

Pathomorphological Changes in the Renal Tissue in Each Group

The results of PAS staining showed that the basement membrane of glomerulus and renal tubules was significantly thickened in the DM group compared to the NC group, and the mesangial area was accompanied by cell proliferation. The results of HE staining showed that the glomerulus and renal tubules of the NC group mice had complete structure and regular morphology, while those of the DM group had glomerulosclerosis, renal tubular atrophy, and epithelial cell abscission. Masson and Sirus red staining showed that collagen fibers were deposited in the renal interstitium of the DM group, while the above pathological changes were alleviated in the AAV-shE2F1 and Met groups (**Figure 2**).

Metformin Improves the Process of Renal Fibrosis and the Degree of DNA Damage and Cellular Senescence in the High-Glucose State

Western blot results showed that the protein expression levels of Fibronectin and COL III were significantly higher in the DM group than in the NC group (**Figure 3A**). Immunohistochemical staining and real-time PCR results showed that the protein and mRNA levels of Fibronectin were significantly higher in the DM group than in the NC group (**Figures 3B,C**). After metformin intervention, the expression of the above indexes decreased markedly. Compared to the NG group, the levels of Fibronectin and COL III proteins were significantly higher in the HG group, compared to the HG group, the levels of Fibronectin and COL III proteins were significantly lower in the HG + Met group (**Figure 3D**). The results of Western blot showed that the phosphorylation levels of DNA damage-related indexes ATM and Chk2 were significantly increased *in vitro* and *in vivo* in the

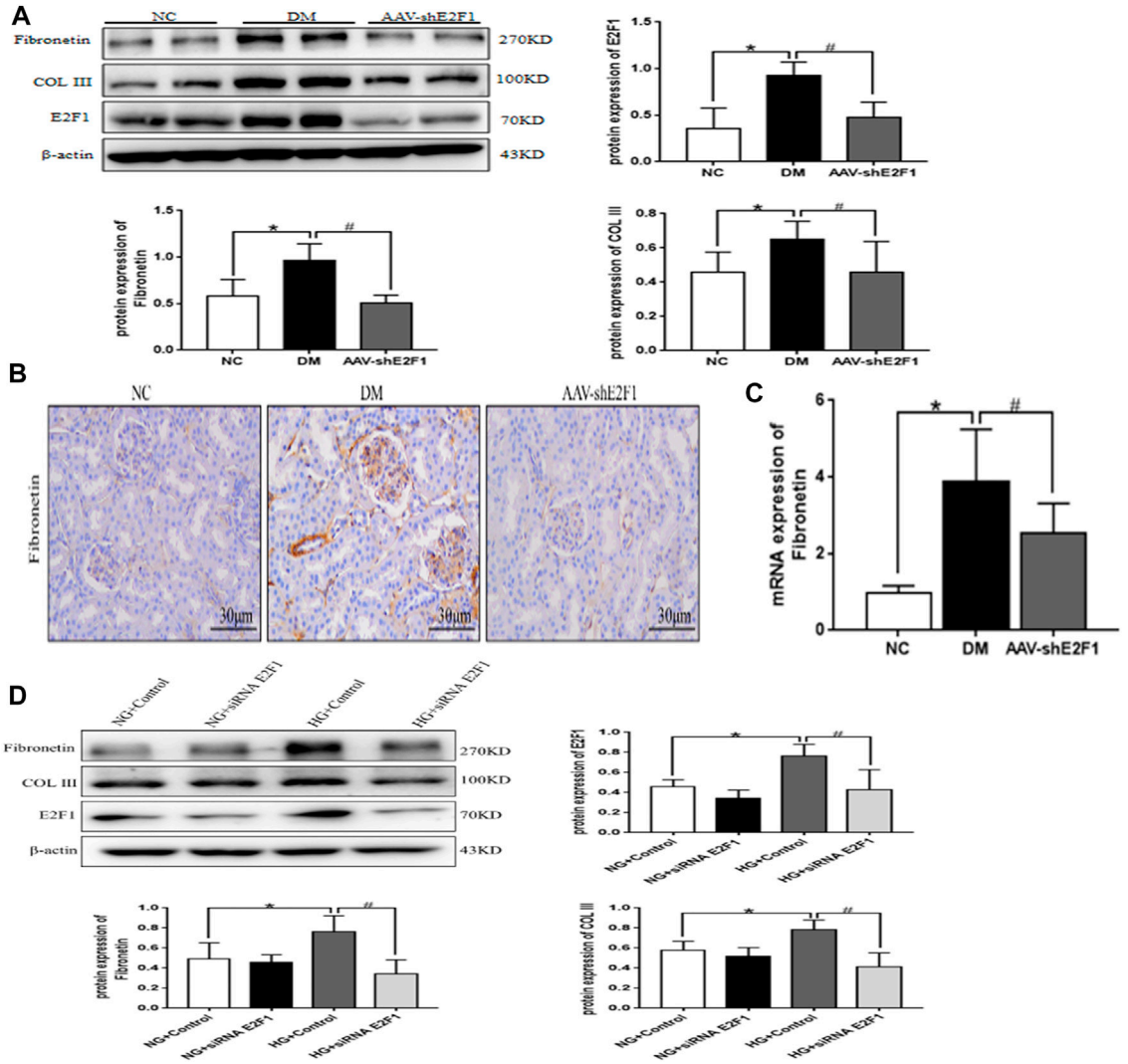

FIGURE 5 | High-expression of E2F1 promotes the fibrosis of renal tubular epithelial cells in the high-glucose state. **(A)** Western blot analysis of E2F1, Fibronectin, and COL III in the renal cortex of mice in each group (n = 6, $^{*}p < 0.05$ vs. NC, $^{\#}p < 0.05$ vs. DM). **(B)** Immunohistochemical staining of Fibronectin in the renal cortex of mice in each group. **(C)** Real-time PCR analysis of Fibronectin in the renal cortex of mice in each group (n = 6, $^{*}p < 0.05$ vs. NC, $^{\#}p < 0.05$ vs. DM). **(D)** Western blot analysis of E2F1, Fibronectin, and COL III in mRTECs (n = 3, $^{*}p < 0.05$ vs. NG + Control, $^{\#}p < 0.05$ vs. HG + Control).

high-glucose environment. The Metformin intervention significantly decreased the expression of the above indexes (**Figures 3E,F**). Western blot, real-time PCR, and tissue immunofluorescence showed that the level of P21 was higher in the DM group than in the NC group (**Figures 3G–I**). According to ELISA, the content of IL-6 and TNF-α was increased markedly in the DM group (**Table 2**), after metformin intervention, the expression of the above indexes decreased markedly. Western blot and cellular immunofluorescence results showed that the expression of P21 was significantly higher in the HG group than the NG group and decreased significantly in the HG + Met group (both $p < 0.05$; **Figures 3J,K**). Interestingly, the β-galactosidase-positive staining was significantly more in the HG group than the NG group but significantly reduced in the HG + Met group (**Figure 3L**). These results suggested that metformin improves the process of renal fibrosis in the high-glucose state, reduces the degree of DNA damage, and delays cellular senescence.

High Expression of E2F1 in Renal Tubular Epithelial Cells in the High-Glucose State

Western blot, tissue immunofluorescence, immunohistochemical staining, and real-time PCR showed significantly higher expression of E2F1 in the DM group than the NC group (**Figures 4A–D**). Western blot and cellular immunofluorescence results showed that the expression of E2F1 was significantly higher in the HG group than in the NG group ($p < 0.05$; **Figures 4E,F**).

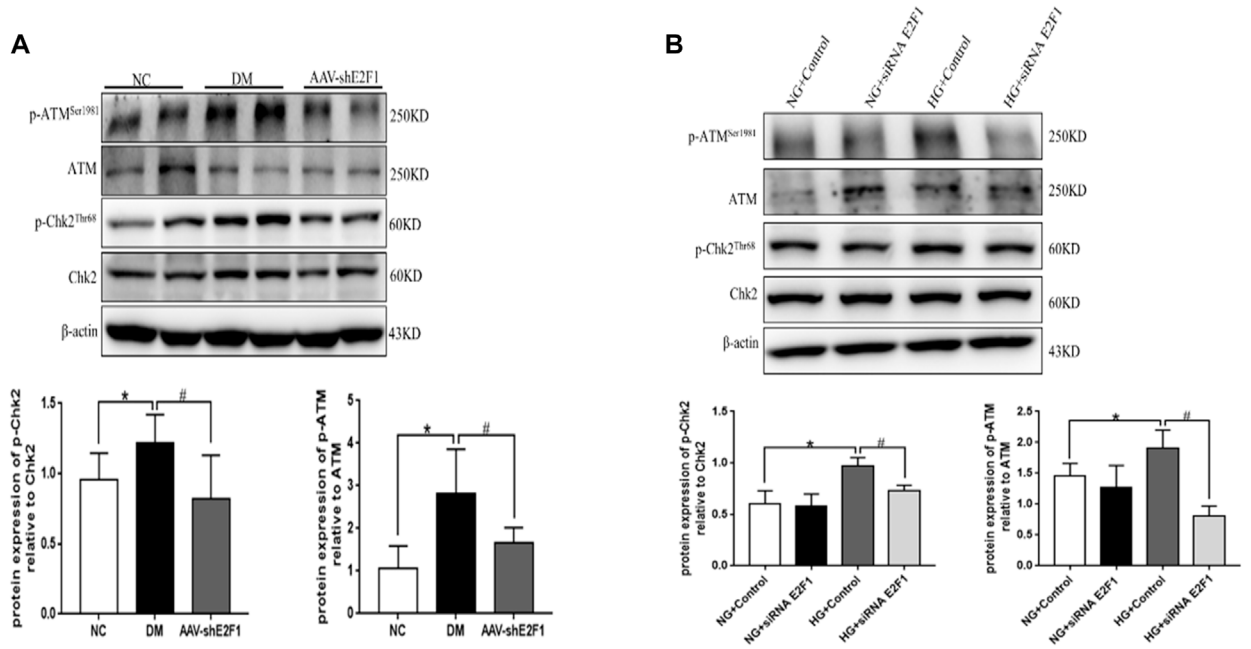

FIGURE 6 | High expression of E2F1 promotes DN damage in renal tubular epithelial cells in the high-glucose state. **(A)** Western blot analysis of ATM, p-ATM^{Ser1981}, Chk2, and p-Chk2^{Thr68} in the renal cortex of mice in each group (n = 6, $^{*}p < 0.05$ vs. NC, $^{\#}p < 0.05$ vs. DM). **(B)** Western blot analysis of ATM, p-ATM^{Ser1981}, Chk2, and p-Chk2^{Thr68} in mRTECs (n = 3, $^{*}p < 0.05$ vs. NG + Control, $^{\#}p < 0.05$ vs. HG + Control).

High Expression of E2F1 Promotes the Fibrosis of Renal Tubular Epithelial Cells in the High-Glucose State

Western blot showed that the levels of Fibronectin and COL III proteins were significantly higher in the DM group than in the NC group (**Figure 5A**). Immunohistochemical staining and real-time PCR revealed that the protein and mRNA levels of Fibronectin were significantly higher in the DM group than those in the NC group (**Figures 5B,C**). However, the expression of the above indexes was significantly decreased in the AAV-shE2F1 group. Compared to the NG + Control and NG + siRNA E2F1 groups. The protein levels of Fibronectin and COL III were significantly higher in the HG group and significantly lower in the HG + siRNA E2F1 group than those in the HG group ($p < 0.05$; **Figure 5D**). Thus, the high expression of E2F1 can promote the fibrosis of renal tubular epithelial cells in the high-glucose state and downregulating the expression can improve the process of fibrosis.

High Expression of E2F1 Promotes the Degree of DNA Damage in Renal Tubular Epithelial Cells in the High-Glucose State

The phosphorylation levels of DNA damage-related indexes, ATM and Chk2, were significantly increased *in vitro* and *in vivo* under the high-glucose environment but reduced after the knockdown of E2F1 ($p < 0.05$; **Figures 6A,B**). This phenomenon suggested that high expression of E2F1 aggravates the DNA damage of renal tubular epithelial cells in the high-glucose state.

High Expression of E2F1 Promotes Cellular Senescence of Renal Tubular Epithelial Cells in the High-Glucose State

Western blot, real-time PCR, and tissue immunofluorescence showed that the expression of P21 was significantly higher in the DM group than the NC group and lower in the AAV-shE2F1 group (**Figures 7A–C**). The results of ELISA revealed that the content of IL-6 and TNF-α was higher in the DM group and significantly lower in the AAV-shE2F1 group than in the NC group (**Table 3**). Compared to the NG + Control and NG + siRNA E2F1 groups, the level of P21 protein was significantly higher in the HG group and significantly lower in the HG + siRNA E2F1 group ($p < 0.05$; **Figure 7D**). This phenomenon suggested that the high expression of E2F1 promotes the senescence of renal tubular epithelial cells in the high-glucose state.

Metformin Improves Renal Injury in the High-Glucose State Through E2F1

Compared to the NG group, the expression of E2F1, Fibronectin, and COL III, the phosphorylation levels of ATM and Chk2, and the expression of P21 was significantly increased in the HG group. After the intervention with metformin, the expression of the above indexes decreased, and the consequent overexpression of E2F1 weakened the effect of metformin on the above indexes in mRTECs (**Figures 8A,B**, $p < 0.05$). Thus, the anti-fibrosis, anti-senescence, and DNA damage repair effects of metformin in the high-glucose state were achieved by downregulating the expression of E2F1.

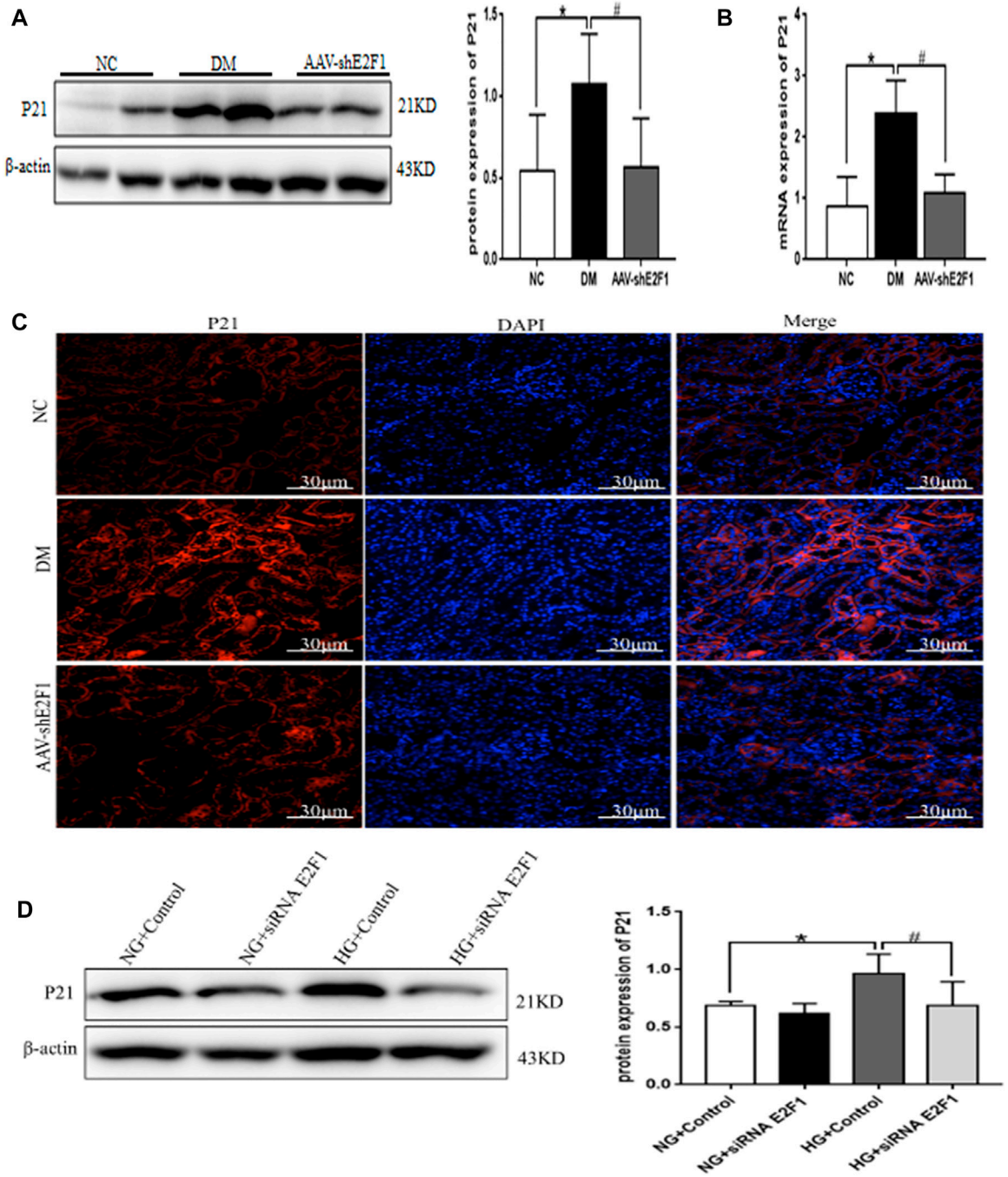

FIGURE 7 | High expression of E2F1 promotes cellular senescence of renal tubular epithelial cells in the high-glucose state. **(A)** Western blot analysis of P21 in the renal cortex of mice in each group (n = 6, $^{*}p < 0.05$ vs. NC, $^{\#}p < 0.05$ vs. DM). **(B)** Real-time PCR analysis of P21 in the renal cortex of mice in each group (n = 6, $^{*}p < 0.05$ vs. NC, $^{\#}p < 0.05$ vs. DM). **(C)** Tissue immunofluorescence of P21 in the renal cortex of mice in each group. **(D)** Western blot analysis of P21 in mRTECs (n = 3, $^{*}p < 0.05$ vs. NG + Control, $^{\#}p < 0.05$ vs. HG + Control).

DISCUSSION

P16 expression and SA-β-Gal activity increased in renal tubular epithelial cells, podocytes, mesangial cells, and endothelial cells in patients with type 2 DKD (Verzola et al., 2008). Also, cellular senescence markers were produced in mesangial cells cultured *in vitro* with high glucose (Zhang et al., 2006) and streptozotocin-induced mice model of type 1 diabetes (Kitada et al., 2014). These results suggested that hyperglycemia is a key driver of cellular senescence and may contribute to DKD progression. Accumulating evidence showed that cellular senescence might be involved in the pathophysiological process of DKD. A large

TABLE 3 | Content of IL-6 and TNF-α in renal tissue supernatant of mice in each group (n = 6,*p < 0.05 vs. NC.$^{\#}p$ < 0.05 vs. DM).

Group	IL-6	TNF-α
NC	303.36 ± 125.87	236.52 ± 150.77
DM	510.29 ± 146.11*	485.83 ± 203.90*
AAV-shE2F1	326.41 ± 66.86$^{\#}$	273.13 ± 81.37$^{\#}$

number of studies reported the putative mechanism of cellular senescence in DKD (Chen et al., 2018; Yi-Chun et al., 2018). However, because the pathogenesis of DKD and cellular senescence is complex, the correlation and regulatory mechanism between DKD and cellular senescence need to be explored further. In the current study, we used *db/db* mice model in the *in vivo* experiments, and the model is a widely used animal model of type 2 DKD. It is a leptin receptor mutation that causes abnormal splicing and adipocyte-derived hormone leptin receptor defects, and the leptin receptor deficiency affects the hypothalamic reaction, which makes the mice appear hyperappetite, obese, hyperlipidemia, and insulin resistant, and the other symptoms are similar to those of patients with type 2 diabetes (Tesch and Lim, 2011). The results of this experiment showed that BG, TG, T-CHO, S-CRE, BUN, and urine microalbumin were significantly increased in *db/db* mice compared to *db/m* mice. HE and PAS staining revealed that the glomerular basement membrane of *db/db* mice was thickened, the mesangial area was accompanied by apparent mesangial cell proliferation, the morphology of renal tubules was irregular, and the epithelial cells of renal tubules were detached. Masson and Sirus red staining showed fibrosis in renal tubulointerstitium. All the above results are consistent with the characteristics of DKD, indicating that type 2 diabetes progressed to DKD in the *db/db* mice model.

Metformin is the most widely used oral hypoglycemic drug, which reduces DKD by inhibiting renal inflammation, oxidative stress, and fibrosis (Kawanami et al., 2020). It also reduces the senescence of renal tubular epithelial cells induced by high glucose, inhibiting high-glucose-induced renal lesions, and plays a renal protective role in DKD (Jiang et al., 2020). Herein, we searched the database to retrieve the putative targets of metformin in the treatment of DKD, involved in aging and DNA damage; the core targets include ATM, CHK2, P21, CDKN1B, MDM2, and TP53. We focused on the altered P21, ATM, and CHK2 expression in renal tubular epithelial cells in the high-glucose state. After 8 weeks of *in vivo* intervention in *db/db* mice, the results showed that metformin reduces BG, TG, T-CHO, S-CRE, BUN, and urinary microalbumin. It could also improve the pathomorphological changes of *db/db* mice. The expression of Fibronectin, COL III, and P21 proteins was decreased in the renal cortex of *db/db* mice, and inhibited the phosphorylation levels of ATM and Chk2, while the content of IL-6 and TNF-α in renal supernatant of *db/db* mice was reduced. This finding suggested that metformin improves the degree of renal tissue fibrosis, inflammation, DNA damage, and cellular senescence in DKD.

E2F1 is involved in cell cycle regulation, apoptosis signal transduction, cell growth, metastasis, autophagy, and other processes (Yuan et al., 2018). The study demonstrated the specific biological function of E2F1 in the progression and related complications of DM. It also promotes hyperlipidemia and hyperglycemia in DM by directly controlling hepatic

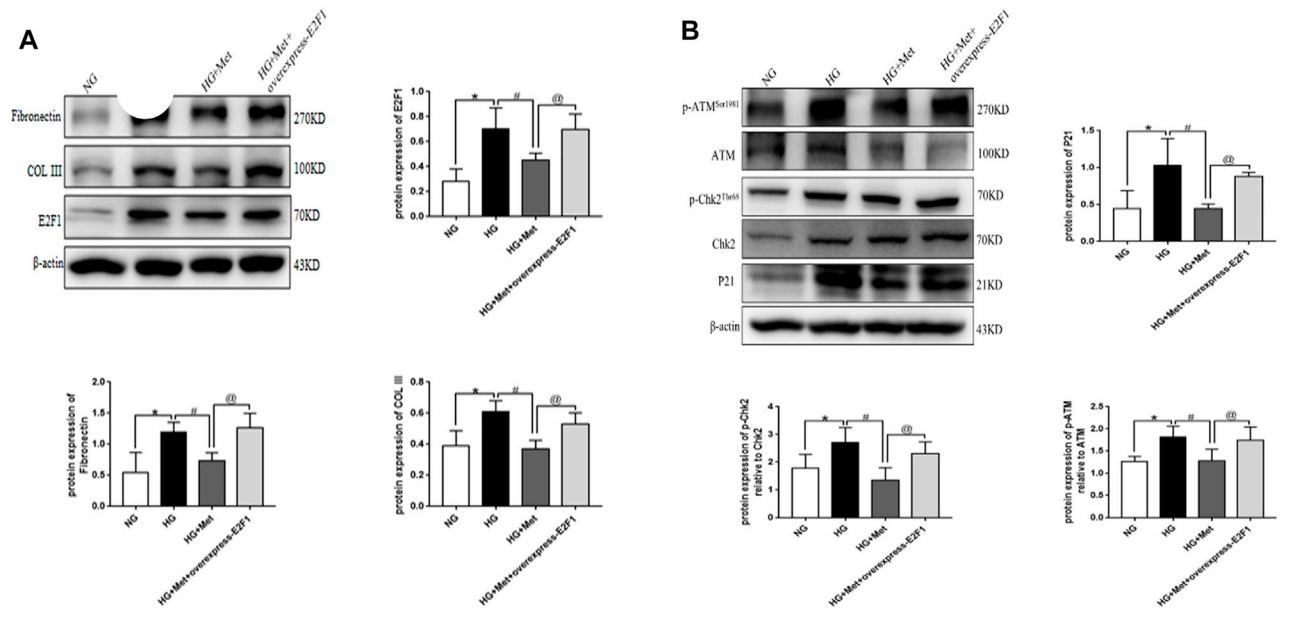

FIGURE 8 | Metformin improves renal injury in the high-glucose state through E2F1. **(A)** Western blot analysis of E2F1, Fibronectin, and COL III in mRTECs (n = 3, *p < 0.05 vs. NG, $^{\#}p$ < 0.05 vs. HG, $^{@}p$ < 0.05 vs. HG + Met). **(B)** Western blot analysis of ATM, p-ATM^{Ser1981}, Chk2, and p-Chk2^{Thr68} in mRTECs (n = 3, *p < 0.05 vs. NG, $^{\#}p$ < 0.05 vs. HG, $^{@}p$ < 0.05 vs. HG + Met).

gluconeogenesis (Giralt et al., 2018). In recent years, the role of E2F1 in cellular senescence has been under intensive focus (Gao et al., 2019). So what is the role of E2F1 in the cellular senescence in DKD? Thus, we used bioinformatics to identify the proteins acting directly with E2F1. The results suggested that E2F1 is directly involved in DNA damage and cellular senescence with respect to the treatment of DKD with metformin. Hence, we injected the adeno-associated virus carrying the *E2F1* knockdown gene into *db/db* mice through the tail vein; animals were sacrificed after 8 weeks. Consequently, the levels of BG, BUN, and urinary microalbumin of adeno-associated virus mice injected with knockdown *E2F1* gene were significantly lower than those of *db/db* mice, the levels of TG, cholesterol-CHO and S-CRE were no significant changes. Moreover, the pathological morphology was improved, and the indexes related to fibrosis, DNA damage, and cellular senescence were reduced, while the levels of IL-6 and TNF-α were significantly reduced in the supernatant of renal tissue. Interestingly, the decrease in E2F1 alleviates the degree of renal tissue fibrosis, the level of inflammation, and the senescence of renal tubular epithelial cells in DKD. In addition, metformin reduces the expression level of E2F1 in the renal tissue of *db/db* mice. To further confirm that E2F1 is directly involved in metformin-alleviated fibrosis, DNA damage, and cellular senescence in DKD, we stimulated mRTECs with high glucose *in vitro* and found that the indexes related to E2F1, fibrosis, DNA damage, and cellular senescence increased significantly, but decreased after transfection with E2F1 siRNA. This phenomenon suggested that the increase in E2F1 affects the occurrence of fibrosis and cellular senescence in DKD, which is consistent with the results *in vivo*. Moreover, the stimulation of mRTECs with high glucose and metformin demonstrated that metformin reduces the expression of E2F1 in the high-glucose state and reverses the increased collagen and fibronectin levels, DNA damage, and senescence-associated markers. Therefore, it could be deduced that metformin exerts an anti-fibrosis role and delays cellular senescence by reducing the expression of E2F1 in the high-glucose state. In order to test this hypothesis, we overexpressed E2F1 after metformin treatment in the high-glucose state. Compared to the metformin treatment alone group, the anti-fibrosis and delayed cell senescence effects of metformin after overexpression of E2F1 were significantly weakened. Together with the *in vivo* results, it was confirmed that metformin is a renal anti-fibrosis and cell aging agent in DKD via decreased expression of E2F1 in the high-glucose state.

In conclusion, the current results suggested that metformin has a protective effect on high glucose-induced renal tubular epithelial cell injury. The mechanism is to reverse the degree of fibrosis of DKD renal tissue, reduce DNA damage, and slow down the aging process of renal tubular epithelial cells by reducing the expression of E2F1. Thus, this study provided a new experimental basis for the mechanism of metformin in renal protection in DKD. It also provides new drug targets for delaying the process and treatment of renal fibrosis and cellular senescence in DKD.

DATA AVAILABILITY STATEMENT

The original contributions presented in the study are included in the article/Supplementary Materials, further inquiries can be directed to the corresponding authors.

ETHICS STATEMENT

The animal study was reviewed and approved by Animal Experimental Ethical Inspection Form of Guizhuo Medical University.

AUTHOR CONTRIBUTIONS

DL and ZL contributed significantly to the work, obtained the main experimental data, analyzed and interpreted the results, and wrote the manuscript. ZF, YD and XW: Assisted in the acquisition and analysis of some experimental data. ZY, FZ, YW, YZ, LL and MS: Reviewed the results and revised manuscript. YiX and BG designed and directed the Experiment, and assured the feasibility of the Experiment.

FUNDING

This study was supported by the National Natural Science Foundation of China (Grant Nos. 81860656 and 81860135) and the Guizhou Province Science and Technology Foundation (Grant Nos. Guizhou Science and Technology Foundation-ZK [2021] Focus 010).

REFERENCES

Burton, D. G. A., and Faragher, R. G. A. (2018). Obesity and Type-2 Diabetes as Inducers of Premature Cellular Senescence and Ageing. *Biogerontology* 19 (6), 447–459. doi:10.1007/s10522-018-9763-7

Calcinotto, A., Kohli, J., Zagato, E., Pellegrini, L., Demaria, M., and Alimonti, A. (2019). Cellular Senescence: Aging, Cancer, and Injury. *Physiol. Rev.* 99 (2), 1047–1078. doi:10.1152/physrev.00020.2018

Chen, K., Dai, H., Yuan, J., Chen, J., Lin, L., Zhang, W., et al. (2018). Optineurin-mediated Mitophagy Protects Renal Tubular Epithelial Cells against Accelerated Senescence in Diabetic Nephropathy. *Cell Death Dis.* 9 (2), 105. doi:10.1038/s41419-017-0127-z

Childs, B. G., Durik, M., Baker, D. J., and van Deursen, J. M. (2015). Cellular Senescence in Aging and Age-Related Disease: from Mechanisms to Therapy. *Nat. Med.* 21 (12), 1424–1435. doi:10.1038/nm.4000

Dick, F. A., and Rubin, S. M. (2013). Molecular Mechanisms Underlying RB Protein Function. *Nat. Rev. Mol. Cell Biol.* 14 (5), 297–306. doi:10.1038/nrm3567

Gao, S., Song, Q., Liu, J., Zhang, X., Ji, X., and Wang, P. (2019). E2F1 Mediates the Downregulation of POLD1 in Replicative Senescence. *Cell Mol. Life Sci.* 76 (14), 2833–2850. doi:10.1007/s00018-019-03070-z

Giralt, A., Denechaud, P. D., Lopez-Mejia, I. C., Delacuisine, B., Blanchet, E., Bonner, C., et al. (2018). E2F1 Promotes Hepatic Gluconeogenesis and Contributes to Hyperglycemia during Diabetes. *Mol. Metab.* 11, 104–112. doi:10.1016/j.molmet.2018.02.011

Hsu, S. K., Cheng, K. C., Mgbeahuruike, M. O., Lin, Y. H., Wu, C. Y., Wang, H. D., et al. (2021). New Insight into the Effects of Metformin on Diabetic Retinopathy, Aging and Cancer: Nonapoptotic Cell Death, Immunosuppression, and Effects beyond the AMPK Pathway. *Int. J. Mol. Sci.* 22 (17), 9453. doi:10.3390/ijms22179453

Jiang, X., Ruan, X. L., Xue, Y. X., Yang, S., Shi, M., Wang, L. N., et al. (2020). Metformin Reduces the Senescence of Renal Tubular Epithelial Cells in Diabetic Nephropathy via the MBNL1/miR-130a-3p/STAT3 Pathway. *Oxid. Med. Cell Longev.* 2020 (6), 8708236–8708322. doi:10.1155/2020/8708236

Kawanami, D., Takashi, Y., and Tanabe, M. (2020). Significance of Metformin Use in Diabetic Kidney Disease. *Int. J. Mol. Sci.* 21 (12), 4239. doi:10.3390/ijms21124239

Kirkland, J. L., and Tchkonia, T. (2017). Cellular Senescence: a Translational Perspective. *EbioMedicine* 21 (C), 21–28. doi:10.1016/j.ebiom.2017.04.013

Kitada, K., Nakano, D., Ohsaki, H., Hitomi, H., Minamino, T., Yatabe, J., et al. (2014). Hyperglycemia Causes Cellular Senescence via a SGLT2- and P21-dependent Pathway in Proximal Tubules in the Early Stage of Diabetic Nephropathy. *J. Diabetes Complicat.* 28 (5), 604–611. doi:10.1016/j.jdiacomp.2014.05.010

Kumar, V., Agrawal, R., Pandey, A., Kopf, S., Hoeffgen, M., Kaymak, S., et al. (2020). Compromised DNA Repair Is Responsible for Diabetes-Associated Fibrosis. *EMBO J.* 39 (11), e103477. doi:10.15252/embj.2019103477

Liang, Y. X., Lu, J. M., Mo, R. J., He, H. C., Xie, J., Jiang, F. N., et al. (2016). E2F1 Promotes Tumor Cell Invasion and Migration through Regulating CD147 in Prostate Cancer. *Int. J. Oncol.* 48 (4), 1650–1658. doi:10.3892/ijo.2016.3364

Lv, Z., and Guo, Y. (2020). Metformin and its Benefits for Various Diseases. *Front. Endocrinol. (Lausanne)* 11, 191. doi:10.3389/fendo.2020.00191

Palmer, A. K., Gustafson, B., Kirkland, J. L., and Smith, U. (2019). Cellular Senescence: at the Nexus between Ageing and Diabetes. *Diabetologia* 62 (10), 1835–1841. doi:10.1007/s00125-019-4934-x

Park, C., Lee, I., and Kang, W. K. (2006). E2F-1 Is a Critical Modulator of Cellular Senescence in Human Cancer. *Int. J. Mol. Med.* 17 (5), 715–720. doi:10.3892/ijmm.17.5.715

Poppy Roworth, A., Ghari, F., and La Thangue, N. B. (2015). To live or let die - complexity within the E2F1 pathway. *Mol. Cell Oncol.* 2 (1), e970480. doi:10.4161/23723548.2014.970480

Ren, H., Shao, Y., Wu, C., Ma, X., Lv, C., and Wang, Q. (2019). Metformin Alleviates Oxidative Stress and Enhances Autophagy in Diabetic Kidney Disease via AMPK/SIRT1-FoxO1 Pathway. *Mol. Cell Endocrinol.* 500, 110628. doi:10.1016/j.mce.201910.1016/j.mce.2019.110628

Rezabakhsh, A., Nabat, E., Yousefi, M., Montazersaheb, S., Cheraghi, O., Mehdizadeh, A., et al. (2017). Endothelial Cells' Biophysical, Biochemical, and Chromosomal Aberrancies in High-Glucose Condition within the Diabetic Range. *Cell Biochem. Funct.* 35 (2), 83–97. doi:10.1002/cbf.3251

Song, A., Zhang, C., and Meng, X. (2021). Mechanism and Application of Metformin in Kidney Diseases: An Update. *Biomed. Pharmacother.* 138, 111454. doi:10.1016/j.biopha.2021.111454

Tesch, G. H., and Lim, A. K. (2011). Recent Insights into Diabetic Renal Injury from the Db/db Mouse Model of Type 2 Diabetic Nephropathy. *Am. J. Physiol. Ren. Physiol.* 300 (2), F301–F310. doi:10.1152/ajprenal.00607.2010

Verzola, D., Gandolfo, M. T., Gaetani, G., Ferraris, A., Mangerini, R., Ferrario, F., et al. (2008). Accelerated Senescence in the Kidneys of Patients with Type 2 Diabetic Nephropathy. *Am. J. Physiol. Ren. Physiol.* 295 (5), F1563–F1573. doi:10.1152/ajprenal.90302.2008

Wang, F., Sun, H., Zuo, B., Shi, K., Zhang, X., Zhang, C., et al. (2021). Metformin Attenuates Renal Tubulointerstitial Fibrosis via Upgrading Autophagy in the Early Stage of Diabetic Nephropathy. *Sci. Rep.* 11 (1), 16362. doi:10.1038/s41598-021-95827-5

Wang, Y., Zhou, Y., Xiao, L., Zheng, S., Yan, N., and Chen, D. (2017). E2F1 Mediates High Glucose-Induced Neuronal Death in Cultured Mouse Retinal Explants. *Cell Cycle* 16 (19), 1824–1834. doi:10.1080/15384101.2017.1361070

Xie, Q., Peng, S., Tao, L., Ruan, H., Yang, Y., Li, T. M., et al. (2014). E2F Transcription Factor 1 Regulates Cellular and Organismal Senescence by Inhibiting Forkhead Box O Transcription Factors. *J. Biol. Chem.* 289 (49), 34205–34213. doi:10.1074/jbc.M114.587170

Xiong, Y., and Zhou, L. (20192019). The Signaling of Cellular Senescence in Diabetic Nephropathy. *Oxid. Med. Cell Longev.* 2019, 7495629–7495716. doi:10.1155/2019/7495629

Xu, B.-H., Sheng, J., You, Y.-K., Huang, X.-R., Ma, R. C. W., Wang, Q., et al. (2020). Deletion of Smad3 Prevents Renal Fibrosis and Inflammation in Type 2 Diabetic Nephropathy. *Metabolism* 103, 154013. doi:10.1016/j.metabol.2019.154013

Xu, J., Xiang, P., Liu, L., Sun, J., and Ye, S. (2020). Metformin Inhibits Extracellular Matrix Accumulation, Inflammation and Proliferation of Mesangial Cells in Diabetic Nephropathy by Regulating H19/miR-143-3p/TGF-B1 axis. *J. Pharm. Pharmacol.* 72 (8), 1101–1109. doi:10.1111/jphp.13280

Yi-Chun, T., Kuo, P. L., Kuo, M. C., Hung, W. W., Wu, L. Y., Chang, W. A., et al. (2018). The Interaction of miR-378i-Skp2 Regulates Cell Senescence in Diabetic Nephropathy. *J. Clin. Med.* 7 (12), 468. doi:10.3390/jcm7120468

Yuan, Y., Li, X., and Li, M. (2018). Overexpression of miR-17-5p P-rotects against H-igh G-lucose-induced E-ndothelial C-ell I-njury by T-argeting E2F1-mediated S-uppression of A-utophagy and P-romotion of A-poptosis. *Int. J. Mol. Med.* 42 (3), 1559–1568. doi:10.3892/ijmm.2018.3697

Zhang, X., Chen, X., Wu, D., Liu, W., Wang, J., Feng, Z., et al. (2006). Downregulation of Connexin 43 Expression by High Glucose Induces Senescence in Glomerular Mesangial Cells. *J. Am. Soc. Nephrol.* 17 (6), 1532–1542. doi:10.1681/ASN.200507077627

Zolali, E., Rezabakhsh, A., Nabat, E., Jaberi, H., Rahbarghazi, R., and Garjani, A. (2019). Metformin Effect on Endocan Biogenesis in Human Endothelial Cells under Diabetic Condition. *Arch. Med. Res.* 50 (5), 304–314. doi:10.1016/j.arcmed.2019.08.012

Conflict of Interest: The authors declare that the research was conducted in the absence of any commercial or financial relationships that could be construed as a potential conflict of interest.

Publisher's Note: All claims expressed in this article are solely those of the authors and do not necessarily represent those of their affiliated organizations, or those of the publisher, the editors and the reviewers. Any product that may be evaluated in this article, or claim that may be made by its manufacturer, is not guaranteed or endorsed by the publisher.

frontiers | Frontiers in Pharmacology

ORIGINAL RESEARCH
published: 06 July 2022
doi: 10.3389/fphar.2022.936853

Tongluo Yishen Decoction Ameliorates Renal Fibrosis *via* NLRP3-Mediated Pyroptosis *In Vivo* and *In Vitro*

Qi Jia[1†], *Xiaoyu Zhang*[1†], *Gaimei Hao*[2], *Yun Zhao*[1], *Scott Lowe*[3], *Lin Han*[4*] *and Jianguo Qin*[1*]

[1]*Department of Nephropathy, Dongfang Hospital, Beijing University of Chinese Medicine, Beijing, China,* [2]*Institute of Basic Theory for Chinese Medicine, China Academy of Chinese Medical Sciences, Beijing, China,* [3]*Kansas City University of Medicine and Biosciences, College of Osteopathic Medicine, Kansas City, MO, United States,* [4]*School of Basic Medicine, Beijing University of Chinese Medicine, Beijing, China*

OPEN ACCESS

Edited by:
Zhiyong Guo,
Second Military Medical University, China

Reviewed by:
Xiao Ma,
Chengdu University of Traditional Chinese Medicine, China
Xie-an Yu,
China Pharmaceutical University, China

***Correspondence:**
Lin Han
hanlinxf89@163.com
Jianguo Qin
qindoctor@163.com

[†]*These authors have contributed equally to this work and share first authorship*

Specialty section:
This article was submitted to Renal Pharmacology, a section of the journal Frontiers in Pharmacology

Received: *05 May 2022*
Accepted: *20 June 2022*
Published: *06 July 2022*

Citation:
Jia Q, Zhang X, Hao G, Zhao Y, Lowe S, Han L and Qin J (2022) Tongluo Yishen Decoction Ameliorates Renal Fibrosis via NLRP3-Mediated Pyroptosis In Vivo and In Vitro. Front. Pharmacol. 13:936853. doi: 10.3389/fphar.2022.936853

Purpose: In this study, we investigated the mechanism of Tongluo Yishen (TLYS) decoction in more detail, from the perspective of pyroptosis in the unilateral ureteral ligation (UUO) model and the hypoxia-induced renal tubular epithelial (NRK-52E) cell.

Method: The UUO model was used, and after 14 days of TLYS intervention, rats were tested for blood creatinine and urea nitrogen, HE staining was used to observe the pathological changes in the kidney, Masson staining was used to assess the degree of interstitial fibrosis, western blot was used to detect the changes of α-smooth muscle actin (α-SMA) protein expression level, immunohistochemistry and western blot detected the changes in protein expression levels of NOD-like receptor protein 3 inflammasome (NLRP3), gasdermin D (GSDMD), cysteinyl aspartate specific proteinase (caspase-1), interleukin 18 (IL-18) and interleukin 1β (I L-1β). A hypoxia model was created using NRK-52E cell, and after different concentrations of TLYS decoction intervention, the changes in the expression levels of pyroptosis were used with immunofluorescence and western blot methods.

Results: TLYS decoction improved renal function, delayed the advancement of renal interstitial fibrosis, and inhibited pyroptosis in UUO rats. Furthermore, we observed that TLYS can mitigate hypoxia-induced NRK-52E cell damage via the suppression of the NLRP3-mediated pyroptosis.

Conclusion: TLYS decoction exert renoprotective effects by inhibiting NLRP3-mediated pyroptosis.

Keywords: Tongluo Yishen decoction, obstruction-induced renal fibrosis, Traditional Chinese Medicine, NRK-52E, pyroptosis

INTRODUCTION

Renal interstitial fibrosis (RIF) is a critical event in the progression of chronic kidney disease (CKD) to end-stage renal disease (ESRD) (Humphreys, 2018). Unilateral ureteral ligation (UUO) is a well-established animal model of RIF, the major pathophysiological changes involved necrosis, inflammation, activation of a variety of macrophages, cytokine release, and a large accumulation of extracellular matrix (ECM) (Chevalier et al., 2009). During the early stages of acute unilateral

obstruction in this mouse model, tubular cells are immediately and dramatically injured (Klahr and Morrissey, 2002). Cell death play a dominant role in the early stages of pathological progression of acute obstructive nephropathy, according to growing evidence (Hosseinian et al., 2017; Zhang B. et al., 2021). Inflammation is a key link in the development of RIF, existing research evidence indicates that epithelial-mesenchymal transition (EMT) and fibroblast activation caused by overexpression of inflammatory factors and inflammatory cell infiltration have important pathological significance in RIF in acute or chronic kidney injury (Meng et al., 2014; Tang et al., 2019). The mobilization and infiltration of macrophages and neutrophils, as well as the subsequent release of cytokines such as interleukin-1β (IL-1β) and IL-18, all contribute significantly to the progression of fibrosis.

Pyroptosis is a newly identified type of programmed inflammatory cell death characterized by excessive cell death and inflammation that can be triggered by canonical caspase-1 inflammasomes or non-canonical caspase-4-, caspase-5-, and caspase-11-mediated pathways (Broz et al., 2020; Kesavardhana et al., 2020). When pyroptosis occurs via canonical signaling, caspase-1 is converted into its active forms (p20 and p10 subunits) by inflammasomes (NLRP3, AIM2, etc.) and then activates proinflammatory cytokines interleukin IL-18 and IL-1β to mature IL-18 and IL-1β (Yu et al., 2021). These have potent pro-inflammatory properties and promote cell vasodilation and extravasation, as well as amplifying the local and systemic inflammatory response (Swanson et al., 2019).

The traditional Chinese medicine Tongluo Yishen (TLYS) decoction has been widely used to treat CKD for decades. TLYS is a compound preparation composed of Salvia, Radix et Rhizoma, Safflower, and Cortex. The components in these herbs could be used to treat kidney disease. Several components of TLYS have been shown in numerous studies to have anti-inflammatory and antioxidant properties (Zhang et al., 2014; Xu et al., 2017; Ye T. et al., 2020; Tang et al., 2020). Our previous research found that TLYS alleviated renal pathological damage by improving oxidative stress in the kidneys of UUO rats (Jia et al., 2021). However, the mechanism of whether TLYS plays a role in pyroptosis remains unclear. Based on previous research, we hypothesized that TLYS might protect renal functions against renal fibrosis via NLRP3 inflammasome-induced pyroptosis. This hypothesis was tested in hypoxic cultures of UUO rats and NRK-52E cells.

MATERIALS AND METHODS

Animal Model and Experimental Design

After fasting without water for 12 h prior to surgery, 2 percent sodium pentobarbital was administered intraperitoneally at 40 mg/kg according to the rat's body weight for anesthesia, the right side of the rat's back was selected for skin preparation and disinfection, an incision was made at 1 cm next to the right rib-spine angle, parallel to the spine, the incision length was about 0.5–0.7 cm, the skin and muscle layer were incised. The UUO group was divided into three groups: the model group, the TLYS group, and the valsartan group, with nine animals in each group receiving gavage administration. The valsartan group received 0.84 mg/100 (g·d) of valsartan. TLYS was given 0.8 g/100 (g·d) to the TLYS group. The treatment period lasted 14 days. The sham-operated and model groups were given 1 ml/100 (g·d) of distilled water daily.

Preparation of Tongluo Yishen Decoction

TLYS decoction contains 25 g Salvia, 15 g Radix Bupleurum, 10 g Safflower, and 10 g Chrysanthemum. The herbal medicine was soaked for 60 min in 600 ml of water (10 times the mass of the herbal medicine), boiled, and then decocted for 40 min twice, combined and blended to remove the dregs, concentrated to contain 1 g of raw herbs per ml, and stored at 4°C. The herbs are used *in vivo* experiments. Place the sterilized TLYS herbs in the freeze-drying mechanism to create a freeze-dried powder. When ready to use, weigh 1 g lyophilized powder with a balance, add 1 ml ultrapure water for redissolution, mix evenly on the shaking table, transfer to a high-temperature resistant container, disinfect and sterilize it under high temperature and high pressure, and store it at 4°C for standby, current use, and distribution. The freeze-dried powder is used *in vitro* experiments.

Measurement of Serum Creatinine (Scr) and Blood Urea Nitrogen (BUN)

Scr and BUN levels were determined using a creatinine assay kit (C011-1, Nanjing Jiancheng Bioengineering Institute, Nanjing, China) and a BUN assay kit (C013-1, Nanjing Jiancheng Bioengineering Institute, Nanjing, China) according to the manufacturer's instructions.

Histology and Immunohistochemistry

Histological Examination: Six kidneys from each group were immediately fixed with 10% formalin, dehydrated, embedded in paraffin, and sectioned to a thickness of 5 μm. These sections were then stained with hematoxylin and eosin (H&E) and Masson's trichrome. Immunohistochemistry (IHC) Staining: Five-micron thick paraffin-embedded kidney sections were deparaffinized, followed by antigen retrieval in ethylenediaminetetraacetic acid (1 mM). The samples were blocked with 0.3% H2O2 in methanol and 5% BSA. Kidney sections were incubated with NLRP3 (1: 200, ab263899, Abcam, United States), GSDMD (1:200, ab255603, Abcam, United States), IL-18 (1:200, 60070-1-Ig, Proteintech, United States) and IL-1β (1:200, 16806-1-AP, Proteintech, United States) primary antibodies overnight at 4°C, followed by horseradish peroxidase (HRP)-conjugated secondary antibodies (PV9001, Beijing Zhongshan Jinqiao Biotechnology Co., Ltd., Beijing). The reaction was visualized with DAB staining using a Leica Aperio Versa 8 system (Leica, Wetzlar, Germany). The cumulative optical density of the area of interest analysis was calculated using ImageJ software.

Cell Culture and Treatment

The rat renal tubular epithelial cells (RTEC, NRK-52E) were obtained from the Chinese Academy of Sciences' Shanghai cell bank (batch No.:20161104). NRK-52E was cultured in a 37°C, 5% CO_2 normal incubator with 10% fetal bovine serum (Gibco, United States) and 1% double antibody (100 U/mL penicillin, 100 G/ml streptomycin, Gibco, United States), 89 percent DMEM high glucose medium (HyClone, United States). To complete the construction of the renal interstitial fibrosis model, NRK-52E was cultured in DMEM high glucose medium in a 37°C, 5% CO_2, and 1% O_2 hypoxia incubator.

The modeling time was 12 h, and the high, middle and low doses of TLYS were 500 μg/ml, 200 μg/ml, and 100 μg/ml, respectively, according to the CCK8 results. The cells were divided into six groups at random: 1) Control group: complete medium containing 10% fetal bovine serum in a normal incubator; 2) Model group: DMEM high glucose medium in a hypoxia incubator; 3) High dose group: DMEM high glucose medium +500 μg/ml of TLYS in a hypoxia incubator; 4) Medium dose group: DMEM high glucose medium +200 μg/ml of TLYS in a hypoxia incubator; 5) Low dose group: DMEM high glucose medium +100 μg/ml of TLYS in a hypoxia incubator; 6) MCC950 group: DMEM high glucose medium in a 10 μmol/L MCC950 in a hypoxia incubator.

Western Blot Analysis

For western blot assays, renal tissues were lysed and homogenized in RIPA buffer supplemented with protease inhibitor cocktail l (C0001-1, Targetmol, China) and quantified with a BCA kit (P0013C, Beyotime, China). Protein sample extracts (30 mg/lane) were separated by SDS-PAGE and transferred onto a polyvinylidene difluoride membrane (PVDF). After the membranes were blocked with 5% BSA, they were incubated with the primary antibodies at 4°C overnight, followed by an HRP-conjugated secondary antibody. Then, the membranes were incubated with HRP-conjugated secondary antibody (Boster Biological Technology Co., Ltd., China) at room temperature for 1 h. Films were scanned by a ChemiScope 6,000 system (Qinxiang, Shanghai, China). ImageJ software was used to measure the protein bands based on that of GAPDH.

Immunofluorescence Staining

Kidney sections were blocked with 10% goat serum at room temperature for 30 min, and then incubated with primary antibodies: GSDMD (1:200, ab255603, Abcam, United States), and IL-18 (1:200, 60070-1-Ig, Proteintech, United States) overnight at 4°C. Later on, the slides were incubated with corresponding secondary antibodies for 30 min. Finally, the slides were stained with DAPI solution for 10 min and captured by a laser scanning confocal fluorescence microscope (Olympus FV 1000, Japan).

Statistical Analysis

For statistical analysis, the GraphPad Prism software was used. The mean standard deviation (SD) is used to express quantitative data. For all experimental data, one-way ANOVA was used, followed by Dunnett's test. A p value of less than 0.05 was deemed significant.

RESULTS

TLYS Alleviated Renal Function, Renal Injury, and Fibrosis in the UUO Rats

In comparison to the sham group, serum creatinine and urea levels were considerably higher in UUO rats, and renal function was dramatically improved after TLYS intervention. (**Figures 1A,B**). When compared to the sham group, HE and Masson's trichrome staining revealed inflammatory cell infiltration and interstitial fibrosis in the kidney tissue of UUO rats, while TLYS intervention markedly alleviated interstitial fibrosis (**Figures 1C,D**). α-SMA is a protein that is commonly found in activated fibroblasts. **Figures 1E,F** shows that α-SMA protein expression was significantly upregulated in kidney tissues of UUO rats and that TLYS intervention improved its abnormal expression. These findings show that TLYS has a more beneficial effect on the kidneys of UUO rats.

TLYS Attenuated Hypoxic NRK-52E Cells Injury and Fibrosis

We further investigated whether TLYS ameliorates hypoxia-induced renal epithelial cell injury. A cell viability experiment demonstrated that TLYS concentrations of 0–500 μg/ml had minimal influence on cell viability (**Figure 2B**). Cell viability was lower in hypoxic-treated NRK-52E cells than in normoxic NRK-52E cells, whereas cell viability was significantly lower in normoxic NRK-52E cells after treatment with 800 and 1000 μg/ml TLYS (**Figure 2B**). These findings suggested that excessive levels of TLYS are harmful to cells. Up to a dosage of 500 μg/ml, treatment with TLYS maintained cell viability in hypoxic NRK-52E cells (**Figure 2B**), whereas greater concentrations of TLYS decreased cell viability. As a result, 500, 200, and 100 μg/ml were chosen as the high, medium, and low concentration groups, respectively. Necrotic cells appeared to be on the rise in the model group, with rounded cell shape and the production of granular material and vacuoles in control cells. TLYS in various doses and MCC950 improved cellular morphology (**Figure 2A**). Western blot was used to assess ECM accumulation (**Figure 2C**). α-SMA was significantly higher in the model group compared to the control group but were reduced by TLYS treatment (**Figures 2C,D**).

TLYS Reverses the Increased Pyroptosis in UUO Rat Renal Injury

Numerous studies have demonstrated that NLRP3-mediated pyroptosis plays a role in the renal inflammatory response and renal injury. Immunohistochemistry and western blot were utilized to further analyze the expression of pyroptosis marker proteins to see if TLYS ameliorates renal interstitial fibrosis by modulating the pyroptosis pathway in renal cells. Immunohistochemistry showed that NLRP3, GSDMD, and the pro-inflammatory cytokines IL-1β and IL-18 protein expression were significantly higher in the model group

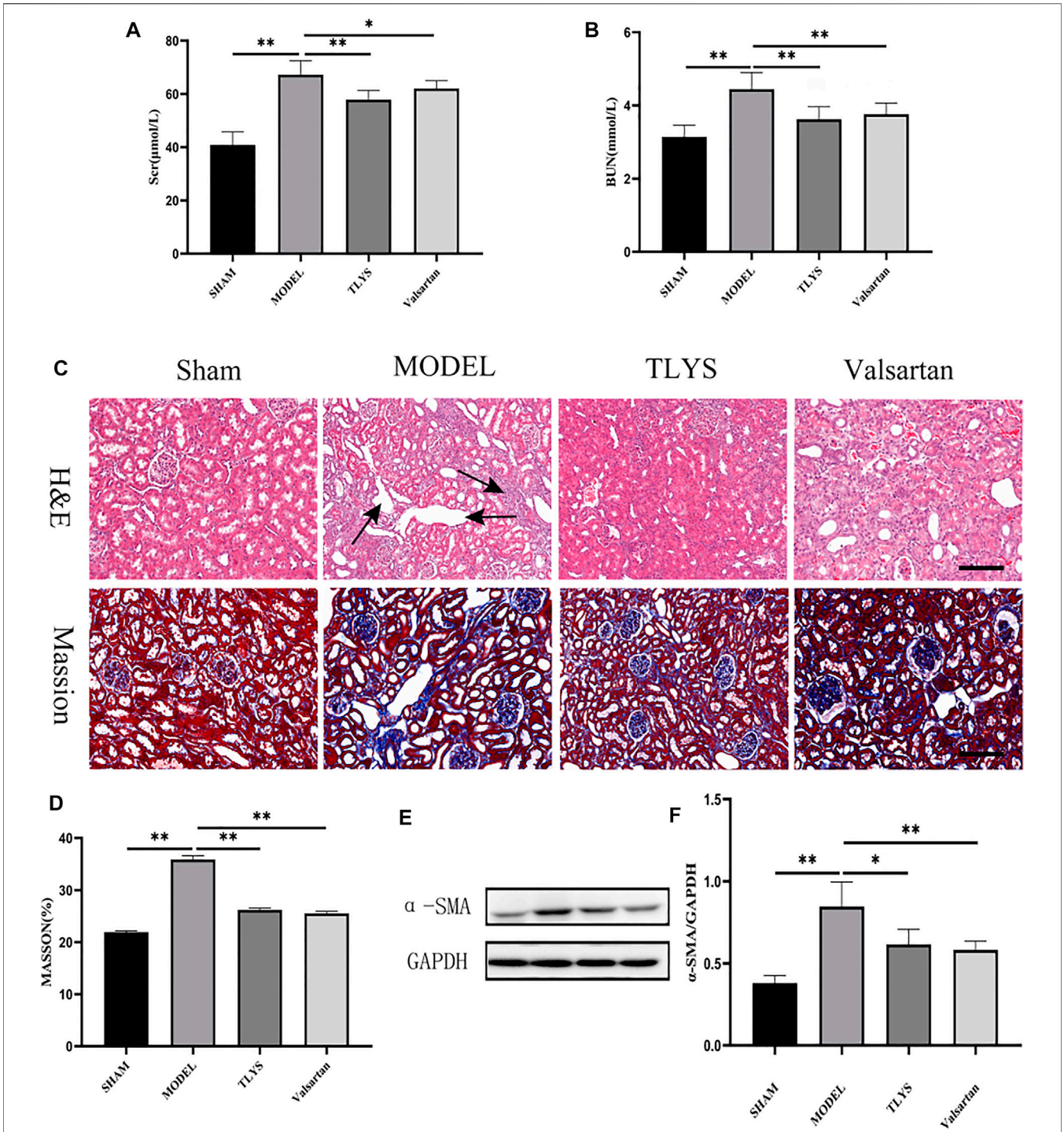

FIGURE 1 | TLYS decoction alleviates the renal function, pathological kidney injuries and renal fibrosis in UUO rats. **(A,B)** serum creatinine and BUN were detected (n = 8). **(C)** H&E and Masson's trichrome were performed to describe and evaluate kidney injury. **(D)** Collagen areas were quantified by Masson's trichrome staining (n = 6). **(E,F)** The protein levels of α-SMA were assayed by Western blot and analyzed semi-quantitatively (n = 6). The magnification of the images is ×200, scale bar = 50 μm. Data were presented as means ± SD. *$p < 0.05$, **$p < 0.01$.

compared to the sham group; Compared to the model group, GSDMD, IL-1β, and IL-18 protein expression were significantly lower in the TLYS and Valsartan groups (**Figures 3A–E**). We then used a Western blot assay to look at the expression levels of NLRP3, GSDMD, IL-1β, IL-18, and caspase-1 proteins, and the results were

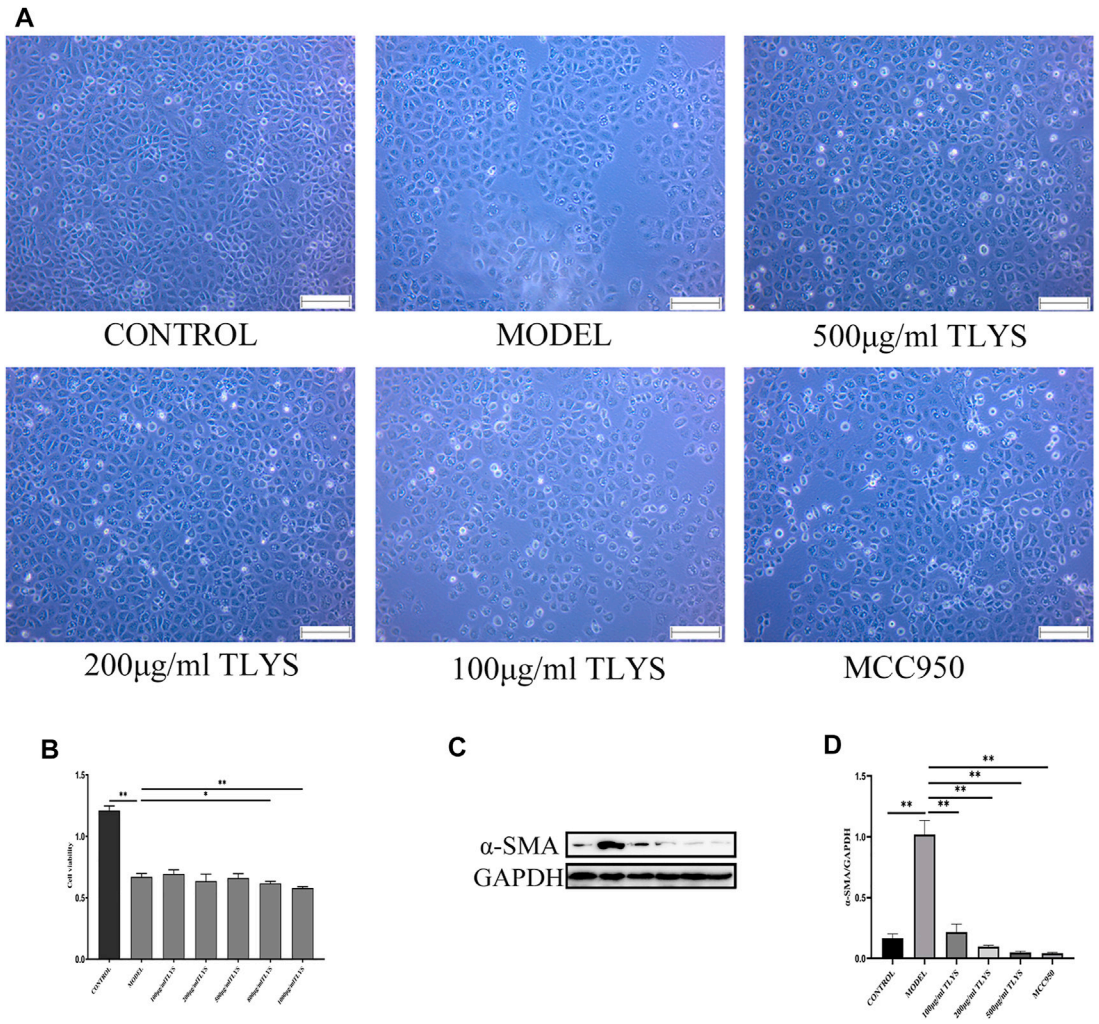

FIGURE 2 | TLYS decoction affects the morphology, viability and fibrosis of NRK-52E cells induced by hypoxia. **(A)** The morphology of NRK-52E cells induced by hypoxia were observed by microscope. **(B)** The viability of NRK-52E cells induced by hypoxia were affected by cck8 test. **(C,D)** The protein levels of α-SMA were assayed by Western blot and analyzed semi-quantitatively (n = 3). The magnification of the images is ×100, scale bar = 50 μm. Data were presented as means ± SD. $^{*}p < 0.05$, $^{**}p < 0.01$.

consistent with the immune tissues, as the levels of NLRP3, GSDMD, IL-1β, IL-18 and caspase-1 proteins in the UUO group were significantly higher than those in the Sham group, while those in the TLYS group were significantly lower than those in the UUO group (**Figures 3F–K**). Similarly, valsartan treatment significantly reduced the level of NLRP3, GSDMD, IL-1, IL-18, and caspase-1 proteins (**Figures 3F–K**).

The Effects of TLYS on Pyroptosis in Hypoxic NRK-52E Cells

To evaluate the effect of TLYS on pyroptosis, we measured the expression of proteins related to pyroptosis activation, including NLRP3, GSDMD, IL-1β, IL-18, and caspase-1 proteins. The protein expression levels of NLRP3, GSDMD, IL-1β, IL-18, and caspase-1 significantly increased in hypoxic NRK-52E cells as compared to those in normoxic NRK-52E cells (**Figures 4A–F**). These decreases were ameliorated by treatment with TLYS at the dose of 500, 200, and 100 μg/ml (**Figures 4A–F**). GSDMD was found primarily in the cell membrane and cytoplasm, while IL-18 was found primarily in the cell plasma, according to immunofluorescence detection results (**Figure 4G**). GSDMD and IL-18 proteins were widely present in hypoxic NRK-52E cells, and their expression was significantly higher in the model group compared to the normal group; however, The expression was significantly lower in the TLYS (500 and 100 μg/ml) and MCC950 group compared to the model group (**Figure 4G**).

DISCUSSION

Inflammation has been proven in numerous studies to be important factor contributing to the progression of interstitial

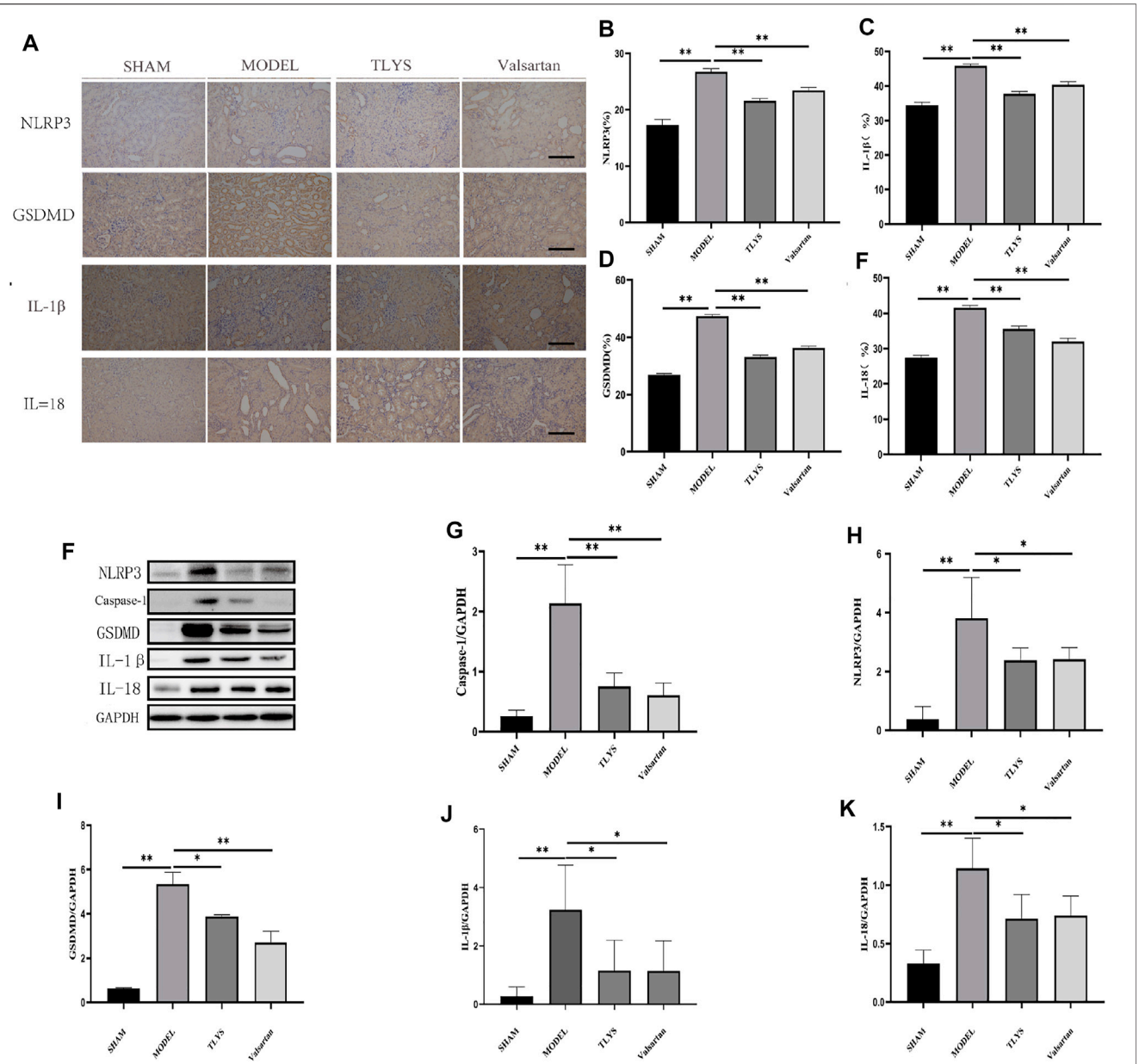

FIGURE 3 | TLYS decoction suppresses the pyroptosis associated protein expressions in UUO rats. **(A–E)** Expression levels of NLRP3, GSDMD, IL-18 and IL-1β in the kidney were detected by immunohistochemistry and the optical intensity of the abovementioned proteins was measured (n = 6). **(F–K)** The protein levels of NLRP3, caspase-1, GSDMD, IL-18 and IL-1β in the kidney were assayed by Western blot and analyzed semi-quantitatively (n = 3). The magnification of the images is ×200, scale bar = 50 μm. Data were presented as means ± SD. $^{*}p < 0.05$, $^{**}p < 0.01$.

fibrosis in the kidney (Liu et al., 2018; Lv et al., 2018; Tang et al., 2019). Following tissue injury, infiltrating inflammatory cells are activated, resulting in the production of tissue-damaging molecules, such as reactive oxygen species (ROS) while inducing the production of fibrogenic cytokines and growth factors (Nathan and Ding, 2010; Schroder and Tschopp, 2010). The onset of pyroptosis in the UUO model may be caused by oxidative stress and inflammation (Chung et al., 2012; Zhang Y. et al., 2021). Recent studies have shown that renal inflammation can activate NLRP3 inflammatory vesicles (Kim et al., 2019; Tajima et al., 2019), which trigger innate immune defenses via pro-inflammatory cytokines such as IL-1β in response to signals such as infection and metabolic dysregulation (Vilaysane et al., 2010).

Our previous research has proved that TLYS has a good therapeutic effect on RIF (Jia et al., 2021). The present experimental study also found that TLYS could protect the kidney function and improve the histopathological damage of the kidney in UUO rats. Following UUO, NLRP3 knockout mice showed reductions in tubular apoptosis, inflammation, and

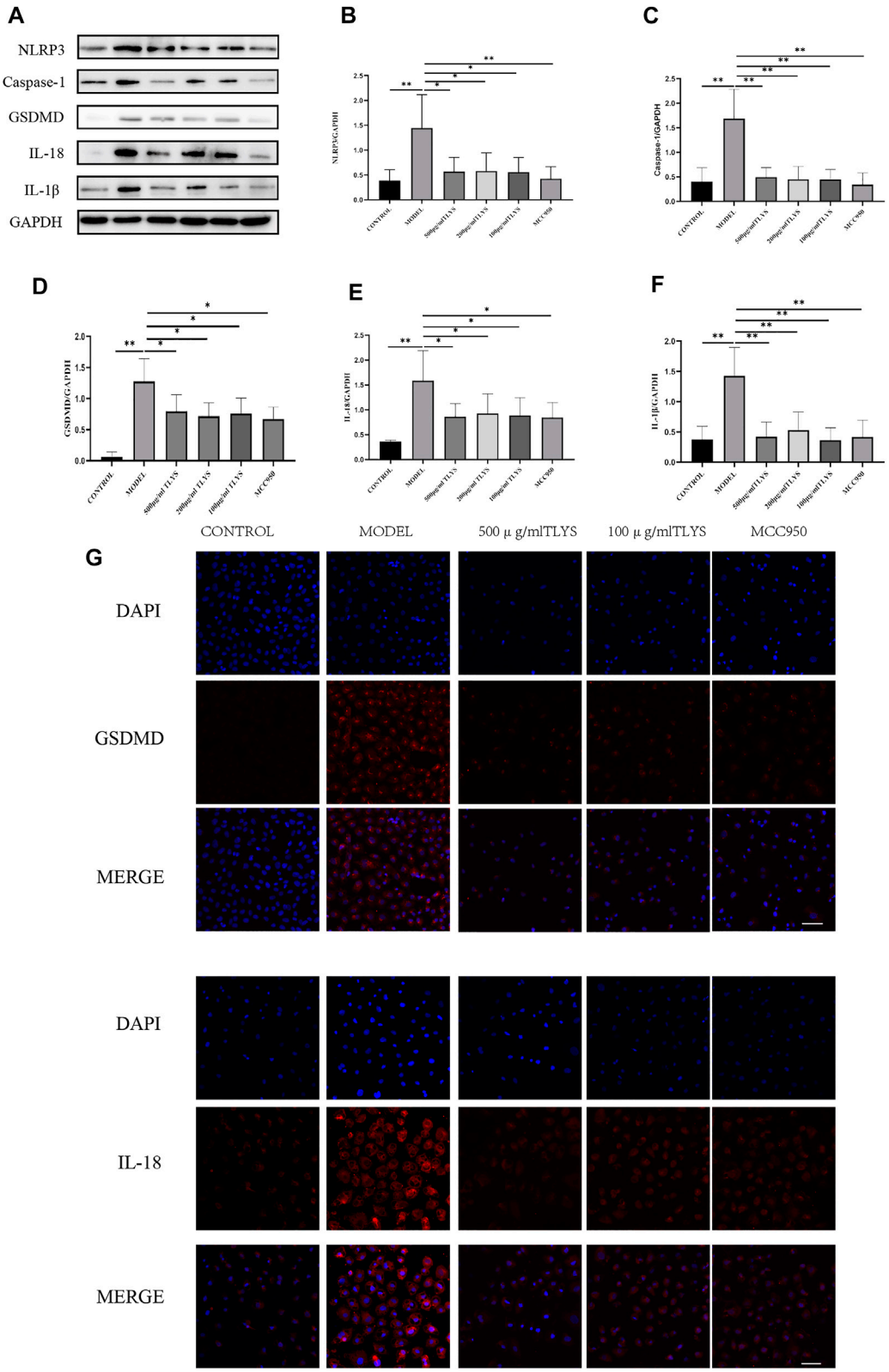

FIGURE 4 | TLYS decoction suppresses the pyroptosis associated protein expressions of NRK-52E cells induced by hypoxia. **(A–F)** The protein levels of NLRP3, caspase-1, GSDMD, IL-18 and IL-1β in NRK-52E cells induced by hypoxia were assayed by Western blot and analyzed semi-quantitatively (n = 3). **(G)** The positions of GSDMD and IL-18 was labeled by immunofluorescence (n = 6). The magnification of the images is ×400, scale bar = 50 μm. Data were presented as means ± SD. $^{*}p < 0.05$, $^{**}p < 0.01$.

fibrosis (Guo et al., 2017; Kim et al., 2018). At 14 days after UUO, leukocyte recruitment to the kidney was reduced, and inflammatory cytokines were reduced (Kim et al., 2018). The findings of this study also revealed that the expression of NLRP3 and caspase-1 was increased in the kidney tissues of rats in the model group, as was the content of inflammatory factors IL-1β and IL-18. TLYS treatment reduced the expression of NLRP3 and caspase-1 in rat kidney tissues, as well as the expression of inflammatory factors, and the interstitial fibrosis of the kidney. Meanwhile, A cell model was established in this study using hypoxia-induced RTEC injury for 12 h. Hypoxia caused cell morphology changes, structural damage, and decreased cell viability in RTEC; however, cell morphology changes and structural damage were improved in different TLYS concentration groups, indicating that TLYS could inhibit hypoxia-induced cell damage. The expression of IL-1β and IL-18 in the model group was significantly higher than in the control group, indicating that inflammation occurred in the model group. It has been reported that NLRP3, GSDMD, and caspase-1 was upregulated in RTEC stimulated by high glucose levels (Xie et al., 2019). We investigated the related proteins to see if hypoxia can cause inflammation by activating the NLRP3 pathway. The model group had higher levels of NLRP3, GSDMD, and caspase-1 expression than the control group, indicating that hypoxia can cause inflammation by activating the NLRP3 pathway. After 12 h of TLYS intervention at various concentrations, NLRP3, GSDMD, IL-1β, IL-18 and caspase-1 proteins were significantly reduced. It suggests that TLYS may inhibit NLRP3 and thus prevent the activation of pro-Caspase-1 to Caspase-1, resulting in the inability of IL-1β and IL-18 precursors to shear into active IL-1β and IL18. The present study found that pyroptosis occurred clearly in hypoxia-induced RTEC, and TLYS may exert its protective effect on hypoxia-induced RTEC by inhibiting the NLRP3-mediated pyroptosis pathway.

Current studies have shown that MCC950, a potent and selective small-molecule inhibitor of NLRP3, has therapeutic effects in several renal diseases, diabetes, and its complications. NLRP3 inflammasome is activated in podocytes of patients with lupus nephritis and mice, and inhibition of NLRP3 by MCC950 attenuates proteinuria, renal pathological damage, and podocyte fusion in mice with lupus nephritis (Fu et al., 2017). MCC950 decreased blood pressure and improved renal inflammation, renal fibrosis, and renal dysfunction in mice with hypertension model (Krishnan et al., 2016; Krishnan et al., 2019). MCC950 was used as a positive control drug in the current study to intervene in hypoxia-induced the tubular epithelial cells injury, and the results showed that cell fibrosis degree, as well as IL-1β and IL-18 levels, decreased in the inhibitor group compared to the model group. MCC950 may influence the development of tubular epithelial cell fibrosis by inhibiting the activation of NLRP3 inflammatory vesicles. MCC950 inhibits hypoxia-induced inflammatory response and fibrosis in RTECs by decreasing NLRP3 expression, Caspase-1 activation, inhibiting inflammatory mediators IL-1β and IL-18 expression, and eventually decreasing α-SMA expression.

Our team conducted the TLYS decoction fingerprint study by UHPLC-MS. A total of 37 compounds were identified (Jia et al., 2021). Studies have also shown that Salvianolic acid B can alleviate I/R injury in mice by inhibiting caspase-1/GSDMD-mediated pyroptosis via the Nrf2/NLRP3 signaling pathway (Pang et al., 2020). Endotoxemia-induced mortality and cardiomyopathy are reduced by Sodium tanshinone IIA sulfonate, which may be linked to NLRP3 inflammasome suppression (Chen et al., 2021). The protective mechanism of Hydroxysafflor yellow A in H/R-induced cardiomyocyte damage is linked to the NLRP3 inflammasome activation (Ye JX. et al., 2020). In Myocardial ischemia/reperfusion injury, Hydroxysafflor yellow A can activate AMPK to reduce the NLRP3 inflammasome via blocking the mTOR pathway (Ye J. et al., 2020). These ingredients may be the basis of TLYS inhibitors of pyroptosis. Herbal compounding, on the other hand, is the combination of several herbs with complex chemical compositions. These chemical components both promote and enhance the action of the drug, while also inhibiting and affecting the overall action of the drug. The glycosides extracted from the original solution of TLYS are primarily Salvianolic acid B, Sodium tanshinone IIA sulfonate, and Hydroxysafflor yellow A, but they may also contain other components. When the drug dosage is increased, these components may inhibit the anti-pyroptosis effect. However, the precise cause must be determined.

In conclusion, this study found that pyroptosis contributes to kidney damage following UUO. Furthermore, the findings demonstrated that TLYS exert significant effects on such injury via a mechanism closely related to the inhibition of the activation of the classical pyroptosis pathway mediated by the NLRP3 inflammasome.

DATA AVAILABILITY STATEMENT

The original contributions presented in the study are included in the article/Supplementary Material, further inquiries can be directed to the corresponding authors.

ETHICS STATEMENT

The animal study was reviewed and approved by the Laboratory Animal Ethics Committee of Dongfang Hospital affiliated with Beijing University of Chinese Medicine.

AUTHOR CONTRIBUTIONS

JQ, LH, and QJ designed the experiments. XZ and YZ performed the animal experiments. QJ and XZ conducted the molecular biology experiments. XZ and QJ analyzed and interpreted the data. QJ and LH wrote the manuscript.

REFERENCES

Broz, P., Pelegrín, P., and Shao, F. (2020). The Gasdermins, a Protein Family Executing Cell Death and Inflammation. *Nat. Rev. Immunol.* 20 (3), 143–157. doi:10.1038/s41577-019-0228-2

Chen, P., An, Q., Huang, Y., Zhang, M., and Mao, S. (2021). Prevention of Endotoxin-Induced Cardiomyopathy Using Sodium Tanshinone IIA Sulfonate: Involvement of Augmented Autophagy and NLRP3 Inflammasome Suppression. *Eur. J. Pharmacol.* 909, 174438. doi:10.1016/j.ejphar.2021.174438

Chevalier, R. L., Forbes, M. S., and Thornhill, B. A. (2009). Ureteral Obstruction as a Model of Renal Interstitial Fibrosis and Obstructive Nephropathy. *Kidney Int.* 75 (11), 1145–1152. doi:10.1038/ki.2009.86

Chung, S. D., Lai, T. Y., Chien, C. T., and Yu, H. J. (2012). Activating Nrf-2 Signaling Depresses Unilateral Ureteral Obstruction-Evoked Mitochondrial Stress-Related Autophagy, Apoptosis and Pyroptosis in Kidney. *PloS one* 7 (10), e47299. doi:10.1371/journal.pone.0047299

Fu, R., Guo, C., Wang, S., Huang, Y., Jin, O., Hu, H., et al. (2017). Podocyte Activation of NLRP3 Inflammasomes Contributes to the Development of Proteinuria in Lupus Nephritis. *Arthritis Rheumatol.* 69 (8), 1636–1646. doi:10.1002/art.40155

Guo, H., Bi, X., Zhou, P., Zhu, S., and Ding, W. (2017). NLRP3 Deficiency Attenuates Renal Fibrosis and Ameliorates Mitochondrial Dysfunction in a Mouse Unilateral Ureteral Obstruction Model of Chronic Kidney Disease. *Mediat. Inflamm.* 2017, 8316560. doi:10.1155/2017/8316560

Hosseinian, S., Rad, A. K., Bideskan, A. E., Soukhtanloo, M., Sadeghnia, H., Shafei, M. N., et al. (2017). Thymoquinone Ameliorates Renal Damage in Unilateral Ureteral Obstruction in Rats. *Pharmacol. Rep.* 69 (4), 648–657. doi:10.1016/j.pharep.2017.03.002

Humphreys, B. D. (2018). Mechanisms of Renal Fibrosis. *Annu. Rev. Physiol.* 80, 309–326. doi:10.1146/annurev-physiol-022516-034227

Jia, Q., Han, L., Zhang, X., Yang, W., Gao, Y., Shen, Y., et al. (2021). Tongluo Yishen Decoction Ameliorates Renal Fibrosis via Regulating Mitochondrial Dysfunction Induced by Oxidative Stress in Unilateral Ureteral Obstruction Rats. *Front. Pharmacol.* 12, 762756. doi:10.3389/fphar.2021.762756

Kesavardhana, S., Malireddi, R. K. S., and Kanneganti, T. D. (2020). Caspases in Cell Death, Inflammation, and Pyroptosis. *Annu. Rev. Immunol.* 38, 567–595. doi:10.1146/annurev-immunol-073119-095439

Kim, S. M., Kim, Y. G., Kim, D. J., Park, S. H., Jeong, K. H., Lee, Y. H., et al. (2018). Inflammasome-Independent Role of NLRP3 Mediates Mitochondrial Regulation in Renal Injury. *Front. Immunol.* 9, 2563. doi:10.3389/fimmu.2018.02563

Kim, Y. G., Kim, S. M., Kim, K. P., Lee, S. H., and Moon, J. Y. (2019). The Role of Inflammasome-dependent and Inflammasome-independent NLRP3 in the Kidney. *Cells* 8 (11). doi:10.3390/cells8111389

Klahr, S., and Morrissey, J. (2002). Obstructive Nephropathy and Renal Fibrosis. *Am. J. Physiol. Ren. PhysiolRenal Physiol.* 283 (5), F861–F875. doi:10.1152/ajprenal.00362.2001

Krishnan, S. M., Dowling, J. K., Ling, Y. H., Diep, H., Chan, C. T., Ferens, D., et al. (2016). Inflammasome Activity Is Essential for One Kidney/deoxycorticosterone Acetate/salt-Induced Hypertension in Mice. *Br. J. Pharmacol.* 173 (4), 752–765. doi:10.1111/bph.13230

Krishnan, S. M., Ling, Y. H., Huuskes, B. M., Ferens, D. M., Saini, N., Chan, C. T., et al. (2019). Pharmacological Inhibition of the NLRP3 Inflammasome Reduces Blood Pressure, Renal Damage, and Dysfunction in Salt-Sensitive Hypertension. *Cardiovasc Res.* 115 (4), 776–787. doi:10.1093/cvr/cvy252

Liu, B. C., Tang, T. T., Lv, L. L., and Lan, H. Y. (2018). Renal Tubule Injury: a Driving Force toward Chronic Kidney Disease. *Kidney Int.* 93 (3), 568–579. doi:10.1016/j.kint.2017.09.033

Lv, W., Booz, G. W., Wang, Y., Fan, F., and Roman, R. J. (2018). Inflammation and Renal Fibrosis: Recent Developments on Key Signaling Molecules as Potential Therapeutic Targets. *Eur. J. Pharmacol.* 820, 65–76. doi:10.1016/j.ejphar.2017.12.016

Meng, X. M., Nikolic-Paterson, D. J., and Lan, H. Y. (2014). Inflammatory Processes in Renal Fibrosis. *Nat. Rev. Nephrol.* 10 (9), 493–503. doi:10.1038/nrneph.2014.114

Nathan, C., and Ding, A. (2010). Nonresolving Inflammation. *Cell* 140 (6), 871–882. doi:10.1016/j.cell.2010.02.029

Pang, Y., Zhang, P. C., Lu, R. R., Li, H. L., Li, J. C., Fu, H. X., et al. (2020). Andrade-Oliveira Salvianolic Acid B Modulates Caspase-1-Mediated Pyroptosis in Renal Ischemia-Reperfusion Injury via Nrf2 Pathway. *Front. Pharmacol.* 11, 541426. doi:10.3389/fphar.2020.541426

Schroder, K., and Tschopp, J. (2010). The Inflammasomes. *Cell* 140 (6), 821–832. doi:10.1016/j.cell.2010.01.040

Swanson, K. V., Deng, M., and Ting, J. P. (2019). The NLRP3 Inflammasome: Molecular Activation and Regulation to Therapeutics. *Nat. Rev. Immunol.* 19 (8), 477–489. doi:10.1038/s41577-019-0165-0

Tajima, T., Yoshifuji, A., Matsui, A., Itoh, T., Uchiyama, K., Kanda, T., et al. (2019). β-Hydroxybutyrate Attenuates Renal Ischemia-Reperfusion Injury through its Anti-pyroptotic Effects. *Kidney Int.* 95 (5), 1120–1137. doi:10.1016/j.kint.2018.11.034

Tang, P., Liu, H., Lin, B., Yang, W., Chen, W., Lu, Z., et al. (2020). Spatholobi Caulis Dispensing Granule Reduces Deep Vein Thrombus Burden through Antiinflammation via SIRT1 and Nrf2. *Phytomedicine* 77, 153285. doi:10.1016/j.phymed.2020.153285

Tang, P. M., Nikolic-Paterson, D. J., and Lan, H. Y. (2019). Macrophages: Versatile Players in Renal Inflammation and Fibrosis. *Nat. Rev. Nephrol.* 15 (3), 144–158. doi:10.1038/s41581-019-0110-2

Vilaysane, A., Chun, J., Seamone, M. E., Wang, W., Chin, R., Hirota, S., et al. (2010). The NLRP3 Inflammasome Promotes Renal Inflammation and Contributes to CKD. *J. Am. Soc. Nephrol.* 21 (10), 1732–1744. doi:10.1681/ASN.2010020143

Xie, C., Wu, W., Tang, A., Luo, N., and Tan, Y. (2019). lncRNA GAS5/miR-452-5p Reduces Oxidative Stress and Pyroptosis of High-Glucose-Stimulated Renal Tubular Cells. *Diabetes Metab. Syndr. Obes.* 12, 2609–2617. doi:10.2147/DMSO.S228654

Xu, X. X., Zhang, X. H., Diao, Y., and Huang, Y. X. (2017). Achyranthes Bidentate Saponins Protect Rat Articular Chondrocytes against Interleukin-1β-Induced Inflammation and Apoptosis In vitro. *Kaohsiung J. Med. Sci.* 33 (2), 62–68. doi:10.1016/j.kjms.2016.11.004

Ye, J., Lu, S., Wang, M., Ge, W., Liu, H., Qi, Y., et al. (2020a). Hydroxysafflor Yellow A Protects against Myocardial Ischemia/Reperfusion Injury via Suppressing NLRP3 Inflammasome and Activating Autophagy. *Front. Pharmacol.* 11, 1170. doi:10.3389/fphar.2020.01170

Ye, J. X., Wang, M., Wang, R. Y., Liu, H. T., Qi, Y. D., Fu, J. H., et al. (2020b). Hydroxysafflor Yellow A Inhibits Hypoxia/reoxygenation-Induced Cardiomyocyte Injury via Regulating the AMPK/NLRP3 Inflammasome Pathway. *Int. Immunopharmacol.* 82, 106316. doi:10.1016/j.intimp.2020.106316

Ye, T., Xiong, D., Chen, L., Li, Y., Gong, S., Zhang, L., et al. (2020c). Effect of Danshen on TLR2-Triggered Inflammation in Macrophages. *Phytomedicine* 70, 153228. doi:10.1016/j.phymed.2020.153228

Yu, P., Zhang, X., Liu, N., Tang, L., Peng, C., and Chen, X. (2021). Pyroptosis: Mechanisms and Diseases. *Signal Transduct. Target Ther.* 6 (1), 128. doi:10.1038/s41392-021-00507-5

Zhang, B., Chen, X., Ru, F., Gan, Y., Li, B., Xia, W., et al. (2021a). Liproxstatin-1 Attenuates Unilateral Ureteral Obstruction-Induced Renal Fibrosis by Inhibiting Renal Tubular Epithelial Cells Ferroptosis. *Cell Death Dis.* 12 (9), 843. doi:10.1038/s41419-021-04137-1

Zhang, Y., Zhang, R., and Han, X. (2021b). Disulfiram Inhibits Inflammation and Fibrosis in a Rat Unilateral Ureteral Obstruction Model by Inhibiting

Gasdermin D Cleavage and Pyroptosis. *Inflamm. Res.* 70 (5), 543–552. doi:10.1007/s00011-021-01457-y

Zhang, Z., Wu, Z., Zhu, X., Hui, X., Pan, J., and Xu, Y. (2014). Hydroxy-safflor Yellow A Inhibits Neuroinflammation Mediated by $A\beta_{1-42}$ in BV-2 Cells. *Neurosci. Lett.* 562, 39–44. doi:10.1016/j.neulet.2014.01.005

Conflict of Interest: The authors declare that the research was conducted in the absence of any commercial or financial relationships that could be construed as a potential conflict of interest.

Publisher's Note: All claims expressed in this article are solely those of the authors and do not necessarily represent those of their affiliated organizations, or those of the publisher, the editors and the reviewers. Any product that may be evaluated in this article, or claim that may be made by its manufacturer, is not guaranteed or endorsed by the publisher.

frontiers | Frontiers in Pharmacology

REVIEW
published: 08 July 2022
doi: 10.3389/fphar.2022.932172

Potential Therapeutic Strategies for Renal Fibrosis: Cordyceps and Related Products

Wei Tan[1†], *Yunyan Wang*[1†], *Hongmei Dai*[2], *Junhui Deng*[1], *Zhifen Wu*[1], *Lirong Lin*[1] *and Jurong Yang*[1*]

[1]Nephrology, The Third Affiliated Hospital of Chongqing Medical University, Chongqing, China, [2]Nephrology, YunYang County People's Hospital, Chongqing, China

At present, there is no effective drug for the treatment of renal fibrosis; in particular, a safe and effective treatment for renal fibrosis should be established. Cordyceps has several medical effects, including immunoregulatory, antitumor, anti-inflammatory, and antioxidant effects, and may prevent kidney, liver, and heart diseases. Cordyceps has also been reported to be effective in the treatment of renal fibrosis. In this paper, we review the potential mechanisms of Cordyceps against renal fibrosis, focusing on the effects of Cordyceps on inflammation, oxidative stress, apoptosis, regulation of autophagy, reduction of extracellular matrix deposition, and fibroblast activation. We also discuss relevant published clinical trials and meta-analyses. Available clinical studies support the possibility that Cordyceps and related products provide benefits to patients with chronic kidney diseases as adjuvants to conventional drugs. However, the existing clinical studies are limited by low quality and significant heterogeneity. The use of Cordyceps and related products may be a potential strategy for the treatment of renal fibrosis. Randomized controlled trial studies with good methodological quality, favorable experimental design, and large sample size are needed to evaluate the efficacy and safety of Cordyceps.

Keywords: cordyceps, renal fibrosis, Chinese herbal medicine, chronic kidney disease, mechanism

OPEN ACCESS

Edited by:
Zhiyong Guo,
Second Military Medical University, China

Reviewed by:
Lianli Shen,
Shanghai University of Traditional Chinese Medicine, China
Noha Mohammed Saeed,
Egyptian Russian University, Egypt
Chengguo Wei,
Mount Sinai Hospital, United States

***Correspondence:**
Jurong Yang
yjr923@163.com

[†]*These authors share first authorship*

Specialty section:
This article was submitted to Renal Pharmacology, a section of the journal Frontiers in Pharmacology

Received: *29 April 2022*
Accepted: *01 June 2022*
Published: *08 July 2022*

Citation:
Tan W, Wang Y, Dai H, Deng J, Wu Z, Lin L and Yang J (2022) Potential Therapeutic Strategies for Renal Fibrosis: Cordyceps and Related Products. Front. Pharmacol. 13:932172. doi: 10.3389/fphar.2022.932172

INTRODUCTION

Renal fibrosis (RF) is a common outcome of the progression of various chronic kidney diseases (CKD) and the main pathological change in the progression of CKD to end-stage renal disease (Humphreys, 2018). It includes glomerulosclerosis (GS), renal interstitial fibrosis (RIF), and arteriosclerosis and perivascular fibrosis (Djudjaj and Boor, 2019). It shows histopathological features of excessive extracellular matrix (ECM) deposition, tubular atrophy, inflammatory cell infiltration, and loss of peritubular microvasculature. Subsequent structural destruction and functional impairment of the organ occurs, with scarring and sclerosis of the renal parenchyma. Cells involved in this event include renal tubular epithelial cells (TECs), endothelial cells (ECs), fibroblasts, pericytes, macrophages, and mast cells (Sun et al., 2016; Yan et al., 2021). In addition, cellular and molecular events such as inflammatory injury, oxidative stress, apoptosis, fibroblast activation, and epithelial–mesenchymal transition (EMT) are closely associated with RF (Liu et al., 2017; Nogueira et al., 2017). Despite significant progress in preclinical research of the mechanisms of RF and its therapeutic targets (Nogueira et al., 2017; Bai et al., 2021; Yan et al., 2021; Ruiz-Ortega et al., 2022), good target effects have not been demonstrated in clinical practice (Vincenti et al., 2017; Voelker et al., 2017). Therefore, there is still a lack of effective

treatment that specifically targets RF. It is especially important to find safe and effective treatments for RF.

Chinese herbal medicines (CHMs) have been used for thousands of years in the treatment of kidney disease. Chinese herbs and fungi with potential kidney benefits include Cordyceps, Sairei-to, *Rheum* spp., *Salvia miltiorrhiza* and its components, and Magnesium lithospermate B (Wojcikowski et al., 2004). Anti-RF mechanisms of CHMs include anti-inflammatory and antioxidant effects, inhibition of EMT, reduction of ECM deposition, immune regulation, regulation of autophagy, inhibition of apoptosis, and control of hemorheology (Zhao et al., 2020). In this paper, we review the mechanisms of Cordyceps and related products in the treatment of RF (**Table 1**), as well as relevant clinical trials and meta-analyses (**Table 2**). We also discuss the possible nephrotoxicity of Cordyceps and the possible antifibrotic effects of the compounded formulation.

Cordyceps is a fungus that colonizes the larvae of moths. It has been used for centuries as a medicine in China, Japan, and other Asian countries. It has several species, including *Cordyceps sinensis*, *Cordyceps militaris*, and *Cordyceps cicadae*. Cordyceps has a variety of medicinal properties or bioactive compounds, including nucleosides, polysaccharides, cyclodepsipeptides, sterols, alkaloids, and phenolics (Olatunji et al., 2018), which show immunomodulatory, antitumor, anti-inflammatory, antioxidant, renoprotective, and other effects (Das et al., 2020). Cordyceps has shown potential promise as an adjunct to conventional medicine to decrease serum creatinine (Scr), increase creatinine clearance, reduce proteinuria, and alleviate CKD-related complications (Zhang et al., 2014). Based on the network pharmacology tools that are used to investigate the molecular mechanism of Cordyceps for the treatment of diabetic nephropathy (DN), seven active ingredients were screened from Cordyceps, 293 putative target genes were identified, and 85 overlapping targets matching DN were identified as potential therapeutic targets, such as tumor necrosis factor (TNF), mitogen-activated protein kinase 1, epidermal growth factor receptor (EGFR), angiotensin-converting enzyme, and Caspase-9. Cordyceps are involved in an inflammatory response, apoptosis, oxidative stress, insulin resistance, and other biological processes through these pathways (Li et al., 2021).

MECHANISMS OF CORDYCEPS AND RELATED PRODUCTS AGAINST RENAL FIBROSIS

Cordyceps Relieves Inflammation

Inflammation is the initiator of RF, and persistent chronic inflammation is considered a hallmark feature of CKD (Meng, 2019). In response to pathogenic factors, damaged renal TECs recruit inflammatory cells to the renal interstitial region, and these inflammatory cells then produce large amounts of proinflammatory and profibrotic cytokines (Gewin et al., 2017). Various active ingredients in Cordyceps have anti-inflammatory effects (Phull et al., 2022). They have been shown to protect against liver fibrosis through anti-inflammatory effects (Xu et al., 2021) (Ying-Mei et al., 2020). Cordyceps extract attenuates renal histological changes, reduces Scr and blood urea nitrogen (BUN) levels, and decreases inflammatory factors in acute kidney injury (AKI), including renal ischemia/reperfusion injury (Han et al., 2020) and cisplatin-induced AKI (Deng et al., 2020). In RF related to streptozotocin (STZ), or alloxan monohydrate–induced DN, the active components of Cordyceps, *Cordyceps cicadae* polysaccharides (CCP) or N^6-(2-hydroxyethyl) adenosine (HEA), are effective in reducing the expression of proinflammatory factors TNF-α, IL-1β, and IL-6 in serum and kidney and in reducing the expression of interstitial fibrosis-associated proteins α-SMA and collagen I (Wang et al., 2019; Yang et al., 2020). *In vitro*, CCP also reduces the release of lipopolysaccharide-induced proinflammatory factors and TGF-β-induced activation of fibroblasts (Yang et al., 2020). Unilateral ureteral obstruction (UUO) is a classical RF model, and Cordyceps extract HEA reduces fibrosis-associated proteins TGF-β1, α-SMA, collagen I, and fibronectin, and inflammatory factors TNF-α, IL-6, and IL-1β in renal tissue 14 days after UUO (Zheng et al., 2018). Zheng et al.'s (2018) study initially explored the effect of HEA on inflammatory cells and found that HEA blocked the accumulation of M1 macrophages and induced the accumulation of M2 macrophages in the kidney as reflected by the positive detection of the F4/80 antigen. The role of M2 macrophages in fibrosis is controversial (Ricardo et al., 2008) (Lin et al., 2010), but the M1/M2 macrophage ratio is an important stage in the development of RIF. However, this study did not further distinguish between the subtypes of M2.

The abovementioned studies have explored the regulatory mechanism of Cordyceps extract against inflammation in RF by inhibiting the TGF-β1/Smad and TLR4/NF-κB signaling pathways (Zheng et al., 2018; Yang et al., 2020). Sun et al. found that p-TLR4, TLR4, p-NF-κB, NF-κB, IL-1 β, and TNF-α levels were effectively reduced by Cordycepin treatment in human embryonic kidney 293T cells. However, Cordycepin did not reduce the levels of these molecules when TLR4 was silenced. These results suggest that Cordycepin may affect the NF-κB signaling pathway through TLR4 (Sun et al., 2019). TLRs/NF-κB activate the downstream inflammasome NOD-like receptor family pyrin domain containing 3 (NLRP3) (Xue et al., 2019), which promotes the maturation of proinflammatory factors IL-1β and IL-18 by activating Caspase-1 (Liston and Masters, 2017). Multiple studies have shown that the NLRP3 inflammasome and its downstream pyroptosis and inflammation play an important role in the development of RF (Ma et al., 2022) (Ram et al., 2022; Wang et al., 2022). It has been shown that *Ophiocordyceps sinensis* causes inhibition of mRNA and protein expression of NLRP3 inflammasome and downstream effectors IL-1β and IL-18 in a rat model of DN (Wang et al., 2018). Thus, Cordyceps and related products are effective in relieving inflammation in RF through multiple mechanisms.

Cordyceps Attenuates Oxidative Stress

The kidney is a highly metabolically active organ with mitochondria rich in oxidative reactions and susceptible to oxidative stress damage. Oxidative stress and inflammation interact to play a key role in renal tissue destruction, irreversible loss of renal function, and progression of RF (Xu et al., 2015; Darby and Hewitson, 2016; Richter and Kietzmann, 2016). Normal cells produce small amounts of reactive oxygen species (ROS), which play an important physiological role. Free

radical–scavenging enzymes and antioxidants maintain oxygen metabolism homeostasis by activating transcription factors, regulating physiologically active substances and inflammatory immunity, and promoting cell proliferation and differentiation. Oxidative stress occurs when the balance between ROS and reactive nitrogen species and the antioxidant defense system is disrupted, that is, when the production of pro-oxidants or ROS exceeds the endogenous antioxidant capacity (Sies et al., 2017). It has been shown that oxidative stress promotes the progression of RF (Aranda-Rivera et al., 2021); if oxidative stress is suppressed, RF can be attenuated (Liao et al., 2022; Lo et al., 2022). Antioxidant enzymes, such as superoxide dismutase (SOD), catalase, and glutathione peroxidase (GSH-Px), protect cells from damage caused by oxygen free radicals. Malondialdehyde (MDA) is one of the products of the reaction between lipids and oxygen free radicals, and it accumulates during oxidative stress. Cordyceps improves the redox properties of CKD by affecting the levels of NO, SOD, and MDA in serum. In rat models of DN (Liu et al., 2016; Wang et al., 2019) and membranous nephropathy (Song et al., 2016), both *C. militaris* and HEA showed excellent ability to attenuate oxidative stress, elevated SOD and GSH, and decreased MDA levels. Using diclofenac or meloxicam to induce oxidative stress, HEA intervention significantly reduced the level of ROS in human proximal tubular cells (HK-2) cells (Chyau et al., 2021). In rats with adenine-induced chronic renal failure, *Cordyceps cicadae* and *Paecilomyces cicadae* effectively reduced serum urea and creatinine levels, improved renal histopathology, inhibited oxidative stress, and enhanced antioxidant capacity (Li et al., 2019). In a CKD mouse model established by adenine gavage, *Ophiocordyceps lanpingensis* polysaccharides elevated SOD and GSH-PX, decreased ROS and MDA, improved histopathological staining, and decreased fibrosis-related proteins TGF-β1, α-SMA, and collagen I (Zhou et al., 2021). Cordyceps and related products have a favorable ability to attenuate oxidative stress, but the mechanisms involved are not well understood.

Cordyceps Inhibits Apoptosis

A variety of kidney injury factors may trigger apoptosis, including ischemia/reperfusion injury (Xu et al., 2019), cisplatin-induced kidney injury (Yang et al., 2018), and DN (Peng et al., 2015). Apoptosis (a programmed cell death) of glomerular ECs, podocytes, and TECs is closely associated with RF (Thomas et al., 1998; Docherty et al., 2006). Inhibition of apoptosis as a therapeutic target can alleviate fibrosis (Chen et al., 2021; Xia et al., 2021; Park et al., 2022). Cordyceps downregulates apoptosis in ischemia/reperfusion injury and Cyclosporine A–induced renal tubular dysfunction (Shahed et al., 2001; Chyau et al., 2014). Apoptosis is also considered an important mechanism in contrast-induced nephropathy (CIN). *C. sinensis* prevents CIN in diabetic rats by decreasing the expression of apoptosis-related proteins Caspase-3 and Bax and increasing the expression of antiapoptotic protein Bcl-2. Mechanistically, *C. sinensis* decreases the expression of JNK protein and increases the expression of ERK protein (Zhao et al., 2018). Renal tubular interstitial fibrosis is a typical pathological feature of hypertensive kidney injury. In a spontaneous hypertension rat model, *C. cicadae* reduces interstitial fiber deposition, α-SMA expression, apoptosis, and Caspase-3 activity by regulating the SIRT1/p53 signaling pathway (Huang et al., 2020). *In vitro*, the major renal damage caused by hepatitis B virus infection is hepatitis B virus X (HBx)–induced apoptosis of renal TECs, which is related to the increased Caspase-3 and Caspase-9 activity and increased PI3K/Akt pathway activity. *C. sinensis* attenuates all of these HBx-induced responses, at least in part by inhibiting the PI3K/Akt signaling pathway (He et al., 2020). Cordyceps and related products have been shown to inhibit apoptosis *in vivo* and *in vitro*, but the mechanisms involved have not been unified.

Cordyceps Regulates Autophagy

Autophagy is a "self-consuming" cell death pathway that degrades most cytoplasmic components by forming autophagosomes and autolysosomes (Yang and Klionsky, 2010). Basal autophagy in the kidney is critical for maintaining renal homeostasis, structure, and function. Namely, basal autophagy removes potentially dysfunctional organelles and long-lived proteins to maintain cellular homeostasis. In response to environmental and intracellular stress, autophagy may serve as an adaptive response to ensure cell survival. However, autophagy may also play a role in cellular dysfunction and organ lesions (Tang et al., 2020), such as AKI (Kaushal and Shah, 2016), AKI-CKD (Baisantry et al., 2016), and DN (Lenoir et al., 2015). The role of autophagy in RF is controversial. It has been reported that sustained activation of autophagy in renal tubular cells promotes interstitial fibrosis, and inhibition of autophagy with chloroquine or selective deletion of Atg7 in proximal tubules alleviates RF in UUO mice (Livingston et al., 2016). Several studies have also reported antifibrotic effects of autophagy, whereas inhibition of autophagy by 3-methyladenine exacerbated RF in a UUO rat model, suggesting that autophagy may exert antifibrotic effects by attenuating renal tubular cell injury (Kim et al., 2012). In STZ-induced DN mice, *C. militaris* polysaccharides (CMP) decrease collagen deposition in the kidney and increase the rate of autophagy; promote the expression of autophagy-specific protein Atg5, Beclin1, and LC3; and decrease the expression of p62 protein in the kidney. This suggests that CMP administration significantly enhances autophagy (Chen et al., 2019a). In a hypertensive nephropathy model, *Cordyceps cicadae* may attenuate the expression of fibrosis-associated proteins. It ameliorates RF induced by hypertension by downregulating autophagy-related proteins LC3II and Beclin-1, thereby significantly inhibiting autophagic vesicles and attenuating autophagic stress. This effect may be attributed to the regulation of SIRT1 pathway-mediated autophagic stress and is achieved by modulating the autophagy regulator forkhead box class O3a (FOXO3a) and oxidative stress (Cai et al., 2021). The regulatory effect of Cordyceps on autophagy is indisputable, but autophagy itself is diverse and can be divided into microautophagy, chaperone-mediated autophagy, and macroautophagy, and macroautophagy can be divided into nonselective autophagy and selective autophagy depending on whether the substrate is selective or not. Because autophagy is environment dependent and may play different roles at different stages of the disease, different cell types do not respond consistently to the autophagy activation, resulting in a bidirectional

TABLE 1 | Mechanisms of Cordyceps and related products against renal fibrosis.

Compound/extract	Animal/cell	Model/ inducer	Outcomes	Targets/pathway	Mode of action	References
CCP	SD rats	HFD + STZ	TNF-α↓, IL-1β↓, IL-6↓ Inflammatory cell infiltration↓ CTGF↓, MMP-2↓, HYP↓ Collagen deposition↓ a-SMA and Collagen I expression↓ Regulation of dysbiosis of gut microbiota	Blocking the TLR4/NF-κB and TGF-β1/Smad signaling pathway	Anti-inflammatory; regulation of dysbiosis of gut microbiota	Yang et al. (2020)
	NRK-52E Cells NRK-49F cells	LPS TGF-β	TNF-α↓, IL-1β↓, IL-6↓ Collagen I↓, Fibronectin↓, α-SMA↓			
HEA	C57BL6/J mice	UUO	Integrity of renal parenchymal cells↑ Collagen deposition↓ TGF-β1↓, α-SMA↓, collagen I↓, Fibronectin↓ TNF-α↓, IL-6↓, IL-1β↓ M1↓, M2↑	Inhibition of TGF-β1/Smad and NF-κB signaling pathways	Anti-inflammatory	Zheng et al. (2018)
	RAW 264.7 cells NRK-49F cells	LPS TGF-β	TNF-α↓,IL-1β↓, IL-10↑ Fibronectin↓,α-SMA↓, collagen I			
HEA	SD rats	Alloxan monohydrate	TNF-α↓, IL-1β↓, IL-6↓ SOD↑, CAT↑, GSH↑, MDA ↓ Tubular necrosis↓, inflammatory infiltration↓, thickening of the membrane basement↓	Inhibition of TGF-β1 and NF-κB	Anti-inflammatory; antioxidative stress	Wang et al. (2019)
Cordycepin	HEK293T cells	—	IL-1 β↓, TNF-α↓	Inhibition of TLR4/NF-κB pathway	Anti-inflammatory	Sun et al. (2019)
Cordyceps cicadae/ Paecilomyces cicadae	SD rats	250 mg/kg adenine	MDA↓, GSH↓, SOD↑ Kidney indices↓, the number of the glomerulus↑ Interstitial inflammation in the proximal and distal convoluted tubules↓	May be related to the downregulated PAI-1	Antioxidative stress; anti-inflammatory	Li et al. (2019)
Ophiocordyceps Lanpingensis	C57BL/6 Mice	0.25% adenine	Ameliorate the CKD pathological Changes Recruitment of macrophages↓ SOD↑, GSH-PX↑, ROS↓, MDA↓ TNF-α↓, IL-1β↓, IL-10↑ Apoptosis cells↓, BAX↓, Caspase-3↓, Caspase-9↓, Bcl-2↑ Tissue fibrosis↓, TGF-β1 expression↓, α-SMA↓, collagen I↓	Inhibition of TLR4-mediated MAPK/NF-κB pathway	Antioxidative stress; anti-inflammatory Antiapoptosis	Zhou et al. (2021)
HEA	HK-2 cells	NSAIDs diclofenac/ meloxicam	ROS↓ Apoptosis cells↓	Regulates the GRP78/ATF6/ PERK/IRE1α/CHOP pathway	Antioxidative stress; antiapoptosis	Chyau et al. (2021)
Cordyceps militaris	SD rats	HFD + STZ	SOD↑, GSH-px↑, ROS↓, MDA↓ Inflammatory infiltrate↓	Phosphor-AKT↓ phosphor-GSK-3β↓	Antioxidative stress; anti-inflammatory	Liu et al. (2016)

(Continued on following page)

TABLE 1 | (*Continued*) Mechanisms of Cordyceps and related products against renal fibrosis.

Compound/extract	Animal/cell	Model/ inducer	Outcomes	Targets/pathway	Mode of action	References
Cordyceps cicadae	SHR/WK rats	SHR	Collagen deposition↓, a-SMA↓	Inhibition of SIRT1/p53 pathway	Antiapoptosis	Huang et al. (2020)
	Primary human RPTEC	AngII	Apoptosis cells↓, Caspase-3↓			
CMP	C57BL/6 mice	STZ	Collagen deposition↓ CD68↓, IL-1β↓, IL-6↓, MCP-1↓ Autophagosome↑ Atg5↑, beclin1↑, LC3↑, p62↓ GSH↑, MDA↓	—	Activation of autophagy; anti-inflammatory; antioxidative stress	Chen et al. (2019a)
Cordyceps cicadae	SHR/WK rats	SHR	Collagen deposition↓ TGFβ1↓, α-SMA↓, fibronectin↓, collagen I↓ Apoptosis cells↓ LC3II↓, beclin-1↓, SQSTM1/p62↓ SOD↑, MDA ↓	Activation of SIRT1/FOXO3a/ROS	Inhibition of autophagy; antioxidative stress	Cai et al. (2021)
	NRK-52E cells	AngII/ rapamycin	Collagen I↓, α-SMA↓ LC3II↓, beclin-1↓			
Nucleoside/ nucleobase extract	C57BL/6 mice	STZ	Collagen deposition↓ Fibronectin↓, collagen I↓ E-cadherin↑, α-SMA↓	Phosphor-p38↓ phosphor-ERK↓	Inhibition of EMT and ECM deposition	Dong et al. (2019)
	HK-2 cells	HG	Morphological and phenotypic changes↓ E-cadherin↑, α-SMA↓ Fibronectin↓, collagen I↓			
Ergosterol peroxide	NRK-49F cells	TGF-β1	Renal fibroblast proliferation rate↓ Fibronectin↓, a-SMA↓, vimentin↓, CTGF↓	Blocking the phosphorylation of ERK1/2, p38, and JNK pathway	Ameliorates TGF-β1-induced activation of kidney fibroblasts	Zhu et al. (2014)
CmNo1 extract	C57BL/6J mice	HFD + STZ	Collagen IV↓	TGF-β1↓	Inhibition of collagen deposition	Yu et al. (2016)
Cordyceps sinensis	SD rats	5/6 nephrectomy	Interstitial fibrosis↓ E-cadherin↑, α-SMA↓, FSP1↓ TGF-β1↓, TβR1↓, TβR2↓, Smad2↓, Smad3↓, Smad7↑	Inhibition of TGF-β1/Smad pathway	Inhibition of EMT and ECM deposition	Pan et al. (2013)
3′-Deoxyadenosine	C57BL/6 mice	UUO	Collagen I↓, α-SMA↓ Interstitial myofibroblasts↓, fibrotic area↓	Reduced phosphorylation and total Smads through transcriptional repression	Inhibition of ECM deposition	Gu et al. (2013)
	NRK-52E	TGF-β/BMP-4	Collagen I↓, collagen IV↓			
Cordyceps sinensis	SD rats	UUO	Interstitial collagen deposition Masson↓, α-SMA↓	BAG3↓	Inhibition of EMT and ECM deposition	Du et al. (2015)
Hirsutella sinensis	C57BL/Ks mice	db/db diabetic	Interstitial fibrosis↓ TGF- β1↓, CTGF↓, VEGF↓, fibronectin↓, collagen I↓, collagen IV↓	Metabolites of the TCA cycle, glycolysis, pentose phosphate pathway, pyrimidine metabolism, and purine metabolism↓	Regulation of disturbed metabolome	Lu et al. (2019)

HFD, high-fat diet; TNF, tumor necrosis factor; IL-1, interleukin 1; IL-6, interleukin 1; CTGF, connective tissue growth factor; MMP-2, matrix metalloproteinase-2; HYP, hydroxyproline; a-Smooth muscle actin, a-shape memory alloy; TLR4, Toll-like receptor 4; NF-κB, Nuclear factor-kappaB; TGF-β1, transforming growth factor beta1; SOD, superoxide dismutase; CAT, catalase; GSH, glutathione; MDA, malondialdehyde; ROS, reactive oxygen species; Bcl-2, B-cell chronic lymphocytic leukemia/lymphoma-2; BAX, Bcl-2-associated X protein; GRP78, glucose-regulated protein 78; ATF6, activating transcription factor 6; PERK, protein kinase R (PKR)-like endoplasmic reticulum kinase; IRE1α, inositol-requiring enzyme 1 alpha; CHOP, C/EBP homologous protein; SHR, spontaneously hypertensive; RPTEC, renal proximal tubular epithelial cells; WK, wistar-kyoto; SIRT1, Sirtuin-1; MCP-1, monocyte chemoattractant protein-1; Atg5, Autophagy Protein 5; LC3, light chain 3; SQSTM1, sequestosome1; FOXO3a, forkhead box class O3a; HG, high glucose; ERK, extracellular signal-regulated kinase; JNK, c-Jun N-terminal kinase; CmNo1, cordyceps militaris No.1; FSP1, ferroptosis suppressor protein 1; EMT, epithelial–mesenchymal transition; ECM, extracellular matrix; BAG3, Bcl-2-associated athanogene 3; VEGF, vascular endothelial growth factor; TCA, tricarboxylic acid.

TABLE 2 | Clinical studies with Cordyceps.

Study type	N	Therapeutic arms	Disease	Duration	Outcomes	References
RCT	98	COG vs. CG	CKD late stage 3 or stage 4	3 months	In COG group Inflammatory state and thickness of glomerular filtration membrane in renal tissue↑ Urinal protein↓ BUN↓, creatinine↓, EGFR↑ ($p < 0.05$) TG↓, TC↓, LDL-C↓, HDL-C↑ ($p < 0.05$) Cys-C ↓, MPO ↓, MDA ↓, NO ↑, SOD ↑ ($p < 0.05$)	Sun et al. (2019)
Study cohort	160	Bailing capsules + losartan vs. losartan	Diabetic glomerulosclerosis	—	In Bailing capsules + losartan group ORR↑, 91.25% vs. 78.75% DBP↓, SBP↓, Scr↓, BUN↓, 24 h UP↓, mALB↓, β2-MG↓,GFR↑ ($p < 0.01$) TCM points↓ ($p < 0.01$) SOD↑, ROS↓, 8-OHdG↓, hs-CRP↓, TGF-β1↓, SAA↓ ($p < 0.01$)	Yu et al. (2021)
Review	1746	Cordyceps vs. placebo, no treatment, or conventional treatment	CKD	—	In Cordyceps group Scr↓ (14 studies, 987 participants), Ccr↑ (6 studies, 362 participants), 24 h UP ↓ (4 studies, 211 participants)	Zhang et al. (2014)
Meta-analysis	3955	JSB capsules + ACEI/ARB vs. ACEI/ARB	Diabetic kidney disease	28 days–4 weeks	In JSB combined with ACEI/ARB group ORR↑ (OR 4.91; 95% CI 3.32–7.25) 24 h UP↓, UAER↓, Scr↓, BUN↓ ($p < 0.0001$) SBP↓, DBP↓,FBG↓, HA1c↓, TC↓, TG↓	Li and Xu, (2020)
Meta-analysis	2198	JSB + ARBs vs. ARBs	Early diabetic Nephropathy	8–28 weeks	In JSB + ARBs group ORR ↑ (OR 3.84; 95% CI: 2.37–6.24; $p < 0.000001$) 24 h UTP↓, UAER↓, ACR↓, Cys-C↓, TG↓ ($p < 0.000001$), BUN↓ ($p = 0.005$), Scr↓ ($p = 0.0006$), SBP↓ ($p = 0.0001$), DBP↓ ($p = 0.03$)	Lu et al. (2018)
Meta-analysis	4288	*Ophiocordyceps sinensis* + ACEI/ARB vs. ACEI/ARB	Diabetic kidney disease	4–24 weeks	In *Ophiocordyceps sinensis* + ACEI/ARB group 24 h UP↓, UAER↓, MAU↓, CRP↓, TG↓, TC↓ ($p < 0.000001$) BUN↓, Scr↓ ($p < 0.0001$) SBP↓ ($p = 0.006$)	Luo et al. (2015)
Meta-analysis	1941	Bailing capsules + control group treatment vs. routine treatment, and/or combined with Western medicine	Type 2 diabetic nephropathy	4–24 weeks	In the group containing Bailing capsules ORR ↑ (OR = 1.24; 95% CI: 1.11–1.38) 24 h urine total protein↓, UAER↓, Scr↓, BUN↓ ($p < 0.01$)	Sheng et al. (2020)
RCT	97	HEA-enriched *Cordyceps cicadae* Mycelium vs. placebo	—	3 months	No differences in symptoms or side effects between participants. There was also no significant difference between baseline measurements and the final analysis of biochemical analysis, such as kidney function, liver function, and blood electrolytes	Tsai et al. (2021)

COG, cordycepin group; CG, control group; GFR, glomerular filtration rates; TG, triglyceride; TC, total cholesterol; LDL-C, low-density lipoprotein cholesterol; HDL-C, low-density lipoprotein cholesterol; Cys-C, cystatin-C; MPO, myeloperoxidase; MDA, malondialdehyde; NO, nitric oxide; SOD, superoxide dismutase; DBP, diastolic blood pressure; SBP, systolic blood pressure; Scr, serum creatinine; BUN, blood urea nitrogen; 24 h UP, 24 h urine protein; mALB, urine microalbumin; β2-MG, β2 microglobulin; TCM, traditional chinese medicine; ROS, reactive oxygen species; 8-OhdG, 8-hydroxydeoxyguanine; hs-CRP, hypersensitive C-reactive protein; TGF-β1, transforming growth factor β1; SAA, serum amyloid A; Ccr, creatinine clearance; FBG, fasting blood glucose; HA1c, hemoglobin A1c; JSB, jinshuibao; CI, confidence interval; MD, mean difference; ORR, overall response rate; ACEI, angiotensin-converting enzyme inhibitors; ARB, angiotensin receptor blockers; 24 h UTP, 24 h urinary total protein; UAER, urinary albumin excretion rate; ACR, albumin-to-creatinine ratio; MAU, microalbuminuria.

effect of cellular autophagy on the process of RF. The regulatory role of autophagy in fibrosis remains to be further investigated.

Cordyceps Reduces Extracellular Matrix Deposition and Fibroblast Activation

Aberrant activation and proliferation of fibroblasts are believed to be key causes of the progression of RF (Zhou et al., 2017). Activated fibroblasts, which promote the production and release of ECM collagens I, III, and IV and fibronectin (Sun et al., 2016), are the main source of ECM during scar tissue formation. Myofibroblasts in RF can be derived from mesenchymal fibroblasts, bone marrow–derived fibroblasts, renal TECs, ECs, pericytes, and macrophages. TECs can produce stroma through the EMT to fibroblasts and myofibroblasts (Yan et al., 2021). In this process, TGF-β is the main driving factor. TGF-β induces fibroblast activation and proliferation as well as excessive synthesis and accumulation of ECM through downstream signaling pathways such as SMAD, BMMP-7, and CTGF, thereby promoting fibrosis. Targeted inhibition of TGF-β and its downstream signaling pathways delay fibrosis (Meng et al., 2016; Walton et al., 2017; Ma and Meng, 2019). In STZ-induced diabetic mice and high glucose–exposed HK-2 cells, the nucleoside/nucleobase–rich extract from Cordyceps increased E-cadherin expression; decreased α-SMA, fibronectin, and collagen I expression; inhibited EMT and ECM deposition; and improved the fibrotic morphology of tissues and cells. Cordyceps extract effectively inhibited the phosphorylation of p38 and ERK, did not affect the phosphorylation level of JNK, and had a synergistic effect on fibrosis with p38 or ERK inhibitors (Dong et al., 2019). Ergosterol peroxide from *Cordyceps cicadae* improves TGF-β1-induced renal fibroblast activation *via* the mitogen-activated protein kinases signaling pathway (Zhu et al., 2014). In DN C57BL/6J mice and 5/6 nephrectomy rats, *C. militaris* (Yu et al., 2016) and *C. sinensis* (Pan et al., 2013) counteracted RF and reduced the expression of fibrosis-associated proteins by inhibiting the TGF-β1 pathway. Further exploring downstream mechanisms, 3′-deoxyadenosine interfered with TGF-β and bone morphogenetic protein signaling by downregulating Smads at the transcriptional level. In that way, it induced decreases in collagen I and α-SMA, mesenchymal myofibroblast number, and fibrotic area (Gu et al., 2013). Cordyceps and its extracts are potential therapeutic strategies against fibrosis *via* the TGF-β/Smad and other pathways.

Other Mechanisms

In addition to the above mechanisms, *C. sinensis* attenuates RF in the UUO model by inhibiting Bcl-2-associated athanogene 3 (BAG3), which has been reported to be involved in cell proliferation, apoptosis, adhesion and migration, and EMT processes (Du et al., 2015).

Recent studies have reported that gut microbiota mediates RF (Liu et al., 2021). CMP reduce renal injury by regulating intestinal flora imbalance (Song and Zhu, 2020). In a study of CCP to attenuate fibrosis in DN, high-throughput pyrophosphate sequencing of 16S rRNA indicated that CCP regulated dysbiosis of the intestinal flora by increasing the relative abundance and proliferation of probiotic bacteria, thereby exerting a beneficial effect on tubulointerstitial fibrosis in DN rats (Yang et al., 2020).

Normal energy metabolism is particularly important for maintaining the structure and function of the kidney, and metabolic reprogramming is generally considered a key process in activating fibrosis in different organs, as it is in the kidney (Barcena-Varela et al., 2021). The balance of fatty acid oxidation and glycolysis directly affects ECM production and degradation or indirectly affects RF through inflammation and hypoxia (Zhu et al., 2021). Metabolomic analysis has been used to explore the metabolic regulatory effects of *C. sinensis* in a db/db diabetic mice model. *Hirsutella sinensis*—the anamorph of the traditional Chinese medicine *C. sinensis*—attenuates RF, ameliorates system-wide disorders of glucolipid metabolism and amino acid deficiency, and regulates excessive activation energy and nucleotide metabolism (Lu et al., 2019). This suggests that Cordyceps may have a potential role in the regulation of renal metabolism and, consequently, may ameliorate fibrosis.

CLINICAL STUDIES OF CORDYCEPS AND RELATED PRODUCTS IN TREATING CHRONIC KIDNEY DISEASES

In this section, we review published clinical studies of Cordyceps and related products, including two randomized controlled trial (RCT) studies, one cohort study, one review, and four meta-analyses (**Table 2**).

One study recruited 98 patients with CKD3 or CKD4 and randomized them to the Cordycepin group (COG, patients received 100 mg of *C. militaris* per day) and the control group (CG, patients received dried chickweed herb placebo per day). After 3 months of treatment, *C. militaris* improved the inflammatory status and thickness of the glomerular filtration membrane of renal tissues. Compared with the CG group, the COG group had lower CKD biomarkers ($p < 0.05$); higher EGFR ($p < 0.05$); lower serum Cys-C, MPO, and MDA levels; and higher NO and SOD levels ($p < 0.05$). *C. sinensis* reduced protein and mRNA levels of the TLR4/NF-κB signaling pathway ($p < 0.05$). This suggests that *C. militaris* improves CKD by affecting the TLR4/NF-κB redox signaling pathway (Sun et al., 2019).

To evaluate the efficacy of the Cordyceps preparation Bailing capsule combined with losartan in the treatment of diabetic GS, a cohort that included 160 patients with diabetic GS was randomly divided into the observation and the CGs; the observation group was treated with losartan and Bailing capsules, and the CG was treated with losartan. The overall effective rate was higher in the observation group than in the CG ($p < 0.05$). After the treatment, the DBP, SBP, Scr, 24 h UP, BUN, mALB, and β2-MG levels were lower, and the GFR was higher in the observation group than in the CG ($p < 0.01$). The traditional Chinese medicine symptom scores were lower in the observation group than in the CG ($p < 0.01$). The observation group also showed higher serum SOD and lower ROS, 8-OHdG, hs-CRP, TGF-β1, and SAA levels than the control group ($p < 0.01$). Bailing capsules combined with losartan improved the efficacy; improved the blood and urine biochemical indexes, the renal function, and the clinical symptoms; and reduced the oxidative stress. However, this

study has the disadvantages of small sample size, short follow-up time, and bias in case selection (Yu et al., 2021).

In another review, 22 studies involving 1,746 participants were included. *C. sinensis* was found to significantly reduce Scr, increase creatinine clearance, and reduce 24 h proteinuria in patients with CKD. All 22 studies were published in Chinese and conducted in Chinese hospitals. The quality of evidence from the included trials in the evaluation was suboptimal; namely, four trials had a high risk of bias because of the lack of clear description of randomization, allocation concealment, and blinding, whereas the remaining 18 trials had an unclear risk of bias. In some of the included trials, there was significant heterogeneity in the conventional treatment as a co-intervention. Since there was no blinding during the study, possible differences in the multiple combined interventions between the treatment and control groups may have introduced bias into the results. Therefore, the poor methodological quality and underreporting of the included studies meant that no definitive conclusions could be drawn regarding the possible effects of Cordyceps preparations in patients with CKD (Zhang et al., 2014).

Four meta-analyses on Cordyceps preparations (JinShuiBao capsule/Bailing capsule) for DN included 51 RCT studies consisting of 3,955 participants (Li and Xu, 2020), 26 RCT studies with 2,198 early DN participants (Lu et al., 2018), 60 studies with 4,288 participants (Luo et al., 2015), and 24 studies with 1,941 participants (Sheng et al., 2020). All four studies showed that the Cordyceps preparation combined with ACEI/ARB was superior to ACEI/ARB alone, as shown by increased overall response rate and decreased 24 h UTP, UAER, BUN, and Scr. None of the studies had serious publication bias. However, all of the participating patients were Chinese with no other ethnicity; most of the included RCTs did not report detailed methodologies; in addition, efficacy assessments were not standardized and rigorous. The low quality of the study design and significant heterogeneity reduced the credibility of the meta-analysis.

To assess the safety of *C. cicadae*, 97 healthy adults were randomized to the treatment group (n = 49) and the placebo group (n = 48) in a double-blind, randomized trial. The treatment group received 1.05 g of *C. cicadae* mycelium granules once a day after a meal for 3 months. The placebo group received 1.05 g granules with the same nutrition, but without additional *C. cicadae* mycelium. Blood samples were collected before and after the treatment for biochemical analysis, including renal function, liver function, blood lipid, and electrolyte levels. No differences in symptoms or side effects were observed between the participants in the trial. There were also no significant differences between the baseline measurements and the final biochemical analyses. The results of the trial indicate that it is safe to consume less than 1.05 g of HEA-rich mycelium per day (Tsai et al., 2021).

In addition to single drugs or extracts, there are many compound preparations of Chinese herbs; some of the compound formulations of Cordyceps also have renal protective effects. WH30+ is a Chinese herb preparation composed of *Rheum palmatum*, *S. miltiorrhiza*, *C. sinensis*, *Leonurus sibiricus*, *Epihedium macranthum*, Radix Astragali, and Radix Codonopsis Pilosulae. It has nephroprotective effects in both glycerol-induced acute renal failure and adenine-induced chronic renal failure rats (Ngai et al., 2005). Cordyceps-related formulations of Novel JY5 formula (Fu et al., 2021), CGA formula (Li et al., 2016; Tian et al., 2019), and Fuzheng Huayu formula (Chen et al., 2019b) all have good effects against liver fibrosis, suggesting that these formulations may also be potential novel therapeutic candidates for RF.

CONCLUSION AND PERSPECTIVE

In this study, we found that Cordyceps and related products could attenuate RF through multiple pathways and targets, but the mechanisms were not independent of each other. Targeting TLR4 could reduce inflammation and oxidative stress *via* NF-κB or activate the downstream TGF-β/Smad signaling pathway to promote ECM deposition and fibroblast activation. Acting on SIRT1 was important in the regulation of autophagy, oxidative stress, energy homeostasis, and apoptosis. Although multitargeting had certain advantages, it could also have more side effects. Toxic side effects associated with Cordyceps have been reported in animals and humans. *C. militaris* was administered to rats at doses of 0, 1, 2, and 3 g/kg per day. Nephrotoxicity characterized by renal tubular epithelial degeneration and necrosis occurred at high doses of 3 g/kg, and the male rats were more susceptible to nephrotoxicity than female rats (Zhou and Yao, 2013). Doan et al. reported 60 cases of apparent Cordyceps fungus poisoning occurring in southern Vietnam during the rainy seasons, between 2008 and 2015. All patients showed symptoms within 60 min of consuming cicada flowers. A 60-year-old male patient died after consuming five cicada flowers and ingesting approximately 200 ml of rice wine. Another patient ingested 15–16 cicada flowers; although he exhibited severe symptoms, he survived after 3 weeks of treatment. These observations suggest that there are individual differences in the doses of cicada flower poisoning (Doan et al., 2017). It is therefore crucial to establish more systematic, complete, and feasible pharmacological and toxicological research methods.

Based on the available preclinical studies, Cordyceps and related products are supported for the treatment of RF. However, the available clinical data are limited. The published study protocol has been improved (Hu et al., 2021); as such, future RCTs with good methodological quality, favorable experimental design, and large sample size are needed to explore the therapeutic effects of Cordyceps and related products on RF to provide more rigorous clinical study data.

AUTHOR CONTRIBUTIONS

WT and YW designed the work of review. HD, JD, ZW, and LL reviewed the literature available on this topic, WT and YW wrote the paper, WT and JY revised the manuscript. All authors approved the paper for publication. As the leader of the project team, JY won the research funding supporting this manuscript.

FUNDING

This project is supported by the Chongqing Talent Program Project (cstc2021ycjh-bgzxm0090).

REFERENCES

Aranda-Rivera, A. K., Cruz-Gregorio, A., Aparicio-Trejo, O. E., Ortega-Lozano, A. J., and Pedraza-Chaverri, J. (2021). Redox Signaling Pathways in Unilateral Ureteral Obstruction (UUO)-induced Renal Fibrosis. *Free Radic. Biol. Med.* 172, 65–81. doi:10.1016/j.freeradbiomed.2021.05.034

Bai, X., Nie, P., Lou, Y., Zhu, Y., Jiang, S., Li, B., et al. (2021). Pirfenidone Is a Renal Protective Drug: Mechanisms, Signalling Pathways, and Preclinical Evidence. *Eur. J. Pharmacol.* 911, 174503. doi:10.1016/j.ejphar.2021.174503

Baisantry, A., Bhayana, S., Rong, S., Ermeling, E., Wrede, C., Hegermann, J., et al. (2016). Autophagy Induces Prosenescent Changes in Proximal Tubular S3 Segments. *J. Am. Soc. Nephrol.* 27 (6), 1609–1616. doi:10.1681/asn.2014111059

Barcena-Varela, M., Paish, H., Alvarez, L., Uriarte, I., Latasa, M. U., Santamaria, E., et al. (2021). Epigenetic Mechanisms and Metabolic Reprogramming in Fibrogenesis: Dual Targeting of G9a and DNMT1 for the Inhibition of Liver Fibrosis. *Gut* 70 (2), 388–400. doi:10.1136/gutjnl-2019-320205

Cai, Y., Feng, Z., Jia, Q., Guo, J., Zhang, P., Zhao, Q., et al. (2021). Cordyceps Cicadae Ameliorates Renal Hypertensive Injury and Fibrosis through the Regulation of SIRT1-Mediated Autophagy. *Front. Pharmacol.* 12, 801094. doi:10.3389/fphar.2021.801094

Chen, C. M., Lin, C. Y., Chung, Y. P., Liu, C. H., Huang, K. T., Guan, S. S., et al. (2021). Protective Effects of Nootkatone on Renal Inflammation, Apoptosis, and Fibrosis in a Unilateral Ureteral Obstructive Mouse Model. *Nutrients* 13 (11). doi:10.3390/nu13113921

Chen, D. D., Xu, R., Zhou, J. Y., Chen, J. Q., Wang, L., Liu, X. S., et al. (2019a). Cordyceps Militaris Polysaccharides Exerted Protective Effects on Diabetic Nephropathy in Mice via Regulation of Autophagy. *Food Funct.* 10 (8), 5102–5114. doi:10.1039/c9fo00957d

Chen, J., Hu, Y., Chen, L., Liu, W., Mu, Y., and Liu, P. (2019b). The Effect and Mechanisms of Fuzheng Huayu Formula against Chronic Liver Diseases. *Biomed. Pharmacother.* 114, 108846. doi:10.1016/j.biopha.2019.108846

Chyau, C. C., Chen, C. C., Chen, J. C., Yang, T. C., Shu, K. H., and Cheng, C. H. (2014). Mycelia Glycoproteins from Cordyceps Sobolifera Ameliorate Cyclosporine-Induced Renal Tubule Dysfunction in Rats. *J. Ethnopharmacol.* 153 (3), 650–658. doi:10.1016/j.jep.2014.03.020

Chyau, C. C., Wu, H. L., Peng, C. C., Huang, S. H., Chen, C. C., Chen, C. H., et al. (2021). Potential Protection Effect of ER Homeostasis of N6-(2-Hydroxyethyl) adenosine Isolated from Cordyceps Cicadae in Nonsteroidal Anti-inflammatory Drug-Stimulated Human Proximal Tubular Cells. *Int. J. Mol. Sci.* 22 (4). doi:10.3390/ijms22041577

Darby, I. A., and Hewitson, T. D. (2016). Hypoxia in Tissue Repair and Fibrosis. *Cell Tissue Res.* 365 (3), 553–562. doi:10.1007/s00441-016-2461-3

Das, G., Shin, H. S., Leyva-Gómez, G., Prado-Audelo, M. L. D., Cortes, H., Singh, Y. D., et al. (2020). Cordyceps spp.: A Review on its Immune-Stimulatory and Other Biological Potentials. *Front. Pharmacol.* 11, 602364. doi:10.3389/fphar.2020.602364

Deng, J. S., Jiang, W. P., Chen, C. C., Lee, L. Y., Li, P. Y., Huang, W. C., et al. (2020). Cordyceps Cicadae Mycelia Ameliorate Cisplatin-Induced Acute Kidney Injury by Suppressing the TLR4/NF-Kb/MAPK and Activating the HO-1/Nrf2 and Sirt-1/AMPK Pathways in Mice. *Oxid. Med. Cell Longev.* 2020, 7912763. doi:10.1155/2020/7912763

Djudjaj, S., and Boor, P. (2019). Cellular and Molecular Mechanisms of Kidney Fibrosis. *Mol. Asp. Med.* 65, 16–36. doi:10.1016/j.mam.2018.06.002

Doan, U. V., Mendez Rojas, B., and Kirby, R. (2017). Unintentional Ingestion of Cordyceps Fungus-Infected Cicada Nymphs Causing Ibotenic Acid Poisoning in Southern Vietnam. *Clin. Toxicol. (Phila)* 55 (8), 893–896. doi:10.1080/15563650.2017.1319066

Docherty, N. G., O'Sullivan, O. E., Healy, D. A., Fitzpatrick, J. M., and Watson, R. W. (2006). Evidence that Inhibition of Tubular Cell Apoptosis Protects against Renal Damage and Development of Fibrosis Following Ureteric Obstruction. *Am. J. Physiol. Ren. Physiol.* 290 (1), F4–F13. doi:10.1152/ajprenal.00045.2005

Dong, Z., Sun, Y., Wei, G., Li, S., and Zhao, Z. (2019). A Nucleoside/Nucleobase-Rich Extract from Cordyceps Sinensis Inhibits the Epithelial-Mesenchymal Transition and Protects against Renal Fibrosis in Diabetic Nephropathy. *Molecules* 24 (22). doi:10.3390/molecules24224119

Du, F., Li, S., Wang, T., Zhang, H. Y., Zong, Z. H., Du, Z. X., et al. (2015). Cordyceps Sinensis Attenuates Renal Fibrosis and Suppresses BAG3 Induction in Obstructed Rat Kidney. *Am. J. Transl. Res.* 7 (5), 932–940.

Fu, Y., Xiao, Z., Tian, X., Liu, W., Xu, Z., Yang, T., et al. (2021). The Novel Chinese Medicine JY5 Formula Alleviates Hepatic Fibrosis by Inhibiting the Notch Signaling Pathway. *Front. Pharmacol.* 12, 671152. doi:10.3389/fphar.2021.671152

Gewin, L., Zent, R., and Pozzi, A. (2017). Progression of Chronic Kidney Disease: Too Much Cellular Talk Causes Damage. *Kidney Int.* 91 (3), 552–560. doi:10.1016/j.kint.2016.08.025

Gu, L., Johno, H., Nakajima, S., Kato, H., Takahashi, S., Katoh, R., et al. (2013). Blockade of Smad Signaling by 3'-deoxyadenosine: a Mechanism for its Anti-fibrotic Potential. *Lab. Invest.* 93 (4), 450–461. doi:10.1038/labinvest.2013.4

Han, F., Dou, M., Wang, Y., Xu, C., Li, Y., Ding, X., et al. (2020). Cordycepin Protects Renal Ischemia/reperfusion Injury through Regulating Inflammation, Apoptosis, and Oxidative Stress. *Acta Biochim. Biophys. Sin. (Shanghai)* 52 (2), 125–132. doi:10.1093/abbs/gmz145

He, P., Lei, J., Miao, J. N., Wu, D., and Wang, C. (2020). Cordyceps Sinensis Attenuates HBx-induced C-ell A-poptosis in HK-2 C-ells through S-uppressing the PI3K/Akt P-athway. *Int. J. Mol. Med.* 45 (4), 1261–1269. doi:10.3892/ijmm.2020.4503

Hu, X., Wang, J., Yang, H., Ji, S., Li, Y., Xu, B., et al. (2021). Bailing Capsule Combined with α-ketoacid Tablets for Stage 3 Chronic Kidney Disease. *Med. Baltim.* 100 (20), e25759. doi:10.1097/md.0000000000025759

Huang, Y. S., Wang, X., Feng, Z., Cui, H., Zhu, Z., Xia, C., et al. (2020). Cordyceps Cicadae Prevents Renal Tubular Epithelial Cell Apoptosis by Regulating the SIRT1/p53 Pathway in Hypertensive Renal Injury. *Evid. Based Complement. Altern. Med.* 2020, 7202519. doi:10.1155/2020/7202519

Humphreys, B. D. (2018). Mechanisms of Renal Fibrosis. *Annu. Rev. Physiol.* 80, 309–326. doi:10.1146/annurev-physiol-022516-034227

Kaushal, G. P., and Shah, S. V. (2016). Autophagy in Acute Kidney Injury. *Kidney Int.* 89 (4), 779–791. doi:10.1016/j.kint.2015.11.021

Kim, W. Y., Nam, S. A., Song, H. C., Ko, J. S., Park, S. H., Kim, H. L., et al. (2012). The Role of Autophagy in Unilateral Ureteral Obstruction Rat Model. *Nephrol. Carlt.* 17 (2), 148–159. doi:10.1111/j.1440-1797.2011.01541.x

Lenoir, O., Jasiek, M., Hénique, C., Guyonnet, L., Hartleben, B., Bork, T., et al. (2015). Endothelial Cell and Podocyte Autophagy Synergistically Protect from Diabetes-Induced Glomerulosclerosis. *Autophagy* 11 (7), 1130–1145. doi:10.1080/15548627.2015.1049799

Li, L., Zhang, T., Li, C., Xie, L., Li, N., Hou, T., et al. (2019). Potential Therapeutic Effects of Cordyceps Cicadae and Paecilomyces Cicadae on Adenine-Induced Chronic Renal Failure in Rats and Their Phytochemical Analysis. *Drug Des. Devel Ther.* 13, 103–117. doi:10.2147/dddt.S180543

Li, X. M., Peng, J. H., Sun, Z. L., Tian, H. J., Duan, X. H., Liu, L., et al. (2016). Chinese Medicine CGA Formula Ameliorates DMN-Induced Liver Fibrosis in Rats via Inhibiting MMP2/9, TIMP1/2 and the TGF-β/Smad Signaling Pathways. *Acta Pharmacol. Sin.* 37 (6), 783–793. doi:10.1038/aps.2016.35

Li, Y., and Xu, G. (2020). Clinical Efficacy and Safety of Jinshuibao Combined with ACEI/ARB in the Treatment of Diabetic Kidney Disease: A Meta-Analysis of Randomized Controlled Trials. *J. Ren. Nutr.* 30 (2), 92–100. doi:10.1053/j.jrn.2019.03.083

Li, Y., Wang, L., Xu, B., Zhao, L., Li, L., Xu, K., et al. (2021). Based on Network Pharmacology Tools to Investigate the Molecular Mechanism of Cordyceps Sinensis on the Treatment of Diabetic Nephropathy. *J. Diabetes Res.* 2021, 1–12. doi:10.1155/2021/8891093

Liao, X., Lv, X., Zhang, Y., Han, Y., Li, J., Zeng, J., et al. (2022). Fluorofenidone Inhibits UUO/IRI-Induced Renal Fibrosis by Reducing Mitochondrial Damage. *Oxid. Med. Cell Longev.* 2022, 2453617. doi:10.1155/2022/2453617

Lin, S. L., Li, B., Rao, S., Yeo, E. J., Hudson, T. E., Nowlin, B. T., et al. (2010). Macrophage Wnt7b Is Critical for Kidney Repair and Regeneration. *Proc. Natl. Acad. Sci. U. S. A.* 107 (9), 4194–4199. doi:10.1073/pnas.0912228107

Liston, A., and Masters, S. L. (2017). Homeostasis-altering Molecular Processes as Mechanisms of Inflammasome Activation. *Nat. Rev. Immunol.* 17 (3), 208–214. doi:10.1038/nri.2016.151

Liu, C., Song, J., Teng, M., Zheng, X., Li, X., Tian, Y., et al. (20162016). Antidiabetic and Antinephritic Activities of Aqueous Extract ofCordyceps militarisFruit Body in Diet-Streptozotocin-Induced Diabetic Sprague Dawley Rats. *Oxidative Med. Cell. Longev.* 2016, 1. doi:10.1155/2016/9685257

Liu, J. R., Miao, H., Deng, D. Q., Vaziri, N. D., Li, P., and Zhao, Y. Y. (2021). Gut Microbiota-Derived Tryptophan Metabolism Mediates Renal Fibrosis by Aryl Hydrocarbon Receptor Signaling Activation. *Cell Mol. Life Sci.* 78 (3), 909–922. doi:10.1007/s00018-020-03645-1

Liu, M., Ning, X., Li, R., Yang, Z., Yang, X., Sun, S., et al. (2017). Signalling Pathways Involved in Hypoxia-Induced Renal Fibrosis. *J. Cell Mol. Med.* 21 (7), 1248–1259. doi:10.1111/jcmm.13060

Livingston, M. J., Ding, H. F., Huang, S., Hill, J. A., Yin, X. M., and Dong, Z. (2016). Persistent Activation of Autophagy in Kidney Tubular Cells Promotes Renal Interstitial Fibrosis during Unilateral Ureteral Obstruction. *Autophagy* 12 (6), 976–998. doi:10.1080/15548627.2016.1166317

Lo, Y. H., Yang, S. F., Cheng, C. C., Hsu, K. C., Chen, Y. S., Chen, Y. Y., et al. (2022). Nobiletin Alleviates Ferroptosis-Associated Renal Injury, Inflammation, and Fibrosis in a Unilateral Ureteral Obstruction Mouse Model. *Biomedicines* 10 (3). doi:10.3390/biomedicines10030595

Lu, Q., Li, C., Chen, W., Shi, Z., Zhan, R., and He, R. (2018). Clinical Efficacy of Jinshuibao Capsules Combined with Angiotensin Receptor Blockers in Patients with Early Diabetic Nephropathy: A Meta-Analysis of Randomized Controlled Trials. *Evid. Based Complement. Altern. Med.* 2018, 6806943. doi:10.1155/2018/6806943

Lu, Z., Li, S., Sun, R., Jia, X., Xu, C., Aa, J., et al. (2019). Hirsutella Sinensis Treatment Shows Protective Effects on Renal Injury and Metabolic Modulation in Db/db Mice. *Evid. Based Complement. Altern. Med.* 2019, 4732858. doi:10.1155/2019/4732858

Luo, Y., Yang, S. K., Zhou, X., Wang, M., Tang, D., Liu, F. Y., et al. (2015). Use of Ophiocordyceps Sinensis (Syn. Cordyceps Sinensis) Combined with Angiotensin-Converting Enzyme Inhibitors (ACEI)/angiotensin Receptor Blockers (ARB) versus ACEI/ARB Alone in the Treatment of Diabetic Kidney Disease: a Meta-Analysis. *Ren. Fail* 37 (4), 614–634. doi:10.3109/0886022x.2015.1009820

Ma, T. T., and Meng, X. M. (2019). TGF-β/Smad and Renal Fibrosis. *Adv. Exp. Med. Biol.* 1165, 347–364. doi:10.1007/978-981-13-8871-2_16

Ma, Z., Wang, F., Wang, H., Sun, T., Sun, W., and Xu, Q. (2022). Quercetin Ameliorates Renal Tubulointerstitial Transformation and Renal Fibrosis by Regulating NLRP3 in Obstructive Nephropathy. *Minerva Med.*. doi:10.23736/s0026-4806.22.08104-6

Meng, X. M. (2019). Inflammatory Mediators and Renal Fibrosis. *Adv. Exp. Med. Biol.* 1165, 381–406. doi:10.1007/978-981-13-8871-2_18

Meng, X. M., Nikolic-Paterson, D. J., and Lan, H. Y. (2016). TGF-β: the Master Regulator of Fibrosis. *Nat. Rev. Nephrol.* 12 (6), 325–338. doi:10.1038/nrneph.2016.48

Ngai, H. H., Sit, W. H., and Wan, J. M. (2005). The Nephroprotective Effects of the Herbal Medicine Preparation, WH30+, on the Chemical-Induced Acute and Chronic Renal Failure in Rats. *Am. J. Chin. Med.* 33 (3), 491–500. doi:10.1142/s0192415x05003089

Nogueira, A., Pires, M. J., and Oliveira, P. A. (2017). Pathophysiological Mechanisms of Renal Fibrosis: A Review of Animal Models and Therapeutic Strategies. *Vivo* 31 (1), 1–22. doi:10.21873/invivo.11019

Olatunji, O. J., Tang, J., Tola, A., Auberon, F., Oluwaniyi, O., and Ouyang, Z. (2018). The Genus Cordyceps: An Extensive Review of its Traditional Uses, Phytochemistry and Pharmacology. *Fitoterapia* 129, 293–316. doi:10.1016/j.fitote.2018.05.010

Pan, M. M., Zhang, M. H., Ni, H. F., Chen, J. F., Xu, M., Phillips, A. O., et al. (2013). Inhibition of TGF-β1/Smad Signal Pathway Is Involved in the Effect of Cordyceps Sinensis against Renal Fibrosis in 5/6 Nephrectomy Rats. *Food Chem. Toxicol.* 58, 487–494. doi:10.1016/j.fct.2013.04.037

Park, J. Y., Yoo, K. D., Bae, E., Kim, K. H., Lee, J. W., Shin, S. J., et al. (2022). Blockade of STAT3 Signaling Alleviates the Progression of Acute Kidney Injury to Chronic Kidney Disease through Antiapoptosis. *Am. J. Physiol. Ren. Physiol.* 322 (5), F553–f572. doi:10.1152/ajprenal.00595.2020

Peng, J., Li, X., Zhang, D., Chen, J. K., Su, Y., Smith, S. B., et al. (2015). Hyperglycemia, P53, and Mitochondrial Pathway of Apoptosis Are Involved in the Susceptibility of Diabetic Models to Ischemic Acute Kidney Injury. *Kidney Int.* 87 (1), 137–150. doi:10.1038/ki.2014.226

Phull, A. R., Ahmed, M., and Park, H. J. (2022). Cordyceps Militaris as a Bio Functional Food Source: Pharmacological Potential, Anti-inflammatory Actions and Related Molecular Mechanisms. *Microorganisms* 10 (2). doi:10.3390/microorganisms10020405

Ram, C., Gairola, S., Syed, A. M., Kulhari, U., Kundu, S., Mugale, M. N., et al. (2022). Biochanin A Alleviates Unilateral Ureteral Obstruction-Induced Renal Interstitial Fibrosis and Inflammation by Inhibiting the TGF-β1/Smad2/3 and NF-kB/NLRP3 Signaling axis in Mice. *Life Sci.* 298, 120527. doi:10.1016/j.lfs.2022.120527

Ricardo, S. D., van Goor, H., and Eddy, A. A. (2008). Macrophage Diversity in Renal Injury and Repair. *J. Clin. Invest.* 118 (11), 3522–3530. doi:10.1172/jci36150

Richter, K., and Kietzmann, T. (2016). Reactive Oxygen Species and Fibrosis: Further Evidence of a Significant Liaison. *Cell Tissue Res.* 365 (3), 591–605. doi:10.1007/s00441-016-2445-3

Ruiz-Ortega, M., Lamas, S., and Ortiz, A. (2022). Antifibrotic Agents for the Management of CKD: A Review. *Am. J. Kidney Dis.* S0272-6386 (21), 01051–01059. doi:10.1053/j.ajkd.2021.11.010

Shahed, A. R., Kim, S. I., and Shoskes, D. A. (2001). Down-regulation of Apoptotic and Inflammatory Genes by Cordyceps Sinensis Extract in Rat Kidney Following Ischemia/reperfusion. *Transpl. Proc.* 33 (6), 2986–2987. doi:10.1016/s0041-1345(01)02282-5

Sheng, X., Dong, Y., Cheng, D., Wang, N., and Guo, Y. (2020). Efficacy and Safety of Bailing Capsules in the Treatment of Type 2 Diabetic Nephropathy: a Meta-Analysis. *Ann. Palliat. Med.* 9 (6), 3885–3898. doi:10.21037/apm-20-1799

Sies, H., Berndt, C., and Jones, D. P. (2017). Oxidative Stress. *Annu. Rev. Biochem.* 86, 715–748. doi:10.1146/annurev-biochem-061516-045037

Song, J., Wang, Y., Liu, C., Huang, Y., He, L., Cai, X., et al. (2016). Cordyceps Militaris Fruit Body Extract Ameliorates Membranous Glomerulonephritis by Attenuating Oxidative Stress and Renal Inflammation via the NF-Kb Pathway. *Food Funct.* 7 (4), 2006–2015. doi:10.1039/c5fo01017a

Song, Q., and Zhu, Z. (2020). Using Cordyceps Militaris Extracellular Polysaccharides to Prevent Pb2+-Induced Liver and Kidney Toxicity by Activating Nrf2 Signals and Modulating Gut Microbiota. *Food Funct.* 11 (10), 9226–9239. doi:10.1039/d0fo01608j

Sun, T., Dong, W., Jiang, G., Yang, J., Liu, J., Zhao, L., et al. (2019). Cordyceps Militaris Improves Chronic Kidney Disease by Affecting TLR4/NF-Kb Redox Signaling Pathway. *Oxid. Med. Cell Longev.* 2019, 7850863. doi:10.1155/2019/7850863

Sun, Y. B., Qu, X., Caruana, G., and Li, J. (2016). The Origin of Renal Fibroblasts/myofibroblasts and the Signals that Trigger Fibrosis. *Differentiation* 92 (3), 102–107. doi:10.1016/j.diff.2016.05.008

Tang, C., Livingston, M. J., Liu, Z., and Dong, Z. (2020). Autophagy in Kidney Homeostasis and Disease. *Nat. Rev. Nephrol.* 16 (9), 489–508. doi:10.1038/s41581-020-0309-2

Thomas, G. L., Yang, B., Wagner, B. E., Savill, J., and El Nahas, A. M. (1998). Cellular Apoptosis and Proliferation in Experimental Renal Fibrosis. *Nephrol. Dial. Transpl.* 13 (9), 2216–2226. doi:10.1093/ndt/13.9.2216

Tian, H., Liu, L., Li, Z., Liu, W., Sun, Z., Xu, Y., et al. (2019). Chinese Medicine CGA Formula Ameliorates Liver Fibrosis Induced by Carbon Tetrachloride Involving Inhibition of Hepatic Apoptosis in Rats. *J. Ethnopharmacol.* 232, 227–235. doi:10.1016/j.jep.2018.11.027

Tsai, Y. S., Hsu, J. H., Lin, D. P., Chang, H. H., Chang, W. J., Chen, Y. L., et al. (2021). Safety Assessment of HEA-Enriched Cordyceps Cicadae Mycelium: A Randomized Clinical Trial. *J. Am. Coll. Nutr.* 40 (2), 127–132. doi:10.1080/07315724.2020.1743211

Vincenti, F., Fervenza, F. C., Campbell, K. N., Diaz, M., Gesualdo, L., Nelson, P., et al. (2017). A Phase 2, Double-Blind, Placebo-Controlled, Randomized Study of Fresolimumab in Patients with Steroid-Resistant Primary Focal Segmental Glomerulosclerosis. *Kidney Int. Rep.* 2 (5), 800–810. doi:10.1016/j.ekir.2017.03.011

Voelker, J., Berg, P. H., Sheetz, M., Duffin, K., Shen, T., Moser, B., et al. (2017). Anti-TGF-β1 Antibody Therapy in Patients with Diabetic Nephropathy. *J. Am. Soc. Nephrol.* 28 (3), 953–962. doi:10.1681/asn.2015111230

Walton, K. L., Johnson, K. E., and Harrison, C. A. (2017). Targeting TGF-β Mediated SMAD Signaling for the Prevention of Fibrosis. *Front. Pharmacol.* 8, 461. doi:10.3389/fphar.2017.00461

Wang, C., Hou, X. X., Rui, H. L., Li, L. J., Zhao, J., Yang, M., et al. (2018). Artificially Cultivated Ophiocordyceps Sinensis Alleviates Diabetic Nephropathy and its Podocyte Injury via Inhibiting P2X7R Expression and NLRP3 Inflammasome Activation. *J. Diabetes Res.* 2018, 1390418. doi:10.1155/2018/1390418

Wang, M. Z., Wang, J., Cao, D. W., Tu, Y., Liu, B. H., Yuan, C. C., et al. (2022). Fucoidan Alleviates Renal Fibrosis in Diabetic Kidney Disease via Inhibition of NLRP3 Inflammasome-Mediated Podocyte Pyroptosis. *Front. Pharmacol.* 13, 790937. doi:10.3389/fphar.2022.790937

Wang, X., Qin, A., Xiao, F., Olatunji, O. J., Zhang, S., Pan, D., et al. (2019). N6 -(2-Hydroxyethyl)-Adenosine from Cordyceps Cicadae Protects against Diabetic Kidney Disease via Alleviation of Oxidative Stress and Inflammation. *J. Food Biochem.* 43 (2), e12727. doi:10.1111/jfbc.12727

Wojcikowski, K., Johnson, D. W., and Gobé, G. (2004). Medicinal Herbal Extracts-Rrenal Friend or Foe? Part Two: Herbal Extracts with Potential Renal Benefits. *Nephrol. Carlt.* 9 (6), 400–405. doi:10.1111/j.1440-1797.2004.00355.x

Xia, W. P., Chen, X., Ru, F., He, Y., Liu, P. H., Gan, Y., et al. (2021). Knockdown of lncRNA XIST Inhibited Apoptosis and Inflammation in Renal Fibrosis via microRNA-19b-Mediated Downregulation of SOX6. *Mol. Immunol.* 139, 87–96. doi:10.1016/j.molimm.2021.07.012

Xu, D., Wang, B., Chen, P. P., Wang, Y. Z., Miao, N. J., Yin, F., et al. (2019). c-Myc Promotes Tubular Cell Apoptosis in Ischemia-Reperfusion-Induced Renal Injury by Negatively Regulating C-FLIP and Enhancing FasL/Fas-Mediated Apoptosis Pathway. *Acta Pharmacol. Sin.* 40 (8), 1058–1066. doi:10.1038/s41401-018-0201-9

Xu, G., Luo, K., Liu, H., Huang, T., Fang, X., and Tu, W. (2015). The Progress of Inflammation and Oxidative Stress in Patients with Chronic Kidney Disease. *Ren. Fail* 37 (1), 45–49. doi:10.3109/0886022x.2014.964141

Xu, Y., Zhang, D., Yang, H., Liu, Y., Zhang, L., Zhang, C., et al. (2021). Hepatoprotective Effect of Genistein against Dimethylnitrosamine-Induced Liver Fibrosis in Rats by Regulating Macrophage Functional Properties and Inhibiting the JAK2/STAT3/SOCS3 Signaling Pathway. *Front. Biosci. (Landmark Ed.* 26 (12), 1572–1584. doi:10.52586/5050

Xue, Y., Enosi Tuipulotu, D., Tan, W. H., Kay, C., and Man, S. M. (2019). Emerging Activators and Regulators of Inflammasomes and Pyroptosis. *Trends Immunol.* 40 (11), 1035–1052. doi:10.1016/j.it.2019.09.005

Yan, H., Xu, J., Xu, Z., Yang, B., Luo, P., and He, Q. (2021). Defining Therapeutic Targets for Renal Fibrosis: Exploiting the Biology of Pathogenesis. *Biomed. Pharmacother.* 143, 112115. doi:10.1016/j.biopha.2021.112115

Yang, C., Guo, Y., Huang, T. S., Zhao, J., Huang, X. J., Tang, H. X., et al. (2018). Asiatic Acid Protects against Cisplatin-Induced Acute Kidney Injury via Anti-apoptosis and Anti-inflammation. *Biomed. Pharmacother.* 107, 1354–1362. doi:10.1016/j.biopha.2018.08.126

Yang, J., Dong, H., Wang, Y., Jiang, Y., Zhang, W., Lu, Y., et al. (2020). Cordyceps Cicadae Polysaccharides Ameliorated Renal Interstitial Fibrosis in Diabetic Nephropathy Rats by Repressing Inflammation and Modulating Gut Microbiota Dysbiosis. *Int. J. Biol. Macromol.* 163, 442–456. doi:10.1016/j.ijbiomac.2020.06.153

Yang, Z., and Klionsky, D. J. (2010). Eaten Alive: a History of Macroautophagy. *Nat. Cell Biol.* 12 (9), 814–822. doi:10.1038/ncb0910-814

Ying-Mei, K. E., Min, J., Shu-Bo, Z., Hong, Y. U., Juan, W., and Feng, G. E. (2020). Component Analysis of Ophiocordyceps Lanpingensis Polysaccharides and Study on Alleviation of Hepatic Fibrosis in Mice by Polysaccharides. *Zhongguo Zhong Yao Za Zhi* 45 (21), 5256–5264. doi:10.19540/j.cnki.cjcmm.20200628.401

Yu, S. H., Dubey, N. K., Li, W. S., Liu, M. C., Chiang, H. S., Leu, S. J., et al. (2016). Cordyceps Militaris Treatment Preserves Renal Function in Type 2 Diabetic Nephropathy Mice. *PLoS One* 11 (11), e0166342. doi:10.1371/journal.pone.0166342

Yu, W., Duan, S., and Yu, Z. (2021). The Effect of Bailing Capsules Combined with Losartan to Treat Diabetic Glomerulosclerosis and the Combination's Effect on Blood and Urine Biochemistry. *Am. J. Transl. Res.* 13 (6), 6873–6880.

Zhang, H. W., Lin, Z. X., Tung, Y. S., Kwan, T. H., Mok, C. K., Leung, C., et al. (2014). Cordyceps Sinensis (A Traditional Chinese Medicine) for Treating Chronic Kidney Disease. *Cochrane Database Syst. Rev.* 12, Cd008353. doi:10.1002/14651858.CD008353.pub2

Zhao, K., Gao, Q., Zong, C., Ge, L., and Liu, J. (2018). Cordyceps Sinensis Prevents Contrast-Induced Nephropathy in Diabetic Rats: its Underlying Mechanism. *Int. J. Clin. Exp. Pathol.* 11 (12), 5571–5580.

Zhao, M., Yu, Y., Wang, R., Chang, M., Ma, S., Qu, H., et al. (2020). Mechanisms and Efficacy of Chinese Herbal Medicines in Chronic Kidney Disease. *Front. Pharmacol.* 11, 619201. doi:10.3389/fphar.2020.619201

Zheng, R., Zhu, R., Li, X., Li, X., Shen, L., Chen, Y., et al. (2018). N6-(2-Hydroxyethyl) Adenosine from Cordyceps Cicadae Ameliorates Renal Interstitial Fibrosis and Prevents Inflammation via TGF-β1/Smad and NF-Kb Signaling Pathway. *Front. Physiol.* 9, 1229. doi:10.3389/fphys.2018.01229

Zhou, D., Fu, H., Zhang, L., Zhang, K., Min, Y., Xiao, L., et al. (2017). Tubule-Derived Wnts Are Required for Fibroblast Activation and Kidney Fibrosis. *J. Am. Soc. Nephrol.* 28 (8), 2322–2336. doi:10.1681/asn.2016080902

Zhou, S., He, Y., Zhang, W., Xiong, Y., Jiang, L., Wang, J., et al. (2021). Ophiocordyceps Lanpingensis Polysaccharides Alleviate Chronic Kidney Disease through MAPK/NF-κB Pathway. *J. Ethnopharmacol.* 276, 114189. doi:10.1016/j.jep.2021.114189

Zhou, X., and Yao, Y. (2013). Unexpected Nephrotoxicity in Male Ablactated Rats Induced by Cordyceps Militaris: The Involvement of Oxidative Changes. *Evid. Based Complement. Altern. Med.* 2013, 786528. doi:10.1155/2013/786528

Zhu, R., Zheng, R., Deng, Y., Chen, Y., and Zhang, S. (2014). Ergosterol Peroxide from Cordyceps Cicadae Ameliorates TGF-B1-Induced Activation of Kidney Fibroblasts. *Phytomedicine* 21 (3), 372–378. doi:10.1016/j.phymed.2013.08.022

Zhu, X., Jiang, L., Long, M., Wei, X., Hou, Y., and Du, Y. (2021). Metabolic Reprogramming and Renal Fibrosis. *Front. Med.* 8, 746920. doi:10.3389/fmed.2021.746920

Conflict of Interest: The authors declare that the research was conducted in the absence of any commercial or financial relationships that could be construed as a potential conflict of interest.

Publisher's Note: All claims expressed in this article are solely those of the authors and do not necessarily represent those of their affiliated organizations, or those of the publisher, the editors, and the reviewers. Any product that may be evaluated in this article, or claim that may be made by its manufacturer, is not guaranteed or endorsed by the publisher.

frontiers | Frontiers in Pharmacology

TYPE Original Research
PUBLISHED 17 August 2022
DOI 10.3389/fphar.2022.964370

OPEN ACCESS

EDITED BY
Zhiyong Guo,
Second Military Medical University, China

REVIEWED BY
Kun Ling Ma,
Zhejiang University, China
Xusheng Liu,
Guangdong Provincial Hospital of Chinese Medicine, China

*CORRESPONDENCE
Xiao-Yong Yu,
gub70725@126.com
Ying-Yong Zhao,
zyy@nwu.edu.cn

SPECIALTY SECTION
This article was submitted to Renal Pharmacology, a section of the journal Frontiers in Pharmacology

RECEIVED 08 June 2022
ACCEPTED 20 July 2022
PUBLISHED 17 August 2022

CITATION
Wang Y-N, Liu H-J, Ren L-L, Suo P, Zou L, Zhang Y-M, Yu X-Y and Zhao Y-Y (2022), Shenkang injection improves chronic kidney disease by inhibiting multiple renin-angiotensin system genes by blocking the Wnt/β-catenin signalling pathway.
Front. Pharmacol. 13:964370.
doi: 10.3389/fphar.2022.964370

Shenkang injection improves chronic kidney disease by inhibiting multiple renin-angiotensin system genes by blocking the Wnt/β-catenin signalling pathway

Yan-Ni Wang[1], Hong-Jiao Liu[1], Li-Li Ren[1], Ping Suo[1], Liang Zou[2], Ya-Mei Zhang[3], Xiao-Yong Yu[4]* and Ying-Yong Zhao[1,3,5]*

[1]Faculty of Life Science and Medicine, Northwest University, Xi'an, Shaanxi, China, [2]Key Disciplines Team of Clinical Pharmacy, School of Food and Bioengineering, Affiliated Hospital of Chengdu University, Chengdu University, Chengdu, Sichuan, China, [3]Clinical Genetics Laboratory, Affiliated Hospital and Clinical Medical College of Chengdu University, Chengdu, Sichuan, China, [4]Department of Nephrology, Shaanxi Traditional Chinese Medicine Hospital, Xi'an, Shaanxi, China, [5]School of Pharmacy, Zhejiang Chinese Medical University, Hangzhou, Zhejiang, China

Chronic kidney disease (CKD) is a major worldwide public health problem. The increase in the number of patients with CKD and end-stage kidney disease requesting renal dialysis or transplantation will progress to epidemic proportions in the next several decades. Although blocking the renin-angiotensin system (RAS) has been used as a first-line standard therapy in patients with hypertension and CKD, patients still progress towards end-stage kidney disease, which might be closely associated with compensatory renin expression subsequent to RAS blockade through a homeostatic mechanism. The Wnt/β-catenin signalling pathway is the master upstream regulator that controls multiple intrarenal RAS genes. As Wnt/β-catenin regulates multiple RAS genes, we inferred that this pathway might also be implicated in blood pressure control. Therefore, discovering new medications to synchronously target multiple RAS genes is necessary and essential for the effective treatment of patients with CKD. We hypothesized that Shenkang injection (SKI), which is widely used to treat CKD patients, might ameliorate CKD by inhibiting the activation of multiple RAS genes *via* the Wnt/β-catenin signalling pathway. To test this hypothesis, we used adenine-induced CKD rats and angiotensin II (AngII)-induced HK-2 and NRK-49F cells. Treatment with SKI inhibited renal function decline, hypertension and renal fibrosis. Mechanistically, SKI abrogated the increased protein expression of multiple RAS elements, including angiotensin-converting enzyme and angiotensin II type 1 receptor, as well as Wnt1, β-catenin and downstream target genes, including Snail1, Twist, matrix metalloproteinase-7, plasminogen activator inhibitor-1 and fibroblast-specific protein 1, in adenine-induced rats, which was verified in AngII-induced HK-2 and NRK-49F cells. Similarly, our results further indicated that treatment with rhein isolated from SKI attenuated renal function decline and epithelial-to-

mesenchymal transition and repressed RAS activation and the hyperactive Wnt/β-catenin signalling pathway in both adenine-induced rats and AngII-induced HK-2 and NRK-49F cells. This study first revealed that SKI repressed epithelial-to-mesenchymal transition by synchronously targeting multiple RAS elements by blocking the hyperactive Wnt/β-catenin signalling pathway.

KEYWORDS

chronic kidney disease, renal fibrosis, Shenkang injection, rhein, renin-angiotensin system, Wnt/β-catenin signalling pathway

Introduction

The worldwide increase in the number of chronic kidney disease (CKD) patients could be reflected in the rising number of end-stage renal disease patients who undergo renal replacement treatment, such as dialysis and transplantation (Hansrivijit et al., 2021; Kalantar-Zadeh et al., 2021; Wang et al., 2022a). CKD affects 13% of adults worldwide (Mantovani and Chiara, 2020; Rashid et al., 2022). Renal fibrosis is the common end-result of CKD (Humphreys, 2018; Bhargava et al., 2021). CKD is associated with a wide range of mechanisms, including aberrant cellular activities such as fibroblast activation, monocyte/macrophage infiltration and epithelial-to-mesenchymal transition (EMT); the activation of molecules such as renin-angiotensin system (RAS), noncoding RNAs and aryl hydrocarbon receptor (Lu et al., 2020; Zhou et al., 2021; Cao et al., 2022); and the dysregulation of pathways such as Wnt/β-catenin and transforming growth factor-β (TGF-β)/Smad signals (Wang et al., 2018a; Yu et al., 2022).

In the last several decades, experimental and clinical findings have indicated that intrarenal RAS activation plays a critical role in the pathogenesis of hypertension and CKD (Yang and Xu, 2017; Luzes et al., 2021). Considerable evidence has demonstrated that intrarenal RAS is activated by the upregulation of multiple RAS element genes, including angiotensinogen, renin, angiotensin-converting enzyme (ACE) and angiotensin II type 1 receptor (AT_1R), after renal damage (Zhou et al., 2015a). Two important enzymes in the RAS, renin and ACE, form the principal active peptide AngII, which induces both blood pressure-dependent and blood pressure-independent renal injury. In addition to regulating blood pressure and haemodynamics, AngII activates TGF-β1 signalling pathways and directly mediates kidney fibrosis. Therefore, angiotensin-converting enzyme inhibitors (ACEIs) and angiotensin receptor blockers (ARBs) have been recommended clinically as first-line therapies in CKD patients (Chen et al., 2019a). These medications could effectively lower proteinuria and CKD progression. However, current targeted RAS treatment using ACEIs or ARBs only exhibits limited efficacy, and chronic administration of ACEIs or ARBs increases AngII and aldosterone levels, which is defined as AngII and aldosterone escape (Wang et al., 2018b). In addition, this effect might partly contribute to the compensatory upregulation of renin expression. Despite these treatments, patients with CKD still have poor outcomes. Currently, there is no effective treatment available; therefore, it is necessary to discover new effective therapies for the prevention and treatment of renal fibrosis.

The Wnt/β-catenin pathway is an evolutionarily conserved developmental signalling cascade that plays a pivotal role in regulating organ development and formation, tissue homeostasis and disease progression (Garg and Maurya, 2019; Zhu et al., 2021). Wnt/β-catenin signalling is relatively silent in the absence of Wnt ligand, and β-catenin is degraded by ubiquitin proteins after being phosphorylated by protein composites (Li et al., 2021). Under physiological conditions, β-catenin is expressed at low levels in the cytoplasm, and most of these molecules are bound to E-cadherin, serving as cell adhesion molecules (Li et al., 2021). When Wnts are activated by ligands, β-catenin is stabilized and translocates into the nucleus, and then β-catenin binds to the T-cell factor (TCF)/lymphoid enhancer-binding factor (LEF) family and forms a complex by recruiting the transcriptional coactivator cyclic adenosine monophosphate response element-binding protein-binding protein to transactivate its target genes, such as Snail1, Twist, matrix metalloproteinase-7 (MMP-7), plasminogen activator inhibitor-1 (PAI-1) and fibroblast-specific protein 1 (FSP1) (Wu et al., 2021). Activation of the Wnt/β-catenin signalling pathway is involved in various forms of CKD, such as adriamycin nephropathy, obstructive nephropathy, diabetic nephropathy (DN), polycystic kidney disease, focal glomerulosclerosis, and chronic allograft nephropathy (Zhou et al., 2015a).

Bioinformatics analysis revealed that the promoter regions of all RAS genes included putative TCF/LEF-binding sites, and β-catenin elicited the binding of LEF-1 to these sites in kidney tubular cells (Zhou et al., 2015a). The overexpression of β-catenin or Wnt ligands mediated the expression of all RAS genes. In contrast, ICG-001, a β-catenin inhibitor, ameliorated RAS induction. Transient treatment or late administration of ICG-001 mitigated the increases in proteinuria and renal damage (Zhou et al., 2015a). Treatment with ICG-001 suppressed intrarenal expression of multiple RAS genes and inhibited the expression of downstream β-catenin target genes in mice induced by adriamycin (Zhou et al., 2015a). These findings demonstrated that all RAS genes were downstream targets of the Wnt/β-catenin signalling pathway (Zuo and Liu, 2018). Inhibiting the Wnt/β-catenin signalling pathway could ameliorate renal fibrosis by synchronously inhibiting the expression of multiple RAS genes.

Many traditional Chinese medicines (TCMs) have been demonstrated to improve CKD and protect against renal fibrosis by inhibiting RAS activation and/or the Wnt/β-catenin signalling pathway (Xue et al., 2017; Chen et al., 2018a; de Souza et al., 2019). Shenkang injection (SKI) is a commonly used herbal formula that contains rhubarb (*R. tanguticum* Maxim. ex Balf. or *Rheum palmatum* L.), safflower (*Carthamus tinctorius* L.), Astragalus (*Astragalus mongholicus* Bunge), and red sage (*Salvia miltiorrhiza* Bunge). SKI quality was determined by fingerprint analysis and high-performance liquid chromatography (HPLC) as described previously (Yao et al., 2015; Xu et al., 2017). The main bioactive anthraquinones, including rhein, aloe-emodin, chrysophanol, emodin and physcion, were used for the quality control of SKI (Wang et al., 2021a). SKI can improve CKD and its complications, such as chronic nephritis, renal insufficiency, glomerulonephritis, chronic renal failure, and DN (Qin et al., 2021). With its obvious therapeutic effects and few side effects, SKI may slow the progression of CKD. Clinical results showed that 73.05% of CKD patients treated with SKI had improved renal function (Zhang et al., 2020). The final metabolite of adenine is uric acid. Excessive adenine is oxidized to 2,8-dihydroxyadenine *via* 8-hydroxyadenine by xanthine dehydrogenase. The low solubility of 2,8-dihydroxyadenine results in a mass of precipitates in renal tubules, which leads to kidney damage. Adenine leads to metabolic dysregulation resembling chronic renal insufficiency in humans. Adenine-treated rats had significantly increased hypertension (Aminzadeh et al., 2013). We hypothesized that SKI could protect kidneys through targeted inhibition of RAS-Wnt/β-catenin axis activation in CKD. To test this hypothesis, we used adenine-induced CKD rats to examine the renoprotective effects of SKI on CKD and assessed the effect of SKI on the RAS-Wnt/β-catenin signalling pathway to reveal its underlying molecular mechanisms.

Materials and methods

Chemicals and reagents

SKI was obtained from Shijishenkang Pharmaceutical Company Ltd. (Xi'an, Shaanxi, China). Adenine (purity ≥99.0%) was purchased from Sigma–Aldrich Company Ltd. (St. Louis, MO, United States). Chrysophanol, emodin and rhein in SKI were isolated and identified and were purchased from Chengdu Pufei De Biotech Co., Ltd. (Chengdu, Sichuan, China). The purities of chrysophanol, emodin and rhein were 99.12%, 98.83%, and 99.25%, respectively. Primary antibodies against collagen I (ab34710, Abcam, United States), α-SMA, (ab7817, Abcam, United States), fibronectin (ab2413, Abcam, United States), E-cadherin (ab76055, Abcam, United States), ACE (sc-23908, Santa Cruz, United States), AT_1R (ab124505, Abcam, United States), Wnt1 (ab85060, Abcam, United States), active β-catenin (05-665, Millipore, United States), β-catenin (610154, BD Transduction Laboratories, United States), Snail1 (ab180714, Abcam, United States), Twist (ab50581, Abcam, United States), MMP-7 (ab5706, Abcam, United States), PAI-1 (612024, BD Transduction Laboratories, United States) and FSP1 (ab197896, Abcam, United States) were purchased from Santa Cruz Biotechnology (Dallas, TX, United States), Proteintech Company (Wuhan, Hubei, China), Abcam Company (Cambridge, MA, United States) and BD Transduction Laboratories (New York, NJ, United States). Glyceraldehyde-3-phosphate dehydrogenase (GAPDH, 10494-1-AP) and α-tubulin (11224-1-AP) were purchased from Proteintech Company (Wuhan, Hubei, China).

Treatment of adenine-induced chronic kidney disease rats with Shenkang injection, chrysophanol, emodin, and rhein

Six- to eight-week-old male Sprague–Dawley rats (body weight 180–210 g) were purchased from the Central Animal Breeding House of Xi'an Jiaotong University (Xi'an, Shaanxi, China). The rats underwent an adaptation for 1 week, during which they were fed commercial feed. The rats were administered adenine by gavage as previously described (Wang et al., 2021b). The rats were divided into eight groups (n = 8/group): control, CKD, low-dose SKI-treated CKD, medium-dose SKI-treated CKD, high-dose SKI-treated CKD, chrysophanol-treated CKD, emodin-treated CKD and rhein-treated CKD. Except for the control group, the other groups of CKD rats were orally administered adenine (200 mg/kg/d) for 3 weeks. The treatment groups were administered SKI (10, 20, and 30 ml/kg/d), chrysophanol (30 mg/kg/d), emodin (100 mg/kg/d) or rhein (150 mg/kg/d) for 3 weeks. After 3 weeks, individual rats were placed in metabolic cages to collect 24-h urine. The rats were anaesthetized with 10% urethane, and then blood and kidneys were collected for subsequent analysis. All animal care and experimental procedures were approved by the Ethics Committee for Animal Experiments of Northwest University.

Blood pressure measurement and renal function assessment

Systolic blood pressure (SBP) and diastolic blood pressure (DBP) were measured by rat tail plethysmography (Techman Soft, Chengdu, China). The levels of serum creatinine were determined by using an Olympus AU6402 automatic analyser.

Cell culture

Human kidney proximal tubular epithelial cells (HK-2 cells), normal rat kidney proximal tubular epithelial cells (NRK-52E cells) and normal rat kidney interstitial fibroblast cells (NRK-49F cells) were purchased from the China Centre for Type Culture Collection. The cells were cultured in DMEM-F12 containing 4 mM L-glutamine, 1.2 g/L $NaHCO_3$, 110 mg/L sodium pyruvate, 15 mM HEPES and 1,000 mg/L glucose supplemented with 10% foetal bovine serum (Gibco, Carlsbad, CA, United States) at 37°C with 5% CO_2.

Cell viability assay

A cell counting kit-8 (CCK-8, EnoGene, Nanjing, China) assay was used to evaluate the viability of HK-2, NRK-52E and NRK-49F cells. The cells were resuspended and seeded in 96-well plates at a density of 1×10^4 cells/well. After 24 h, HK-2, NRK-52E and NRK-49F cells were treated with SKI (0.125, 0.25, 0.5, 1.0, 2.0, 4.0, 6.0, 8.0, 12.0, and 16.0 mg/ml) for 24 h. In addition, HK-2 cells were treated with rhein (1.0, 2.5, 5.0, 7.5, 10.0, and 12.5 μM) for 24 h. Subsequently, CCK-8 was added to each well and incubated at 37°C for 3 h. The absorbance was measured at 450 nm on a microplate reader (Thermo, New York, United States). There were six replicates for each experimental condition.

Cell treatment with Shenkang injection and rhein

Different concentrations of SKI (0.125, 0.25, 0.5, 1.0, 2.0, and 6.0 mg/ml) or rhein (10 μM) were used to treat HK-2 cells stimulated by AngII (1.0 μM). In addition, SKI (1.0 mg/ml) or rhein (10 μM) was used to treat NRK-49F cells stimulated by AngII (1.0 μM). The angiotensin II type 1 receptor blocker losartan (LOS, 1 mM, Selleck Chemicals, Houston, United States) was used as a standard positive control.

Light microscopy

The effects of different concentrations of SKI on the morphological changes of HK-2 cells treated with AngII (1.0 μM) were visualized with a Leica Microsystems CMS GmbH (Leica, Wetzlar, Germany) using ToupView 3.7 software.

Immunohistochemical staining

The expression of specific proteins, including ACE, AT_1R, Wnt1, β-catenin and FSP1, in paraffin sections of kidney tissues was performed as previously described (Miao et al., 2020).

Immunofluorescence staining

The *in situ* expression of fibronectin, Wnt1 and β-catenin was assessed by immunofluorescence staining using an established procedure (Chen et al., 2019b). The slides were visualized with an Olympus laser-scanning confocal microscope (FV1000, Tokyo, Japan) using FV10-ASW 4.0 VIEW software.

Western blot analysis

All solutions, tubes, and centrifuges were maintained at 0–4°C. Total proteins were extracted from the renal cortex as previously described (Choi et al., 2010). Protein levels were determined by Western blotting as previously described (Miao et al., 2020). The blots were exposed by using enhanced chemiluminescence reagent, and the levels of the target proteins were normalized to the level of GAPDH or α-tubulin. Semiquantitative analyses of specific bands were performed by using ImageJ software (version 1.48).

Statistical analysis

The results are expressed as the mean ± SEM. Statistical analyses were performed using GraphPad Prism software (version 6.0). A two-tailed unpaired Student's *t* test was used for comparisons between two groups. Statistically significant differences among more than two groups were analysed by one-way analysis of variance followed by Dunnett's post-hoc tests. $p < 0.05$ was considered significant.

Results

Shenkang injection controlled blood pressure and inhibited intrarenal renin-angiotensin system activation in chronic kidney disease rats

First, we examined the effects of different doses of SKI on CKD rats induced by adenine. As shown in Figure 1A, all three doses of SKI (10, 20, and 30 ml/kg/d) reduced serum creatinine levels in CKD rats, while 20 and 30 ml/kg/d SKI induced stronger effects than 10 ml/kg/d SKI. However, there were no significant differences between the effects of 20 ml/kg/d and 30 ml/kg/d SKI. Therefore, 20 ml/kg/d SKI was subsequently used for all *in vivo* experiments. Oral administration of exogenous adenine increased SBP and DBP in rats, which was accompanied by activation of the RAS, including the upregulation of intrarenal ACE and AT_1R protein expression in adenine-induced rats (Figures 1C,D), and treatment with SKI significantly decreased

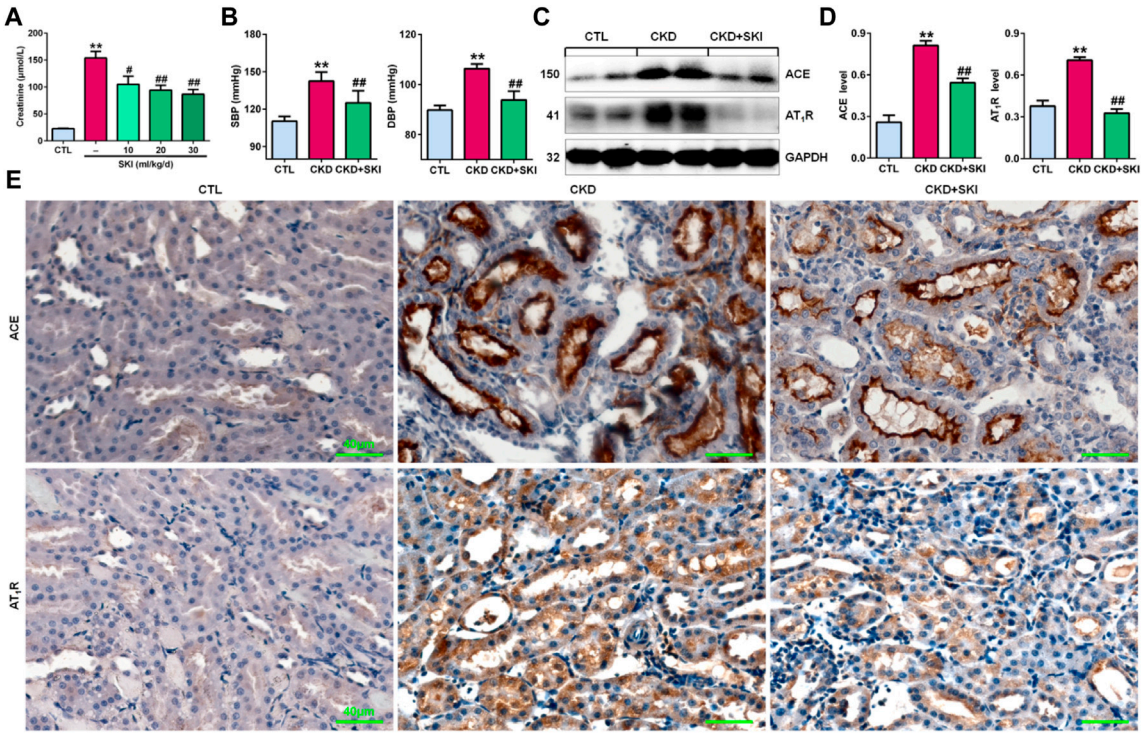

FIGURE 1
SKI controlled blood pressure and inhibited RAS activation in CKD rats. **(A)** Serum creatinine levels in adenine-induced rats treated with three doses of SKI (10, 20, 30 ml/kg/d). **(B)** SBP and DBP in adenine-induced rats treated with SKI. **(C)** Protein expression of intrarenal RAS components, including ACE and AT_1R, in adenine-induced rats treated with SKI. **(D)** Quantitative analysis of the protein expression of intrarenal RAS components, including ACE and AT_1R, in adenine-induced rats treated with SKI. **(E)** Immunohistochemical analysis of intrarenal ACE and AT_1R in adenine-induced rats treated with SKI. Scale bar, 40 μm $^{**}p < 0.01$ compared with CTL rats; $^{\#}p < 0.05$, $^{\#\#}p < 0.01$ compared with CKD rats. Abbreviations: DBP, diastolic blood pressure; SBP, systolic blood pressure; SKI, shenkang injection.

blood pressure and inhibited the upregulation of ACE and AT_1R protein expression in adenine-induced rats (Figures 1B–D). Additionally, immunohistochemistry showed that treatment with SKI significantly inhibited the upregulation of intrarenal ACE and AT_1R protein expression in adenine-induced CKD rats (Figure 1E). Taken together, these findings demonstrated that SKI inhibited the activation of the intrarenal RAS.

Shenkang injection suppressed the Wnt1/β-catenin signalling pathway in chronic kidney disease rats

A seminal publication indicated that all RAS genes were novel downstream targets of Wnt/β-catenin in a mouse model of nephropathy induced by adriamycin (Zhou et al., 2015a). Our previous study showed that chrysophanol, emodin, and rhein, which are anthraquinones that are major components of SKI, could ameliorate renal fibrosis in adenine-induced CKD rats (Luo et al., 2021). We further examined whether SKI and these three anthraquinones had inhibitory effects on the activation of the Wnt1/β-catenin signalling pathway in adenine-induced CKD rats. Immunohistochemical analysis showed that adenine upregulated intrarenal Wnt1 protein expression (Figure 2A), which was accompanied by the upregulation of intrarenal β-catenin protein expression in CKD rats (Figure 2B). However, treatment with SKI and the three anthraquinones significantly inhibited the upregulation of intrarenal Wnt1 and β-catenin protein expression in CKD rats (Figures 2A,B). Similarly, upregulated protein expression of intrarenal Wnt1 and β-catenin was observed in CKD rats by Western blotting, while treatment with SKI and the three anthraquinones significantly inhibited the upregulation of these intrarenal proteins in adenine-induced CKD rats (Figures 2C,D). The upregulation of intrarenal β-catenin protein expression was accompanied by the upregulation of downstream β-catenin proteins, including Snail1, Twist, MMP-7, PAI-1, and FSP1, in CKD rats, while treatment with SKI and the three anthraquinones significantly inhibited this upregulation of protein expression in CKD rats (Figures 3A,B). Additionally, immunohistochemical analysis showed

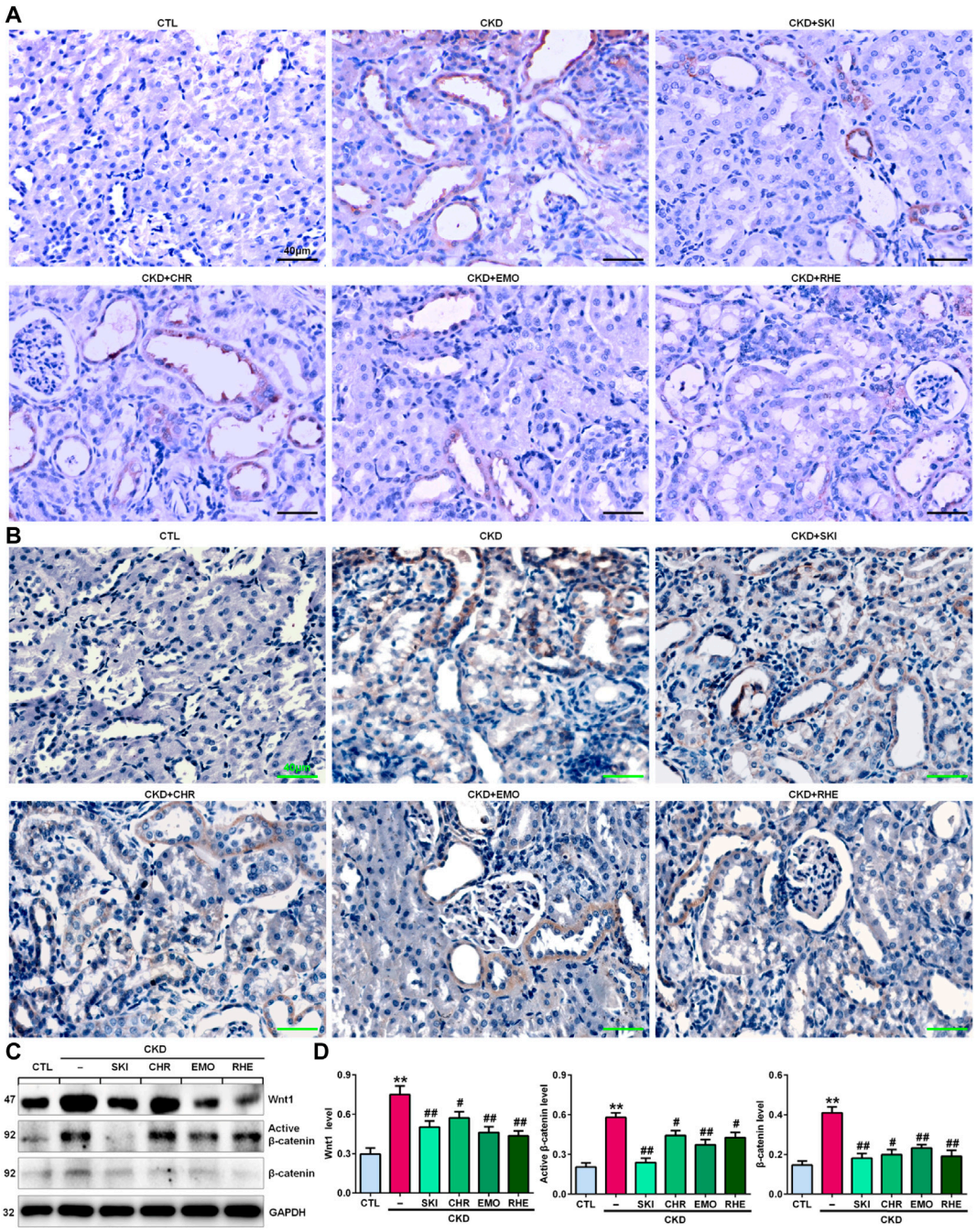

FIGURE 2
SKI suppressed Wnt1/β-catenin signalling in CKD rats. **(A)** Immunohistochemical analysis of intrarenal Wnt1 expression in the different groups. **(B)** Immunohistochemical analysis of intrarenal β-catenin expression in the different groups. **(C)** Protein expression levels of intrarenal Wnt1, active β-catenin and β-catenin in the different groups. **(D)** Quantitative analysis of the protein expression of intrarenal Wnt1, active β-catenin and β-catenin in the different groups. Scale bar, 40 μm $^{**}p < 0.01$ compared with CTL rats; $^{\#}p < 0.05$, $^{\#\#}p < 0.01$ compared with CKD rats. Abbreviations: CHR, chrysophanol; EMO, emodin; RHE, rhein.

that treatment with SKI and the three anthraquinones significantly inhibited intrarenal FSP1 expression in CKD rats (Figure 3C). Intriguingly, rhein exerted the strongest inhibitory effect on the Wnt1/β-catenin signalling pathway among the three anthraquinones. Therefore, rhein was selected for further bioactivity evaluation *in vitro*. Overall,

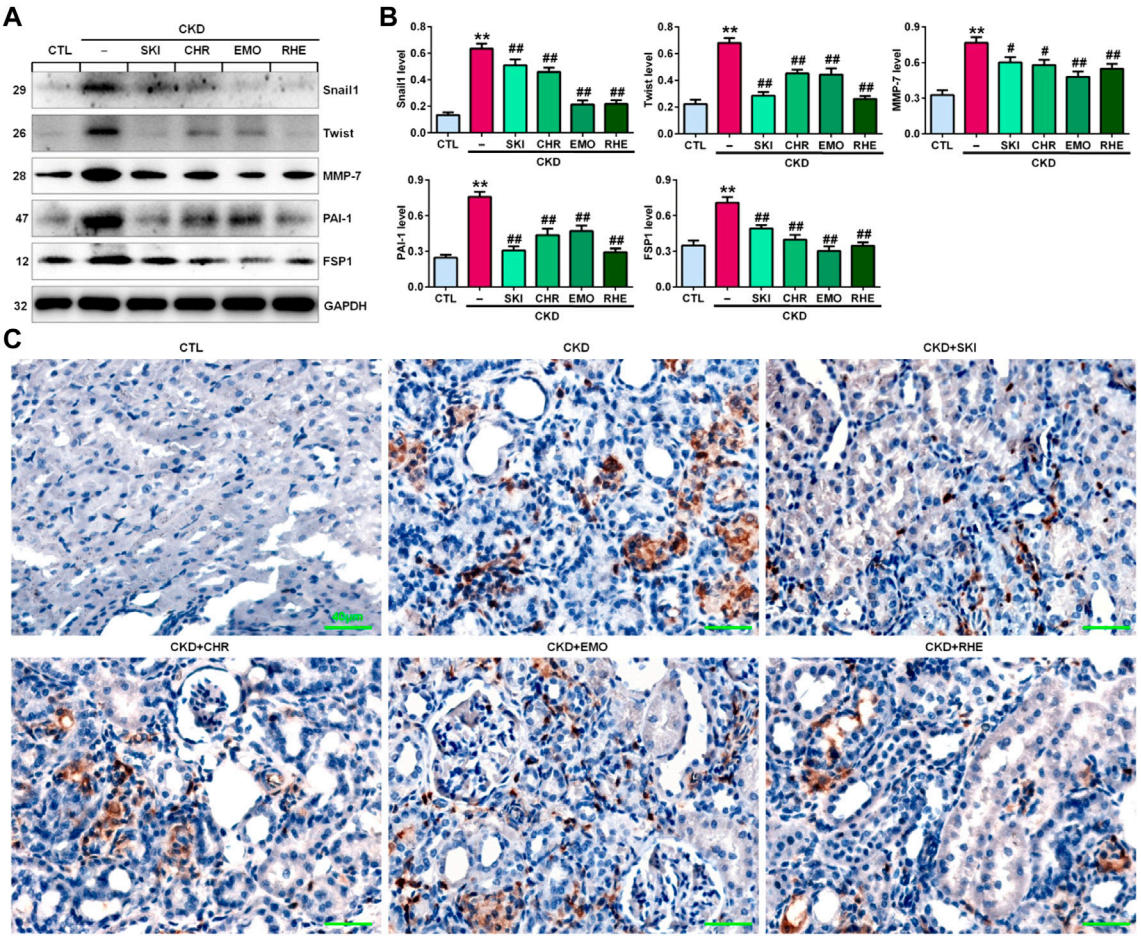

FIGURE 3
SKI inhibited the downstream target genes of β-catenin in CKD rats. **(A)** Protein expression levels of intrarenal Snail1, Twist, MMP-7, PAI-1, and FSP1 in the different groups. **(B)** Quantitative analysis of the protein expression of intrarenal Snail1, Twist, MMP-7, PAI-1, and FSP1 in the different groups. **(C)** Immunohistochemical analysis of intrarenal FSP1 expression in the different groups. Scale bar, 40 μm $^{**}p < 0.01$ compared with CTL rats; $^{\#}p < 0.05$, $^{\#\#}p < 0.01$ compared with CKD rats.

these findings demonstrated that SKI inhibited activation of the intrarenal Wnt1/β-catenin signalling pathway.

Effects of Shenkang injection on cell viability

To investigate the toxicity of SKI to cells, we cultured HK-2, NRK-52E and NRK-49F cells with SKI (0.125–16.0 mg/ml) and examined cell viability. As shown in Figure 4A, 0.125–16.0 mg/ml, 0.125–6.0 mg/ml and 0.125–2.0 mg/ml SKI had no significant effects on the viability of HK-2, NRK-52E and NRK-49F cells, respectively, but 8.0 mg/ml SKI 4.0 mg/ml SKI significantly reduced the viability of NRK-52E cells and NRK-49F cells, respectively. Therefore, SKI concentrations between 0.125 and 6.0 mg/ml were used to assess the effect of SKI on morphological changes in HK-2 cells stimulated with AngII.

Shenkang injection inhibited AngII-induced morphological changes and injury in intrarenal cells

High blood pressure led to RAS activation in adenine-induced rats. Therefore, we used AngII stimulation to investigate the effect of SKI on HK-2 cells. As shown in Figure 4B, HK-2 cells in the control group exhibited a pebble-like appearance, while the cells showed a decrease in cell–cell contacts and became a more elongated following stimulation with AngII (1.0 μM) for 48 h. Treatment with

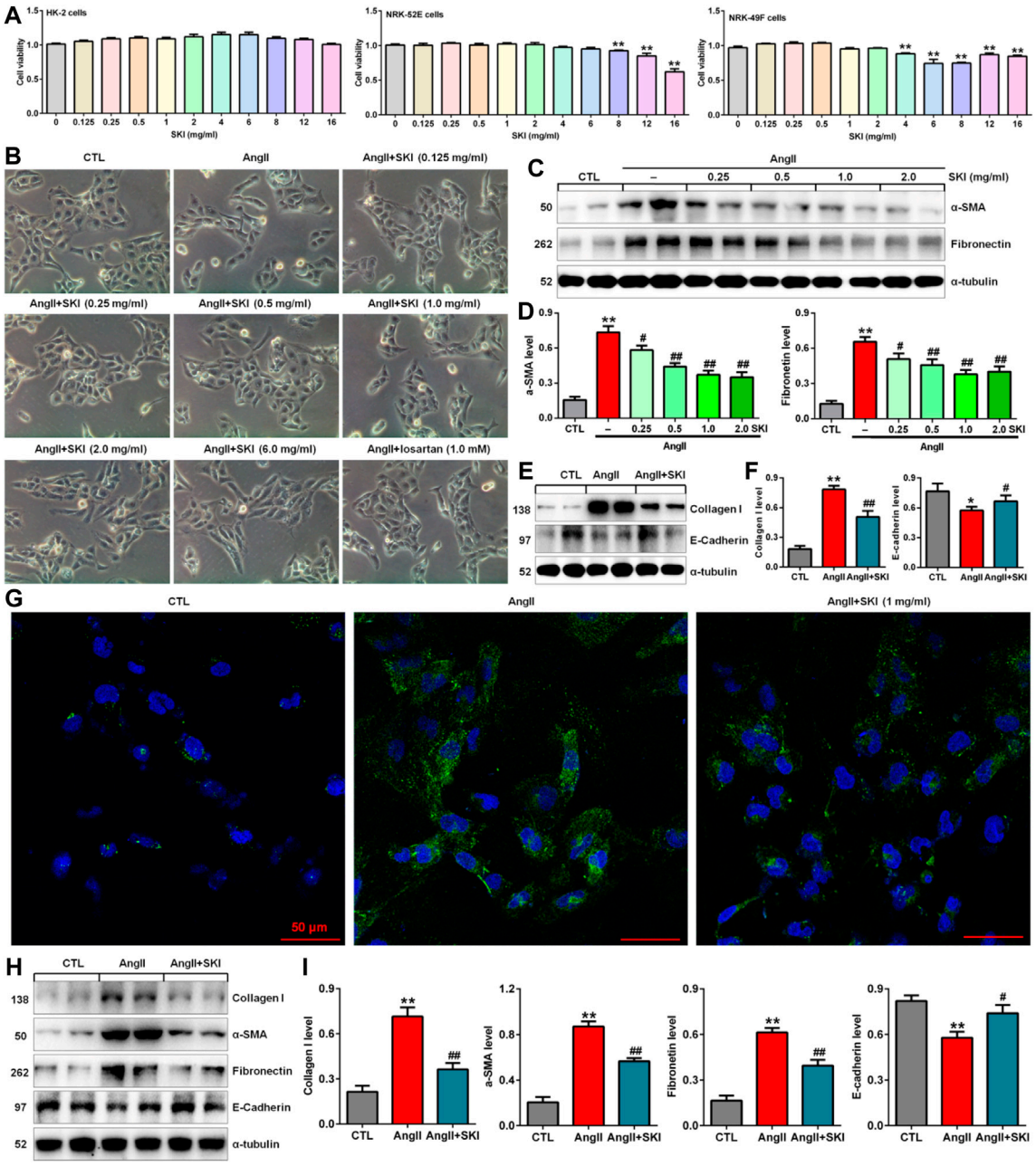

FIGURE 4
SKI improved morphological changes and injury in AngII-induced HK-2 cells. **(A)** Cell viability analysis after HK-2, NRK-52E and NRK-49F cells were treated with increasing concentrations of SKI (0–16 mg/ml). **(B)** Morphological observation in AngII-induced HK-2 cells treated with different concentrations of SKI (0–6.0 mg/ml) and losartan (1.0 mM) at 48 h. **(C)** Protein expression of α-SMA and fibronectin in AngII-induced HK-2 cells treated with different concentrations of SKI (0.25, 0.5, 1.0, 2.0 mg/ml). **(D)** Quantitative analysis of the protein expression of α-SMA and fibronectin in AngII-induced HK-2 cells treated with different concentrations of SKI (0.25, 0.5, 1.0, 2.0 mg/ml) for 48 h. **(E)** Protein expression of collagen I and E-cadherin in AngII-induced HK-2 cells treated with SKI. **(F)** Quantitative analysis of the protein expression of collagen I and E-cadherin in AngII-induced HK-2 cells treated with SKI. **(G)** Representative immunofluorescent analysis of fibronectin in AngII-induced HK-2 cells treated with SKI. **(H)** Protein expression of collagen I, α-SMA, E-cadherin and fibronectin in AngII-induced NRK-49F cells treated with SKI. **(I)** Quantitative analysis of the protein expression of collagen I, α-SMA, E-cadherin and fibronectin in AngII-induced NRK-49F cells treated with SKI. $^{*}p < 0.05$, $^{**}p < 0.01$ compared with the control group; $^{\#}p < 0.05$, $^{\#\#}p < 0.01$ compared with the AngII-induced group.

SKI could improve renal cell injury. Notably, treatment with SKI (0.25–2.0 mg/ml) significantly ameliorated AngII-induced morphological changes in HK-2 cells. We further determined the effect of SKI on profibrotic proteins such as α-SMA and fibronectin in AngII-induced HK-2 cells. Treatment with SKI exhibited a concentration-dependent inhibitory

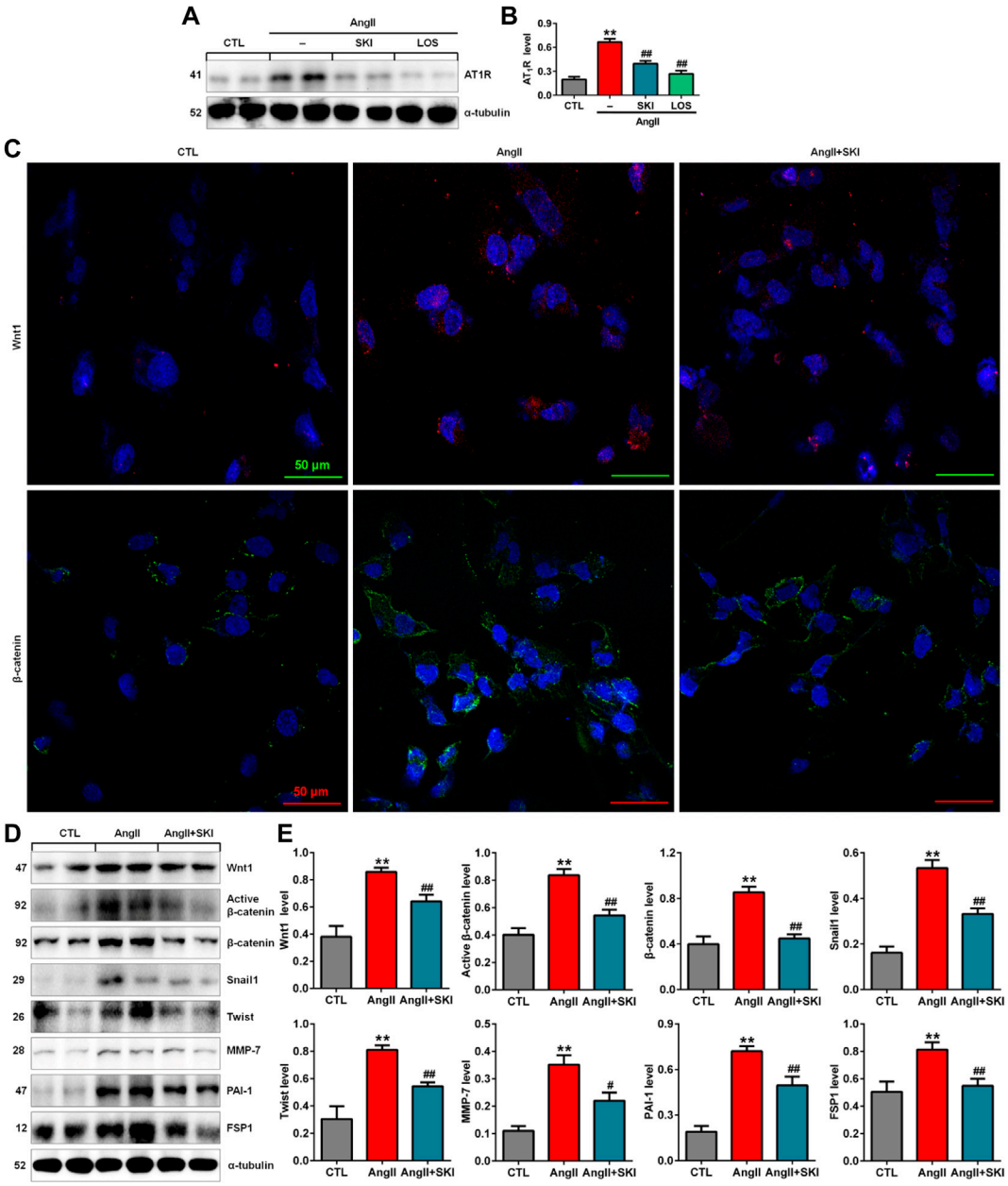

FIGURE 5
SKI inhibited the RAS/Wnt/β-catenin signalling axis in AngII-induced HK-2 cells. **(A)** Protein expression of AT_1R in AngII-induced HK-2 cells treated with SKI and losartan. **(B)** Quantitative analysis of the protein expression of AT_1R in AngII-induced HK-2 cells treated with SKI and losartan. **(C)** Representative immunofluorescent analysis of Wnt1 and β-catenin in AngII-induced HK-2 cells treated with SKI. **(D)** Protein expression of Wnt1, active β-catenin and β-catenin, as well as its downstream target gene products, including Snail1, Twist, MMP-7, PAI-1, and FSP1, in AngII-induced HK-2 cells treated with SKI. **(E)** Quantitative analysis of Wnt/β-catenin signalling pathway protein expression in AngII-induced HK-2 cells treated with SKI. $^{**}p < 0.01$ compared with the control group; $^{\#}p < 0.05$, $^{\#\#}p < 0.01$ compared with the AngII-induced group.

effect on the protein expression of α-SMA and fibronectin in HK-2 cells stimulated by AngII (Figures 4C,D). Of note, 1.0 mg/ml SKI showed a stronger inhibitory effect on profibrotic protein expression than the other concentrations of SKI. Collectively, 1.0 mg/ml SKI was selected to analyse the molecular mechanism by which SKI protects against renal fibrosis *in vitro*.

Our results further showed that treatment with SKI significantly inhibited the protein expression of collagen I and E-cadherin in AngII-induced HK-2 cells (Figures 4E,F).

Additionally, immunofluorescent analysis showed that treatment with SKI (1.0 mg/ml) significantly inhibited the protein expression of fibronectin in HK-2 cells stimulated by AngII (Figure 4G). Similarly, treatment with SKI significantly inhibited the protein expression of collagen I, α-SMA, fibronectin and E-cadherin in AngII-induced NRK-49F cells (Figures 4H,I). These results demonstrated that SKI could inhibit EMT in from HK-2 and NRK-49F cells. Collectively, our findings demonstrated that SKI exerted a significant inhibitory effect on profibrotic protein expression.

Shenkang injection inhibited the renin-angiotensin system/Wnt/β-catenin signalling axis in AngII-induced HK-2 cells

Our *in vivo* experiment demonstrated that SKI inhibited intrarenal RAS activation in adenine-induced rats. We further investigated the effect of SKI on the RAS in AngII-induced HK-2 cells. The upregulation of AT1R protein expression was observed in AngII-induced HK-2 cells, while SKI significantly abrogated the increase in AT_1R protein expression, which was consistent with the inhibitory effect of losartan (Figures 5A,B). A previous study demonstrated that all RAS components were downstream targets of Wnt/β-catenin signalling. Immunofluorescence analysis showed that treatment with SKI significantly inhibited the protein expression of Wnt1 and β-catenin in HK-2 cells stimulated by AngII, and treatment with SKI significantly inhibited the expression of these two proteins in AngII-treated HK-2 cells (Figure 5C). Western blot analysis showed that the protein expression of Wnt1, active β-catenin and β-catenin was upregulated in AngII-induced HK-2 cells, which was accompanied by upregulated expression of downstream β-catenin targets, including Snail1, Twist, MMP-7, PAI-1. and FSP1, while treatment with SKI significantly inhibited this upregulation in protein expression in AngII-induced HK-2 cells (Figures 5D,E). These results demonstrate that SKI exerted its renoprotective effect by inhibiting the RAS/Wnt/β-catenin signalling axis.

Rhein inhibited epithelial-to-mesenchymal transition by blocking renin-angiotensin system activation in AngII-induced HK-2 cells

The previous *in vivo* experiments demonstrated that rhein exerted the strongest inhibitory effects on renal fibrosis and the Wnt/β-catenin signalling pathway among the three anthraquinones. Therefore, the effect of rhein on AngII-induced HK-2 cells was further investigated. Treatment with 1.0–10.0 μM rhein for at 24 h had no significant effect on HK-2 cell viability, while 12.5 μM rhein significantly reduced cell viability (Figure 6A). Therefore, 10 μM rhein was ultimately selected to examine the molecular mechanism *in vitro*.

Treatment with rhein significantly inhibited the increase in AT_1R protein expression, which was consistent with the inhibitory effect of losartan (Figures 6B,C). Treatment with rhein significantly inhibited the protein expression of collagen I, α-SMA, fibronectin and E-cadherin AngII-induced HK-2 cells (Figures 6D,E). Additionally, immunofluorescent analysis showed that treatment with rhein significantly inhibited the protein expression of fibronectin in HK-2 cells stimulated by AngII (Figure 6F). Similarly, treatment with rhein significantly inhibited the protein expression of collagen I, α-SMA, fibronectin and E-cadherin in AngII-induced NRK-49F cells (Figures 6G,H). These results indicated that rhein could inhibit EMT.

Rhein inhibited the Wnt/β-catenin signalling pathway in AngII-induced HK-2 cells

Immunofluorescence analysis showed that treatment with rhein significantly inhibited the protein expression of β-catenin in HK-2 cells stimulated with AngII (Figure 7A). Western blot analysis also showed that treatment with rhein significantly inhibited the upregulation of Wnt1, active β-catenin and β-catenin protein expression in AngII-induced HK-2 cells, which was accompanied by inhibition of the downstream β-catenin targets including Snail1, Twist, MMP-7, PAI-1, and FSP1 (Figures 7B,C). These results demonstrated that rhein exerted its renoprotective effect by inhibiting the Wnt/β-catenin signalling pathway.

Discussion

The current study demonstrates that SKI and its three components chrysophanol, emodin, and rhein inhibit tubulointerstitial fibrosis by inhibiting the RAS/Wnt/β-catenin signalling axis in adenine-induced CKD rats. Recent studies show that emodin ameliorates tubulointerstitial fibrosis (Wang et al., 2022b; Xu et al., 2022). In addition, several publications revealed that rhein improves renal fibrosis and is associated with the nuclear factor kappa B and Twist1 pathways (Chen et al., 2022; Song et al., 2022). Many studies have demonstrated that RAS activation is closely associated with various diseases (Bakhle, 2020; Bhullar et al., 2021; Lizaraso-Soto et al., 2021; Mikusic et al., 2021; Walther et al., 2021). The presence of a local or tissue-based RAS has been well documented and is considered to be a pivotal player in the pathogenesis of CKD and its complications (Yang and Xu, 2017). The kidneys express all RAS elements, and intrarenal AngII production not only regulates glomerular haemodynamics and tubular sodium transport but also mediates many inflammatory and fibrotic pathways (Kobori

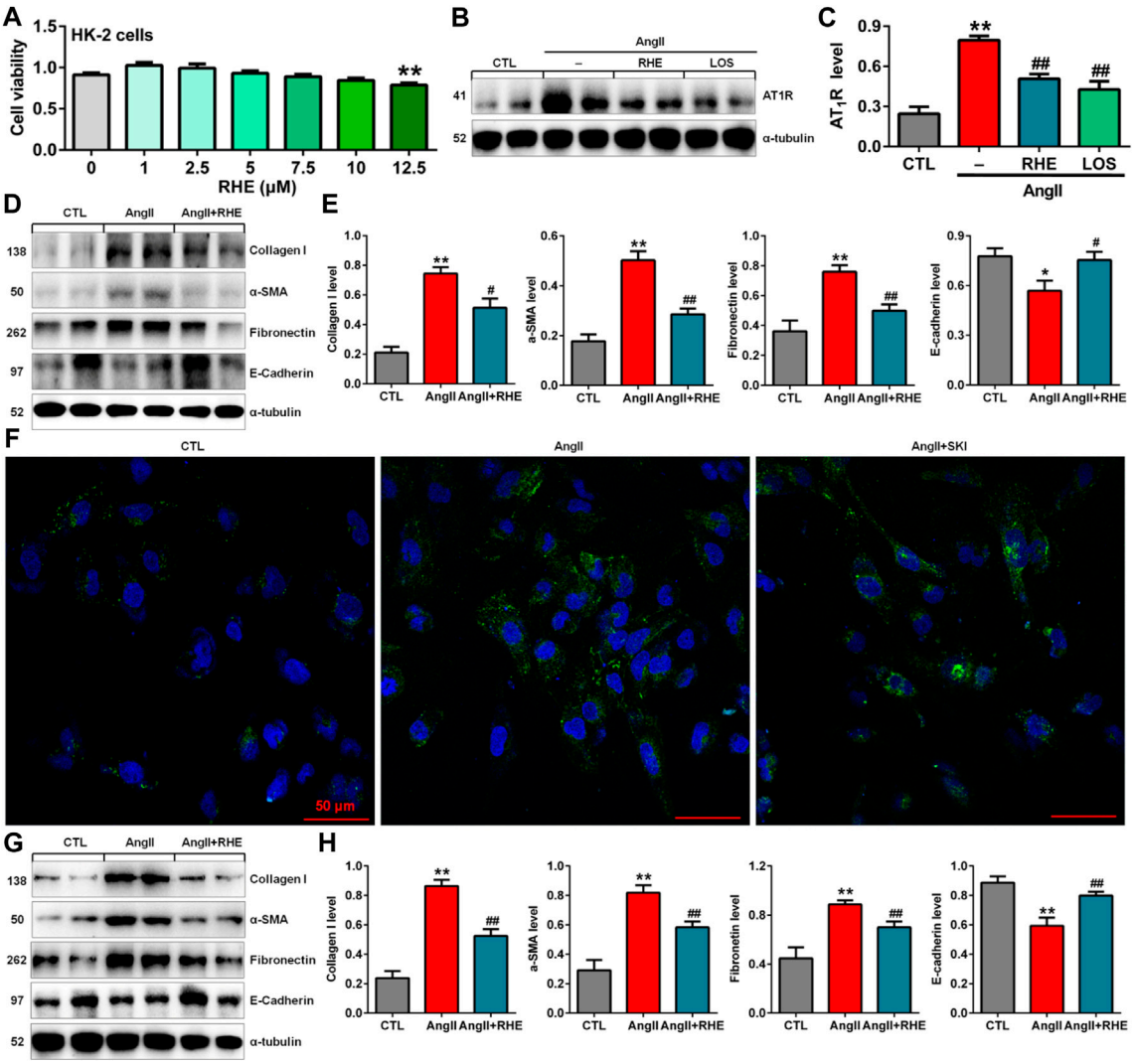

FIGURE 6
Rhein inhibited EMT by blocking the RAS in AngII-induced HK-2 cells. **(A)** Cell viability analysis after HK-2 cells were treated with increasing concentrations of rhein (0–12.5 μM). **(B)** Protein expression of AT_1R in AngII-induced HK-2 cells treated with rhein and losartan. **(C)** Quantitative analysis of the protein expression of AT_1R in AngII-induced HK-2 cells treated with rhein and losartan. **(D)** Protein expression of collagen I, α-SMA, E-cadherin and fibronectin in AngII-induced HK-2 cells treated with rhein. **(E)** Quantitative analysis of the protein expression of collagen I, α-SMA, E-cadherin and fibronectin in AngII-induced NRK-49F cells treated with rhein. **(F)** Representative immunofluorescent analysis of fibronectin in AngII-induced HK-2 cells treated with SKI. **(G)** Protein expression of collagen I, α-SMA, E-cadherin and fibronectin in AngII-induced NRK-49F cells treated with rhein. **(H)** Quantitative analysis of the protein expression of collagen I, α-SMA, E-cadherin and fibronectin in AngII-induced NRK-49F cells treated with rhein. $^{*}p < 0.05$, $^{**}p < 0.01$ compared with the control group; $^{\#}p < 0.05$, $^{\#\#}p < 0.01$ compared with the AngII-induced group.

et al., 2007). Over the past several decades, blood pressure control and RAS blockade have been considered cornerstones of preventing CKD or slowing disease progression, following key background and clinical evidence on the correlation among hypertension and activation of RAS with kidney damage (Kobori et al., 2007; Hsu and Tain, 2021). On the one hand, increased blood pressure is a major risk factor for CKD, and on the other hand, renal damage can lead to hypertension (Kobori et al., 2007). The published findings indicated a strong relationship between hypertension and the risk of renal functional decline or ESRD (Kobori et al., 2007). Therefore, numerous studies have suggested that ACEIs and ARBs are recommended as first-line therapies for hypertension in CKD patients (Hsu and Tain, 2021). Although ACEIs and ARBs can ameliorate CKD progression, the results are often unsatisfactory, and many patients progress to ESRD or even die. One of the important potential reasons is compensatory renin levels followed by RAS inhibition through a homeostatic mechanism (Zhang et al., 2008). Increased renin expression mediates the profibrotic effect though an angiotensin-independent

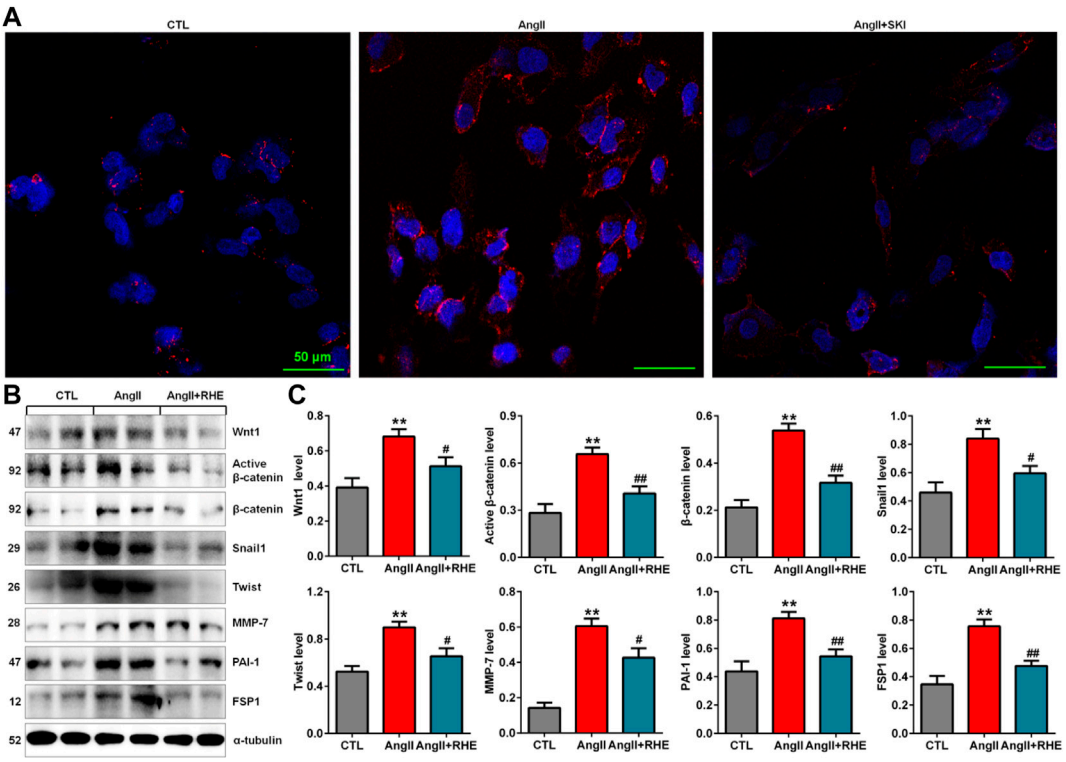

FIGURE 7
Rhein inhibited the Wnt/β-catenin signalling pathway in AngII-induced HK-2 cells. **(A)** Representative immunofluorescent analysis of β-catenin in AngII-induced HK-2 cells treated with rhein. **(B)** Protein expression of Wnt1, active β-catenin and β-catenin, as well as its downstream target gene products, including Snail1, Twist, MMP-7, PAI-1, and FSP1, in AngII-induced HK-2 cells treated with rhein. **(C)** Quantitative analysis of the protein expression of Wnt/β-catenin signalling pathway factors in AngII-induced HK-2 cells treated with rhein. $^{**}p < 0.01$ compared with the control group; $^{\#}p < 0.05$, $^{\#\#}p < 0.01$ compared with the AngII-induced group.

mechanism involving binding to the prorenin/renin receptor (Nguyen et al., 2002). The active renin inhibitor aliskiren was shown to effectively treat hypertension and CKD (Jhund et al., 2015; Zuo and Liu, 2018). However, aliskiren did not show significant beneficial effects on renal and cardiovascular diseases compared with ARB alone but markedly increased the risk of side effects based on the ONTARGET and aliskiren in left ventricular hypertrophy trials (Mann et al., 2008). Furthermore, ACEIs and ARBs repressed the activity of RAS elements but did not inhibit their expression. Therefore, there is still a clear need for additional strategies to synchronously block multiple RAS genes more effectively to reduce the progression of CKD.

A seminal publication revealed that multiple RAS genes were direct downstream targets of the Wnt/β-catenin signalling pathway (Zhou et al., 2015a). After being activated, β-catenin translocated to the nucleus, where it bound to and activated transcription factors in the TCF and LEF families to mediate the transcription of target genes. The common TCF/LEF binding sequence was (A/T)(A/T)CAA(A/T)G. The bioinformatics results indicated the presence of presumptive TCF/LEF-binding sites in promoter areas of RAS genes, including AGT, renin, ACE, AT_1R, and AT_2R (Zhou et al., 2015a). An *in vitro* study showed that increased β-catenin expression promoted the binding of LEF-1 to sites in these RAS genes, and the activation of β-catenin or many Wnt ligands could induce the expression of AGT, renin, ACE, and AT_1R (Zhou et al., 2015a). Collectively, these findings indicated that canonical Wnt/β-catenin signalling was a master upstream mediator that could synchronously modulate the expression of these RAS genes in diseased kidneys.

The β-catenin inhibitor ICG-001 effectively inhibited the upregulation of four RAS elements in kidneys. Therefore, mechanism of the inhibitory effect of ICG-001 was fully different from that of RAS intervention therapy. Although ACEIs or ARBs target one specific element of the RAS, ICG-001 inhibited the upregulation of all RAS genes. Further analysis indicated that ICG-001 could lower blood pressure (Xiao et al., 2019). ICG-001 treatment could lower AngII-induced hypertension through the Wnt/β-catenin signalling pathway. Interestingly, chronic AngII infusion could trigger the expression of multiple Wnt genes in rats and rat kidney interstitial fibroblasts (NRK-49F), thereby forming a vicious

cycle between RAS and Wnt/β-catenin (Xiao et al., 2019). In 5/6 nephrectomised rats, intrarenal β-catenin expression was significantly increased, and ICG-001 treatment could inhibit the increase in blood pressure and the protein expression of AGT, renin, ACE, and AT_1R. Moreover, ICG-001 treatment could reduce the levels of albuminuria, serum creatinine and urea, inhibit intrarenal protein expression of PAI-1, collagen I and fibronectin and repress the infiltration of inflammatory cells, including $CD3^+$ T cells and $CD68^+$ monocytes/macrophages (Xiao et al., 2019). In human kidney proximal tubular epithelial cells (HKC-8), losartan could inhibit Wnt/β-catenin-induced expression of α-SMA, Snail1 and fibronectin, indicating that the expression of fibrotic genes associated with Wnt/β-catenin signalling was dependent on RAS activation (Xiao et al., 2019). In addition, the antiaging protein Klotho, which is highly expressed in the tubular epithelium of normal adult kidneys, could bind to and functionally sequester Wnt ligands; therefore, Klotho is an endogenous Wnt antagonist that inhibits Wnt/β-catenin signalling activity (Zhou et al., 2013). Exogenous Klotho expression suppressed the upregulation of AGT, renin, ACE, and AT_1R protein expression and normalized blood pressure in 5/6 nephrectomised rats and unilateral ureteral obstruction (UUO) mice (Zhou et al., 2015b). Klotho can also repress β-catenin expression and ameliorate renal fibrosis (Zhou et al., 2013). Collectively, these findings uncovered a mechanistic link between the Wnt/β-catenin signalling pathway and blood pressure regulation. Hyperactivity of the Wnt/β-catenin signalling pathway could promote hypertension and renal injury through RAS activation.

A growing body of evidence suggested that inhibiting RAS activation by a number of TCMs, including TCM formulas, single herbs and identified compounds, could slow CKD and renal fibrosis (Yang et al., 2019). For example, Zhen-wu-tang is a classic TCM formula that is specifically used to treat CKD. Treatment with Zhen-wu-tang could blunt hyperglycaemia-induced intrarenal AngII levels in rats with DN induced by streptozotocin (Cai et al., 2010). Yiqi Huaju formula could lower arterial pressure and downregulate the mRNA expression of intrarenal renin, ACE and AT_1R in rats with salt-sensitive hypertension induced by a high-salt and high-fat diet, but this formula did not affect the activities of plasma renin, ACE or AngII (He et al., 2015). Wulingsan has long been used to regulate body fluid homeostasis. Treatment with Wulingsan could lower adriamycin-induced intrarenal angII levels in rats with nephrotic syndrome. In addition, treatment with Wulingsan could lower plasma renin activity and aldosterone levels in rats (Ahn et al., 2012). Two previous studies have demonstrated the effect of SKI components, including *Astragali Radix* and *C. tinctorius,* on RAS elements, such as ACE, AngII, and AT_1R, in renal injury rats. A previous study indicated that total flavonoids of *A. Radix*, one of the major components of SKI, could inhibit intrarenal ACE mRNA expression in rats with adriamycin-induced nephropathy (Zhang et al., 2018). Another study indicated that the ethanol extract of *C. tinctorius*, one of the major components of SKI, could inhibit serum ACE activity, plasma AngII levels, and aortic AT_1R protein expression in 2K-1C hypertensive rats (Bunbupha et al., 2018). Treatment with *Nigella sativa* extract repressed AngII expression in rats with UUO (Hosseinian et al., 2018). 2,3,5,4′-Tetrahydroxystilbene-2-O-β-d-glucoside is one of the important components of *Polygonum multiflorum* Thunb. Treatment with 2,3,5,4′-tetrahydroxystilbene-2-O-β-d-glucoside could inhibit hyperglycaemia-induced mRNA and protein expression of AGT, renin, ACE, and AT_1R in mice with DN induced by streptozotocin (Chen et al., 2016). Collectively, these findings suggest that TCM protects against renal injury by modulating RAS activation.

Although RAS activation is associated with various pathways, the most compelling evidence highlighted that the Wnt/β-catenin signalling pathway was the master upstream regulator that controlled the expression of all RAS elements (Zhou et al., 2015a), suggesting that targeting this upstream factor might be an effective strategy to prevent and treat CKD in patients with hypertension. Our latest review showed that targeting the Wnt/β-catenin signalling pathway was a viable therapeutic strategy to treat renal fibrosis (Liu et al., 2019; Li et al., 2021). Based on clinical observations and experimental studies, several TCM formulas have been demonstrated to inhibit the Wnt/β-catenin signalling pathway in renal injury. Clinically, a randomized controlled trial showed that treatment with Qingshen granules could lower the levels of serum Wnt1, β-catenin, α-SMA, and E-cadherin in patients with chronic renal failure (Wang et al., 2019). In cell- and rat/mouse-based models, several studies have demonstrated the effect of TCM formulas on the Wnt/β-catenin signalling pathway in renal injury. For example, Huang Gan formula, a new TCM compound, could lower serum creatinine and urea levels, inhibit oxidative stress and ameliorate tubulointerstitial fibrosis in rats with adenine-induced CKD (Mo et al., 2015). Treatment with the Huang Gan formula improved renal function by decreasing the levels of serum creatinine and urea, as well as urine protein, and increasing the creatinine clearance rate in 5/6 nephrectomised rats. Huang Gan formula could modulate the Wnt/β-catenin signalling pathway by inhibiting the expression of Wnt1, β-catenin, TCF4 and fibronectin (Mo et al., 2015). In addition, Mahuang Fuzi and Shenzhuo decoction inhibited β-catenin expression and phosphorylation in high glucose-induced podocytes (Dai et al., 2020). Moreover, Huayu Tongluo herbs could reduce proteinuria by inhibiting the protein expression of Wnt4, glycogen synthase kinase-3 beta (GSK3β), phosphorylated GSK3β and β-catenin in diabetic rats induced by streptozotocin (Bai et al., 2017). A previous study indicated that root water and ethanol extracts, as well as stem and leaf water and ethanol extracts of *S. miltiorrhiza*, one of the major components of SKI, could repress the protein expression of Wnt4 and β-catenin in DN rats induced by a high-fat diet and streptozotocin (Xiang

et al., 2019). Although these findings indicated that activation of the Wnt/β-catenin signalling pathway was involved in the inhibitory effect of TCM formulas on renal fibrosis, no publications have demonstrated that TCM formulas protect against renal fibrosis by modulating both the hyperactive Wnt/β-catenin signalling pathway and RAS activation. Our current study was the first to demonstrate that SKI could lower hypertension and abolish RAS activation by inhibiting the hyperactive Wnt/β-catenin signalling pathway.

In contrast to TCM formulas, our previous studies have indicated that a number of isolated compounds from diuretic TCMs, such as *Poria cocos*, *Alismatis rhizome*, and *Polyporus umbellatus,* could abolish RAS activation by inhibiting the hyperactive Wnt/β-catenin signalling pathway (Chen et al., 2018a). *P. cocos* (Schw.) Wolf (Polyporaceae), a well-known edible mushroom, is typically used in functional foods, nutraceuticals, dietary supplements and medications. *P. cocos* exerted various pharmacological effects, such as anti-inflammatory, antioxidant, diuretic and antifibrotic effects. We have isolated and identified a number of novel tetracyclic triterpenoids, such as poricoic acid ZC, poricoic acid ZD, poricoic acid ZE, poricoic acid ZG, poricoic acid ZH, poricoic acid ZI, poricoic acid ZM and poricoic acid ZP, from *P. cocos* (Wang et al., 2018a; Wang et al., 2018b; Chen et al., 2019c; Wang M. et al., 2020). Further pharmacological experiments have demonstrated that poricoic acid ZC, poricoic acid, ZD poricoic acid ZG, and poricoic acid ZH exhibit robust inhibitory effects on the protein expression of all RAS elements, including AGT, renin, ACE, and AT_1R, in TGF-β1- and AngII-induced HK-2 cells and/or UUO mice. Treatment with these compounds could also inhibit the protein expression of Wnt1 and β-catenin, as well as downstream target genes, including Snail1, Twist, MMP-7, PAI-1, and FSP1 (Wang et al., 2018a; Wang et al., 2018b). In addition, our studies demonstrated that poricoic acid ZE showed a strong inhibitory effect on renin compared with poricoic acid ZC and poricoic acid ZD in TGF-β1- and AngII-induced HK-2 cells and UUO mice (Wang et al., 2018a). Similarly, *A. rhizome*, a diuretic TCM, exerts renoprotective effects (Tian et al., 2014). 25-O-Methylalisol F was isolated and identified from *A. rhizome* and could ameliorate renal injury by repressing multiple RAS elements by inhibiting the hyperactive Wnt/β-catenin signalling pathway (Chen et al., 2018b). In addition, our previous *in vitro* experiment indicated that pachymic acid B from *P. cocos*, alisol B 23-acetate from *A. rhizome* and ergone from *P. umbellatus* could inhibit the protein expression of Snail1, Twist, MMP-7, PAI-1, and FSP1 (Chen et al., 2017). In addition, our recent studies showed that poricoic acid A, as a modulator of tryptophan hydroxylase-1 expression, inhibited renal fibrosis by regulating β-catenin protein stability and induced transcription (Chen et al., 2020). Increased evidence has indicated that acute kidney injury (AKI) is one of the major risk factors for renal fibrosis progression (Xiao et al., 2016). Our previous studies showed that poricoic acid A could block AKI-to-CKD progression and renal fibrosis by modulating the Wnt/β-catenin pathway in renal ischaemia–reperfusion injury and hypoxia/reoxygenation- or TGF-β1-induced HK-2 cells (Chen et al., 2019d). Taken together, these findings indicated that these diuretic TCM-derived components could abolish kidney damage by inhibiting multiple RAS elements *via* the Wnt/β-catenin signalling pathway. In addition, several publications have demonstrated the inhibitory effects of isolated compounds on the hyperactive Wnt/β-catenin signalling pathway in diabetes-induced renal injury. For example, rhein is an anthraquinone that is extracted from rhubarb, which is one of the major components of SKI. Treatment with rhein inhibited the upregulation of Wnt1 protein expression and the phosphorylation of β-catenin and GSK3β in db/db mice with DN (Duan et al., 2016). *In vitro* experiments from the same research group further revealed that treatment with rhein could inhibit the upregulation of Wnt3a, β-catenin and phosphorylated GSK3β protein expression in high glucose-induced podocytes (Duan et al., 2017). Astragaloside IV is a saponin extracted from *A. mongholicus*, which is another herb in SKI. Treatment with astragaloside IV inhibited the protein expression of Wnt1 and β-catenin in DN rats induced by a high-fat diet and streptozotocin (Wang et al., 2020b). Similarly, treatment with *Tripterygium wilfordii* significantly inhibited the hyperglycaemia-induced expression of Wnt1 and β-catenin at both the mRNA and protein levels in diabetic rats induced by streptozotocin (Chang et al., 2018; Huang et al., 2020). Moreover, treatment with mycelium polysaccharides from *Coprinus comatus* could attenuate the protein expression of Wnt1 and β-catenin in DN rats induced by a high-fat diet and streptozotocin (Gao et al., 2021). Sinomenine, an active alkaloid extracted from the climbing plant *Sinomenium acutum*, inhibited the expression of profibrotic proteins, including α-SMA and fibronectin, in TGF-β1-treated HEK293 human embryonic kidney cells and ameliorated tubulointerstitial fibrosis by inhibiting the protein expression of α-SMA and fibronectin in UUO mice, which was associated with the inhibition of β-catenin protein expression in TGF-β1-treated HEK293 cells (Qin et al., 2016). Collectively, our current and previous work and that of others suggest that synchronous inhibition of multiple RAS genes by blocking the hyperactive Wnt/β-catenin signalling pathway is a therapeutic strategy by which TCMs can be used to protect against renal fibrosis.

Conclusion

In summary, our current study was the first to demonstrate that SKI could lower elevated blood pressure, improve impaired renal function and ameliorate renal fibrosis. Mechanistically, SKI could lower hypertension and abolish RAS activation by inhibiting the hyperactive Wnt/β-catenin signalling pathway. Three anthraquinones blocked multiple RAS elements by

inhibiting the hyperactive Wnt/β-catenin signalling pathway. Inhibiting multiple RAS genes by blocking the activated Wnt/β-catenin signalling pathway might be considered a therapeutic strategy by which TCMs can be used to protect against renal fibrosis.

Data availability statement

The original contributions presented in the study are included in the article/supplementary materials, further inquiries can be directed to the corresponding authors.

Ethics statement

The animal study was reviewed and approved by Northwest University.

Author contributions

Y-YZ was responsible for the conception and design of the study; and Y-NW, H-JL, L-LR, PS, and X-YY were responsible for the data collection, analysis, and image processing. Y-YZ wrote the manuscript. LZ, Y-MZ, and X-YY revised the manuscript. Y-NW and Y-YZ were responsible for the final approval of the version to be submitted. All authors read and approved the final manuscript.

Funding

This study was supported by the Shaanxi Key Science and Technology Plan Project (No. 2019ZDLSF04-04-02), the ShaanXi Science and Technology Innovation Team (No. 2019TD-016) and the National Natural Science Foundation of China (Nos. 82074002, 81872985).

Conflict of interest

The authors declare that the research was conducted in the absence of any commercial or financial relationships that could be construed as a potential conflict of interest.

Publisher's note

References

Ahn, Y. M., Cho, K. W., Kang, D. G., and Lee, H. S. (2012). Oryeongsan (Wulingsan), a traditional Chinese herbal medicine, induces natriuresis and diuresis along with an inhibition of the renin-angiotensin-aldosterone system in rats. *J. Ethnopharmacol.* 141 (3), 780–785. doi:10.1016/j.jep.2012.02.021

Aminzadeh, M. A., Nicholas, S. B., Norris, K. C., and Vaziri, N. D. (2013). Role of impaired Nrf2 activation in the pathogenesis of oxidative stress and inflammation in chronic tubulo-interstitial nephropathy. *Nephrol. Dial. Transpl.* 28 (8), 2038–2045. doi:10.1093/ndt/gft022

Bai, L., Huo, B., Chen, Z., Guo, Q., Xu, J., Fang, J., et al. (2017). Effect of Huayu Tongluo herbs on reduction of proteinuria via inhibition of Wnt/β-catenin signaling pathway in diabetic rats. *Evid. Based. Complement. Altern. Med.* 2017, 3054145. doi:10.1155/2017/3054145

Bakhle, Y. S. (2020). How ACE inhibitors transformed the renin-angiotensin system. *Br. J. Pharmacol.* 177 (12), 2657–2665. doi:10.1111/bph.15045

Bhargava, V., Singh, K., Meena, P., and Sanyal, R. (2021). Nephrogenic systemic fibrosis: a frivolous entity. *World J. Nephrol.* 10 (3), 29–36. doi:10.5527/wjn.v10.i3.29

Bhullar, S. K., Shah, A. K., and Dhalla, N. S. (2021). Role of angiotensin II in the development of subcellular remodeling in heart failure. *Explor. Med.* 2, 352–371. doi:10.37349/emed.2021.00054

Bunbupha, S., Wunpathe, C., Maneesai, P., Berkban, T., Kukongviriyapan, U., Kukongviriyapan, V., et al. (2018). Carthamus tinctorius L. extract improves hemodynamic and vascular alterations in a rat model of renovascular hypertension through Ang II-AT_1R-NADPH oxidase pathway. *Ann. Anat.* 216, 82–89. doi:10.1016/j.aanat.2017.11.005

Cai, Y., Chen, J., Jiang, J., Cao, W., and He, L. (2010). Zhen-wu-tang, a blended traditional Chinese herbal medicine, ameliorates proteinuria and renal damage of streptozotocin-induced diabetic nephropathy in rats. *J. Ethnopharmacol.* 131 (1), 88–94. doi:10.1016/j.jep.2010.06.004

Cao, G., Miao, H., Wang, Y. N., Chen, D. Q., Wu, X. Q., Chen, L., et al. (2022). Intrarenal 1-methoxypyrene, an aryl hydrocarbon receptor agonist, mediates progressive tubulointerstitial fibrosis in mice. *Acta Pharmacol. Sin.*. doi:10.1038/s41401-022-00914-6

Chang, B., Chen, W., Zhang, Y., Yang, P., and Liu, L. (2018). Tripterygium wilfordii mitigates hyperglycemia-induced upregulated Wnt/β-catenin expression and kidney injury in diabetic rats. *Exp. Ther. Med.* 15 (4), 3874–3882. doi:10.3892/etm.2018.5901

Chen, D. Q., Cao, G., Chen, H., Argyopoulos, C. P., Yu, H., Su, W., et al. (2019d). Identification of serum metabolites associating with chronic kidney disease progression and anti-fibrotic effect of 5-methoxytryptophan. *Nat. Commun.* 10 (1), 1476. doi:10.1038/s41467-019-09329-0

Chen, D. Q., Cao, G., Zhao, H., Chen, L., Yang, T., Wang, M., et al. (2019b). Combined melatonin and poricoic acid A inhibits renal fibrosis through modulating the interaction of Smad3 and β-catenin pathway in AKI-to-CKD continuum. *Ther. Adv. Chronic Dis.* 10, 2040622319869116. doi:10.1177/2040622319869116

Chen, D. Q., Feng, Y. L., Cao, G., and Zhao, Y. Y. (2018a). Natural products as a source for antifibrosis therapy. *Trends Pharmacol. Sci.* 39 (11), 937–952. doi:10.1016/j.tips.2018.09.002

Chen, D. Q., Wu, X. Q., Chen, L., Hu, H. H., Wang, Y. N., and Zhao, Y. Y. (2020). Poricoic acid A as a modulator of TPH-1 expression inhibits renal fibrosis via modulating protein stability of β-catenin and β-catenin-mediated transcription. *Ther. Adv. Chronic Dis.* 11, 2040622320962648. doi:10.1177/2040622320962648

Chen, G. T., Yang, M., Chen, B. B., Song, Y., Zhang, W., and Zhang, Y. (2016). 2, 3, 5, 4'-Tetrahydroxystilbene-2-O-β-d-glucoside exerted protective effects on diabetic nephropathy in mice with hyperglycemia induced by streptozotocin. *Food Funct.* 7 (11), 4628–4636. doi:10.1039/c6fo01319h

Chen, H., Yang, T., Wang, M. C., Chen, D. Q., Yang, Y., and Zhao, Y. Y. (2018b). Novel RAS inhibitor 25-O-methylalisol F attenuates epithelial-to-mesenchymal transition and tubulo-interstitial fibrosis by selectively inhibiting TGF-β-mediated Smad3 phosphorylation. *Phytomedicine* 42, 207–218. doi:10.1016/j.phymed.2018.03.034

Chen, L., Cao, G., Wang, M., Feng, Y. L., Chen, D. Q., Vaziri, N. D., et al. (2019c). The Matrix Metalloproteinase-13 inhibitor poricoic acid ZI ameliorates renal fibrosis by mitigating epithelial-mesenchymal transition. *Mol. Nutr. Food Res.* 63 (13), e1900132. doi:10.1002/mnfr.201900132

Chen, L., Chen, D. Q., Wang, M., Liu, D., Chen, H., Dou, F., et al. (2017). Role of RAS/Wnt/β-catenin axis activation in the pathogenesis of podocyte injury and tubulo-interstitial nephropathy. *Chem. Biol. Interact.* 273, 56–72. doi:10.1016/j.cbi.2017.05.025

Chen, Q., Guo, H., Hu, J., and Zhao, X. (2022). Rhein inhibits NF-κB signaling pathway to alleviate inflammatory response and oxidative stress of rats with chronic glomerulonephritis. *Appl. Bionics Biomech.* 2022, 9671759. doi:10.1155/2022/9671759

Chen, T. K., Knicely, D. H., and Grams, M. E. (2019a). Chronic kidney disease diagnosis and management: a review. *JAMA* 322 (13), 1294–1304. doi:10.1001/jama.2019.14745

Choi, H. Y., Lim, J. E., and Hong, J. H. (2010). Curcumin interrupts the interaction between the androgen receptor and Wnt/β-catenin signaling pathway in LNCaP prostate cancer cells. *Prostate Cancer Prostatic Dis.* 13 (4), 343–349. doi:10.1038/pcan.2010.26

Dai, H., Liu, F., Qiu, X., Liu, W., Dong, Z., Jia, Y., et al. (2020). Alleviation by Mahuang Fuzi and Shenzhuo decoction in high glucose-induced podocyte injury by inhibiting the activation of wnt/β-catenin signaling pathway, resulting in activation of podocyte autophagy. *Evid. Based. Complement. Altern. Med.* 2020, 7809427. doi:10.1155/2020/7809427

De Souza, P., da Silva, L. M., de Andrade, S. F., and Gasparotto Junior, A. (2019). Recent advances in the knowledge of naturally-derived bioactive compounds as modulating agents of the renin-angiotensin-aldosterone system: therapeutic benefits in cardiovascular diseases. *Curr. Pharm. Des.* 25 (6), 670–684. doi:10.2174/1381612825666190329122443

Duan, S., Wu, Y., Zhao, C., Chen, M., Yuan, Y., Xing, C., et al. (2016). The Wnt/β-catenin signaling pathway participates in rhein ameliorating kidney injury in DN mice. *Mol. Cell. Biochem.* 411 (1-2), 73–82. doi:10.1007/s11010-015-2569-x

Duan, S., Zhang, S., Zhang, C., Wu, Y., Huang, Z., Xing, C., et al. (2017). Therapeutic effect of rhein on high glucose-induced podocyte injury via GSK3β-wnt/β-Catenin-PPARγ signaling pathway. *Int. J. Clin. Exp. Pathol.* 10 (6), 6279–6289.

Gao, Z., Kong, D., Cai, W., Zhang, J., and Jia, L. (2021). Characterization and anti-diabetic nephropathic ability of mycelium polysaccharides from Coprinus comatus. *Carbohydr. Polym.* 251, 117081. doi:10.1016/j.carbpol.2020.117081

Garg, M., and Maurya, N. (2019). Wnt/β-catenin signaling in urothelial carcinoma of bladder. *World J. Nephrol.* 8 (5), 83–94. doi:10.5527/wjn.v8.i5.83

Hansrivijit, P., Chen, Y. J., Lnu, K., Trongtorsak, A., Puthenpura, M. M., Thongprayoon, C., et al. (2021). Prediction of mortality among patients with chronic kidney disease: a systematic review. *World J. Nephrol.* 10 (4), 59–75. doi:10.5527/wjn.v10.i4.59

He, Y. M., Yang, H. J., Yang, Q., Cui, J. G., Wang, T. Z., Chen, Y., et al. (2015). Yiqi Huaju formula, a Chinese herbal medicine, reduces arterial pressure in salt-sensitive hypertension by inhibiting renin-angiotensin system activation. *Mol. Med. Rep.* 12 (4), 5321–5327. doi:10.3892/mmr.2015.4095

Hosseinian, S., Ebrahimzadeh Bideskan, A., Shafei, M. N., Sadeghnia, H. R., Soukhtanloo, M., Shahraki, S., et al. (2018). Nigella sativa extract is a potent therapeutic agent for renal inflammation, apoptosis, and oxidative stress in a rat model of unilateral ureteral obstruction. *Phytother. Res.* 32 (11), 2290–2298. doi:10.1002/ptr.6169

Hsu, C. N., and Tain, Y. L. (2021). Targeting the renin-angiotensin-aldosterone system to prevent hypertension and kidney disease of developmental origins. *Int. J. Mol. Sci.* 22 (5), 2298. doi:10.3390/ijms22052298

Huang, W. J., Liu, W. J., Xiao, Y. H., Zheng, H. J., Xiao, Y., Jia, Q., et al. (2020). Tripterygium and its extracts for diabetic nephropathy: Efficacy and pharmacological mechanisms. *Biomed. Pharmacother.* 121, 109599. doi:10.1016/j.biopha.2019.109599

Humphreys, B. D. (2018). Mechanisms of renal fibrosis. *Annu. Rev. Physiol.* 80, 309–326. doi:10.1146/annurev-physiol-022516-034227

Jhund, P. S., McMurray, J. J., Chaturvedi, N., Brunel, P., Desai, A. S., Finn, P. V., et al. (2015). Mortality following a cardiovascular or renal event in patients with type 2 diabetes in the ALTITUDE trial. *Eur. Heart J.* 36 (36), 2463–2469. doi:10.1093/eurheartj/ehv295

Kalantar-Zadeh, K., Jafar, T. H., Nitsch, D., Neuen, B. L., and Perkovic, V. (2021). Chronic kidney disease. *Lancet* 398 (10302), 786–802. doi:10.1016/s0140-6736(21)00519-5

Kobori, H., Nangaku, M., Navar, L. G., and Nishiyama, A. (2007). The intrarenal renin-angiotensin system: from physiology to the pathobiology of hypertension and kidney disease. *Pharmacol. Rev.* 59 (3), 251–287. doi:10.1124/pr.59.3.3

Li, S. S., Sun, Q., Hua, M. R., Suo, P., Chen, J. R., Yu, X. Y., et al. (2021). Targeting the Wnt/β-catenin signaling pathway as a potential therapeutic strategy in renal tubulointerstitial fibrosis. *Front. Pharmacol.* 12, 719880. doi:10.3389/fphar.2021.719880

Liu, D., Chen, L., Zhao, H., Vaziri, N. D., Ma, S. C., and Zhao, Y. Y. (2019). Small molecules from natural products targeting the Wnt/β-catenin pathway as a therapeutic strategy. *Biomed. Pharmacother.* 117, 108990. doi:10.1016/j.biopha.2019.108990

Lizaraso-Soto, F., Gutiérrez-Abejón, E., Bustamante-Munguira, J., Martín-García, D., Chimeno, M. M., Nava-Rebollo, Á., et al. (2021). Binding potassium to improve treatment with renin-angiotensin-aldosterone system inhibitors: results from multiple one-stage pairwise and network meta-analyses of clinical trials. *Front. Med.* 8, 686729. doi:10.3389/fmed.2021.686729

Lu, C. C., Hu, Z. B., Wang, R., Hong, Z. H., Lu, J., Chen, P. P., et al. (2020). Gut microbiota dysbiosis-induced activation of the intrarenal renin-angiotensin system is involved in kidney injuries in rat diabetic nephropathy. *Acta Pharmacol. Sin.* 41 (8), 1111–1118. doi:10.1038/s41401-019-0326-5

Luo, L. P., Suo, P., Ren, L. L., Liu, H. J., Zhang, Y., and Zhao, Y. Y. (2021). Shenkang injection and its three anthraquinones ameliorates renal fibrosis by simultaneous targeting IκB/NF-κB and Keap1/Nrf2 signaling pathways. *Front. Pharmacol.* 12, 800522. doi:10.3389/fphar.2021.800522

Luzes, R., Muzi-filho, H., Pereira-Acacio, A., Crisostomo, T., and Vieyra, A. (2021). Angiotensin-(3-4) modulates the overweight- and undernutritioninduced ACE2 downregulation in renal proximal tubule cells: implications for COVID-19? *Explor. Med.* 2, 134–145. doi:10.37349/emed.2021.00038

Mann, J. F., Schmieder, R. E., McQueen, M., Dyal, L., Schumacher, H., Pogue, J., et al. (2008). Renal outcomes with telmisartan, ramipril, or both, in people at high vascular risk (the ONTARGET study): a multicentre, randomised, double-blind, controlled trial. *Lancet* 372 (9638), 547–553. doi:10.1016/s0140-6736(08)61236-2

Mantovani, A., and Chiara, Z. (2020). PNPLA3 gene and kidney disease. *Explor. Med.* 1, 42–50. doi:10.37349/emed.2020.00004

Miao, H., Cao, G., Wu, X. Q., Chen, Y. Y., Chen, D. Q., Chen, L., et al. (2020). Identification of endogenous 1-aminopyrene as a novel mediator of progressive chronic kidney disease via aryl hydrocarbon receptor activation. *Br. J. Pharmacol.* 177 (15), 3415–3435. doi:10.1111/bph.15062

Mikusic, N. L. R., Pineda, A. M., and Gironacci, M. M. (2021). Angiotensin-(1-7) and mas receptor in the brain. *Explor. Med.* 2, 268–293. doi:10.37349/emed.2021.00046

Mo, L., Xiao, X., Song, S., Miao, H., Liu, S., Guo, D., et al. (2015). Protective effect of Huang Gan formula in 5/6 nephrectomized rats by depressing the Wnt/β-catenin signaling pathway. *Drug Des. Devel. Ther.* 9, 2867–2881. doi:10.2147/dddt.s81157

Nguyen, G., Delarue, F., Burcklé, C., Bouzhir, L., Giller, T., and Sraer, J. D. (2002). Pivotal role of the renin/prorenin receptor in angiotensin II production and cellular responses to renin. *J. Clin. Invest.* 109 (11), 1417–1427. doi:10.1172/jci14276

Qin, T., Wu, Y., Liu, T., and Wu, L. (2021). Effect of Shenkang on renal fibrosis and activation of renal interstitial fibroblasts through the JAK2/STAT3 pathway. *BMC Complement. Med. Ther.* 21 (1), 12. doi:10.1186/s12906-020-03180-3

Qin, T., Yin, S., Yang, J., Zhang, Q., Liu, Y., Huang, F., et al. (2016). Sinomenine attenuates renal fibrosis through Nrf2-mediated inhibition of oxidative stress and TGFβ signaling. *Toxicol. Appl. Pharmacol.* 304, 1–8. doi:10.1016/j.taap.2016.05.009

Rashid, I., Katravath, P., Tiwari, P., D'Cruz, S., Jaswal, S., and Sahu, G. (2022). Hyperuricemia-a serious complication among patients with chronic kidney disease: a systematic review and meta-analysis. *Explor. Med.* 3 (3), 249–259. doi:10.37349/emed.2022.00089

Song, X., Du, Z., Yao, Z., Tang, X., and Zhang, M. (2022). Rhein improves renal fibrosis by restoring Cpt1a-mediated fatty acid oxidation through SirT1/STAT3/twist1 pathway. *Molecules* 27 (7), 2344. doi:10.3390/molecules27072344

Tian, T., Chen, H., and Zhao, Y. Y. (2014). Traditional uses, phytochemistry, pharmacology, toxicology and quality control of alisma orientale (sam.) juzep: a review. *J. Ethnopharmacol.* 158, 373–387. doi:10.1016/j.jep.2014.10.061

Walther, C. P., Winkelmayer, W. C., Richardson, P. A., Virani, S. S., and Navaneethan, S. D. (2021). Renin-angiotensin system blocker discontinuation and adverse outcomes in chronic kidney disease. *Nephrol. Dial. Transpl.* 36 (10), 1893–1899. doi:10.1093/ndt/gfaa300

Wang, E., Wang, L., Ding, R., Zhai, M., Ge, R., Zhou, P., et al. (2020b). Astragaloside IV acts through multi-scale mechanisms to effectively reduce diabetic nephropathy. *Pharmacol. Res.* 157, 104831. doi:10.1016/j.phrs.2020.104831

Wang, M., Chen, D. Q., Chen, L., Cao, G., Zhao, H., Liu, D., et al. (2018a). Novel inhibitors of the cellular renin-angiotensin system components, poricoic acids, target Smad3 phosphorylation and Wnt/β-catenin pathway against renal fibrosis. *Br. J. Pharmacol.* 175 (13), 2689–2708. doi:10.1111/bph.14333

Wang, M., Chen, D. Q., Chen, L., Zhao, H., Liu, D., Zhang, Z. H., et al. (2018b). Novel RAS Inhibitors poricoic acid ZG and poricoic acid ZH attenuate renal fibrosis via a wnt/β-catenin pathway and targeted phosphorylation of smad3 signaling. *J. Agric. Food Chem.* 66 (8), 1828–1842. doi:10.1021/acs.jafc.8b00099

Wang, M., Hu, H. H., Chen, Y. Y., Chen, L., Wu, X. Q., and Zhao, Y. Y. (2020a). Novel poricoic acids attenuate renal fibrosis through regulating redox signalling and aryl hydrocarbon receptor activation. *Phytomedicine* 79, 153323. doi:10.1016/j.phymed.2020.153323

Wang, W. W., Liu, Y. L., Wang, M. Z., Li, H., Liu, B. H., Tu, Y., et al. (2021a). Inhibition of renal tubular epithelial mesenchymal transition and endoplasmic reticulum stress-induced apoptosis with Shenkang injection attenuates diabetic tubulopathy. *Front. Pharmacol.* 12, 662706. doi:10.3389/fphar.2021.662706

Wang, Y., Liu, Q., Cai, J., Wu, P., Wang, D., Shi, Y., et al. (2022b). Emodin prevents renal ischemia-reperfusion injury via suppression of CAMKII/DRP1-mediated mitochondrial fission. *Eur. J. Pharmacol.* 916, 174603. doi:10.1016/j.ejphar.2021.174603

Wang, Y. N., Feng, H. Y., Nie, X., Zhang, Y. M., Zou, L., Li, X., et al. (2022a). Recent advances in clinical diagnosis and pharmacotherapy options of membranous nephropathy. *Front. Pharmacol.* 13, 907108. doi:10.3389/fphar.2022.907108

Wang, Y. N., Wu, X. Q., Zhang, D. D., Hu, H. H., Liu, J. L., Vaziri, N. D., et al. (2021b). Polyporus umbellatus protects against renal fibrosis by regulating intrarenal fatty acyl metabolites. *Front. Pharmacol.* 12, 633566. doi:10.3389/fphar.2021.633566

Wang, Y., Zhang, L., Jin, H., and Wang, D. (2019). Based on HIF-1α/Wnt/β-catenin pathway to explore the effect of Qingshen granules on chronic renal failure patients a randomized controlled trial. *Evid. Based. Complement. Altern. Med.* 2019, 7656105. doi:10.1155/2019/7656105

Wu, X., Zhong, Y., Meng, T., Ooi, J. D., Eggenhuizen, P. J., Tang, R., et al. (2021). Patient survival between hemodialysis and peritoneal dialysis among end-stage renal disease patients secondary to myeloperoxidase-ANCA-associated vasculitis. *Front. Med.* 8, 775586. doi:10.3389/fmed.2021.775586

Xiang, X., Cai, H. D., Su, S. L., Dai, X. X., Zhu, Y., Guo, J. M., et al. (2019). Salvia miltiorrhiza protects against diabetic nephropathy through metabolome regulation and Wnt/β-catenin and TGF-β signaling inhibition. *Pharmacol. Res.* 139, 26–40. doi:10.1016/j.phrs.2018.10.030

Xiao, L., Xu, B., Zhou, L., Tan, R. J., Zhou, D., Fu, H., et al. (2019). Wnt/β-catenin regulates blood pressure and kidney injury in rats. *Biochim. Biophys. Acta. Mol. Basis Dis.* 1865 (6), 1313–1322. doi:10.1016/j.bbadis.2019.01.027

Xiao, L., Zhou, D., Tan, R. J., Fu, H., Zhou, L., Hou, F. F., et al. (2016). Sustained activation of Wnt/β-catenin signaling drives AKI to CKD progression. *J. Am. Soc. Nephrol.* 27 (6), 1727–1740. doi:10.1681/asn.2015040449

Xu, T., Zuo, L., Sun, Z., Wang, P., Zhou, L., Lv, X., et al. (2017). Chemical profiling and quantification of ShenKang injection, a systematic quality control strategy using ultra high performance liquid chromatography with Q Exactive hybrid quadrupole orbitrap high-resolution accurate mass spectrometry. *J. Sep. Sci.* 40 (24), 4872–4879. doi:10.1002/jssc.201700928

Xu, Z., Hou, Y., Sun, J., Zhu, L., Zhang, Q., Yao, W., et al. (2022). Deoxycholic acid-chitosan coated liposomes combined with *in situ* colonic gel enhances renal fibrosis therapy of emodin. *Phytomedicine.* 101, 154110. doi:10.1016/j.phymed.2022.154110

Xue, R., Gui, D., Zheng, L., Zhai, R., Wang, F., and Wang, N. (2017). Mechanistic insight and management of diabetic nephropathy: recent progress and future perspective. *J. Diabetes Res.* 2017, 1839809. doi:10.1155/2017/1839809

Yang, T., Chen, Y. Y., Liu, J. R., Zhao, H., Vaziri, N. D., Guo, Y., et al. (2019). Natural products against renin-angiotensin system for antifibrosis therapy. *Eur. J. Med. Chem.* 179, 623–633. doi:10.1016/j.ejmech.2019.06.091

Yang, T., and Xu, C. (2017). Physiology and pathophysiology of the intrarenal renin-angiotensin system: an update. *J. Am. Soc. Nephrol.* 28 (4), 1040–1049. doi:10.1681/asn.2016070734

Yao, S., Zhang, J., Wang, D., Hou, J., Yang, W., Da, J., et al. (2015). Discriminatory components retracing strategy for monitoring the preparation procedure of Chinese patent medicines by fingerprint and chemometric analysis. *PLoS One* 10 (3), e0121366. doi:10.1371/journal.pone.0121366

Yu, X. Y., Sun, Q., Zhang, Y. M., Zou, L., and Zhao, Y. Y. (2022). TGF-β/Smad signaling pathway in tubulointerstitial fibrosis. *Front. Pharmacol.* 13, 860588. doi:10.3389/fphar.2022.860588

Zhang, B., Zhang, X. L., Zhang, C. Y., Sun, G. B., and Sun, X. B. (2020). Shenkang Injection protects against diabetic nephropathy in streptozotocin (STZ)-induced mice through enhancement of anti-oxidant and anti-inflammatory activities. *Chin. Herb. Med.* 12 (3), 289–296. doi:10.1016/j.chmed.2020.05.004

Zhang, W. N., Li, A. P., Qi, Y. S., Qin, X. M., and Li, Z. Y. (2018). Metabolomics coupled with system pharmacology reveal the protective effect of total flavonoids of Astragali Radix against adriamycin-induced rat nephropathy model. *J. Pharm. Biomed. Anal.* 158, 128–136. doi:10.1016/j.jpba.2018.05.045

Zhang, Z., Zhang, Y., Ning, G., Deb, D. K., Kong, J., and Li, Y. C. (2008). Combination therapy with AT1 blocker and vitamin D analog markedly ameliorates diabetic nephropathy: blockade of compensatory renin increase. *Proc. Natl. Acad. Sci. U. S. A.* 105 (41), 15896–15901. doi:10.1073/pnas.0803751105

Zhou, L., Li, Y., Hao, S., Zhou, D., Tan, R. J., Nie, J., et al. (2015a). Multiple genes of the renin-angiotensin system are novel targets of Wnt/β-catenin signaling. *J. Am. Soc. Nephrol.* 26 (1), 107–120. doi:10.1681/asn.2014010085

Zhou, L., Li, Y., Zhou, D., Tan, R. J., and Liu, Y. (2013). Loss of Klotho contributes to kidney injury by derepression of Wnt/β-catenin signaling. *J. Am. Soc. Nephrol.* 24 (5), 771–785. doi:10.1681/asn.2012080865

Zhou, L., Mo, H., Miao, J., Zhou, D., Tan, R. J., Hou, F. F., et al. (2015b). Klotho ameliorates kidney injury and fibrosis and normalizes blood pressure by targeting the renin-angiotensin system. *Am. J. Pathol.* 185 (12), 3211–3223. doi:10.1016/j.ajpath.2015.08.004

Zhou, X. F., Wang, Y., Luo, M. J., and Zhao, T. T. (2021). Tangshen formula attenuates renal fibrosis by downregulating transforming growth factor β1/Smad3 and LncRNA-MEG3 in rats with diabetic kidney disease. *Integr. Med. Nephrol. Androl.* 8, 2. doi:10.4103/imna.imna_22_21

Zhu, Z., Ruan, S., Jiang, Y., Huang, F., Xia, W., Chen, J., et al. (2021). α-Klotho released from HK-2 cells inhibits osteogenic differentiation of renal interstitial fibroblasts by inactivating the Wnt-β-catenin pathway. *Cell. Mol. Life Sci.* 78 (23), 7831–7849. doi:10.1007/s00018-021-03972-x

Zuo, Y., and Liu, Y. (2018). New insights into the role and mechanism of Wnt/β-catenin signalling in kidney fibrosis. *Nephrology* 23 (4), 38–43. doi:10.1111/nep.13472

frontiers | Frontiers in Pharmacology

TYPE Review
PUBLISHED 02 September 2022
DOI 10.3389/fphar.2022.968226

OPEN ACCESS

EDITED BY
Dan-Qian Chen,
Northwest University, China

REVIEWED BY
Milad Ashrafizadeh,
Sabancı University, Turkey
Yaser Hosny Ali Elewa,
Zagazig University, Egypt
Maria Russo,
Institute of Food Sciences (CNR), Italy

*CORRESPONDENCE
Fu-Hua Lu,
lufuhua@gzucm.edu.cn
Yue-Yu Gu,
guyy@gzucm.edu.cn

†These authors have contributed equally to this work

SPECIALTY SECTION
This article was submitted to Renal Pharmacology, a section of the journal Frontiers in Pharmacology

RECEIVED 13 June 2022
ACCEPTED 28 July 2022
PUBLISHED 02 September 2022

CITATION
Chen Y-Q, Chen H-Y, Tang Q-Q, Li Y-F, Liu X-S, Lu F-H and Gu Y-Y (2022), Protective effect of quercetin on kidney diseases: From chemistry to herbal medicines.
Front. Pharmacol. 13:968226.
doi: 10.3389/fphar.2022.968226

Protective effect of quercetin on kidney diseases: From chemistry to herbal medicines

Yi-Qin Chen[1†], Hao-Yin Chen[1†], Qin-Qi Tang[1†], Yi-Fan Li[1], Xu-Sheng Liu[1], Fu-Hua Lu[1*] and Yue-Yu Gu[1,2*]

[1]Department of Nephrology, Guangdong Provincial Hospital of Chinese Medicine, The Second Affiliated Hospital of Guangzhou University of Chinese Medicine, Guangzhou, China, [2]Department of Pharmacology, School of Pharmaceutical Sciences, Guangzhou University of Chinese Medicine, Guangzhou, China

Kidney injuries may trigger renal fibrosis and lead to chronic kidney disease (CKD), but effective therapeutic strategies are still limited. Quercetin is a natural flavonoid widely distributed in herbal medicines. A large number of studies have demonstrated that quercetin may protect kidneys by alleviating renal toxicity, apoptosis, fibrosis and inflammation in a variety of kidney diseases. Therefore, quercetin could be one of the promising drugs in the treatment of renal disorders. In the present study, we review the latest progress and highlight the beneficial role of quercetin in kidney diseases and its underlying mechanisms. The pharmacokinetics and bioavailability of quercetin and its proportion in herbal medicine will also be discussed.

KEYWORDS

quercetin, natural product, herbal medicine, kidney injury, renal disease

1 Introduction

Kidney diseases are one of the life-threatening diseases with high mortality rates (Li et al., 2021b). Renal injuries could be triggered by various insults such as nephrotoxins, oxidative stress, or inflammation. These pathogenic factors act as the major driving force to promote renal injuries towards fibrosis (Gu et al., 2020b), which may eventually lead to chronic kidney disease (CKD) or end-stage renal disease (ESRD). To date, the effective drugs and therapeutic strategies for renal injury are still limited.

Natural products have been used in the clinical management of the renal disease. The constituent compounds of herbal medicine receive considerable attention in experimental models of kidney disease both *in vivo* and *in vitro* (Chen et al., 2018). Quercetin is one of the most abundant flavonoids present in natural plants. Due to its antioxidative, anti-hypertensive, and anti-diabetic effects, quercetin has been suggested as an effective flavonoid that plays a beneficial role in the treatment of cancer, cardiovascular disease, and metabolic disease (Sok Yen et al., 2021).

Although quercetin has been studied in many studies, we could not locate a recent overview of quercetin's action in kidney diseases. In the present review, we discuss and explore the biological effects of quercetin on kidney injuries such as nephrotoxicity, renal inflammation, fibrosis, hyperglycemia damage, and oxidative stress. We also identified the

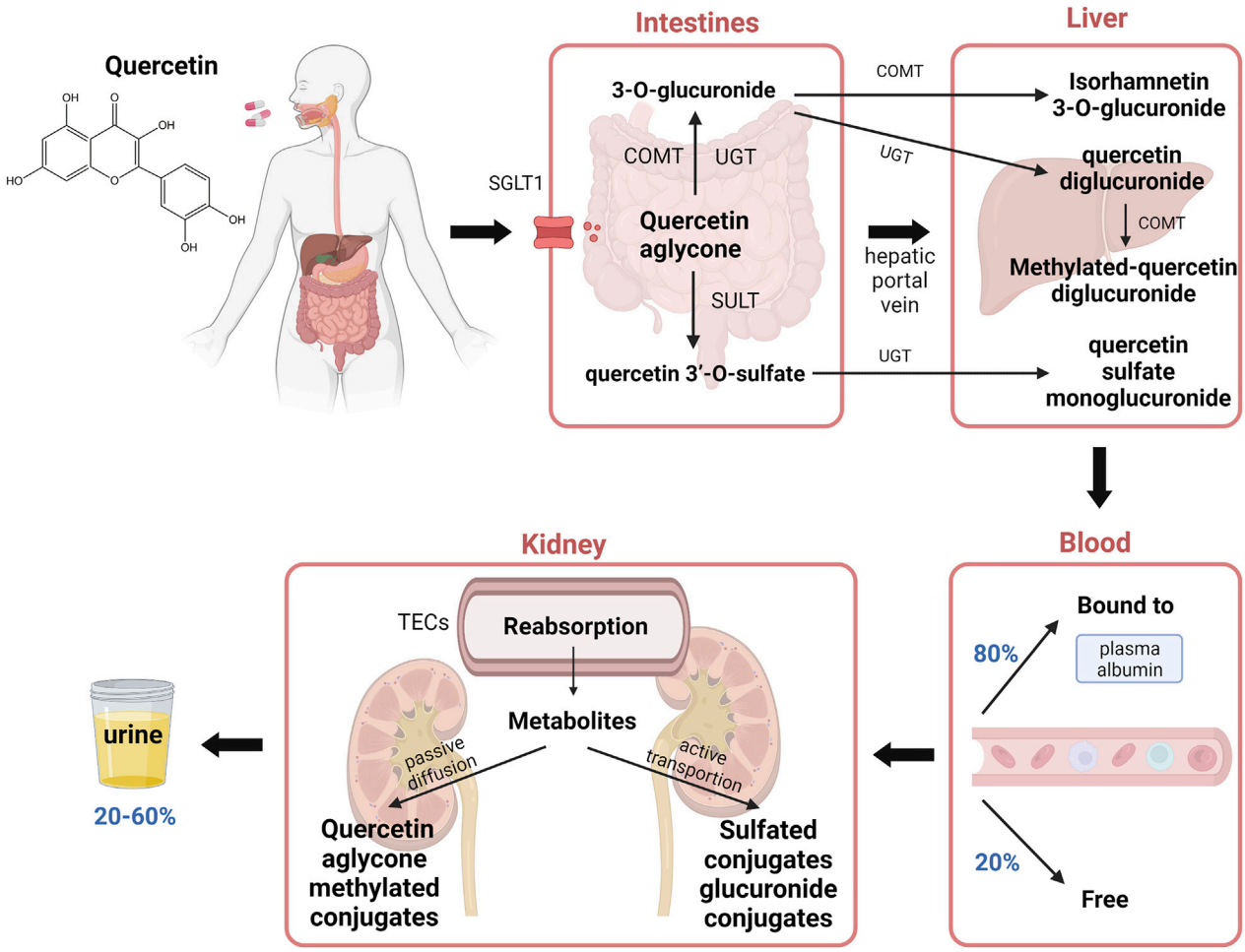

FIGURE 1
Chemical structure of quercetin and its pharmacokinetics in the body. Quercetin is transported by SGLT1, the process begins with hydrolysis in the gastrointestinal tract and releases quercetin aglycone. Biotransformation reactions include glucuronidation, methylation, and sulfation of quercetin aglycone are catalyzed by UGT, COMT, and SULT, respectively. Main metabolites such as 3-O-glucuronide and quercetin 3′-O-sulfate undergo a second transformation in the liver and 80% of the metabolites are bound to plasma albumin and the remaining 20% are free to enter tissues. The metabolites are reabsorbed in the TECs and enter cells by passive diffusion or active transportation. Up to 20%–60% of the quercetin intake may be secreted into the urine. Abbreviations: SGLT1, sodium-dependent glucose transporter 1; UGT, UDP-glucuronyltransferases; COMT, catechol O-methyltransferases; SULT, sulfotransferases; TECs, tubular epithelial cells.

pathogenic mechanisms of renal disease and focused on the signaling pathways that are potentially associated with quercetin treatment.

2 Pharmacokinetics and bioavailability of quercetin

Quercetin, also known as 3,5,7,3′,4′-pentahydroxyflavone, is a natural flavonoid compound. In nature, it exists in various forms in different plants and can be found as either quercetin aglycone or derivatives, while the most abundant form in the diet is glycosides (Owumi et al., 2019). Quercetin is highly soluble in lipids and alcohol. Due to its hydrophobicity, quercetin has relatively poor solubility in water (0.17–7 μg/ml), gastric fluids (5.5 μg/ml) and small intestine fluids (28.9 μg/ml), which have reduced its bio-accessibility (Bağdatlıoğlu, 2016). Quercetin aglycone exhibit a poor oral bioavailability of about 2%. However, depending on different radicals bound to the quercetin aglycone backbone, the solubility and biochemical activity of quercetin derivatives vary. The glycoside is much more soluble compared to aglycone, as the glycosyl group increases the water solubility. After the intake of quercetin-rich supplements in human bodies, quercetin quickly disappeared in the body with a 1–2 h removal half-life (Graefe et al., 1999).

Quercetin can be transported through sodium-dependent glucose transporter 1(SGLT1). The process begins with the hydrolysis of quercetin glycosides by lactase phloridzin hydrolase (LPH) and intracellular *ß*-Glucosidases and releases quercetin aglycone. Quercetin aglycone is then primarily metabolized in the gastrointestinal tract (Graf et al., 2006). In enterocytes, the biotransformation of quercetin includes glucuronidation by UDP-glucuronyltransferases (UGT), methylation by catechol O-methyltransferases (COMT), and sulfation by sulfotransferases (SULT). 3-O-glucuronide and quercetin 3′-O-sulfate are the two main metabolites passing from the enterocyte and diffusing into the hepatic portal vein to undergo a second transformation in the liver before returning to the bloodstream (Figure 1). Afterward, about 80% of aglycone or metabolites are bound to plasma albumin and the remaining 20% free form can enter the tissues, therefore the aglycone amount is relatively low in the blood. The metabolism process takes place in the intestines, liver and kidneys and the accumulation tends to happen in those organs.

In the kidney, the metabolites from the plasma go through the glomerular filtration process, followed by dispersion into the tubular. The metabolites are partially reabsorbed by tubular epithelial cells (TECs), and the remaining part passes into the urine. The transportation to proximal TECs primarily occurs in the basolateral membrane and apical membrane (Wong et al., 2011). Quercetin aglycone and methylated conjugates across the basolateral membrane by passive diffusion, while sulfated conjugates and glucuronide conjugates use active transport to enter the cells, due to their high affinity for organic anion transporters (OATs). The metabolites are formed in the tubular cells and secreted into the urine. In the human body, the quercetin metabolites excreted through urine take up 20%–60% of total quercetin intake and they are mainly composed of monoglucuronide sulfates, methylated quercetin monoglucuronides, and quercetin diglucuronide (Graf et al., 2006; Mullen et al., 2006).

Previous experiments and studies have revealed the pharmacodynamics of quercetin, it is found that due to its chemical structure, it has low water solubility, oral absorption rate, rapid elimination, and low bioavailability (Diniz et al., 2020). Such characteristics greatly hindered the application of quercetin in pre-employment drug testing and clinical practice (Heeba and Mahmoud, 2016). Casanova et al. (2021) encapsulated quercetin with Pluronic F127 to make micelles and found that it had higher water solubility with good bioavailability, and the protective effect on the kidney had been greatly improved (Gu et al., 2020a). Although more in-depth drug experiments and clinical trials are needed, it is believed that the utilization of quercetin can be improved in the future.

3 Quercetin in traditional herbal medicines

Except for various food and supplements, quercetin is widely abundant in flowers, leaves and fruits of plants. It was determined in nearly 200 kinds of traditional Chinese herbal medicines, such as *Sophora japonicum, Radix Bupleuri* (Sen-ming, 2013), *Gynostemmae Pentaphylli Herba* (Conglei Pan, 2019).

High-performance liquid chromatography (HPLC) was mainly used to determine the content of quercetin in herbal medicine. As shown in Table 1, the content of quercetin in different species can vary from less than 1 mg/g to more than 300 mg/g. According to the theory of traditional Chinese medicine (TCM), the efficacy of these herbal medicines containing quercetin can be summarized as follows: 1) heat clearing: the heat described in TCM is somehow related to the inflammatory response in the body and due to quercetin's significant antioxidant property, it can relieve pain and inflammation. For instance, stranguria is a common urologic disease that is considered to cause by excessive damp heat in the lower energizer. In clinical practice, *Houttuyniae cordata* (Arky Jane Langstieh et al., 2021), *Pyrrosiae lingua* (Chen Junhua et al., 2014), and *Centella asiatica* (Mohammad Azmin and Mat Nor, 2020) are frequently selected, which contained 315.8 mg/g, 234.6 mg/g, and 77.6 mg/g quercetin, respectively. Other representative herbal medicines with heat-clearing effect include *Mori follum*, *Sophora japonica* L., and *Fallopia multiflora Herba* (Vetrova et al., 2017), and *Fallopia multiflora Herba* (Bao Lidao et al., 2015); 2) urination promotion, swelling, or edema reduction: by dilating the renal arteries, quercetin can increase blood and urine volume, therefore alleviating the edema. The common ingredients are *Ephedra Herba* (Saida Ibragic, 2015), *Hedysarum Multijugum Maxim* (Fu Juan and Huang, 2013), and *Plantaginis Semen* (Cao Xuesong and Huang, 2019); 3) promoting kidney recovery: other herbal medicines also exert a nourishing and strengthening effect on the kidney, such as *Lycii Fructus* (Kim Le and Ng, 2007), *Herba Taxilli* (Zhu Kaixin et al., 2011), and *Rubi Fructus* (Zhang Jing and Yan, 2020). *Crataegi Folium* (Deng Ting et al., 2021) (12.73 mg/g) was reported to attain a cardiovascular protection effect by lowering blood lipid, while the contents of quercetin in *Ginkgo Folium* (Qiu et al., 2017) and *Inulae Flos* (Hongmei, 2008) are relatively low (less than 1 mg/g).

4 Renal protective effects of quercetin in kidney disease

4.1 Nephrotoxicity

When exposed to certain toxic substances or harmful pollution for a long period, one may occur nephrotoxicity. Due to the special biological structure and physiological role,

TABLE 1 The content of quercetin commonly used in traditional Chinese medicine.

Name	Latin name	Active portion	Quercetin content (mg/g)	Reference
Chai Hu	*Radix Bupleuri*	Root	1.7127	Sen-ming (2013)
Che Qian Zi	*Plantaginis Semen*	Seed	0.81	Cao Xuesong and Huang (2019)
Fu Pen Zi	*Rubi Fructus*	Fruit	0.9451	Zhang Jing and Yan (2020)
He Shou Wu	*Fallopia multiflora Harald*	Aerial part	0.55	Bao Lidao et al. (2015)
Huai hua	*S. japonica L.*	Flower	13.7	Vetrova et al. (2017)
Jiao Gu Lan	*Gynostemmae Pentaphylli Herba*	Leaf	14.78	Conglei Pan (2019)
Sang Ji Sheng	*Herba Taxilli*	Leaf	5.27	Zhu Kaixin et al. (2011)
Sang Ye	*Mori Follum*	Leaf	1.784–3.645	Zhong Yuekui and Qiu (2021)
Shan Zha Ye	*Crataegi Folium*	Leaf	12.73	Deng Ting et al. (2021)
Yu Xing Cao	*H. cordata*	Leaf	315.8	Arky Jane Langstieh et al. (2021)
Yin Xing Ye	*Ginkgo Folium*	Leaf	0.609	Qiu et al. (2017)
Xuan Fu Hua	*Inulae Flos*	Flower	0.86	Hongmei (2008)
Gou Qi Zi	*Lycii Fructus*	Fruit	0.296	Kim Le and Ng (2007)
Huang Qi	*Hedysarum Multijugum Maxim*	Root	0.6–1.1	Fu Juan and Huang (2013)
Ji Xue Cao (Asiatic Pennywort Herb)	*C. asiatica (L.)* (Hydro-Cotyle *Asiatica L.*)	Leaf	77.6 (dry)	Mohammad Azmin and Mat Nor (2020)
Ma Huang	*Ephedra Herba*	Stem	2.8 (dry)	Saida Ibragic (2015)
Shi Wei	*P. lingua*	Leaf	234.6	Chen Junhua et al. (2014)

the kidneys are important organs for drug metabolism and are susceptible to toxins including antineoplastics, antibiotics and many kinds of agents. As summarized in Table 2, many experimental studies and mechanism exploration of multifaceted signal transduction and pathways suggest that quercetin has great potential in reducing renal toxicity.

Antineoplastic agents such as cisplatin (Li et al., 2016a), methotrexate (Erboga et al., 2015), doxorubicin (Heeba and Mahmoud, 2016), and cyclophosphamide may cause side effects in clinical treatment due to dose-related nephrotoxicity. The nephroprotective effect of quercetin against cisplatin-induced oxidative stress was demonstrated by Almaghrabi (2015). In cisplatin-treated rats, quercetin can reduce tubular injury, downregulate the pro-inflammatory mediators and maintain renal blood flow. Moreover, quercetin also exhibited antioxidant and anti-apoptotic effects, therefore reducing the apoptosis of non-tumor cells caused by cisplatin treatment (Almaghrabi, 2015; Casanova et al., 2021). It is worth mentioning that quercetin did not interfere with the antitumor activity of cisplatin (Sánchez-González et al., 2017). Furthermore, experimental results have shown that quercetin may enhance the activity of cisplatin against cancer (Li et al., 2016a). Likewise, quercetin may protect against cyclophosphamide-induced hepatic and renal injury by immunosuppressing the IDO/TDO pathway (Ebokaiwe et al., 2021). It is hypothesized that this effect may be due to the combination of quercetin's ability to scavenge reactive oxygen species (ROS) and inhibition of malondialdehyde (MDA) formation. The production of free radicals and ROS are key triggers for the activation of Nrf2 (nuclear factor erythroid 2-related factor 2) and HO-1 (renal heme oxygenase 1). Regarding nephrotoxicity, Nrf2/HO-1 pathway may play an important role in boosting the GSH, GPx, and SOD antioxidant moieties (Arab et al., 2021). Quercetin supplementation could markedly activate the mRNA expression of Nrf2 and HO-1 in copper sulfate-induced renal injury mice (Peng et al., 2020).

Dosage is of great importance in the understanding of the pharmacological effects of quercetin. Of note, evidence also support that when applied with high dose, such as 100 mg/kg/d, quercetin did not show significant improvement in renal function or protection against doxorubicin-induced renal injury (Heeba and Mahmoud, 2016). Nevertheless, quercetin protects kidneys against antineoplastic drugs through the inhibition of inflammatory response, enhancement of the antioxidant system, and exertion of anti-apoptotic effects.

Oral pretreatment of quercetin in rats with gentamicin-induced renal injury (50 mg/kg) for 10 days revealed an improvement in renal injury. The mechanisms of the protective effect of quercetin could be the rebalancing of the antioxidant system and the modulation of renal biomarkers (Rahdar et al., 2021). A study reported by Dallak et al. (2020) showed that toxic doses of acetaminophen formed severe damage to glomerular ultrastructural compartments after 24 h, and apoptosis was observed in renal tissues. Pretreatment with resveratrol and quercetin exerted a protective effect, namely the reduction of p53 expression in the renal tissue, as well as the decrease of blood urea, creatinine, and oxidative biomarkers.

TABLE 2 Protective effects and mechanism of quercetin against renal toxins.

Toxins	Model	Quercetin Dose (mg/kg)	Effects/Mechanisms	References
Cisplatin		50, 100	Anti-inflammatory, maintained renal blood flow, anti-oxidative and enhanced the antitumor activity, reduced renal injury	Sánchez-González et al. (2017), Casanova et al. (2021), Li et al. (2016a), Almaghrabi (2015)
Methotrexate		15, 50	Anti-oxidative, reduced renal injury, scavenged free radicals	Yuksel et al. (2017)
Cyclophosphamide		50	Anti-inflammatory, anti-oxidative	Ebokaiwe et al. (2021)
Doxorubicin		10, 50	Anti-oxidative, anti-inflammatory, protected podocytes	Khalil et al. (2018), Heeba and Mahmoud (2016)
Cadmium		10, 50	Anti-inflammatory, anti-oxidative, reduced renal injury, regulated the metabolism of lipids, amino acids, and purine, anti-oxidative	Jia et al. (2020), Liu et al. (2020), Guan et al. (2021)
Sodium nitrite		200	Anti-inflammatory	Alshanwani et al. (2020)
Diesel exhaust particles		60	Anti-oxidative, anti-inflammatory, promoted autophagy	Morsi et al. (2022)
Ferrous sulfate		50	Reduced renal injury	Gholampour and Saki (2019)
Acrylamide	rats	5, 10, 20, 40, 50	Reduced urea, uric acid levels, anti-oxidative, anti-apoptotic	Bao et al. (2017), Uthra et al. (2017), Bo et al. (2018)
$NTiO_2$		75	Anti-inflammatory, anti-oxidative, anti-apoptotic	Alidadi et al. (2018)
Gold nanoparticles		100	Anti-inflammatory, anti-oxidative	Abdelhalim et al. (2018)
Organophosphate pesticides		10, 50	Regulated the metabolism of fatty acids, energy, and sex hormones, anti-oxidative, anti-apoptotic	Qi et al. (2017), Li et al. (2016b)
Ochratoxin A		50	Anti-inflammatory, anti-oxidative, anti-apoptotic	Abdel-Wahhab et al. (2017)
Combination antiretroviral therapy		50	Anti-inflammatory, anti-oxidative, improved the cytoarchitecture and biochemical activities of the organs	Gu et al. (2020a)
Acetaminophen		50	Anti-inflammatory, anti-oxidative, reduced renal injury	Dallak et al. (2020)
Echis pyramidum venom		10	Anti-oxidative, anti-edema, and wound healing effects	Al-Asmari et al. (2018)
Gentamicin		50	Attenuated lipid peroxidation, antioxidative, reduced renal injury	Rahdar et al. (2021)
Valproic acid	Supernatant, renal, tissue	0.05 mM	Cleaned the free radicals, anti-oxidative	Chaudhary et al. (2015)
Contrast media	Human	500 mg	Reduced renal injury	Vicente-Vicente et al. (2019)
	HK-2 cells	10, 100 μm	Reduced renal injury	Andreucci et al. (2018)

In addition, quercetin also exerts renoprotective effects on antiretroviral combination therapy involving multiple drugs. Valproic acid (VPA) is widely used to intervene in epilepsy and control multiple seizures. It was deduced from experimental studies that the effectiveness of quercetin in protecting against VPA-induced kidney injury and toxicity relies on its ability to scavenge free radicals and alter antioxidant status (Chaudhary et al., 2015). Quercetin showed the potential to improve kidney damage caused by cArt through inhibiting oxidative stress and inflammatory processes. As a result, quercetin participates in the scavenging of toxins, improves the cellular structure of organs and maintains normal biological chemical activity (Gu et al., 2020a).

Specifically, with the development of industrial technology and the progress of science and technology, the damage of chemical raw materials to the kidney has grown immensely prominent. Data from animal models have shown that the protective effect of quercetin is closely related to the clearance of free radicals and reduction of lipid peroxidation in both industrial chemical raw materials and heavy metal and diesel particulate pollution (Li et al., 2016b; Qi et al., 2017; Uthra et al., 2017; Alshanwani et al., 2020; Morsi et al., 2022). Moreover, Quercetin was also found to reduce organophosphorus pesticide mixture-induced nephrotoxicity by regulating fatty acid, energy and sex hormone metabolism, protecting antioxidant defense systems and reducing DNA damage (Qi et al., 2017). Quercetin may regulate the metabolism of phospholipids, energy, fatty acids and amino acids to protect the kidney against acrylamide-induced nephrotoxicity (Bao et al., 2017;

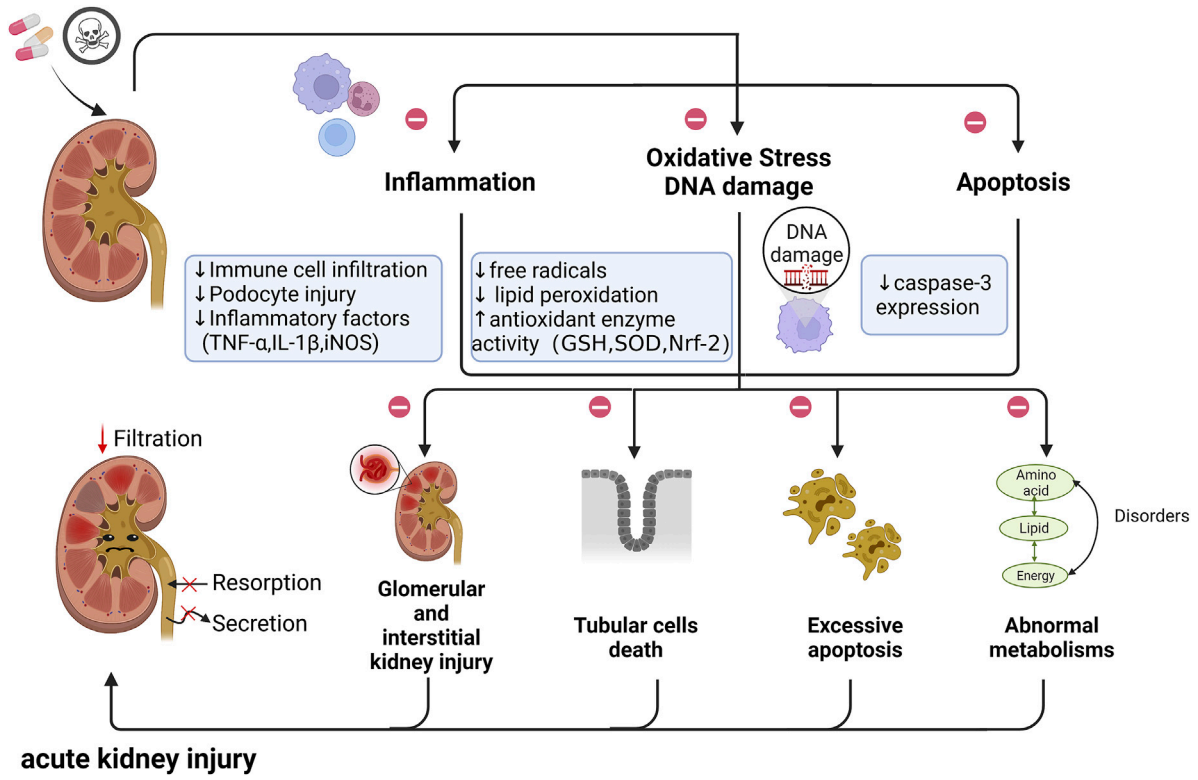

FIGURE 2
The potential role of renal toxins in the pathogenesis of AKI. Nephrotoxins may cause glomerular and interstitial kidney injury, tubular cell necrosis, and excessive apoptosis. In addition, the normal metabolism of the body can also be disrupted. This contributes to the reduction of kidney filtration and the impaired function of reabsorption and secretion, and eventually leads to acute kidney injury. (⊖ indicates therapeutic targets of quercetin; ↑ and ↓ indicates the regulatory role of quercetin on pathogenic changes); Abbreviations: TNF-α, tumor necrosis factor α; IL-1β, interleukin 1β; iNOS, inducible nitric oxide synthase; GSH, glutathione; SOD, superoxide dismutase; Nrf-2,Nuclear factor erythroid 2-related factor 2.

Bo et al., 2018). All these findings have shown that quercetin can produce significant protective effects in alleviating nephrotoxicity and renal insults caused by drug treatments (Figure 2).

4.2 Acute and chronic renal injury

4.2.1 Acute kidney injury

Injuries from mesangial cells, endothelial cells (ECs), podocytes, TECs, and inflammatory cells could also lead to glomerular and interstitial fibrosis. Unresolved renal inflammation could also trigger cell apoptosis and fibrosis by releasing pro-apoptotic, pro-fibrotic growth factors, cytokines, and chemokines (Gu et al., 2021a).

Cell apoptosis and glomerular injuries are observed during renal ischemia. Quercetin can effectively prevent glomerular loss caused by renal hypochlorous ischemia (Gonçalves et al., 2021). The pathogenesis of renal ischemia/reperfusion injury (IRI) involves oxidative stress responses in the kidneys and distal organs, and the antioxidant effect of quercetin can prevent partial IRI (Gholampour and Sadidi, 2018). Regarding apoptosis, iron apoptosis is the iron-dependent regulatory necrosis that contributes to the progression of acute kidney injury (AKI), quercetin inhibits iron apoptosis in proximal renal TECs, thereby reducing AKI (Wang et al., 2021).

Carvedilol can relieve AKI caused by renal IRI and quercetin restores renal function by reducing inflammation (Rezk et al., 2021). Quercetin may also prevent AKI by regulating Mincle/Syk/NF-κB signaling to inhibit macrophage inflammation (Tan et al., 2020). Quercetin improves kidney damage by regulating macrophage polarization (Lu et al., 2018). Lipopolysaccharide (LPS) induces AKI in mice, and quercetin pretreatment protects mice from LPS-induced renal inflammation by inhibiting the TLR4/NF-κB signaling pathway (Tan et al., 2019). Quercetin may prevent sepsis-associated AKI by inhibiting NF-κB activation and upregulating Sirt1 expression (Lu et al., 2021). Besides, CD38 plays an important role in macrophage activation during sepsis-induced AKI. In the

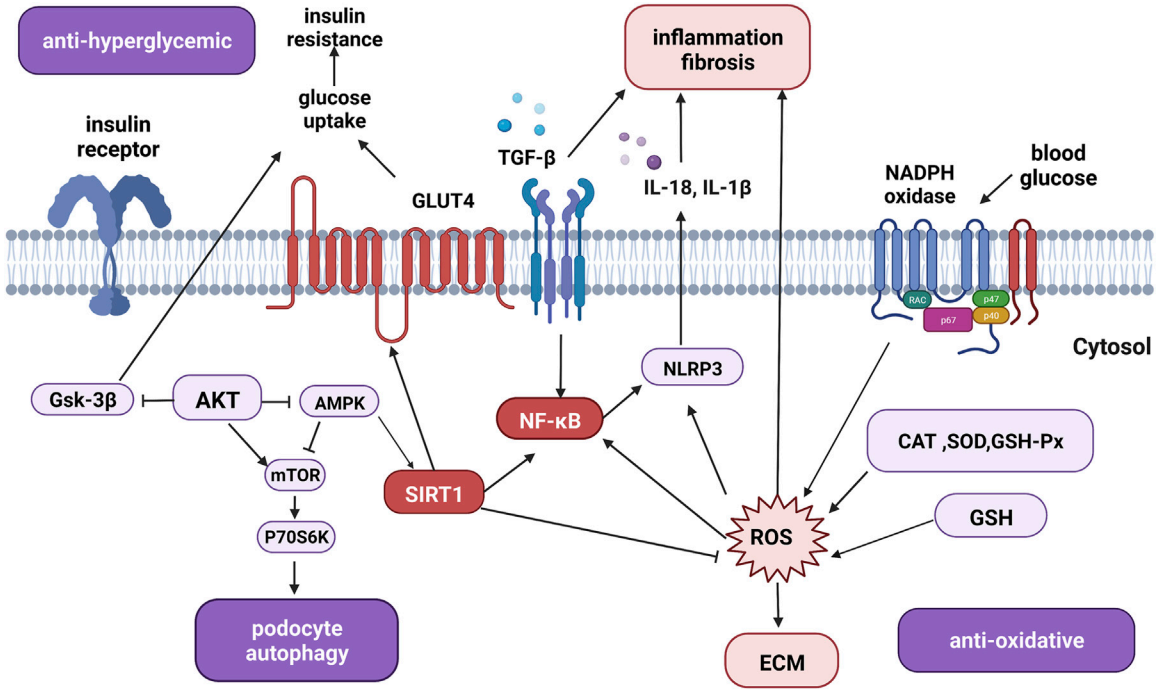

FIGURE 3
The overview of signaling pathways and therapeutic targets of quercetin in the treatment of diabetic nephropathy. Quercetin acts as an anti-hyperglycemic agent by regulating glucose-related signaling pathways. Quercetin also targets fibrotic, inflammatory, and oxidative mediators such as TGF-β, SIRT1, AKT, and NF-κB to inhibit inflammation, fibrosis, oxidative stress, apoptosis, and promote autophagy to exert renal protective effects. Abbreviations: Gsk-3β, glycogen synthase kinase-3; AKT, protein kinase B; AMPK, AMP-activated protein kinase; mTOR, mammalian target of rapamycin; P70S6K, 70-kDa ribosomal protein S6 kinase; GLUT4, glucose transporter protein type-4; TGF-β, transforming growth factor beta; NF-κB, nuclear factor κ-light-chain-enhancer of activated B cells; SIRT1, silent information regulator 1; NLRP3, NLR family pyrin domain containing 3; CAT, catalase; SOD, superoxide dismutase; GSH-Px, glutathione peroxidase; GSH, glutathione; ROS, reactive oxygen species; ECM, extracellular matrix; IL-18, interleukin-18; IL-1β, interleukin-1β; (Figure created with BioRender.com).

LPS-induced AKI mouse model, quercetin induces the blockade of CD38, thus significantly alleviating renal dysfunction and the infiltration of inflammatory cells (Shu et al., 2018).

Interestingly, as kidneys are one of the targets of SARS-CoV-2, up to 36% of SARS-CoV-2-infected patients develop AKI. COVID-19-induced inflammation is closely associated with AKI. Quercetin restores renal function by inhibiting the inflammatory and apoptosis-related signaling pathways (Gu et al., 2021b). Quercetin may potentially target SARS-CoV-2 3Clpro, which might inhibit the invasion of coronavirus, the life-threatening inflammation and cytokines storm in AKI (Diniz et al., 2020).

4.2.2 Chronic kidney injury and renal fibrosis

One of the notable pathological characteristics of CKD is renal fibrosis, a prolonged wound-healing process that responds to multiple tissue injuries in the kidney. This process is characterized by glomerulosclerosis, tubular atrophy, and interstitial fibrosis. Studies have shown that renal fibrosis could be triggered by chronic inflammation. Renal injuries promote the recruitment of inflammatory cells and the release of related cytokines, chemokines, and ROS. This inflammatory process eventually activates fibroblasts and promotes the synthesis and accumulation of extracellular matrix (ECM) proteins. It is demonstrated that quercetin alleviated inflammation by upregulating the miR-124/NF-κB pathway in LPS-stimulated TECs (Guo et al., 2020). Of note, quercetin can also reduce macrophage accumulation and the expression of inflammatory cytokines in the kidneys of obstructive, therefore inhibiting renal fibrosis (Ren et al., 2016).

Transforming growth factor beta (TGF-β) is a major cytokine that promotes ECM accumulation. It may also induce the apoptosis of podocytes and promote epithelial to mesenchymal transition (EMT) progression (Arauz et al., 2015). One study has demonstrated that quercetin downregulated TGF-β signaling and reduced the expression of EMT-related proteins to halt the progression of glomerulosclerosis (Liu et al., 2019b). Other studies have also suggested that quercetin suppressed TGF-β signaling *via* Sonic Hedgehog, PTEN/TIMP3 and PI3k/Akt signaling pathways (Cao et al., 2018; Liu et al., 2019a; Tu et al., 2021). All the studies have suggested the anti-fibrotic role of quercetin in chronic kidney injury.

4.3 Diabetic nephropathy

4.3.1 Anti-hyperglycemic effect

As shown in Figure 3, the regulatory roles of the signaling pathways involved in diabetic nephropathy (DN) are complex. Both hyperglycemia and dyslipidemia can induce structural and functional damage in diabetic kidneys (Sun et al., 2019). On one hand, quercetin decreases blood glucose levels by increasing the release of insulin while reducing hepatic glucose production. Mechanistically, quercetin may also enhance glucose uptake by regulating the expression and function of GLUT4 and the insulin receptor beta subunit (Ali et al., 2020).

On the other, hyperglycemia also induces metabolic alterations, resulting in the disturbance of protein, fat, and carbohydrate metabolism. Disorders of these metabolites also increase the burden on the diabetic kidneys. Quercetin at a dosage of 10 mg/kg/d can reduce blood glucose and triglycerides serum levels (Gomes et al., 2015). Likewise, at the early stage of DN, 50 or 100 mg/kg/d quercetin could improve lipid metabolism by alleviating albuminuria and renal function. In terms of lipid metabolism, quercetin reduces serum cholesterol, and triglycerides, and increases low-density lipoprotein cholesterol through the SCAP-SREBP2-LDLr signaling pathway in the diabetic rat model (Jiang et al., 2019).

4.3.2 Anti-oxidative effect

The excessive expression of intracellular ROS is one of the significant changes in DN. ROS induces the activity of apoptosis-related enzymes, causing damage to the podocytes and promoting the proliferation of fibrotic cells to induce the synthesis of ECM (Ma et al., 2018). These processes result in renal fibrosis and inflammation and turn out to the progression of DN. Quercetin has acted as a free radical scavenger in DN animal models. For instance, one study measured the antioxidant-related enzymes and histopathological changes in kidneys and found that quercetin alleviated the damage by preventing oxidative stress (Elbe et al., 2015). As reported by other studies, dihydro quercetin exerts a renal protective effect on DN rats at the dose of 100 mg/kg/day, with the downregulated expression of ROS-related proteins and NLRP3 inflammasome (Ding et al., 2018). Besides, another study has revealed that both quercetin and quercetin-nanoparticle complex reduced structural damage to the kidney, improved renal function and alleviated oxidative stress by downregulating the expression of ICAM-1 (Tong et al., 2017).

4.3.3 Autophagy promotion

Autophagy plays a crucial role in the intracellular degradation system for cellular homeostasis. As for kidney diseases, autophagy may protect functions in both glomerular and tubular compartments by suppressing excessive inflammation and fibrosis in AKI, CKD, and DN (Kimura et al., 2017; Bhatia and Choi, 2020). For example, hyperglycemia induces the dysregulation of autophagy in major types of resident kidney cells, mainly the impairment of podocytes. Autophagy is primarily regulated by signaling pathways such as the serine/threonine protein kinase mammalian target of rapamycin (mTOR), AMP activated protein kinase (AMPK), and sirtuins. High glucose can inhibit podocyte autophagy through AMPK pathway (Platé et al., 2020) and activate the mTOR signaling to inhibit podocyte autophagy. Evidence has suggested a quercetin-rich fruit, guava, is able to protect against type 2 diabetes mellitus-induced renal and pancreatic dysfunction by preventing cell apoptosis, autophagy, and pyroptosis (Lin et al., 2016). More studies have also demonstrated quercetin regulating blood glucose/lipid levels and improving renal fibrosis, potential mechanisms could be the modulation of the AMPK-dependent autophagy process, inhibition of mTORC1/p70S6K signaling, or the activation of Hippo pathways *in vitro* and *in vivo* (Lu et al., 2015; Lei et al., 2019; Lai et al., 2021). Further studies should focus on the glycemic regulating role and underlying mechanisms of quercetin treatment on DN.

4.4 Senolytic therapy for kidney disease

As clinical interest in kidney aging rapidly arises, the progression of cellular senescence relates closely to the stable cell cycle arrest. The accumulation of renal senescent cells (SCs) promotes inflammation and fibrosis, leading to multiple kidney disorders. The senolytics are a class of drugs that may selectively clear SCs. Quercetin, together with dasatinib, acts as the novel pharmacological senolytic agent for a number of kidney diseases (Kirkland and Tchkonia, 2020).

Senescent TECs are the driving force in renal fibrosis progression, which may activate fibroblasts. The combination of quercetin and dasatinib may specifically induce apoptosis of senescent TECs, therefore restoring renal function and ameliorating fibrosis (Li et al., 2021a). Another study has also shown that the combination of quercetin and dasatinib can alleviate renal insufficiency and damage in animal models of renal ischemia. *In vivo* study has revealed that senolytic therapy of quercetin and dasatinib improved renal artery stenosis by reducing the p21 positive stenotic TECs and attenuating mesenchymal transition (Kim et al., 2021). Notably, obesity could promote cellular senescence and impair renal function. Researchers have found an increased expression of renal markers of senescence, such as p16, p19, and p53, in a high-fat-diet-induced mouse model. Renal function and fibrosis are improved in quercetin-treated mice (Kim et al., 2019). Similarly, an open-label Phase 1 pilot study (NCT02848131) in patients with diabetic kidney disease showed that the combination of quercetin and dasatinib can eliminate senescent cells and significantly reduce senescent cell burden in adipose and skin

tissues within 11 days. The possible mechanisms of their protective effects may be associated with the decrease of p16-, p21 expressing cells and the downregulation of senescence-associated secretory phenotype (including the expression of pro-inflammatory cytokines IL-6, IL-1α, and MMP-9) (Hickson et al., 2019). More explorations are needed to investigate the mechanism of analytic therapy and verify its efficacy and safety. The combination of quercetin and dasatinib could serve as new therapeutic agents to hinder renal senescence.

4.5 Other renal disorders

Dietary intake of the flavonoid quercetin has been proven effective in lowering blood pressure and restoring endothelial dysfunction in animal models of hypertension. Quercetin intake improves endothelium-dependent relaxation and inhibits α1-adrenoceptor mediated contractions in aortic rings from hypertensive rats. In addition, quercetin treatment in high dose promotes a significant reduction in blood pressure in spontaneously hypertensive rats compared to the control group (Choi et al., 2016; Elbarbry et al., 2020). These data not only demonstrate the anti-hypertensive effect of quercetin but also provide evidence for its role as a novel cardioprotective compound.

Renal cell carcinoma (RCC) has become a common subtype of kidney cancer, which has the highest propensity to manifest as metastatic disease. We lack knowledge of the correlation between migration and invasion in RCC, thus few therapeutic options are available (Meng et al., 2015). Intriguingly, recent studies have found that quercetin has anti-tumor effects against diverse types of cancers *via* multiple signaling pathways (Zhu et al., 2018). For example, a study explored the anti-tumoral effect of a potential chemopreventive effect of quercetin, the combination of quercetin and anti-sense oligo gene therapy provides stronger suppressive effects on RCC cells rather than a solo treatment. These studies have provided the possibility of quercetin as a novel treatment for renal cancer (Meng et al., 2015).

Autosomal dominant polycystic kidney disease (ADPKD) is a monogenic disease characterized by the massive enlargement of fluid-filled cysts in the kidney. One study has found that quercetin dramatically inhibited the formation and growth of the cyst, suggesting that quercetin could hinder renal cyst progression and should be represented as a novel candidate strategy for the treatment of ADPKD (Zhu et al., 2018). Nevertheless, speaking of kidney stones, quercetin also reduces the reabsorption of sodium, calcium, and water, thereby preventing the formation of a kidney stone in the urinary tract (Nirumand et al., 2018).

5 Conclusion and future perspectives

Quercetin, an active compound from natural products, has shown a significant protective effect in various models of kidney diseases. However, most of the studies have reported observational results and phenotype changes rather than the mechanisms of action related to the crucial pathogenesis. Besides, although experimental research has focused on the therapeutic effects and mechanisms of quercetin, it could hardly be used in the clinical setting due to its poor solubility and low oral bioavailability. Nevertheless, further research on nanoparticles, liposomes, micelles, or novel materials is in urgent need to improve the drug delivery system of quercetin and bring this natural compound to the forefront of therapeutic agents for the treatment of kidney disease.

Author contributions

Y-QC, H-YC, and Q-QT contributed equally to writing and revising the manuscript. Y-FL wrote and checked the manuscript. F-HL and X-SL supervised and conducted the study. Y-YG conducted, wrote, and revised the manuscript. All authors contributed to the manuscript conception development and discussed the manuscript writing and revising.

Funding

This work was supported by the National Natural Science Foundation of China (No. 81903956), the China Postdoctoral Science Foundation (2021M690042, 2022T150148), the Basic and Applied Basic Research Project of Guangzhou Science and Technology Department (202102020011) and the Research Fund for Bajian Talents of Guangdong Provincial Hospital of Chinese Medicine (No. BJ2022KY03).

Conflict of interest

The authors declare that the research was conducted in the absence of any commercial or financial relationships that could be construed as a potential conflict of interest.

Publisher's note

References

Abdel-Wahhab, M. A., Aljawish, A., El-Nekeety, A. A., Abdel-Aziem, S. H., and Hassan, N. S. (2017). Chitosan nanoparticles plus quercetin suppress the oxidative stress, modulate DNA fragmentation and gene expression in the kidney of rats fed ochratoxin A-contaminated diet. *Food Chem. Toxicol.* 99, 209–221. doi:10.1016/j.fct.2016.12.002

Abdelhalim, M. A. K., Qaid, H. A., Al-Mohy, Y., and Al-Ayed, M. S. (2018). Effects of quercetin and arginine on the nephrotoxicity and lipid peroxidation induced by gold nanoparticles *in vivo*. *Int. J. Nanomedicine* 13, 7765–7770. doi:10.2147/ijn.S183281

Al-Asmari, A. K., Khan, H. A., Manthiri, R. A., Al-Khlaiwi, A. A., Al-Asmari, B. A., and Ibrahim, K. E. (2018). Protective effects of a natural herbal compound quercetin against snake venom-induced hepatic and renal toxicities in rats. *Food Chem. Toxicol.* 118, 105–110. doi:10.1016/j.fct.2018.05.016

Ali, A. M., Gabbar, M. A., Abdel-Twab, S. M., Fahmy, E. M., Ebaid, H., Alhazza, I. M., et al. (2020). Antidiabetic potency, antioxidant effects, and mode of actions of citrus reticulata fruit peel hydroethanolic extract, hesperidin, and quercetin in nicotinamide/streptozotocin-induced wistar diabetic rats. *Oxid. Med. Cell. Longev.* 2020, 1730492. doi:10.1155/2020/1730492

Alidadi, H., Khorsandi, L., and Shirani, M. (2018). Effects of quercetin on tubular cell apoptosis and kidney damage in rats induced by titanium dioxide nanoparticles. *Malays. J. Med. Sci.* 25 (2), 72–81. doi:10.21315/mjms2018.25.2.8

Almaghrabi, O. A. (2015). Molecular and biochemical investigations on the effect of quercetin on oxidative stress induced by cisplatin in rat kidney. *Saudi J. Biol. Sci.* 22 (2), 227–231. doi:10.1016/j.sjbs.2014.12.008

Alshanwani, A. R., Shaheen, S., Faddah, L. M., Alhusaini, A. M., Ali, H. M., Hasan, I., et al. (2020). Manipulation of quercetin and melatonin in the down-regulation of HIF-1α, HSP-70 and VEGF pathways in rat's kidneys induced by hypoxic stress. *Dose. Response.* 18 (3), 1559325820949797. doi:10.1177/1559325820949797

Andreucci, M., Faga, T., Pisani, A., Serra, R., Russo, D., De Sarro, G., et al. (2018). Quercetin protects against radiocontrast medium toxicity in human renal proximal tubular cells. *J. Cell. Physiol.* 233 (5), 4116–4125. doi:10.1002/jcp.26213

Arab, H. H., Eid, A. H., Gad, A. M., Yahia, R., Mahmoud, A. M., and Kabel, A. M. (2021). Inhibition of oxidative stress and apoptosis by camel milk mitigates cyclosporine-induced nephrotoxicity: Targeting Nrf2/HO-1 and AKT/eNOS/NO pathways. *Food Sci. Nutr.* 9 (6), 3177–3190. doi:10.1002/fsn3.2277

Arauz, J., Rivera-Espinoza, Y., Shibayama, M., Favari, L., Flores-Beltrán, R. E., and Muriel, P. (2015). Nicotinic acid prevents experimental liver fibrosis by attenuating the prooxidant process. *Int. Immunopharmacol.* 28 (1), 244–251. doi:10.1016/j.intimp.2015.05.045

Arky Jane Langstieh, J. B. W., Jane Lyngdoh, C., Jaba, I., Sarkar, C., and Brahma, D. K. (2021). Estimation of quercetin and rutin content in hyouttunia cordata and *Centella asiatica* plant extracts using UV-spectrophotometer. *Int. J. Pharm. Sci. Rev. Res.* 71 (2), 130–132. doi:10.47583/ijpsrr.2021.v71i02.021

Bağdatlıoğlu, M. B. K. (2016). Bioavailability of quercetin. *Curr. Res. Nutr. Food Sci.* 4, 1. doi:10.12944/CRNFSJ.4.Special-Issue-October.20

Bao Lidao, D. H., Zhao, Y., Wu, L., and Song, J. (2015). Simultaneous determination of four active components in polygonum aviculare L by HPLC. *Liaoning J. Traditional Chin. Med.* 43 (06), 1266–1268.

Bao, W., Cao, C., Li, S., Bo, L., Zhang, M., Zhao, X., et al. (2017). Metabonomic analysis of quercetin against the toxicity of acrylamide in rat urine. *Food Funct.* 8 (3), 1204–1214. doi:10.1039/c6fo01553k

Bhatia, D., and Choi, M. E. (2020). Autophagy in kidney disease: Advances and therapeutic potential. *Prog. Mol. Biol. Transl. Sci.* 172, 107–133. doi:10.1016/bs.pmbts.2020.01.008

Bo, L., Liu, Y., Jia, S., Liu, Y., Zhang, M., Li, S., et al. (2018). Metabonomics analysis of quercetin against the nephrotoxicity of acrylamide in rats. *Food Funct.* 9 (11), 5965–5974. doi:10.1039/c8fo00902c

Cao Xuesong, W. J., and Huang, Z. (2019). Determination of quercetin, kaempferol, luteolin, apigenin in semen Plantaginis by RP-HPLC. *China Pharm.* 18 (12), 32–34.

Cao, Y., Hu, J., Sui, J., Jiang, L., Cong, Y., and Ren, G. (2018). Quercetin is able to alleviate TGF-β-induced fibrosis in renal tubular epithelial cells by suppressing miR-21. *Exp. Ther. Med.* 16 (3), 2442–2448. doi:10.3892/etm.2018.6489

Casanova, A. G., Prieto, M., Colino, C. I., Gutiérrez-Millán, C., Ruszkowska-Ciastek, B., de Paz, E., et al. (2021). A micellar formulation of quercetin prevents cisplatin nephrotoxicity. *Int. J. Mol. Sci.* 22 (2), E729. doi:10.3390/ijms22020729

Chaudhary, S., Ganjoo, P., Raiusddin, S., and Parvez, S. (2015). Nephroprotective activities of quercetin with potential relevance to oxidative stress induced by valproic acid. *Protoplasma* 252 (1), 209–217. doi:10.1007/s00709-014-0670-8

Chen, D. Q., Hu, H. H., Wang, Y. N., Feng, Y. L., Cao, G., and Zhao, Y. Y. (2018). Natural products for the prevention and treatment of kidney disease. *Phytomedicine.* 50, 50–60. doi:10.1016/j.phymed.2018.09.182

Chen Junhua, Z. G., Peng, G., Qin, H., Cheng, H., and Shen, J. (2014). Content determination of chlorogenic acid, quercetin and kaempferol in pyrrosia lingua(thumb.) farwell by HPLC. *Chin. J. Inf. Traditional Chin. Med.* 21 (8), 67–69.

Choi, S., Ryu, K. H., Park, S. H., Jun, J. Y., Shin, B. C., Chung, J. H., et al. (2016). Direct vascular actions of quercetin in aorta from renal hypertensive rats. *Kidney Res. Clin. Pract.* 35 (1), 15–21. doi:10.1016/j.krcp.2015.12.003

Conglei Pan, H. L., and Lu, H. (2019). Preparative separation of quercetin, ombuin and kaempferide from Gynostemma pentaphyllum by high-speed countercurrent chromatography. *J. Chromatogr. Sci.* 57 (3), 265–271. doi:10.1093/chromsci/bmy110

Dallak, M., Dawood, A. F., Haidara, M. A., Abdel Kader, D. H., Eid, R. A., Kamar, S. S., et al. (2020). Suppression of glomerular damage and apoptosis and biomarkers of acute kidney injury induced by acetaminophen toxicity using a combination of resveratrol and quercetin. *Drug Chem. Toxicol.* 45, 1–7. doi:10.1080/01480545.2020.1722156

Deng Ting, Q. T., Xu, Y., and Sun, T. (2021). Simultaneous detection of 6 flavonoids in Hawthorn Leave total flavonoids and evaluation of antioxidant activity *in vitro*. *Pharm. Clin. Chin. Materia Medica* 12 (05), 27–32.

Ding, T., Wang, S., Zhang, X., Zai, W., Fan, J., Chen, W., et al. (2018). Kidney protection effects of dihydroquercetin on diabetic nephropathy through suppressing ROS and NLRP3 inflammasome. *Phytomedicine.* 41, 45–53. doi:10.1016/j.phymed.2018.01.026

Diniz, L. R. L., Souza, M. T. S., Duarte, A. B. S., and Sousa, D. P. (2020). Mechanistic aspects and therapeutic potential of quercetin against COVID-19-associated acute kidney injury. *Molecules* 25 (23), E5772. doi:10.3390/molecules25235772

Ebokaiwe, A. P., Obasi, D. O., Njoku, R. C. C., Osawe, S., Olusanya, O., and Kalu, W. O. (2021). Cyclophosphamide instigated hepatic-renal oxidative/inflammatory stress aggravates immunosuppressive indoleamine 2, 3-dioxygenase in male rats: Abatement by quercetin. *Toxicology* 464, 153027. doi:10.1016/j.tox.2021.153027

Elbarbry, F., Abdelkawy, K., Moshirian, N., and Abdel-Megied, A. M. (2020). The antihypertensive effect of quercetin in young spontaneously hypertensive rats; role of arachidonic acid metabolism. *Int. J. Mol. Sci.* 21 (18), E6554. doi:10.3390/ijms21186554

Elbe, H., Vardi, N., Esrefoglu, M., Ates, B., Yologlu, S., and Taskapan, C. (2015). Amelioration of streptozotocin-induced diabetic nephropathy by melatonin, quercetin, and resveratrol in rats. *Hum. Exp. Toxicol.* 34 (1), 100–113. doi:10.1177/0960327114531995

Erboga, M., Aktas, C., Erboga, Z. F., Donmez, Y. B., and Gurel, A. (2015). Quercetin ameliorates methotrexate-induced renal damage, apoptosis and oxidative stress in rats. *Ren. Fail.* 37 (9), 1492–1497. doi:10.3109/0886022x.2015.1074521

Fu Juan, Y. S., and Huang, L. (2013). Simultaneous determination of six flavonoid active components in Radix astragali by UPLC. *Chin. Pharm. J.* 48 (11), 916–919.

Gholampour, F., and Sadidi, Z. (2018). Hepatorenal protection during renal ischemia by quercetin and remote ischemic perconditioning. *J. Surg. Res.* 231, 224–233. doi:10.1016/j.jss.2018.05.036

Gholampour, F., and Saki, N. (2019). Hepatic and renal protective effects of quercetin in ferrous sulfateinduced toxicity. *Gen. Physiol. Biophys.* 38 (1), 27–38. doi:10.4149/gpb_2018038

Gomes, I. B., Porto, M. L., Santos, M. C., Campagnaro, B. P., Gava, A. L., Meyrelles, S. S., et al. (2015). The protective effects of oral low-dose quercetin on diabetic nephropathy in hypercholesterolemic mice. *Front. Physiol.* 6, 247. doi:10.3389/fphys.2015.00247

Gonçalves, G. F. B., Silva, M. E. M., Sampaio, F. J. B., Pereira-Sampaio, M. A., and de Souza, D. B. (2021). Quercetin as a nephroprotector after warm ischemia: Histomorphometric evaluation in a rodent model. *Int. Braz J. Urol.* 47 (4), 796–802. doi:10.1590/s1677-5538.Ibju.2020.0358

Graefe, E. U., Derendorf, H., and Veit, M. (1999). Pharmacokinetics and bioavailability of the flavonol quercetin in humans. *Int. J. Clin. Pharmacol. Ther.* 37 (5), 219–233.

Graf, B. A., Ameho, C., Dolnikowski, G. G., Milbury, P. E., Chen, C. Y., and Blumberg, J. B. (2006). Rat gastrointestinal tissues metabolize quercetin. *J. Nutr.* 136 (1), 39–44. doi:10.1093/jn/136.1.39

Gu, Y., Huang, X., Wu, Y., Liu, X., and Lan, H. (2020a). Quercetin alleviates cisplatin-induced acute kidney injury by rebalancing TGF-beta/Smad signaling. *Nephrology* 25 (S1), 478.

Gu, Y. Y., Dou, J. Y., Huang, X. R., Liu, X. S., and Lan, H. Y. (2021a). Transforming growth factor-β and long non-coding RNA in renal inflammation and fibrosis. *Front. Physiol.* 12, 684236. doi:10.3389/fphys.2021.684236

Gu, Y. Y., Liu, X. S., Huang, X. R., Yu, X. Q., and Lan, H. Y. (2020b). Diverse role of TGF-β in kidney disease. *Front. Cell Dev. Biol.* 8, 123. doi:10.3389/fcell.2020.00123

Gu, Y. Y., Zhang, M., Cen, H., Wu, Y. F., Lu, Z., Lu, F., et al. (2021b). Quercetin as a potential treatment for COVID-19-induced acute kidney injury: Based on network pharmacology and molecular docking study. *PLoS One* 16 (1), e0245209. doi:10.1371/journal.pone.0245209

Guan, T., Xin, Y., Zheng, K., Wang, R., Zhang, X., Jia, S., et al. (2021). Metabolomics analysis of the effects of quercetin on renal toxicity induced by cadmium exposure in rats. *Biometals.* 34 (1), 33–48. doi:10.1007/s10534-020-00260-2

Guo, S., Sun, J., and Zhuang, Y. (2020). Quercetin alleviates lipopolysaccharide-induced inflammatory responses by up-regulation miR-124 in human renal tubular epithelial cell line HK-2. *Biofactors* 46 (3), 402–410. doi:10.1002/biof.1596

Heeba, G. H., and Mahmoud, M. E. (2016). Dual effects of quercetin in doxorubicin-induced nephrotoxicity in rats and its modulation of the cytotoxic activity of doxorubicin on human carcinoma cells. *Environ. Toxicol.* 31 (5), 624–636. doi:10.1002/tox.22075

Hickson, L. J., Langhi Prata, L. G. P., Bobart, S. A., Evans, T. K., Giorgadze, N., Hashmi, S. K., et al. (2019). Senolytics decrease senescent cells in humans: Preliminary report from a clinical trial of Dasatinib plus Quercetin in individuals with diabetic kidney disease. *EBioMedicine* 47, 446–456. doi:10.1016/j.ebiom.2019.08.069

Hongmei, G. (2008). Simultaneous determination of 4 flavonoids in inula britannica by RP-HPLC. *China Pharm.* 20 (27), 2122–2123.

Jia, S., Guan, T., Zhang, X., Liu, Y., Liu, Y., and Zhao, X. (2020). Serum metabonomics analysis of quercetin against the toxicity induced by cadmium in rats. *J. Biochem. Mol. Toxicol.* 34 (4), e22448. doi:10.1002/jbt.22448

Jiang, X., Yu, J., Wang, X., Ge, J., and Li, N. (2019). Quercetin improves lipid metabolism via SCAP-SREBP2-LDLr signaling pathway in early stage diabetic nephropathy. *Diabetes Metab. Syndr. Obes.* 12, 827–839. doi:10.2147/dmso.S195456

Khalil, S. R., Mohammed, A. T., Abd El-Fattah, A. H., and Zaglool, A. W. (2018). Intermediate filament protein expression pattern and inflammatory response changes in kidneys of rats receiving doxorubicin chemotherapy and quercetin. *Toxicol. Lett.* 288, 89–98. doi:10.1016/j.toxlet.2018.02.024

Kim Le, F. C., and Ng, K. (2007). Identification and quantification of antioxidants in Fructus lycii. *Food Chem.* 105 (1), 353–363. doi:10.1016/j.foodchem.2006.11.063

Kim, S. R., Jiang, K., Ogrodnik, M., Chen, X., Zhu, X. Y., Lohmeier, H., et al. (2019). Increased renal cellular senescence in murine high-fat diet: Effect of the senolytic drug quercetin. *Transl. Res.* 213, 112–123. doi:10.1016/j.trsl.2019.07.005

Kim, S. R., Puranik, A. S., Jiang, K., Chen, X., Zhu, X. Y., Taylor, I., et al. (2021). Progressive cellular senescence mediates renal dysfunction in ischemic nephropathy. *J. Am. Soc. Nephrol.* 32 (8), 1987–2004. doi:10.1681/asn.2020091373

Kimura, T., Isaka, Y., and Yoshimori, T. (2017). Autophagy and kidney inflammation. *Autophagy* 13 (6), 997–1003. doi:10.1080/15548627.2017.1309485

Kirkland, J. L., and Tchkonia, T. (2020). Senolytic drugs: From discovery to translation. *J. Intern. Med.* 288 (5), 518–536. doi:10.1111/joim.13141

Lai, L. L., Lu, H. Q., Li, W. N., Huang, H. P., Zhou, H. Y., Leng, E. N., et al. (2021). Protective effects of quercetin and crocin in the kidneys and liver of obese Sprague-Dawley rats with Type 2 diabetes: Effects of quercetin and crocin on T2DM rats. *Hum. Exp. Toxicol.* 40 (4), 661–672. doi:10.1177/0960327120954521

Lei, D., Chengcheng, L., Xuan, Q., Yibing, C., Lei, W., Hao, Y., et al. (2019). Quercetin inhibited mesangial cell proliferation of early diabetic nephropathy through the Hippo pathway. *Pharmacol. Res.* 146, 104320. doi:10.1016/j.phrs.2019.104320

Li, C., Shen, Y., Huang, L., Liu, C., and Wang, J. (2021a). Senolytic therapy ameliorates renal fibrosis postacute kidney injury by alleviating renal senescence. *Faseb J.* 35 (1), e21229. doi:10.1096/fj.202001855RR

Li, Q. C., Liang, Y., Hu, G. R., and Tian, Y. (2016a). Enhanced therapeutic efficacy and amelioration of cisplatin-induced nephrotoxicity by quercetin in 1, 2-dimethyl hydrazine-induced colon cancer in rats. *Indian J. Pharmacol.* 48 (2), 168–171. doi:10.4103/0253-7613.178834

Li, S., Cao, C., Shi, H., Yang, S., Qi, L., Zhao, X., et al. (2016b). Effect of quercetin against mixture of four organophosphate pesticides induced nephrotoxicity in rats. *Xenobiotica.* 46 (3), 225–233. doi:10.3109/00498254.2015.1070443

Li, X., Chen, W., Feng, J., and Zhao, B. (2021b). Incidence of death from kidney diseases among cancer patients: A US population-based analysis. *Int. Urol. Nephrol.* 53 (12), 2627–2633. doi:10.1007/s11255-021-02801-1

Lin, C. F., Kuo, Y. T., Chen, T. Y., and Chien, C. T. (2016). Quercetin-rich guava (psidium guajava) juice in combination with trehalose reduces autophagy, apoptosis and pyroptosis formation in the kidney and pancreas of type II diabetic rats. *Molecules* 21 (3), 334. doi:10.3390/molecules21030334

Liu, X., Sun, N., Mo, N., Lu, S., Song, E., Ren, C., et al. (2019a). Quercetin inhibits kidney fibrosis and the epithelial to mesenchymal transition of the renal tubular system involving suppression of the Sonic Hedgehog signaling pathway. *Food Funct.* 10 (6), 3782–3797. doi:10.1039/c9fo00373h

Liu, Y., Dai, E., and Yang, J. (2019b). Quercetin suppresses glomerulosclerosis and TGF-β signaling in a rat model. *Mol. Med. Rep.* 19 (6), 4589–4596. doi:10.3892/mmr.2019.10118

Liu, Y., Zhang, X., Guan, T., Jia, S., Liu, Y., and Zhao, X. (2020). Effects of quercetin on cadmium-induced toxicity in rat urine using metabonomics techniques. *Hum. Exp. Toxicol.* 39 (4), 524–536. doi:10.1177/0960327119895811

Lu, H., Wu, L., Liu, L., Ruan, Q., Zhang, X., Hong, W., et al. (2018). Quercetin ameliorates kidney injury and fibrosis by modulating M1/M2 macrophage polarization. *Biochem. Pharmacol.* 154, 203–212. doi:10.1016/j.bcp.2018.05.007

Lu, Q., Ji, X. J., Zhou, Y. X., Yao, X. Q., Liu, Y. Q., Zhang, F., et al. (2015). Quercetin inhibits the mTORC1/p70S6K signaling-mediated renal tubular epithelial-mesenchymal transition and renal fibrosis in diabetic nephropathy. *Pharmacol. Res.* 99, 237–247. doi:10.1016/j.phrs.2015.06.006

Lu, S., Zhou, S., Chen, J., Zheng, J., Ren, J., Qi, P., et al. (2021). Quercetin nanoparticle ameliorates lipopolysaccharide-triggered renal inflammatory impairment by regulation of Sirt1/NF-KB pathway. *J. Biomed. Nanotechnol.* 17 (2), 230–241. doi:10.1166/jbn.2021.3031

Ma, Y., Chen, F., Yang, S., Chen, B., and Shi, J. (2018). Protocatechuic acid ameliorates high glucose-induced extracellular matrix accumulation in diabetic nephropathy. *Biomed. Pharmacother.* 98, 18–22. doi:10.1016/j.biopha.2017.12.032

Meng, F. D., Li, Y., Tian, X., Ma, P., Sui, C. G., Fu, L. Y., et al. (2015). Synergistic effects of snail and quercetin on renal cell carcinoma Caki-2 by altering AKT/mTOR/ERK1/2 signaling pathways. *Int. J. Clin. Exp. Pathol.* 8 (6), 6157–6168.

Mohammad Azmin, S. N. H., and Mat Nor, M. S. (2020). Chemical fingerprint of Centella Asiatica's bioactive compounds in the ethanolic and aqueous extracts. *Adv. Biomark. Sci. Technol.* 2, 35–44. doi:10.1016/j.abst.2020.10.001

Morsi, A. A., Fouad, H., Alasmari, W. A., and Faruk, E. M. (2022). The biomechanistic aspects of renal cortical injury induced by diesel exhaust particles in rats and the renoprotective contribution of quercetin pretreatment: Histological and biochemical study. *Environ. Toxicol.* 37 (2), 310–321. doi:10.1002/tox.23399

Mullen, W., Edwards, C. A., and Crozier, A. (2006). Absorption, excretion and metabolite profiling of methyl-glucuronyl-glucosyl- and sulpho-conjugates of quercetin in human plasma and urine after ingestion of onions. *Br. J. Nutr.* 96 (1), 107–116. doi:10.1079/bjn20061809

Nirumand, M. C., Hajialyani, M., Rahimi, R., Farzaei, M. H., Zingue, S., Nabavi, S. M., et al. (2018). Dietary plants for the prevention and management of kidney stones: Preclinical and clinical evidence and molecular mechanisms. *Int. J. Mol. Sci.* 19 (3), E765. doi:10.3390/ijms19030765

Owumi, S. E., Danso, O. F., and Effiong, M. E. (2019). Dietary quercetin abrogates hepatorenal oxidative damage associated with dichloromethane exposure in rats. *Acta Biochim. Pol.* 66 (2), 201–206. doi:10.18388/abp.2018_2771

Peng, X., Dai, C., Zhang, M., and Das Gupta, S. (2020). Molecular mechanisms underlying protective role of quercetin on copper sulfate-induced nephrotoxicity in mice. *Front. Vet. Sci.* 7, 586033. doi:10.3389/fvets.2020.586033

Platé, M., Guillotin, D., and Chambers, R. C. (2020). The promise of mTOR as a therapeutic target pathway in idiopathic pulmonary fibrosis. *Eur. Respir. Rev.* 29 (157), 200269. doi:10.1183/16000617.0269-2020

Qi, L., Cao, C., Hu, L., Chen, S., Zhao, X., and Sun, C. (2017). Metabonomic analysis of the protective effect of quercetin on the toxicity induced by mixture of organophosphate pesticides in rat urine. *Hum. Exp. Toxicol.* 36 (5), 494–507. doi:10.1177/0960327116652460

Qiu, J., Chen, X., Netrusov, A. I., Zhou, Q., Guo, D., Liu, X., et al. (2017). Screening and identifying antioxidative components in Ginkgo biloba pollen by DPPH-HPLC-PAD coupled with HPLC-ESI-MS2. *PLoS One* 12 (1), e0170141. doi:10.1371/journal.pone.0170141

Rahdar, A., Hasanein, P., Bilal, M., Beyzaei, H., and Kyzas, G. Z. (2021). Quercetin-loaded F127 nanomicelles: Antioxidant activity and protection against renal injury induced by gentamicin in rats. *Life Sci.* 276, 119420. doi:10.1016/j.lfs.2021.119420

Ren, J., Li, J., Liu, X., Feng, Y., Gui, Y., Yang, J., et al. (2016). Quercetin inhibits fibroblast activation and kidney fibrosis involving the suppression of mammalian target of rapamycin and β-catenin signaling. *Sci. Rep.* 6, 23968. doi:10.1038/srep23968

Rezk, A. M., Ibrahim, I., Mahmoud, M. F., and Mahmoud, A. A. A. (2021). Quercetin and lithium chloride potentiate the protective effects of carvedilol against renal ischemia-reperfusion injury in high-fructose, high-fat diet-fed Swiss albino mice independent of renal lipid signaling. *Chem. Biol. Interact.* 333, 109307. doi:10.1016/j.cbi.2020.109307

Saida Ibragic, E. S., and Sofic, E. (2015). Chemical composition of various Ephedra species. *Bosn. J. Basic Med. Sci.* 15 (3), 21–27. doi:10.17305/bjbms.2015.539

Sánchez-González, P. D., López-Hernández, F. J., Dueñas, M., Prieto, M., Sánchez-López, E., Thomale, J., et al. (2017). Differential effect of quercetin on cisplatin-induced toxicity in kidney and tumor tissues. *Food Chem. Toxicol.* 107 (1), 226–236. doi:10.1016/j.fct.2017.06.047

Sen-ming, Z. (2013). Improvements of flavonoids and saponins determination in Radix Bupleuri by HPLC method. *Mod. Chin. Med.* 15 (09), 744–747.

Shu, B., Feng, Y., Gui, Y., Lu, Q., Wei, W., Xue, X., et al. (2018). Blockade of CD38 diminishes lipopolysaccharide-induced macrophage classical activation and acute kidney injury involving NF-κB signaling suppression. *Cell. Signal.* 42, 249–258. doi:10.1016/j.cellsig.2017.10.014

Sok Yen, F., Shu Qin, C., Tan Shi Xuan, S., Jia Ying, P., Yi Le, H., Darmarajan, T., et al. (2021). Hypoglycemic effects of plant flavonoids: A review. *Evid. Based. Complement. Altern. Med.* 2021, 2057333. doi:10.1155/2021/2057333

Sun, H. J., Wu, Z. Y., Cao, L., Zhu, M. Y., Liu, T. T., Guo, L., et al. (2019). Hydrogen sulfide: Recent progression and perspectives for the treatment of diabetic nephropathy. *Molecules* 24 (15), E2857. doi:10.3390/molecules24152857

Tan, J., He, J., Qin, W., and Zhao, L. (2019). Quercetin alleviates lipopolysaccharide-induced acute kidney injury in mice by suppressing TLR4/NF-κB pathway. *Nan Fang. Yi Ke Da Xue Xue Bao* 39 (5), 598–602. doi:10.12122/j.issn.1673-4254.2019.05.16

Tan, R. Z., Wang, C., Deng, C., Zhong, X., Yan, Y., Luo, Y., et al. (2020). Quercetin protects against cisplatin-induced acute kidney injury by inhibiting Mincle/Syk/NF-κB signaling maintained macrophage inflammation. *Phytother. Res.* 34 (1), 139–152. doi:10.1002/ptr.6507

Tong, F., Liu, S., Yan, B., Li, X., Ruan, S., and Yang, S. (2017). Quercetin nanoparticle complex attenuated diabetic nephropathy via regulating the expression level of ICAM-1 on endothelium. *Int. J. Nanomedicine* 12, 7799–7813. doi:10.2147/ijn.S146978

Tu, H., Ma, D., Luo, Y., Tang, S., Li, Y., Chen, G., et al. (2021). Quercetin alleviates chronic renal failure by targeting the PI3k/Akt pathway. *Bioengineered* 12 (1), 6538–6558. doi:10.1080/21655979.2021.1973877

Uthra, C., Shrivastava, S., Jaswal, A., Sinha, N., Reshi, M. S., and Shukla, S. (2017). Therapeutic potential of quercetin against acrylamide induced toxicity in rats. *Biomed. Pharmacother.* 86, 705–714. doi:10.1016/j.biopha.2016.12.065

Vetrova, E. V., Maksimenko, E. V., Borisenko, S. N., Lekar, A. V., Borisenko, N. I., and Minkin, V. I. (2017). Extraction of rutin and quercetin antioxidants from the buds of Sophora Japonica (Sophora japonica L.) by subcritical water. *Russ. J. Phys. Chem. B* 11, 1202–1206. doi:10.1134/s1990793117070193

Vicente-Vicente, L., González-Calle, D., Casanova, A. G., Hernández-Sánchez, M. T., Prieto, M., Rama-Merchán, J. C., et al. (2019). Quercetin, a promising clinical candidate for the prevention of contrast-induced nephropathy. *Int. J. Mol. Sci.* 20 (19), E4961. doi:10.3390/ijms20194961

Wang, Y., Quan, F., Cao, Q., Lin, Y., Yue, C., Bi, R., et al. (2021). Quercetin alleviates acute kidney injury by inhibiting ferroptosis. *J. Adv. Res.* 28, 231–243. doi:10.1016/j.jare.2020.07.007

Wong, C. C., Botting, N. P., Orfila, C., Al-Maharik, N., and Williamson, G. (2011). Flavonoid conjugates interact with organic anion transporters (OATs) and attenuate cytotoxicity of adefovir mediated by organic anion transporter 1 (OAT1/SLC22A6). *Biochem. Pharmacol.* 81 (7), 942–949. doi:10.1016/j.bcp.2011.01.004

Yuksel, Y., Yuksel, R., Yagmurca, M., Haltas, H., Erdamar, H., Toktas, M., et al. (2017). Effects of quercetin on methotrexate-induced nephrotoxicity in rats. *Hum. Exp. Toxicol.* 36 (1), 51–61. doi:10.1177/0960327116637414

Zhang Jing, T. C., and Yan, F. (2020). Simultaneous determination of seven constituents in rubus chingii by HPLC. *China Pharm.* 23 (12), 2496–2499. doi:10.1016/S1674-6384(16)60051-5

Zhong Yuekui, C. Q., and Qiu, Z. (2021). Determination of 4 flavonoids in mulberry leaves from different habitats by ultra performance liquid chromatography. *J. Food Saf. Qual.* 12 (05), 1855–1860.

Zhu Kaixin, Z. X., Zhao, M., Pei, H., Su, B., and Li, Y. (2011). Determination of quarcetin from four kinds of Herba Taxilli parasiticed in mulberry. *Lishizhen Med. Materia Medica* 22 (10), 2395–2397.

Zhu, Y., Teng, T., Wang, H., Guo, H., Du, L., Yang, B., et al. (2018). Quercetin inhibits renal cyst growth *in vitro* and via parenteral injection in a polycystic kidney disease mouse model. *Food Funct.* 9 (1), 389–396. doi:10.1039/c7fo01253e

frontiers | Frontiers in Pharmacology

TYPE Original Research
PUBLISHED 14 September 2022
DOI 10.3389/fphar.2022.968980

OPEN ACCESS

EDITED BY
Dan-Qian Chen,
Northwest University, China

REVIEWED BY
Senyan Liu,
Shanghai Changzheng Hospital, China
Cunyun Min,
Guangdong Provincial People's Hospital, China

*CORRESPONDENCE
Xuezhong Gong,
shnanshan@yeah.net

SPECIALTY SECTION
This article was submitted to Renal Pharmacology, a section of the journal Frontiers in Pharmacology

RECEIVED 14 June 2022
ACCEPTED 22 August 2022
PUBLISHED 14 September 2022

CITATION
Li T, Xu Y, Yuan G, Lu W, Jian G and Gong X (2022), Efficacy and safety of tailin formulation combined with continuous low-dose antibiotic therapy in patients with recurrent urinary tract infection: A multicenter, randomized, controlled clinical trial.
Front. Pharmacol. 13:968980.
doi: 10.3389/fphar.2022.968980

Efficacy and safety of tailin formulation combined with continuous low-dose antibiotic therapy in patients with recurrent urinary tract infection: A multicenter, randomized, controlled clinical trial

Tonglu Li[1], Yingru Xu[1], Gang Yuan[1], Wen Lu[2], Guihua Jian[3] and Xuezhong Gong[1]*

[1]Department of Nephrology, Shanghai Municipal Hospital of Traditional Chinese Medicine, Shanghai University of Traditional Chinese Medicine, Shanghai, China, [2]Department of Nephrology, Shanghai Baoshan District Hospital of Integrated Traditional Chinese and Western Medicine, Shanghai University of Traditional Chinese Medicine, Shanghai, China, [3]Department of Nephrology, Shanghai Sixth People's Hospital, Shanghai Jiaotong University, Shanghai, China

Persistent inflammation associated with recurrent urinary tract infection (rUTI) is a crucial inducement of inflammation-driven renal fibrosis (IDRF). Although continuous low-dose antibiotic therapy (CLAT) is the common treatment for rUTI, its clinical efficacy remains unsatisfactory. Tailin formulation (TLF), a Chinese herbal formulation prescribed for treating rUTI, is effective in alleviating symptoms and reducing recurrence. This study was to evaluate the efficacy and safety of TLF combined with CLAT compared with CLAT used alone in patients with rUTI. In this multicenter, randomized, controlled clinical trial, patients were assigned (1:1) to receive either TLF + CLAT or CLAT for 12 weeks. The primary outcome was the effective rate at week 12 of the treatment. The secondary outcomes were the recurrent rate at week 4 and week 12 post treatment; the post-treatment changes in renal tubular injury markers (urinary N-acetyl-β-D-glucosaminidase (NAG) and β2-microglobulin (β2-MG)), profibrotic factors (urinary monocyte chemoattractant protein-1 (MCP-1) and transforming growth factor beta1 (TGF-β1)), and traditional Chinese medicine (TCM) symptoms, and vital signs indicators and serious adverse events (SAEs) were also monitored throughout the trial. A total of 195 patients were included in the final analysis. The TLF + CLAT group had a higher effective rate and a lower recurrence rate than the CLAT group ($p < 0.01$). Significant decrease of urinary NAG and β2-MG was observed in the TLF + CLAT group vs. CLAT group ($p < 0.01$), and similar changes were observed in profibrotic factors (urinary MCP-1 and TGF-β1) ($p < 0.05$), which indicated that TLF might have potential renal tubular protection and anti-fibrosis effects. Additionally, a positive correlation within a certain range was shown in the correlation analysis of medical history (months) of rUTI patients with urinary MCP-1 ($r = 0.50$, $p < 0.05$) and TGF-β1 ($r = 0.78$, $p < 0.01$). A significant difference

was also observed in TCM symptoms ($p < 0.01$). There were no obvious adverse reactions that occurred during this study. We conclude that TLF combined with CLAT was superior to CLAT used alone in reducing rUTI recurrence, alleviating the non-infection-related physical symptoms and protecting renal tubular and anti-fibrosis, which suggests this novel therapy might be an available treatment with great promise in treating rUTI.

KEYWORDS

recurrent urinary tract infection, renal fibrosis, tailin formulation, continuous low-dose antibiotic therapy, traditional Chinese medicine, randomized controlled trial

1 Introduction

rUTI is a common clinical refractory disease affecting millions of people across the globe annually (Geerlings, 2016), exerting considerable impact on patient's quality of life (Wagenlehner et al., 2018).

Inflammation of the urinary tract is the critical pathological mechanism of rUTI (Kaur and Kaur, 2021), which might result in renal tubular damage (Lorenzo-Gomez et al., 2020) and renal fibrosis (Lv et al., 2018) in those patients. However, there is insufficient evidence to reflect renal damage and inflammation-driven renal fibrosis (IDRF) as subsequent issues due to the rUTI. Urinary NAG and β2-MG are sensitive markers of tubular injury to predict acute kidney injury (AKI) (Ix and Shlipak, 2021). Elevated urinary NAG and β2-MG values have been described in patients suffering risk factors, including nephrotoxic drugs (Raduly et al., 2021). Therefore, presumably, renal damage attributable to rUTI could be evidenced by the increase of urinary NAG and β2-MG.

Persistent inflammation associated with rUTI is a crucial inducement of IDRF (Humphreys, 2018; Lv et al., 2018), involving complex interactions among multiple inflammatory cells and profibrotic cytokine signaling pathways. Critical profibrotic factors include MCP-1 and TGF-β1. Inflammation might promote fibrosis by inflammatory cells, which is tightly regulated by TGF-β1 (Humphreys, 2018). MCP-1 also plays an important role in the process of inflammation for it could attract other inflammatory factors/cells and has been found to be associated with renal fibrosis (Singh et al., 2021). Given that, changes of critical profibrotic factors (urinary MCP-1 and TGF-β1) in rUTI patients should be paid more attention.

In addition to the high prevalence and economic burden of rUTI, the presumable renal damage and IDRF attributed to rUTI in those patients bring an even greater challenge in the treatment of rUTI.

Antibiotic treatment including CLAT is the most common treatment for rUTI globally (Anger et al., 2019). Although CLAT is effective in inhibiting uropathogenic bacteria and shortening the duration of the infection-related symptoms in episodes, the clinical efficacy and safety of CLAT still remain unsatisfactory due to the presumable side effects and lack of long-term efficacy (Flower et al., 2016; Forbes et al., 2018). Consequently, alternative treatments are being considered, such as Chinese herbal medicine (CHM).

Based on 5,000 years of practice and experience, Chinese medicine is an essential part of healthcare in China. Comparable beneficial outcomes have also been reported for CHM products administered to patients with rUTI (Flower et al., 2019).

TLF (Gong et al., 2006) is a herbal prescription developed by Professor Gong Xuezhong for the treatment of rUTI, consisting of Radix Pseudostellariae (Taizishen), Radix Rehmanniae Recen (Shengdihuang), Sargentodoxa Cuneata (Daxueteng), and Polygonum Cuspidatum (Huzhang). Previous studies by our group have shown the possible roles for TLF in the treatment of rUTI (Gong et al., 2006; Gong et al., 2007; Gong et al., 2010). In animal experiments, we have built rat models of cystitis, acute pyelonephritis (APN), and chronic pyelonephritis (CPN) by *E. coli* $O_{111}B_4$ successfully (Gong et al., 2003; Gong et al., 2004) and found that TLF might effectively protect renal tubules from injury, inhibit renal tubular and interstitial inflammation, and cures renal fibrosis in rats with UTI (Gong et al., 2006; Gong et al., 2010). In the clinical trial (Gong et al., 2007), we have found that compared with the levofloxacin group, urine NAG/Cr and β2-MG decreased significantly in the TLF group, suggesting that TLF could protect the renal tubular function of CPN patients.

Since the clinical efficacy of CLAT in the rUTI population is unsatisfactory, this study attempted to determine if there was a more effective alternative in patients with rUTI using LTF combined with CLAT. Moreover, given that persistent inflammation associated with rUTI is a crucial inducement of IDRF, we also explored the possible relationship between the critical profibrotic factors (TGF-β1, MCP-1) and the medical history (months) of rUTI patients in the present study to clarify if renal fibrosis can be associated with rUTI.

Here, we report the results of this study, hoping to provide reliable evidence-based medical evidence for treatment of rUTI and ease the burden for patients with rUTI.

2 Materials and methods

2.1 Study design

This trial ran from January 2021 to March 2022 and involved three tertiary hospitals (Shanghai Municipal

Hospital of Traditional Chinese Medicine, Shanghai University of Traditional Chinese Medicine; Shanghai Sixth People's Hospital, Shanghai Jiaotong University; Shanghai Baoshan District Hospital of Integrated Traditional Chinese and Western Medicine, Shanghai University of Traditional Chinese Medicine). Patients eligible for the trial in each trial site were assigned a randomized 1:1 ratio to receive LTF + CLAT or CLAT for 12 weeks. This study protocol was approved by the Institutional Ethics Committee (record number: 2020SHL-KY-47) and registered at the Chinese Clinical Trial Registry (registration number: ChiCTR-TRC-10001518).

2.2 Sample size

The sample size was calculated by PASS (version 15.0). Based on the previous trial (Li, 2018), 91 patients per group were needed to achieve 90% power to detect a difference between the group proportions of 0.18. Assuming an attrition rate of 10%, a planned recruitment target of 100 patients per group will be set.

2.3 Participants

According to the inclusion and exclusion criteria, rUTI patients diagnosed with the qi-yin of spleen and kidney deficiency and damp-heat adhesion syndrome by TCM will be considered potential participants.

2.4 Diagnostic criteria

2.4.1 For UTI

Patients would be diagnosed with UTI if

1) urine culture: $\geq 10^5$ cfu/ml bacteria;
2) urinary sediment: white blood cell (WBC) > 10/HP, or with clinical symptoms of UTI.

2.4.2 For rUTI

rUTI is defined as more than two UTIs in the last 6 months or more than three UTIs in the last 12 months, and the course of the disease is more than 2 years.

2.5 Inclusion/exclusion criteria

Eligibility criteria for inclusion were patients who were aged 18–70 years; history of rUTI (at least two episodes in the last 6 months or more than three episodes in the last 12 months); diagnosed with the qi-yin of spleen and kidney deficiency and damp-heat adhesion syndrome by TCM; no known allergies to the drugs to be prescribed; agreed to take part in the trial and sign informed consent.

Exclusion criteria were pregnancy or lactation; with an in-dwelling catheter; urethral syndrome; chronic kidney disease (CKD) stages IV–V (eGFR<30 ml/min); combined with serious heart and liver function damage or diabetes and other diseases which need immediate treatment; severe central nervous system disease; participating in other drug clinical trials or have participated in other clinical trials in the last 3 months.

2.6 Randomization and blinding

Patients eligible in each trial site were assigned randomly, using a computer-generated random number sequence. The division of the groups in this study will be blinded to all participants, investigators, and statisticians. The placebo and TLF are the same in the appearance of the drug package.

2.7 Intervention

Participants randomly assigned to the treatment group were administered TLF + CLAT for 12 weeks, and the participants assigned to the control group received CLAT + placebo for 12 weeks. Dosage and duration are shown in Table 1.

2.8 Outcomes

The primary outcome was the effective rate at week 12 of treatment. The second outcomes were the recurrence rate at weeks 4 and 12 after treatment; post-treatment changes in urinary NAG/Cr, β2-MG, TGF-β1, and MCP-1; furthermore, traditional Chinese medicine (TCM) symptoms were also scored; meanwhile, vital sign indicators and serious adverse events (SAEs) were monitored throughout the trial.

2.9 Follow-up

After treatment was completed, all patients had a follow-up of 12 weeks. Efficacy-related examinations and safety indicators were performed and collected during the treatment and follow-up period. Routine urine examination was conducted at week 0 of the treatment period and every 2 weeks during the treatment period and the follow-up period; cleaning middle urine cultivation was conducted at weeks 0 and 4 and 8 and 12 of the treatment period and weeks 4 and 12 post treatment. Urinary NAG/Cr, β2-MG, TGF-β1, and MCP-1 were measured at weeks 0 and 12 of the treatment period.

TABLE 1 Dosage and duration of drugs for the two group.

Treatment	Time					
	Week 1 and 2	Week 3 and 4	Week 5 and 6	Week 7 and 8	Week 9 and 10	Week 11 and 12
TLF	◇	◇	◇	◇	◇	◇
TLF Placebo	◆	◆	◆	◆	◆	◆
CLAT						
Levofloxacin (0.1g, QN, po)	◇◆			◇◆		
Nitrofurantoin (0.1g, QN, po)		◇◆			◇◆	
Cefdinir (0.1g, QN, po)			◇◆			◇◆

◇represents the administration of the TLF + CLAT group, ◆represents the administration of the CLAT group.

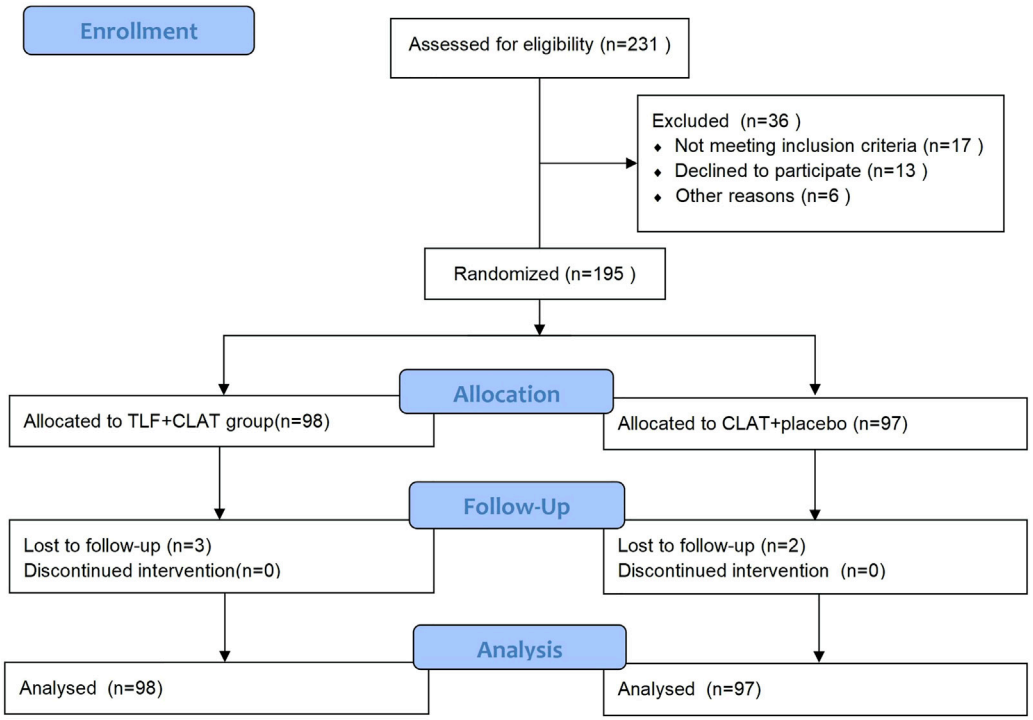

FIGURE 1
Participant flowchart.

2.10 Statistical analysis

Original data were collected and verified by monitors at every visit. Continuous variables of the endpoints were compared with those at the baseline using an analysis of variance or Student's t-test. After processing the categorical variables, the researchers used Fisher's exact test, the chi-square test, or the Cochran–Mantel–Haenszel test to analyze the results. The continuous variables conforming to normality will be analyzed using Pearson's correlation test, and those that do not conform to normality will be analyzed using the Spearman correlation test.

3 Results

During the recruitment period, patients with uncomplicated rUTI were randomized with a 1:1 ratio into two groups to receive TLF + CLAT or CLAT. Figure 1 shows a CONSORT flow chart.

TABLE 2 Baseline characteristics of the rUTI participants at enrollment.

Item	TLF + CLAT (n = 98)	CLAT (n = 97)
Demographic characteristics		
Age (years), mean ± SD	52.24 ± 13.92	53.01 ± 13.90
Female [n (%)]	68 (69.39)	66 (68.04)
Medical history (months), mean ± SD	43.85 ± 14.24	43.06 ± 12.76
Disease characteristics [Case (%)]		
Urine white blood cells	94 (95.91)	92 (94.85)
Urine protein	95 (96.94)	93 (95.88)
Uropathogenic culture	96 (97.96)	96 (98.97)
Urine frequency	94 (95.91)	90 (92.78)
Urinary urgency	95 (96.94)	92 (94.85)
Urinary pain	92 (93.88)	91 (93.81)
Renal tubular injury markers, mean ± SD		
Urinary NAG/Cr (U/mmol)	3.14 ± 1.20	3.02 ± 1.19
Urinary β2-MG (mg/L)	0.43 ± 0.12	0.40 ± 0.15
Renal fibrosis markers, mean ± SD		
Urinary TGF-β1 (pg/ml)	25.56 ± 8.60	26.44 ± 8.97
Urinary MCP-1 (ng/L)	11.47 ± 3.40	11.90 ± 3.43
TCM syndrome score, mean ± SD	21.15 ± 1.89	20.71 ± 2.32

The final data analysis included 98 patients in the TLF + CLAT group and 97 in the CLAT group.

3.1 Baseline characteristics of patients

The patients were comparable between the three groups in terms of demographic and disease characteristics.

Table 2 shows that the mean age was 52.24 years (SD 13.92) in the TLF group and 53.01 years (SD 13.90) in the CLAT group; the percentage of females present was 69.39% (68/98) in the TLF group and 68.04% (66/97) in CLAT group; the mean medical history (recorded from the first diagnosis of rUTI) of rUTI patients was 43.85 months (SD 14.24) in the TLF group and 43.06 months (SD 12.76) in the CLAT group; the mean composite TCM syndrome score was 21.15 points (SD 1.89) in the TLF group and 20.71 points (SD 2.32) in the CLAT group.

3.2 Efficacy results

The primary and secondary outcomes are shown in Table 3. The clinical effective rate of the two groups was calculated at week 12 of treatment. The recurrent rate of the two groups was calculated at weeks 4 and 12 post treatment, separately. Urinary NAG/Cr, β2-MG, TGF-β1, MCP-1, and TCM syndrome of the patients in the two groups were measured at weeks 0 and 12 of the treatment period.

Urinary NAG/Cr was above the normal range before the treatment both in the TLF + CLAT group and CLAT group, with no significant difference ($p = 0.116$). After 12 weeks of treatment, NAG/Cr decreased in the TLF + CLAT group but not in the CLAT group (mean (SD) 1.74 (1.01) U. mmolCr (−1) vs. 3.18 (1.03) U. mmolCr (−1), respectively; $p < 0.01$). Similar changes were observed in urinary β2-MG (mean (SD) 0.22 (0.11) U. mmolCr (−1) vs. 0.41 (0.20) U. mmolCr (−1), respectively; $p < 0.01$).

Urinary TGF-β1 decreased in the TLF + CLAT group but not in the CLAT group (mean (SD) 17.51 (8.38) pgml (−1) vs. 21.11 (8.59) pgml (−1), respectively; $p < 0.05$). Similar changes were observed in urinary MCP-1 (mean (SD) 6.68 (3.41) ngL (−1) vs. 8.92 (3.46) ngL (−1), respectively; $p < 0.05$). Additionally, a positive correlation within a certain range was shown in correlation analysis of medical history (months) of rUTI patients with urinary MCP-1 ($r = 0.50$, $p < 0.05$) and TGF-β1 ($r = 0.78$, $p < 0.01$) (Figures 2, 3).

3.3 Comprehensive efficacy

Compared with patients treated with CLAT alone, TLF combined with CLAT resulted in a higher clinical effective rate and lower recurrence rate and was sustained thereafter. For long-term clinical efficacy, the total effective rates were 90.82% (89/98) in the TLF + CLAT group and 74.23% (72/97) in the CLAT group, $p < 0.05$. For long-term clinical efficacy, the

TABLE 3 Primary and secondary outcomes.

Item	TLF + CLAT (n = 98)	CLAT (n = 97)	p-Value
Clinical efficacy [n (%)]			
Complete recovery	53 (54.08)	40 (41.24)**	<0.001
Significant recovery	30 (30.61)	27 (27.84)	-
Symptomatic improvement	6 (6.12)	5 (5.15)	-
No recovery	9 (9.19)	25 (25.77)**	<0.001
Recurrence rate [n (%)]			
At week 4 post treatment	14 (14.29)	35 (36.08)**	<0.001
At week 12 post treatment	19 (19.39)	46 (47.42)**	<0.001
Renal tubular injury markers, mean ± SD			
Urinary NAG/Cr (U/mmol)	1.74 ± 1.01	3.18 ± 1.03**	<0.001
Urinary β2-MG (mg/L)	0.22 ± 0.11	0.41 ± 0.20**	<0.001
Renal fibrosis markers, mean ± SD			
Urinary TGF-β1 (pg/ml)	17.51 ± 8.38	21.11 ± 8.59**	0.003
Urinary MCP-1 (ng/L)	6.68 ± 3.41	8.92 ± 3.46**	<0.001
TCM syndrome score, mean ± SD	6.22 ± 4.09	11.44 ± 5.52**	<0.001

*p < 0.05, **p < 0.01 vs. the TLF + CLAT group.

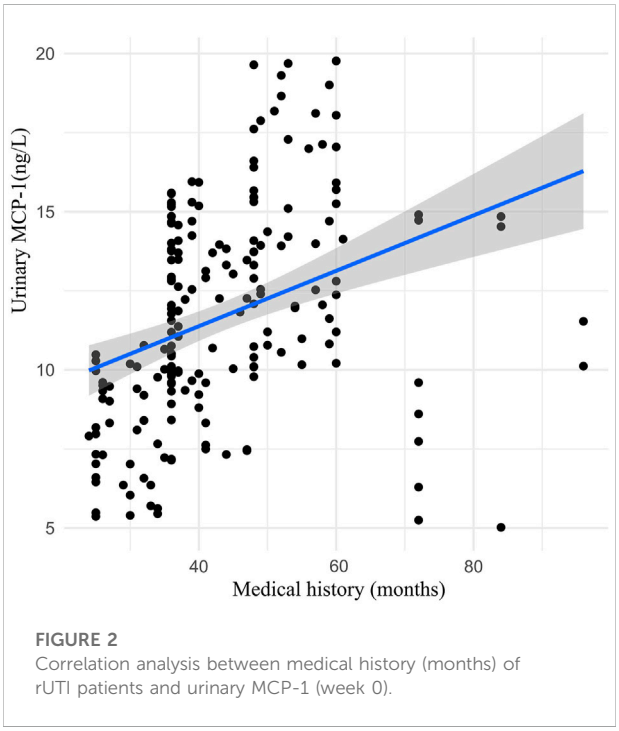

FIGURE 2
Correlation analysis between medical history (months) of rUTI patients and urinary MCP-1 (week 0).

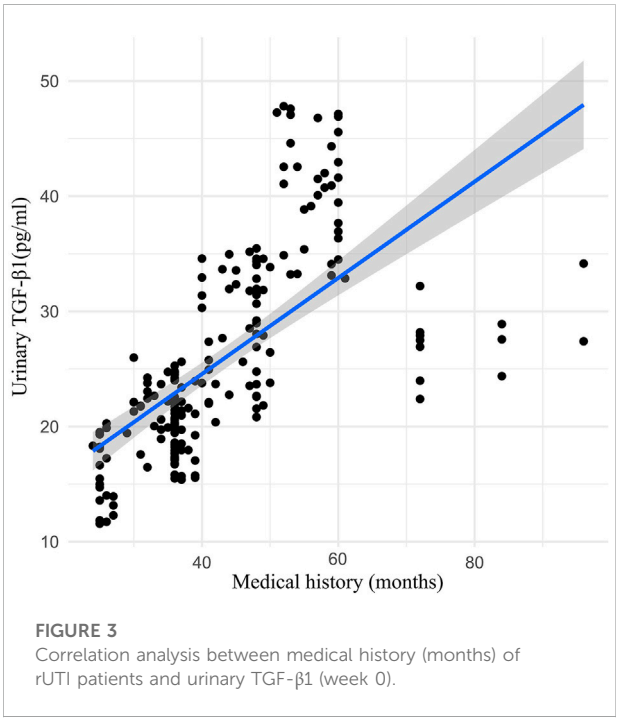

FIGURE 3
Correlation analysis between medical history (months) of rUTI patients and urinary TGF-β1 (week 0).

recurrent rate at week 4 post treatment was 14.29% (14/98) in the TLF + CLAT group and 36.08% (36/97) in the CLAT group; the recurrent rate at week 12 post treatment was 19.39% (19/98) in the TLF + CLAT group and 47.42% (46/97) in the CLAT group. Clinical efficacy is evaluated by the disappearance or improvement of clinical symptoms and uropathogenic clearance. More details could be found in Table 4.

Groups were similar in TCM syndrome scores before the treatment, with a mean composite symptom score of 21.15 points (SD 1.89) in the TLF + CLAT group and 20.71 points (SD 2.32) in the CLAT group. After 12 weeks of treatment, groups showed significant differences, with a mean composite symptom score of 6.22 points (SD 4.09) in the TLF + CLAT group and 11.44 points (SD 5.52) in the CLAT group, p < 0.01.

TABLE 4 Evaluation of clinical efficacy.

Clinical efficacy	Indicators		
	Clinical symptom and sign	Urine routine (for two consecutive times)	Clean-catch midstream urine culture
Complete recovery	Disappeared	Normal	Negative
Significant recovery	Disappeared or nearly disappeared	Normal or almost normal	Negative
Symptomatic improvement	Alleviated	Significantly improved	Occasionally positive
No recovery	No significant improvement	No significant improvement	Colony count≥10^5/ml 4 weeks after medication

3.4 Safety results

There were no significant changes in the safety results, including blood routine, liver and kidney function, and electrocardiogram before and after treatment in the two groups, and no obvious adverse reactions occurred. CLAT-related laboratory abnormalities were not observed during this trial.

4 Discussion

In this study, we found that compared with CLAT, TLF combined with CLAT resulted in a significantly higher clinical effective rate and lower recurrence rate. Notably, additional benefits in protecting renal tubule, inhibiting renal fibrosis, and alleviating the non-infection-related physical signs and subjective symptoms were also observed in patients treated with TLF + CLAT. There were no obvious adverse reactions that occurred during this study.

CHM has been shown to be either used alone or combined with antibiotics, which may be more effective than antibiotics alone in treating (Yu et al., 2018). Equally, our previous studies showed relatively good clinical efficacy of TLF compared with CLAT in the treatment of rUTI (Gong et al., 2003; Gong et al., 2004; Gong et al., 2006; Gong et al., 2007; Gong et al., 2010). In the present study, we combined TLF with CLAT to treat rUTI and evaluated the clinical efficacy of this novel therapy. Compared with patients administrated with CLAT alone, a higher clinical effective rate was observed in TLF + CLAT group at week 12 of treatment. Furthermore, recurrent rates were monitored respectively at week 4 and week 12 post treatment to observe the long-term efficacy of the two treatments. Our results showed that TLF combined with CLAT has a longer and more stable effect; indirectly, it also suggested that TLF might have benefits to enhance the long-term efficacy.

RUTI involves inflammation of the urinary tract, which might result in renal tubular damage and ultimately kidney failure in those patients (Ichino et al., 2009; Lorenzo-Gomez et al., 2020). Urinary NAG and β2-MG are sensitive markers of tubular injury (Ix and Shlipak, 2021). The study has shown that abnormal expression of the urinary kidney injury marker (NAG) was also observed in rUTI patients (Lorenzo-Gomez et al., 2020). Therefore, quantitative detection of urinary renal tubular injury markers in patients with rUTI should be paid more attention, which might be helpful for early prevention of renal damage attributable to rUTI. In the present study, increased urinary renal tubular injury markers (NAG/Cr and β2-MG) were observed in rUTI patients and were reduced more after TLF + CLAT treatment compared with CLAT. Accordingly, TLF + CLAT might have an effect on renal tubular protection in rUTI patients.

Persistent inflammation associated with rUTI is a crucial inducement of IDRF, which is a complicated process involving proinflammatory and profibrotic paracrine mediators, such as growth factors, TGF-β1, MCP-1, and cytokines (Humphreys, 2018; Gu et al., 2020; Singh et al., 2021). As the critical profibrotic factors, urinary MCP-1 and TGF-β1 were monitored to evaluate the anti-fibrosis effects of the two treatments in the present study. Urinary TGF-β1 and MCP-1 were tested at week 0 and week 12 of treatment. Correlation analysis showed that the medical history (months) of rUTI patients was positively correlated with the level of profibrotic factors at week 0, suggesting that rUTI might be a risk factor for IDRF. Also, after 12 weeks of treatment, compared with CLAT, the expression of urinary TGF-β1 and MCP-1 decreased significantly in the TLF + CLAT group, which showed that TLF combined with CLAT has benefits in protecting against renal fibrosis. Therefore, attention should be paid to early prevention of renal fibrosis in the treatment of patients with rUTI. However, the specificity and sensitivity of urinary TGF-β1 and MCP-1 in the diagnosis of renal fibrosis attributable to rUTI still need more support from evidence-based clinical research, which already became a trigger for our subsequent experiments.

Furthermore, benefits in alleviating the non-infection-related physical signs and subjective symptoms were also observed in rUTI patients treated with TLF + CLAT. In clinical practice, we find that symptoms such as abdominal distention and fatigue would persist for a considerable time even after the infection is under control, which would result in significant inconvenience to those patients. The guidelines for rUTI showed that, since 2011,

the non-infection-related physical signs and subjective symptoms have been recognized as part of the diagnosis criteria, along with "self-diagnosis of UTI" (Dason et al., 2011; Anger et al., 2019). This suggests that treatment of RUTI should not only focus on the negative result of urine culture but also pay attention to eradicate or alleviate the non-infection-related physical signs and subjective symptoms of rUTI patients. Therefore, this novel treatment is also a promising strategy helping to improve the health-related quality of life of rUTI patients.

In conjunction with the previous evidences (Gong et al., 2006; Gong et al., 2007; Gong et al., 2010; Lorenzo-Gomez et al., 2020), our results suggest that renal injury and IDRF might be the consequences due to rUTI in those patients, which involves complex interactions among multiple inflammatory cells and profibrotic cytokine signaling pathways. Given that, it is becoming more and more challenging to treat rUTI since it may not be possible to treat this disease by targeting one single molecular pathway. In other words, a multi-pharmacological approach involving several anti-inflammatory and antifibrotic molecules may need to be employed.

Chinese herbal is a natural medicine, contains a variety of effective ingredients, and has long been used to treat rUTI (Flower et al., 2015). TLF is an effective herbal prescription developed for treating rUTI. With the characteristics of the multi-ingredients, the mechanism of action and targets of Chinese herbal prescription TLF in patients with rUTI are also diverse. Studies by our group have shown the possible roles for TLF in the treatment of rUTI, including effects on reducing recurrence rate, alleviating symptoms, protecting renal tubular function, and inhibiting renal fibrosis (Gong et al., 2003; Gong et al., 2004; Gong et al., 2006; Gong et al., 2007; Gong et al., 2010). Consequently, TLF might be the multi-pharmacological approach with great promise in treating rUTI. However, further studies are still needed to investigate the mechanism of TLF against rUTI.

This study was designed as a double-blind RCT, with strict quality control processes for manufacturing TLF and placebo. The major contribution of our research is to demonstrate that rUTI is a significant threat that could cause renal damage and fibrosis, and TLF might be a multi-pharmacological approach involving anti-inflammatory and antifibrotic molecules and with great promise in treating rUTI. Since our study duration was relatively short (24 weeks), further investigation with longer follow-up is warranted to validate the role of urinary TGF-β1 and MCP-1 in the IDRF diagnosis and the impact of TLF in renal damage and fibrosis attributable to rUTI.

5 Conclusion

TLF combined with CLAT was superior to CLAT used alone in rUTIs in alleviating symptoms and decreasing recurrence and might have renal tubular protection and anti-fibrosis effects, which suggests TLF combined with CLAT might be an available treatment for rUTI. Moreover, TLF might be a multi-pharmacological approach involving anti-inflammatory and antifibrotic molecules and with great promise in treating rUTI.

Data availability statement

The original contributions presented in the study are included in the article/Supplementary Material; further inquiries can be directed to the corresponding author.

Ethics statement

The studies involving human participants were reviewed and approved by the Ethics Committee of Shanghai Municipal Hospital of Traditional Chinese Medicine. The patients/participants provided their written informed consent to participate in this study.

Author contributions

XG is the chief investigator of the trial and contributed to conceive the research, organize, and supervise the study. TL carried out the trial registration, drafted the manuscript, and participated in the data collection. GJ and WL contributed in enrolling patients at sub-centers of this research; YX and GY participated in the clinical data monitoring and the organization of study visits. All authors revised the protocol critically for important intellectual content and approved the final version of the manuscript.

Funding

This trial is funded by the National Natural Science Foundation of China (No. 82074387 and No. 81873280) and Shanghai Municipal Education Commission Gaofeng Gaoyuan Discipline Construction Project (No. 02.ZY05.191311N). The funders had no role in study design and conduction, data collection and analysis, decision to publish, or preparation of the manuscript.

Acknowledgments

The authors thank GJ and WL for their efforts in enrolling patients at Shanghai Sixth People's Hospital, Shanghai Baoshan District Hospital of Integrated Traditional Chinese and Western Medicine, respectively. We are also thankful to all of the patients

who participated in the study and the staff of the participating hospitals for their support.

Conflict of interest

The authors declare that the research was conducted in the absence of any commercial or financial relationships that could be construed as a potential conflict of interest.

Publisher's note

All claims expressed in this article are solely those of the authors and do not necessarily represent those of their affiliated organizations, or those of the publisher, the editors, and the reviewers. Any product that may be evaluated in this article, or claim that may be made by its manufacturer, is not guaranteed or endorsed by the publisher.

References

Anger, J., Lee, U., Ackerman, A. L., Chou, R., Chughtai, B., Clemens, J. Q., et al. (2019). Recurrent uncomplicated urinary tract infections in women: AUA/CUA/SUFU guideline. *J. Urol.* 202 (2), 282–289. doi:10.1097/JU.0000000000000296

Dason, S., Dason, J. T., and Kapoor, A. (2011). Guidelines for the diagnosis and management of recurrent urinary tract infection in women. *Can. Urol. Assoc. J.* 5 (5), 316–322. doi:10.5489/cuaj.11214

Flower, A., Harman, K., Lewith, G., Moore, M., Bishop, F. L., Stuart, B., et al. (2016). Standardised Chinese herbal treatment delivered by GPs compared with individualised treatment administered by practitioners of Chinese herbal medicine for women with recurrent urinary tract infections (RUTI): Study protocol for a randomised controlled trial. *Trials* 17, 358. doi:10.1186/s13063-016-1471-5

Flower, A., Harman, K., Willcox, M., Stuart, B., and Moore, M. (2019). The RUTI trial: A feasibility study exploring Chinese herbal medicine for the treatment of recurrent urinary tract infections. *J. Ethnopharmacol.* 243, 111935. doi:10.1016/j.jep.2019.111935

Flower, A., Wang, L. Q., Lewith, G., Liu, J. P., and Li, Q. (2015). Chinese herbal medicine for treating recurrent urinary tract infections in women. *Cochrane Database Syst. Rev.* 6, CD010446. doi:10.1002/14651858.CD010446.pub2

Forbes, R., Ali, A., Abouhajar, A., Brennand, C., Brown, H., Carnell, S., et al. (2018). ALternatives to prophylactic antibiotics for the treatment of recurrent urinary tract infection in women (ALTAR): Study protocol for a multicentre, pragmatic, patient-randomised, non-inferiority trial. *Trials* 19 (1), 616. doi:10.1186/s13063-018-2998-4

Geerlings, S. E. (2016). Clinical presentations and epidemiology of urinary tract infections. *Microbiol. Spectr.* 4 (5), 1–11. doi:10.1128/microbiolspec.UTI-0002-2012

Gong, X. Z., Yang, J., Meng, Q., Zheng, P. D., and He, L. Q. (2003). Comparision of pathological morphology in two rat model of acute pyelonephritis. *Shenzhen J. Integr. Traditional Chin. West. Med.* 13 (2), 74–77. doi:10.16458/j.cnki

Gong, X. Z., Zheng, P. D., Yang, J., and Feng, Z. (2007). Effect of the Qi-tonifying Kidney-nourishing and Damp-heat-relieving Method on the tubular function in patients with chronic pyelonephritis. *Jiangsu J. Traditional Chin. Med.* 39 (8), 19–21. doi:10.3969/j.issn.1672-397X.2007.08.014

Gong, X. Z., Zheng, P. D., Yang, J., and Meng, Q. (2004). Building rat model of chronic pyelonephritis. *Beijing Med. Journal(Chin)* 26 (6), 391–394. doi:10.15932/j.0253

Gong, X. Z., Zheng, P. D., Yang, J., Meng, Q., and Li, H. Y. (2006). Effect of tailinfang on renal tubular function of chronic pyelonephritis rats. *Chin. J. Integr. Traditional West. Nephrol.* 7 (3), 138–140.

Gong, X. Z., Zheng, P. D., Yang, J., Zhou, J. J., and He, L. Q. (2010). Effects of "Tailin Decoction" on renal scarring suppression in chronic pyelonephrits rats. *Shanghai J. Traditional Chin. Med.* 44 (4), 72–75. doi:10.16305/j.1007

Gu, Y., Liu, X., Huang, X., Yu, X., and Lan, H. (2020). TGF-β in renal fibrosis triumphs and challenges. *Future Med. Chem.* 12 (9), 853–866. doi:10.4155/fmc-2020-0005

Humphreys, B. D. (2018). Mechanisms of renal fibrosis. *Annu. Rev. Physiol.* 80, 309–326. doi:10.1146/annurev-physiol-022516-034227

Ichino, M., Kuroyanagi, Y., Kusaka, M., Mori, T., Ishikawa, K., Shiroki, R., et al. (2009). Increased urinary neutrophil gelatinase associated lipocalin levels in a rat model of upper urinary tract infection. *J. Urol.* 181 (5), 2326–2331. doi:10.1016/j.juro.2009.01.010

Ix, J. H., and Shlipak, M. G. (2021). The promise of tubule biomarkers in kidney disease: A review. *Am. J. Kidney Dis.* 78 (5), 719–727. doi:10.1053/j.ajkd.2021.03.026

Kaur, R., and Kaur, R. (2021). Symptoms, risk factors, diagnosis and treatment of urinary tract infections. *Postgrad. Med. J.* 97 (1154), 803–812. doi:10.1136/postgradmedj-2020-139090

Li, L. w. (2018). *Clinical observation on the treatment of recurrent urinary tract infection by Bushen Tonglin prescription combined with antimicrobial drugs*. China: Liaoning University of TCM.

Lorenzo-Gomez, M. F., Flores-Fraile, M. C., Marquez-Sanchez, M., Flores-Fraile, J., Gonzalez-Casado, I., Padilla-Fernandez, B., et al. (2020). Increased urinary markers of kidney damage in the institutionalized frail elderly due to recurrent urinary tract infections. *Ther. Adv. Urol.* 12, 1756287220974133. doi:10.1177/1756287220974133

Lv, W., Booz, G. W., Wang, Y., Fan, F., and Roman, R. J. (2018). Inflammation and renal fibrosis: Recent developments on key signaling molecules as potential therapeutic targets. *Eur. J. Pharmacol.* 820, 65–76. doi:10.1016/j.ejphar.2017.12.016

Raduly, Z., Price, R. G., Dockrell, M. E. C., Csernoch, L., and Pocsi, I. (2021). Urinary biomarkers of mycotoxin induced nephrotoxicity-current status and expected future trends. *Toxins (Basel)* 13 (12), 848. doi:10.3390/toxins13120848

Singh, S., Anshita, D., and Ravichandiran, V. (2021). MCP-1: Function, regulation, and involvement in disease. *Int. Immunopharmacol.* 101, 107598. doi:10.1016/j.intimp.2021.107598

Wagenlehner, F., Wullt, B., Ballarini, S., Zingg, D., and Naber, K. G. (2018). Social and economic burden of recurrent urinary tract infections and quality of life: A patient web-based study (GESPRIT). *Expert Rev. pharmacoecon. Outcomes Res.* 18 (1), 107–117. doi:10.1080/14737167.2017.1359543

Yu, G. Y., Xie, Y. M., Gao, N., Sun, Y., Miao, R. P., Han, S. J., et al. (2018). Clinical application evaluation of clinical practice guideline on traditional Chinese medicine therapy alone or combined with antibiotics for uncomplicated lower urinary tract infection. *Zhongguo Zhong Yao Za Zhi(Chin)* 43 (24), 4746–4752. doi:10.19540/j.cnki.cjcmm.2018.0126

frontiers | Frontiers in Pharmacology

TYPE Hypothesis and Theory
PUBLISHED 21 September 2022
DOI 10.3389/fphar.2022.968256

OPEN ACCESS

EDITED BY
Dan-Qian Chen,
Northwest University, China

REVIEWED BY
Vladimir Tesar,
Charles University, Czechia
Lin Chen,
Northwest University, China

*CORRESPONDENCE
Yang Zheng,
154202536@qq.com
Baoli Liu,
liubaoli@bjzhongyi.com

SPECIALTY SECTION
This article was submitted to Renal Pharmacology,
a section of the journal
Frontiers in Pharmacology

RECEIVED 13 June 2022
ACCEPTED 29 August 2022
PUBLISHED 21 September 2022

CITATION
Zhou X, Dai H, Jiang H, Rui H, Liu W, Dong Z, Zhang N, Zhao Q, Feng Z, Hu Y, Hou F, Zheng Y and Liu B (2022), MicroRNAs: Potential mediators between particulate matter 2.5 and Th17/Treg immune disorder in primary membranous nephropathy.
Front. Pharmacol. 13:968256.
doi: 10.3389/fphar.2022.968256

MicroRNAs: Potential mediators between particulate matter 2.5 and Th17/Treg immune disorder in primary membranous nephropathy

Xiaoshan Zhou[1,2], Haoran Dai[3], Hanxue Jiang[1], Hongliang Rui[1,4], Wenbin Liu[5], Zhaocheng Dong[2], Na Zhang[6], Qihan Zhao[1,6], Zhendong Feng[7], Yuehong Hu[1,6], Fanyu Hou[8], Yang Zheng[1]* and Baoli Liu[1,3]*

[1]Beijing University of Chinese Medicine, Beijing, China, [2]Beijing Hospital of Traditional Chinese Medicine, Capital Medical University, Beijing, China, [3]Shunyi Branch, Beijing Hospital of Traditional Chinese Medicine, Beijing, China, [4]Beijing Institute of Chinese Medicine, Beijing, China, [5]School of Life Sciences, Beijing University of Chinese Medicine, Beijing, China, [6]School of Traditional Chinese Medicine, Capital Medical University, Beijing, China, [7]Pinggu Hospital, Beijing Hospital of Traditional Chinese Medicine, Beijing, China, [8]School of Traditional Chinese Medicine, Changchun University of Chinese Medicine, Changchun, China

Primary membranous nephropathy (PMN), is an autoimmune glomerular disease and the main reason of nephrotic syndrome in adults. Studies have confirmed that the incidence of PMN increases yearly and is related to fine air pollutants particulate matter 2.5 (PM2.5) exposure. These imply that PM2.5 may be associated with exposure to PMN-specific autoantigens, such as the M-type receptor for secretory phospholipase A2 (PLA2R1). Emerging evidence indicates that Th17/Treg turns to imbalance under PM2.5 exposure, but the molecular mechanism of this process in PMN has not been elucidated. As an important indicator of immune activity in multiple diseases, Th17/Treg immune balance is sensitive to antigens and cellular microenvironment changes. These immune pathways play an essential role in the disease progression of PMN. Also, microRNAs (miRNAs) are susceptible to external environmental stimulation and play link role between the environment and immunity. The contribution of PM2.5 to PMN may induce Th17/Treg imbalance through miRNAs and then produce epigenetic affection. We summarize the pathways by which PM2.5 interferes with Th17/Treg immune balance and attempt to explore the intermediary roles of miRNAs, with a particular focus on the changes in PMN. Meanwhile, the mechanism of PM2.5 promoting PLA2R1 exposure is discussed. This review aims to clarify the potential mechanism of PM2.5 on the pathogenesis and progression of PMN and provide new insights for the prevention and treatment of the disease.

KEYWORDS

PM2.5, PLA2R1, microRNA, Th17/Treg, primary membranous nephropathy (PMN)

1 Introduction

Membranous nephropathy (MN) is a pathological pattern of primary glomerular disease and has developed into the main pathological type of adult nephrotic syndrome. Primary membranous nephropathy (PMN) is a part of membranous nephropathy with unknown etiology, accounting for about 75% (Lai et al., 2015). The occurrence of PMN results from complex interactions of environment, genetics, and immunity as a classic model of autoimmune glomerular disease. However, the specific mechanism of air pollution components and risk loci inducing PMN pathological injury pattern formation has not been confirmed. About 25% of the remaining patients are secondary MN, associated with various diseases such as malignancy, systemic lupus erythematosus, drug reactions, and infections (Akiyama et al., 2019). Unlike other kidney diseases, the incidence of MN has been substantially increasing in recent 10 years. MN has passed IgA nephropathy to become the leading cause of adult nephrotic syndrome (Hu et al., 2020). Spontaneous remission of proteinuria occurs in 30%–40% of patients, while slow progression to end-stage renal disease (ESRD) occurs in the remaining patients after 5–15 years (Lai et al., 2015). Early diagnosis and reasonable intervention of PMN are essential.

The clinical manifestations of PMN are mostly nephrotic syndrome or asymptomatic proteinuria. And its pathology is characterized by diffuse thickening of the basement membrane. Its immunofluorescence is a diffuse granular deposition of IgG and complements C3 on glomerular capillary walls, with IgG4 being the predominant IgG subtype (Fogo et al., 2015; Ahmad and Appel, 2020). At present, the renal biopsy result is used as the gold standard for diagnosing MN. Pathogenic podocyte autoantigens can be found in the glomerular immune deposits as the incentives to stimulate the formation of *in situ* immune complexes (Couser et al., 1978). As pro-inflammatory factors of autoimmune response, helper T (Th) cells promote B cell differentiation and antibody production upstream. In contrast, regulatory T (Treg) cells inhibit this effect and maintain immune tolerance. The formation of initial damage may also further promote the expression of autoantigens and trigger new immune activities (Ronco and Debiec, 2012), yet that hypothesis has not been confirmed. MN recurrence after renal transplantation may be related to circulating autoantibodies reaching the renal binding donor autoantigens (Stahl et al., 2010). These antigens are essential for disease diagnosis, disease progression, and prognosis. Among them, PLA2R1 accounts for about 70% and acts as a characteristic and diagnostic autoantigen of PMN. Some evidences show that PLA2R1 can reflect disease immune activity and is more sensitive and quicker than proteinuria remission, which also indicates that PMN immune remission occurs before clinical remission (Beck et al., 2011; Du et al., 2014). There are good reasons to speculate that the rising incidence of PMN is inextricably linked to increased exposure to self-antigens. From an epidemiological point of view, there are regional differences in disease incidence. It can also be found in clinical practice that some PMN patients still relapse after the regular application of immunosuppressive therapy. Our team proposed that fine air pollutants PM2.5 act as an unstable factor to stimulate continuous autoantigen exposure and lead to autoimmune disorders (Liu et al., 2019). Thus, autoantibodies against ectopic antigens bind to situ antigens in podocytes. This review will also introduce several hypotheses about how PM2.5 causes antigen exposure. Th17/Treg imbalance has been confirmed of great significance in PMN. Correlation studies have shown that PM2.5 exposure relocates the immune response to the Th17 immune pathway (Cremoni et al., 2020). The effect of PM2.5 on Th17/Treg immune balance has been confirmed to have multiple tracks, such as polycyclic aromatic hydrocarbons (PAH), NF-κB, Notch, et al. These intermediate links interact with microRNAs. In multi-system such as respiratory and cardiovascular, the response of microRNA to external pollution stimuli significantly affects Th17/Treg balance. PM2.5 regulating Th17/Treg from upstream *via* microRNA is also considered to be important in PMN. In PMN, antigen exposure by PM2.5 ultimately targets the glomerulus. This feature is different from other types of diseases. Alterations of miRNAs in this process may contribute to this property.

2 Primary membranous nephropathy

2.1 The exposure of primary membranous nephropathy autoantigens

Heymann et al. (1959) proposed an active Heymann nephritis model. By intraperitoneal injection of the supernatant of rat kidney extract, the animal model exhibits a more pronounced MN-like clinical response (Heymann et al., 1959). Couser et al. (1978) confirmed the existence of antigens on human podocytes as the target of circulating autoantibodies. It is speculated that the pathological model of PMN also has the process of antigen-antibody binding. Beck et al. (2009) found that PLA2R1 is present in normal podocytes and immune deposits of PMN patients. PLA2R1 triggers autoimmune responses under its special intramolecular disulfide bond configuration and colocalizes with IgG (Beck et al., 2009). Anti-PLA2R1 antibodies are found in 70%–80% of patients from different ethnic groups (Du et al., 2014). Autoantigens such as THSD7A (Tomas et al., 2014), Nell-1 (Sethi et al., 2020), and Exostosin1or Exostosin2 (Sethi et al., 2019) were subsequently identified. The pathogenesis of PMN is associated with antibodies binding to podocyte autoantigens. However, PMN-specific autoantigens are not only expressed in podocytes. As early as 2017, a study on PLA2R1 and asthma found that PLA2R1 is expressed in endobronchial tissue and epithelial brushings (Nolin et al., 2016); In 2018, a clinical study in Hamburg,

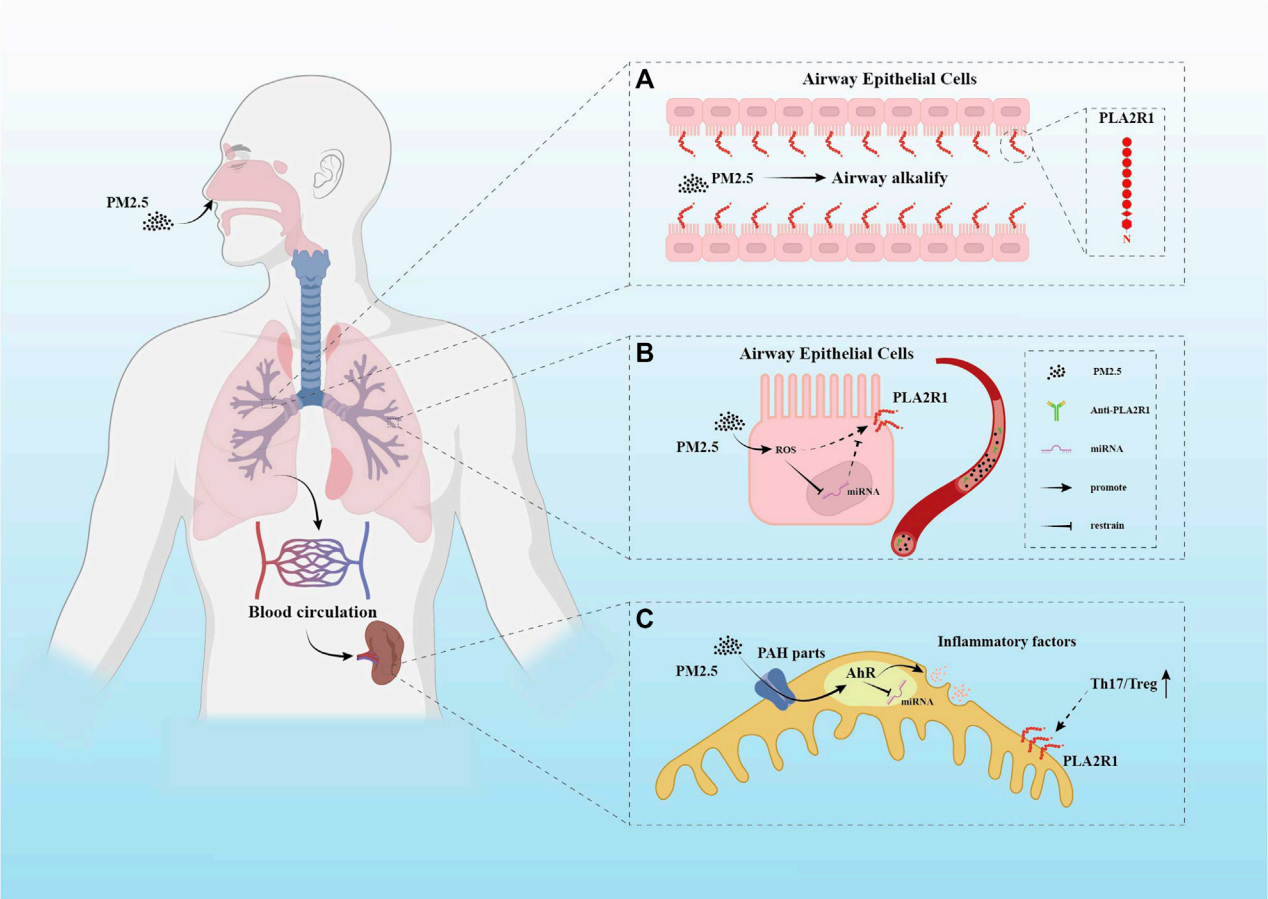

FIGURE 1
Several different hypothetical mechanisms of PM2.5 pathogenicity. **(A)** PLA2R1 has been demonstrated to be expressed in human respiratory epithelial cells. PM2.5 is mainly composed of polycyclic aromatic hydrocarbons (PAHs) and metals. After entering the respiratory tract, the alkalinization effect of PM2.5 on the airway may enhance the expression of PLA2R1. This conjecture has not been supported by direct evidence. **(B)** The oxidative stress response caused by PM2.5 in the respiratory system may cause changes in miRNAs. The promotion of ROS and the inhibition of miRNAs by PM2.5 may increase the expression of PLA2R1. **(C)** PAH components in PM2.5 have been shown to play a role in the imbalance of Th17/Treg ratio. This component uses AhR as a channel. It is not clear how AhR affects the enhancement of Th17 immune pathway, but miRNAs may be one of them.

Germany, confirmed that two antigens, PLA2R1 and THSD7A, are stably expressed in bronchioles and podocytes (von Haxthausen et al., 2018). And PLA2R1 expression is not limited to PMN patients. It is also less expressed in normal podocytes (Beck et al., 2009).

Academician Hou Fanfan's team discovered the relationship between PM2.5 concentration and the increased incidence of PMN in 2016 (Xu et al., 2016). Based on a large number of studies in China, Zhang et al. (2018a) concluded that the growth trend of the disease is closely related to gene-environment interactions. According to our hypothesis of increased PLA2R1 autoantigen exposure under environmental pollution (Liu et al., 2019), extrarenal autoantigens may trigger circulating antibody production.

MiRNAs are sensitive to external stimuli. A study found that downregulation of miR-130a-5p in MN kidney biopsy specimens promoted podocyte apoptosis. The same phenomenon occurs in a model of AngII-induced podocyte injury. Downregulated miR-130a-5p targeting increases the expression of PLA2R1 (Liu et al., 2018). miR-130a-5p is sensitive to oxidative stress induced by external stimuli. And miR-130a-5p is upregulated in an H_2O_2-induced oxidative stress environment (Ayaz and Dinç, 2018). However, there is no direct evidence to prove the variation of miR-130a-5p under PM pollutants. It is known that under the contamination of PM, bronchial epithelial cells can cause significant oxidative stress, and the oxidative stress effect of PM2.5 seems to change with the seasons (Longhin et al., 2016). It is speculated that airborne fine particle pollutants

represented by PM2.5 can alter microRNA expression, thereby promoting the exposure of PMN autoantigens. Combined with previous studies, this process may be achieved through oxidative stress (Figure1B), but it has not been confirmed. The entry of PM2.5 into the human body can cause increased levels of oxidative stress. Epigenetic changes often accompany this process. Eleonora Longhin et al. (2016) confirmed the link between oxidative stress and related miRNAs under the molecular network activated by PM2.5; Jin Li et al. (2018a) found that PM2.5 intervention in human alveolar epithelial cells led to increased reactive oxygen species (ROS) generation with downregulation of miR-486. And upregulation of miR-486 can inhibit oxidative stress response; In 2016, Rodosthenis S. Rodosthenous et al. (2016) studied the effect of PM2.5 on the abnormal miRNA expression of extracellular vesicles, which means circulating miRNAs. They demonstrated that PM2.5 exposure-related miRNAs in the circulation are associated with oxidative stress, inflammation, and arteriosclerosis pathways in cardiovascular disease populations. This also led us to think that PM2.5 could not only bind to the important related protein Dicer during miRNAs production to hinder pre-miRNA maturation (Izzotti and Pulliero, 2014), but also affect the function of circulating miRNAs at the post-mature level and cause systemic responses. However, PLA2R1 is not static, and epitope spread occurs as the disease progresses. Moreover, this epitope expansion is associated with renal prognosis stratification in PMN patients (Seitz-Polski et al., 2016). After discovering the relationship between disease activity and epitope spread, no studies have identified factors or pathways associated with changes in the PLA2R1 epitope in PMN.

2.2 Major immune pathways of primary membranous nephropathy

The characterization of PMN as an autoimmune disease is the activation of Th17, Th2, and Treg, et al. Research about PM2.5 currently focuses on its contribution to the incidence of PMN and induction of Th17/Treg balance dysregulation. However, the specific immune process of PM2.5 particles entering the body has not been elucidated. PM2.5 particles enter the lung from the respiratory tract and can reach the bottom of the alveoli due to their tiny diameter. Parts of it are taken up and processed by innate immune cells. Others can enter the blood circulation and act on the whole body (Krauskopf et al., 2018). Inflammation and oxidative stress caused by PM2.5 take place through multiple pathways. Although dendritic cells (DCs) are potent antigen-presenting cells (APCs), they can monitor the environment, uptake antigens, and initiate new $CD4^+$ T cells in lymph nodes (Hilligan and Ronchese, 2020). However, its role in the entry of PM2.5 into the body is unclear. PM2.5 particle stimulation can induce increased expression of DEC205, a surface receptor present in APCs such as DCs and macrophages, which can influence the maturation of APCs (Honda et al., 2021). However, Zheng et al. (2020) showed that although PM2.5 increased the proportion of mature DCs, it did not enhance the response of lymphocytes, yet it could stimulate the Th17 phenotype. We speculate that PM2.5 particles may not only be taken up and presented by DCs after entering the body. Other APC types may be involved in PM2.5-activated $CD4^+$ T cells differentiating into Th17. Changes in macrophages seem to play an important role in studies of immune cell responses to PM2.5. The survey of Soi Jeong et al. (2019) flow cytometry showed that pulmonary macrophages significantly increased after PM2.5 treatment. Taking the liver as an example, it has been proved that PM2.5 particles can cause secondary organ inflammation through blood exposure after entering the human body from the respiratory tract. Fu et al. (2020) demonstrated that PM2.5 could activate macrophages in a dose-dependent manner and cause respiratory system inflammation through TLR4/NF-κB/COX-2 signaling pathway. Macrophages are critical to PM2.5 disrupting immune homeostasis. After being stimulated by foreign pollutants, macrophages play a role in phagocytosis and release inflammatory cytokines, such as NF-κB, and increase the level of oxidative stress (Bekki et al., 2016). Several studies have confirmed that PM2.5 can upregulate the expression of NF-κB, IFN-γ, et al. (Table 1). These phenomena also further confirmed the role of macrophages in PM2.5 particle uptake and Th17/Treg immune imbalance. PM2.5 mediates IFN-γ production. Th17-related immune pathways are enhanced after IFN-γ-induced macrophage activation. In human autoimmune diseases, IFN-γ can target APC to promote the expression of IL-17 (Kryczek et al., 2008). The effects of PM2.5 particles on the polarization of the Th17 immune pathway are not limited to this pathway. Sun et al. (2020) demonstrated that the PAH components in PM2.5 can directly act on $CD4^+$ naive T cells from the spleen through aromatic hydrocarbon receptors (AhR) to affect Th17 and Treg immune pathways. And the most apparent different expression of this process is the environmental information processing related genes. PM2.5 particles, especially their adsorbed PAH components, can directly cause changes in the proportion of immune cells in the spleen, increase T cells and decrease B cells (Honda et al., 2017).

2.2.1 Th17

In the presence of pro-inflammatory cytokines IL-6, IL-1, TGF-β, and IL-23, IL-21, and $CD4^+$ T cells induce the expression of the RORγt gene through STAT3 and then differentiate into Th17 cells (Zhang et al., 2021). The experiment confirmed that cytokines, such as IL-23 are necessary to produce Th17. Cytokine deficiency can induce autoimmunity disorders (Cua et al., 2003). In addition, after activation of the PI3K/Akt signaling pathway, mTOR stimulates glycolysis supported by HIF-1, which also

TABLE 1 The effects of PM2.5 treatment on microRNA expression in different models and the changes of corresponding immune inflammatory factors.

Model	microRNA change	Changes in inflammatory factors	References
BALB/c mice	miR-224↓	Treg↓/Th17↑,TLR2/TLR4/MYD88↑	Ping Li et al. (2020)
BALB/c mice	miR-146↑	IL-6, IFN-γ, TNF-α↑	Hou et al. (2021)
ApoE$^{-/-}$ mice	miR-326-3p↑	NF-κB↑	Gao et al. (2022)
Beas-2B cells	miR-331↓	NF-κB, IL-6, IL-8↑	Song et al. (2017)
HAEC	miR-939-5p↓	HIF-1α↑	Liang et al. (2021)
BALB/c mice	10 miRs	Th1↑/Th2↓, IL-4, IFN-γ↑	Hou et al. (2018)
COPD mice	miR-149-5p↓	NF-κB↑	Qiuyue Li et al. (2021)
A549 cells	miR-582-3p↑	Wnt/β-catenin↑	Yang et al. (2022)
16HBE cells	miR-218↓	IL-1β, IL-6, TNF-α↑	Song et al. (2020)
Beas-2B/HBE cells	miR-582-5p↓	HIF-1α↑	Jiang et al. (2021)

Beas-2B cells, human bronchial epithelial cell line; HAEC, human aortic endothelial cells; A549 cells, human alveolar basal epithelial cell line; 16HBE cells, human bronchial epithelial cell line; COPD, chronic obstructive pulmonary disease.

essentially drives Th17 type expression (Cong et al., 2020). Th17 cells can express a variety of pro-inflammatory cytokines, such as IL-17A, IL-17F, IL-22, and GM-CSF (Yasuda et al., 2019). It can be defined that Th17 is the hinge of autoimmune diseases (Murphy et al., 2003). Th17 immune pathway can recruit other inflammatory cells, thereby causing direct damage to the tissue.

Several studies have confirmed the vital role of Th17 in the pathogenesis of PMN. Huimin Li et al. observed that IL-17A was significantly upregulated in MN patients. Simultaneously MDSCs, part of peripheral blood mononuclear cells (PBMC), participated in disease progression through the Th17 immune pathway and inhibited Th2 polarization under the mediation of IL-6 and IL-10 (Li H. et al., 2020); Marion Cremoni et al. observed a significant increase in the expression of IL-17A in MN through *in vitro* stimulation and verified the activation of Th17, Th2, and Th1 pathway in MN after vivo stimulation, which manifested as variety expression of related cytokines (Cremoni et al., 2020). And Th17 cells are more flexible and sensitive to changes in the immune microenvironment than other effector T cell subsets (Bluestone et al., 2009). The tissue damage phenotype caused by Th17 cells is not static. But the timing of Th17 responses playing a significant role in PMN remains to be excavated, which may be more involved during relapse and progression. Roza Motavalli et al. (2021) examined the ratio of Th17/Treg in PBMCs of 30 newly diagnosed and unsuppressed PMN patients and 30 healthy people. They did not find significant changes in Th17 numbers in newly diagnosed MN patients but observed a differential reduction in Treg, resulting in an increased Th17/Treg ratio. PM2.5 particles can stimulate the production of IL-1a, which is involved in the production of inducible bronchial-associated lymphoid tissue (iBALTs). This potency is sustained (Kuroda et al., 2016), which can trigger the transition of T-cell immunity to the Th17 immune pathway. Rheumatoid arthritis, an autoimmune disease mediated by genetics and environment, is also closely related to this process (Sigaux et al., 2019). The entry of PM2.5 into the lung through the airway can induce the upregulation of IL-17A and activate the immune-inflammatory pathway to participate in the induction of lung injury (Cong et al., 2020). The increase of IL-17A is macrophage-dependent. The pro-inflammatory effects of T-cytokines under the action of macrophages are persistent (Ma et al., 2017).

2.2.2 Th2

After naive T cells are stimulated by antigens and signal transduction such as T cell receptor (TCR) *in vivo*, they differentiate into Th1, Th2, Treg, and other subsets. Th2 cells mainly produce IL-4, IL-5, IL-10, and IL-13. They can mediate humoral immunity, trigger B cell activation and promote immunoglobulin synthesis.

Since the immune complex deposited in the glomerular capillary wall of PMN is accounted for IgG4 for the main part. Therefore, it is considered that Th2 is one of the main immune pathways in PMN (Kuroki et al., 2005). An evaluation of Th subgroup mRNA expression also proved that IL-4 and IL-5 mRNA were significantly increased in MN renal biopsy specimens compared with other types of glomerular diseases (Ifuku et al., 2013). A study found that Th2 immune pathway-related factors peaked between 4 and 6 h after stimulation. Then Th2 showed a downward trend (Openshaw et al., 1995; Hirayama et al., 2002; Masutani et al., 2004), thus speculating that the polarization of Th2 may be closely related to the immune activity in the early stage of MN. The initial Th2 polarization phenomenon will increase the response of B cells to promote the production of IgG4 (Kuroki et al., 2005). So Th2 is involved in the mechanism of MN immunoglobulin generation.

2.2.3 Treg

Different from immune pathways such as Th17, Th2, and Th1, Treg cells differentiated from $CD4^+$ naive T cells are crucial in suppressing autoimmune responses (Strom and Koulmanda, 2009). TGF-β, IL-2, and Foxp3 are cytokines necessary for differentiation into Treg. Treg cells are rapidly recruited to the injured site when inflammation occurs, secreting TGF-β and IL-10 to inhibit immune overactivation.

Treg's percentage decreased significantly in PMN patients compared to the healthy control group. Also, Treg increased significantly 8 days after rituximab stimulation. This phenomenon means the clinical response of Treg to the drug is sensitive (Rosenzwajg et al., 2017). In addition to PMN, Treg and IL-10 also serve as critical therapeutic factors in systemic lupus erythematosus (SLE). And the severity of SLE can be reduced by increasing the number of Treg cells and the production of IL-10 (Lee et al., 2019). The PAH components in PM2.5 can damage the Foxp3 locus necessary for Treg cell differentiation by binding to cell surface AhR (Sun et al., 2020). Another study also observed a decrease in Treg cell differentiation under exposure to PM2.5 (Gu et al., 2017).

2.2.4 Th17/Treg immune balance

Th17 and Treg cells are differentiated from naive $CD4^+$ T cells under the influence of a microenvironment composed of shared and different cytokines. They are a novel and classic paradigm for understanding autoimmune regulation. Following Th1 and Th2, Th17 and Treg cell subsets are more representative and flexible for understanding the immune status, proving that effector T cells have a more refined division of labor. Th17 and Treg are interrelated. A variety of cellular microenvironmental factors are the most critical factors in regulating the metabolic reprogramming of CD4+T cells. For example, Foxp3, which is necessary for Treg differentiation and development, interacts with RORγt to inhibit Treg binding to DNA, thereby changing Th17 differentiation into Treg (Sun et al., 2017); TGF-β, as an initial differentiation signal, which is involved in two kinds of differentiation of immune cell lines (Zhang et al., 2021), induces iTreg cells to convert to Th17 cells under the conditions of IL-6 (Bettelli et al., 2006).

Microarray data showed that the expression of IL-17 signaling pathway mRNA in lung tissue increased under the action of PM2.5. The expression of IL-17 in lung tissue was significantly increased after PM2.5 exposure (Jeong et al., 2019). Lin et al. (2020) showed that PM2.5 intratracheal perfusion could lead to an increase in the number of lymphocytes in the lungs and a decrease in the number of TGF-β cytokines; metabolic responses and costimulatory signals are also involved in affecting this balance. Such as blocking glucose glycolysis can promote the generation of Treg cells and inhibit the development of Th17 cells (Shi et al., 2011). Dynamic changes in Th17/Treg immune balance can reflect changes in the local immune microenvironment and represent an epigenetically unstable variable whole (Strom and Koulmanda, 2009) to induce the occurrence and aggravation of PMN. Studies have confirmed the phenomenon of increased Th17 cells and decreased Treg cells in MN, showing the existence of a Th17/Treg immune imbalance, and this balance is restored after immunotherapy (Ma et al., 2021). However, the mechanism underlying PM2.5 disrupts this balance in PMN remains unclear.

There are many speculations about the key pathogenic mechanism of air fine particle pollutant PM2.5. First, they enter the respiratory system, penetrate deep into the alveoli, and diffuse to other organs through the blood-air barrier (Falcon-Rodriguez et al., 2016), resulting in the local immune-inflammatory response. They can induct pro-inflammatory cytokines release or oxidative stress in the respiratory system. These cytokines directly enter the blood circulation, thus activating NF-κB, STAT1 pathways, et al. (Falcon-Rodriguez et al., 2016), triggering a systemic inflammatory cascade (Krauskopf et al., 2018). After PM2.5 suspension was instilled in mice trachea, the increase of Th17 immune pathway polarizing factor IL-6 was observed in peripheral blood circulation. And the increase in IL-6 was PM2.5 dose-dependent (Hou et al., 2018). The cellular and molecular mechanisms of MN pathogenicity after PM2.5 enter the blood circulation have not been elucidated. There are studies evaluating the effects of PM2.5 incubation on podocytes and found that podocyte cell homeostasis and immune-related molecules were significantly affected (Wan et al., 2020); Air pollutants use the lung as the starting point of autoimmunity and can regulate Th17/Treg; Studies found that prolonged exposure to fine particulate pollutants can lead to inflammation and endothelial function-related markers in the blood intercellular adhesion molecule-1 (ICAM-1) and vascular cell adhesion molecule-1 (VCAM-1) elevate (Rui et al., 2016), which also explains the increase in blood coagulation indexes in patients with PMN. Air pollution fine particles not only affect the local but also trigger systemic effects; PM2.5 treatment of $CD4^+$ naïve T cells in healthy human PBMC, similar inflammatory stimulation was observed, which can interfere with Th17/Treg balance through HIF-1α, glutamate oxaloacetate transaminase 1, as described before. Taking the complex transcriptional response of HIF-1α under hypoxia as an example, miR-210 is a hotspot closely related to it, also mediating macrophage apoptosis (Karshovska et al., 2020), Th17 differentiation (Wu et al., 2018), NF-κB pathway (Jia et al., 2020), and other effects.

As a stimulatory molecule from the external environment, PM2.5 has been confirmed to be associated with a high incidence of PMN. In terms of immunity, it has been confirmed that it can regulate microRNA and cause Th17/Treg immune imbalance in multi-system diseases. To our knowledge, there is currently no direct evidence for this pathway in PMN. There is also no data on miRNAs changes in PMN models under the effect of PM2.5. Taking miR-194 as an example, *in vitro* cell experiments confirmed the impact of PM2.5 on the downregulation of miR-194-3p (Zhou et al., 2018). qPCR analysis of renal biopsy

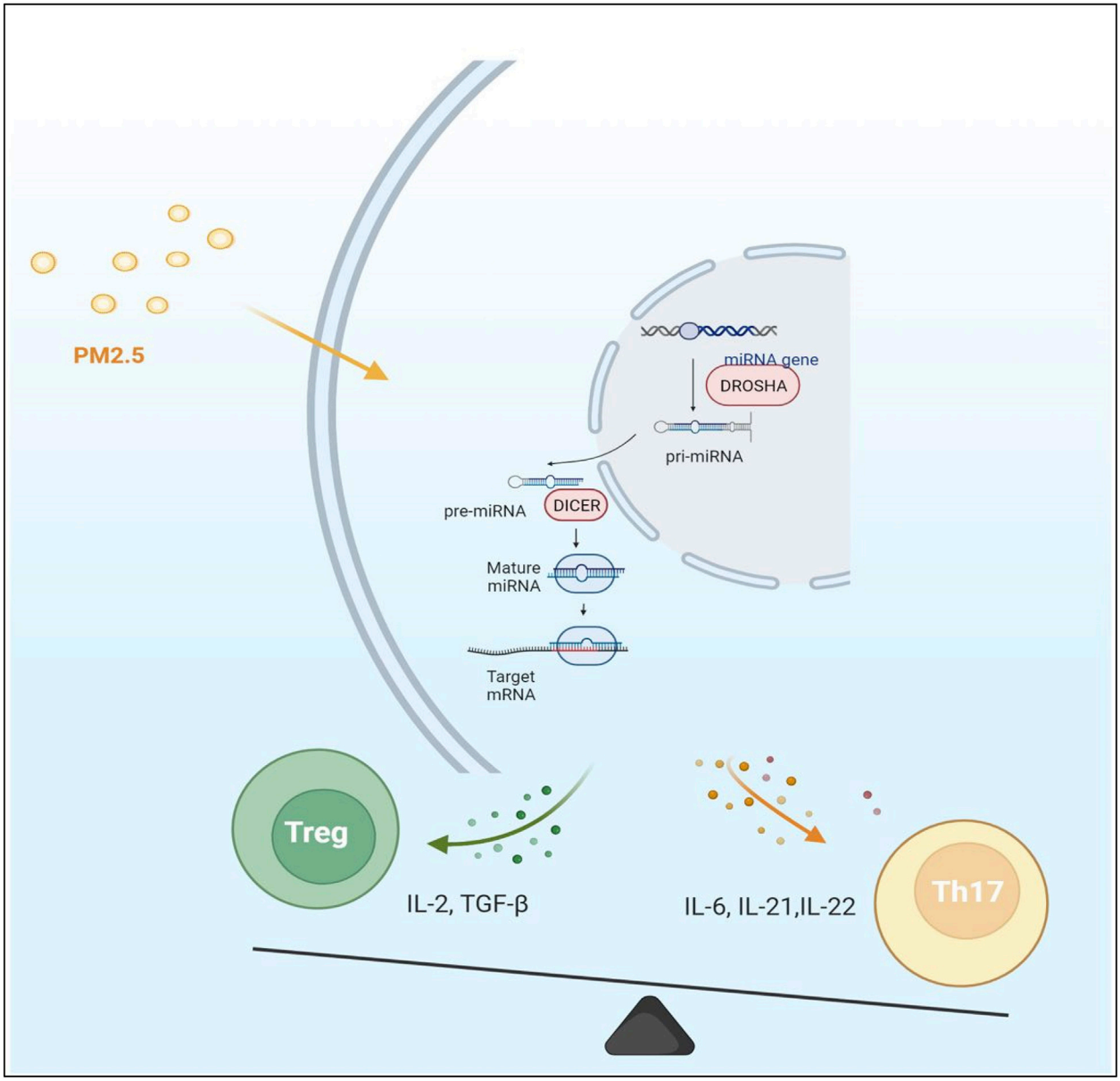

FIGURE 2
The expression of microRNA and mRNA in cells was changed under the effect of PM2.5 particles. Most of the immune factors secreted by cells are proinflammatory factors under PM2.5 stimulation. The immune balance of Th17/Treg was disturbed. The Th17 immune pathway is polarized. However, it is not clear which step of microRNA production is significantly affected by PM2.5.

samples from CKD patients with different disease types revealed that miR-194 was significantly downregulated in the advanced stage. MN patients were also included in the discovery cohort of this study (Rudnicki et al., 2016). However, this data on miRNAs expression in MN patients need further analysis. These two studies were tested in different tissues and did not prove our conjecture. MicroRNA is a kind of communication medium between cells and tissues. And its expression at specific sites may also provide signals. As an essential part of the epigenetic mechanism, miRNAs are also susceptible to the stimulation of PM2.5, affecting critical components of immune pathways by binding to target mRNAs (Bartel, 2004) (Figure 2). The inspiration of foreign molecules creates a stressful environment, and many baroreceptors, such as p53, direct regulatory effects on miRNAs (Krauskopf et al., 2017). In addition, other studies have found that PM2.5 can directly penetrate the placenta. Parental exposure to PM2.5 directly affects the parental Th17 and Treg immune pathways and

may change the immune microenvironment in offspring. The expression of IL-17A, IL-6, and IL-10 in offspring significantly increases with or without exposure to PM2.5, suggesting that the Th17/Treg balance was indirectly affected, which is called genetic susceptibility (Zhang et al., 2019).

3 Composition and mechanism of particulate matter 2.5

PM2.5 is a kind of fine particle pollutant with an aerodynamic diameter ≤2.5 μm, which is the main component of smog, mainly released from mineral combustion, automobile exhaust emissions, and construction industry processes. Its large surface area can absorb various toxic substances (Perrone et al., 2013). Taking Hangzhou, China, as an example, PM2.5 in this city is primarily composed of metals and organic ingredients like PAH. The concentration of PM2.5 increases in Hangzhou is related to the increase in construction sites, traffic emissions, and road asphalt particles (Fu et al., 2020); In rural and suburban areas, however, the harmfulness of PM2.5 pollution is sometimes overlooked. Taking the rural and remote mountainous areas of Milan and Italy as examples, in this study, the metal components of PM2.5 are mainly produced from aerosols and natural dust sources, also including organic elements such as PAH. But the biological effect of PM2.5 may be higher than that of PM1. It is easier for PM2.5 to cause DNA damage (Perrone et al., 2013); In a specific working environment, taking the subway as an example, the components of PM2.5 are mainly iron, copper, manganese, and other metals. The concentration of PM2.5 particles is thicker than the surface, affected by season and the burning of minerals. The concentration will increase in winter when the need for warmth is higher (Chang et al., 2021). PM2.5 particles have a large surface area. They enter the lung through the respiratory system and act on other human body organs. The results of a prospective study spanning 2005 to 2018 and covering 121 counties in Hunan, China, showed a strong positive correlation between high-level PM2.5 exposure and chronic kidney disease (Duan et al., 2022). Animal studies have shown that the kidney is a toxicological target of particulate pollutants inhaled from the lungs (Nemmar et al., 2010). PM2.5 exposure is associated with early kidney injury. This effect is not only reflected in the damage to the endocrine function of the kidney (Aztatzi-Aguilar et al., 2015) but also in the increase of the renal damage markers β-2-microglobulin and cystatin-C (Aztatzi-Aguilar et al., 2016). The toxic effects of metal and PAH elements are closely related to oxidative stress (Greenwell et al., 2002), Th17 immune pathway activation (Zhang et al., 2018b), and gene transcription changes (Mehta et al., 2008). Previous studies on PM2.5 hazards used filters to collect PM2.5 particles. They can analyze the components carried on the surface of the particles. It is achieved by conducting *in vivo* or *in vitro* experiments such as tracheal instillation of PM2.5 suspensions or real-world ventilation. As a particulate matter that can enter the alveoli, PM2.5's significant impact on human immunity and epigenetics is not only related to the toxicity of its surface adsorption components. Akiko Honda et al. (2021) avoided the contamination of PM2.5 ingredients by extracting materials through cyclone separation technology, thus analyzing the effect of PM2.5 as a powder itself on immune cells and factors. Compared with the organic components of PM2.5, it has a more noticeable impact on reducing cell viability and promoting the release of IL-6.

3.1 Particulate matter 2.5 and the onset of primary membranous nephropathy

Due to its small diameter, unlike the large particles cleared away by mucociliary, PM2.5 can accumulate in inhaled alveoli, be phagocytosed by alveolar macrophages, be absorbed by pulmonary vascular endothelial cells, or along with the lung's air exchange entering the circulatory system (Xing et al., 2016). Air pollution is closely related to the pathogenesis of multi-system diseases such as respiratory and cardiovascular systems. This capability has a significant impact in many developing countries. The impact of PM2.5 on the incidence and progression of many diseases has been confirmed. It is known that both PM2.5 pathogenicity and glomerular diseases have regional and ethnic differences. However, the role of PM2.5 from different regional sources is different. This phenomenon may be related to varying sources of PM2.5 (Table 2). Related articles have confirmed that higher concentrations of PM2.5 in different regions will increase the risk of MN. A study covering a database of 43.7 million hospitalized patients in China confirmed the influence of environmental and geographical factors on the incidence of PMN. This study takes the Yangtze River as the geographical boundary. The incidence of PMN in the north of the Yangtze River was positively correlated with PM2.5 exposure. While the incidence in the south of the Yangtze River is positively correlated with the proportion of the Zhuang population, but not PM2.5 exposure (Li et al., 2018b). A study covering 938 hospitals in 282 cities in China showed that in areas where PM2.5 concentrations >0.70 mg/m3, every 10 mg/m3 increase in PM2.5 concentration increases the risk of MN by 14%. In addition, during the past 10 years, unlike other kinds of glomerular diseases that remained stable disease incidence, the incidence of MN has increased by

TABLE 2 The disturbed miRNAs and their target mRNA after exposure with PM2.5 in different areas.

Source of PM2.5	microRNA change	Target mRNA	Changed factor	References
SRM 1648a	miR138-1-3p↓	—	IL-6, IL-8, NF-κB↑	Jin et al. (2021)
Beijing, China	miR-21-5p↑	SOX7	VE-cadherin↓	Shiwen Wang et al. (2020)
SRM 1648a	miR-582-5p↓	HIF-1α	HIF-1α↑	Jiang et al. (2021)
Boston area, United States	8 miRs↓	—	HMGB1/RAGE↑	Fossati et al. (2014)
Wuhan, China	miR-182/185↓	SLC30A1, SERPINB2, AKR1C1	SLC30A1, SERPINB2, AKR1C1↑	Liu et al. (2015b)
Hong Kong SAR, China	miR-125a-3p↓	TCTP	TCTP↑	Liu et al. (2020)
Beijing, China	miR-326-3p↑	IκBα	TNF-α, NF-κB, VCAM1↑	Gao et al. (2022)
Beijing, China	6 miRs	—	E-cadherin↓ Vimentin↑	Yunxia Wang et al. (2021)
Purchased from United States	miR-16-1-3p↓	Twist1	Twist1↑	Zhang and Li, (2019)
Jiangsu, China	miR-29b-3p↑	PI3K(P85a)	P53↑PEAMIR↓ PI3K(P85a)/ATK/GSK3b↓	Pei et al. (2020)
Shenyang, China	miR-32↑	Smad1	Smad1↓	Yang et al. (2017)
Beijing, China	miR-139-5p↓	Notch1	Notch1↑	Yunxia Wang et al. (2020)
Beijing, China	3 miRs↑	—	IL-4↓, IFN-γ↑	Hou et al. (2018)
Beijing, China	miR-149-5p↓	TAB2	MAPK, NF-κB↑	Qiuyue Li et al. (2021)
Zhengzhou, China	miR-155↑	FOXO3a	FOXO3a↓	Jiansheng Li et al. (2021)
Shijiazhuang, China	miR-183/96/182↑	FOXO1	NACHT, LRR, NALP3↑	Lixiao Zhou et al. (2019)
Taiyuan, China	miR-206↑	SOD1	CAT/GSH/GSH-Px/T-SO↓ ROS↑	Lei Wang et al. (2019)
Changchun, China	miR-331↓	IKK-β	NF-κB↑	Song et al. (2017)
Shanghai, China	miR-338-3p↓	UBE2Q1	UBE2Q1/AKT/mTOR↑	Jin-Chao Wang et al. (2021)
Purchased from United States	miR-486↓	PTEN, FOXO1	PTEN, FOXO1↑	Jin Li et al. (2018)
Taiyuan, China	miR-574-5p↓	BACE1	BACE1↑	Ku et al. (2017)

SRM, 1648a: The standard reference material (SRM) is atmospheric particulate matter collected in an urban area and acts as a control material used in the inorganic analysis of atmospheric particulate matter. A unit of SRM, 1648a consists of a bottle containing 2 g of atmospheric particulate matter.

13% every year (Xu et al., 2016). It is possibly related to the increased air pollution condition in recent years.

Current studies believe that genetic risk factors determine most glomerulonephritis; MN is no exception which has been shown to have susceptibility to HLA-DQ, HLA-DR, and PLA2R1 genes. More importantly, anti-PLA2R1 antibodies were detectable in 73% of patients with high-risk genotypes of PLA2R1 and HLA-DQA1, which differed from the low-risk population (Stanescu et al., 2011; Gupta et al., 2018). The effect of PM2.5 on PMN incidence may also be premised on genetic susceptibility through stimulation of immunity or exposure to self-antigens. Risk amino acids encoded by risk alleles DRB1*1501 and DRB1*0301 of PMN have been reported to promote the role of T cell epitopes in the presentation of PLA2R1 antigen by MHC class II molecules in the Chinese Han population (Cui et al., 2017). Currently, no evidence shows whether PM2.5 is more related to PLA2R1-positive MN. Perhaps because of its large proportion, unique biological characteristics, and different conformation, most studies have focused on PLA2R1. The relationship between other specific antigens of MN and environmental pollution needs more studies to verify. We hypothesized that the effect of PM2.5 on the increased incidence of MN may not be limited to specific autoantigens but may be related to the population with risk genes. And this susceptibility may be achieved through epigenetic pathways.

Although epidemiological evidence suggests that PM2.5 contributes to the increased incidence of PMN, no convincing data has confirmed the molecular mechanism of this process. Studies observe that PM2.5 can deposit in the kidney through macrophage endocytosis or adsorption of proteins, resulting in damage to the glomerulus (Saint-Georges et al., 2008). But the onset and progression of PMN are inseparable from exposure to self-antigens. Therefore, the speculation that air pollution can lead to self-antigen exposure is more valuable. The resulting anti-PLA2R1 antibodies first bind with high affinity to the antigen in the kidney. Circulating anti-PLA2R1 antibody concentrations are not detectable until the kidney binding sites are saturated (van de Logt et al., 2015). In addition to the relationship between its antibody concentration and disease progression (Beck et al., 2011), changes in the PLA2R1 epitope are also closely related to disease progression and patient subgroups (Fresquet et al., 2015). There are several hypotheses about how PM2.5 causes PLA2R1 exposure. PM2.5 can trigger vascular endothelial cell inflammation through toll-like receptors (TLRs) or by stimulating macrophages to make them a potential phospholipase A2 (sPLA2) target. These effects may contribute to the exposure of PLA2R1 that

circulates continuously between the plasma membrane and the endosome (East and Isacke, 2002; Ronco and Debiec, 2012); Studies by Paul D. Boyce et al. (2006) demonstrate that inhalable metal particles alkalize the airways and increase pH. Compared with an acidic environment, PLA2R1 will appear conformational extension in the alkaline environment (Dong et al., 2017) (Figure 1A); PM2.5 causes oxidative stress, and the oxidative cellular microenvironment may cause PLA2R1 to retain disulfide bonds (Liu et al., 2019). In addition, the PAH components in PM2.5 can cause polarization of the Th17 immune pathway through AhR (Sun et al., 2020), reducing Tregs (Figure 1C). The balance of immune tolerance is disrupted. Small amounts of anti-PLA2R1 antibodies are inherently present in the circulation. Under the premise that the tolerance balance is broken, PM2.5 particles disturb the balance of PLA2R1 and antibodies, which may make the kidneys more severely hit. PM2.5 may also promote PLA2R1 exposure by activating AhR on podocytes (Li et al., 2018b). And AhR is believed to be involved in various responses such as immune inflammation by altering the epigenetic mechanism of miRNAs (Disner et al., 2021). However, there are few studies on this process in PMN.

PM2.5 particles first act on the human body through the lung tissue. And the PLA2R1 formed in the lung stimulates the immune system to generate anti-PLA2R1 antibodies, which then act on the kidneys through circulation. It is unclear whether organs other than the lung express PMN autoantigens represented by PLA2R1. However, the roles of PM2.5 particles are limited. No studies have confirmed that PM2.5 is necessary for the pathogenesis of PMN. Whether large inhalation or chronic exposure to PM2.5 particles, the major impact is the occurrence of respiratory diseases such as asthma (Yu et al., 2022). Therefore, the contribution of PM2.5 to the incidence of PMN may be achieved based on the production of nephrogenic antibodies.

3.2 Intervention of particulate matter 2.5 on immune balance and miRNAs expression

PM2.5 particles are inhaled into the lung from the airway. Part of them can be directly translocated to the alveolar extravascular matrix and vascular endothelial cells. Thereby PM2.5 particles enter the systemic circulation and cause miRNAs changes related to various inflammatory pathways. Bioinformatics analysis showed that changes in respiratory system function caused by short-term exposure to PM2.5 are mainly concentrated in immune pathways (Lin et al., 2022). After passing through the respiratory system, PM2.5 can enter the blood circulation. Studies confirmed that PM2.5 particles are related to the increased expression of Th17 immune pathway-related factor IL-17A in MN. Marion Cremoni et al. found that PM2.5 can be used as a threshold for distinguishing IL-17A positivity at the concentration was 58 pg/ml (Cremoni et al., 2020). In the case of the podocyte *in situ* antigen exposure in PMN patients, changes in immune activity represented by Th17/Treg immune balance can form autoantibodies against situ antigen. The role of PM2.5 in influencing Th cell differentiation in multiple ways has been confirmed by many studies, such as acting on Th17/Treg balance through AhR (Sun et al., 2020), NF-κB (Wan et al., 2020), Notch (Gu et al., 2017), et al. Oxidative stress is one of the important responses of PM2.5 intervention. Elevation of NF-κB under PM2.5 stimulation activates pro-inflammatory responses under oxidative stress (Longhin et al., 2016). The abnormal expressions of miRNAs caused by PM2.5 mainly focus on the changes in NF-κB. What is the significance of miRNAs in the differentiation of Th cells? How do miRNAs work?

Epigenetic regulation regulates gene expression at the transcriptional and translational levels without altering the nucleotide sequence (Balasubramanian et al., 2020). The occurrence and progression of MN are closely related to the environment, genetics, and immunity. These different factors all contain the abnormal expression of miRNAs stimulated by external environmental toxins. As a critical mediator in regulating gene expression at the transcriptional translational level, miRNAs function as an essential aspect of epigenetics (Bartel, 2004). Several studies have confirmed the connection between miRNAs and external toxins, such as ethanol (Pasqualotto et al., 2021) and cigarette smoke (Donate et al., 2021), et al.

The differentiation of Th cells, which have plasticity, is affected by antigens and co-stimulatory factors in the cellular microenvironment. Different types of Th cell differentiation are often accompanied by relatively specific miRNAs molecular patterns. After the stimulation of TCR, downstream signaling levels are activated in multiple ways. In this process, miRNAs act as regulatory targets and upstream regulatory factors to control the differentiation of effector T cells (Zhou et al., 2007). The regulation of critical factors' mRNA that governs signal threshold plays a considerable role in the differentiation and development of T cells (Baumjohann and Ansel, 2013). The previous study about the changes of miRNAs in PMN has found that downregulation trend in most cases. Mechanistically, it may be explained that T cells are stimulated to induce AGO2 ubiquitination and its proteasome-dependent reversal, shortening the half-life and leading to an overall decrease in the abundance of miRNAs (Bronevetsky et al., 2013). That is why the expression of corresponding stress factors and mRNA will increase. In the state of pathological stress, the role of microRNA can be said to be small because it has a considerable number of targets and has multiple

regulatory effects on the downstream multi-level cascade after TCR activation (Baumjohann and Ansel, 2013). The diversity of its roles and the coincidence with the target also makes its function impossible to detect by conventional experimental means, obscuring its important regulatory significance.

4 MicroRNA: Biological function and action formation

4.1 MicroRNA production and biological function

MiRNAs are a class of small endogenous single-stranded non-coding RNAs about 22 nucleotides in length, repressors of post-transcriptional gene regulation. MiRNAs first experience gene encoding in the nucleus and form the classical hairpin precursor. However, they are not directly involved in encoding proteins since they negatively regulate gene expression through complementary pairing with the 3′UTR region of mRNA, causing mRNA translation inhibition or inducing its degradation to negatively regulate gene expression (O'Brien et al., 2018) (Figure 2). Single miRNA can target multiple mRNAs, yet multiple miRNAs also can synergistically work on one single mRNA, hinting the roles of miRNAs in life processes are diverse and complex. Considering such features, changes in multiple signaling pathways stimulated by environmental pollution can be displayed by miRNAs and act downstream. Therefore, miRNAs may represent the body's stress response to stimulation. MiRNAs themselves are not easily degraded, primarily located inside cells. Another part called circulating miRNAs is located in the extracellular environment, which can circulate in body fluids related to RNA-binding proteins or in exosome-like lipid vesicles. As regulators of post-transcriptional processes, miRNAs play crucial roles in various cellular processes of development, proliferation, differentiation, and apoptosis, as well as stress responses (Iorio et al., 2010). They are thought to be involved in epigenetic mechanisms as an important player in gene expression regulation. Studies have found that the progression of MN and immune disorders are closely related to the functional changes of some miRNAs. Environmental and health research results indicate that epigenetics may mediate environmental factors' effects at the gene regulation level. Liu et al. (2015a) prove that epigenetic differential markers caused by environmental pollution exist in genes and are related to immune activation. MiRNAs are epigenetically sensitive response molecules to external pollutant stimuli (Balasubramanian et al., 2020). They can link air pollution with induced immune activity. MiRNAs play a vital role in the inflammatory activity of macrophages involved in the phagocytosis of PM2.5 (Hamidzadeh et al., 2017). The abnormal expression of miRNAs caused by exogenous pollutants can be reflected in circulating miRNAs (Balasubramanian et al., 2020).

4.2 MicroRNAs as membranous nephropathy diagnostic markers

Diagnosis of MN and other types of kidney disease largely depends on the typical injury pattern in biopsy tissue shown by microscopy. Renal biopsy, although important in confirming the type of disease, can still cause a certain degree of kidney damage as an invasive test. There is an urgent need for a non-invasive method to judge and predict disease progression. MiRNAs have made some progress in this field. A group of highly kidney-specific miRNAs cluster molecules has been found by K-means clustering, which are miR-192, miR-194, miR-204, miR-215, and miR-216 (Sun et al., 2004). Possibly because of the close distance, they regulate gene expression as a common transcriptional unit. MiR135a-5p, 146b5p, 150-5p, and 155-5p can be used as risk markers for chronic kidney disease (CKD) nephropathy progression by reflecting the degree of renal fibrosis or established renal failure (Pawluczyk et al., 2021). Unlike healthy people or other diseases, PMN patients have many differentially expressed miRNAs. Research results in recent years have shown that differentially expressed miRNAs have important roles in mediating inflammation, immune response and provide diagnostic value. Many studies have found that multiple miRNAs expression and function are altered in MN patients. In a 2018 study, ten microRNAs were found differentially expressed in biopsies from patients with MN compared with healthy controls. They target IL-6 and MYC, which are related to immune response; Among them, miR-204 can not be ignored in the immune process of MN for suppressing T cell proliferation (Barbagallo et al., 2019). MiR-27b-3p and miR-1228-3p were significantly upregulated in renal biopsy tissue of diabetic membranous nephropathy patients instead of diabetic nephropathy patients (Conserva et al., 2019). However, in this study, there was no direct analysis of the difference in expression of these two miRNAs between diabetic membranous nephropathy patients and healthy subjects. At present, no more studies on miR-27b-3p in MN have been retrieved. Based on the miRNAs microarray dataset GSE51674 downloaded from GEO, Yawei Hou et al. (2021a) extracted the MN and healthy control group information and combined it with the mRNA microarray dataset GSE108109 for target gene prediction. Finally, they screened out ten differentially expressed miRNAs involved in processes such as podocyte autophagy and renal fibrosis in MN by targeting mRNA regulatory networks. There is also a significant downregulation of miR-217 in MN compared with healthy people, which targets the expression of tumor

necrosis factor superfamily member 11 (TNFSF11). MiR-217 has sensitivity and specificity for distinguishing MN patients from healthy people (Li et al., 2017). Based on the detection value of serum anti-PLA2R1 antibody for disease, the serological detection method, as a non-invasive method, can play an important role in predicting the occurrence and prognosis of PMN (De Vriese et al., 2017). Different from the invasive detection method of kidney biopsy tissue, the detection of diagnostically valuable factors in serum is less invasive to the human body. miRNAs can exist stably in various body fluids. The studies of miRNAs sequencing in serum as a biomarker have also found a lot. InO.Sun et al. (2022) detected the expression of miRNAs in serum extracellular vesicles by RNA sequencing method. The identification results showed that the expression levels of miR-1229-3p, miR-340-3p, and miR-99b-5p in PMN differed from those in idiopathic nephrotic syndrome and healthy people. Differentially expressed miRNAs in extracellular vesicles can reflect the clinical treatment response of patients. Different humoral-derived miRNAs are differentially expressed in PMN. MicroRNA database analysis revealed differentially expressed miR-195-5p and miR-328-5p in MN and healthy people target PPM1A and BRSK1, respectively. These two target genes are associated with MAPK pathway activation. In addition, there is also miR-192-3p involved in the p53 signaling pathway by targeting RAB1A (Zhou et al., 2019a). MicroRNAs exist stably in peripheral blood. These miRNAs released from cells into the circulation may represent an overall profile of differential expression under stress. PBMCs from 30 adult patients with MN were collected from the nephrology department of a hospital in Iran and compared with healthy controls. MiRNAs-sequencing of collected PBMC samples by real-time PCR revealed a significant increase in miR-30c and miR-186 (Hejazian et al., 2020). MiRNAs in PBMC can not only distinguish MN from healthy people but can also distinguish MN from other glomerular lesions. For example, miR-106a-5p and miR-30a-5p can distinguish mesangial proliferative glomerulonephritis from MN (Wang et al., 2020a). By analyzing morning urine samples, Jinshi Zhang et al. (2020) found 28 specifically expressed miRNAs in the urinary exosomes of PMN patients. The target genes of these miRNAs are widely involved in pathway responses such as podocyte autophagy and macrophage inflammation. 2022, in Datong, Shanxi, Songjia Guo et al. (2022) run high-throughput miRNAs sequencing of urinary exosomes. Results showed that miR-30b-5p and miR-9-5p were significantly downregulated in PMN patients compared with healthy people. Moreover, in this study, miR-30b-5p in urinary exosomes was significantly correlated with the clinical indicator anti-PLA2R1 in serum. By analyzing the urinary sediment microRNA database GSE64306 in previous studies, Guangyu Zhou et al. (2021) compared the data of MN and healthy people. Data analysis showed that five miRNAs, miR-145-5p, miR-148a-3p, miR-148b-3p, miR-3605-5p, and miR-497-5p, could participate in the immunity and metabolism of MN through their target mRNAs Regulatory Network.

4.3 MicroRNAs and immune system cells

MiRNAs are essential kinds of immune cell regulators. As a kind of factor that has a clear effect on the stability of Th cells (Zhou et al., 2008), miRNAs have an important impact on the development and function of the immune system. They participate in the disease process by targeting a variety of mRNAs. PM2.5 first invades the respiratory system. In some lung diseases, it has been confirmed that miRNAs affect the balance of immune pathways such as Th1 and Th2, which occupy the leading position and further damage the immune system (Hou et al., 2018). MiRNAs can participate in the effect of PM2.5 by targeting immune-inflammatory-related factors, which has been demonstrated in multiple systems. PM2.5 inhaled into the lungs has been confirmed to play oxidative stress on lung tissue through miRNAs targeting function, activating NF-κB, NLRP3 (Zhou et al., 2020), and M1 polarization (Zhong et al., 2019). While causing lung damage, inflammatory factors secreted by these processes can enter the bloodstream and cause changes in miRNAs. Gene-environment interactions in PMN are important regulators of immune imbalance. The expression of genes involved in the inflammatory signaling pathway response is significantly increased in active PMN (Xu et al., 2021), which is considered to be related to the post-transcriptional negative regulation of miRNAs. Studies have shown that miR-16 can regulate various immune-related factors, such as IL-6, TNF-α, IL-4, IL-8, et al. These factors can affect the balance of Th17 and Treg. MiR-16 is involved in the immune process of SLE. It is highly expressed in PBMC and can be used as a recurrence marker of SLE (Yan et al., 2019). As mentioned above, miR-27b-3p was significantly upregulated in diabetic membranous nephropathy patients compared with patients with diabetic nephropathy. However, in a recent study on the function of miR-27b-3p, it was found that miR-27b-3p was significantly downregulated in chicken peripheral blood lymphocytes treated with ammonia, a component of PM2.5 aerosol, *in vitro*. Treg immune pathway-related protein gene expression was significantly decreased. Th2 and Th17 immune pathway-related protein expression were significantly increased (Zhang et al., 2022). In the treatment aspect of MN, studies have reported that tacrolimus, a calcineurin inhibitor, has an immunosuppressive effect on the disease. But its efficacy varies significantly among individuals, which may be related to the regulatory effect of miR-582-5p. MiR-582-5p is altered to affect the expression of PPP3R1 (Zhu et al., 2018).

4.4 MicroRNAs' damage to podocytes and kidneys

Podocytes are important presenting cells for *in situ* antigens as a relatively fully differentiated cell line. MN is marked by podocyte apoptosis. Although miRNAs are not much involved in developing human cell lineages and tissues, they play a central regulatory role in fully developed cells under stress and injury conditions (Mendell and Olson, 2012). MiRNAs can affect podocytes through multiple pathways. As previously described, miR-217 is downregulated in MN. MiR-217 can target TNFSF11 to participate in podocyte apoptosis. Upregulation of this miRNA *in vitro* attenuates damage to podocytes. Ling-wei Jin et al. (2019) demonstrated that the effect of miR-217 on podocyte apoptosis in MN could also be achieved through TLR4. Sha et al. (2015) revealed that miR-186 was significantly downregulated in MN and promoted podocyte apoptosis. This phenomenon is accompanied by an increase in the receptor family TLR4, which is crucial for immune system activation. MiR-124 induces podocyte adhesion damage by targeting integrin α3 and β1 under stress (Li et al., 2013); Downregulation of miR-500a-5p in MN is associated with promoting podocyte apoptosis. This effect is achieved through the Circ_0000524/miR-500a-5p/CXCL16 signaling pathway (Sun et al., 2021). MiRNAs have also been proved by many studies that their normal expression plays an important role in mature podocyte homeostasis. Such as podocyte-specific deletion of Dicer or Drosha, reduced miRNAs expression can cause podocyte and glomerular dysfunction (Zhou et al., 2008). There are also miR-30 that protect podocytes by inhibiting the toxic Notch1 or p53 pathways (Wu et al., 2014). Kidney biopsies from both MN and focal stage glomerulosclerosis (FSGS) patients showed increased expression of miR-378a-3p, distinguishable from diabetic nephropathy and IgA glomerulonephritis. MiR-378a-3p can increase in podocytes under TGF-β stress and target glomerular nephronectin (NPNT) inhibition, which is associated with podocyte reduction and proteinuria in active glomerular disease (Müller-Deile et al., 2017). Podocyte-derived miR-378a-3p and glomerular-derived miR-192-5p can also jointly upregulate NPNT (Müller-Deile et al., 2021). MiR-106a, miR-19b, and miR-17 are important regulators of pro-apoptotic gene expression. Lina Wu et al. (2021) found that these miRNAs in serum targeted inhibit phosphatase and tensin homolog deleted on chromosome ten (PTEN) expression. This process may be related to the decline of glomerular filtration function by promoting podocyte apoptosis in the early stage of MN. Peng Li et al. (2021a) searched the GSE133288 database and found 20 miRNAs that were differentially expressed in the tubulointerstitial transcriptome of MN and healthy individuals. They analyzed that the SRY-Box Transcription Factor4 (Sox4) gene was significantly upregulated in MN and was targeted by miR-204-5p. In 2014, high-throughput sequencing analyzed the expression profiles of miRNAs in PBLC of MN patients and healthy people. 286 of the 326 differentially expressed miRNAs were downregulated. This is different from other kidney diseases, where upregulated miRNAs are predominant. However, like other kidney diseases, downregulation of miR-23b, miR-24, and miR-26a also leads to rapid progression of marked glomerular and tubular damage in MN (Chen et al., 2014). MiR-150-5p positivity was observed in proliferating mesangial cells, atrophic tubules, and nodular infiltrates in MN (Pawluczyk et al., 2021). The expression of this miRNA is closely related to the development and differentiation of T and B cells (Zhou et al., 2007). In a rat model of MN, upregulation of miR-193a may affect the expression of important proteins in the cleft septum of podocytes by targeting WTI. Inhibition of miR-193a is helpful for the stability of podocyte structure and glomerular barrier function (Li et al., 2019).

4.5 Particulate matter 2.5 and microRNA

Based on environmental epidemiological studies, it has been demonstrated that exposure to PM2.5 has a clear association with the expression of some inflammation-related miRNAs (Bhargava et al., 2019). The toxicogenomics of microRNA is closely related to the pathogenesis and progression of the disease (Piletič and Kunej, 2016). By studying the analysis of circulating miRNAs genes in human populations exposed to PM2.5, it has been summarized by Julian Krauskopf et al. that PM2.5 can target the lung, heart, kidney, and brain. Rigorous statistical analysis has demonstrated dose and pollutant species-dependent changes in circulating miRNome after 2 h of ambient air pollution (Krauskopf et al., 2018). Multiple studies demonstrated that PM2.5 exposure could affect Th17/Treg balance by affecting microRNA expression. For example, PM2.5 exposure can downregulate miR-338-3p, miR-338-3p targets UBE2Q1 to inhibit autophagy, thus disrupt Treg/Th17 balance (Wang et al., 2021a).

PM2.5 and other ultrafine particle pollutants acting on cells *in vitro* can cause oxidative stress and lead to prolonged activation of the NF-κB pathway. NF-κB pathway consistently mediates pro-inflammatory responses that release IL-6, as the switch of epigenetic changes (Bhargava et al., 2019). And vice versa is also true. For example, PM2.5 indirectly targets and participates in FoxO and P13K/Akt signaling pathways by regulating some miRNAs (Wang et al., 2019a), which are also involved in the differentiation of Th cells. Lei Song et al. (2016)

demonstrated the pro-inflammatory effect of the miR-let-7 family under PM2.5 particle pollution induction. In bronchial cells, PM2.5 exposure significantly suppressed the expression level of miR-let-7a. Let-7a can inhibit arginase 2 (ARG2) to reduce oxidative stress caused by air pollution. Additionally, Iliopoulos et al. (2009) described a positive feedback loop of inflammatory factors involving the let-7 family. Activation of NF-κB and IL-6 inhibits the let-7 family. Therefore, the targeted inhibition of IL-6 and RAS by the Let-7 family is weakened. And RAS can further activate IL-6. Finally, let-7 is further inhibited. Moreover, it has been confirmed that the entry of PM2.5 particles into the body can activate the NF-κB pathway. Therefore, even a tiny amount of PM2.5 stimulation may trigger huge physiological effects driven by microRNA (Ebert and Sharp, 2012). Cytokines produced by these immune responses in the respiratory system can enter the circulation or reach the kidneys. The significant contribution of PM2.5 to PMN incidence highlights the promoting regulatory effect of miRNAs.

PM2.5 has a significant impact on the expression of immune factor-related miRNAs. The regulation of miRNAs can also directly change the expression of immune-inflammatory factors. They also have the effect of reducing the susceptibility to air pollutants in the opposite direction. Under the influence of PM2.5, sICAM-1 and sVCAM-1 levels were lower in rs1062923 homozygous carriers (Wilker et al., 2011). Some western or traditional Chinese medicine ingredients also reduce the effects of PM2.5, such as apigenin. Apigenin can regulate IL-17 and NF-κB to balance the Th2/Th17 immune disorder caused by PM2.5 (Pang et al., 2019). Indirect exposure to PM2.5 in a short time may not result in significant changes in microRNA levels. In contrast, direct exposure to PM2.5 can typically be observed with significant effects on cells, tissues, and related factors in renal and cardiovascular studies. Considering during a short exposure time, the irritating effect may not be noticeable. However, in the respiratory system, indirect exposure to high concentrations of PM2.5 in the environment can lead to significant changes in microRNA expression in nasal mucosa or endothelial cells. As previously mentioned, the regulation of PM2.5 significantly affects miRNAs expression. This is also consistent with significant changes in miRNAs in PMN. However, no detailed studies have confirmed the specific role of miRNAs in the PMN process. The effect of PM2.5 on morbidity and immune disorders *in vivo* is presumed to be related to PLA2R1 exposure. While the exposure of PLA2R1 is usually inhibited by miRNAs and stimulated by ROS (Sukocheva et al., 2019) (Figure 1B). Currently, there are few studies on the related miRNAs targeting PLA2R1 in PMN. And it is unclear which immune sites are targeted by the differentially expressed miRNAs in PMN. For example, whether miRNAs targeting PLA2R1 in PMN are involved in the Th17/Treg immune pathway remains obscure.

5 Conclusion

MN is an autoimmune disease mediated by environment, heredity, and immunity. PM2.5, an air pollutant that can be deposited at the bottom of alveoli, can trigger oxidation, release inflammation-related factors and promote the expression of pathogenic antigens *in situ* in trachea, bronchus, and alveoli. These products entering the bloodstream can alter the immune microenvironment and may even induce the production of circulating autoantibodies. PM2.5 particles entering the circulation can also cause Th immune imbalance, which acts on podocytes and destroys kidney function. However, the renal toxicity of PM2.5 may require the guidance of genetic susceptibility. But this effect may be related to racial genetic differences. The obvious correlation between PM2.5 and the incidence of multiracial PMN may be reflected by miRNAs. MicroRNA, a highly conserved molecule in the human body and an intermediary factor of environmental effects, is sensitive to stress responses caused by external poisons. The disturbances in microRNA are closely related to Th17/Treg immune imbalance. According to existing studies, PM2.5 can enter the human blood circulation through the respiratory system to stimulate the glomerulus, the placenta, and other trachea or viscera, leading to oxidative stress, autophagy, and immune response. They even have the effect of immune directional induction. Metal component on the surface of PM2.5 particles is related to oxidative stress through free radical action. At the same time, PAH may triggers T cell polarization or affect antigen expression through the AhR receptor. Different components of PM2.5 may also influence its pathogenic effect on PMN. However, the role of miRNAs in PMN needs more research and exploration.

Data availability statement

The original contributions presented in the study are included in the article/supplementary material, further inquiries can be directed to the corresponding author.

Author contributions

BL and YZ were responsible for conception of the study. HD, HJ, HR, WL, and ZD participated in the collection and summary of literature. XZ participated in the drafting of the

manuscript. NZ, QZ, and ZF were responsible for critical revision of important content. YH and FH participated in the drawing of tables and pictures respectively. BL and YZ were responsible for approving the final version to be published and agree to be responsible for all aspects of the work and to ensure that issues relating to the accuracy or completeness of any part of the work are properly investigated and resolved. All authors listed have made a substantial, direct, and intellectual contribution to the work and approved it for publication.

Funding

This work is supported by grants from Capital's Funds for Health Improvement and Research (No. 2020-2-2234 to BL), the National Key Research and Development Project of China (No. 2019YFC1709402 to BL), the General project of the National Natural Science Foundation of China (No. 81973793 to BL), and Youth Foundation of National Natural Science Foundation of China (No. 82004269 to HD).

Acknowledgments

Figure 2 was created with Biorender (Agreement number: ST245ELZA8).

Conflict of Interest

The authors declare that the research was conducted in the absence of any commercial or financial relationships that could be construed as a potential conflict of interest.

Publisher's note

References

Ahmad, S. B., and Appel, G. B. (2020). Antigens, antibodies, and membranous nephropathy: A decade of progress. *Kidney Int.* 97 (1), 29–31. doi:10.1016/j.kint.2019.10.009

Akiyama, S., Imai, E., and Maruyama, S. (2019). Immunology of membranous nephropathy. *F1000Res* 8, F1000 Faculty Rev-734. doi:10.12688/f1000research.17589.1

Ayaz, L., and Dinç, E. (2018). Evaluation of microRNA responses in ARPE-19 cells against the oxidative stress. *Cutan. Ocul. Toxicol.* 37 (2), 121–126. doi:10.1080/15569527.2017.1355314

Aztatzi-Aguilar, O. G., Uribe-Ramirez, M., Arias-Montano, J. A., Barbier, O., and De Vizcaya-Ruiz, A. (2015). Acute and subchronic exposure to air particulate matter induces expression of angiotensin and bradykinin-related genes in the lungs and heart: Angiotensin-II type-I receptor as a molecular target of particulate matter exposure. *Part. Fibre Toxicol.* 12, 17. doi:10.1186/s12989-015-0094-4

Aztatzi-Aguilar, O. G., Uribe-RaMirezM.Narvaez-Morales, J., De VizcAyA-Ruiz, A., and Barbier, O. (2016). Early kidney damage induced by subchronic exposure to PM(2.5) in rats. *Part. Fibre Toxicol.* 13 (1), 68. doi:10.1186/s12989-016-0179-8

Balasubramanian, S., Gunasekaran, K., Sasidharan, S., Jeyamanickavel Mathan, V., and Perumal, E. (2020). MicroRNAs and xenobiotic toxicity: An overview. *Toxicol. Rep.* 7, 583–595. doi:10.1016/j.toxrep.2020.04.010

Barbagallo, C., Passanisi, R., Mirabella, F., Cirnigliaro, M., Costanzo, A., Lauretta, G., et al. (2019). Upregulated microRNAs in membranous glomerulonephropathy are associated with significant downregulation of IL6 and MYC mRNAs. *J. Cell. Physiol.* 234 (8), 12625–12636. doi:10.1002/jcp.27851

Bartel, D. P. (2004). MicroRNAs: Genomics, biogenesis, mechanism, and function. *Cell.* 116 (2), 281–297. doi:10.1016/s0092-8674(04)00045-5

Baumjohann, D., and Ansel, K. M. (2013). MicroRNA-mediated regulation of T helper cell differentiation and plasticity. *Nat. Rev. Immunol.* 13 (9), 666–678. doi:10.1038/nri3494

Beck, L. H., Jr., Bonegio, R. G. B., Lambeau, G., Beck, D. M., Powell, D. W., Cummins, T. D., et al. (2009). M-type phospholipase A2 receptor as target antigen in idiopathic membranous nephropathy. *N. Engl. J. Med.* 361 (1), 11–21. doi:10.1056/NEJMoa0810457

Beck, L. H., Jr., Fervenza, F. C., Beck, D. M., Bonegio, R. G. B., Malik, F. A., Erickson, S. B., et al. (2011). Rituximab-induced depletion of anti-PLA2R autoantibodies predicts response in membranous nephropathy. *J. Am. Soc. Nephrol.* 22 (8), 1543–1550. doi:10.1681/ASN.2010111125

Bekki, K., Ito, T., Yoshida, Y., He, C., Arashidani, K., He, M., et al. (2016). PM2.5 collected in China causes inflammatory and oxidative stress responses in macrophages through the multiple pathways. *Environ. Toxicol. Pharmacol.* 45, 362–369. doi:10.1016/j.etap.2016.06.022

Bettelli, E., Carrier, Y., Gao, W., Korn, T., Strom, T. B., Oukka, M., et al. (2006). Reciprocal developmental pathways for the generation of pathogenic effector TH17 and regulatory T cells. *Nature* 441 (7090), 235–238. doi:10.1038/nature04753

Bhargava, A., Shukla, A., Bunkar, N., Shandilya, R., Lodhi, L., Kumari, R., et al. (2019). Exposure to ultrafine particulate matter induces NF-κβ mediated epigenetic modifications. *Environ. Pollut.* 252, 39–50. doi:10.1016/j.envpol.2019.05.065

Bluestone, J. A., Mackay, C. R., O'Shea, J. J., and Stockinger, B. (2009). The functional plasticity of T cell subsets. *Nat. Rev. Immunol.* 9 (11), 811–816. doi:10.1038/nri2654

Boyce, P. D., Kim, J. Y., Weissman, D. N., Hunt, J., and Christiani, D. C. (2006). pH increase observed in exhaled breath condensate from welding fume exposure. *J. Occup. Environ. Med.* 48 (4), 353–356. doi:10.1097/01.jom.0000205988.50907.d8

Bronevetsky, Y., Villarino, A. V., Eisley, C. J., Barbeau, R., Barczak, A. J., Heinz, G. A., et al. (2013). T cell activation induces proteasomal degradation of Argonaute and rapid remodeling of the microRNA repertoire. *J. Exp. Med.* 210 (2), 417–432. doi:10.1084/jem.20111717

Chang, L., Chong, W. T., Wang, X., Pei, F., Zhang, X., Wang, T., et al. (2021). Recent progress in research on PM(2.5) in subways. *Environ. Sci. Process. Impacts* 23 (5), 642–663. doi:10.1039/d1em00002k

Chen, W., Lin, X., Huang, J., Tan, K., Chen, Y., Peng, W., et al. (2014). Integrated profiling of microRNA expression in membranous nephropathy using high-throughput sequencing technology. *Int. J. Mol. Med.* 33 (1), 25–34. doi:10.3892/ijmm.2013.1554

Cong, L. H., Li, T., Wang, H., Wu, Y. N., Wang, S. P., Zhao, Y. Y., et al. (2020). IL-17A-producing T cells exacerbate fine particulate matter-induced lung inflammation and fibrosis by inhibiting PI3K/Akt/mTOR-mediated autophagy. *J. Cell. Mol. Med.* 24 (15), 8532–8544. doi:10.1111/jcmm.15475

Conserva, F., Barozzino, M., Pesce, F., Divella, C., Oranger, A., Papale, M., et al. (2019). Urinary miRNA-27b-3p and miRNA-1228-3p correlate with the progression of kidney fibrosis in diabetic nephropathy. *Sci. Rep.* 9 (1), 11357. doi:10.1038/s41598-019-47778-1

Couser, W. G., Steinmuller, D. R., Stilmant, M. M., Salant, D. J., and Lowenstein, L. M. (1978). Experimental glomerulonephritis in the isolated perfused rat kidney. *J. Clin. Invest.* 62 (6), 1275–1287. doi:10.1172/JCI109248

Cremoni, M., Brglez, V., Perez, S., Decoupigny, F., Zorzi, K., Andreani, M., et al. (2020). Th17-Immune response in patients with membranous nephropathy is associated with thrombosis and relapses. *Front. Immunol.* 11, 574997. doi:10.3389/fimmu.2020.574997

Cua, D. J., Sherlock, J., Chen, Y., Murphy, C. A., Joyce, B., Seymour, B., et al. (2003). Interleukin-23 rather than interleukin-12 is the critical cytokine for autoimmune inflammation of the brain. *Nature* 421 (6924), 744–748. doi:10.1038/nature01355

Cui, Z., Xie, L. J., Chen, F. J., Pei, Z. Y., Zhang, L. J., Qu, Z., et al. (2017). MHC class II risk alleles and amino acid residues in idiopathic membranous nephropathy. *J. Am. Soc. Nephrol.* 28 (5), 1651–1664. doi:10.1681/ASN.2016020114

De Vriese, A. S., Glassock, R. J., Nath, K. A., Sethi, S., and Fervenza, F. C. (2017). A proposal for a serology-based approach to membranous nephropathy. *J. Am. Soc. Nephrol.* 28 (2), 421–430. doi:10.1681/ASN.2016070776

Disner, G. R., Lopes-Ferreira, M., and Lima, C. (2021). Where the aryl hydrocarbon receptor meets the microRNAs: Literature review of the last 10 years. *Front. Mol. Biosci.* 8, 725044. doi:10.3389/fmolb.2021.725044

Donate, P. B., Alves de Lima, K., Peres, R. S., Almeida, F., Fukada, S. Y., Silva, T. A., et al. (2021). Cigarette smoke induces miR-132 in Th17 cells that enhance osteoclastogenesis in inflammatory arthritis. *Proc. Natl. Acad. Sci. U. S. A.* 118 (1), e2017120118. doi:10.1073/pnas.2017120118

Dong, Y., Cao, L., Tang, H., Shi, X., and He, Y. (2017). Structure of human M-type phospholipase A2 receptor revealed by cryo-electron microscopy. *J. Mol. Biol.* 429 (24), 3825–3835. doi:10.1016/j.jmb.2017.10.019

Du, Y., Li, J., He, F., Lv, Y., Liu, W., Wu, P., et al. (2014). The diagnosis accuracy of pla2r-AB in the diagnosis of idiopathic membranous nephropathy: A meta-analysis. *PLoS One* 9 (8), e104936. doi:10.1371/journal.pone.0104936

Duan, J. W., Li, Y. L., Li, S. X., Yang, Y. P., Li, F., Li, Y., et al. (2022). Association of long-term ambient fine particulate matter ($PM_{2.5}$) and incident CKD: A prospective cohort study in China. *Am. J. Kidney Dis.* S0272-6386(22), 00623–0. doi:10.1053/j.ajkd.2022.03.009

East, L., and Isacke, C. M. (2002). The mannose receptor family. *Biochim. Biophys. Acta* 1572 (2-3), 364–386. doi:10.1016/s0304-4165(02)00319-7

Ebert, M. S., and Sharp, P. A. (2012). Roles for microRNAs in conferring robustness to biological processes. *Cell.* 149 (3), 515–524. doi:10.1016/j.cell.2012.04.005

Falcon-Rodriguez, C. I., Osornio-Vargas, A. R., Sada-Ovalle, I., and Segura-Medina, P. (2016). Aeroparticles, composition, and lung diseases. *Front. Immunol.* 7, 3. doi:10.3389/fimmu.2016.00003

Fogo, A. B., Lusco, M. A., Najafian, B., and Alpers, C. E. (2015). AJKD atlas of renal pathology: Membranous nephropathy. *Am. J. Kidney Dis.* 66 (3), e15–7. doi:10.1053/j.ajkd.2015.07.006

Fossati, S., Baccarelli, A., Zanobetti, A., Hoxha, M., Vokonas, P. S., Wright, R. O., et al. (2014). Ambient particulate air pollution and microRNAs in elderly men. *Epidemiology* 25 (1), 68–78. doi:10.1097/EDE.0000000000000026

Fresquet, M., Jowitt, T. A., Gummadova, J., Collins, R., O'Cualain, R., McKenzie, E. A., et al. (2015). Identification of a major epitope recognized by PLA2R autoantibodies in primary membranous nephropathy. *J. Am. Soc. Nephrol.* 26 (2), 302–313. doi:10.1681/ASN.2014050502

Fu, H., Liu, X., Li, W., Zu, Y., Zhou, F., Shou, Q., et al. (2020). PM2.5 exposure induces inflammatory response in macrophages via the TLR4/COX-2/NF-κB pathway. *Inflammation* 43 (5), 1948–1958. doi:10.1007/s10753-020-01269-y

Gao, Y., Zhang, Q., Sun, J., Liang, Y., Zhang, M., Zhao, M., et al. (2022). Extracellular vesicles derived from PM2.5-exposed alveolar epithelial cells mediate endothelial adhesion and atherosclerosis in ApoE(-/-) mice. *Faseb J.* 36 (2), e22161. doi:10.1096/fj.202100927RR

Greenwell, L. L., Moreno, T., Jones, T. P., and Richards, R. J. (2002). Particle-induced oxidative damage is ameliorated by pulmonary antioxidants. *Free Radic. Biol. Med.* 32 (9), 898–905. doi:10.1016/s0891-5849(02)00782-7

Gu, X. Y., Chu, X., Zeng, X. L., Bao, H. R., and Liu, X. J. (2017). Effects of PM2.5 exposure on the Notch signaling pathway and immune imbalance in chronic obstructive pulmonary disease. *Environ. Pollut.* 226, 163–173. doi:10.1016/j.envpol.2017.03.070

Guo, S., Hao, H., Li, S., Zhang, L., and Li, R. (2022). Differential expression of urinary exosomal miRNA in idiopathic membranous nephropathy and evaluation of its diagnostic value. *Tohoku J. Exp. Med.* 256 (4), 327–336. doi:10.1620/tjem.2022.J002

Gupta, S., Kottgen, A., Hoxha, E., Brenchley, P., Bockenhauer, D., Stanescu, H. C., et al. (2018). Genetics of membranous nephropathy. *Nephrol. Dial. Transpl.* 33 (9), 1493–1502. doi:10.1093/ndt/gfx296

Hamidzadeh, K., Christensen, S. M., Dalby, E., Chandrasekaran, P., and Mosser, D. M. (2017). Macrophages and the recovery from acute and chronic inflammation. *Annu. Rev. Physiol.* 79, 567–592. doi:10.1146/annurev-physiol-022516-034348

Hejazian, S. M., Ardalan, M., Shoja, M. M., Samadi, N., and Zununi Vahed, S. (2020). Expression levels of miR-30c and miR-186 in adult patients with membranous glomerulonephritis and focal segmental glomerulosclerosis. *Int. J. Nephrol. Renov. Dis.* 13, 193–201. doi:10.2147/IJNRD.S258624

Heymann, W., Hackel, D. B., Harwood, S., Wilson, S. G., and Hunter, J. L. (1959). Production of nephrotic syndrome in rats by Freund's adjuvants and rat kidney suspensions. *Proc. Soc. Exp. Biol. Med.* 100 (4), 660–664. doi:10.3181/00379727-100-24736

Hilligan, K. L., and Ronchese, F. (2020). Antigen presentation by dendritic cells and their instruction of CD4+ T helper cell responses. *Cell. Mol. Immunol.* 17 (6), 587–599. doi:10.1038/s41423-020-0465-0

Hirayama, K., Ebihara, I., Yamamoto, S., Kai, H., Muro, K., Yamagata, K., et al. (2002). Predominance of type-2 immune response in idiopathic membranous nephropathy. Cytoplasmic cytokine analysis. *Nephron* 91 (2), 255–261. doi:10.1159/000058401

Honda, A., Fukushima, W., Oishi, M., Tsuji, K., Sawahara, T., Hayashi, T., et al. (2017). Effects of components of PM(2.5) collected in Japan on the respiratory and immune systems. *Int. J. Toxicol.* 36 (2), 153–164. doi:10.1177/1091581816682224

Honda, A., Okuda, T., Nagao, M., Miyasaka, N., Tanaka, M., and Takano, H. (2021). PM2.5 collected using cyclonic separation causes stronger biological responses than that collected using a conventional filtration method. *Environ. Res.* 198, 110490. doi:10.1016/j.envres.2020.110490

Hou, T., Chen, Q., and Ma, Y. (2021). Elevated expression of miR-146 involved in regulating mice pulmonary dysfunction after exposure to PM2.5. *J. Toxicol. Sci.* 46 (10), 437–443. doi:10.2131/jts.46.437

Hou, T., Liao, J., Zhang, C., Sun, C., Li, X., and Wang, G. (2018). Elevated expression of miR-146, miR-139 and miR-340 involved in regulating Th1/Th2 balance with acute exposure of fine particulate matter in mice. *Int. Immunopharmacol.* 54, 68–77. doi:10.1016/j.intimp.2017.10.003

Hou, Y., Li, Y., Wang, Y., Li, W., and Xiao, Z. (2021). Screening and analysis of key genes in miRNA-mRNA regulatory network of membranous nephropathy. *J. Healthc. Eng.* 2021, 5331948. doi:10.1155/2021/5331948

Hu, R., Quan, S., Wang, Y., Zhou, Y., Zhang, Y., Liu, L., et al. (2020). Spectrum of biopsy proven renal diseases in central China: A 10-year retrospective study based on 34, 630 cases. *Sci. Rep.* 10 (1), 10994. doi:10.1038/s41598-020-67910-w

Ifuku, M., Miyake, K., Watanebe, M., Ito, K., Abe, Y., Sasatomi, Y., et al. (2013). Various roles of Th cytokine mRNA expression in different forms of glomerulonephritis. *Am. J. Nephrol.* 38 (2), 115–123. doi:10.1159/000353102

Iliopoulos, D., Hirsch, H. A., and Struhl, K. (2009). An epigenetic switch involving NF-kappaB, Lin28, Let-7 MicroRNA, and IL6 links inflammation to cell transformation. *Cell.* 139 (4), 693–706. doi:10.1016/j.cell.2009.10.014

Iorio, M. V., Piovan, C., and Croce, C. M. (2010). Interplay between microRNAs and the epigenetic machinery: An intricate network. *Biochim. Biophys. Acta* 1799 (10-12), 694–701. doi:10.1016/j.bbagrm.2010.05.005

Izzotti, A., and Pulliero, A. (2014). The effects of environmental chemical carcinogens on the microRNA machinery. *Int. J. Hyg. Environ. Health* 217 (6), 601–627. doi:10.1016/j.ijheh.2014.01.001

Jeong, S., Park, S. A., Park, I., Kim, P., Cho, N. H., Hyun, J. W., et al. (2019). PM2.5 exposure in the respiratory system induces distinct inflammatory signaling in the lung and the liver of mice. *J. Immunol. Res.* 2019, 3486841. doi:10.1155/2019/3486841

Jia, S., Yang, X., Yang, X., and Zhang, F. (2020). MicroRNA-210 protects against periodontitis through targeting HIF-3α and inhibiting p38MAPK/NF-κB pathway. *Artif. Cells Nanomed. Biotechnol.* 48 (1), 129–136. doi:10.1080/21691401.2019.1699818

Jiang, P., Hao, S., Xie, L., Xiang, G., Hu, W., Wu, Q., et al. (2021). LncRNA NEAT1 contributes to the acquisition of a tumor like-phenotype induced by PM 2.5 in lung bronchial epithelial cells via HIF-1α activation. *Environ. Sci. Pollut. Res. Int.* 28 (32), 43382–43393. doi:10.1007/s11356-021-13735-7

Jin, L. W., Pan, M., Ye, H. Y., Zheng, Y., Chen, Y., Huang, W. W., et al. (2019). Down-regulation of the long non-coding RNA XIST ameliorates podocyte apoptosis in membranous nephropathy via the miR-217-TLR4 pathway. *Exp. Physiol.* 104 (2), 220–230. doi:10.1113/EP087190

Jin, X., Wang, L., and Yang, M. (2021). circ_0038467 promotes PM2.5-induced bronchial epithelial cell dysfunction. *Open Med.* 16 (1), 854–863. doi:10.1515/med-2021-0213

Karshovska, E., Wei, Y., Subramanian, P., Mohibullah, R., GeiBler, C., Baatsch, I., et al. (2020). HIF-1α (Hypoxia-Inducible factor-1α) promotes macrophage

necroptosis by regulating miR-210 and miR-383. *Arterioscler. Thromb. Vasc. Biol.* 40 (3), 583–596. doi:10.1161/ATVBAHA.119.313290

Krauskopf, J., Caiment, F., van Veldhoven, K., Chadeau-Hyam, M., Sinharay, R., Chung, K. F., et al. (2018). The human circulating miRNome reflects multiple organ disease risks in association with short-term exposure to traffic-related air pollution. *Environ. Int.* 113, 26–34. doi:10.1016/j.envint.2018.01.014

Krauskopf, J., de Kok, T. M., Hebels, D. G., Bergdahl, I. A., Johansson, A., Spaeth, F., et al. (2017). MicroRNA profile for health risk assessment: Environmental exposure to persistent organic pollutants strongly affects the human blood microRNA machinery. *Sci. Rep.* 7 (1), 9262. doi:10.1038/s41598-017-10167-7

Kryczek, I., Bruce, A. T., Gudjonsson, J. E., Johnston, A., Aphale, A., Vatan, L., et al. (2008). Induction of IL-17+ T cell trafficking and development by IFN-gamma: Mechanism and pathological relevance in psoriasis. *J. Immunol.* 181 (7), 4733–4741. doi:10.4049/jimmunol.181.7.4733

Ku, T., Li, B., Gao, R., Zhang, Y., Yan, W., Ji, X., et al. (2017). NF-κB-regulated microRNA-574-5p underlies synaptic and cognitive impairment in response to atmospheric PM(2.5) aspiration. *Part. Fibre Toxicol.* 14 (1), 34. doi:10.1186/s12989-017-0215-3

Kuroda, E., Ozasa, K., Temizoz, B., Ohata, K., Koo, C. X., Kanuma, T., et al. (2016). Inhaled fine particles induce alveolar macrophage death and interleukin-1α release to promote inducible bronchus-associated lymphoid tissue formation. *Immunity* 45 (6), 1299–1310. doi:10.1016/j.immuni.2016.11.010

Kuroki, A., Iyoda, M., Shibata, T., and Sugisaki, T. (2005). Th2 cytokines increase and stimulate B cells to produce IgG4 in idiopathic membranous nephropathy. *Kidney Int.* 68 (1), 302–310. doi:10.1111/j.1523-1755.2005.00415.x

Lai, W. L., Yeh, T. H., Chen, P. M., Chan, C. K., Chiang, W. C., Chen, Y. M., et al. (2015). Membranous nephropathy: A review on the pathogenesis, diagnosis, and treatment. *J. Formos. Med. Assoc.* 114 (2), 102–111. doi:10.1016/j.jfma.2014.11.002

Lee, S. Y., Lee, S. H., Seo, H. B., Ryu, J. G., Jung, K., and Choi, J. W. (2019). Inhibition of IL-17 ameliorates systemic lupus erythematosus in Roquin(san/san) mice through regulating the balance of TFH cells, GC B cells, Treg and Breg. *Sci. Rep.* 9 (1), 5227. doi:10.1038/s41598-019-41534-1

Li, D., Lu, Z., Jia, J., Zheng, Z., and Lin, S. (2013). Changes in microRNAs associated with podocytic adhesion damage under mechanical stress. *J. Renin. Angiotensin. Aldosterone. Syst.* 14 (2), 97–102. doi:10.1177/1470320312460071

Li, H., Wu, H., Guo, Q., Yu, H., Xu, Y., Yu, J., et al. (2020). Myeloid-derived suppressor cells promote the progression of primary membranous nephropathy by enhancing Th17 response. *Front. Immunol.* 11, 1777. doi:10.3389/fimmu.2020.01777

Li, J., Chen, Y., Shen, L., and Deng, Y. (2019). Improvement of membranous nephropathy by inhibition of miR-193a to affect podocytosis via targeting WT1. *J. Cell. Biochem.* 120 (3), 3438–3446. doi:10.1002/jcb.27616

Li, J., Cui, Z., Long, J., Huang, W., Wang, J., Zhang, H., et al. (2018b). Primary glomerular nephropathy among hospitalized patients in a national database in China. *Nephrol. Dial. Transpl.* 33 (12), 2173–2181. doi:10.1093/ndt/gfy022

Li, J., Liu, B., Xue, H., Zhou, Q. Q., and Peng, L. (2017). miR-217 is a useful diagnostic biomarker and regulates human podocyte cells apoptosis via targeting TNFSF11 in membranous nephropathy. *Biomed. Res. Int.* 2017, 2168767. doi:10.1155/2017/2168767

Li, J., Wang, J., Li, Y., Zhao, P., Tian, Y., Liu, X., et al. (2021). Effective-component compatibility of Bufei Yishen formula protects COPD rats against PM2.5-induced oxidative stress via miR-155/FOXO3a pathway. *Ecotoxicol. Environ. Saf.* 228, 112918. doi:10.1016/j.ecoenv.2021.112918

Li, J., Zhou, Q., Liang, Y., Pan, W., Bei, Y., Zhang, Y., et al. (2018a). miR-486 inhibits PM2.5-induced apoptosis and oxidative stress in human lung alveolar epithelial A549 cells. *Ann. Transl. Med.* 6 (11), 209. doi:10.21037/atm.2018.06.09

Li, P., Wang, J., Guo, F., Zheng, B., and Zhang, X. (2020). A novel inhibitory role of microRNA-224 in particulate matter 2.5-induced asthmatic mice by inhibiting TLR2. *J. Cell. Mol. Med.* 24 (5), 3040–3052. doi:10.1111/jcmm.14940

Li, P., Zhong, X., Zhang, L., Yu, Y., and Niu, J. (2021). Bioinformatic investigation for candidate genes and molecular mechanism in the pathogenesis of membranous nephropathy. *Nephrol. Carlt.* 26 (3), 262–269. doi:10.1111/nep.13833

Li, Q., Li, S., Xu, C., Zhao, J., Hou, L., Jiang, F., et al. (2021). microRNA-149-5p mediates the PM(2.5)-induced inflammatory response by targeting TAB2 via MAPK and NF-κB signaling pathways *in vivo* and *in vitro*. *Cell. Biol. Toxicol.* doi:10.1007/s10565-021-09638-5

Liang, S., Ning, R., Zhang, J., Liu, J., Zhang, J., Shen, H., et al. (2021). MiR-939-5p suppresses PM(2.5)-induced endothelial injury via targeting HIF-1α in HAECs. *Nanotoxicology* 15 (5), 706–720. doi:10.1080/17435390.2021.1917716

Lin, C. H., Tseng, C. Y., and Chao, M. W. (2020). Administration of Lactobacillus paracasei HB89 mitigates PM2.5-induced enhancement of inflammation and allergic airway response in murine asthma model. *PLoS One* 15 (12), e0243062. doi:10.1371/journal.pone.0243062

Lin, Z., Chen, P., Yuan, Z., Yang, L., Miao, L., Wang, H., et al. (2022). Fine particulate matter, airway inflammation, stress response, non-specific immune function and buccal microbial diversity in young adults. *Environ. Pollut.* 308, 119692. doi:10.1016/j.envpol.2022.119692

Liu, C., Guo, H., Cheng, X., Shao, M., Wu, C., Wang, S., et al. (2015b). Exposure to airborne PM2.5 suppresses microRNA expression and deregulates target oncogenes that cause neoplastic transformation in NIH3T3 cells. *Oncotarget* 6 (30), 29428–29439. doi:10.18632/oncotarget.5005

Liu, C., Xu, J., Chen, Y., Guo, X., Zheng, Y., Wang, Q., et al. (2015a). Characterization of genome-wide H3K27ac profiles reveals a distinct PM2.5-associated histone modification signature. *Environ. Health* 14, 65. doi:10.1186/s12940-015-0052-5

Liu, D., Liu, F., Wang, X., Qiao, Y., Pan, S., Yang, Y., et al. (2018). MiR-130a-5p prevents angiotensin II-induced podocyte apoptosis by modulating M-type phospholipase A2 receptor. *Cell. Cycle* 17 (21-22), 2484–2495. doi:10.1080/15384101.2018.1542901

Liu, L. Z., Wang, M., Xin, Q., Wang, B., Chen, G. G., and Li, M. Y. (2020). The permissive role of TCTP in PM(2.5)/NNK-induced epithelial-mesenchymal transition in lung cells. *J. Transl. Med.* 18 (1), 66. doi:10.1186/s12967-020-02256-5

Liu, W., Gao, C., Dai, H., Zheng, Y., Dong, Z., Gao, Y., et al. (2019). Immunological pathogenesis of membranous nephropathy: Focus on PLA2R1 and its role. *Front. Immunol.* 10, 1809. doi:10.3389/fimmu.2019.01809

Longhin, E., Capasso, L., Battaglia, C., Proverbio, M. C., Cosentino, C., Cifola, I., et al. (2016). Integrative transcriptomic and protein analysis of human bronchial BEAS-2B exposed to seasonal urban particulate matter. *Environ. Pollut.* 209, 87–98. doi:10.1016/j.envpol.2015.11.013

Ma, D. H., Yang, X. D., Hua, Q. J., Hou, Y. L., Liu, Y., Xu, Q. Y., et al. (2021). Changes and significance of Treg and Th17 in adult patients with primary membranous nephropathy. *Clin. Nephrol.* 96 (3), 155–164. doi:10.5414/CN110333

Ma, Q. Y., Huang, D. Y., Zhang, H. J., Wang, S., and Chen, X. F. (2017). Exposure to particulate matter 2.5 (PM2.5) induced macrophage-dependent inflammation, characterized by increased Th1/Th17 cytokine secretion and cytotoxicity. *Int. Immunopharmacol.* 50, 139–145. doi:10.1016/j.intimp.2017.06.019

Masutani, K., Taniguchi, M., Nakashima, H., Yotsueda, H., Kudoh, Y., Tsuruya, K., et al. (2004). Up-regulated interleukin-4 production by peripheral T-helper cells in idiopathic membranous nephropathy. *Nephrol. Dial. Transpl.* 19 (3), 580–586. doi:10.1093/ndt/gfg572

Mehta, M., Chen, L. C., Gordon, T., Rom, W., and Tang, M. S. (2008). Particulate matter inhibits DNA repair and enhances mutagenesis. *Mutat. Res.* 657 (2), 116–121. doi:10.1016/j.mrgentox.2008.08.015

Mendell, J. T., and Olson, E. N. (2012). MicroRNAs in stress signaling and human disease. *Cell.* 148 (6), 1172–1187. doi:10.1016/j.cell.2012.02.005

Motavalli, R., Etemadi, J., Soltani-Zangbar, M. S., Ardalan, M. R., Kahroba, H., Roshangar, L., et al. (2021). Altered Th17/Treg ratio as a possible mechanism in pathogenesis of idiopathic membranous nephropathy. *Cytokine* 141, 155452. doi:10.1016/j.cyto.2021.155452

Müller-Deile, J., Dannenberg, J., Schroder, P., Lin, M. H., Miner, J. H., Chen, R., et al. (2017). Podocytes regulate the glomerular basement membrane protein nephronectin by means of miR-378a-3p in glomerular diseases. *Kidney Int.* 92 (4), 836–849. doi:10.1016/j.kint.2017.03.005

Müller-Deile, J., Sopel, N., Ohs, A., Rose, V., Groner, M., Wrede, C., et al. (2021). Glomerular endothelial cell-derived microRNA-192 regulates nephronectin expression in idiopathic membranous glomerulonephritis. *J. Am. Soc. Nephrol.* 32 (11), 2777–2794. doi:10.1681/ASN.2020121699

Murphy, C. A., Langrish, C. L., Chen, Y., Blumenschein, W., McClanahan, T., Kastelein, R. A., et al. (2003). Divergent pro- and antiinflammatory roles for IL-23 and IL-12 in joint autoimmune inflammation. *J. Exp. Med.* 198 (12), 1951–1957. doi:10.1084/jem.20030896

Nemmar, A., Al-Salam, S., Zia, S., Yasin, J., Al Husseni, I., and Ali, B. H. (2010). Diesel exhaust particles in the lung aggravate experimental acute renal failure. *Toxicol. Sci.* 113 (1), 267–277. doi:10.1093/toxsci/kfp222

Nolin, J. D., Ogden, H. L., Lai, Y., Altemeier, W. A., Frevert, C. W., Bollinger, J. G., et al. (2016). Identification of epithelial phospholipase A(2) receptor 1 as a potential target in asthma. *Am. J. Respir. Cell. Mol. Biol.* 55 (6), 825–836. doi:10.1165/rcmb.2015-0150OC

O'Brien, J., Hayder, H., Zayed, Y., and Peng, C. (2018). Overview of MicroRNA biogenesis, mechanisms of actions, and circulation. *Front. Endocrinol.* 9, 402. doi:10.3389/fendo.2018.00402

Openshaw, P., Murphy, E. E., Hosken, N. A., Maino, V., Davis, K., Murphy, K., et al. (1995). Heterogeneity of intracellular cytokine synthesis at the single-cell level in polarized T helper 1 and T helper 2 populations. *J. Exp. Med.* 182 (5), 1357–1367. doi:10.1084/jem.182.5.1357

Pang, L., Zou, S., Shi, Y., Mao, Q., and Chen, Y. (2019). Apigenin attenuates PM2.5-induced airway hyperresponsiveness and inflammation by down-regulating NF-κB in murine model of asthma. *Int. J. Clin. Exp. Pathol.* 12 (10), 3700–3709.

Pasqualotto, A., Ayres, R., Longo, L., Del Duca Lima, D., Losch de Oliveira, D., Alvares-da-Silva, M. R., et al. (2021). Chronic exposure to ethanol alters the expression of miR-155, miR-122 and miR-217 in alcoholic liver disease in an adult zebrafish model. *Biomarkers.* 26 (2), 146–151. doi:10.1080/1354750X.2021.1874051

Pawluczyk, I. Z. A., Didangelos, A., Barbour, S. J., Er, L., Becker, J. U., Martin, R., et al. (2021). Differential expression of microRNA miR-150-5p in IgA nephropathy as a potential mediator and marker of disease progression. *Kidney Int.* 99 (5), 1127–1139. doi:10.1016/j.kint.2020.12.028

Pei, Y. H., Chen, J., Wu, X., He, Y., Qin, W., He, S. Y., et al. (2020). LncRNA PEAMIR inhibits apoptosis and inflammatory response in PM2.5 exposure aggravated myocardial ischemia/reperfusion injury as a competing endogenous RNA of miR-29b-3p. *Nanotoxicology* 14 (5), 638–653. doi:10.1080/17435390.2020.1731857

Perrone, M. G., GualtieriM.Consonni, V., Ferrero, L., SanGiorGi, G., Longhin, E., et al. (2013). Particle size, chemical composition, seasons of the year and urban, rural or remote site origins as determinants of biological effects of particulate matter on pulmonary cells. *Environ. Pollut.* 176, 215–227. doi:10.1016/j.envpol.2013.01.012

Piletič, K., and Kunej, T. (2016). MicroRNA epigenetic signatures in human disease. *Arch. Toxicol.* 90 (10), 2405–2419. doi:10.1007/s00204-016-1815-7

Rodosthenous, R. S., Coull, B. A., Lu, Q., Vokonas, P. S., Schwartz, J. D., and Baccarelli, A. A. (2016). Ambient particulate matter and microRNAs in extracellular vesicles: A pilot study of older individuals. *Part. Fibre Toxicol.* 13, 13. doi:10.1186/s12989-016-0121-0

Ronco, P., and Debiec, H. (2012). Pathogenesis of membranous nephropathy: Recent advances and future challenges. *Nat. Rev. Nephrol.* 8 (4), 203–213. doi:10.1038/nrneph.2012.35

Rosenzwajg, M., Languille, E., Debiec, H., Hygino, J., Dahan, K., Simon, T., et al. (2017). B- and T-cell subpopulations in patients with severe idiopathic membranous nephropathy may predict an early response to rituximab. *Kidney Int.* 92 (1), 227–237. doi:10.1016/j.kint.2017.01.012

Rudnicki, M., Perco, P., D Haene, B., Leierer, J., Heinzel, A., Muhlberger, I., et al. (2016). Renal microRNA- and RNA-profiles in progressive chronic kidney disease. *Eur. J. Clin. Invest.* 46 (3), 213–226. doi:10.1111/eci.12585

Rui, W., Guan, L., Zhang, F., Zhang, W., and Ding, W. (2016). PM2.5-induced oxidative stress increases adhesion molecules expression in human endothelial cells through the ERK/AKT/NF-κB-dependent pathway. *J. Appl. Toxicol.* 36 (1), 48–59. doi:10.1002/jat.3143

Saint-Georges, F., Abbas, I., Billet, S., Verdin, A., Gosset, P., Mulliez, P., et al. (2008). Gene expression induction of volatile organic compound and/or polycyclic aromatic hydrocarbon-metabolizing enzymes in isolated human alveolar macrophages in response to airborne particulate matter (PM2.5). *Toxicology* 244 (2-3), 220–230. doi:10.1016/j.tox.2007.11.016

Seitz-Polski, B., Dolla, G., Payre, C., Girard, C. A., Polidori, J., Zorzi, K., et al. (2016). Epitope spreading of autoantibody response to PLA2R associates with poor prognosis in membranous nephropathy. *J. Am. Soc. Nephrol.* 27 (5), 1517–1533. doi:10.1681/ASN.2014111061

Sethi, S., Debiec, H., Madden, B., Charlesworth, M. C., Morelle, J., Gross, L., et al. (2020). Neural epidermal growth factor-like 1 protein (NELL-1) associated membranous nephropathy. *Kidney Int.* 97 (1), 163–174. doi:10.1016/j.kint.2019.09.014

Sethi, S., Madden, B. J., Debiec, H., Charlesworth, M. C., Gross, L., Ravindran, A., et al. (2019). Exostosin 1/exostosin 2-associated membranous nephropathy. *J. Am. Soc. Nephrol.* 30 (6), 1123–1136. doi:10.1681/ASN.2018080852

Sha, W. G., Shen, L., Zhou, L., Xu, D. y., and Lu, G. y. (2015). Down-regulation of miR-186 contributes to podocytes apoptosis in membranous nephropathy. *Biomed. Pharmacother.* 75, 179–184. doi:10.1016/j.biopha.2015.07.021

Shi, L. Z., Wang, R., Huang, G., Vogel, P., Neale, G., Green, D. R., et al. (2011). HIF1alpha-dependent glycolytic pathway orchestrates a metabolic checkpoint for the differentiation of TH17 and Treg cells. *J. Exp. Med.* 208 (7), 1367–1376. doi:10.1084/jem.20110278

Sigaux, J., Biton, J., Andre, E., Semerano, L., and Boissier, M. C. (2019). Air pollution as a determinant of rheumatoid arthritis. *Jt. Bone Spine* 86 (1), 37–42. doi:10.1016/j.jbspin.2018.03.001

Song, B., Ye, L., Wu, S., and Jing, Z. (2020). Long non-coding RNA MEG3 regulates CSE-induced apoptosis and inflammation via regulating miR-218 in 16HBE cells. *Biochem. Biophys. Res. Commun.* 521 (2), 368–374. doi:10.1016/j.bbrc.2019.10.135

Song, L., Li, D., Gu, Y., Li, X., and Peng, L. (2016). Let-7a modulates particulate matter (≤ 2.5 μm)-induced oxidative stress and injury in human airway epithelial cells by targeting arginase 2. *J. Appl. Toxicol.* 36 (10), 1302–1310. doi:10.1002/jat.3309

Song, L., Li, D., Li, X., Ma, L., Bai, X., Wen, Z., et al. (2017). Exposure to PM2.5 induces aberrant activation of NF-κB in human airway epithelial cells by downregulating miR-331 expression. *Environ. Toxicol. Pharmacol.* 50, 192–199. doi:10.1016/j.etap.2017.02.011

Stahl, R., Hoxha, E., and Fechner, K. (2010). PLA2R autoantibodies and recurrent membranous nephropathy after transplantation. *N. Engl. J. Med.* 363 (5), 496–498. doi:10.1056/NEJMc1003066

Stanescu, H. C., Arcos-Burgos, M., Medlar, A., Bockenhauer, D., Kottgen, A., Dragomirescu, L., et al. (2011). Risk HLA-DQA1 and PLA(2)R1 alleles in idiopathic membranous nephropathy. *N. Engl. J. Med.* 364 (7), 616–626. doi:10.1056/NEJMoa1009742

Strom, T. B., and Koulmanda, M. (2009). Recently discovered T cell subsets cannot keep their commitments. *J. Am. Soc. Nephrol.* 20 (8), 1677–1680. doi:10.1681/ASN.2008101027

Sukocheva, O., Menschikowski, M., Hagelgans, A., Yarla, N. S., Siegert, G., Reddanna, P., et al. (2019). Current insights into functions of phospholipase A2 receptor in normal and cancer cells: More questions than answers. *Semin. Cancer Biol.* 56, 116–127. doi:10.1016/j.semcancer.2017.11.002

Sun, I. O., Bae, Y. U., Lee, H., Kim, H., Jeon, J. S., Noh, H., et al. (2022). Circulating miRNAs in extracellular vesicles related to treatment response in patients with idiopathic membranous nephropathy. *J. Transl. Med.* 20 (1), 224. doi:10.1186/s12967-022-03430-7

Sun, L., Fu, J., Lin, S. H., Sun, J. L., Xia, L., Lin, C. H., et al. (2020). Particulate matter of 2.5 μm or less in diameter disturbs the balance of T(H)17/regulatory T cells by targeting glutamate oxaloacetate transaminase 1 and hypoxia-inducible factor 1α in an asthma model. *J. Allergy Clin. Immunol.* 145 (1), 402–414. doi:10.1016/j.jaci.2019.10.008

Sun, L., Fu, J., and Zhou, Y. (2017). Metabolism controls the balance of Th17/T-regulatory cells. *Front. Immunol.* 8, 1632. doi:10.3389/fimmu.2017.01632

Sun, Y., Koo, S., White, N., Peralta, E., Esau, C., Dean, N. M., et al. (2004). Development of a micro-array to detect human and mouse microRNAs and characterization of expression in human organs. *Nucleic Acids Res.* 32 (22), e188. doi:10.1093/nar/gnh186

Sun, Z., Xu, Q., Ma, Y., Yang, S., and Shi, J. (2021). Circ_0000524/miR-500a-5p/CXCL16 axis promotes podocyte apoptosis in membranous nephropathy. *Eur. J. Clin. Invest.* 51 (3), e13414. doi:10.1111/eci.13414

Tomas, N. M., Beck, L. H., Meyer-Schwesinger, C., Seitz-Polski, B., Ma, H., Zahner, G., et al. (2014). Thrombospondin type-1 domain-containing 7A in idiopathic membranous nephropathy. *N. Engl. J. Med.* 371 (24), 2277–2287. doi:10.1056/NEJMoa1409354

van de Logt, A. E., Hofstra, J. M., and Wetzels, J. F. (2015). Serum anti-pla2r antibodies can be initially absent in idiopathic membranous nephropathy: Seroconversion after prolonged follow-up. *Kidney Int.* 87 (6), 1263–1264. doi:10.1038/ki.2015.34

von Haxthausen, F., Reinhard, L., Pinnschmidt, H. O., Rink, M., Soave, A., Hoxha, E., et al. (2018). Antigen-specific IgG subclasses in primary and malignancy-associated membranous nephropathy. *Front. Immunol.* 9, 3035. doi:10.3389/fimmu.2018.03035

Wan, Q., Liu, Z., Yang, M., Deng, P., Tang, N., and Liu, Y. (2020). Triptolide ameliorates fine particulate matter-induced podocytes injury via regulating NF-κB signaling pathway. *BMC Mol. Cell. Biol.* 21 (1), 4. doi:10.1186/s12860-020-0248-6

Wang, J. C., Huang, Y., Zhang, R. X., Han, Z. J., Zhou, L. L., Sun, N., et al. (2021). miR-338-3p inhibits autophagy in a rat model of allergic rhinitis after PM2.5 exposure through AKT/mTOR signaling by targeting UBE2Q1. *Biochem. Biophys. Res. Commun.* 554, 1–6. doi:10.1016/j.bbrc.2021.03.085

Wang, L., Lin, J., Yu, T., Zuo, Q., Shen, B., Zhang, H., et al. (2020). Identification of plasma miR-106a-5p and miR-30a-5p as potential biomarkers for mesangial proliferative glomerulonephritis. *Clin. Biochem.* 84, 79–86. doi:10.1016/j.clinbiochem.2020.07.001

Wang, L., Xu, J., Liu, H., Li, J., and Hao, H. (2019). PM2.5 inhibits SOD1 expression by up-regulating microRNA-206 and promotes ROS accumulation and disease progression in asthmatic mice. *Int. Immunopharmacol.* 76, 105871. doi:10.1016/j.intimp.2019.105871

Wang, S., Lin, Y., Zhong, Y., Zhao, M., Yao, W., Ren, X., et al. (2020). The long noncoding RNA HCG18 participates in PM2.5-mediated vascular endothelial

barrier dysfunction. *Aging (Albany NY)* 12 (23), 23960–23973. doi:10.18632/aging.104073

Wang, Y., Zhong, Y., Sun, K., Fan, Y., Liao, J., and Wang, G. (2021). Identification of exosome miRNAs in bronchial epithelial cells after PM2.5 chronic exposure. *Ecotoxicol. Environ. Saf.* 215, 112127. doi:10.1016/j.ecoenv.2021.112127

Wang, Y., Zhong, Y., Zhang, C., Liao, J., and Wang, G. (2020). PM2.5 downregulates MicroRNA-139-5p and induces EMT in bronchiolar epithelium cells by targeting Notch1. *J. Cancer* 11 (19), 5758–5767. doi:10.7150/jca.46976

Wang, Y., Zou, L., Wu, T., Xiong, L., Zhang, T., Kong, L., et al. (2019). Identification of mRNA-miRNA crosstalk in human endothelial cells after exposure of PM2.5 through integrative transcriptome analysis. *Ecotoxicol. Environ. Saf.* 169, 863–873. doi:10.1016/j.ecoenv.2018.11.114

Wilker, E. H., Alexeeff, S. E., Suh, H., Vokonas, P. S., Baccarelli, A., and Schwartz, J. (2011). Ambient pollutants, polymorphisms associated with microRNA processing and adhesion molecules: The normative aging study. *Environ. Health* 10, 45. doi:10.1186/1476-069X-10-45

Wu, J., Zheng, C., Fan, Y., Zeng, C., Chen, Z., Qin, W., et al. (2014). Downregulation of microRNA-30 facilitates podocyte injury and is prevented by glucocorticoids. *J. Am. Soc. Nephrol.* 25 (1), 92–104. doi:10.1681/ASN.2012111101

Wu, L., Zhang, X., Luo, L., Li, X., Liu, Y., and Qin, X. (2021). Altered expression of serum miR-106a, miR-19b, miR-17, and PTEN in patients with idiopathic membranous nephropathy. *J. Clin. Lab. Anal.* 35 (4), e23737. doi:10.1002/jcla.23737

Wu, R., Zeng, J., Yuan, J., Deng, X., Huang, Y., Chen, L., et al. (2018). MicroRNA-210 overexpression promotes psoriasis-like inflammation by inducing Th1 and Th17 cell differentiation. *J. Clin. Invest.* 128 (6), 2551–2568. doi:10.1172/JCI97426

Xing, Y. F., Xu, Y. H., Shi, M. H., and Lian, Y. X. (2016). The impact of PM2.5 on the human respiratory system. *J. Thorac. Dis.* 8 (1), E69–E74. doi:10.3978/j.issn.2072-1439.2016.01.19

Xu, J., Shen, C., Lin, W., Meng, T., Ooi, J. D., Eggenhuizen, P. J., et al. (2021). Single-cell profiling reveals transcriptional signatures and cell-cell crosstalk in anti-pla2r positive idiopathic membranous nephropathy patients. *Front. Immunol.* 12, 683330. doi:10.3389/fimmu.2021.683330

Xu, X., Wang, G., Chen, N., Lu, T., Nie, S., Xu, G., et al. (2016). Long-term exposure to air pollution and increased risk of membranous nephropathy in China. *J. Am. Soc. Nephrol.* 27 (12), 3739–3746. doi:10.1681/ASN.2016010093

Yan, L., Liang, M., Hou, X., Zhang, Y., Zhang, H., Guo, Z., et al. (2019). The role of microRNA-16 in the pathogenesis of autoimmune diseases: A comprehensive review. *Biomed. Pharmacother.* 112, 108583. doi:10.1016/j.biopha.2019.01.044

Yang, D., Ma, M., Zhou, W., Yang, B., and Xiao, C. (2017). Inhibition of miR-32 activity promoted EMT induced by PM2.5 exposure through the modulation of the Smad1-mediated signaling pathways in lung cancer cells. *Chemosphere* 184, 289–298. doi:10.1016/j.chemosphere.2017.05.152

Yang, M., Ju, L., Li, C., Cheng, H., Li, N., Zhang, Q., et al. (2022). MiR-582-3p participates in the regulation of biological behaviors of A549 cells by ambient PM(2.5) exposure. *Environ. Sci. Pollut. Res. Int.* 29 (9), 13624–13634. doi:10.1007/s11356-021-16801-2

Yasuda, K., Takeuchi, Y., and Hirota, K. (2019). The pathogenicity of Th17 cells in autoimmune diseases. *Semin. Immunopathol.* 41 (3), 283–297. doi:10.1007/s00281-019-00733-8

Yu, Z., Koppelman, G. H., Boer, J. M. A., Hoek, G., Kerckhoffs, J., Vonk, J. M., et al. (2022). Ambient ultrafine particles and asthma onset until age 20: The PIAMA birth cohort. *Environ. Res.* 214, 113770. doi:10.1016/j.envres.2022.113770

Zhang, H., and Li, Z. (2019). microRNA-16 via Twist1 inhibits EMT induced by PM2.5 exposure in human hepatocellular carcinoma. *Open Med.* 14, 673–682. doi:10.1515/med-2019-0078

Zhang, J., Cui, J., Wang, Y., Lin, X., Teng, X., and Tang, Y. (2022). Complex molecular mechanism of ammonia-induced apoptosis in chicken peripheral blood lymphocytes: miR-27b-3p, heat shock proteins, immunosuppression, death receptor pathway, and mitochondrial pathway. *Ecotoxicol. Environ. Saf.* 236, 113471. doi:10.1016/j.ecoenv.2022.113471

Zhang, J., Fulgar, C. C., Mar, T., Young, D. E., Zhang, Q., Bein, K. J., et al. (2018). TH17-Induced neutrophils enhance the pulmonary allergic response following BALB/c exposure to house dust mite allergen and fine particulate matter from California and China. *Toxicol. Sci.* 164 (2), 627–643. doi:10.1093/toxsci/kfy127

Zhang, J., Zeng, X., Du, X., Pan, K., Song, L., Song, W., et al. (2019). Parental PM2.5 exposure-promoted development of metabolic syndrome in offspring is associated with the changes of immune microenvironment. *Toxicol. Sci.* 170 (2), 415–426. doi:10.1093/toxsci/kfz109

Zhang, J., Zhu, Y., Cai, R., Jin, J., and He, Q. (2020). Differential expression of urinary exosomal small RNAs in idiopathic membranous nephropathy. *Biomed. Res. Int.* 2020, 3170927. doi:10.1155/2020/3170927

Zhang, S., Gang, X., Yang, S., Cui, M., Sun, L., Li, Z., et al. (2021). The alterations in and the role of the Th17/treg balance in metabolic diseases. *Front. Immunol.* 12, 678355. doi:10.3389/fimmu.2021.678355

Zhang, X. D., Cui, Z., and Zhao, M. H. (2018). The genetic and environmental factors of primary membranous nephropathy: An overview from China. *Kidney Dis.* 4 (2), 65–73. doi:10.1159/000487136

Zheng, X. Y., Tong, L., Shen, D., Yu, J. E., Hu, Z. Q., Li, Y. J., et al. (2020). Airborne bacteria enriched PM2.5 enhances the inflammation in an allergic adolescent mouse model induced by ovalbumin. *Inflammation* 43 (1), 32–43. doi:10.1007/s10753-019-01071-5

Zhong, Y., Liao, J., Hu, Y., Wang, Y., Sun, C., Zhang, C., et al. (2019). PM(2.5) upregulates MicroRNA-146a-3p and induces M1 polarization in RAW264.7 cells by targeting Sirtuin1. *Int. J. Med. Sci.* 16 (3), 384–393. doi:10.7150/ijms.30084

Zhou, B., Wang, S., Mayr, C., Bartel, D. P., and Lodish, H. F. (2007). miR-150, a microRNA expressed in mature B and T cells, blocks early B cell development when expressed prematurely. *Proc. Natl. Acad. Sci. U. S. A.* 104 (17), 7080–7085. doi:10.1073/pnas.0702409104

Zhou, G., Jiang, N., Zhang, W., Guo, S., and Xin, G. (2021). Biomarker identification in membranous nephropathy using a long non-coding RNA-mediated competitive endogenous RNA network. *Interdiscip. Sci.* 13 (4), 615–623. doi:10.1007/s12539-021-00466-z

Zhou, G., Zhang, X., Wang, W., Zhang, W., Wang, H., and Xin, G. (2019). Both peripheral blood and urinary miR-195-5p, miR-192-3p, miR-328-5p and their target genes PPM1A, RAB1A and BRSK1 may Be potential biomarkers for membranous nephropathy. *Med. Sci. Monit.* 25, 1903–1916. doi:10.12659/MSM.913057

Zhou, L., Li, P., Zhang, M., Han, B., Chu, C., Su, X., et al. (2020). Carbon black nanoparticles induce pulmonary fibrosis through NLRP3 inflammasome pathway modulated by miR-96 targeted FOXO3a. *Chemosphere* 241, 125075. doi:10.1016/j.chemosphere.2019.125075

Zhou, L., Su, X., Li, B., Chu, C., Sun, H., Zhang, N., et al. (2019). PM2.5 exposure impairs sperm quality through testicular damage dependent on NALP3 inflammasome and miR-183/96/182 cluster targeting FOXO1 in mouse. *Ecotoxicol. Environ. Saf.* 169, 551–563. doi:10.1016/j.ecoenv.2018.10.108

Zhou, T., Zhong, Y., Hu, Y., Sun, C., Wang, Y., and Wang, G. (2018). PM(2.5) downregulates miR-194-3p and accelerates apoptosis in cigarette-inflamed bronchial epithelium by targeting death-associated protein kinase 1. *Int. J. Chron. Obstruct. Pulmon. Dis.* 13, 2339–2349. doi:10.2147/COPD.S168629

Zhou, X., Jeker, L. T., Fife, B. T., Zhu, S., Anderson, M. S., McManus, M. T., et al. (2008). Selective miRNA disruption in T reg cells leads to uncontrolled autoimmunity. *J. Exp. Med.* 205 (9), 1983–1991. doi:10.1084/jem.20080707

Zhu, Y., Zhang, M., Wang, F., Lu, J., Chen, R., Xie, Q., et al. (2018). The calcineurin regulatory subunit polymorphism and the treatment efficacy of tacrolimus for idiopathic membranous nephropathy. *Int. Immunopharmacol.* 65, 422–428. doi:10.1016/j.intimp.2018.10.038

frontiers | Frontiers in Pharmacology

TYPE Correction
PUBLISHED 27 February 2023
DOI 10.3389/fphar.2023.1166591

OPEN ACCESS

APPROVED BY
Frontiers Editorial Office,
Frontiers Media SA, Switzerland

*CORRESPONDENCE
Yang Zheng,
154202536@qq.com
Baoli Liu,
liubaoli@bjzhongyi.com

SPECIALTY SECTION
This article was submitted to Renal Pharmacology, a section of the journal Frontiers in Pharmacology

RECEIVED 15 February 2023
ACCEPTED 16 February 2023
PUBLISHED 27 February 2023

CITATION
Zhou X, Dai H, Jiang H, Rui H, Liu W, Dong Z, Zhang N, Zhao Q, Feng Z, Hu Y, Hou F, Zheng Y and Liu B (2023), Corrigendum: MicroRNAs: Potential mediators between particulate matter 2.5 and Th17/Treg immune disorder in primary membranous nephropathy. *Front. Pharmacol.* 14:1166591. doi: 10.3389/fphar.2023.1166591

Corrigendum: MicroRNAs: Potential mediators between particulate matter 2.5 and Th17/Treg immune disorder in primary membranous nephropathy

Xiaoshan Zhou[1,2], Haoran Dai[3], Hanxue Jiang[2], Hongliang Rui[2,4], Wenbin Liu[5], Zhaocheng Dong[1], Na Zhang[6], Qihan Zhao[2,6], Zhendong Feng[7], Yuehong Hu[2,6], Fanyu Hou[8], Yang Zheng[2]* and Baoli Liu[2]*

[1]Beijing University of Chinese Medicine, Beijing, China, [2]Beijing Hospital of Traditional Chinese Medicine, Capital Medical University, Beijing, China, [3]Shunyi Branch, Beijing Hospital of Traditional Chinese Medicine, Beijing, China, [4]Beijing Institute of Chinese Medicine, Beijing, China, [5]School of Life Sciences, Beijing University of Chinese Medicine, Beijing, China, [6]School of Traditional Chinese Medicine, Capital Medical University, Beijing, China, [7]Pinggu Hospital, Beijing Hospital of Traditional Chinese Medicine, Beijing, China, [8]School of Traditional Chinese Medicine, Changchun University of Chinese Medicine, Changchun, China

KEYWORDS

PM2.5, PLA2R1, microRNA, Th17/Treg, primary membranous nephropathy (PMN)

A Corrigendum on
MicroRNAs: Potential mediators between particulate matter 2.5 and Th17/Treg immune disorder in primary membranous nephropathy

by Zhou X, Dai H, Jiang H, Rui H, Liu W, Dong Z, Zhang N, Zhao Q, Feng Z, Hu Y, Hou F, Zheng Y, Liu B (2022). Front Pharmacol. 13:968256. doi: 10.3389/fphar.2022.968256

In the published article, there was an error in **Affiliations** [1, 2]. Instead of "[1]Beijing Hospital of Traditional Chinese Medicine, Capital Medical University, Beijing, China, [2]School of Traditional Chinese Medicine, Beijing University of Chinese Medicine, Beijing, China," it should be "[1]Beijing University of Chinese Medicine, Beijing, China, [2]Beijing Hospital of Traditional Chinese Medicine, Capital Medical University, Beijing, China."

In the published article, there was an error in the **Funding** statement. The number of the first fund was incorrect. The correct **Funding** statement appears below.

Funding

This work is supported by grants from Capital's Funds for Health Improvement and Research (No. 2020-2-2234 to BL), the National Key Research and Development Project of

China (No. 2019YFC1709402 to BL), the General project of the National Natural Science Foundation of China (No. 81973793 to BL), and Youth Foundation of National Natural Science Foundation of China (No. 82004269 to HD).

The authors apologize for this error and state that this does not change the scientific conclusions of the article in any way. The original article has been updated.

Publisher's note

frontiers | Frontiers in Pharmacology

TYPE Original Research
PUBLISHED 26 September 2022
DOI 10.3389/fphar.2022.897167

OPEN ACCESS

EDITED BY
Zhiyong Guo,
Second Military Medical University, China

REVIEWED BY
Xiao-Liang Zhang,
Southeast University, China
Pravin C. Singhal,
North Shore Long Island Jewish Health System, United States
Manman Shi,
Kunshan Traditional Chinese Medicine Hospital, China

*CORRESPONDENCE
Zhanzheng Zhao,
zhanzhengzhao@zzu.edu.cn
Jin Shang,
fccshangj2@zzu.edu.cn

SPECIALTY SECTION
This article was submitted to Renal Pharmacology, a section of the journal Frontiers in Pharmacology

RECEIVED 15 March 2022
ACCEPTED 23 August 2022
PUBLISHED 26 September 2022

CITATION
Guo R, Wang P, Zheng X, Cui W, Shang J and Zhao Z (2022), SGLT2 inhibitors suppress epithelial–mesenchymal transition in podocytes under diabetic conditions via downregulating the IGF1R/PI3K pathway.
Front. Pharmacol. 13:897167.
doi: 10.3389/fphar.2022.897167

SGLT2 inhibitors suppress epithelial–mesenchymal transition in podocytes under diabetic conditions *via* downregulating the IGF1R/PI3K pathway

Ruixue Guo[1,2], Peipei Wang[1,2], Xuejun Zheng[1,2], Wen Cui[1,2], Jin Shang[1,3,4]* and Zhanzheng Zhao[1,3,4]*

[1]Department of Nephrology, The First Affiliated Hospital of Zhengzhou University, Zhengzhou, China, [2]Zhengzhou University, Zhengzhou, China, [3]Laboratory of Nephrology, The First Affiliated Hospital of Zhengzhou University, Zhengzhou, China, [4]Laboratory Animal Platform of Academy of Medical Sciences, Zhengzhou University, Zhengzhou, China

Loss of podocyte is a characteristic pathological change of diabetic nephropathy (DN) which is associated with increased proteinuria. Many studies have shown that novel inhibitors of sodium–glucose cotransporter 2 (SGLT2-is), such as dapagliflozin, exert nephroprotective effect on delaying DN progression. However, the mechanisms underlying SGLT2-associated podocyte injury are still not fully elucidated. Here, we generated streptozotocin-induced DN models and treated them with dapagliflozin to explore the possible mechanisms underlying SGLT2 regulation. Compared to mice with DN, dapagliflozin-treated mice exhibited remission of pathological lesions, including glomerular sclerosis, thickening of the glomerular basement membrane (GBM), podocyte injury in the glomeruli, and decreased nephrotoxin levels accompanied by decreased SGLT2 expression. The mRNA expression profiles of these treated mice revealed the significance of the insulin-like growth factor-1 receptor (IGF1R)/PI3K regulatory axis in glomerular injury. KEGG analysis confirmed that the phosphatidylinositol signaling system and insulin signaling pathway were enriched. Western blotting showed that SGLT2-is inhibited the increase of mesenchymal markers (α-SMA, SNAI-1, and ZEB2) and the loss of podocyte markers (nephrin and E-cad). Additionally, SGLT2, IGF1R, phosphorylated PI3K, α-SMA, SNAI-1, and ZEB2 protein levels were increased in high glucose-stimulated human podocytes (HPC) and significantly decreased in dapagliflozin-treated (50 nM and 100 nM) or OSI-906-treated (inhibitor of IGF1R, 60 nM) groups. However, the use of both inhibitors did not enhance this protective effect. Next, we analyzed urine and plasma samples from a cohort consisting of 13 healthy people and 19 DN patients who were administered with (n = 9) or without (n = 10) SGLT2 inhibitors. ELISA results showed decreased circulating levels of IGF1 and IGF2 in SGLT2-is-treated DN patients compared with DN patients. Taken together, our study reported the key role of SGLT2/IGF1R/PI3K signaling in

regulating podocyte epithelial–mesenchymal transition (EMT). Modulating IGF1R expression may be a novel approach for DN therapy.

KEYWORDS

diabetic nephropathy, sodium–glucose cotransporter-2 inhibitors, insulin-like growth factor-1 receptor, podocyte, epithelial–mesenchymal transition

1 Introduction

Diabetic nephropathy (DN) is associated with increasing incidence (Zhang et al., 2010; Ogurtsova et al., 2017) and poor prognosis (Alicic et al., 2017; Cheng et al., 2021). Patients identified as having diabetes mellitus (DM) exhibit higher filtration and reabsorption of glucose in the kidney, which is associated with the upregulated expression of sodium–glucose cotransporter 2 (SGLT2) in the proximal convoluted tubules (Vallon and Verma, 2021). This excessive increase in SGLT2 expression further promotes the accumulation of glucose in the host, which forms a vicious cycle and causes lasting kidney damage. The glomerular pathology that occurs secondary to diabetes is characterized by the thickening of the glomerular basement membrane (GBM) and podocyte injury (Rabkin, 2003). In the early stage of DN, podocytes can become hypertrophic to respond to the tractive effects of the thickened GBM. However, constant stimulation ultimately leads to the dissociation of the foot process and basement membrane, as well as the loss of cell proliferation ability (Xu et al., 2010). Podocytes are the last and most critical components of the glomerular filtration barrier, and the loss of this function is closely associated with the onset of proteinuria (Mundel and Reiser, 2010). According to reports, an elevated level of proteinuria is positively correlated with adverse renal outcomes (Lambers Heerspink and Gansevoort, 2015). Therefore, blocking SGLT2-mediated glucose transport in DN, even DM, helps attenuate the progression of proteinuria.

Recently, numerous studies reported the reno-protective effects of SGLT2-is, a new hypoglycemic drug, such as dapagliflozin, in treating DN and its cardiovascular complications (Kovesdy et al., 2022; Liu et al., 2022). These beneficial effects can be attributed to the effects of SGLT2-is on the decreased regulation of glomerular filtration and proteinuria (Korbut et al., 2020; Ravindran and Munusamy, 2022). For instance, dapagliflozin dilates the efferent arteriole, reduces intravascular pressure, and alleviates shear force injury to the filtration barrier (van Bommel et al., 2020). In BTBR ob/ob mice, empagliflozin decreased the expression of SGLT2 in podocytes and further improved the microvascular endothelial ultrastructure by inhibiting the secretion of podocyte-derived VEGF-A (Locatelli et al., 2022). Cassis et al. (2018) reported a high level of SGLT2 in protein-overloaded human podocytes (HPC), and inhibition of SGLT2 could help normalize podocyte cytoskeleton and function. However, much evidence regarding the possible molecular mechanisms by which SGLT2-is affect glomeruli, especially in podocytes, is still needed.

For this purpose, we established SGLT2-is-treated diabetic models and found that kidney injury caused by SGLT2 upregulation was mediated by insulin-like growth factor 1 receptor (IGF1R). In parallel, we reconfirmed the causal relationship between SGLT2 and IGF1R in HPC cultured with high glucose. SGLT2/IGF1R signaling mainly mediated EMT in podocytes. Moreover, efficacy evaluations in DN patients revealed the direct effect of SGLT2 on IGF1R ligands. All these results showed that inhibition of IGF1R might be an alternative approach to normalize the function of podocytes and reduce proteinuria, which provided a new idea for DN therapy.

2 Materials and methods

2.1 Management of animal models

A total of 18 six-week-old specific pathogen-free (SPF) male C57BL6J mice were purchased from Huafukang Laboratory Animals Center (Beijing, China) and were randomly divided into Con (n = 6), DN (n = 6), and dapagliflozin-treated DN groups (DA, n = 6). Prior to our experiment, the mice were allowed to adapt to the suitable laboratory conditions (room temperature of 22°C; 12 h light/dark cycle) for 2 weeks. Meanwhile, the mice designed as diabetes models (the DN and DA groups) were given a high-fat diet (fat content: 60%). In the eighth week, the mice that were assigned to diabetic groups were intraperitoneally injected with streptozotocin (50 mg/kg/d, Sigma), and the mice in the Con group were given an equal volume of saline for five consecutive days. Diabetic mice were defined as having a blood glucose (BG) level >=17.6 mmol/L in the tenth week. In the subsequent 4 weeks, dapagliflozin was dissolved in sodium hydroxymethyl cellulose and delivered to the mice (DA group) by oral gavage (1 mg/kg/d). The rest of the mice (DN and Con groups) were treated with equal amounts of normal saline. All the mice were euthanized at 18th weeks. The Institutional Review Board of the Experimental Animal Center of Zhengzhou University approved our animal experiment (ZZU-LAC20210402 [09]).

2.2 Measurement of laboratory parameters

Laboratory parameters such as body weight (BW), BG, and protein/creatinine ratio (PCR) were recorded in the 8th, 10th, 14th, and 18th weeks. Mouse tails were punctured to collect blood for BG measurements. The PCR was measured on a platform in our hospital laboratory department. In addition, we obtained the jugular venous blood to measure the biochemical indexes. Biochemical detection kits for serum creatinine (50 ul/well, sarcosine oxidase method) (Liang et al., 2017) and blood urea nitrogen (BUN) (10 ul/well) were obtained from Shanghai Meilian Biotechnology Co., Ltd., (Shanghai, China).

2.3 Histological analysis of the animal renal cortex

After blood collection, we immediately blanched the mouse kidney by perfusing the left ventricle using normal saline (NS). When both kidneys were white, we resected and isolated sections of the renal cortex from the medulla and placed them in a -80°C environment for subsequent mRNA sequencing and WB analysis. In addition, another small piece of the cortex was collected and stored in fixative to perform TEM as previously described (Veron et al., 2011). The remaining renal cortex was incubated in 4% paraformaldehyde (PFA), embedded in paraffin for 48 h, and finally processed into 4-μm-thick sections for hematoxylin/eosin (HE), periodic acid–Schiff's reagent (PAS), Masson (Veron et al., 2021) and immunohistochemical (IHC) staining. IHC of frozen kidney sections was performed using primary antibodies against SGLT2 (1:100), IGF1R (1:1000), IGF1 (1:500), and collagen IV (1:500)) (Veron et al., 2014). As previously described, we also focused on SGLT2 expression in glomeruli using immunofluorescence staining (Kato et al., 2006).

2.4 mRNA assay

mRNA sequencing was performed on the renal cortex of all mice ($n = 18$). Total RNA was isolated following the instructions of the RNAeasy Mini Kit (Qiagen, Germany). Poly-T oligo-conjugated magnetic beads were used to purify mRNA molecules containing poly-A. We first fragmented the mRNA under high temperature and then performed reverse transcription to generate a cDNA library. The Qubit® 2.0 Fluorometer (Life Technologies, United States) and Agilent 2100 bioanalyzer (Agilent Technologies, United States) were used to confirm the gene concentration. Clusters of mRNAs were further sequenced on an Illumina NovaSeq 6000 (Illumina, United States). Total RNA isolation, cDNA library establishment, and Illumina sequencing were all conducted by Sinotech Genomics Co., Ltd., (Shanghai, China). The RNA concentration was assessed using FPKM, which is defined as fragments per kilobase of exon per million reads mapped. The fragments within each gene were counted using StringTie software and then normalized using the TMM algorithm. Differentially expressed genes (DEGs) were selected using the edgeR R package. PCA/heatmap/volcano plots visualized the expression levels of the DEGs among the three groups. SangerBox was used to analyze Kyoto Encyclopedia of Genes and Genomes (KEGG) pathway enrichment. The construction of a protein–protein interaction (PPI) with IGF1R as the core was performed using the following steps: first, Cytoscape software was used to identify the top 20 core genes from 1957 DEGs (|log2(FC)| value >1 and p-adjusted value/q < 0.05), which were coexpressed in Con vs. DN and DN vs. DA comparisons. The results suggested that the IGF1R/PI3K pathway was the most significantly modulated by SGLT2. Second, genes with combined scores larger than 0.9 with IGF1R were selected for PPI in analysis using the STRING website (https://string-db.org/).

2.5 Cell culture and inhibitor use

Conditionally, immortalized HPC referred to in our study were donated by Shandong University. HPC and human glomerular endothelial cells (HGRECs) were normally expanded in 1640 medium supplemented with 1% penicillin–streptomycin, 10% FBS, and 5.6 mM glucose. Mesangial cells (HMCs) and HK-2 cells (a kind of tubular epithelial cell) were cultured in DMEM. To explore the optimal experimental conditions, $2*10^6$ cells were seeded in six-well plates, serum-starved for 24 h, and stimulated with 20 mM or 40 mM glucose for 24 h (cell density: 50%) or 48 h (cell density: 30%). Inhibitor-treated groups were set with different doses of inhibitors: dapagliflozin (Macklin, 461432-26-8; 50 nM, 100 nM, or 250 nM), OSI-906 (IGF1R antagonist, MedChemExpress, HY-10191; 30 nM or 60 nM), and Da+OSI-906 (50 nM + 60 nM).

2.6 Western blotting

The extracts from the renal cortex or cultured cells were incubated with antibodies against SGLT2 (ab37296, 2 ug/ml), IGF1R (ab182408, 1/2000), PI3K-p85 alpha (AF6241, 1/2000), p-PI3K-p85 (Tyr458/p55Try199) (AF3242, 1:1000), α-SMA (ab21027, 1/400), nephrin (ab58968, 1/1000), E-cadherin (60335-1-AP, 1:1000), SNAI-1 (26183-1-AP, 1:1000), and ZEB2 (14026-1-AP, 1:1000). Protein expression *in vitro* and *in vivo* was quantified using ImageJ (https://imagej.nih.gov/ij/) and processed using Prism 8 software.

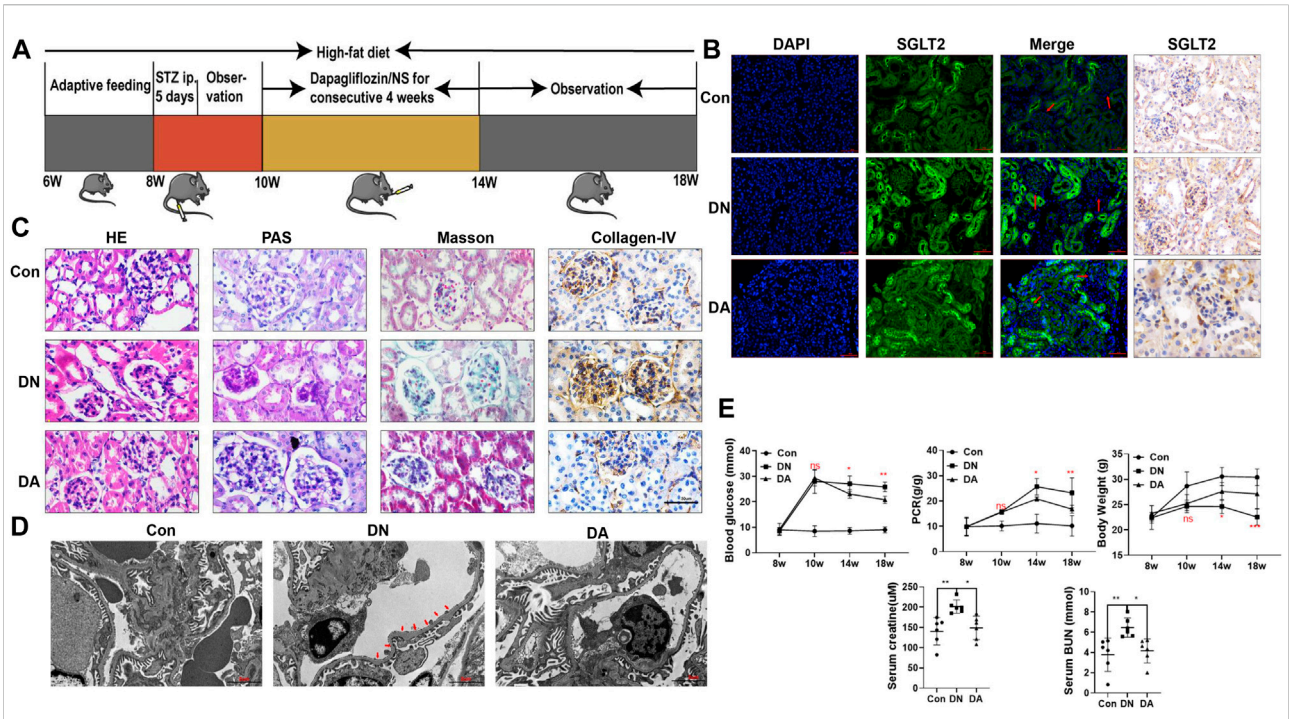

FIGURE 1
Dapagliflozin attenuated STZ-induced diabetic kidney injury. **(A)** Flowchart of the animal experiment (n = 6/group). **(B)** IF and IHC staining of SGLT2. **(C)** Pathological staining: light micrographs of HE, PAS, and Masson staining and IHC of collagen IV. **(D)** Representative electron micrographs of glomeruli. Areas of basement membrane thickening and podocyte injury are indicated by red arrows. **(E)** Statistical significance of BG levels, BW, and PCR among the three groups in the 8th, 10th, 14th, and 18th weeks was performed using two-way ANOVA, and Tukey's algorithm for subsequent multiple comparisons between two groups. In parallel, one-way ANOVA was performed for SCr and BUN levels. STZ: streptozotocin; Con: control group; DN: diabetic nephropathy; DA: dapagliflozin-treated DN group: NS: normal saline; SGLT2: sodium–glucose cotransporter 2; IF: immunofluorescent staining; IHC: immunohistochemical staining; one-way ANOVA: one-way analysis of variance; BG: blood glucose; BW: body weight; PCR: urinary total protein to creatinine ratio; SCr: serum creatinine; BUN: blood urea nitrogen.

2.7 Human specimen collection

Study design: from 2018 to 2020, urine and plasma samples from 1030 patients who were diagnosed with DN were collected and stored in the Biobank of The First Affiliated Hospital of Zhengzhou University. After strict screening criteria described in the following paragraph, 10 patients with DN and 9 SGLT2-is-treated DN patients were ultimately included in our study. Thirteen-year-old/sex-matched healthy people were recruited as controls from the Physical Examination Center of our hospital.

Inclusion criteria: there were two evaluative criteria for the control groups: 1) with normal laboratory tests including kidney and liver function tests and routine blood examination and 2) no drug treatment. The diagnostic criteria of DN were in accordance with the 2012 KDIGO (Levey et al., 2011). Based on the former requirement, the SGLT2-is-treated group should have completed taking SGLT2-is (i.e., dapagliflozin, empagliflozin, and canagliflozin) for more than 1 month.

Exclusion criteria: subjects who suffered cancer, hepatic diseases, endocrine system diseases (i.e., pituitary tumor), and a combination of other urinary system diseases (e.g., ANCA-associated vasculitis with renal damage, IgA nephropathy, membranous nephropathy, and end-stage renal disease) or who received dialysis-related treatments were excluded. Notably, we also excluded DN patients who were treated with exogenous insulin.

Others: the use of these patients' specimens was approved by the Institutional Review Board of The First Affiliated Hospital of Zhengzhou University (2019-KY-361) and followed the Declaration of Helsinki. All the participants signed written informed consent forms.

The levels of IGF1 and IGF2 in all obtained specimens were tested using ELISA kits according to the manufacturer's instructions.

2.8 Statistical analysis

The statistical significance of BG, BW, and PCR among the three groups was calculated using two-way ANOVA followed by

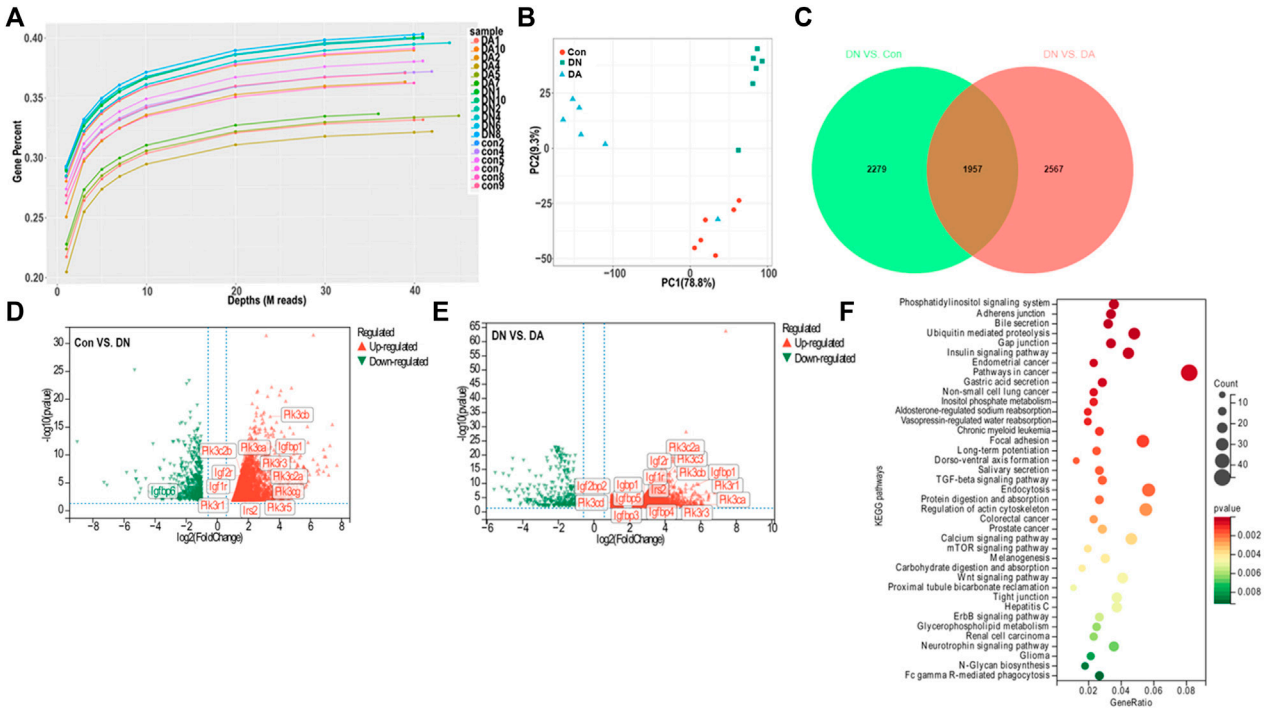

FIGURE 2
Gene expression profile of dapagliflozin-treated diabetic models. **(A)** Gene saturation analysis. **(B)** PCA plot within groups. The values of principal components 1 and 2 were 78.8% and 9.3%, respectively. **(C)** Venn diagram of all the DEGs between Con vs. DN and DN vs. DA. Volcano plots of the DEGs between DN and Con **(D)** and between DN and DA **(E)**. Red dots: upregulated in DN; green dots: downregulated in DN. **(F)** KEGG analysis revealed enriched pathways modulated by the DEGs among the three groups (p-adjusted<0.05). X-axis: gene-ratio = genes with significance/all involved genes; circle color represents significance, and circle size represents counts of the DEGs. PCA: principal component analysis; IGF1R: insulin-like growth factor-1 receptor; DEGs: differentially expressed genes (p/q < 0.05 and |log2(FC)| >1).

Tukey's *post hoc* method, while one-way ANOVA was used for the other statistical analysis.

3 Results

3.1 Sodium–glucose cotransporter 2-is attenuated the pathological progression and improved laboratory parameters in mice with diabetic nephropathy

To evaluate the reno-protective effect of SGLT2 inhibitors on kidney pathology and function in diabetic mice, we established Con, DN, and dapagliflozin-treated groups (Figure 1A). First, IHC and IF staining both indicated a wider distribution of SGLT2 in the glomeruli of the DN group than in the Con or DA group (Figure 1B, Supplementary Figure S1). The diabetic mice exhibited smaller and sclerotic glomeruli with an expanded mesangial matrix, increased glycogen deposition, and obvious collagen fiber after 2 months, while all these lesions were improved in the dapagliflozin-treated mice with DN (Figure 1C, Supplementary Figure S2). Measurement of the GBM in the DN group showed an irregular thickening and missing podocyte processes, but no significant differences were observed between the DA group and Con group (Figure 1D and Supplementary Figure S3). Laboratory variables, including BG levels, PCR, Scr levels, and BUN levels were lower and BW was higher in the DA group than in the DN group (Figure 1E). These results suggested that suppression of SGLT2 could alleviate glucose-induced DN progression.

3.2 mRNA profile in dapagliflozin-treated mice

We first explored the molecular effects of dapagliflozin on the basis of transcriptomics. Gene-depth curves showed that the depth of the estimated genes approached saturation in each sample (Figure 2A). The PCA plot indicated a relatively concentrated distribution within groups (Figure 2B). As shown in the Venn diagram, 1957 genes were shared between the Con vs. DN and DA vs. DN comparisons (p/q < 0.05 and |log2(FC)|>1, Figure 2C, Supplementary Figure S4). The expression profiles of the 1957 genes among the three groups were shown in a heatmap (Supplementary Figure S5, Supplementary Table S1). The volcano

10.3389/fphar.2022.897167

TABLE 1 Using Cytoscape to determine the top 20 hub genes from 1957 DEGs.

Scorename method	Closeness	Degree	EPC	MCC	MNC	Radiality
Pten	766.05	148	156.627	2.2026E+11	145	7.708313115
Cdh1	726.88333	121	146.143	—	120	7.580855815
Pik3ca	713.9	114	151.778	2.27117E+11	114	7.53963828
Mapk1	703.4	93	137.49	—	93	7.523785382
Ep300	700.68333	105	131.263	—	102	7.493981934
Cltc	700.08333	84	—	—	80	7.526955962
Pik3r1	694.6	94	148.31	2.26976E+11	93	7.487006659
Nina	694.1	81	124.133	—	77	7.501591325
Igfir	690.43333	75	138.306	19488251184	75	7.497152514
Atm	685.46667	79	—	—	77	7.473690225
Erbb4	684.36667	78	134.207	2.2702E+11	77	7.467983181
Smad4	683.83333	82	132.157	—	82	7.457203211
Arf6	679.8	84	123.035	—	81	7.437545617
Yes1	679.55	83	132.845	1.22932E+11	78	7.438179733
Htt	677.56667	—	—	—	—	7.465446718
Prkacb	672.75	77	—	—	75	7.417253908
Pik3cb	670.55	79	133.311	2.26923E+11	79	—
Traf6	670.25	—	—	—	—	7.421058603
Ptk2b	669.78333	83	129.637	2.00279E+11	81	—
Lrrk2	669.75	—	—	—	—	7.43564327
Kdr	—	78	129.232	1.82683E+11	75	—
Pik3r3	—	76	132.562	2.26932E+11	74	—
Ptpn11	—	74	130.379	2.27085E+11	71	—
Erbb3	—	—	131.252	2.27017E+11	—	7.410278633
Map2k1	—	—	126.476	10276488566	—	7.409644517
Frk	—	—	124.383	1.0408E+11	—	—
Sos1	—	—	—	2.26385E+11	—	—
Sos2	—	—	—	2.26374E+11	—	—
Cbl	—	—	—	2.14613E+11	—	—
Flt1	—	—	—	1.75403E+11	—	—
Jak1	—	—	—	28052807594	—	—
Lyn	—	—	—	16332161318	—	—

plot showed the upregulated and downregulated genes in the DN vs. DA and Con vs. DN comparisons (Figures 2D,E). After KEGG enrichment analysis of 1957 DEGs, 39 signaling pathways, including inositol phosphate metabolism, phosphatidylinositol signaling system, insulin signaling pathway, mTOR signaling pathway, and TGF-β signaling pathway, remained significantly associated with dapagliflozin use (p-adjusted<0.05, Figure 2F).

3.3 Upregulation of sodium–glucose cotransporter 2 caused glomerular injury mainly *via* the insulin-like growth factor 1 receptor/PI3K pathway

Through six algorithms provided using Cytoscape software, we observed a core status of IGF1R among the 1957 DEGs (Table 1). Moreover, PI3K signaling exhibited strong crosstalk with IGF1R (Figure 3A; Supplementary Figure S6). Compared with those in the DA or Con group, the expression levels of factors related to the IGF system, PI3K subunits, and markers of epithelial–interstitial trans-differentiation (EMT) were all increased in the DN group (Supplementary Figure S7). A study reported that IGF1-receptor expression was significantly increased in diabetic models with kidney damage, and this receptor partly activated downstream PI3K signaling in a phosphatase-dependent manner, ultimately leading to the accumulation of toxic substances in podocytes (Korbut et al., 2020). Therefore, we proposed the hypothesis that inhibition of SGLT2/IGF1R/PI3K signaling plays an important role in protecting against DN progression.

To verify the effects of dapagliflozin on IGF1R signals, we measured the expression of relevant proteins in the renal cortex

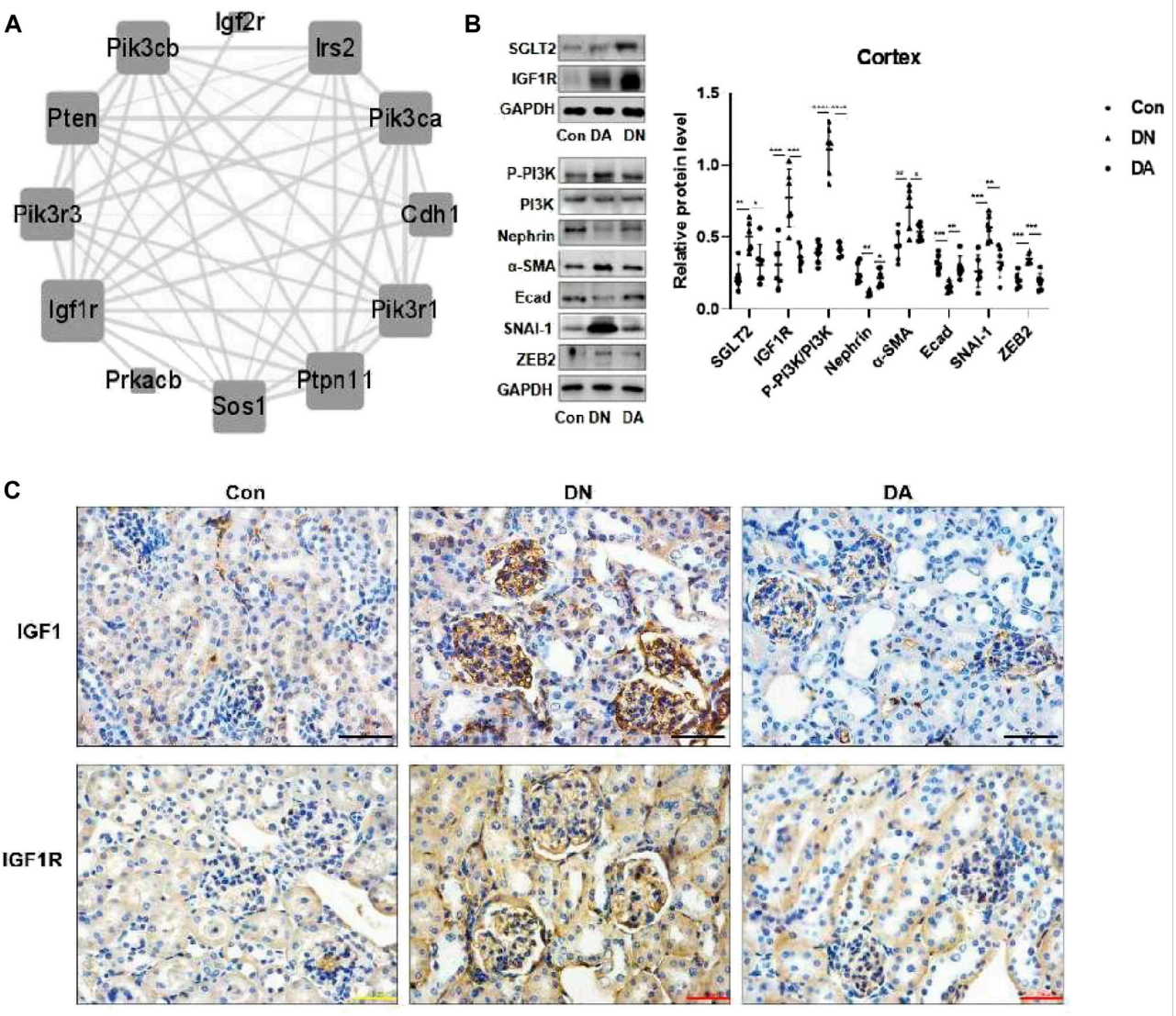

FIGURE 3
In DN models, upregulation of SGLT2 activated IGF1R/PI3K signaling. **(A)** IGF1R-centered PPI network (combined score>0.9). **(B)** Protein expression levels of SGLT2, IGF1R, phosphorylated PI3K, and EMT markers were analyzed using Western blotting. The data were analyzed by ANOVA with Tukey's post hoc test. **(C)** IHC images of IGF1 and IGF1R. PPI: protein–protein interaction; $*p < 0.05$, $**p < 0.01$.

in response to high-glucose simulation. Western blotting revealed that dapagliflozin decreased the protein levels of IGF1R and phosphorylated PI3K but prevented the loss of nephrin, a marker of podocytes, and E-cad. Moreover, diabetic mice treated with dapagliflozin exhibited a reduction in the expression of α-SMA, SNAI-1, and ZEB2, which were implicated in EMT (Figure 3B). IHC staining revealed a wide distribution of IGF1 and IGF1R expression in DN glomeruli, compared with dapagliflozin-treated models (Figure 3C, Supplementary Figure S8).

3.4 Inhibition of the sodium–glucose cotransporter 2/insulin-like growth factor 1 receptor pathway reduced epithelial–interstitial trans-differentiation in high-glucose-stimulated podocytes

After 24 h or 48 h of stimulation under high-glucose conditions (20 mM and 40 mM), the protein expression of IGF1R in HPC or HGREC was dramatically increased, but the change in the expression of the latter was mainly

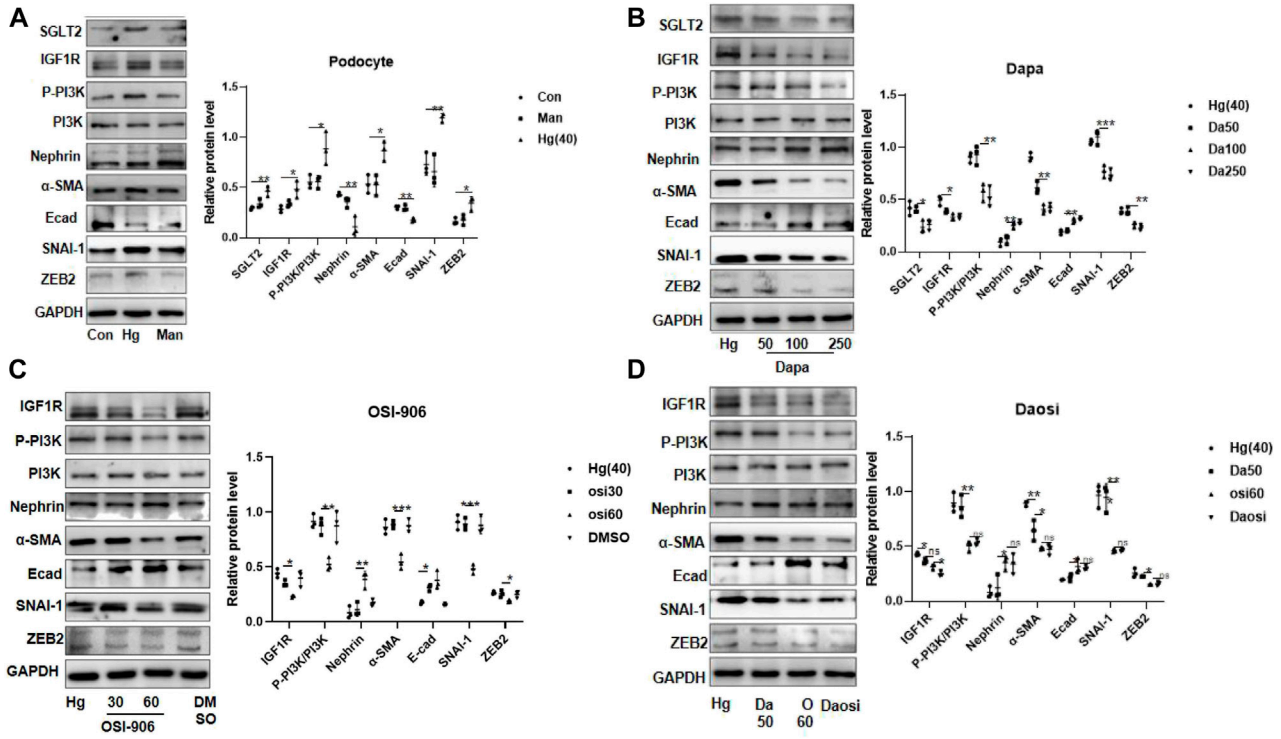

FIGURE 4
SGLT2 directly regulated podocyte EMT *via* IGF1R/PI3K signaling. **(A)** Representative WB images and densitometric analysis of the expression of SGLT2, IGF1R, phosphorylated PI3K, and EMT markers in high-glucose-stimulated podocytes (Hg: 40 nM, 24 h). **(B)** Podocytes treated with different doses of dapagliflozin (50 nM, 100 nM, and 250 nM) and **(C)** OSI-906 (30 nM and 60 nM). **(D)** Combination of OSI60 and Da50. EMT: epithelial–mesenchymal transition. The data were analyzed by ANOVA with Tukey's post hoc test. N = 3; $*p < 0.05$, $**p < 0.01$, $***p < 0.001$, $****p < 0.001$.

attributed to the effects of hyper-osmosis. In addition, we did not observe obvious glucose-induced alterations in IGF1R protein expression in HMC or HK-2 cells (Supplementary Figure S9). Therefore, we chose HPC for further analysis. HPC were exposed to 40 mM glucose for 24 h. Consistent with the results in diabetic mice, we observed similar trends of protein expression in the high-glucose-stimulated podocytes (Figure 4A). Interestingly, dapagliflozin-treated podocytes presented a dose-dependent reduction in the levels of IGF1R, phosphorylated PI3K, α-SMA, SNAI-1, and ZEB2 and an upregulation of the levels of nephrin and E-cad (Figure 4B). We further cultured high-glucose-stimulated podocytes with OSI-906 (30 or 60 nM), a selective IGF1R inhibitor, to elucidate the relationship between IGF1R and PI3K. As expected, OSI-906 downregulated phosphorylated PI3K, α-SMA, SNAI-1, and ZEB2 and upregulated nephrin and E-cad levels in a dose-dependent manner (Figure 4C). Additional cotreatment with OSI-906 (60 nM) and dapagliflozin (50 nM) was performed to explore the favorable effect on podocyte repair. The combined process failed to enhance the reno-protective effects (Figure 4D). Altogether, our results demonstrated a critical role of SGLT2/IGF1R signaling in suppressing podocyte injury.

3.5 Sodium–glucose cotransporter 2-is alleviated the progression of diabetic nephropathy accompanied by decreased circulation and excretion of insulin-like growth factor-1 levels

After a strict screening process, a total of 19 volunteers with DN who were taking SGLT2 inhibitors ($n = 9$) or not ($n = 10$) were enrolled. The statistical significance of the biochemical variables of all the included participants is shown in Supplementary Table S2. We found increased circulation of IGF1 and IGF2 in the patients with DN compared with the healthy controls, which could be reversed after SGLT2-is use (Figure 5A–D). This suggested that SGLT2-is might inhibit hepatic synthesis of IGF1 and IGF2, thereby reducing the secretion and excretion of IGF1R ligands.

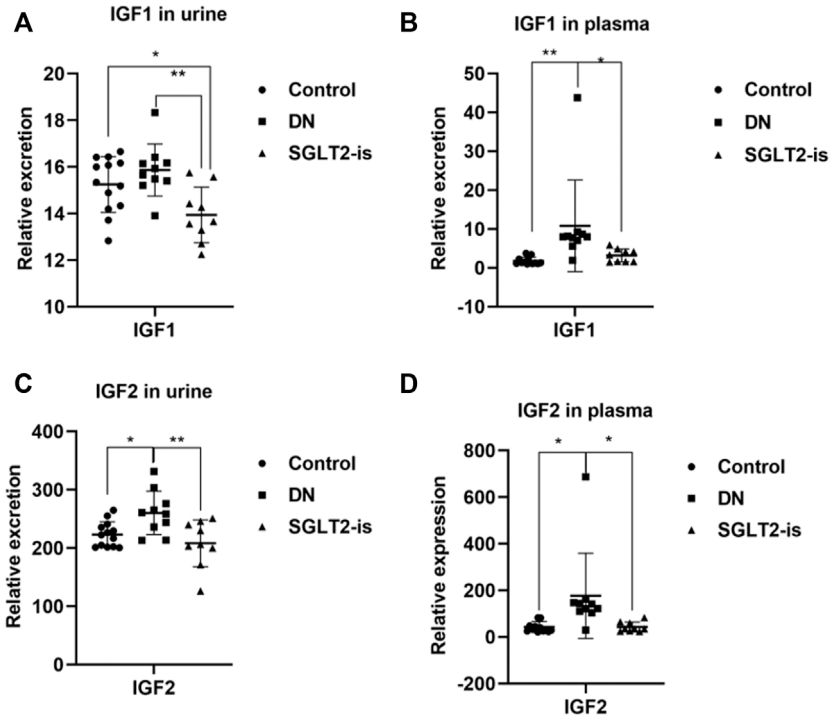

FIGURE 5
IGF1 and IGF2 expression in DN patients with or without SGLT2-is use. Excreted and circulating levels of IGF1 **(A,B)** and **(C,D)** IGF2 in human urine and plasma. Healthy controls: $n = 13$; DN patients without SGLT2-is use: $n = 10$; DN patients with SGLT2-is use: $n = 9$. The data were analyzed by ANOVA with Tukey's post hoc test. * $p < 0.05$, ** $p < 0.01$.

4 Discussion

In our study, we provided substantial evidence to verify that SGLT2-is limited podocyte EMT by decreasing IGF1R/PI3K activity in *in vitro* and *in vivo* experiments. To some extent, the finding helped explain the anti-proteinuria effect of SGLT2-is, which suggested that podocytes might also be a major target of SGLT2 (Figure 6). Considering the specific expression of SGLT2 in the proximal tubules, previous studies about DN mainly focused on its beneficial effects by maintaining normal glycemia, thereby delaying DN progression (Kim et al., 2021; Sen et al., 2022). Several studies recently reported a direct role of SGLT2 in interfering with podocyte dysfunction. For instance, in mice with DN, the reno-protective effect of empagliflozin against proteinuria was primarily due to the decreased release of substances that damaged endothelial cells after SGLT2 downregulation in podocytes (Locatelli et al., 2022). Particularly, Cassis et al. (2018) reported increased SGLT2 expression in the HPC of proteinuric CKD patients as well as podocytes cultured with repeated BSA exposure. In support of this observation, our experiments found that intervention with dapagliflozin could limit podocyte SGLT2 upregulation and EMT-induced damage in a dose-dependent manner. As we all know, hyperglycemia is the major contributor to DN, which is clinically characterized by proteinuria (DeFronzo et al., 2021). Although SGLT2 inhibitors, which are well-recognized glucose-lowering agents, are involved in improving every pathological aspect of DN (Gnudi et al., 2016), more studies are needed to better verify the direct effect of SGLT2 inhibition on improving podocyte function.

Another important finding was that dapagliflozin modulated the EMT of podocytes *via* the IGF1R/PI3K pathway, which provided a conceivable connection between SGLT2 inhibition and reduced proteinuria. In dapagliflozin-treated DN mice or high-glucose-stimulated podocytes, the mRNA and protein expression profiles in the isolated renal cortex showed downregulation of IGF1R. IGF1R binds with high affinity to IGF1, followed by IGF2, which is activated to promote cellular glucose uptake and utilization by cells (Li et al., 2018). The compensatory upregulation of IGF1R in the early stage of DN promotes the energy use of target cells, while long-term excessive increases in IGF1R expression result in metabolic damage. For example, aminoguanidine, which inhibits glycosylation, was reported to decrease the renal expression of IGF1 and further improve mesangial expansion (Lupia et al., 1999; Peiris et al., 2017). In STZ-induced diabetic mice, activation of IGF-1

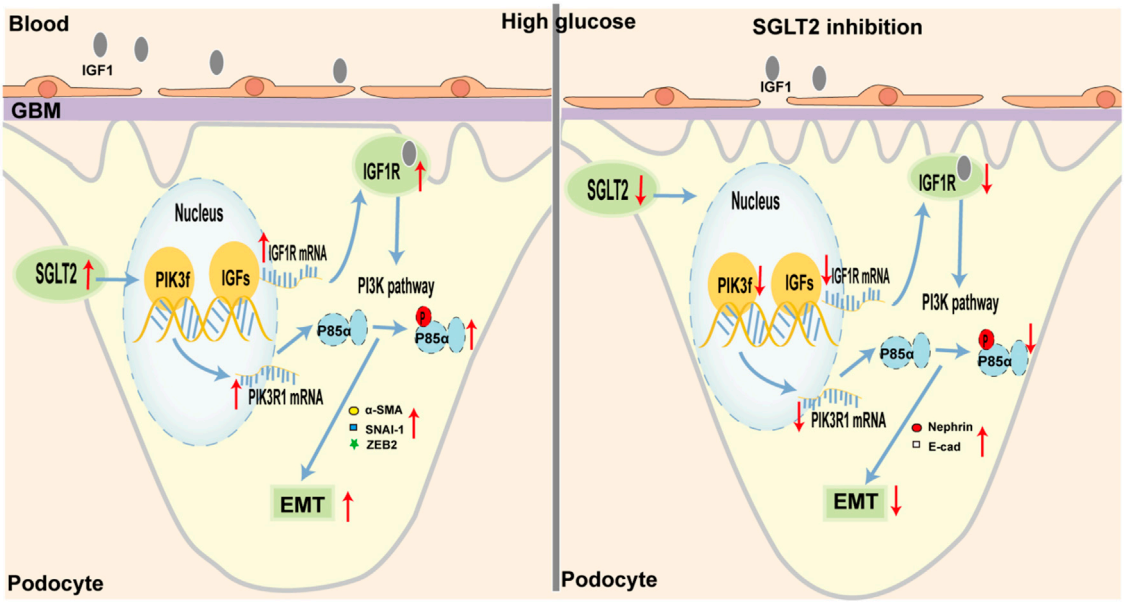

FIGURE 6
Schematic representation of SGLT2/IGF1R/PI3K-regulated EMT in podocytes under diabetic conditions. (Left) In diabetes, glycemic dysregulation caused the overexpression of SGLT2 in podocytes, which then promoted the formation of an intracellular hyperglycemic microenvironment. In response to high-glucose stimulation, the transcriptional and translational capacities of IGF1R/PI3K signaling were enhanced. At the molecular level, IGF1 and IGF2 expression was increased and closely bound to IGF1 receptors, further activated the phosphorylation of PI3K, and finally led to podocyte dysfunction, such as enhanced EMT. Microscopically, podocyte loss or fusion and glomerular fibrosis occurred. Macroscopically, proteinuria appeared. (Right) When SGLT2 was inhibited, podocyte damage mediated by the IGF1R/PI3K signaling pathway was inhibited, such as decreased IGF1 and IGF2 circulating levels, and increased nephrin and E-cad.

promoted renal fibrosis by upregulating SNAI-1 (Dong et al., 2019). When translating this observation to the *in vitro* experiments, we observed a marked upregulation of IGF1R and EMT markers, such as α-SMA, SNAI-1, and ZEB2, in cultured HPC exposed to high-glucose concentrations. This effect was not observed in HK-2, HMC, or HGREC, which suggested that the SGLT2/IGF1R axis functioned mainly in podocytes. In particular, when SGLT2 or IGF1R was inhibited, the effects on downstream factors and EMT markers were all gradually alleviated. A consistent previous study demonstrated that the IGF system helped to maintain the integrity of podocytes and glomeruli. Histological analysis of IGF1 transgenic mice showed obvious nuclear condense and foot process fusion (Bridgewater et al., 2008). Another study revealed that IGF-binding protein-3 enhanced TGF-β-mediated apoptosis and decreased BM7-induced anti-apoptotic signaling, which altogether resulted in podocyte loss (Peters et al., 2006). The insulin/IGF1R signaling pathway could promote mitochondrial fusion in podocytes, which further affected energy utilization (Ising et al., 2015). Thus, it is reasonable that we hypothesized that the high expression of SGLT2 in podocytes could promote the transition to the epithelium and become dysfunctional and thus contributed to and aggravated proteinuria.

Moreover, among the various molecular mechanisms regulated by IGF1R, the most common mechanism is the autophosphorylation of downstream protein kinases, which triggers signal transduction and results in disease development (Peiris et al., 2017; Qiao et al., 2021). For instance, the PI3K/AKT/mTOR pathway, which is a classical pathway of IGF1R action, is activated to inhibit cell apoptosis and stimulate protein synthesis (Wang et al., 2020). Consistent with these studies, we also observed enhanced transcription and translation of PI3K in high-glucose-stimulated podocytes. EMT is a characteristic feature of podocyte damage. Xing et al. (2015) reported that the PTEN/PI3K/AKT pathway mediated EMT in high-glucose-stimulated podocytes, and inhibition of this pathway prevented phenotypic transition. PI3K/AKT phosphorylation is involved in the signal transduction of proinflammatory and fibrogenic factors, which affected podocyte homeostasis (Luo et al., 2021). In STZ-induced DN models, islet transplantation increased the expression of the podocyte marker, nephrin, and decreased the protein level of the mesenchymal marker, α-SMA (Guo et al., 2014). Consistent with these results, we observed the upregulation of α-SMA, SNAI-1, ZEB2 and the downregulation of nephrin and E-cad in both DN mice and high-glucose-stimulated podocytes. Consistent with this view, the KEGG analysis in our study also revealed enrichment of the phosphatidylinositol signaling system and insulin signaling pathway,

which contributed to the EMT of podocytes (Zhang et al., 2019; Zheng et al., 2020).

SGLT2-is-treated DN patients exhibited decreased circulating levels of IGF1 and IGF2, possibly due to the reduction of its synthesis in the liver. In addition, the expression level of IGF2 was significantly higher than that of IGF1, and this suggested a possible role of IGF2 in mediating IGF1R activation. Several clinical studies have observed increased expression of IGF1 and IGF2 in patients with DN (Sireesha et al., 2009; Shao et al., 2016), but the central roles of the two ligands remain controversial and need further study. As IGF1R inhibitors have not entered the clinical trial stage yet, it is not feasible to assess the clinical effects of these inhibitors in patients with DN. In our *in vitro* trial, OSI-906 helped to stabilize podocyte integrity, in combination with dapagliflozin or not, which provided evidence for its protective role in DN.

In summary, through mRNA-seq, we discovered the anti-EMT effect of IGF1R/PI3K signaling in dapagliflozin-treated DN mice. We inferred that enhanced expression of components of the IGF1R/PI3K pathway could accelerate the EMT of podocytes, ultimately leading to progressive proteinuria. Our study supported the use of IGF1R inhibitors in reducing glomerular proteinuria.

Data availability statement

.The datasets presented in this study can be found in https://www.ncbi.nlm, and the accession number is GSE200322.

Ethics statement

The study involving human participants was reviewed and approved by the Institutional Review Board of The First Affiliated Hospital of Zhengzhou University (2019-KY-361). The animal study was reviewed and approved by the Institutional Review Board of the Experimental Animal Center of Zhengzhou University (ZZU-LAC20210402).

Author contributions

ZZ and JS provided financial support. JS contributed to the design and supervised this study. RG completed the experiment and wrote the manuscript. PW, XZ, and WC helped in animal trials. All authors read and approved the final manuscript.

Funding

This work was supported by the National Natural Science Foundation of China (Grant Nos. 81873611 and 82170738) and the 2020 key project of Medical Science and Technology to JS.

Acknowledgments

The authors thank all volunteers for donating samples for our study. The authors also thank their colleagues' work for this study.

Conflict of interest

The authors declare that the research was conducted in the absence of any commercial or financial relationships that could be construed as a potential conflict of interest.

Publisher's note

Supplementary material

The Supplementary Material for this article can be found online at: https://www.frontiersin.org/articles/10.3389/fphar.2022.897167/full#supplementary-material

SUPPLEMENTARY FIGURE S1
Representative IHC images of SGLT2 expression in glomeruli from the Con, DN, and DA groups.

SUPPLEMENTARY FIGURE S2
Representative images of HE, PAS, Masson staining, and IHC of collagen IV in glomeruli from the Con, DN, and DA groups.

SUPPLEMENTARY FIGURE S3
Representative electron micrographs of Con, DN, and DA mice. Red arrow: thickened GBM and damaged podocyte.

SUPPLEMENTARY FIGURE S4
Venn diagram of all 1957 DEGs. DEGs: differentially expressed genes.

SUPPLEMENTARY FIGURE S5
Heatmap of all 1957 DEGs. Red: upregulated; green: downregulated.

SUPPLEMENTARY FIGURE S6
IGF1R-centered PPI network (combined score >0.4).

SUPPLEMENTARY FIGURE S7
IGF system and EMT-related DEGs among the three groups.

SUPPLEMENTARY FIGURE S8
Representative IHC images of IGF1 and IGF1R expression in glomeruli from the Con, DN, and DA groups.

SUPPLEMENTARY FIGURE S9
IGF1R expression levels in cultured HMC **(A)**, HGREC **(B)**, HK-2 cells **(C)**, and HPC **(D)**. HMC: human mesangial cell; HGREC: human glomerular endothelial cell; HK-2: human tubular epithelial cell line; HPC: human podocytes; Man: mannitol-treated group (34.4 mM). Data were analyzed by ANOVA followed by Tukey's post hoc test. N=3; * $P<0.05$, ** $P<0.01$, and * $P<0.05$, ns: no significance.

References

Alicic, R. Z., Rooney, M. T., and Tuttle, K. R. (2017). Diabetic kidney disease: Challenges, progress, and possibilities. *Clin. J. Am. Soc. Nephrol.* 12 (12), 2032–2045. doi:10.2215/CJN.11491116

Bridgewater, D. J., Dionne, J. M., Butt, M. J., Pin, C. L., and Matsell, D. G. (2008). The role of the type I insulin-like growth factor receptor (IGF-IR) in glomerular integrity. *Growth Horm. IGF Res.* 18 (1), 26–37. doi:10.1016/j.ghir.2007.06.003

Cassis, P., Locatelli, M., Cerullo, D., Corna, D., Buelli, S., Zanchi, C., et al. (2018). SGLT2 inhibitor dapagliflozin limits podocyte damage in proteinuric nondiabetic nephropathy. *JCI Insight* 3 (15), 98720. doi:10.1172/jci.insight.98720

Cheng, H. T., Xu, X., Lim, P. S., and Hung, K. Y. (2021). Worldwide epidemiology of diabetes-related end-stage renal disease, 2000-2015. *Diabetes Care* 44 (1), 89–97. doi:10.2337/dc20-1913

DeFronzo, R. A., Reeves, W. B., and Awad, A. S. (2021). Pathophysiology of diabetic kidney disease: Impact of SGLT2 inhibitors. *Nat. Rev. Nephrol.* 17 (5), 319–334. doi:10.1038/s41581-021-00393-8

Dong, R., Yu, J., Yu, F., Yang, S., Qian, Q., and Zha, Y. (2019). IGF-1/IGF-1R blockade ameliorates diabetic kidney disease through normalizing Snail1 expression in a mouse model. *Am. J. Physiol. Endocrinol. Metab.* 317 (4), E686–E98. doi:10.1152/ajpendo.00071.2019

Gnudi, L., Coward, R. J. M., and Long, D. A. (2016). Diabetic nephropathy: Perspective on novel molecular mechanisms. *Trends Endocrinol. Metab.* 27 (11), 820–830. doi:10.1016/j.tem.2016.07.002

Guo, J., Xia, N., Yang, L., Zhou, S., Zhang, Q., Qiao, Y., et al. (2014). GSK-3β and vitamin D receptor are involved in β-catenin and snail signaling in high glucose-induced epithelial-mesenchymal transition of mouse podocytes. *Cell. Physiol. biochem.* 33 (4), 1087–1096. doi:10.1159/000358678

Ising, C., Koehler, S., Brahler, S., Merkwirth, C., Hohne, M., Baris, O. R., et al. (2015). Inhibition of insulin/IGF-1 receptor signaling protects from mitochondria-mediated kidney failure. *EMBO Mol. Med.* 7 (3), 275–287. doi:10.15252/emmm.201404916

Kato, M., Yuan, H., Xu, Z. G., Lanting, L., Li, S. L., Wang, M., et al. (2006). Role of the akt/FoxO3a pathway in TGF-beta1-mediated mesangial cell dysfunction: A novel mechanism related to diabetic kidney disease. *J. Am. Soc. Nephrol.* 17 (12), 3325–3335. doi:10.1681/ASN.2006070754

Kim, M. N., Moon, J. H., and Cho, Y. M. (2021). Sodium-glucose cotransporter-2 inhibition reduces cellular senescence in the diabetic kidney by promoting ketone body-induced NRF2 activation. *Diabetes Obes. Metab.* 23 (11), 2561–2571. doi:10.1111/dom.14503

Korbut, A. I., Taskaeva, I. S., Bgatova, N. P., Muraleva, N. A., Orlov, N. B., Dashkin, M. V., et al. (2020). SGLT2 inhibitor empagliflozin and DPP4 inhibitor linagliptin reactivate glomerular autophagy in db/db mice, a model of type 2 diabetes. *Int. J. Mol. Sci.* 21 (8), E2987. doi:10.3390/ijms21082987

Kovesdy, C., Schmedt, N., Folkerts, K., Bowrin, K., Raad, H., Batech, M., et al. (2022). Predictors of cardio-kidney complications and treatment failure in patients with chronic kidney disease and type 2 diabetes treated with SGLT2 inhibitors. *BMC Med.* 20 (1), 2. doi:10.1186/s12916-021-02191-2

Lambers Heerspink, H. J., and Gansevoort, R. T. (2015). Albuminuria is an appropriate therapeutic target in patients with CKD: The Pro view. *Clin. J. Am. Soc. Nephrol.* 10 (6), 1079–1088. doi:10.2215/CJN.11511114

Levey, A. S., de Jong, P. E., Coresh, J., El Nahas, M., Astor, B. C., Matsushita, K., et al. (2011). The definition, classification, and prognosis of chronic kidney disease: A KDIGO controversies conference report. *Kidney Int.* 80 (1), 17–28. doi:10.1038/ki.2010.483

Li, J., Dong, R., Yu, J., Yi, S., Da, J., Yu, F., et al. (2018). Inhibitor of IGF1 receptor alleviates the inflammation process in the diabetic kidney mouse model without activating SOCS2. *Drug Des. devel. Ther.* 12, 2887–2896. doi:10.2147/DDDT.S171638

Liang, H., Xin, M., Zhao, L., Wang, L., Sun, M., and Wang, J. (2017). Serum creatinine level and ESR values associated to clinical pathology types and prognosis of patients with renal injury caused by ANCA-associated vasculitis. *Exp. Ther. Med.* 14 (6), 6059–6063. doi:10.3892/etm.2017.5306

Liu, H., Sridhar, V. S., Boulet, J., Dharia, A., Khan, A., Lawler, P. R., et al. (2022). Cardiorenal protection with SGLT2 inhibitors in patients with diabetes mellitus: From biomarkers to clinical outcomes in heart failure and diabetic kidney disease. *Metabolism.* 126, 154918. doi:10.1016/j.metabol.2021.154918

Locatelli, M., Zoja, C., Conti, S., Cerullo, D., Corna, D., Rottoli, D., et al. (2022). Empagliflozin protects glomerular endothelial cell architecture in experimental diabetes through the VEGF-A/caveolin-1/PV-1 signaling pathway. *J. Pathol.* 256 (4), 468–479. doi:10.1002/path.5862

Luo, J., Jiang, J., Huang, H., Jiang, F., Xu, Z., Zhou, Z., et al. (2021). C-peptide ameliorates high glucose-induced podocyte dysfunction through the regulation of the Notch and TGF-beta signaling pathways. *Peptides* 142, 170557. doi:10.1016/j.peptides.2021.170557

Lupia, E., Elliot, S. J., Lenz, O., Zheng, F., Hattori, M., Striker, G. E., et al. (1999). IGF-1 decreases collagen degradation in diabetic NOD mesangial cells: Implications for diabetic nephropathy. *Diabetes* 48 (8), 1638–1644. doi:10.2337/diabetes.48.8.1638

Mundel, P., and Reiser, J. (2010). Proteinuria: An enzymatic disease of the podocyte? *Kidney Int.* 77 (7), 571–580. doi:10.1038/ki.2009.424

Ogurtsova, K., da Rocha Fernandes, J. D., Huang, Y., Linnenkamp, U., Guariguata, L., Cho, N. H., et al. (2017). IDF Diabetes Atlas: Global estimates for the prevalence of diabetes for 2015 and 2040. *Diabetes Res. Clin. Pract.* 128, 40–50. doi:10.1016/j.diabres.2017.03.024

Peiris, D., Spector, A. F., Lomax-Browne, H., Azimi, T., Ramesh, B., Loizidou, M., et al. (2017). Cellular glycosylation affects Herceptin binding and sensitivity of breast cancer cells to doxorubicin and growth factors. *Sci. Rep.* 7, 43006. doi:10.1038/srep43006

Peters, I., Tossidou, I., Achenbach, J., Woroniecki, R., Mengel, M., Park, J. K., et al. (2006). IGF-binding protein-3 modulates TGF-beta/BMP-signaling in glomerular podocytes. *J. Am. Soc. Nephrol.* 17 (6), 1644–1656. doi:10.1681/ASN.2005111209

Qiao, C., Huang, W., Chen, J., Feng, W., Zhang, T., Wang, Y., et al. (2021). IGF1-mediated HOXA13 overexpression promotes colorectal cancer metastasis through upregulating ACLY and IGF1R. *Cell Death Dis.* 12 (6), 564. doi:10.1038/s41419-021-03833-2

Rabkin, R. (2003). Diabetic nephropathy. *Clin. Cornerstone* 5 (2), 1–11. doi:10.1016/s1098-3597(03)90014-7

Ravindran, S., and Munusamy, S. (2022). Renoprotective mechanisms of sodium-glucose co-transporter 2 (SGLT2) inhibitors against the progression of diabetic kidney disease. *J. Cell. Physiol.* 237 (2), 1182–1205. doi:10.1002/jcp.30621

Sen, T., Koshino, A., Neal, B., Bijlsma, M. J., Arnott, C., Li, J., et al. (2022). Mechanisms of action of the sodium-glucose cotransporter-2 (SGLT2) inhibitor canagliflozin on tubular inflammation and damage: A post hoc mediation analysis of the canvas trial. *Diabetes Obes. Metab.* 24 (10), 1950–1956. doi:10.1111/dom.14779

Shao, Y., Lv, C., Yuan, Q., and Wang, Q. (2016). Levels of serum 25(OH)VD3, HIF-1α, VEGF, vWf, and IGF-1 and their correlation in type 2 diabetes patients with different urine albumin creatinine ratio. *J. Diabetes Res.* 2016, 1925424. doi:10.1155/2016/1925424

Sireesha, M., Sambasivan, V., Kumar, V. K., Radha, S., Raj, A. Y., and Qurratulain, H. (2009). Relevance of insulin-like growth factor 2 in the etiopathophysiology of diabetic nephropathy: Possible roles of phosphatase and tensin homolog on chromosome 10 and secreted protein acidic and rich in cysteine as regulators of repair. *J. Diabetes* 1 (2), 118–124. doi:10.1111/j.1753-0407.2009.00025.x

Vallon, V., and Verma, S. (2021). Effects of SGLT2 inhibitors on kidney and cardiovascular function. *Annu. Rev. Physiol.* 83, 503–528. doi:10.1146/annurev-physiol-031620-095920

van Bommel, E. J. M., Muskiet, M. H. A., van Baar, M. J. B., Tonneijck, L., Smits, M. M., Emanuel, A. L., et al. (2020). The renal hemodynamic effects of the SGLT2 inhibitor dapagliflozin are caused by post-glomerular vasodilatation rather than pre-glomerular vasoconstriction in metformin-treated patients with type 2 diabetes in the randomized, double-blind RED trial. *Kidney Int.* 97 (1), 202–212. doi:10.1016/j.kint.2019.09.013

Veron, D., Aggarwal, P. K., Li, Q., Moeckel, G., Kashgarian, M., and Tufro, A. (2021). Podocyte VEGF-A knockdown induces diffuse glomerulosclerosis in diabetic and in eNOS knockout mice. *Front. Pharmacol.* 12, 788886. doi:10.3389/fphar.2021.788886

Veron, D., Aggarwal, P. K., Velazquez, H., Kashgarian, M., Moeckel, G., and Tufro, A. (2014). Podocyte-specific VEGF-a gain of function induces nodular glomerulosclerosis in eNOS null mice. *J. Am. Soc. Nephrol.* 25 (8), 1814–1824. doi:10.1681/ASN.2013070752

Veron, D., Bertuccio, C. A., Marlier, A., Reidy, K., Garcia, A. M., Jimenez, J., et al. (2011). Podocyte vascular endothelial growth factor (Vegf(1)(2)(3)) overexpression

causes severe nodular glomerulosclerosis in a mouse model of type 1 diabetes. *Diabetologia* 54 (5), 1227–1241. doi:10.1007/s00125-010-2034-z

Wang, Y., Yin, L., and Sun, X. (2020). CircRNA hsa_circ_0002577 accelerates endometrial cancer progression through activating IGF1R/PI3K/Akt pathway. *J. Exp. Clin. Cancer Res.* 39 (1), 169. doi:10.1186/s13046-020-01679-8

Xing, L., Liu, Q., Fu, S., Li, S., Yang, L., Liu, S., et al. (2015). PTEN inhibits high glucose-induced phenotypic transition in podocytes. *J. Cell. Biochem.* 116 (8), 1776–1784. doi:10.1002/jcb.25136

Xu, L., Yang, H. C., Hao, C. M., Lin, S. T., Gu, Y., and Ma, J. (2010). Podocyte number predicts progression of proteinuria in IgA nephropathy. *Mod. Pathol.* 23 (9), 1241–1250. doi:10.1038/modpathol.2010.110

Zhang, L., Shen, Z. Y., Wang, K., Li, W., Shi, J. M., Osoro, E. K., et al. (2019). C-reactive protein exacerbates epithelial-mesenchymal transition through Wnt/β-catenin and ERK signaling in streptozocin-induced diabetic nephropathy. *FASEB J.* 33 (5), 6551–6563. doi:10.1096/fj.201801865RR

Zhang, P., Zhang, X., Brown, J., Vistisen, D., Sicree, R., Shaw, J., et al. (2010). Global healthcare expenditure on diabetes for 2010 and 2030. *Diabetes Res. Clin. Pract.* 87 (3), 293–301. doi:10.1016/j.diabres.2010.01.026

Zheng, Z. C., Zhu, W., Lei, L., Liu, X. Q., and Wu, Y. G. (2020). Wogonin ameliorates renal inflammation and fibrosis by inhibiting NF-κB and TGF-β1/smad3 signaling pathways in diabetic nephropathy. *Drug Des. devel. Ther.* 14, 4135–4148. doi:10.2147/DDDT.S274256

Nomenclature

DM diabetic mellitus
DN diabetic nephropathy
SGLT2 sodium–glucose cotransporter 2
SGLT2-is inhibitors of SGLT2
IGF1 insulin-like growth factor-1
IGF2 insulin-like growth factor-2
IGF1R IGF1 receptor
IGFs IGF system
EMT epithelial–mesenchymal transition
HPC human podocytes
HRGEC human renal glomerular endothelial cell
HMC human mesangial cell
HK-2 human tubular epithelial cell line
DA dapagliflozin
OSI-906 inhibitor of IGF1R
STZ streptozotocin
BW body weight
BG blood glucose
SCr serum creatinine
PCR protein and creatinine ratio
BUN blood urea nitrogen
IHC immunohistochemical staining
IF immunofluorescence
PCA principal component analysis
KEGG Kyoto Encyclopedia of Genes and Genomes
ANOVA analysis of variance
DEG differentially expressed genes
FPKM fragments per kilobase of exon per million reads
PPI protein–protein interaction

frontiers | Frontiers in Pharmacology

TYPE Correction
PUBLISHED 22 December 2022
DOI 10.3389/fphar.2022.1074294

OPEN ACCESS

EDITED AND REVIEWED BY
Zhiyong Guo,
Second Military Medical University, China

*CORRESPONDENCE
Jin Shang,
fccshangj2@zzu.edu.cn
Zhanzheng Zhao,
zhanzhengzhao@zzu.edu.cn

SPECIALTY SECTION
This article was submitted to Renal Pharmacology, a section of the journal Frontiers in Pharmacology

RECEIVED 19 October 2022
ACCEPTED 23 November 2022
PUBLISHED 22 December 2022

CITATION
Guo R, Wang P, Zheng X, Cui W, Shang J and Zhao Z (2022), Corrigendum: SGLT2 inhibitors suppress epithelial-mesenchymal transition in podocytes under diabetic conditions *via* downregulating the IGF1R/PI3K pathway.
Front. Pharmacol. 13:1074294.
doi: 10.3389/fphar.2022.1074294

Corrigendum: SGLT2 inhibitors suppress epithelial-mesenchymal transition in podocytes under diabetic conditions *via* downregulating the IGF1R/PI3K pathway

Ruixue Guo[1,2], Peipei Wang[1,2], Xuejun Zheng[1,2], Wen Cui[1,2], Jin Shang[1,3,4]* and Zhanzheng Zhao[1,3,4]*

[1]Department of Nephrology, The First Affiliated Hospital of Zhengzhou University, Zhengzhou, China, [2]Zhengzhou University, Zhengzhou, China, [3]Nephropathy Laboratory, The First Affiliated Hospital of Zhengzhou University, Zhengzhou, China, [4]Laboratory Animal Platform of Academy of Medical Sciences, Zhengzhou, China

KEYWORDS

diabetic nephropathy, sodium-glucose cotransporter-2 inhibitors, insulin-like growth factor-1 receptor, podocyte, epithelial-mesenchymal transition

A Corrigendum on
SGLT2 inhibitors suppress epithelial-mesenchymal transition in podocytes under diabetic conditions *via* downregulating the IGF1R/PI3K pathway

by Guo R, Wang P, Zheng X, Cui W, Shang J and Zhao Z (2022). Front Pharmacol. 13:897167. doi: 10.3389/fphar.2022.897167

In the original article, there was a mistake in Figure 1C, **Supplementary Figure S2**, Figure 3B, and Figure 4 as published:

(1) In Figure 1C and **Supplementary Figure S2**, the IHC images of IGF1R were erroneously used as the results of Collagen IV. The corrected IHC images of Collagen IV were displayed as below.

(2) In Figure 3B, WB gels related to SGLT2 and IGF1R should be annotated according to Con-DA-DN. The corrected Figure 3B was displayed as below.

(3) In Figure 4A, the annotation of WB gel for Nephrin and α-SMA was reversed. The corrected Figure 4A was displayed as below.

(4) In Figures 4B,D, the annotation of the bar for Nephrin and α-SMA was reversed. The corrected Figure 4 was displayed as below.

(5) **Supplemenary Figures S10–S12** are added as the raw data of Figures 3, 4 and **Supplemenary Figure S9**.

The authors apologize for this error and state that this does not change the scientific conclusions of the article in any way. The original article has been updated.

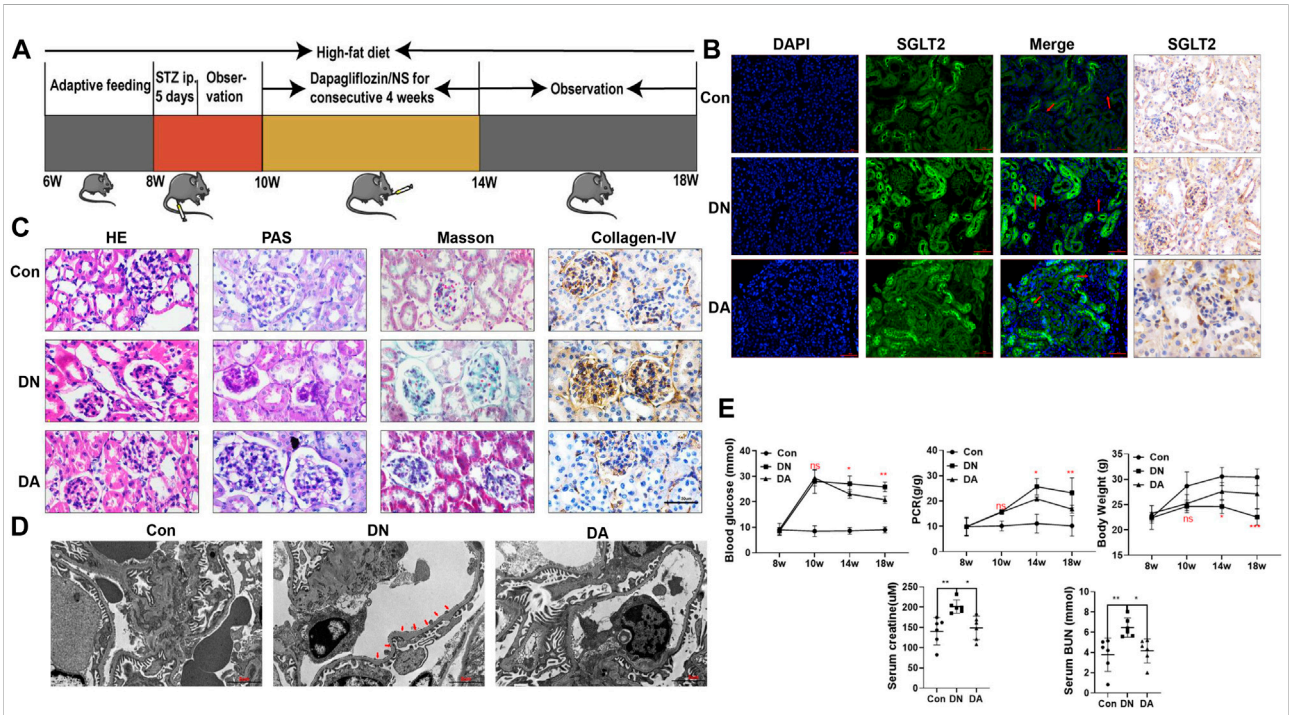

FIGURE 1
Dapagliflozin attenuated STZ-induced diabetic kidney injury. **(A)** Flowchart of the animal experiment (*n* = 6/group). **(B)** IF and IHC staining of SGLT2. **(C)** Pathological staining: light micrographs of HE, PAS, and Masson staining and IHC of collagen IV. **(D)** Representative electron micrographs of glomeruli. Areas of basement membrane thickening and podocyte injury are indicated by red arrows. **(E)** Statistical significance of BG levels, BW, and PCR among the three groups in the 8th, 10th, 14th, and 18th weeks was performed using two-way ANOVA, and Tukey's algorithm for subsequent multiple comparisons between two groups. In parallel, one-way ANOVA was performed for SCr and BUN levels. STZ: streptozotocin; Con: control group; DN: diabetic nephropathy; DA: dapagliflozin-treated DN group: NS: normal saline; SGLT2: sodium–glucose cotransporter 2; IF: immunofluorescent staining; IHC: immunohistochemical staining; one-way ANOVA: one-way analysis of variance; BG: blood glucose; BW: body weight; PCR: urinary total protein to creatinine ratio; SCr: serum creatinine; BUN: blood urea nitrogen.

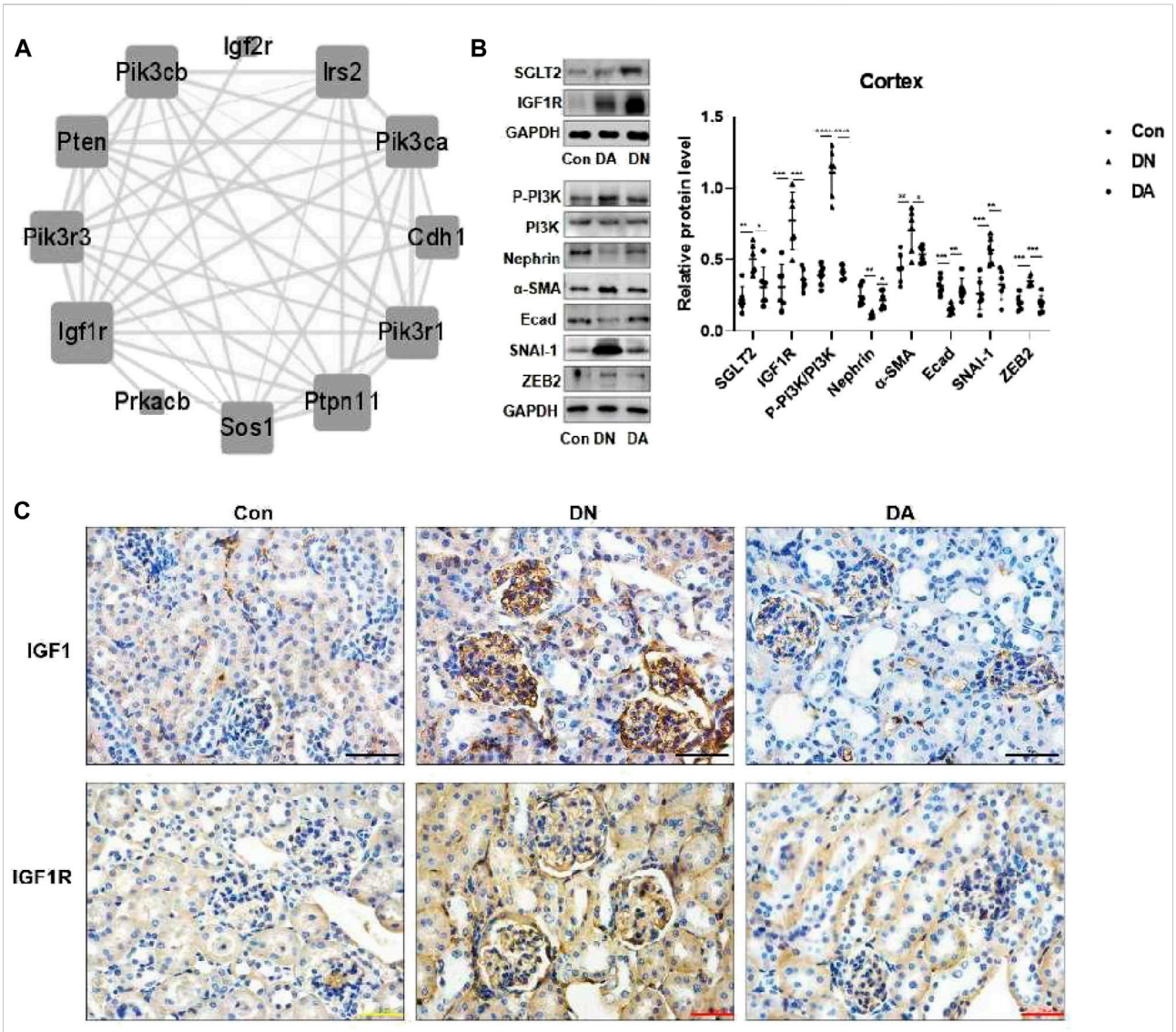

FIGURE 3
In DN models, upregulation of SGLT2 activated IGF1R/PI3K signaling. **(A)** IGF1R-centered PPI network (combined score>0.9). **(B)** Protein expression levels of SGLT2, IGF1R, phosphorylated PI3K, and EMT markers were analyzed using Western blotting. The data were analyzed by ANOVA with Tukey's post hoc test. **(C)** IHC images of IGF1 and IGF1R. PPI: protein–protein interaction; $*p < 0.05$, $**p < 0.01$.

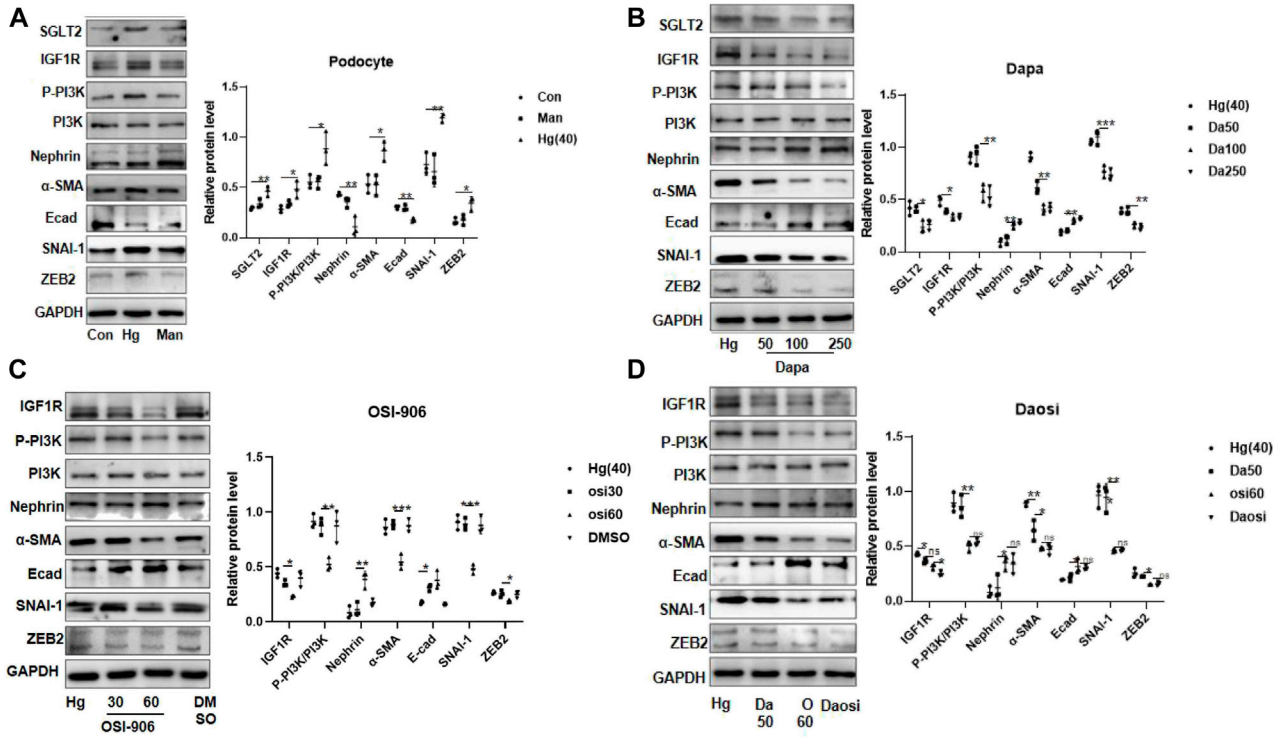

FIGURE 4
SGLT2 directly regulated podocyte EMT *via* IGF1R/PI3K signaling. **(A)** Representative WB images and densitometric analysis of the expression of SGLT2, IGF1R, phosphorylated PI3K, and EMT markers in high-glucose-stimulated podocytes (Hg: 40 nM, 24 h). **(B)** Podocytes treated with different doses of dapagliflozin (50 nM, 100 nM, and 250 nM) and **(C)** OSI-906 (30 nM and 60 nM). **(D)** Combination of OSI60 and Da50. EMT: epithelial–mesenchymal transition. The data were analyzed by ANOVA with Tukey's post hoc test. N = 3; $^{*}p < 0.05$, $^{**}p < 0.01$, $^{***}p < 0.001$, $^{****}p < 0.001$.

Publisher's Note

frontiers | Frontiers in Pharmacology

TYPE Original Research
PUBLISHED 03 October 2022
DOI 10.3389/fphar.2022.969107

OPEN ACCESS

EDITED BY
Dan-Qian Chen,
Northwest University, China

REVIEWED BY
Na Liu,
Tongji University, China
Fujun Lin,
Shanghai Jiao Tong University, China

*CORRESPONDENCE
Xuezhong Gong,
shnanshan@yeah.net

SPECIALTY SECTION
This article was submitted to Renal Pharmacology,
a section of the journal
Frontiers in Pharmacology

RECEIVED 14 June 2022
ACCEPTED 12 September 2022
PUBLISHED 03 October 2022

CITATION
Chen L, Ye Z, Wang D, Liu J, Wang Q, Wang C, Xu B and Gong X (2022), Chuan Huang Fang combining reduced glutathione in treating acute kidney injury (grades 1–2) on chronic kidney disease (stages 2–4): A multicenter randomized controlled clinical trial. *Front. Pharmacol.* 13:969107. doi: 10.3389/fphar.2022.969107

Chuan Huang Fang combining reduced glutathione in treating acute kidney injury (grades 1–2) on chronic kidney disease (stages 2–4): A multicenter randomized controlled clinical trial

Ling Chen[1], Zi Ye[1], Danjun Wang[1], Jianlian Liu[1], Qian Wang[1], Chen Wang[2], Bing Xu[3] and Xuezhong Gong[1]*

[1]Department of Nephrology, Shanghai Municipal Hospital of Traditional Chinese Medicine, Shanghai University of Traditional Chinese Medicine, Shanghai, China, [2]Department of Nephrology, Shuguang Hospital Affiliated to Shanghai University of Traditional Chinese Medicine, Shanghai, China, [3]Department of Nephrology, Minhang Branch of Yueyang Hospital of Integrative Chinese and Western Medicine Affiliated to Shanghai University of Traditional Chinese Medicine, Shanghai, China

Lack of effective drugs for acute kidney injury (AKI) grades 1–2 is a crucial challenge in clinic. Our previously single-center clinical studies indicated Chuan Huang Fang (CHF) might have nephroprotection in AKI on chronic kidney disease (CKD) (A on C) patients by preventing oxidant damage and inhibiting inflammation. Reduced glutathione (RG) has recently been shown to increase the clinical effectiveness of high-flux hemodialysis among patients with severe AKI. In this multicenter randomized controlled clinical study, we designed a new protocol to assess the efficacy and safety of CHF combining RG in patients with A on C. We also explored therapeutic mechanisms from renal fibrosis biomarkers. 98 participants were randomly and equally divided into the RG and RG + CHF subgroups. The RG and RG + CHF groups received general treatments with RG and a combination of RG and CHF, respectively. The therapy lasted for 2 weeks. In this study, the primary assessment result was a difference in the slope of serum creatinine (Scr) over the course of 2 weeks. The secondary evaluation outcomes were alterations in blood urea nitrogen (BUN), uric acid (UA), estimated glomerular filtration rate (eGFR), urinary AKI biomarkers, renal fibrosis biomarkers (transforming growth factor-β_1 (TGF-β_1), connective tissue growth factor (CTGF)), and traditional Chinese medicine (TCM) symptoms. Furthermore, vital signs and adverse events (AEs) were observed. Both groups had a slower renal function decline after treatment than before treatment. Compared with RG group, more reductions of Scr, BUN, UA, and better improvement of eGFR were observed in RG + CHF group ($p < 0.05$). Additionally, the levels of urinary AKI biomarkers, renal fibrosis biomarkers, and TCM syndromes were decreased in RG + CHF group versus RG group ($p < 0.05$). No significant between-group differences were observed of AEs. We thus concluded this

novel therapy of CHF combining RG might be a useful method for treating A on C patients.

KEYWORDS

acute kidney injury, chuan huang fang, chronic kidney disease, renal fibrosis, reduced glutathione, traditional Chinese medicine

Clinical Trial Registration: http://www.chictr.org.cn, ChiCTR2100043311

1 Introduction

Acute kidney injury (AKI) is described as a sudden deterioration in renal function that encompasses both structural failure and loss of functionality (Makris and Spanou, 2016). As a serious complication induced by a variety of critical conditions, AKI might result in significant morbidity and death in both the short and long run (Sawhney and Fraser, 2017). Renal replacement therapy (RRT) ought to be initiated as early as feasible in severe AKI (grade 3), however, there is still a lack of effective drugs for AKI grades 1–2 (Gong et al., 2014; Kellum and Ronco, 2016; Meersch et al., 2018).

Chronic kidney disease (CKD) is a combination of chronic illnesses attributed to a variety of indicators, particularly, inflammation, oxidative stress, and metabolic abnormalities (Hoerger et al., 2015; Yan et al., 2021). AKI and CKD are strongly linked to each other. Furthermore, CKD is an unignorable pathogenic factor for the advancement of AKI (He et al., 2017). Studies have shown that the presence of CKD impaired renal function in individuals with AKI and delayed their recovery after AKI (He et al., 2017; Acosta-Ochoa et al., 2019). It is widely recognized that treating AKI on CKD (A on C) is extremely challenging. Renal fibrosis, which is characterized by glomerulosclerosis and tubulointerstitial fibrosis, is a progressive and chronic condition that affects renal function of CKD patients throughout aging (Bhargava et al., 2021; Li et al., 2021). Renal fibrosis is the most prevalent consequence in practically all instances of progressive CKD, which has few therapeutic choices (Djudjaj and Boor, 2019). With regard to treating renal fibrosis, TCM might be a useful alternative treatment option (Zhou et al., 2020).

According to historical records, Chinese physicians utilized traditional Chinese medicine (TCM) to treat AKI during the era when RRT was absent (Li et al., 2019). In China, TCM has been extensively indicated for the management of renal problems (Norgren and Gong, 2018). Chuan Huang Fang (CHF) is a Chinese herbal formulation synthesized by Professor Xuezhong Gong in Shanghai Municipal Hospital of Traditional Chinese Medicine for the treatment of A on C (Tang et al., 2015; Chen and Gong, 2022b). Our previously single-center clinical studies indicated Chuan Huang Fang (CHF) might have nephroprotection in A on C patients via mechanisms of reducing oxidative damage and decreasing inflammatory reactions (Gong et al., 2014; Gong et al., 2020; Gong et al., 2021). Reduced glutathione (RG) has been shown to be beneficial in controlling local inflammation, reducing accumulation of reactive oxygen species, decreasing inflammatory markers, and lowering oxidative stress in the tissues and organs (Matsubara et al., 2019; Zhang and Bai, 2019; Wang and Wu, 2021). Recently, it has been ascertained that RG could increase the therapeutic efficacy of high-flux hemodialysis among patients with severe AKI (Hu, 2015; Yang et al., 2020). Thus, we subsequently optimized the original protocol by utilizing a new drug treatment method involving the combination of CHF and RG.

We undertook a multicenter randomized controlled trial (RCT) for assessing the clinical efficacy and safety of CHF combing RG against A on C. By completing this trial in a timely manner, a unique pharmacological treatment method for AKI grades 1–2 would be developed.

2 Materials and methods

2.1 Study design

A multicenter randomized controlled clinical trial was performed in this study. The study duration for this research were ranged from 26 December2016- 13 April2020. Approval for the trial was granted by the international review board and ethical committees of each participating hospital and the Ethics Committee of Shanghai Municipal Hospital of Traditional Chinese Medicine (No.2020SHL-KYYS-60). This trial was registered in the Chinese Clinical Trials Register (No. ChiCTR2100043311) before the enrolment of the first participant.

2.2 Participants

Three hospitals enrolled participants in this study: 1) Shanghai Municipal Hospital of Traditional Chinese Medicine, 2) Shuguang Hospital Affiliated to Shanghai University of Traditional Chinese Medicine, and 3) Minhang Branch of Yueyang Hospital of Integrative

Chinese & Western Medicine Affiliated to Shanghai University of Traditional Chinese Medicine. Overall, 98 participants were classified randomly and equally into the RG and RG + CHF groups. This study enrolled patients who had CKD stages 2–4 complicated with AKI grades 1–2 and toxicity stasis inter-combination syndrome, as well as spleen–kidney qi deficit.

2.3 Criteria for inclusion

The following were the criteria for participation in the study: 1) patients satisfied all clinical guidelines for chronic kidney disease stages 2–4 and acute kidney injury grades 1–2, 2) patients satisfied the criteria for a diagnosis for the classification of TCM syndromes, 3) 24 h U-pro of patients ≤2.5 g, 4) ages of patients were range from 18 to 70 years, and 5) patients should be volunteered to participate and signed informed consent.

2.4 Exclusion criteria

The following were the criteria for excluding participants from the study: 1) patients who were pregnant or lactating, 2) patients with acute primary illnesses of other organs requiring immediate treatment, including active *tuberculosis*, malignant tumors, or consumption disorders, 3) patients suffering from anorectal disorders who failed to receive enema, 4) patients who had received a kidney transplant, 5) patients who were psychopaths or who had poor compliance, 6) those with an allergic reaction to the therapeutic medication, and 7) those who were enrolled in other clinical trials within the past 3 months.

2.5 Criteria for differentiating TCM syndromes

Based on the *Guidelines for Clinical Research of Chinese Medicine (New Drug)* (Zheng, 2002)and *Diagnosis, Syndrome Differentiation and Efficacy Evaluation of Chronic Renal Failure (Trial Protocol)* (He 2006), participants exhibited the following four major symptoms and one to two secondary symptoms, all of which might be indicative of toxicity stasis inter-combination syndrome and spleen–kidney qi deficit. The primary symptoms were: 1) feeling fatigued, having shortness of breath, and being reluctant to talk, 2) a feeling of nausea and vomiting, 3) a dim complexion, and 4) soreness in the knees and waist. The following were the secondary symptoms: 1) discomfort and distention in the abdomen, 2) a loss of appetite, as well as numbness to respond, 3) having skin that is dry and squamous, 4) greasy and thick tongue coating, 5) purple and dark tongue or petechia, and 6) fine tart or slow sunken pulse.

2.6 Blinding and randomization

To produce random number sequences, independent biostatisticians used the SPSS (version 21.0) program, which was used to establish these sequences using a simple random approach. The subjects agreed to take part in the research and completed a formal informed consent immediately. Participants also gave their informed permission before being randomly assigned to groups. Participants were assigned a random number and equally classified into two groups by the investigators depending on the order in which they were enrolled in this study: the RG and RG + CHF groups. During the random sampling process, closed envelopes labeled with sequential coding numerals were employed to keep track of allocation information during randomization, and participants, biostatisticians, and investigators were kept blind to the group allocation. Since there was no use of a placebo in the control group, it was not feasible to keep individuals completely unaware of the therapy. It was, however, concealed from all laboratory personnel who were involved in the investigations.

2.7 Study interventions

Participants were recruited for the study after providing formal informed permission. They were categorized at random into the RG and the RG + CHF groups. The participants underwent training for study behavior and health to reduce the possibility of loss and ensure that they could follow the experiment without difficulty. Furthermore, they were informed about potential hazards, their rights, and responsibilities, as well as how to deal with an emergency. All of the patients were given a low-protein, high-quality, and low-salt meal plan to follow (protein consumption of 0.6–0.8 g/kg/day). They received basic therapies with the goal of restoring normal water and electrolyte levels as well as acid-base balance abnormalities, controlling blood pressure, improving anemia, and correcting renal bone illnesses. Certain investigators regularly followed up with participants and assisted them to adhere to treatment procedures and undergo tests as per schedule.

The control group received an intravenous injection (IV) of RG 1.8 g mixed with 0.9 percent normal saline or 5 percent glucose in a volume of 250 ml once every day for a period of 2 weeks. The treatment group additionally received 200 ml CHF twice daily for a total of 2 weeks. Simultaneously, they received an enema of the concentrated solution of CHF once a day for 5 days (i.e., 5 times a week), followed by 2 days of rest. RG was obtained from Chongqing Yaoyou Pharmaceutical

TABLE 1 Composition and action of Chuan Huang Fang.

Ingredient	TCM action	Medicinal parts	Dose (g)
Prepared rhubarb (Zhidahuang)	1. Clear heat-fire 2. Promote diuresis 3. Remove jaundice 4. Detoxify	Root	18
Ligusticum wallichii (Chuanxiong)	1. Benefit qi 2. Promote blood circulation	Root	9
Codonopsis pilosula (Dangshen)	1. Invigorate the spleen 2. Replenish qi	Root	9
Salvia miltiorrhiza (Danshen)	1. Promote blood circulation 2. Remove blood stasis 3. Promote tissue regeneration 4. Regulate menstruation	Root	18
Coptidis rhizome (Huanglian)	1. Clear heat 2. Dry dampness 3. Detoxify	Root	3
Smilacis glabrae (Tufuling)	1. Detoxify 2. Calm endogenous wind 3. Promote diuresis 4. Remove turbid poison	Root	18
Rhizoma Pinellinae Praeparata (Zhibanxia)	1. Eliminate dampness and phlegm 2. Lower adverse qi 3. Prevent vomiting 3. Dissolve lumps and resolve masses	Stem	6
Pericarpium citri reticulatae (Chenpi)	1. Regulate qi 2. Dry dampness to tonify the spleen 3. Lower adverse qi 4. Prevent vomiting	Pericarp	3
Cordyceps sinensis (Chongcaojunsi)	1. Tonify deficiency	Sclerotium	3

TCM, traditional Chinese medicine.

Co. Ltd. The quality standards of CHF were controlled as follows: 1) All herbal medicines were from Shanghai Municipal Hospital of Traditional Chinese Medicine pharmacy, which were traceable; 2) CHF decoction was produced by the pharmacy; 3) Our team had professional pharmaceutical staff to detect the main monomer content of CHF (emodin and TMP, etc) using fingerprints method regularly. The principal pharmaceutical ingredients of CHF are *Prepared rhubarb (Zhidahuang), Ligusticum wallichii (Chuanxiong), Smilacis glabrae (Tufuling), Coptidis rhizome (Huanglian), Codonopsis pilosula (Dangshen), Salviae miltiorrhizae (Danshen), Rhizoma Pinellinae Praeparata (Zhibanxia), Pericarpium citri reticulatae (Chenpi), Cordyceps sinensis (Chongcaojunsi)*, etc (Gong et al., 2021; Chen and Gong, 2022b). Major composition and action of CHF are demonstrated below (Table 1).

Enema were performed by a professional clinician. A clinician took 100 ml concentrated medicine solution of CHF, waiting for the medicine solution close to almost human temperature, and put it into an enema bag. The patient was told to lie on the side of the operating bed, the clinician inserted enema tube to the patient's anus 20–30 cm deep and then injected the medicine solution slowly, each dripping time for 20 min. After enema operation, the patient was instructed to lie on his pillow with buttocks rising 10–15 cm. The medical liquid should be maintained in the patient's intestine for more than 1 h.

A series of related studies were carried out, and data were recorded at baseline and every week throughout the duration of therapy. Patient data was gathered, efficacy-related exams were carried out, and indicators of mechanism and safety, as well as medication administration, were meticulously observed throughout the study.

2.8 Outcome measures

The primary assessment result was measured and represented as the alteration in the slope of serum creatinine (Scr). The secondary assessment outcomes were post-treatment alterations in blood urea nitrogen (BNU), uric acid (UA), estimated glomerular filtration rate (eGFR), urinary AKI biomarkers including neutrophil gelatinase associated lipocalin (NGAL) and interleukin-18 (IL-18), as well as TCM syndromes. Besides, levels of renal fibrosis biomarkers from serum samples, notably, transforming growth factor-β_1 (TGF-β_1), and connective tissue growth factor (CTGF) were assessed both before and after treatment. Moreover, 1 week before and 2 weeks following the treatment, safety results and vital signs indices (hemoglobin, serum potassium, urine routine, blood routine, and electrocardiogram) were documented for each participant. In the meantime, adverse events (AEs) were continuously observed, precisely documented, and appropriately addressed by researchers throughout the trial.

2.9 Evaluation criteria for TCM syndromes

Statistical analysis of the improvement in clinical symptoms score was performed in strict compliance with the Guidelines for Clinical Research of Chinese Medicine (New Drug) (Zheng, 2002). The primary and secondary symptoms of toxicity stasis inter-combination syndrome and spleen–kidney qi deficiency were categorized as mild, moderate, and severe with 2, 4, 8 points, and 4, 8, 12 points, respectively. The two values of total scores generated by the measuring scale depending on TCM symptoms for each patient were added together and employed to compute the efficacy indicator (EI).

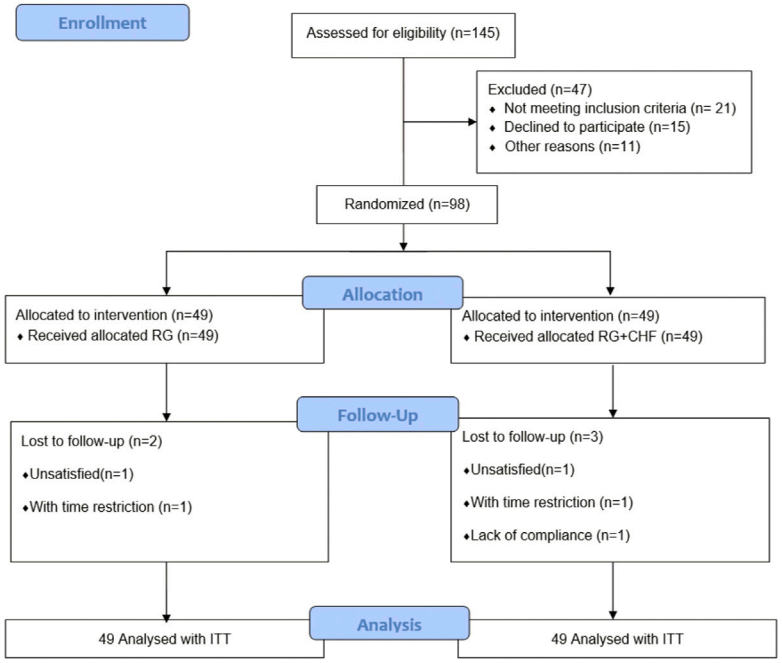

FIGURE 1
Participants flowchart.

TABLE 2 Baseline characteristics of the study participants.

Characteristics	Total (n = 98)	RG group (n = 49)	RG + CHF group (n = 49)
Male, n (%)	58 (59.2)	28 (57.1)	30 (61.2)
Age (years), mean ± SD	62.2 ± 9.9	62.9 ± 9.4	61.4 ± 10.5
Concomitant diseases			
Hypertension, n (%)	79 (80.6)	41 (83.7)	38 (77.6)
2-Diabetes mellitus, n (%)	47 (48.0)	23 (46.9)	24 (49.0)

RG, reduced glutathione; CHF, chuan huang fang.

EI = (Total symptom score before treatment − Total symptom score after treatment)/Total symptom score before treatment × 100%

The treatment efficacy was evaluated using EI. Symptom improvement levels were defined as follows: clinical control (EI ≥ 95%), significant effect (94% > EI ≥ 70%), and effectiveness (69% > EI ≥ 30%) to inefficacy (EI < 30%).

2.10 Determination of the sample size

In this study, we used baseline Scr change to estimate sample size. Premised on previous studies (Zhang and Bai, 2019; Gong et al., 2020), we computed the mean Scr value (160.39 μmol/L), and the standard deviation (44.43 μmol/L). Thus, we hypothesized that the Scr level in the RG + CHF group would be obviously lowered (by over 30 μmol/L) as opposed to that in the control group. SPSS (version 21.0) software was utilized to generate a random number table, and the included participants were randomly and equally divided into the control and treatment groups. It was computed with the help of the sample size estimation program PASS (version 15.0.3) to obtain significant difference α = 0.05 (one-sided test) and test efficacy 1–β = 0.90. Premised on a 20% drop-out rate, the predicted sample size for random sampling was 49 cases within every group for 98 cases in the study.

TABLE 3 The comparison of primary outcome between two groups.

Variable	RG group (n = 49)		RG + CHF group (n = 49)	
	before treatment	after treatment	before treatment	after treatment
Scr (μmol/L), mean ± SD	221.1 ± 71.7	207.3 ± 63.4*	228.3 ± 66.3	177.4 ± 54.6*#

RG, reduced glutathione; CHF, chuan huang fang; Scr, serum creatinine.
*Statistically significant difference from before treatment; $p < 0.05$ was considered statistically significant.
#Statistically significant difference from RG group; $p < 0.05$ was considered statistically significant.

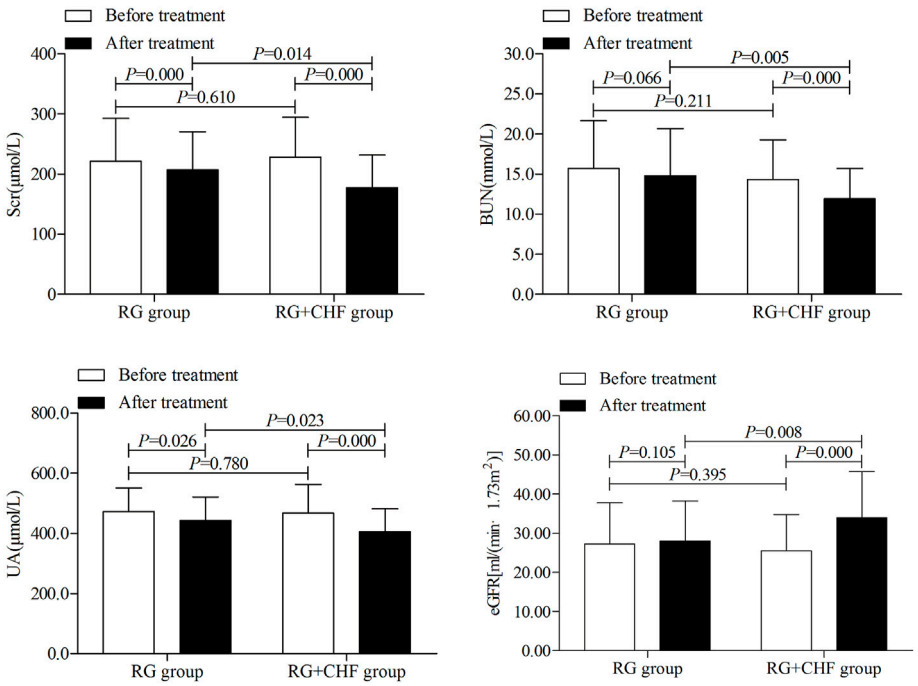

FIGURE 2
The comparison of renal function indicators between two groups before and after treatment.

2.11 Statistical analysis

Regarding the Full Analysis Set (FAS), which is made up of individuals who were randomly assigned into two groups, the principal analysis was carried out. Participants who successfully completed the research protocol and had good compliance were defined as the per-protocol sample. In conformity with the Intend-to-Treat (ITT) principle, all subjects receiving test medications were included in a safety analysis.

Continuous variables were presented as mean ± standard deviation or by the median. In this case, categorical variables were displayed in the form of numbers and percentages. Student's *t*-tests or one-way ANOVA were applied for continuous data exhibiting normal distribution; in contrast, Pearson's chi-square test (or Fisher's exact test for cell count <5 in any cell) was employed for comparisons involving categorical variables. All statistical analyses were conducted using a two-sided design. $p < 0.05$ was established as a determinant of statistical significance. The analyses of statistical data were carried out by a biostatistician who was not engaged in the research with the aid of the SPSS (version 21.0) software package. There were no further analyses or interim analyses carried out in this study.

3 Results

3.1 Participants' characteristics

After screening 145 patients, 98 participants were enrolled in the study with 21 patients not meeting inclusion criteria, 15 patients declining to participant and 11 patients for other reasons (Figure 1). RG group included

TABLE 4 The comparison of secondary outcomes between two groups.

Variables	RG group (n = 49)		RG + CHF group (n = 49)	
	Before treatment	After treatment	Before treatment	After treatment
Renal function indicators				
BUN (mmol/L), mean ± SD	15.7 ± 5.9	14.8 ± 5.9	14.3 ± 5.0	11.9 ± 3.8*#
UA (μmol/L), mean ± SD	472.8 ± 78.4	442.7 ± 79.2*	467.9 ± 94.9	406.6 ± 75.4*#
eGFR [mL/(min·1.73m^2)], mean ± SD	27.3 ± 10.5	28.0 ± 10.2	25.5 ± 9.3	34.0 ± 11.8*#
Urinary AKI biomarkers				
NGAL (ng/ml), mean ± SD	174.0 ± 100.0	138.4 ± 82.3*	177.4 ± 92.0	107.6 ± 42.0*#
IL-18 (pg/ml), mean ± SD	120.5 ± 37.5	104.7 ± 30.8*	126.0 ± 37.4	85.6 ± 27.2*#
Renal fibrosis biomarkers				
TGF-β_1 (μg/L), mean ± SD	187.0 ± 20.8	155.2 ± 21.6*	190.7 ± 25.1	143.9 ± 25.3*#
CTGF (ng/L), mean ± SD	277.1 ± 29.5	232.4 ± 28.1*	281.6 ± 32.4	215.2 ± 37.2*#
TCM syndrome scores	57.9 ± 11.2	34.2 ± 12.0*	57.0 ± 10.4	28.7 ± 10.1*#

RG, reduced glutathione; CHF, chuan huang fang; BUN, blood urea nitrogen; UA, uric acid; eGFR, estimated glomerular filtration rate; NGAL, neutrophil gelatinase-associated lipocalin; IL-18, interleukin-18; TGF-β_1, transforming growth factor-β_1; CTGF, connective tissue growth factor.
*Statistically significant difference from before treatment; $p < 0.05$ was considered statistically significant.
#Statistically significant difference from RG group; $p < 0.05$ was considered statistically significant.

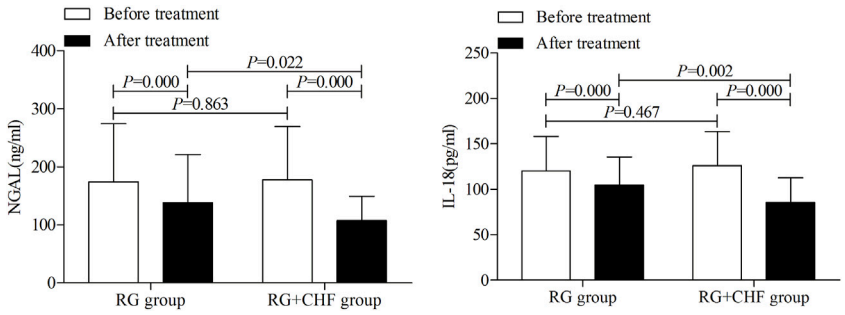

FIGURE 3
The comparison of urinary AKI biomarkers between two groups before and after treatment.

28 male patients and 21 female participants with an average age of (62.9 ± 9.4) years. In RG + CHF group, there were 30 male participants and 19 female participants with an average age of (61.4 ± 10.5) years. The concomitant diseases were also demonstrated below. According to the statistical results, there were no significant difference in gender, age, and concomitant diseases between two groups ($p > 0.05$). It indicated that the baseline characteristics of two groups were balanced and the efficacy of this clinical study was comparable (Table 2).

3.2 Primary outcome

Statistical results showed that mean ± SD of the primary outcome Scr after treatment were 207.3 ± 63.4, 177.4 ± 54.6 in RG group and RG + CHF group respectively. Both groups had a significant Scr decline after treatment than before treatment ($p < 0.01$). Compared with RG group, Scr in RG + CHF group was lower and the difference was statistically significant ($p < 0.05$) (Table 3; Figure 2).

3.3 Secondary outcomes

3.3.1 The comparison of renal function indicators between two groups

According to statistical results, it showed that mean ± SD of BUN after treatment were 14.8 ± 5.9,11.9 ± 3.8 in RG group and RG + CHF group respectively. Compared with RG group, BUN in RG + CHF group were lower and the difference was statistically significant ($p < 0.01$). Besides,

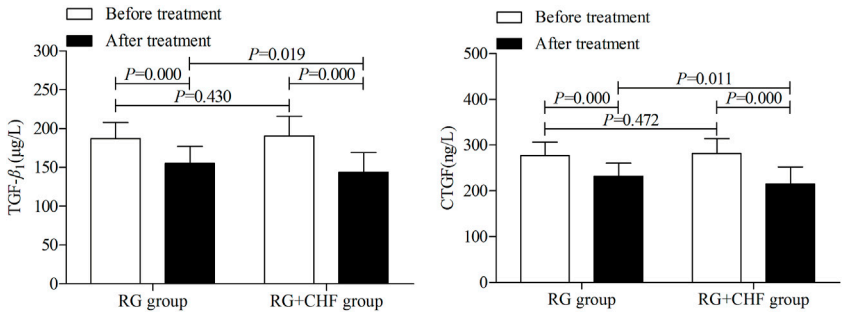

FIGURE 4
The comparison of renal fibrosis biomarkers between two groups before and after treatment.

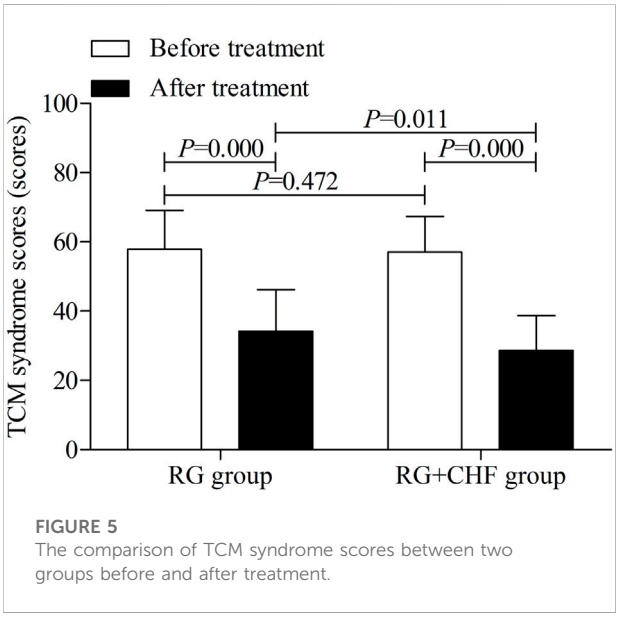

FIGURE 5
The comparison of TCM syndrome scores between two groups before and after treatment.

UA in RG + CHF group were lower and the difference was statistically significant ($p < 0.05$), eGFR was improved and the difference was statistically significant ($p < 0.01$) (Table 4 and Figure 2).

3.3.2 The comparison of urinary AKI biomarkers between two groups

According to statistical results, it showed that mean ± SD of NGAL after treatment were 138.4 ± 82.3, 107.6 ± 42.0 in RG group and RG + CHF group respectively. Compared with RG group, NGAL in RG + CHF group was lower and the difference was statistically significant ($p < 0.05$). Besides, IL-18 in RG + CHF group was lower and the difference was statistically significant ($p < 0.01$) (Table 4 and Figure 3).

3.3.3 The comparison of renal fibrosis biomarkers between two groups

Statistical results showed that mean ± SD of TGF-β_1 after treatment were 115.2 ± 21.6, 143.9 ± 25.3 in RG group and RG + CHF group respectively. Compared with RG group, TGF-β_1 in RG + CHF group was lower and the difference was statistically significant ($p < 0.05$). Besides, CTGF in RG + CHF group was lower and the difference was statistically significant ($p < 0.05$) (Table 4 and Figure 4).

3.3.4 The comparison of TCM syndrome scores between two groups

Statistical results showed that mean ± SD of TCM syndrome scores respectively were 34.2 ± 12.0, 28.7 ± 10.1 in RG group and RG + CHF group after treatment. Compared with RG group, TCM syndrome scores in RG + CHF group were lower and the difference was statistically significant ($p < 0.05$) (Table 4 and Figure 5).

3.3.5 The comparison of effective rate between two groups

As shown in the table below, significantly effective rate and effective rate in RG group respectively were 12 (24.5%) and 6 (12.2%). While the significantly effective rate and effective rate were 24 (49.0%) and 13 (26.5%) in RG + CHF group. Total effective rate (75.5%) in RG + CHF group were obviously higher than that (36.7%) in RG group, and there was significant statistically difference between two groups ($p < 0.01$) (Table 5).

3.5 Safety evaluation

The AEs occurred in the RG and RG + CHF group were demonstrated below (Table 6). There were no SAEs requiring withdrawal reported during the whole treatment period in any group.

TABLE 5 The comparison of effective rate between two groups.

Effective rate	RG group (n = 49)	RG + CHF group (n = 49)	Chi-square value	p value
Significantly effective, n (%)	12(24.5)	24(49.0)	6.323	0.012
Effective, n (%)	6(12.2)	13(26.5)	3.199	0.074
Stable, n (%)	16(32.7)	10(20.4)	1.885	0.170
Ineffective, n (%)	15(30.6)	2(4.1)	12.028	0.001
Total effective rate, n (%)	18(36.7)	37(75.5)	14.959	0.000

RG, reduced glutathione; CHF, chuan huang fang.

TABLE 6 Adverse events during treatment period.

Adverse events	RG group (n = 49)	RG + CHF group (n = 49)
Overall Severe adverse events Gastrointestinal reactions Dizziness or headache Arrhythmia Skin rash Other adverse events	2 0 1 0 0 1 0	3 0 2 1 0 0 0

Adverse events (AEs) were recognized as negative or unpredictable medical manifestations throughout the whole study. Serious adverse events (SAEs) were defined as: 1) critical or life-threatening complications; 2) hospitalization or disability, even death; and 3) other serious hazards and events.
RG, reduced glutathione; CHF, Chuan Huang Fang.

4 Discussion

Compared with RG group, more reductions of Scr, BUN, UA, and better improvement of eGFR were observed in RG + CHF group. Additionally, the levels of urinary AKI biomarkers, renal fibrosis biomarkers, and TCM syndromes were decreased in RG + CHF group versus RG group. RG + CHF group demonstrated better renal protective effects than RG subgroup.

AKI is a clinical condition hallmarked by a sudden decrease of renal function, whereas CKD is hallmarked by renal functional or structural impairments. As a consequence of AKI, a significant number of oxygen free radicals are produced, endogenous antioxidants are continually depleted, and high levels of inflammatory substances are secreted, all of which contribute to kidney damage progression (Han and Lee, 2019). Moreover, A on C might be caused by the combination of multiple factors such as decreased prostaglandin synthesis, inflammatory reaction, oxidative stress, abnormal hemodynamics, and increases in the production of thromboxane by the kidney cortex (Gong et al., 2012; Gong et al., 2014; Ruedig and Johnson, 2015; Barnett and Cummings, 2018). Despite the fact that the shift from AKI to CKD has previously been shown in multiple studies, researches of A on C is still in its infancy (Sawhney and Fraser, 2017; Cooper et al., 2018; Bagshaw and Wald, 2021).

According to our published papers (Gong et al., 2014; Gong et al., 2020; Gong et al., 2021), the common precipitating factors of A on C include infection, electrolyte disturbance, hypertension, and stress state, etc. But inflammation and oxidative stress play a crucial role in the underlying molecular mechanisms of such an acute kidney damage. Addressing inflammatory reactions is a viable approach in the treatment of both CKD and AKI (Nikolic-Paterson et al., 2021). AKI can potentially elicit reactions comparable to those observed in CKD, including enhanced cytokine production, higher level of inflammatory cell infiltration, epithelial to mesenchymal transition, and activation of fibroblasts (Lv et al., 2018; Black et al., 2019). Oxidative stress is a condition caused by an imbalance between antioxidants and oxidants (Daenen et al., 2019). Mounting evidence has revealed that oxidative stress performs a fundamental function in the advancement of renal disorders and the progression of kidney-related problems (Zhou et al., 2021). Oxidative stress and inflammation are inextricably related, jointly causing and exacerbating the effects of the other (Luo et al., 2021).

Our previously single-center clinical studies indicated CHF might have nephroprotection in A on C patients (Gong et al., 2014; Gong et al., 2020; Gong et al., 2021). Besides, we published papers about CHF against AKI in animal and cell models as well. Previous research (Gong et al., 2019b) explored clinical dosage of trivalent arsenic inhibition effect and mechanism of renal toxicity. We found CHF could effectively suppressed clinical dose of trivalent arsenic of the kidney toxicity, and its molecular mechanism were associated with the inhibition of caspase three induced renal tubular epithelial cell apoptosis. We also conducted a research on the mechanism of Zhidahuang-Chuanxiong drug pair on tubular epithelial cell apoptosis in contrast-induced acute kidney injury (CI-AKI) rats (Gong et al., 2013). Thus, it was found that activation of p38MAPK pathway

played an important role in pathogenesis of CI-AKI, and Zhidahuang-Chuanxiong drug pair might alleviate renal damage in CI-AKI rats through inhibiting the activation of pathway. Based on this result, we further explored the mechanism of the drug pair from nuclear factor erythroid 2-related factor2/Hemeoxygenase-1(Nrf2/HO-1) pathway (Gong et al., 2017). Nrf2/HO-1 pathway was activated and involved in the process, and Zhidahuang-Chuanxiong drug pair could activate and have renal protective effects of CI-AKI rats by inhibiting this pathway. Tetramethylpyrazine (TMP), an active component in both CHF and the medicinal herbs *Ligusticum wallichii (Chuanxiong)*, has the potential to prevent AKI via a variety of processes, including ameliorating oxidative stress damage, suppressing inflammatory responses, deterring apoptotic cell death of intrinsic renal cells, and modulating autophagy (Gong, 2018; Gong et al., 2019a; Gong, 2020; Chen and Gong, 2022a).

Renal fibrosis is by far the most important mechanism that leads to CKD (Gu et al., 2020). It is originally induced by a variety of biophysiological shocks or inflammatory mediators, and it serves as a protective response in the case of kidney injury. Nevertheless, when kidney injuries are prolonged and overreacted, this reaction becomes pathogenic, ultimately contributing to the emergence of ESRD (Inker et al., 2014). TGF-β_1 is the primary profibrotic facilitator in kidney disorders due to its role as a key modulator of fibrosis (Meng et al., 2016). Research findings on the upregulation of active TGF-β_1 have additionally validated the profibrotic function of TGF-β_1 in the etiology of progressive renal fibrosis in a variety of kidney illnesses (Wong et al., 2017; Humphreys, 2018; Kim et al., 2018). Consequently, it has been hypothesized that TGF-β_1 might be a possible treatment target for the clinical management of renal fibrosis. CTGF is an essential component in the onset of renal fibrosis. Although CTGF exists in healthy kidneys as a form of low level, the level is dramatically elevated in a variety of renal illnesses, and it has a substantial impact on the progression of progressive kidney illness (Toda et al., 2018). The gene of CTGF, a matricellular protein, is a straightforward downstream initial response gene of the TGF-β_1 (Lee et al., 2015). According to research results, the treatment group could effectively reduce the level of TGF-β_1 and CTGF, which might provide clinical evidence for early prevention and treatment of A on C patients.

RRT is predominantly applied to treat severe AKI (grade 3). However, there is currently no recognized medication therapy strategy for AKI grades 1–2 (Gong et al., 2014; Kellum and Ronco, 2016; Meersch et al., 2018; Peters et al., 2018). As indicated by the KDIGO recommendations, the primary therapeutic approach for AKI is to regulate the body's internal milieu, and the vast majority of therapies are supportive rather than curative. Identifying the underlying cause of AKI, maintaining hemodynamic stability, and dealing with severe consequences are all critical throughout the early stages of the disease (Moore et al., 2018). The maintenance of hemodynamic stability needs to be given extensive consideration in AKI because of the impaired autoregulation mechanisms that are present (Ostermann et al., 2019). As previously stated, RG has the potential to attenuate the damaging peroxide metabolites, decrease oxidative stress, and perform specific metabolic functions in the production of inflammatory components (Matsubara et al., 2019; Zhang and Bai, 2019; Wang and Wu, 2021).

Premised on our previously clinical evidence and recent breakthroughs in clinical therapy of A on C, we designed a new protocol with the combination of CHF and RG. And this study tried to explore the medical mechanism of CHF combining RG treating A on C from the aspect of renal fibrosis. The current research would be beneficial in resolving this clinical dilemma in the future. The combination might successfully minimize renal damage of A on C patients, enhance restoration of kidney functionality, and relieve clinical symptoms in these individuals. As a result, we consider that the clinical application values of this therapy method are satisfactory. Based on the findings of this study, we will continue to explore therapeutic effects of CHF combining RG for patients with A on C to gather more relevant clinical data.

5 Conclusion

CHF combining RG showed better therapeutic effects than RG alone, and its renal protective effects were associated with reducing Scr, BUN, UA, and improving eGFR, as well as preventing renal fibrosis. We thus concluded that this novel therapy of combining CHF and RG might be a useful method for treating A on C patients.

Data availability statement

The original contributions presented in the study are included in the article/supplementary material, further inquiries can be directed to the corresponding author.

Ethics statement

The studies involving human participants were reviewed and approved by the Ethics Committee of Shanghai Municipal Hospital of Traditional Chinese Medicine. The patients/participants provided their written informed consent to participate in this study.

Author contributions

XG was the chief investigator in charge of this trial program. He designed this study, and coordinated various personnel and material resources to ensure the smooth implementation of the program. In addition, he participated in, instructed, and supervised the whole study. CW and BX were responsible for the enrollment of participants in other two hospitals, and they

coordinated related affairs with XG. LC and ZY understood the task of data collection, analysis, and interpretation. Besides, LC mainly drafted the manuscript and assisted the implement of subsequent trial program. DW, JL, and QW assisted to consult relevant literatures, and they contributed many useful advices to this manuscript. The manuscript is critically revised by XG and finally approved by all authors for publication.

Funding

This work was supported by grants from National Natural Science Foundation of China (Nos. 82074387 and 81873280), Shanghai Municipal Science and Technology Commission Project (No. 20Y21902200), and Shanghai Municipal Health Commission Project (No. ZY(2021-2023)-0207-01).

Conflict of interest

The authors declare that the research was conducted in the absence of any commercial or financial relationships that could be construed as a potential conflict of interest.

Publisher's note

References

Acosta-Ochoa, I., Bustamante-Munguira, J., Mendiluce-Herrero, A., Bustamante-Bustamante, J., and Coca-Rojo, A. (2019). Impact on outcomes across KDIGO-2012 AKI criteria according to baseline renal function. *J. Clin. Med.* 8 (9), E1323. doi:10.3390/jcm8091323

Bagshaw, S. M., and Wald, R. (2021). Starting kidney replacement therapy in critically III patients with acute kidney injury. *Crit. Care Clin.* 37 (2), 409–432. doi:10.1016/j.ccc.2020.11.005

Barnett, L. M. A., and Cummings, B. S. (2018). Nephrotoxicity and renal pathophysiology: A contemporary perspective. *Toxicol. Sci.* 164 (2), 379–390. doi:10.1093/toxsci/kfy159

Bhargava, V., Singh, K., Meena, P., and Sanyal, R. (2021). Nephrogenic systemic fibrosis: A frivolous entity. *World J. Nephrol.* 10 (3), 29–36. doi:10.5527/wjn.v10.i3.29

Black, L. M., Lever, J. M., and Agarwal, A. (2019). Renal inflammation and fibrosis: A double-edged sword. *J. Histochem. Cytochem.* 67 (9), 663–681. doi:10.1369/0022155419852932

Chen, L., and Gong, X. (2022a). Drug-induced acute kidney injury: Epidemiology, mechanisms, risk factors, and preventive treatment of traditional Chinese medicine. *Integr. Med. Nephrol. Androl.* 9 (5), 5. doi:10.4103/2773-0387.345767

Chen, L., and Gong, X. (2022b). Efficacy and safety of chuan Huang Fang combining reduced glutathione in treating acute kidney injury (grades 1-2) on chronic kidney disease (stages 2-4): Study protocol for a multicenter randomized controlled clinical trial. *Evid. Based. Complement. Altern. Med.* 2022, 1099642. doi:10.1155/2022/1099642

Cooper, D. J., Plewes, K., Grigg, M. J., Rajahram, G. S., Piera, K. A., William, T., et al. (2018). The effect of regularly dosed paracetamol versus no paracetamol on renal function in plasmodium knowlesi malaria (PACKNOW): Study protocol for a randomised controlled trial. *Trials* 19 (1), 250. doi:10.1186/s13063-018-2600-0

Daenen, K., Andries, A., Mekahli, D., Van Schepdael, A., Jouret, F., and Bammens, B. (2019). Oxidative stress in chronic kidney disease. *Pediatr. Nephrol.* 34 (6), 975–991. doi:10.1007/s00467-018-4005-4

Djudjaj, S., and Boor, P. (2019). Cellular and molecular mechanisms of kidney fibrosis. *Mol. Asp. Med.* 65, 16–36. doi:10.1016/j.mam.2018.06.002

Gong, X., Duan, Y., Wang, Y., Ye, Z., Zheng, J., Lu, W., et al. (2020). Effects of Chuanhuang Decoction on renal function and oxidative stress in patients of chronic kidney disease at stage 2-4 complicated with acute kidney injury. *J. Shanghai Univ. Trad. Chin. Med. Sci.* 34 (1), 11–16. doi:10.16306/j.1008-861x.2020.01.002

Gong, X., Duan, Y., Zheng, J., Ye, Z., and Hei, T. K. (2019a). Tetramethylpyrazine prevents contrast-induced nephropathy via modulating tubular cell mitophagy and suppressing mitochondrial fragmentation, CCL2/CCR2-mediated inflammation, and intestinal injury. *Oxid. Med. Cell. Longev.* 2019, 7096912. doi:10.1155/2019/7096912

Gong, X., Qiu, A., Duan, Y., Ye, Z., Zheng, J., Wang, Q., et al. (2017). Effects of Couplet Medicines of Prepared Radix et Rhizoma Rhei-Rhizoma Ligustici Chuanxiong on Nrf2/HO-1 Signaling Pathway in Renal Tissue of Contrast-induced Nephropathy Rats. *J. Shanghai Univ. Trad. Chin. Med. Sci.* 31 (06), 58–61. doi:10.16306/j.1008-861x.2017.06.014

Gong, X., Tang, X., Wang, Q., Wang, Y., and Zhou, J. (2014). Observe the clinical efficacy of chuanhuang decoction combined with lipo PGE1 in treating acute kidney injury (AKI) on phase 2~4 chronic kidney disease (CKD) patients. *Chin. J. Integr. Trad. West Med. Nephrol.* 15 (9), 784–787.

Gong, X., Wang, Q., Fu, D., Tang, X., Wang, Y., Wang, G., et al. (2013). Research on Radix et Rhizoma Rhei-Rhizoma Ligustici Chuanxiong restraining renal tubular epithelial cell apoptosis in contrast-induced nephropathy rats. *Shanghai J. Trad. Chin. Med.* 47 (03), 69–71. doi:10.16305/j.1007-1334.2013.03.023

Gong, X., Wang, Y., Fu, D., Wang, Q., Wang, G., Tang, X., et al. (2012). Effects of Zhidahuang - chuanxiong drug pair on tubular epithelial cell apoptosis in contrast - induced nephropathy rats. *Chin. J. Integr. Trad. West Med. Nephrol.* 13 (8), 675–677.

Gong, X., Ye, Z., Xu, X., Chen, L., Xu, Y., Yuan, D., et al. (2021). Effects of Chuanhuang Formula combined with prostaglandin E1 in treating patients of chronic kidney disease complicated with acute kidney injury and its influence on NLRP3. *J. Shanghai Univ. Trad. Chin. Med. Sci.* 35 (06), 12–16. doi:10.16306/j.1008-861x.2021.06.002

Gong, X. Z. (2020). Chinese medicine might Be A promising way for A solution to arsenic nephrotoxicity. *Chin. J. Integr. Med.* 26 (2), 83–87. doi:10.1007/s11655-019-3210-8

Gong, X., Zheng, J., Duan, Y., and Ye, Z. (2019b). Effect of Chuanhuang Fang on apoptosis of renal tubular epithelial cells in rats with trivalent arsenic nephrotoxicity. *Beijing Med. J.* 41, 1089–1093. doi:10.15932/j.0253-9713.2019.12.009

Gong, X. Z. (2018). Recent advances in Chinese medicine for contrast-induced nephropathy. *Chin. J. Integr. Med.* 24 (1), 6–9. doi:10.1007/s11655-017-2906-x

Gu, Y. Y., Liu, X. S., Huang, X. R., Yu, X. Q., and Lan, H. Y. (2020). TGF-B in renal fibrosis: Triumphs and challenges. *Future Med. Chem.* 12 (9), 853–866. doi:10.4155/fmc-2020-0005

Han, S. J., and Lee, H. T. (2019). Mechanisms and therapeutic targets of ischemic acute kidney injury. *Kidney Res. Clin. Pract.* 38 (4), 427–440. doi:10.23876/j.krcp.19.062

He, L. Q. (2006). Diagnosis, syndrome differentiation and efficacy evaluation of chronic renal failure (trial protocol). *Shanghai J. Tradit. Chin. Med.* 40 (8), 8–9.

He, L., Wei, Q., Liu, J., Yi, M., Liu, Y., Liu, H., et al. (2017). AKI on CKD: Heightened injury, suppressed repair, and the underlying mechanisms. *Kidney Int.* 92 (5), 1071–1083. doi:10.1016/j.kint.2017.06.030

Hoerger, T. J., Simpson, S. A., Yarnoff, B. O., Pavkov, M. E., Ríos Burrows, N., Saydah, S. H., et al. (2015). The future burden of CKD in the United States: A simulation model for the CDC CKD initiative. *Am. J. Kidney Dis.* 65 (3), 403–411. doi:10.1053/j.ajkd.2014.09.023

Hu, D. J. (2015). Reduced glutathione with high flux hemodialysis therapy of acute renal injury in clinical study. *J. Clin. Nephrol.* 15 (1), 39–41.

Humphreys, B. D. (2018). Mechanisms of renal fibrosis. *Annu. Rev. Physiol.* 80, 309–326. doi:10.1146/annurev-physiol-022516-034227

Inker, L. A., Astor, B. C., Fox, C. H., Isakova, T., Lash, J. P., Peralta, C. A., et al. (2014). KDOQI US commentary on the 2012 KDIGO clinical practice guideline for the evaluation and management of CKD. *Am. J. Kidney Dis.* 63 (5), 713–735. doi:10.1053/j.ajkd.2014.01.416

Kellum, J. A., and Ronco, C. (2016). The 17th acute disease quality initiative international consensus conference: Introducing precision renal replacement therapy. *Blood Purif.* 42 (3), 221–223. doi:10.1159/000448500

Kim, K. K., Sheppard, D., and Chapman, H. A. (2018). TGF-β1 signaling and tissue fibrosis. *Cold Spring Harb. Perspect. Biol.* 10 (4), a022293. doi:10.1101/cshperspect.a022293

Lee, S. Y., Kim, S. I., and Choi, M. E. (2015). Therapeutic targets for treating fibrotic kidney diseases. *Transl. Res.* 165 (4), 512–530. doi:10.1016/j.trsl.2014.07.010

Li, H. D., Meng, X. M., Huang, C., Zhang, L., Lv, X. W., and Li, J. (2019). Application of herbal traditional Chinese medicine in the treatment of acute kidney injury. *Front. Pharmacol.* 10, 376. doi:10.3389/fphar.2019.00376

Li, S. S., Sun, Q., Hua, M. R., Suo, P., Chen, J. R., Yu, X. Y., et al. (2021). Targeting the wnt/β-catenin signaling pathway as a potential therapeutic strategy in renal tubulointerstitial fibrosis. *Front. Pharmacol.* 12, 719880. doi:10.3389/fphar.2021.719880

Luo, L. P., Suo, P., Ren, L. L., Liu, H. J., Zhang, Y., and Zhao, Y. Y. (2021). Shenkang injection and its three anthraquinones ameliorates renal fibrosis by simultaneous targeting IκB/NF-κB and keap1/nrf2 signaling pathways. *Front. Pharmacol.* 12, 800522. doi:10.3389/fphar.2021.800522

Lv, W., Booz, G. W., Wang, Y., Fan, F., and Roman, R. J. (2018). Inflammation and renal fibrosis: Recent developments on key signaling molecules as potential therapeutic targets. *Eur. J. Pharmacol.* 820, 65–76. doi:10.1016/j.ejphar.2017.12.016

Makris, K., and Spanou, L. (2016). Acute kidney injury: Definition, pathophysiology and clinical phenotypes. *Clin. Biochem. Rev.* 37 (2), 85–98.

Matsubara, A., Oda, S., Jia, R., and Yokoi, T. (2019). Acute kidney injury model established by systemic glutathione depletion in mice. *J. Appl. Toxicol.* 39 (6), 919–930. doi:10.1002/jat.3780

Meersch, M., Küllmar, M., Schmidt, C., Gerss, J., Weinhage, T., Margraf, A., et al. (2018). Long-term clinical outcomes after early initiation of RRT in critically ill patients with AKI. *J. Am. Soc. Nephrol.* 29 (3), 1011–1019. doi:10.1681/asn.2017060694

Meng, X. M., Nikolic-Paterson, D. J., and Lan, H. Y. (2016). TGF-B: The master regulator of fibrosis. *Nat. Rev. Nephrol.* 12 (6), 325–338. doi:10.1038/nrneph.2016.48

Moore, P., Hsu, R., and Liu, K. (2018). Management of acute kidney injury: Core curriculum 2018. *Am. J. Kidney Dis.* 72, 136–148. doi:10.1053/j.ajkd.2017.11.021

Nikolic-Paterson, D. J. G. K., and Ma, F. Y. (2021). JUN amino (2021). JUN amino terminal kinase in cell death and inflammation in acute and chronic kidney disease. *Integr. Med. Nephrol. Androl.* 8 (10). doi:10.4103/imna.imna_35_21

Norgren, S., and Gong, X. Z. (2018). Contrast-induced nephropathy-time for Western medicine and Chinese medicine to team up. *Chin. J. Integr. Med.* 24 (1), 3–5. doi:10.1007/s11655-017-2905-y

Ostermann, M., Liu, K., and Kashani, K. (2019). Fluid management in acute kidney injury. *Chest* 156, 594–603. doi:10.1016/j.chest.2019.04.004

Peters, E., Antonelli, M., Wittebole, X., Nanchal, R., François, B., Sakr, Y., et al. (2018). A worldwide multicentre evaluation of the influence of deterioration or improvement of acute kidney injury on clinical outcome in critically ill patients with and without sepsis at ICU admission: Results from the intensive care over nations audit. *Crit. Care* 22 (1), 188. doi:10.1186/s13054-018-2112-z

Ruedig, E., and Johnson, T. E. (2015). An evaluation of health risk to the public as a consequence of *in situ* uranium mining in Wyoming, USA. *J. Environ. Radioact.* 150, 170–178. doi:10.1016/j.jenvrad.2015.08.004

Sawhney, S., and Fraser, S. D. (2017). Epidemiology of AKI: Utilizing large databases to determine the burden of AKI. *Adv. Chronic Kidney Dis.* 24 (4), 194–204. doi:10.1053/j.ackd.2017.05.001

Tang, X., Gong, X., and Wang, Q. (2015). Experiences of professor Gong Xuezhong in treating acute kidney injury on chronic kidney disease based on toxicity and blood stasis. *Shenzhen J. Integr. Trad. Chin. West Med.* 25 (17), 40–42. doi:10.16458/j.cnki.1007-0893.2015.17.021

Toda, N., Mukoyama, M., Yanagita, M., and Yokoi, H. (2018). CTGF in kidney fibrosis and glomerulonephritis. *Inflamm. Regen.* 38, 14. doi:10.1186/s41232-018-0070-0

Wang, W. M., and Wu, Y. (2021). Clinical effect of reduced glutathione combined with jinshuibao in the treatment of acute renal injury. *Guide China Med.* 19 (24), 7–9.

Wong, E. B., Ndung'u, T., and Kasprowicz, V. O. (2017). The role of mucosal-associated invariant T cells in infectious diseases. *Immunology* 150 (1), 45–54. doi:10.1111/imm.12673

Yan, H., Xu, J., Xu, Z., Yang, B., Luo, P., and He, Q. (2021). Defining therapeutic targets for renal fibrosis: Exploiting the biology of pathogenesis. *Biomed. Pharmacother.* 143, 112115. doi:10.1016/j.biopha.2021.112115

Yang, F., Tong, J., Li, H., Chen, J., and Dai, L. (2020). Effects of reduced glutathione combined with high-flux hemodialysis on serum CysC, KIM-1 and Scr in patients with acute kidney injury. *Med. J. West China* 32 (6), 863–867.

Zhang, L., and Bai, L. (2019). Therapeutic effect of Reduced Glutathione on acute kidney injury in patients with sepsis. *Chin. Mode Med.* 26 (9), 54–60.

Zheng, X. (2002). *Guidelines for clinical research of Chinese medicine (new drug)*. Beijing: Chinese Medicine and Science Publication House.

Zhou, F., Zou, X., Zhang, J., Wang, Z., Yang, Y., and Wang, D. (2021). Jian-pi-yi-shen formula ameliorates oxidative stress, inflammation, and apoptosis by activating the Nrf2 signaling in 5/6 nephrectomized rats. *Front. Pharmacol.* 12, 630210. doi:10.3389/fphar.2021.630210

Zhou, S., Ai, Z., Li, W., You, P., Wu, C., Li, L., et al. (2020). Deciphering the pharmacological mechanisms of taohe-chengqi decoction extract against renal fibrosis through integrating network Pharmacology and experimental validation *in vitro* and *in vivo*. *Front. Pharmacol.* 11, 425. doi:10.3389/fphar.2020.00425

Frontiers in Pharmacology

Explores the interactions between chemicals and living beings

The most cited journal in its field, which advances access to pharmacological discoveries to prevent and treat human disease.

Discover the latest Research Topics

See more →

Frontiers

Avenue du Tribunal-Fédéral 34
1005 Lausanne, Switzerland
frontiersin.org

Contact us

+41 (0)21 510 17 00
frontiersin.org/about/contact